THE ROLE OF GLYCANS IN INFECTIOUS DISEASE

EDITED BY: Ivan Martinez Duncker, Fabrizio Chiodo, Hector Mora Montes and Gerardo R. Vasta

PUBLISHED IN: Frontiers in Microbiology and Frontiers in Immunology

frontiers Research Topics

ISSN 1664-8714
ISBN 978-2-88976-312-2
DOI 10.3389/978-2-88976-312-2

About Frontiers

Frontiers is more than just an open-access publisher of scholarly articles: it is a pioneering approach to the world of academia, radically improving the way scholarly research is managed. The grand vision of Frontiers is a world where all people have an equal opportunity to seek, share and generate knowledge. Frontiers provides immediate and permanent online open access to all its publications, but this alone is not enough to realize our grand goals.

Frontiers Journal Series

The Frontiers Journal Series is a multi-tier and interdisciplinary set of open-access, online journals, promising a paradigm shift from the current review, selection and dissemination processes in academic publishing. All Frontiers journals are driven by researchers for researchers; therefore, they constitute a service to the scholarly community. At the same time, the Frontiers Journal Series operates on a revolutionary invention, the tiered publishing system, initially addressing specific communities of scholars, and gradually climbing up to broader public understanding, thus serving the interests of the lay society, too.

Dedication to Quality

Each Frontiers article is a landmark of the highest quality, thanks to genuinely collaborative interactions between authors and review editors, who include some of the world's best academicians. Research must be certified by peers before entering a stream of knowledge that may eventually reach the public - and shape society; therefore, Frontiers only applies the most rigorous and unbiased reviews.
Frontiers revolutionizes research publishing by freely delivering the most outstanding research, evaluated with no bias from both the academic and social point of view. By applying the most advanced information technologies, Frontiers is catapulting scholarly publishing into a new generation.

What are Frontiers Research Topics?

Frontiers Research Topics are very popular trademarks of the Frontiers Journals Series: they are collections of at least ten articles, all centered on a particular subject. With their unique mix of varied contributions from Original Research to Review Articles, Frontiers Research Topics unify the most influential researchers, the latest key findings and historical advances in a hot research area! Find out more on how to host your own Frontiers Research Topic or contribute to one as an author by contacting the Frontiers Editorial Office: frontiersin.org/about/contact

THE ROLE OF GLYCANS IN INFECTIOUS DISEASE

Topic Editors:
Ivan Martinez Duncker, Universidad Autónoma del Estado de Morelos, Mexico
Fabrizio Chiodo, National Research Council (CNR), Italy
Hector Mora Montes, University of Guanajuato, Mexico
Gerardo R. Vasta, University of Maryland, Baltimore, United States

Citation: Duncker, I. M., Chiodo, F., Montes, H. M., Vasta, G. R., eds. (2022). The Role of Glycans in Infectious Disease. Lausanne: Frontiers Media SA.
doi: 10.3389/978-2-88976-312-2

Table of Contents

frontiers | Frontiers in Microbiology

EDITORIAL
published: 12 May 2022
doi: 10.3389/fmicb.2022.921436

Editorial: The Role of Glycans in Infectious Disease

Iván Martínez-Duncker[1]*, *Fabrizio Chiodo*[2,3], *Héctor M. Mora-Montes*[4] and *Gerardo R. Vasta*[5]*

[1] Laboratorio de Glicobiología Humana y Diagnóstico Molecular, Centro de Investigación en Dinámica Celular, Instituto de Investigación en Ciencias Básicas y Aplicadas, Universidad Autónoma del Estado de Morelos, Cuernavaca, Mexico, [2] Department of Molecular Cell Biology and Immunology, Amsterdam UMC, Vrije Universiteit Amsterdam, Amsterdam, Netherlands, [3] Institute of Biomolecular Chemistry, National Research Council (CNR) Pozzuoli Napoli, Pozzuoli Napoli, Italy, [4] División de Ciencias Naturales y Exactas, Departamento de Biología, Universidad de Guanajuato, Guanajuato, Mexico, [5] Department of Microbiology and Immunology, University of Maryland School of Medicine, UMB and Institute of Marine and Environmental Technology, University of Maryland, Baltimore, MD, United States

Keywords: tuberculosis, Chagas, toxoplasmosis, galectins, *Sporothrix*, fungal, HIV, COVID

Editorial on the Research Topic

The Role of Glycans in Infectious Disease

Virtually all eukaryotic and bacterial cells, as well as many enveloped viruses, display carbohydrates of variable complexity associated to their macromolecules (e.g., glycoproteins, glycolipids), as well as polysaccharides. The carbohydrate moieties of both soluble and cell-associated glycoconjugates encode complex information that is "decoded" by specific carbohydrate–binding proteins. These protein–carbohydrate interactions are ubiquitous and essential to all biological systems.

In metazoans, for example, recognition of endogenous ("self") glycans, either soluble or displayed on the cell surface, is critical not only for specific interactions between cells that facilitate cell adhesion and migration, but as the initiator of a functional crosstalk that modulates cell homeostatic balance, including the regulation of both innate and adaptive immune functions. In contrast, recognition of exogenous ("non-self") carbohydrates on the surface of viruses, microbes, and parasites by the host's glycan-binding proteins frequently constitutes the first step in the innate immune response to infectious challenge.

As microbes, parasites and some viruses are also endowed of a diverse repertory of adhesins, lectins, hemagglutinins, and other glycan-binding proteins that facilitate their adhesion and host entry, the outcome of this interplay of reciprocal glycan recognition may result in either infectious disease, a successful host immune response, or the establishment of a mutualistic association, such as the commensal microbiota.

Volume 1 of "*The Role of Glycans in Infectious Disease*" Research Topic offers a series of high-quality articles that share an ample view of glycan host-pathogen interactions involving bacterial, fungal, parasitic, and viral infections, as well as the different approaches used to study them and to develop diagnostic and therapeutic applications.

A wide number of glycoproteins across different bacterial species are involved in pathogenicity and virulence. Tuberculosis, caused by infection with *Mycobacterium tuberculosis* (Mtb), is a communicable disease that is a major cause of ill health and one of the leading causes of death worldwide. Until the coronavirus (COVID-19) pandemic, tuberculosis was the leading cause of death from a single infectious agent (World Health Organization, 2021a). It is known that Mtb expresses a wide range of *O*-mannosylated proteins involved in the pathogenesis and immune response to tuberculosis. In an original research article, Jia et al. highlight this role by using *Mycobacterium smegmatis* as a study model, demonstrating that the mycobacterium protein *O*-mannosyltransferase, that catalyzes the initial step of protein *O*-mannosylation, is required for

OPEN ACCESS

Edited and reviewed by:
Axel Cloeckaert,
Institut National de recherche pour l'agriculture, l'alimentation et l'environnement (INRAE), France

***Correspondence:**
Iván Martínez-Duncker
duncker@uaem.mx
Gerardo R. Vasta
gvasta@som.umaryland.edu

Specialty section:
This article was submitted to Infectious Agents and Disease, a section of the journal Frontiers in Microbiology

Received: *15 April 2022*
Accepted: *22 April 2022*
Published: *12 May 2022*

Citation:
Martínez-Duncker I, Chiodo F, Mora-Montes HM and Vasta GR (2022) Editorial: The Role of Glycans in Infectious Disease. Front. Microbiol. 13:921436. doi: 10.3389/fmicb.2022.921436

growth and resistance to lysozyme and acidic stress, determining survival within macrophages, as well as in modulating the host innate immune responses.

Endogenous lectins such as galectins, a large family of carbohydrate binding proteins with members in nearly every lineage of multicellular life, are known to play important roles in modulating host cell function, but also in the binding of non-self glycans on the surface of potentially pathogenic microorganisms, mediating recognition and effector functions in innate immunity (Verkerke et al., 2022). In an original research article, Wu et al. present data regarding the binding specificities of galectin-3 (Gal-3), the first galectin shown to engage bacterial glycans, as well as its C-terminal domain, indicating that differently from other galectins, such as Gal-8, the C-terminal domain of Gal-3 is not sufficient to kill bacteria, and that the N-terminal is required for both high-affinity microbial glycan interactions and the ability to kill microbes.

Antimicrobial resistance is a global threat to the very core of modern medicine and the sustainability of an effective, global public health response to the enduring threat from infectious diseases (Regional Office for South-East Asia WHO, 2016). Since bacterial glycosylation is different from human glycosylation, these metabolic pathways constitute promising antibacterial targets. In a timely review, Yakovlieva et al. describe the current status and promise for the future of using bacterial glycosylation to develop novel antibacterial strategies by focusing on unique glycosylation systems in bacterial pathogens and their role in bacterial homeostasis and infection, with an emphasis on virulence factors and highlighting recent advances to inhibit the enzymes involved in these glycosylation systems.

Fungal diseases have been continually neglected over the years (Rodrigues and Nosanchuk, 2020) and understanding the immune response to fungal infection is key in unraveling their pathogenesis. The fungal cell wall is a robust and dynamic structure that protects the cell from the changes in the extracellular environment, but that also is the immediate contact point with host cells, containing antigenic determinants, glycoproteins involved in the adhesion to host tissues, and most of the pathogen-associated molecular patterns that are recognized by the host immune system. In an original research article, Villalobos-Duno et al. share a comparative study on the cell wall glycosylation of *Sporothrix schenckii* and *Sporothrix brasiliensis* strains, the main causative agents of sporotrichosis, a human subcutaneous mycosis. Important differences regarding rhamnose-to-β-glucan ratio and structural differences in rhamnomannan were observed and the authors associated changes to the different virulence degrees of the studied strains, interestingly expressing them through a linear equation.

Infections caused by parasitic protozoans and helminths are among the world's leading causes of death, including malaria, one of the leading global health burdens, estimated in 2020 to have caused 241 million cases of malaria worldwide and an estimated number of 627 000 deaths (World Health Organization, 2021b). In a detailed review, Goerdeler et al. describe the role of glycans and lectins in the pathogenesis and host defense mechanisms of plasmodium parasites that cause malaria, explaining the basics of the pathogen glycosylation pathways and the host glycans that participate in the disease, sharing their perspectives on intervention sites for malaria therapy, including vaccine development and glycan-based drug targets. Also in an original research article, Ricci-Azevedo et al. reveal a mechanism by which *Toxoplasma gondii* lectin type microneme proteins inhibit the host inflammatory response to favor its success in the early stage of toxoplasmosis, a widely distributed parasitic zoonotic infection of importance to public health and animal production (de Barros et al., 2022). Chagas disease is a neglected tropical disease caused by infection with the parasite *Trypanosoma cruzi*, endemic to Latin America, but found in immigrant populations worldwide (Álvarez-Hernández et al., 2021). In a focused review, Poncini et al. discuss the role of galectin-driven circuits in modulating both *T. cruzi* infection and immunoregulation, clearly articulating the decisive roles that galectins play during the life cycle of *T. cruzi*.

The COVID-19 pandemic and the study of the pathogenic mechanisms involving SARS-CoV-2 infection have highlighted the importance of glycans as key participants in the interphase of virus-host interactions. An interesting aspect shared in an original research article by Breiman et al. shed light into the potential protective role against COVID-19 infection of naturally occurring antibodies against common glycan epitopes. COVID-19 patients were found to present lower levels of anti-Tn antibodies than controls, pointing to the potential protective role of these antibodies. This finding contributes to the ongoing and complex discussion regarding differences in susceptibility amongst the human population and if boosting this natural protection through anti-glycan antibody epitopes could be considered a prophylactic therapy. Also, in an original research article, Schwedler et al. report on the *N*-glycosylation of total IgG1, total IgG2, and anti-Spike IgG1 isolated from plasma of severe COVID-19 patients by means of MALDI-TOF-MS, showing that anti-Spike IgG1 fucosylation and galactosylation had the strongest variation during the disease course.

Another viral pathogen included in this Research Topic is the Human Immunodeficiency Virus (HIV), well-known to use glycans and host lectins at different stages of its life cycle. In a focused review, Segura et al. discuss the pathogenic mechanisms involving the interaction between HIV-1 envelope glycans and their binding to L-selectin on CD4+ T lymphocytes to facilitate viral adhesion and entry and the role of L-selectin shedding in viral release, suggesting that the regulation of L-selectin is a promising target for developing anti-HIV therapies.

A physiological perspective regarding the study of the glycan host-pathogen interactions offers a better understanding of the processes involving different types of cells and tissues that come into place during infection. In a detailed mini-review, Argüeso et al. describe the ocular glycocalyx barrier that occurs in the interface between the ocular surface epithelia and the external environment and its role in the pathogenesis of bacterial, viral, fungal and parasitic infection. Also, in a dedicated review, Jung and Kim describe the intestinal models for studying normal and disease host-microbiome interactions and pathways, including the current state of the art for *in vitro* cell-based models of the small intestine system to replace animal models,

including *ex vivo*, 2D culture, organoid, lab-on-a-chip, and 3D culture models.

An important benefit of understanding the role of glycans and glycan-binding proteins in host-pathogen interactions is to develop novel diagnostic tools and therapeutics that can positively impact prompt diagnosis and better outcomes. McKitrick et al. present a very interesting perspective, reporting on a workshop organized jointly by the National Institute of Allergy and Infectious Diseases and the National Institute of Dental and Craniofacial Research that addressed the use of emerging glycoscience tools and resources to advance the investigation of glycans and their roles in microbe-host interactions, immune-mediated diseases, and immune cell recognition and function.

Although most contributions involved human pathogens, we had the opportunity to include an extensive review by Villa-Rivera et al. that describes the beneficial plant-microbe interactions and defense mechanisms established by arabinogalactans and arabinogalactan proteins found in the plant cell wall or plasma membrane, including the interplay with pathogenic fungal and bacterial enzymes that degrade them to establish infections and that result in plant defense responses.

This Research Topic underscores the diverse and expanding role of glycans and glycan-binding proteins in different infectious diseases, presenting it as a promising field to discover novel mechanisms involved in host-pathogen interactions, that harbor the potential for improved design of novel diagnostic tools and therapeutics against infectious diseases.

AUTHOR CONTRIBUTIONS

All authors listed have made a substantial, direct, and intellectual contribution to the work and approved it for publication.

FUNDING

GV was supported by grants IOS-1656720 from the National Science Foundation, and grant R01 GM070589 from the National Institutes of Health. HM-M was supported by grants from the Consejo Nacional de Ciencia y Tecnología FC2015-02-834; Ciencia de Frontera 2019-6380 and Red Temática Glicociencia en Salud.

REFERENCES

Álvarez-Hernández, D. A., García-Rodríguez-Arana, R., Ortiz-Hernández, A., Álvarez-Sánchez, M., Wu, M., Mejia, R., et al. (2021). A systematic review of historical and current trends in Chagas disease. *Ther. Adv. Infect. Dis.* 8, 20499361211033715. doi: 10.1177/20499361211033715

de Barros, R. A. M., Torrecilhas, A. C., Marciano, M. A. M., Mazuz, M. L., Pereira-Chioccola, V. L., and Fux, B. (2022). Toxoplasmosis in human and animals around the world. Diagnosis and Perspectives in the One Health Approach. *Acta Trop.* 231:106432. doi: 10.1016/j.actatropica.2022.106432

Regional Office for South-East Asia WHO. (2016). *Global Action Plan on Antimicrobial Resistance*. WHO Regional Office for South-East Asia. Available online at: https://apps.who.int/iris/handle/10665/254352 (accessed April 15, 2022).

Rodrigues, M. L., and Nosanchuk, J. D. (2020). Fungal diseases as neglected pathogens: a wake-up call to public health officials. *PLoS Negl. Trop. Dis.* 14, e0007964. doi: 10.1371/journal.pntd.0007964

Verkerke, H., Dias-Baruffi, M., Cummings, R. D., Arthur, C. M., and Stowell, S. R. (2022). Galectins: an ancient family of carbohydrate binding proteins with modern functions. *Methods Mol. Biol.* 2442:1–40. doi: 10.1007/978-1-0716-2055-7_1

World Health Organization. (2021a). *Global Tuberculosis Report 2021*. World Health Organization. Avaialble online at: https://apps.who.int/iris/handle/10665/346387 (accessed April 15, 2022).

World Health Organization. (2021b). *World Malaria Report 2021*. World Health Organization. Available online at: https://apps.who.int/iris/handle/10665/350147 (accessed April 15, 2022).

Conflict of Interest: The authors declare that the research was conducted in the absence of any commercial or financial relationships that could be construed as a potential conflict of interest.

Publisher's Note: All claims expressed in this article are solely those of the authors and do not necessarily represent those of their affiliated organizations, or those of the publisher, the editors and the reviewers. Any product that may be evaluated in this article, or claim that may be made by its manufacturer, is not guaranteed or endorsed by the publisher.

frontiers in Microbiology

ORIGINAL RESEARCH
published: 11 February 2021
doi: 10.3389/fmicb.2021.641460

Low Levels of Natural Anti-α-*N*-Acetylgalactosamine (Tn) Antibodies Are Associated With COVID-19

*Adrien Breiman[1,2], Nathalie Ruvoën-Clouet[1,3], Marie Deleers[4,5], Tiffany Beauvais[1,2], Nicolas Jouand[6], Jézabel Rocher[1], Nicolai Bovin[7], Nathalie Labarrière[1], Hanane El Kenz[4,5] and Jacques Le Pendu[1]**

[1] Université de Nantes, INSERM, CRCINA, Nantes, France, [2] CHU de Nantes, Nantes, France, [3] Oniris, Ecole Nationale Vétérinaire, Agroalimentaire et de l'Alimentation, Nantes, France, [4] Department of Transfusion, CHU Brugmann, Université Libre de Bruxelles (ULB), Brussels, Belgium, [5] Laboratory of Immunology, LHUB-ULB, Brussels, Belgium, [6] Platform Cytocell, SFR François Bonamy, Nantes, France, [7] Shemyakin-Ovchinnikov Institute of Bioorganic Chemistry, Russian Academy of Sciences, Moscow, Russia

Human serum contains large amounts of anti-carbohydrate antibodies, some of which may recognize epitopes on viral glycans. Here, we tested the hypothesis that such antibodies may confer protection against COVID-19 so that patients would be preferentially found among people with low amounts of specific anti-carbohydrate antibodies since individual repertoires vary considerably. After selecting glycan epitopes commonly represented in the human anti-carbohydrate antibody repertoire that may also be expressed on viral glycans, plasma levels of the corresponding antibodies were determined by ELISA in 88 SARS-CoV-2 infected individuals, including 13 asymptomatic, and in 82 non-infected controls. We observed that anti-Tn antibodies levels were significantly lower in patients as compared to non-infected individuals. This was not observed for any of the other tested carbohydrate epitopes, including anti-αGal antibodies used as a negative control since the epitope cannot be synthesized by humans. Owing to structural homologies with blood groups A and B antigens, we also observed that anti-Tn and anti-αGal antibodies levels were lower in blood group A and B, respectively. Analyses of correlations between anti-Tn and the other anti-carbohydrates tested revealed divergent patterns of correlations between patients and controls, suggesting qualitative differences in addition to the quantitative difference. Furthermore, anti-Tn levels correlated with anti-S protein levels in the patients' group, suggesting that anti-Tn might contribute to the development of the specific antiviral response. Overall, this first analysis allows to hypothesize that natural anti-Tn antibodies might be protective against COVID-19.

Keywords: COVID-19, *O*-glycans, natural antibodies, Tn antigen, histo-blood group antigens

OPEN ACCESS

Edited by:
Ivan Martinez Duncker, Universidad Autónoma del Estado de Morelos, Mexico

Reviewed by:
Marcin Czerwiński, Hirszfeld Institute of Immunology and Experimental Therapy, Polish Academy of Sciences, Poland
Fernando Roger Esquivel-Guadarrama, Autonomous University of the State of Morelos, Mexico

****Correspondence:***
Jacques Le Pendu
jacques.le-pendu@inserm.fr

Specialty section:
This article was submitted to Infectious Diseases, a section of the journal Frontiers in Microbiology

Received: *14 December 2020*
Accepted: *18 January 2021*
Published: *11 February 2021*

Citation:
Breiman A, Ruvoën-Clouet N, Deleers M, Beauvais T, Jouand N, Rocher J, Bovin N, Labarrière N, El Kenz H and Le Pendu J (2021) Low Levels of Natural Anti-α-N-Acetylgalactosamine (Tn) Antibodies Are Associated With COVID-19. Front. Microbiol. 12:641460. doi: 10.3389/fmicb.2021.641460

INTRODUCTION

Viral envelope proteins, including those of the severe acute respiratory syndrome coronavirus 2 SARS-CoV-2 are extensively glycosylated (Watanabe et al., 2020). Since these glycans are synthesized by the host cell enzymatic machinery, they are part of the self and have little immunogenic potential. Alongside other functions, the glycan shield masks the protein surface from potential peptide specific antibodies (Bagdonaite and Wandall, 2018). Glycosylation is therefore exploited by enveloped viruses as a protection mechanism (Watanabe et al., 2019). Yet, it might also constitute a Trojan horse. Indeed, several carbohydrate antigenic epitopes may be present on viral envelope glycoproteins. The αGal antigen is the most extensively studied example of a carbohydrate epitope that can lead to the elimination of viruses through natural antibodies (Galili, 2019). This carbohydrate antigen is expressed by many cell types in most mammalian species, but is lacking in humans, apes and old-world monkeys due to pseudogenization of the *GGTA1* gene that encodes the galactosyltransferase required for its synthesis. As a result, species unable to express the αGal antigen produce natural anti-αGal antibodies in response to bacteria of the microbiota that carry mimicking carbohydrate structures. It has been established that several types of enveloped viruses, including influenza virus, murine C retrovirus, porcine endogenous retrovirus, lymphocytic choriomeningitis virus, Newcastle disease virus, Sindbis virus, vesicular stomatitis virus, measles virus, and paramyxovirus present the αGal antigen when produced in cells that synthesize it (Galili, 2020). Anti-αGal antibodies can directly neutralize these viruses or opsonize them leading to complement-mediated destruction or to amplification of the immune response by targeting antigen presenting cells. It is thus believed that these xenogenic natural antibodies contribute to protect our species from zoonotic transmission of enveloped viruses (Galili, 2019). Likewise, enveloped viruses can be decorated with allogeneic carbohydrate epitopes of the ABO blood group type. Thus, measles viruses produced by cells expressing either the A or B blood group antigens was neutralized by the natural cognate antibodies in a complement-dependent manner (Preece et al., 2002). Moreover, anti-A antibodies could block the interaction between SARS-CoV S protein and its cellular receptor, the angiotensin-converting enzyme ACE2, when the viral protein was produced by cells expressing the A blood group antigen (Guillon et al., 2008). This was consistent with the expression of blood group antigens by respiratory tract epithelial cells where the virus replicates and the lesser risk of infection of blood group O individuals by SARS-CoV observed in a Hong Kong hospital outbreak (Cheng et al., 2005). Indeed, group O individuals possess anti-A and anti-B antibodies that could have protected them from viral particles emitted by either blood group A or B patients. Interestingly, a large number of observations indicate that blood group O individuals have a lower risk of COVID-19, whereas blood group A individuals appear to be at a higher risk (Cheng et al., 2005; Abdollahi et al., 2020; Ahmed et al., 2020; Aljanobi et al., 2020; Barnkob et al., 2020; Chegni et al., 2020; Delanghe et al., 2020; Dzik et al., 2020; Ellinghaus et al., 2020; Fan et al., 2020; Franchini et al., 2020; Gallian et al., 2020; Göker et al., 2020; Hoiland et al., 2020; Latz et al., 2020; Leaf et al., 2020; Li et al., 2020; Muniz-Diaz et al., 2020; Niles et al., 2020; Padhi et al., 2020; Ray et al., 2020; Roberts et al., 2020; Shelton et al., 2020; Sohlpour et al., 2020; Valenti et al., 2020; Wu et al., 2020; Zeng et al., 2020; Zhang et al., 2020; Zhao J. et al., 2020; Zietz et al., 2020). Only a few studies failed to find any association between ABO types and COVID-19, likely depending on study design (Boudin et al., 2020; Focosi et al., 2020; Pairo-Castineira et al., 2020). Coherent with the notion that natural anti-carbohydrate could have a protective effect, we recently observed that COVID-19 patients present lower levels of anti-A and/or anti-B blood group antibodies than controls (Deleers et al., 2020).

In addition to anti-xenogenic or anti-allogenic antibodies such as the anti-αGal, anti-A and anti-B antibodies, humans possess a large repertoire of natural anti-carbohydrate antibodies (New et al., 2016). Although most of them recognize bacterial structures, some have the potential to recognize viral glycans. Glycan structural analyses of the SARS-CoV-2 S protein produced in HEK-293T cells or of the virus produced in Vero cells have recently been described. They mainly include *N*-glycans of the oligomannose, hybrid and complex types that broadly cover the protein surface (Gao et al., 2020; Sanda et al., 2020; Shajahan et al., 2020; Sun et al., 2020; Watanabe et al., 2020). Yet, simple *O*-glycans have also been found either at the junction between the N-terminal domain (NTD) and the receptor binding domain (RBD) of the S1 domain or surrounding the furin cleavage site of the S2 domain (Antonopoulos et al., 2020; Gao et al., 2020; Sanda et al., 2020; Shajahan et al., 2020; Zhao P. et al., 2020). Based on these data, we selected a set of carbohydrate structures potentially present on virions produced by epithelial cells and known to constitute major epitopes of the human natural anti-carbohydrate repertoire (Huflejt et al., 2009; Stowell et al., 2014; Schneider et al., 2015; Muthana and Gildersleeve, 2016; Purohit et al., 2018; Khasbiullina et al., 2019).

Regardless of their specificity, levels of natural anti-glycans are highly variable between individuals (Tendulkar et al., 2017; Luetscher et al., 2020). Thus, we reasoned that if some natural anti-carbohydrate antibodies present an anti-viral activity, akin to what has been shown for anti-αGal antibodies in xenogenic situations (Galili, 2020), protection should not take place when they are present at low levels. Accordingly, patients should present lower levels of a protective anti-carbohydrate antibody specificity. In this work we thus compared levels of the selected anti-carbohydrate epitopes in the plasma of a group of COVID-19 patients and of a group of uninfected controls in order to reveal a potentially protective glycan epitope.

MATERIALS AND METHODS

Study Design and Patients

For this study, the recruited individuals represented a subset from a study approved by the ethics committees of the Centre Hospitalier Universitaire Brugmann (CHU Brugmann, Bruxelles) and the Hôpital Universitaire Des Enfants Reine

Fabiola (HUDERF, Bruxelles) in Belgium (the number "CHUB-BDS-Covid19 ClinicalTrials.gov: NCT04462627"). The study was carried out in accordance with the principles of the Declaration of Helsinki. The authors assume responsibility for the accuracy and completeness of the data and analyses.

Briefly, the study carried out between 11 March 2020 and 16 June 2020 in Brussels, Belgium, at the Brugmann University Hospital and the HUDERF, enabled the recruitment of 290 patients with or without symptoms of COVID 19, and with a positive RT-PCR test for SARS-CoV-2 on nasal and pharyngeal swab specimens. A control group (n = 276) included asymptomatic ambulatory patients or hospitalized patients without COVID symptoms and a negative RT-PCR test for SARS-CoV-2. For all these individuals, blood samples on EDTA were obtained on which standard anti-A and/or anti-B IgM agglutination scores were performed.

As shown on **Table 1**, to test our hypothesis about the involvement of other natural carbohydrate antibodies other than A and B in SARS-Cov-2 susceptibility, a random selection of 30 individuals from each of the patients and control groups A, B, and O types was performed (total target number = 180). The lack of left-over plasma from 10 selected individuals reduced our study sample to 170.

Quantification of anti-SARS-CoV-2 antibodies (see method below) on the plasmas of individuals in the control group (with no apparent sign of COVID at the time of sampling and negative RT-PCR) showed that seven control individuals had antibodies indicating that they had been infected. For our analysis, these individuals were thus repositioned according to their ABO blood type in the patients' group.

The patients' group (88) was then subdivided into 2 subgroups: 75 COVID patients (RT-PCR positive and symptomatic), and 13 asymptomatic patients (RT-PCR positive or RT-PCR negative with positive serology resulting from the reclassification of the control individuals).

Quantification of Natural Anti-carbohydrate Antibodies

Anti-carbohydrate antibodies were assessed with the enzyme-linked immunosorbent assay (ELISA). ELISA plates (Maxisorp, Nunc, Thermo Fisher Scientific, Roskilde, Denmark) were coated with synthetic sugars (structures shown on **Figure 1**) conjugated to polyacrylamide (PAA neoglycoconjugates) at 5 μg/mL in 0.1 M Carbonate buffer pH 9.0 overnight at 4°C. The plates were washed three times with phosphate-buffered saline (PBS)−0.05% Tween 20 (PBS-T), and unbound sites were blocked with PBS-5% bovine serum albumin (BSA) for 2 h at 37°C. After three additional washes with PBS-T, plasma samples (EDTA) from patients with Covid-19 or controls were added to the plate at a 1:30 dilution in PBS-1% BSA for 1 h at 37°C, except in the case of anti-αGal where plasma samples were diluted 1:50. Optimal dilutions had been chosen based on preliminary analyses performed using plasma samples from healthy blood donors. The plates were then washed 3 times with PBS-T and Donkey anti-human IgG (H + L)-conjugated horseradish peroxidase (Jackson ImmunoResearch Laboratories Inc., Ely, United Kingdom) was added at a 1:5000 dilution in PBS-1% BSA for 1 h at 37°C. This secondary antibody recognizes all classes of immunoglobulins, including IgM, IgG and IgA. Finally, after three last washes with PBS-T and one with plain PBS, revelation was performed with 50 μL/well of 3,3′,5,5′-Tetramethylbenzidine (Sigma Aldrich, St Louis, MO, United States) and the reaction was stopped with 50 μL/well of 1 M Phosphorous acid. Optical densities were read twice at 450 nm with a SPECTROstar Nano spectrophotometer (BMG Labtech, Champigny-sur-Marne, France).

Flow Cytometry Quantification of Anti-SARS-CoV-2 Antibodies

The S-flow assay described by Grzelak et al. (2020) was used to detect anti-S viral protein in both controls and patients plasma samples. Briefly, detached HEK-293T cells (5×10^5) stably expressing the S protein following transfection of a codon-optimized SARS-CoV-2 S gene were incubated for 30 min at 4°C with 50 μL of plasma samples at a 1/300 dilution in PBS containing 2 mM EDTA and 0.5% BSA. Untransfected HEK-293T cells used as negative controls were treated similarly. Following washings with PBS, cells were then incubated 30 min at 4°C with 35 μL of anti-Hu IgG (H + L) AlexaFluor 647 antibody (A21445, Invitrogen) diluted 1:600 in Staining Buffer. After washings in PBS, cells were fixed with PFA 2% (15714, Electron Microscopy Sciences, Hatfield, PA, United States), 15 min at room temperature, washed in PBS and analyzed by Flow cytometry, on a FACS Canto cytometer. Results were normalized according the formula: % of positive cells = 100 × [(%

TABLE 1 | Constitution of the controls and cases groups.

	Controls				Cases				
	A	B	O	Total controls	A	B	O	Total cases	Total samples
Complete study	108	52	116	276	126	48	116	290	566
Sub-study randomization	30	30	30	90	30	30	30	90	180
Tested samples	30	30	29	89	29	22	30	81	170
Actual sub study[a]	28 (−2)	28 (−2)	26 (−3)	82	31 (29 + 2)	24 (22 + 2)	33 (30 + 3)	88[b]	170

[a] *Seven controls were reclassified as cases because of anti-SARS-CoV-2 seropositivity.*
[b] *Among cases, 75 were symptomatic and 13 were asymptomatic.*

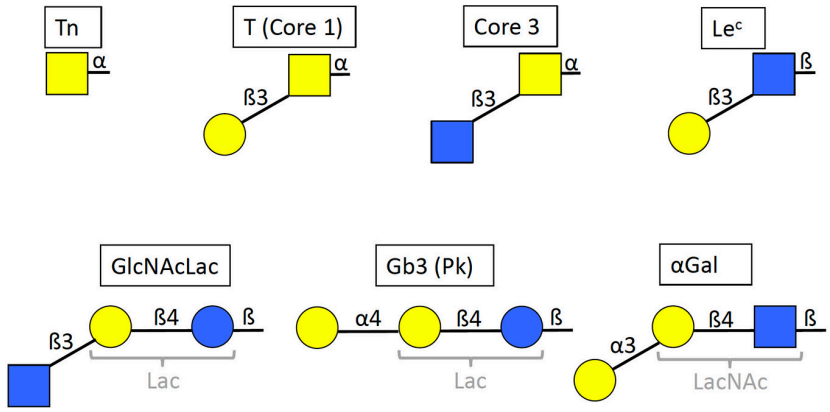

FIGURE 1 | Structures of the selected glycan motifs. The Tn, T or core 1 and core 3 motifs correspond to short *O*-glycans in alpha linkage to either serine or threonine of the peptide chain. The Le^c (Lewis c), GlcNAcLac and αGal epitopes can be present either on N– and O–linked glycans of glycoproteins, or on glycolipids, whilst the Gb3 trisaccharide (globotrihexosyl), also called Pk antigen, is only known on glycosphingolipids. The GlcNAcLac, Gb3 and αGal motifs contain either a lactose or an *N*-acetyllactosamine inner core (Lac and LacNAc, respectively, in gray). Yellow squares = GalNAc (*N*-acetylgalactosamine), yellow circles = Gal (galactose), blue squares = GlcNAc (N-acetylglucosamine), blue circles = Glc (glucose). Linkages are indicated as α or β anomers on either position 3 or 4 of the subjacent monosaccharide unit.

in 293T-S)−(% in 293T-CTRL)/100−(% in 293T-CTRL)]. The cut-off for positivity was fixed at 30%.

Specificity Assay for the Anti-Tn NAM217-2A9 by ELISA

Maxisorp ELISA plates were coated with PAA-conjugated glycans at 10 μg/ml, human salivary mucins at 1:1000 dilution or bovine submaxillary mucins (Sigma) at 5 μg/ml in PBS at 4°C overnight. The sialyl-Tn-rich bovine mucins had been chemically de-sialylated by incubation in 2M H_2SO_4 for 30 min at 80°C followed by neutralization with NaOH. After three washes with PBS-0,05% Tween20 (PBS-T), the wells were blocked with PBS-5% BSA for 2 h at 37°C and washed another three times with PBS-T. Three-fold serial dilutions (1:50 to 1:1350) of mouse anti-Tn NAM217-2A9 in PBS-1%BSA were then loaded onto the plate and incubated for 1 h at 37°C. Washes, incubation with anti-mouse-HRP (Uptima, Interchim, Montluçon, France; 1:1000), revelation and OD measurement were then performed as described above.

Flow Cytometry Detection of the Tn Antigen

Vero green monkey kidney cells and HEK293T human embryonic kidney cells were detached using trypsin or PBS-EDTA, respectively, and resuspended in PBS-0.1% BSA. Jurkat cells were cultivated in suspension. 250.000 cells were stained with anti-Tn monoclonal mouse antibodies for 30–60 min at 4°C followed by anti-mouse-FITC 1:200. Analysis was performed on a Celesta flow cytometer using the DIVA software (BD Biosciences).

Immunohistological Analysis of the Expression of the Tn Antigen in the Respiratory Tract

The ethanol-fixed human tissue sections, collected and stored before the French law 88–138 of the 20th of December 1988 on tissue resection for scientific investigation, were obtained from the Nantes University Hospital Center for Biological Resources[1] (approval DC-2011-1399).

Immunohistochemistry was performed as described elsewhere (Lopes et al., 2018). Briefly, the slides were deparaffinized and blocked for endogenous peroxidase activity and non-specific protein binding and incubated with the IgM mouse monoclonal antibodies against Tn NaM217-2A9 that was raised against human Tn erythrocytes (Duk et al., 2001) overnight at 4°C. The slides were then successively incubated with HRP-conjugated anti-mouse IgG (H + L) (Uptima; Interchim, Montluçon, France) and AEC substrate (Vector Laboratories, Burlingame, CA, United States) with three PBS washes in-between and conterstained with hematoxylin (Vector Laboratories) before mounting and imaging with a Nanozoomer slide-scanner using a ×20 objective (Hamamatsu Photonics, Massy, France).

STATISTICAL ANALYSES

Analyses were performed using GraphPad Prism 8. Between groups differences were calculated using two-tailed Mann-Whitney test and correlation were assessed using Pearson correlation coefficient. To account for multiple testing, Holm correction was applied were necessary. $P < 0.05$ was considered significant.

RESULTS

Low Levels of Natural Anti-Tn Are Associated With COVID-19 Status

In order to select carbohydrate epitopes that may be present on SARS-CoV-2 and correspond to epitopes of the human natural

[1]http://relib.fr

anti-carbohydrate repertoire, we first examined published glycan microarray data that describe this repertoire (Huflejt et al., 2009; Stowell et al., 2014; Schneider et al., 2015; Muthana and Gildersleeve, 2016; Purohit et al., 2018; Khasbiullina et al., 2019). We looked for epitopes that could both be present on SARS-CoV-2 and give strong IgM and IgG signals with the serum of many healthy donors. The analysis revealed six potentially interesting epitopes, the short *O*-glycans Tn, T and core 3 as well as the Le^c and GlcNAcLac motifs of either complex *O*-glycans or *N*-glycans that can be synthesized by upper respiratory tract cells (**Figure 1**). In addition, we selected the Gb3 trisaccharide which corresponds to a widely distributed glycolipid highly reactive with healthy human serum natural antibodies (Volynsky et al., 2017).

Individual levels of the selected natural anti-carbohydrate antibodies were then tested in a group of COVID-19 patients and compared to those in a group of controls of similar size. Since some of the tested antigens show similarity with either the A or B blood group antigens, the patients and controls groups were constituted so as to comprise nearly even numbers of A, B and O phenotypes. The αGal antigen was used as a control since it is not expressed in humans. We therefore anticipated that anti-αGal antibodies do not play any direct role in COVID-19 infection. Considering the structural relationship with the A blood group antigen, levels of anti-Tn were expected to be lower in blood group A individuals in comparison with blood group O and B and this was verified both for the control and COVID-19 groups (**Figure 2**). Interestingly, anti-Tn levels were significantly lower in COVID-19 patients as compared with controls since patients' values were mainly distributed in the low range ($p = 0.003$). A similar, albeit less prominent effect was also visible when comparing SARS-CoV-2 infected individuals and controls ($p = 0.012$). Yet, no difference between controls and the subgroup of asymptomatic infected individuals was visible. It should be stressed, however, that the latter comprises 13 individuals only. The anti-αGal antibodies revealed a distinct picture. They appeared at lower levels in blood group B than in blood groups A and O individuals, both in the controls and SARS-CoV-2 infected groups. This was expected since the αGal epitope is closely related to blood group B. Yet, there was no difference related to the SARS-CoV-2 infectious status or COVID-19 status. Analyzing anti-T, anti-core-3, anti-Le^c, anti-GlcNAcLac and anti-Gb3 revealed either no or only marginal between-group differences that vanished when using a threshold of significance lower than 0.02 (**Figure 3**). Thus, anti-Tn levels appear to be specifically low in COVID-19 patients.

Recently published data indicated that natural anti-glycan antibodies, including anti-Tn show cross-reactivity with a variety of other carbohydrate structures (Bovin et al., 2012; Dobrochaeva et al., 2020). Based on the premises that specific antibodies may cross-react with closely related structures, whilst less specific antibodies would cross-react more broadly, to get a more qualitative comparison of the natural antibodies from COVID-19 patients and controls, we performed correlation analyses of anti-Tn with the other tested anti-carbohydrates in both groups. In controls, strong correlations were found between anti-Tn levels and anti-T, anti-core 3 and anti-Le^c levels. A weaker correlation was additionally found with anti-GlcNAcLac. By contrast, in patients, anti-Tn strongly correlated with anti-GlcNAcLac and Gb3 only (**Figure 4** and **Table 2**). These divergent relationships between levels of anti-Tn and those of the other anti-glycans in patients and controls indicate differences in natural antibodies repertoires between the two groups. Thus, not only do patients have lower levels of anti-Tn antibodies than controls, but these antibodies also appear qualitatively distinct.

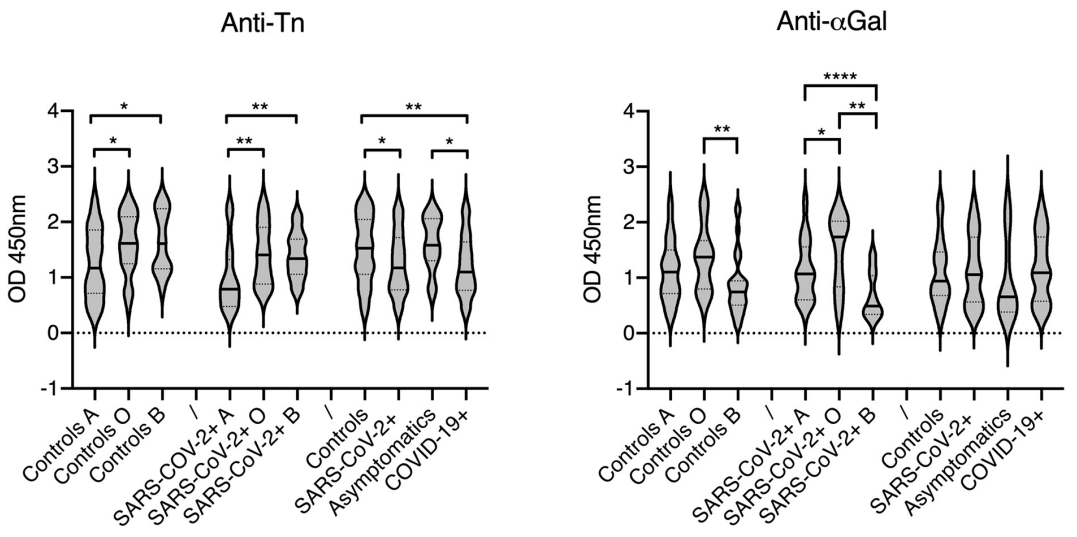

FIGURE 2 | Relationships between the anti-Tn and anti-αGal levels, ABO phenotypes and infection status. Antibodies levels are shown as OD450 nm values at 1: 30 and 1: 50 plasma dilutions, respectively. Infected patients are defined as SARS-CoV-2 +, regardless of their clinical status or subdivided as asymptomatic and symptomatic COVID-19 +. Controls presented no sign of disease, were RT-PCR negative and anti-S negative. Violin plots show median values and quartiles (horizontal bars) for each group. *P*-values from Mann-Whitney between-groups comparisons are indicated: $*p < 0.05$, $**p < 0.01$, $****p < 0.0001$.

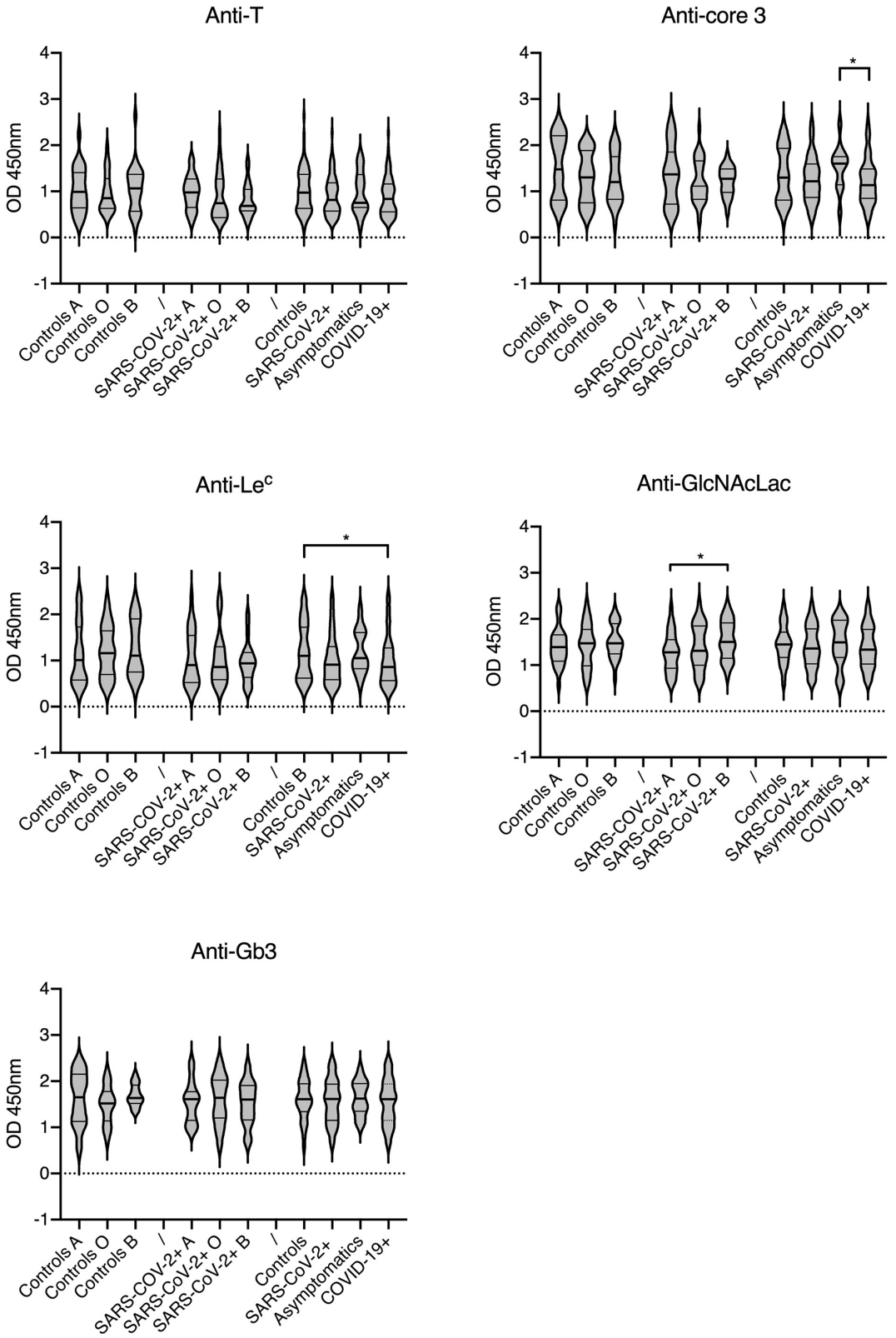

FIGURE 3 | Relationships between natural anti-carbohydrate antibodies, ABO phenotypes and infection status. Analyzed carbohydrate antigens are indicated on each panel. Antibodies levels are shown as OD450 nm values at 1: 30 plasma dilutions. Infected patients are defined as SARS-CoV-2 +, regardless of their clinical status or subdivided as asymptomatic and symptomatic COVID-19 +. Controls presented no sign of disease, were RT-PCR negative and anti-S negative. Plots show median values and quartiles (horizontal bars). *P*-values from Mann-Whitney between-groups comparisons are indicated: $^{*}p < 0.05$.

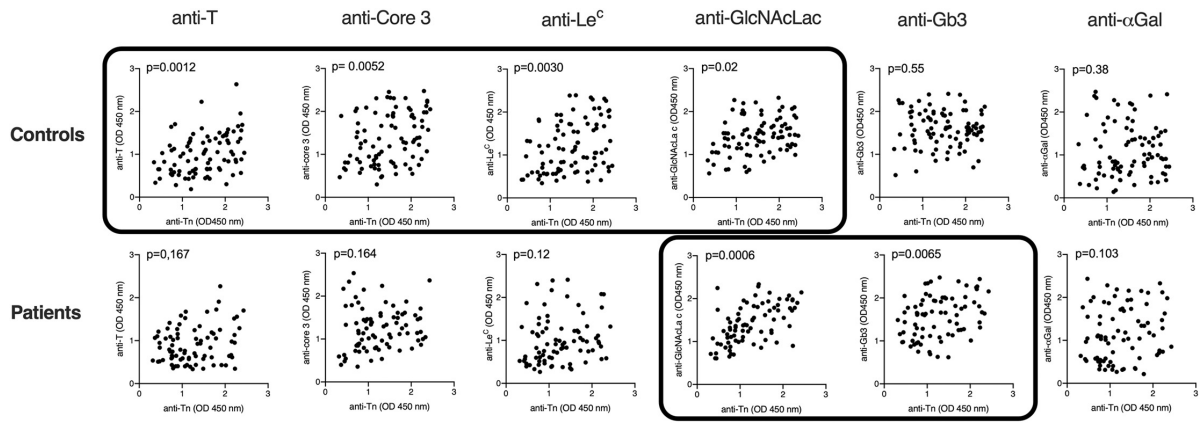

FIGURE 4 | Correlations between levels of anti-Tn natural antibodies and the other assayed natural anti-carbohydrate antibodies. Antibodies levels are shown as OD450 nm values at 1: 30 or 1: 50 (αGal) plasma dilutions. Correlations were assessed using Spearman *r* and two-tailed *p*-values after Holm correction for multiple testing are shown. Data sets with *p*-values <0.05 are boxed.

TABLE 2 | Correlations between levels of anti-Tn and levels of the other assayed natural anti-carbohydrates.

	Anti-T	Anti-core 3	Anti-Le^c	Anti-GlcNAcLac	Anti-Gb3	Anti-αGal
Controls	0.38	0.34	0.36	0.29	−0.06	0.09
N = 82	(0.0002)	(0.0013)	(0.0006)	(0.0067)	(0.5514)	(0.3826)
Patients	0.16	0.16	0.24	0.58	0.35	0.18
N = 88	(0.1666)	(0.1644)	(0.0303)	(0.00001)	(0.0013)	(0.1032)

Correlations were assessed using Spearman r and non-corrected for multiple testing two-tailed p values in parentheses are shown both for controls and patients. R values above 0.3 are boxed in red.

Correlation Between Anti-Tn and Anti-SARS-CoV-2 S Protein

Having observed that anti-Tn levels were lower in patients than in controls, we wondered if their levels within patients might have a relationship with the development of the specific anti-viral immune response. Anti-S protein antibodies were quantified using the previously described S-flow assay that shows high correlation with the neutralization assay (Grzelak et al., 2020). Anti-S antibodies were found in 45 out of 75 symptomatic patients, a rather low percentage (60%), likely resulting from the early sampling at the time of diagnosis of some patients. Interestingly, anti-S antibodies levels correlated with those of anti-Tn, unlike anti-αGal (**Figures 5A,B**) and the remaining tested anti-carbohydrates (not shown). Consistent with the lower levels of anti-Tn in blood group A individuals, it appeared that anti-S antibodies were also lower in blood group A individuals as compared to blood group O and blood group B patients (**Figure 5C**).

Expression of the Tn Epitope in the Respiratory Tract

The Tn antigen has been detected on SARS-CoV-2 S protein produced in HEK-293T cells (Gao et al., 2020; Sanda et al., 2020; Shajahan et al., 2020). Their *O*-glycosylation capability unlikely represents that of epithelial cells of the respiratory tract which are the main viral target cells contributing to transmission. Respiratory as well as digestive epithelial cells produce large amounts of *O*-glycans and express a broad set of the polypeptide GalNAc transferases that add the first *N*-acetylgalatosamine unit to the peptide chain constituting the Tn epitope (Bennett et al., 2012). In normal tissues, the Tn antigen is masked by elongation of *O*-glycan chains and it is known to be over-expressed in carcinoma (Rodrigues et al., 2018). Nonetheless, in order to determine if indeed the Tn antigen could be produced by respiratory epithelial cells, we tested its expression by immunohistochemistry on fixed tracheal and lung tissue from three individuals of the A, B and O blood types, respectively. First, the anti-Tn specificity was validated by ELISA on PAA neoglycoconjugates and on mucins presenting high levels of either the Tn epitope or A, B and H blood group antigens. We observed a specific binding to the Tn-PAA conjugate and to Tn-rich desialylated bovine submaxillary mucin, but not to other conjugates or to human salivary mucin, although a small reactivity was detected on blood group A containing mucin or neoglycoconjugate (**Figure 6A**). In addition, the antibody had previously been shown to recognize glycophorins from Tn erythrocytes, as well as ovine submaxillary mucin (OSM) (Duk et al., 2001). Thus, the anti-Tn that we used recognizes the Tn antigen independently of the underlying peptide while showing only little cross-reactivity with related structures such as blood group A antigen. Flow cytometry experiments additionally showed that the anti-Tn strongly bound to Jurkat cells known to strongly express the Tn epitope due

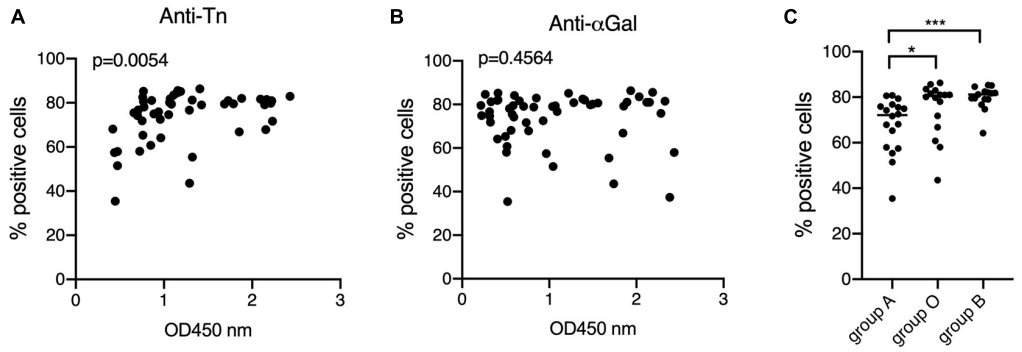

FIGURE 5 | Relationships between the anti-Tn and anti-αGal levels, ABO phenotypes and the levels of anti-S protein. Anti-S protein antibodies of COVID-19 patients were detected and quantified by the S-Flow assay at a plasma dilution of 1: 300. Data are shown as percentage of positive cells. Only positive plasma samples were considered. **(A)** Correlation between anti-S and anti-Tn, Spearman *r p* value is shown; **(B)** correlation between anti-S and anti-αGal, Spearman *r P*-value is shown; **(C)** relationship between ABO phenotypes and anti-S. Only anti-S positive individuals (with cut-off values >30%) were considered. *P*-values from Mann-Whitney comparisons are indicated: $*p < 0.05$, $***p < 0.001$.

to a genetic defect that impairs *O*-glycans elongation. In the same conditions, HEK-293T cells and Vero cells were not recognized by the antibody (**Figure 6B**). When tested on tissue sections, the antibody revealed a strong intracellular binding to the tracheal and bronchial epithelia, but not to any other cell type in the respiratory tract, regardless of the donor ABO phenotype (**Figure 6C**).

DISCUSSION

Here we tested the possibility that in addition to anti-A and anti-B blood group antibodies, natural anti-carbohydrate antibodies could play a protective role against SARS-CoV-2 infection. Consistent with the initial hypothesis, we observed that COVID-19 patients presented lower levels of anti-Tn antibodies than controls, whilst none of the other tested anti-carbohydrates showed significant differences in levels between the two groups. Tn antigen is constituted by a single *N*-acetylgalactosamine linked to either a serine or a threonine residue. It constitutes the basis of all mucin-type *O*-glycans to which additional monosaccharide units are generally added. It is therefore not normally detected at the cell surface and is considered a tumor marker in several types of carcinoma where elongation of *O*-glycosylation is impaired (Rodrigues et al., 2018). It is also considered a blood group isoantigen since there exist rare individuals who express the Tn antigen on their erythrocytes due to a genetic defect in the *O*-glycosylation elongation pathway and since natural anti-Tn antibodies agglutinate these rare erythrocytes, causing a so-called polyagglutinability (Dahr et al., 1975).

The SARS-CoV-2 S protein possesses several documented *O*-glycosylation sites located at the hinge between the RBD and NTD domains and surrounding the furin cleavage site (Antonopoulos et al., 2020; Gao et al., 2020; Sanda et al., 2020; Shajahan et al., 2020; Zhao P. et al., 2020). Blocking of *O*-glycosylation resulted in partial inhibition of SARS-CoV-2 cell entry *in vitro*, indicating the functional importance of *O*-glycans in the infection process (Yang et al., 2020). Epithelial cells of the upper respiratory tract, nasopharynx, trachea and large bronchi, appear to be the main producers of virions involved in inter-individual transmission (Wolfel et al., 2020). In accordance with the notion that epithelial cells synthesize large amounts of *O*-glycans, we observed that these cells in the respiratory epithelia present intracellular Tn epitopes, unlike the remaining cell types present in these tissues. Initiation of GalNAc-type *O*-glycosylation is performed by polypeptide *N*-acetylgalatosaminyltransferases (GalNAc-Ts) (Bennett et al., 2012). Twenty isoforms of GalNAc-Ts are known that show both overlapping and non-redundant specific functions to orchestrate the patterns of *O*-glycans on proteins. Inspection of the Human Protein Atlas[2] indicates that epithelial cells of the nasopharynx and of bronchi express strong to moderate amounts of at least 11 of these enzymes. This confirmed the strong potential for epithelial cells of the nasopharynx, trachea and bronchi to produce *O*-glycosylated glycoproteins. At present, only small amounts of *O*-glycans, including the Tn epitope, have been detected on SARS-CoV-2 recombinant S protein produced in HEK-293 cells, indicating that the major viral envelope protein can be *O*-glycosylated. Rapidly replicating viruses being expected to carry a large fraction of immature glycan structures, it is thus plausible that authentic infectious SARS-CoV-2 carries Tn epitopes.

Confirmation will await the complete structural characterization of native expectorated virions. In addition, it will be necessary in future experiments to show that purified natural anti-Tn antibodies can bind to native virions.

Since blood group A antigen is characterized by a terminal *N*-acetylgalactosamine in alpha linkage, it was expected that the levels of anti-Tn antibodies would be lower in blood group A individuals owing to the structural homology between the two epitopes. Likewise, due to the homology between blood group B and the αGal antigen, it was expected that blood group B individuals should show lower anti-αGal

[2]www.proteinatlas.org

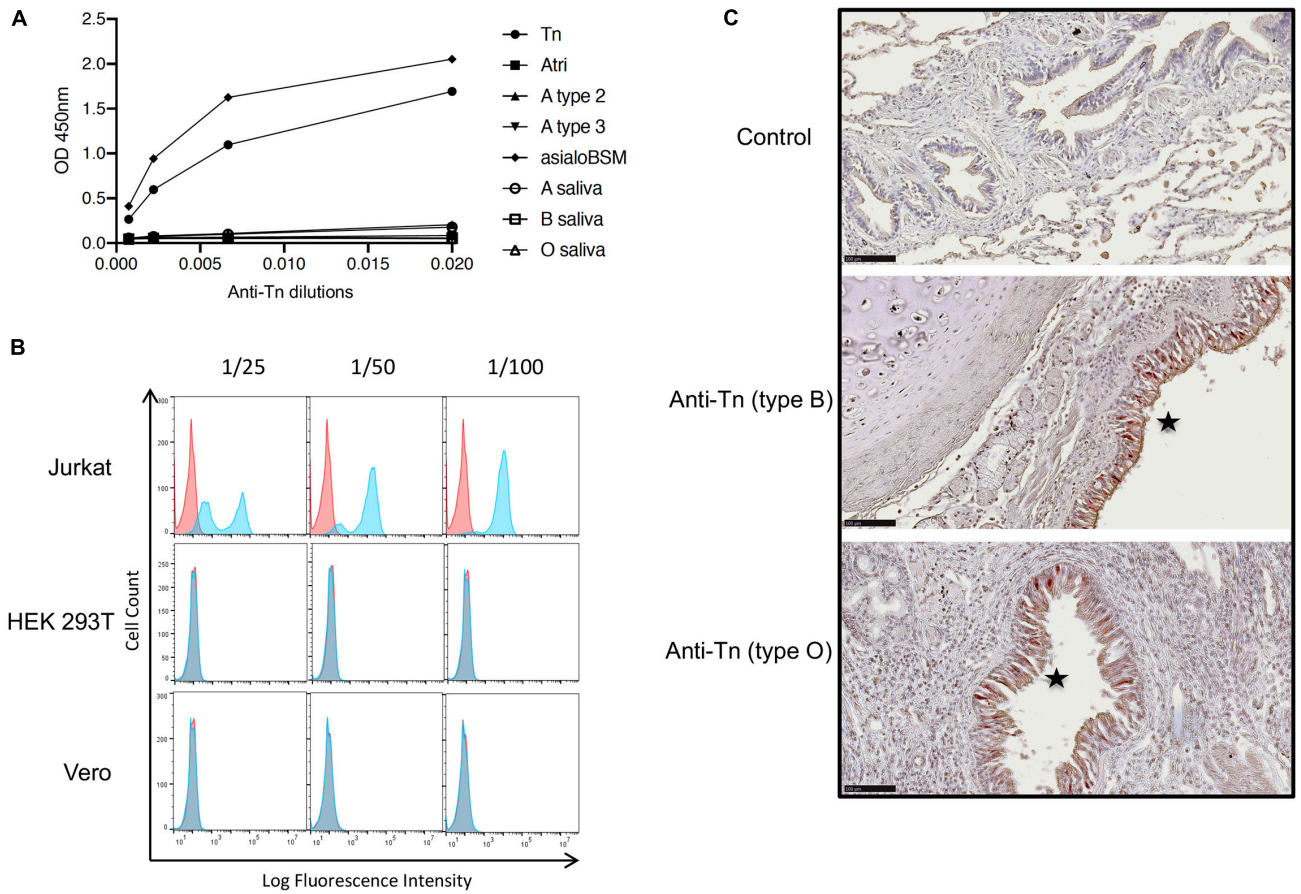

FIGURE 6 | Expression of the Tn epitope in lung and trachea. **(A)** Binding of the anti-Tn monoclonal antibody NaM217-2A9 to immobilized polyacrylamide-conjugated carbohydrate epitopes (Tn, A blood group trisaccharide, A type 2 and A type 3), human salivary mucins from A, B or O secretor individuals and desialylated bovine submaxillary mucin (asialoBSM) were assayed by ELISA. Strong reactivity was observed with the Tn-PAA conjugate, and asialoBSM that contains large amounts of Tn epitope. **(B)** Reactivity of the anti-Tn on cell lines detected by flow cytometry. Jurkat cells known to express large amounts of Tn epitope were used as a positive control. Negative controls are shown as red plots the blue plots showing data in the presence of the anti-Tn NaM217-2A9. **(C)** Staining of tracheal (middle panel) and bronchial epithelial cells (lower panel) by the anti-Tn NaM217-2A9 shown by the brown-red color (stars) in a blood group B and a blood group O donor, respectively (type B, type O). The upper panel (negative control) shows the lack of staining in absence of the primary anti-Tn antibody. Black bar = 100 μm.

levels. These associations with ABO phenotypes were indeed observed for the Tn and αGal antigens, respectively, but not for any of the other tested carbohydrate epitopes, which validated the method of quantification that we used. Regarding analyses of correlations with COVID-19 status, only the anti-Tn antigen showed significant lower amounts in patients in comparison with the control group, indicating that the effect did not stem from a general decrease of natural anti-carbohydrate in patients following infection. Thus, the data suggest that patients had lower anti-Tn prior to being infected. However, at this stage we cannot eliminate other potential causes that might contribute to the difference in anti-Tn levels between patients and controls. Besides the quantitative difference, there was a qualitative difference between patients and controls anti-Tn antibodies. The qualitative difference was indirectly observed through analysis of correlations with the other carbohydrate epitopes, revealing an absence of correlation with Tn-related motifs for patients, unlike for controls. A previous study performed using purified anti-Tn antibodies from pooled plasma samples revealed cross-reactivities with several related oligosaccharides or unrelated polysaccharides, indicating a rather broad polyreactivity (Bovin et al., 2012; Dobrochaeva et al., 2020). It is possible that the divergent patterns of correlation with other anti-carbohydrates between patients and control groups reflect distinct cross-reactivities of the anti-Tn. Alternatively, the observed divergent correlations between patients and controls for several anti-carbohydrates could reflect divergent immunogens composition from the microbiota. Direct evidence for this could be obtained by a specificity analysis following purification of patients and controls anti-Tn antibodies in future studies. In addition, it will be important to distinguish between different immunoglobulin subclasses, which was not done in this preliminary study.

Levels of natural anti-carbohydrate antibodies may decrease with aging (Muthana and Gildersleeve, 2016). Since patients and controls groups were not matched for age, the lower anti-Tn observed in patients may have originated from the higher mean age of patients (68 years) compared to that of controls (42 years). Again, this seems unlikely since the same effect should have been observed for the other anti-carbohydrates that were tested. In addition, within the patients' cohort there was a relationship between the levels of anti-Tn, but not of the other tested anti-carbohydrate antibodies, and those of anti-S viral protein. Although the underlying reason for this correlation remains unknown, it is noteworthy that similar to anti-Tn antibodies, the anti-S antibodies were lower in blood group A patients, suggesting that anti-Tn may have contributed to the development of the specific anti-viral response, akin to what has previously been observed for the anti-αGal antibodies in models of xenogenic viral infections (Galili, 2020).

It is now rather well documented through a large set of studies that blood group A individuals are at a higher risk of COVID-19 than individuals of blood group O, whilst blood group B seldom shows significant odd ratios relative to the other blood groups (Aktimur et al., 2020; Barnkob et al., 2020; Chegni et al., 2020; Ellinghaus et al., 2020; Göker et al., 2020; Latz et al., 2020; Leaf et al., 2020; Li et al., 2020; Muniz-Diaz et al., 2020; Shelton et al., 2020; Sohlpour et al., 2020; Valenti et al., 2020; Wu et al., 2020; Zeng et al., 2020; Zhang et al., 2020; Zhao J. et al., 2020; Zietz et al., 2020). We recently observed that anti-A and anti-B agglutinating natural antibodies were significantly lower in COVID-19 patients compared with controls (Deleers et al., 2020). Together with the present observations on anti-Tn antibodies, this may explain the ABO effect on COVID-19 epidemiology. Indeed, blood group O individuals, possess natural anti-A, anti-B and anti-Tn antibodies, B blood group individuals possess anti-A and anti-Tn antibodies, but blood group A individuals possess anti-B and low levels of anti-Tn only. The degree of protection conferred by these natural anti-carbohydrates would thus be minimal for blood group AB individuals who should possess only low levels of anti-Tn, followed by blood group A, then blood group B and finally by blood group O individuals who could benefit from all three types of antibodies. The anti-Tn antibodies could be particularly important as they could provide protection regardless of the ABO type of the virus transmitters, unlike anti-A and anti-B that may only protect during transmission events in an ABO incompatible situation.

In conclusion, in a first exploratory study, we observed that natural anti-Tn antibodies differ between COVID-19 patients and controls both quantitatively and qualitatively and that their levels are lower in blood group A individuals and associated with the levels of anti-S protein. These results suggest that natural anti-carbohydrate antibodies that target *O*-glycans may confer some protection against COVID-19. Nonetheless, it should be stressed that our study is preliminary and requires validation by further studies including age and gender matching of patients and controls, as well as *in vitro* experiments aimed at characterizing the mechanisms whereby anti-Tn antibodies could be protective. If validated, it would indicate that a significant fraction of the population with sufficient natural anti-Tn antibodies could benefit from a natural immunity conferred by these antibodies against COVID-19 and it would offer a prophylactic perspective by boosting the anti-Tn titers in everyone.

DATA AVAILABILITY STATEMENT

The raw data supporting the conclusions of this article will be made available by the authors, without undue reservation.

ETHICS STATEMENT

The studies involving human participants were reviewed and approved by Centre Hospitalier Universitaire Brugmann (CHU Brugmann, Bruxelles) and the Hôpital Universitaire Des Enfants Reine Fabiola (HUDERF, Bruxelles). The patients/participants provided their written informed consent to participate in this study.

AUTHOR CONTRIBUTIONS

AB, NR-C, TB, NJ, and JR performed the experiments. MD and HE provided the patients samples, their ABO blood groups and COVID-19 status. NB provided reagents and discussed the data. NL, AB, and NRV analyzed the data. JLP conceived the work, analyzed the data and wrote the manuscript. All authors corrected the manuscript and approved the final version.

FUNDING

This work was supported by Inserm, the University of Nantes, the University Hospital of Nantes. NB was supported by grant #20-04-60335 of the Russian Foundation for Basic Research.

ACKNOWLEDGMENTS

The authors were grateful to Dr. D. Blanchard (Etablissement Français du Sang, Pays de la Loire, Nantes) for his kind gift of the monoclonal anti-Tn antibody and to Drs O. Schwartz and T. Bruel (Pasteur Institute, Paris) for their gift of S protein stably expressing and control HEK-293T cells. The authors also thank the Cytometry Facility Cytocell (SFR Sante Francois Bonamy, Nantes) for expert technical assistance.

REFERENCES

Abdollahi, A., Mahmoudi-Aliabadi, M., Mehrtash, V., Jafarzadeh, B., and Salehi, M. (2020). The novel coronavirus SARS-CoV-2 vulnerabiloty association with ABO/Rh blood types. *Iran. J. Pathol.* 15, 156–160. doi: 10.30699/ijp.2020.125135.2367

Ahmed, I., Quinn, L., and Tan, B. K. (2020). COVID-19 and the ABO blood group in pregnancy: a tale of two multiethnic cities. *Int. J. Lab. Hematol.* 43, e45–e47. doi: 10.1111/ijlh.13355

Aktimur, S. H., Sen, H., Yazicioglu, B., Gunes, A. K., and Genc, S. (2020). The assessment of the relationship between ABO blood groups and Covid-19 infection. *Int. J. Hematol. Oncol.* 30, 121–125. doi: 10.4999/uhod.204348

Aljanobi, G., Alhajjaj, A., Alkhabbaz, F., and Al-Jishi, J. (2020). The relationship between ABO blood group type and the covid-19 susceptibility in qatif central hospital, eastern province, saudi arabia: a retrospective cohort study. *Open J. Intern. Med.* 10, 232–238. doi: 10.4236/ojim.2020.102024

Antonopoulos, A., Broome, S., Sharov, V., Ziegenfuss, C., Easton, R. L., Panico, M., et al. (2020). Site-specific characterisation of SARS-CoV-2 spike glycoprotein receptor binding domain. *Glycobiology* doi: 10.1093/glycob/cwaa085

Bagdonaite, I., and Wandall, H. H. (2018). Global aspects of viral glycosylation. *Glycobiology* 28, 443–467. doi: 10.1093/glycob/cwy021

Barnkob, M. B., Pottegard, A., Stovring, H., Haunstrup, T. M., Homburg, K., Larsen, R., et al. (2020). Reduced prevalence of SARS-CoV-2 infection in ABO blood group O. *Blood Adv.* 4, 4990–4993. doi: 10.1182/bloodadvances.2020002657

Bennett, E. P., Mandel, U., Clausen, H., Gerken, T. A., Fritz, T. A., and Tabak, L. A. (2012). Control of mucin-type O-glycosylation: a classification of the polypeptide GalNAc-transferase gene family. *Glycobiology* 22, 736–756. doi: 10.1093/glycob/cwr182

Boudin, L., Janvier, F., Bylicki, O., and Dutasta, F. (2020). ABO blood groups are not associated with risk of acquiring the SARS-CoV-2 infection in young adults. *Haematologica* 105, 2841–2843. doi: 10.3324/haematol.2020.265066

Bovin, N., Obukhova, P., Shilova, N., Rapoport, E., Popova, I., Navakouski, M., et al. (2012). Repertoire of human natural anti-glycan immunoglobulins. do we have auto-antibodies? *Biochim. Biophys. Acta* 1820, 1373–1382. doi: 10.1016/j.bbagen.2012.02.005

Chegni, H., Pakravan, N., Saadati, M., Ghaffari, A. D., Shirzad, H., and Hassan, Z. M. (2020). Is There a link between COVID-19 mortality with genus, age, ABO blood group type, and ACE2 gene polymorphism? *Iran. J. Public Health* 49, 1582–1584.

Cheng, Y., Cheng, G., Chui, C. H., and Lau, F. Y. (2005). ABO blood group and susceptibility to severe acute respiratory syndrome. *JAMA* 293, 1450–1451.

Dahr, W., Uhlenbruck, G., Gunson, H. H., and Van Der Hart, M. (1975). Molecular basis of Tn-polyaggutinability. *Vox. Sang.* 29, 36–50. doi: 10.1111/j.1423-0410.1975.tb00475.x

Delanghe, J. R., De Buyzere, M. L., and Speeckaert, M. M. (2020). C3 and ACE1 polymorphisms are more important confounders in the spread and outcome of COVID-19 in comparison with ABO polymorphism. *Eur. J. Prev. Cardiol.* 27, 1331–1332. doi: 10.1177/2047487320931305

Deleers, M., Breiman, A., Daubie, V., Maggetto, C., Barreau, I., Besse, T., et al. (2020). Covid-19 and blood groups: ABO antibody levels may also matter. *Int. J. Infect. Dis.* 104, 242–249. doi: 10.1016/j.ijid.2020.12.025

Dobrochaeva, K., Khasbiullina, N., Shilova, N., Antipova, N., Obukhova, P., Ovchinnikova, T., et al. (2020). Specificity of human natural antibodies referred to as anti-Tn. *Mol. Immunol.* 120, 74–82. doi: 10.1016/j.molimm.2020.02.005

Duk, M., Blanchard, D., and Lisowska, E. (2001). Anti-T and anti-Tn antibodies. *Trans. Clin. Biol.* 8, 253.

Dzik, S., Eliason, K., Morris, E. B., Kaufman, R. M., and North, C. M. (2020). COVID-19 and ABO blood groups. *Transfusion* 60, 1883–1884.

Ellinghaus, D., Degenhardt, F., Bujanda, L., Buti, M., Albillos, A., Invernizzi, P., et al. (2020). Genomewide association study of severe covid-19 with respiratory failure. *N. Engl. J. Med.* 383, 1522–1534. doi: 10.1056/nejmoa2020283

Fan, Q., Zhang, W., Li, B., Li, D. J., Zhang, J., and Zhao, F. (2020). Association between ABO blood group system and COVID-19 susceptibility in Wuhan. *Front. Cell Infect. Microbiol.* 10:404.

Focosi, D., Iorio, M. C., and Lanza, M. (2020). ABO blood group correlations with COVID-19: cohort choice makes a difference. *Clin. Infect. Dis.* 361:ciaa1495. doi: 10.1093/cid/ciaa1495

Franchini, M., Glingani, C., Del Fante, C., Capuzzo, M., Di Stasi, V., Rastrelli, G., et al. (2020). The protective effect of O blood type against SARS-CoV-2 infection. *Vox Sang* (in press). doi: 10.1111/vox.13003

Galili, U. (2019). Evolution in primates by "Catastrophic-selection" interplay between enveloped virus epidemics, mutated genes of enzymes synthesizing carbohydrate antigens, and natural anticarbohydrate antibodies. *Am. J. Phys. Anthropol.* 168, 352–363. doi: 10.1002/ajpa.23745

Galili, U. (2020). Human natural antibodies to mammalian carbohydrate antigens as unsung heroes protecting against past, present, and future viral infections. *Antibodies (Basel)* 9:25. doi: 10.3390/antib9020025

Gallian, P., Pastorino, B., Morel, P., Chiaroni, J., Ninove, L., and Lamballerie, X. (2020). Lower prevalence of antibodies neutralizing SARS-CoV-2 in group O French blood donors. *Antiviral. Res.* 181:104880. doi: 10.1016/j.antiviral.2020.104880

Gao, C., Zeng, J., Jia, N., Stavenhagen, K., Matsumoto, Y., Zhang, H., et al. (2020). SARS-CoV-2 spike protein interacts with multiple innate immune receptors. *bioRxiv* [Preprint]. doi: 10.1101/2020.1107.1129.227462

Göker, H., Aladağ, K. E., Demiroğlu, H., Ayaz Ceylan, ÇM., Büyükaşik, Y., Inkaya, A. Ç, et al. (2020). The effects of blood group types on the risk of COVID-19 infection and its clinical outcome. *Turk. J. Med. Sci.* 50, 679–683. doi: 10.3906/sag-2005-395

Grzelak, L., Temmam, S., Planchais, C., Demeret, C., Tondeur, L., Huon, C., et al. (2020). A comparison of four serological assays for detecting anti-SARS-CoV-2 antibodies in human serum samples from different populations. *Sci. Transl. Med.* 12:3103. doi: 10.1126/scitranslmed.abc3103

Guillon, P., Clément, M., Sébille, V., Rivain, J.-G., Chou, C.-F., Ruvoën-Clouet, N., et al. (2008). Inhibition of the interaction beteen the SARS-CoV spike protein and its cellular receptor by anti-histo-blood group antibodies. *Glycobiology* 18, 1085–1093. doi: 10.1093/glycob/cwn093

Hoiland, R. L., Fergusson, N. A., Mitra, A. R., Griesdale, D. E. G., Devine, D. V., Stukas, S., et al. (2020). The association of ABO blood group with indices of disease severity and multiorgan dysfunction in COVID-19. *Blood Adv.* 4, 4981–4989. doi: 10.1182/bloodadvances.2020002623

Huflejt, M. E., Vuskovic, M., Vasiliu, D., Xu, H., Obukhova, P., Shilova, N., et al. (2009). Anti-carbohydrate antibodies of normal sera: findings, surprises and challenges. *Mol. Immunol.* 46, 3037–3049. doi: 10.1016/j.molimm.2009.06.010

Khasbiullina, N. R., Shilova, N. V., Navakouski, M. J., Nokel, A. Y., Blixt, O., Kononov, L. O., et al. (2019). The repertoire of human antiglycan antibodies and its dynamics in the first year of life. *Biochemistry (Mosc)* 84, 608–616. doi: 10.1134/s0006297919060038

Latz, C. A., Decarlo, C., Boitano, L., Png, C. Y. M., Patell, R., Conrad, M. F., et al. (2020). Blood type and outcomes in patients with COVID-19. *Ann. Hematol.* 99, 2113–2118.

Leaf, R. K., Al-Samkari, H., Brenner, S. K., Gupta, S., and Leaf, D. E. (2020). ABO phenotype and death in critically ill patients with COVID-19. *Br. J. Haematol.* 190, e204–e208. doi: 10.1111/bjh.16984

Li, J., Wang, X., Chen, J., Cai, Y., Deng, A., and Yang, M. (2020). Association between ABO blood groups and risk of SARS-CoV-2 pneumonia. *Br. J. Haematol.* 190, 24–27. doi: 10.1111/bjh.16797

Lopes, A. M., Breiman, A., Lora, M., Le Moullac-Vaidye, B., Galanina, O., Nystrom, K., et al. (2018). Host-specific glycans are correlated with susceptibility to infection by lagoviruses, but not with their virulence. *J. Virol.* 92:e001759-17.

Luetscher, R. N. D., Mckitrick, T. R., Gao, C., Mehta, A. Y., Mcquillan, A. M., Kardish, R., et al. (2020). Unique repertoire of anti-carbohydrate antibodies in individual human serum. *Sci. Rep.* 10:15436.

Muniz-Diaz, E., Llopis, J., Parra, R., Roig, I., Ferrer, G., Grifols, J., et al. (2020). Relationship between the ABO blood group and COVID-19 susceptibility, severity and mortality in two cohorts of patients. *Blood Transfus* 11, 462–465. doi: 10.2450/2020.0256-2420

Muthana, S. M., and Gildersleeve, J. C. (2016). Factors affecting anti-glycan IgG and IgM repertoires in human serum. *Sci. Rep.* 6:19509.

New, J. S., King, R. G., and Kearney, J. F. (2016). Manipulation of the glycan-specific natural antibody repertoire for immunotherapy. *Immunol. Rev.* 270, 32–50. doi: 10.1111/imr.12397

Niles, J. K., Karnes, H. E., Dlott, J. S., and Kaufman, H. W. (2020). Association of ABO/Rh with SARS-CoV-2 positivity: The role of race and ethnicity in a female cohort. *Am. J. Hematol.* 96, E23–E26. doi: 10.1002/ajh.26019

Padhi, S., Suvankar, S., Dash, D., Panda, V. K., Pati, A., Panigrahi, J., et al. (2020). ABO blood group system is associated with COVID-19 mortality: an epidemiological investigation in the Indian population. *Transfus Clin. Biol.* 27, 253–258. doi: 10.1016/j.tracli.2020.08.009

Pairo-Castineira, E., Clohisey, S., Klaric, L., Bretherick, A., Rawlik, K., Parkinson, N., et al. (2020). Genetic mechanisms of critical illness in Covid-19. *MedRxiv* [Preprint]. doi: 10.1101/2020.1109.1124.20200048

Preece, A. F., Strahan, K. M., Devitt, J., Yamamoto, F. F., and Gustavson, K. (2002). Expression of ABO or related antigenic carbohydrates on viral envelopes leads to neutralization in the presence of serum containing specific natural antibodies and complement. *Blood* 99, 2477–2482. doi: 10.1182/blood.v99.7.2477

Purohit, S., Li, T., Guan, W., Song, X., Song, J., Tian, Y., et al. (2018). Multiplex glycan bead array for high throughput and high content analyses of glycan binding proteins. *Nat. Commun.* 9:258.

Ray, J. G., Schull, M. J., Vermeulen, M. J., and Park, A. L. (2020). Association between ABO and Rh blood groups and SARS-CoV-2 infection or severe COVID-19 Illness. a population-based cohort study. *Ann. Int. Med.* (in press). doi: 10.7326/M7320-4511

Roberts, G. H. L., Park, D. S., Coignet, M. V., Mccurdy, S. R., Knight, S. C., Partha, R., et al. (2020). AncestryDNA COVID-19 host genetic study I 1 dentifies three novel loci. *medRxiv* [Preprint]. doi: 10.1101/2020.1110.1106.2020 5864

Rodrigues, J. G., Balmana, M., Macedo, J. A., Pocas, J., Fernandes, A., De-Freitas-Junior, J. C. M., et al. (2018). Glycosylation in cancer: selected roles in tumour progression, immune modulation and metastasis. *Cell Immunol.* 333, 46–57. doi: 10.1016/j.cellimm.2018.03.007

Sanda, M., Morrison, L., and Goldman, R. (2020). N and O glycosylation of the SARS-CoV-2 spike protein. *bioRxiv* [Preprint]. doi: 10.1101/2020.1107.1105. 187344

Schneider, C., Smith, D. F., Cummings, R. D., Boligan, K. F., Hamilton, R. G., Bochner, B. S., et al. (2015). The human IgG anti-carbohydrate repertoire exhibits a universal architecture and contains specificity for microbial attachment sites. *Sci. Transl. Med.* 7:269ra261.

Shajahan, A., Supekar, N. T., Gleinich, A. S., and Azadi, P. (2020). Deducing the N- and O- glycosylation profile of the spike protein of novel coronavirus SARS-CoV-2. *Glycobiology* 30, 981–988. doi: 10.1093/glycob/cwaa042

Shelton, J. F., Shastri, A. J., Ye, C., Weldon, C. H., Filshtein-Somnez, T., Coker, D., et al. (2020). Trans-ethnic analysis reveals genetic and non-genetic associations with COVID-19 susceptibility and severity. *medRxiv* [Preprint]. doi: 10.1101/2020.1109.1104.20188318

Sohlpour, A., Jafari, A., Apourhoseingholi, M. A., and Soltani, F. (2020). Corona COVID-19 virus and severe hypoxia in young patients without underlying disease: high prevalence rate with blood group A. *Trends Anesth Crit. Care* 34, 63–64. doi: 10.1016/j.tacc.2020.1008.1005

Stowell, S. R., Arthur, C. M., Mcbride, R., Berger, O., Razi, N., Heimburg-Molinaro, J., et al. (2014). Microbial glycan microarrays define key features of host-microbial interactions. *Nat. Chem. Biol.* 10, 470–476. doi: 10.1038/nchembio. 1525

Sun, Z., Ren, K., Zhang, X., Chen, J., Jiang, Z., Jiang, J., et al. (2020). Mass spectrometry analysis of newly emerging coronavirus HCoV-19 spike protein and human ACE2 reveals camouflaging glycans and unique post-translational modifications. *Engineering (Beijing)* (in press). doi: 10.1016/j.eng.2020.1007. 1014

Tendulkar, A. A., Jain, P. A., and Velaye, S. (2017). Antibody titers in Group O platelet donors. *Asian J. Transfus. Sci.* 11, 22–27. doi: 10.4103/0973-6247. 200765

Valenti, L., Villa, S., Baselli, G., Temporiti, R., Bandera, A., Scudeller, L., et al. (2020). Association of ABO blood groups and secretor phenotype with severe COVID-19. *Transfusion* 60, 3067–3070. doi: 10.1111/trf.16130

Volynsky, P., Efremov, R., Mikhalev, I., Dobrochaeva, K., Tuzikov, A., Korchagina, E., et al. (2017). Why human anti-Galalpha1-4Galbeta1-4Glc natural antibodies do not recognize the trisaccharide on erythrocyte membrane? Molecular dynamics and immunochemical investigation. *Mol. Immunol.* 90, 87–97. doi: 10.1016/j.molimm.2017.06.247

Watanabe, Y., Allen, J. D., Wrapp, D., Mclellan, J. S., and Crispin, M. (2020). Site-specific glycan analysis of the SARS-CoV-2 spike. *Science* 369, 330–333.

Watanabe, Y., Bowden, T. A., Wilson, I. A., and Crispin, M. (2019). Exploitation of glycosylation in enveloped virus pathobiology. *Biochim. Biophys. Acta Gen. Subj.* 1863, 1480–1497. doi: 10.1016/j.bbagen.2019.05.012

Wolfel, R., Corman, V. M., Guggemos, W., Seilmaier, M., Zange, S., Muller, M. A., et al. (2020). Virological assessment of hospitalized patients with COVID-2019. *Nature* 581, 465–469. doi: 10.1038/s41586-020-2196-x

Wu, Y., Feng, Z., Li, P., and Yu, Q. (2020). Relationship between ABO blood group distribution and clinical characteristics in patients with COVID-19. *Clin. Chim. Acta* 509, 220–223. doi: 10.1016/j.cca.2020.06.026

Yang, Q., Hughes, T. A., Kelkar, A., Yu, X., Cheng, K., Park, S., et al. (2020). Inhibition of SARS-CoV-2 viral entry upon blocking N- and O-glycan elaboration. *Elife* 9:e61552.

Zeng, X., Fan, H., Lu, D., Meng, F., Zhuo, L., Tang, M., et al. (2020). Association between ABO blood groups and clinical outcome of coronavirus disease 2019: evidence from two cohorts. *medRxiv* [Preprint]. doi: 10.1101/2020.1104.1115. 20063107

Zhang, L., Huang, B., Xia, H., Fan, H., Zhu, M., Zhu, L., et al. (2020). Retrospective analysis of clinical features in 134 coronavirus disease 2019 cases. *Epidemiol. Infect.* 148:e199.

Zhao, J., Yang, Y., Huang, H.-P., Li, D., Gu, D.-F., and Lu, X.-F. (2020). Relationship between the ABO blood group and the COVID-19 susceptibility. *Clin. Infect. Dis.* 4:ciaa1150. doi: 10.1093/cid/ciaa1150

Zhao, P., Praissman, J. L., Grant, O. C., Cai, Y., Xiao, T., Rosenbalm, K. E., et al. (2020). Virus-receptor interactions of glycosylated SARS-CoV-2 spike and human ACE2 receptor. *Cell Host. Microbe.* 28, 586–601.e586.

Zietz, M., Zucker, J., and Tatonetti, M. P. (2020). Associations between blood type and COVID-19 infection, intubation, and death. *Nat. Commun.* 11:5761.

Conflict of Interest: The authors declare that the research was conducted in the absence of any commercial or financial relationships that could be construed as a potential conflict of interest.

frontiers in Immunology

ORIGINAL RESEARCH
published: 12 April 2021
doi: 10.3389/fimmu.2021.655371

Microneme Proteins 1 and 4 From *Toxoplasma gondii* Induce IL-10 Production by Macrophages Through TLR4 Endocytosis

Rafael Ricci-Azevedo[1†‡], *Flavia Costa Mendonça-Natividade*[1‡], *Ana Carolina Santana*[2], *Juliana Alcoforado Diniz*[3] *and Maria Cristina Roque-Barreira*[1*]

[1] *Laboratory of Immunochemistry and Glycobiology, Department of Cell and Molecular Biology and Pathogenic Bioagents, Ribeirão Preto Medical School, University of São Paulo, Ribeirão Preto, Brazil,* [2] *Laboratory of Cellular and Molecular Biology of Mast Cells, Department of Cell and Molecular Biology and Pathogenic Bioagents, Ribeirão Preto Medical School, University of São Paulo, Ribeirão Preto, Brazil,* [3] *Laboratory of Molecular Parasitology, Department of Cell and Molecular Biology and Pathogenic Bioagents, Ribeirão Preto Medical School, University of São Paulo, Ribeirão Preto, Brazil*

The protozoan parasite *Toxoplasma gondii* modulates host cell responses to favor its success in the early stage of infections by secreting proteins from its apical organelles. Some of these proteins, including microneme proteins (MICs) 1 and 4, trigger pro-inflammatory host cell responses. The lectins MIC1 and MIC4 interact with N-linked glycans on TLR2 and TLR4, activating NF-κB and producing IL-12, TNF-α, and IL-6. Interestingly, MIC1 and MIC4 also trigger secretion of the anti-inflammatory cytokine IL-10 through mechanisms as yet unknown. Herein, we show that the ability of these MICs to induce macrophages to produce IL-10 depends on TLR4 internalization from the cell surface. Macrophages subjected to blockade of endocytosis by Dynasore continued to release TNF-α, but failed to produce IL-10, in response to MIC1 or MIC4 exposure. Similarly, IL-10 was not produced by Dynasore-conditioned *T. gondii*-infected macrophages. Furthermore, MIC1- or MIC4-stimulated macrophages gained transient tolerance to LPS. We report a previously undiscovered mechanism by which well-defined *T. gondii* components inhibit a host inflammatory response.

Keywords: *Toxoplasma gondii*, MIC1, MIC4, TLR4 (Toll-like receptor 4), Dynasore, endocytosis, IL-10 (Interleukin 10)

OPEN ACCESS

Edited by:
Hector Mora Montes, University of Guanajuato, Mexico

Reviewed by:
Françoise Debierre-Grockiego, Université de Tours, France
Emma Harriet Wilson, University of California, Riverside, United States

****Correspondence:***
Maria Cristina Roque-Barreira
mcrbarre@fmrp.usp.br

†Present address:
Rafael Ricci-Azevedo, EA 3878 Groupe D'étude De La Thrombose De Bretagne Occidentale (GETBO), Brest Hospital, Univ Brest, Brest, France

‡These authors share first authorship

Specialty section:
This article was submitted to Microbial Immunology, a section of the journal Frontiers in Immunology

Received: *18 January 2021*
Accepted: *22 March 2021*
Published: *12 April 2021*

Citation:
Ricci-Azevedo R, Mendonça-Natividade FC, Santana AC, Alcoforado Diniz J and Roque-Barreira MC (2021) Microneme Proteins 1 and 4 From Toxoplasma gondii *Induce IL-10 Production by Macrophages Through TLR4 Endocytosis. Front. Immunol. 12:655371. doi: 10.3389/fimmu.2021.655371*

INTRODUCTION

Toxoplasma gondii is a protozoan obligate intracellular parasite of the phylum Apicomplexa, that causes toxoplasmosis. *T. gondii* infects a range of warm-blooded animals, including humans (1). From the estimated 1/3 of the world's population chronically infected with *T. gondii*, most of them are clinically asymptomatic. There are relevant exceptions. Reactivation of latent disease in immunocompromised patients frequently causes life-threatening encephalitis, and acute infection acquired during pregnancy can be fatal to the fetus (2–4). *T. gondii* invades host cells *via* several mechanisms (5, 6), including recognition of carbohydrates on a host cell surface (7, 8). The host cell response to contact with the parasite plays a crucial role in deciding infection outcome (9).

Studies of *T. gondii* components capable of inducing cytokine production by innate immune cells have made progress in recent years. Most reports have focused on the role of profilin in activating TLR11 (10) and TLR12 (11). This activation results in release of the pro-inflammatory cytokine IL-12 (12). The ability to induce IL-12 secretion *via* TLR activation has been attributed to other *T. gondii* components, including glycosylphosphatidylinositol (GPI) anchors (13) and heat shock protein 70 (TgHSP70) (14). Granule dense proteins (GRA) 24 account for cytokine release by macrophages, which occurs through a TLR-independent pathway (15, 16). Finally, our laboratory has shown that the complex LAC+, containing the microneme proteins (MICs) 1, 4, and 6 from *T. gondii* induce cytokine release by innate immune cells (17, 18), which was later confirmed to be happening due to the interaction of MIC1 and MIC4 with both TLR2 and TLR4 (19, 20).

We and others have previously reported that MIC1 and MIC4 possess lectin domains (17, 21, 22) that recognize oligosaccharides with terminal α (2, 3)-sialyl residues linked to β-galactosides (MIC1) (17, 19) or terminal β(1–4)- or β(1–3)-galactose (MIC4) (19, 23). These carbohydrate recognition domains (CRDs) account for the interaction of MICs with glycans that are N-linked to receptors, such as TLR2 and TLR4, on innate immune cells (24). The interactions of isolated MIC1 or MIC4 with TLR2 are sufficient to trigger pro-inflammatory cytokine production. This response is optimized in the presence of the co-receptor CD14, or upon TLR2 heterodimerization with TLR1 or TLR6 (20). Remarkably, MIC1 and MIC4 also induce production of the anti-inflammatory cytokine IL-10 in addition to release of pro-inflammatory cytokines, including IL-12, IL-6, and TNF-α (19).

Following *T. gondii* infection, the IL-12 produced by mononuclear phagocytes stimulates release of IFN-γ by NK and CD4+ T cells, driving the host immune response toward a Th1 axis (12, 25, 26). Although beneficial, an exaggerated Th1 response intensifies inflammation, potentiating tissue injury unless increased IL-10 release regulates this response (27, 28). The key role of IL-10 in *T. gondii* infection was demonstrated by inoculating an avirulent parasite strain in IL-10 knock-out (KO) mice, which yielded 100% mortality within the first two weeks, although the level of parasite proliferation was similar to that detected in WT mice, which survived the infection. Compared to controls, IL-10 KO mice had four- to six-fold higher serum levels of IL-12 and IFN-γ, and their death was attributed to enhanced liver pathology, consisting of intense inflammatory cell infiltration and necrosis (29).

Some mechanisms by which MIC1 and MIC4 prime innate immune cells have been elucidated, including structural requirements and signaling cascades underlying TLR2 activation (20), but many details of cell-priming remain unknown. This study characterizes TLR4 dependent IL-10 production by MIC1- or MIC4-stimulated macrophages. MIC1/TLR4 or MIC4/TLR4 complex formation on the cell surface is sufficient to stimulate inflammatory cytokines. However, these complexes must undergo endosomal internalization to induce production of the anti-inflammatory cytokine IL-10, which can reproducibly confer cell tolerance to a subsequent inflammatory stimulus in *T. gondii*-infected macrophages. We provide the first report of a mechanism underlying production of anti-inflammatory cytokines in response to *T. gondii* proteins.

MATERIALS AND METHODS

Animals and Ethics

All experiments were performed in accordance with the ethical principles in animal research described by the Brazilian Society of Laboratory Animal Science, and were approved by the Ethics Committee on Animal Experimentation and Research of the Ribeirão Preto Medical School (FMRP), University of São Paulo (USP) (protocol number 191/2017). C57BL/6 mice, Wild type (WT) or genetically lacking CD14 (CD14-/-), TLR2 (TLR2-/-), or TLR4 (TLR4-/-) genes, 8 to 12 weeks old, were obtained from the Central Animal Facility of the University of São Paulo in Ribeirão Preto and housed in the bioterium of the Department of Cellular and Molecular Biology – FMRP.

MIC1 and MIC4 Recombinant Proteins

The procedures for obtaining highly purified and endotoxin-free recombinant lectins were made accordingly to the protocol previously published by us (30). Briefly, for the recombinant proteins expression, *mic1* and *mic4* sequences were amplified from cDNA of the *T. gondii* strain ME49 with a 6—histidine-tagged added on the N-terminal, cloned into pDEST17 vector (Gateway Cloning, Thermo Fisher Scientific, Grand Island, NY) under T7 promoter inducible by isopropyl-β-D-1-thiogalactopyranoside (IPTG) (Sigma Aldrich, St. Louis, MO). The MIC1 and MIC4 were then purified from inclusion bodies and refolded by gradient dialysis. The concentrations of recombinant proteins were determined by bicinchoninic acid assay (BCA) (Pierce, Thermo Fisher Scientific Inc.) and stored at –20°C. Endotoxin was removed by passing through polymyxin-B columns (Affi-Prep Polymyxin Resin; Bio-Rad, Hercules, CA) and any residual concentration were measured in all protein samples for quality control, using the Limulus Amebocyte Lysate Kit–QCL-1000 (Lonza, Basel). MIC1 and MIC4 were only used when the concentration of endotoxin was less than 3 UE/ug. Additionally, prior their use to all *in vitro* assays aliquots of the recombinant proteins were incubated with 50 μg/mL polymyxin B sulfate salt (Sigma-Aldrich) for 30 min at 37°C to neutralize any residual endotoxin. Biotinylation of MIC1 and MIC4 with Sulfo-NHS-LC-biotin (Pierce, Thermo Fisher Inc.) was performed according to the manufacturer's recommendations kit.

Toxoplasma gondii Culture

Toxoplasma gondii was cultured as previously described (31). Briefly, type I RH strain parasites were maintained on human foreskin fibroblast (HFF-1) monolayers, grown in Dulbecco's modified Eagle's medium (DMEM) supplemented with 10% (vol/vol) fetal bovine serum (FBS), 0.25 mM gentamicin, 10 U/mL penicillin, and 10 μg/mL streptomycin (Gibco, Thermo

Fisher Scientific Inc.). For *in vitro* infections, parasites were recovered from HFF monolayers as previously described (19). In brief, cells were centrifuged for 5 min at 50 × g to remove HFF cell debris. Supernatant containing parasites was transferred to a new tube and centrifuged for 10 min at 1,000 × g. The pellet was resuspended in RPMI-1640 medium (Gibco,Thermo Fisher Scientific Inc.) for parasite counting.

Macrophage Culture

WT, $CD14^{-/-}$, $TLR2^{-/-}$, and $TLR4^{-/-}$ bone marrow derived macrophages (BMDMs) were obtained as previously described (32). Briefly, bone marrow cells were cultured for 7–9 days in RPMI 20/30, which consists of RPMI-1640 medium (Gibco, Thermo Fisher Scientific Inc.), supplemented with 20% (vol/vol) FBS and 30% (vol/vol) L-Cell Conditioned Media (LCCM) as a source of macrophage colony-stimulating factor (M-CSF) on non-treated Petri dishes (Optilux - Costar, Corning Inc. Corning, NY). Twenty-four hours before experiments, BMDM monolayers were detached using cold phosphate-buffered saline (PBS) (Hyclone, GE Healthcare Inc. South Logan, UT) and cultured, as specified, in RPMI-1640 (Gibco,Thermo Fisher Scientific Inc.) supplemented with 10% (vol/vol) FBS, 10 U/mL penicillin, and 10 µg/mL streptomycin, (2 mM) L-glutamine, (25 mM) HEPES, pH 7.2 (Gibco,Thermo Fisher Scientific Inc.) at 37°C in 5% CO2 for the indicated periods.

Macrophage Endocytosis Blockage With Dynasore

For endocytosis blockage using dynasore, 5×10^5 BMDMs (500 µL/well – 24 well plates) were washed with serum-free RPMI-1640 (Gibco,Thermo Fisher Scientific Inc.) and incubated for 1 hour. Then cells were cooled to 17°C and pretreated with Dynasore (80 µM, Sigma-Aldrich) for 30 minutes in serum-free RPMI-1640. Then cells were stimulated or infected as described below. The BMDMs were incubated at 37°C in 5% CO_2 and, for 24 hours incubation, 40 µM of Dynasore was added to each 9 h of incubation period.

Macrophage Stimulation and *In Vitro T. gondii* Infection

BMDMs were pre-treated or not with Dynasore as previously mentioned. 1×10^6 BMDMs/mL were stimulated with MIC1 or MIC4 at 5 µg/mL. It was established a sub-optimal lectin concentration based on dose-response experiments, following previous studies of our group (19, 20). LPS (standard LPS, *E. coli* 0111: B4; Sigma-Aldrich, 500 ng/mL) and medium alone were used respectively as the positive and negative controls. For *in vitro* infection assay, after counted as previously mentioned, 3 tachyzoites per BMDM were added into wells (multiplicity of infection, MOI = 3). The plates were immediately centrifuged for 3 min at 200 × g to synchronize infection within BMDMs and incubated at 37°C in 5% CO2. After incubation, culture supernatants were collected for analyzing cytokine secretion, RNA was isolated for gene expression studies, and cell lysates were prepared for western analysis.

TLR4 Surface Detection

To detect cell surface displayed TLR4, 1×10^5 BMDMs cultured in black 96-well plates with clear bottoms were stimulated with medium only, LPS, MIC1, or MIC4 for the indicated periods, then fixed with 2% (vol/vol) paraformaldehyde (Sigma Aldrich). Wells were rinsed with phosphate buffered saline solution (PBS) pH 7 to 7.2 (Hyclone, GE Healthcare Inc.) supplemented with 1M glycine (Sigma Aldrich) and blocked using anti-mouse CD16/32 (FcBlock) for 1 h at room temperature. This was followed by incubation overnight at 4°C with 0.5 ng/mL rat anti-mouse TLR4 (Biolegend San Diego, CA - 117601), followed by five washes with 200 µL PBS. Secondary antibodies conjugated with Alexa Fluor 488 (Invitrogen, Thermo Fisher Scientific Inc - A21208) were added to the wells (1:1000) and incubated for 1 h at room temperature. Wells were washed 7 times with 200 µL PBS. TLR4 was detected in an FLx800 Fluorescence Microplate Reader (BioTek Instruments, Winooski, VT); excitation 485 nm, emission 528 nm). Results are expressed as median fluorescence intensity (MFI).

Confocal Microscopy and Colocalization Analysis

To analyze the distribution of biotinylated MIC1 and MIC4 after incubation with macrophages, 2×10^4 BMDMs were cultured on 13 mm diameter glass coverslips placed in 24-well plates for 18 h at 37°C in 5% CO_2. Cells were then stimulated with 5 µg/mL biotinylated MIC1 or MIC4 and immediately incubated for 5, 10, or 15 min at 37°C in 5% CO_2. After incubation, cells were fixed for 20 min in 2% (vol/vol) paraformaldehyde (Sigma-Aldrich) in PBS (Hyclone, GE Healthcare Inc.), washed twice with PBS, and incubated with 0.1 M glycine (in PBS) for 10 min. Cells were then permeabilized with 0.01% (vol/vol) saponin (Sigma-Aldrich) in PBS for 20 min and blocked with 7 µg/mL polyclonal donkey anti-mouse IgG (Jackson Immuno Research, West Grove, PA, 715-007-003) plus 1% (vol/vol) bovine serum albumin (BSA) (Sigma Aldrich) in PBS for 45 min. Coverslips were washed with PBS and incubated for 1 h with a mixture of mouse monoclonal IgG2b anti- TLR4 (Abcam ab22048, 1:500) and rabbit polyclonal IgG anti- EEA1 (Abcam – ab2900, 1:500), (diluted in PBS containing 1% BSA). Cells were then washed 5 X 5 min in PBS, and then incubated with a mixture of Goat anti-mouse IgG2b conjugated with Alexa Fluor 647 (Invitrogen, Thermo Fisher Scientific Inc - A-21242, 1:1000), Goat anti-rabbit IgG conjugated with Alexa Fluor 488 (Invitrogen, Thermo Fisher Scientific Inc, A-11008, 1:1000) as secondary antibodies and, Alexa Fluor 594 conjugated streptavidin (Invitrogen, Thermo Fisher Scientific Inc, S32356, 1:1000). Finally, cells were washed 10 X 5 min in PBS, rinsed quickly with ultrapure water (Milli-Q, Merck Millipore, Watford WD), and mounted with Fluoromount G (Electron Microscopy Sciences, Hatfield, PA). Cells incubated without primary antibody were used as controls, and were all negative. Cells were analyzed using a conventional Olympus BX50 fluorescence microscope (Olympus, Waltham, MA), and a Leica TCS SP5 confocal microscope (Leica Microsystems, Wetzlar). The images were obtained by a

sequential acquisition of the three fluorophores to avoid crosstalk/overlap. Colocalization studies were performed in serial cuts (Z axis) of 0.17 µm each, followed by calculation of Manders coefficients. Coefficients of colocalization tM1/tM2 were calculated using FIJI software (33) and the Colocalization Threshold Plug-in developed by Tony Collins (Wright Cell Imaging Facility, Toronto, Canada). These coefficients vary from 0 to 1, corresponding to a lack of correlation and a perfect correlation, respectively. tM1 is the number of pixels (above the background) in the green channel that overlaps the pixels (above the background) in the red channel. tM2 is the number of pixels (above the background) in the red channel that overlaps the pixels (above the background) in the green channel. For immunostaining analysis of MIC1 and MIC4, the red channel was used, and for the TLR4 and EEA-1 markers, the green channel was used. Trough LUT (Look-up Table, FIJI/ImageJ) Magenta was chosen as pseudo-color for TLR4, for better visualization.

Western Blotting Analysis

To evaluate p38 and IRF3 phosphorylation, 1×10^7 BMDMs were stimulated with MIC1, MIC4, LPS, or medium for the indicated periods of time. Cells were lysed in a buffer containing 100 mM NaCl, 20 mM Tris (pH 7.6), 10 mM EDTA (pH 8), 0.5% SDS, 1% Triton X-100, and a protease inhibitor cocktail (Sigma-Aldrich). Cells were immediately transferred into liquid nitrogen, and stored at -80°C. Laemmli sample buffer was added to lysates, and samples were boiled for 10 min. Proteins were separated by SDS-PAGE on 10% (vol/vol) polyacrylamide resolving gels and transferred to nitrocellulose membranes. The membranes were blocked for 16 h at 4°C in PBS containing 0.05% (vol/vol) de Tween-20 (Sigma Aldrich) and 3% (vol/vol) BSA (Sigma Aldrich), and were then incubated for 1 h at room temperature with primary antibodies: anti-phospho-p38 MAPK (Thr180/Tyr182, 28B10, 1:100; Cell Signaling Technology, Danvers, MA -9216), anti-p38 MAPK (1:1000; Cell Signaling-9212), anti-phospho-IRF3 (Ser396 - 4D4G; 1:1000; Cell Signaling-4947), anti-IRF3 (D83B9; 1:1000; Cell Signaling-4302), and anti-β-actin (1:1000; Santa Cruz Biotechnology Santa Cruz, CA -4778) for a loading control. The same nitrocellulose membrane was then subjected to secondary probing anti-mouse IgG-HRP (1:2000) or anti-rabbit HRP (1:2000) (Invitrogen) for 30 min. The membranes were developed using chemiluminescence (0.1M Tris-HCl pH 8.5, 2.5 mM de luminol, 0.9 mM p-coumaric acid e 1% de hydrogen peroxide solution). For stripping, the immunoblot was immersed in mild stripping buffer (15 g glycine, 1 g SDS, 10 mL Tween 20 in 1000 mL distilled water. pH 2.2), incubated at room temperature for 10 min and the immunoblot was repeat as described. The chemiluminescence detection was performed using ChemiDoc Imaging Systems (Bio-Rad Laboratories).

ELISA

TNF-α, IL-10 (OptEIA set; BD Biosciences, San Jose, CA), and IFN-β (R&D Systems, Minneapolis, MN) concentrations in cell culture supernatants were determined by ELISA in accordance with the manufacturer's instructions. Standard curves generated from serial dilution of a provided set of recombinant cytokines were used to determine the respective cytokine concentrations in the supernatant samples. Absorbance at 450 nm was measured using a Power Wave-X spectrophotometer (BioTek Instruments, Inc.).

Quantitative Real-Time PCR

BMDMs (2×10^7) were stimulated for 5 h with MIC1, MIC4, LPS, or medium only. RNA was extracted using Trizol Reagent (Invitrogen) and purified using the Direct-zol RNA MiniPrep Plus Kit (Zymo Research, Irvine, CA) according to the manufacturer's instructions. cDNA was synthesized from 1.5 µg of RNA using SuperScript Reverse Transcriptase (Invitrogen) according to the manufacturer's instructions. Quantitative real-time PCR was performed using Power SYBR Green (Applied Biosystems, Thermo Fisher Scientific Inc.) on a 7500 Real-Time PCR thermocycler (Applied Biosystems). Relative expression of transcripts was quantified using the ΔΔCt method, and *β-actin* was used as an endogenous control. The following primers were used for quantification: *β-actin* F: 5'-GATGCAGAAGGAGATCACAGCC-3' and *β-actin* R: 5'-ACA ATGAGGCCAGAATGGAGC-3'; *Il-10* F: 5'-GCTCTTACTGA CTGGCATGAG-3' and *Il-10* R: 5'-CGCAGCTCTAGGAGC ATGTG-3'; *Cxcl10* F: 5'-TTTACCCAGTGGATGGCTAGTC-3' and *Cxcl10* R: 5'-GCTTGACCATCATCCTGCA-3; *Tnf-α* F: 5'-GACGTGGAACTGGCAGAAGAG-3' and *Tnf-α* R: 5'-GCCAC AAGCAGGAATGAGAAG-3'; and *Ifn-β* F: 5'-GCACTGGGTG GAATGAGACT-3' and *Ifn-β* R: 5'AGTGGAGAGCAGTTG AGGACA-3'.

Statistical Analysis

Statistical analyses were performed by one-way ANOVA followed by Bonferroni's post-test, or two-way ANOVA followed by Tukey's post-test, as indicated. Analyses were performed using GraphPad Prism software version 8 (GraphPad, La Jolla, CA). Differences were considered significant when P values were <0.05.

RESULTS

MIC1 and MIC4 Colocalize With Early Endosomes After Interacting With TLR4

As previously demonstrated, *T. gondii* lectins MIC1 and MIC4 interact physically with TLR4 N-glycans on the surface of mononuclear phagocytes (19). We thus investigated the localization of the complexes following their initial contact. Using an immunofluorescence plate assay, we first detected TLR4 on the surface of vehicle control treated and MIC1, MIC4, or LPS stimulated bone marrow-derived macrophages (BMDMs). There was a significant decay in the presence of cell surface TLR4 over time, which was fastest on MIC1-stimulated cells, followed by similar rates on MIC4- and LPS-stimulated cells (**Figure 1A**).

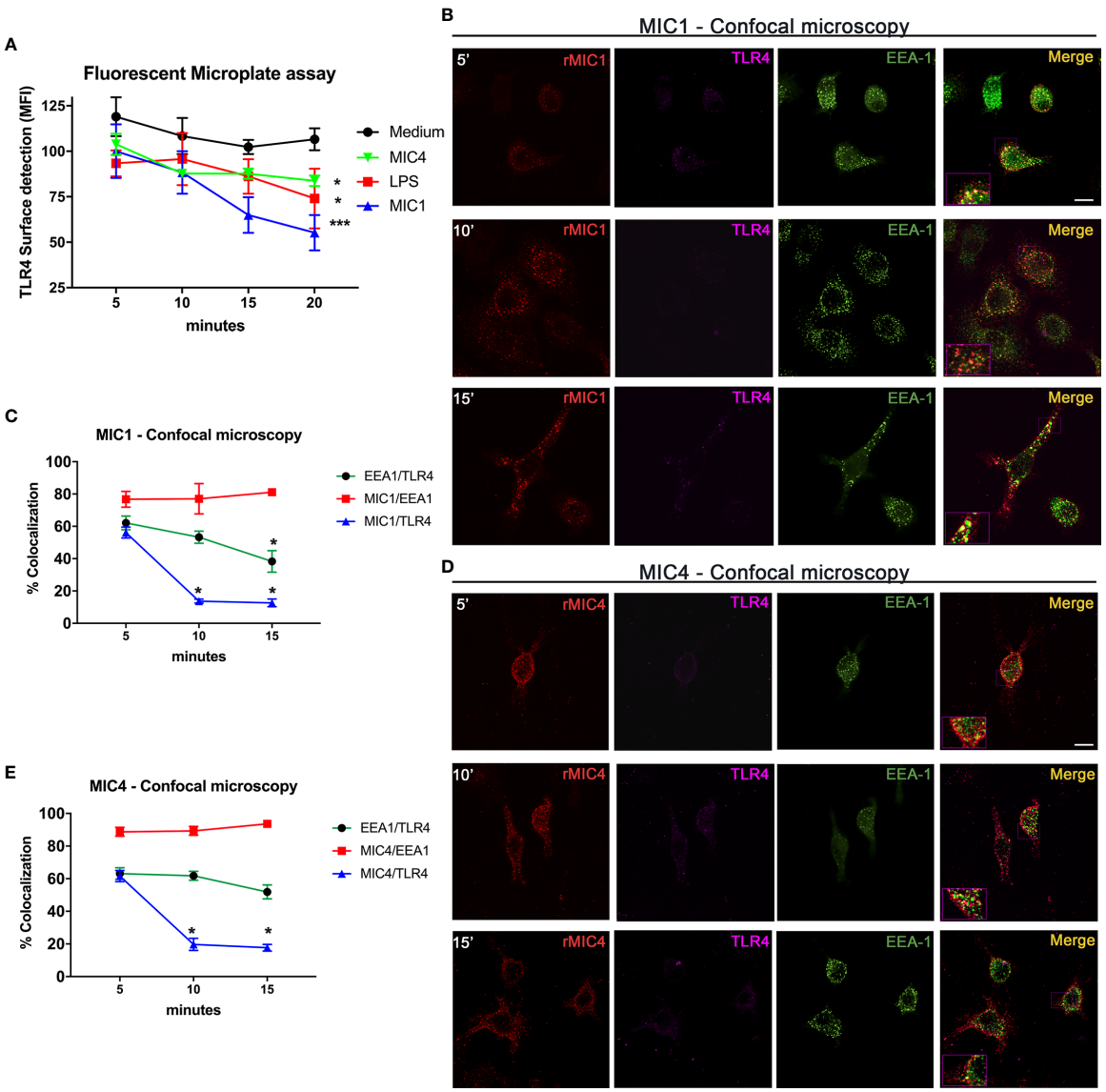

FIGURE 1 | MIC1 and MIC4 colocalize with early endosomes concurrent with TLR4 downregulation on the cell surface. **(A)** BMDMs were stimulated with medium only, LPS, MIC1, or MIC4 for the indicated periods. After fixing, cells were blocked (Fcblock) and stained with anti-TLR4 antibodies. Cell surface TLR4 was quantified using an FLx800 Fluorescence Microplate Reader (BioTek Instruments, USA; excitation 485 nm, emission 528 nm). Results were expressed as MFI + SD. *$p < 0.05$ and *** $p < 0.001$ (One-way ANOVA and Bonferroni post-test). For confocal microscopy, BMDMs were incubated with biotin-MIC1 or with biotin-MIC4 for 5, 10, or 15 min **(B, D)**. After fixing and permeabilization, cells were immunostained with anti-TLR4 (Alexa-647, pseudo-color -LUT magenta), or anti-EEA-1 (Alexa-488, green). Biotinylated lectins were detected by reaction with fluorescent streptavidin (Alexa-594, red). Merge = yellow. Bar = 10 µM. Insets: 2.5-fold increased magnification. **(C, E)** Percentages of colocalization of MIC1 or MIC4 with EEA-1 (red line) or TLR4 (blue line) were determined at 5, 10, and 15 min after stimulation. Additionally, the percentage of EEA1 colocalization with TLR4 was determined (green line) for both MIC1 and MC4 stimulation at the same time points. Results were obtained by calculating the Manders Colocalization Coefficient (MCC) and expressed as averages + SD. Representative data from experiments performed in triplicate. *$p < 0.05$ (one-way ANOVA and Bonferroni post-test).

To measure internalization of microneme protein/TLR4 complexes putatively formed on the cell surface, we performed quantitative analysis of complex component colocalization by confocal microscopy of BMDMs stimulated with biotinylated MIC1 or MIC4 for 5, 10, and 15 min. The colocalization profiles of MIC1 and MIC4 with TLR4 were similar, as shown in **Figures 1B, D**. Five minutes after stimulation, high colocalization with TLR4 was observed for MIC1 (55.2%, **Figures 1B, C**) and MIC4 (61.6% **Figures 1D, E**). These proportions decreased rapidly and significantly after longer time points: MIC1 colocalization with TLR4 was 13.7% at 10 min and 12.6% at 15 min after stimulation (**Figure 1C**). At the same time points, MIC4/TLR4 colocalization

was 19.7% and 17.6% (**Figure 1E**). MIC1 and MIC4 displayed a punctate distribution throughout the cytoplasm and within various subcellular compartments, but primarily in regions cortical to the cell membrane, in a pattern that suggested endosomal encapsulation (**Figures 1B, D**). We evaluated MIC1 and MIC4 colocalization with endosomes in microneme protein-stimulated BMDMs. As expected, we did not observe colocalization of MIC1 or MIC4 with EEA1 immediately after stimulation (time zero, not shown). At 5 min, we observed approximately 80% colocalization of each MIC with EEA1. MIC1 and MIC4 maintained high-level colocalization with EEA1 for the remainder of the experimental period (**Figures 1C, E**).

We next examined TLR4 colocalization with EEA-1 in MIC1- or MIC4-stimulated BMDMs. We found 60% colocalization between TLR4 and EEA-1 at 5 min post-stimulation (**Figures 1C, E**). This proportion decayed significantly to 38.2% by 15 min after the MIC1-stimulus (**Figure 1C**) but was maintained at higher than 50% over time in MIC4-stimulated BMDMs (**Figure 1E**).

We conclude that microneme protein/TLR4 complexes are found early and for a brief period within stimulated cells, colocalized inside early endosomes. Although they remain within endosomes longer, MIC1 and MIC4 segregate quickly from TLR4, and are then cleared slowly and progressively from the endosome.

TLR4 Endocytosis Is Critical for IL-10 Release From MIC1- and MIC4-Stimulated BMDMs

We have previously verified that interaction between MIC1 or MIC4 and TLR4 induces mononuclear phagocytes to release cytokines (19, 20). Herein, we showed that both MICs induce TLR4 uptake from the BMDM surface, followed by colocalization with EEA1. To evaluate the impact of TLR4 internalization on cytokine release by microneme-protein-stimulated BMDMs, we blocked their endocytic pathway with Dynasore, a dynamin inhibitor.

We evaluated the impact of endocytic pathway blockade on different intracellular signaling pathways in BMDMs untreated with MICs. The impact was indirectly assessed by quantitating *Cxcl10* (dependent on JAK/STAT1), *Tnf-α* (dependent on MyD88/NF-κB), and *Il-10* (dependent on IRF3/AKT) mRNA levels. Pretreatment with Dynasore did not affect *Cxcl10* mRNA levels in MIC1-, MIC4-, or LPS-stimulated BMDMs (**Figure 2A**). While *Tnf-α* mRNA levels increased with blockade of endocytosis in MIC-stimulated BMDMs after endocytosis blockage (**Figure 2B**), *Il-10* mRNA levels decreased significantly. Maximal reduction was observed in MIC1-stimulated cells (**Figure 2C**). Upon identify a possible modulation of *Il-10* and *Tnf-α* through the qPCR assay, we also proceeded to the investigation of effect of blocking endocytosis on protein levels of these cytokines released by BMDMs. We confirmed our previous finding that MIC1 and MIC4, similar to LPS, induce increased release of pro-inflammatory TNF-α and anti-inflammatory IL-10 (**Figures 2D, E**, blue bars). Distinct from what was observed in the qPCR results, the pretreatment with Dynasore mildly antagonized MIC induction of TNF-α release (**Figure 2D**, red bars). On the other hand, corroborating with qPCR results, Dynasore treatment effectively quenched IL-10 release by MIC1-, MIC4-, and LPS-stimulated BMDMs (**Figure 2E**, red bars).

We also assayed BMDMs obtained from TLR2-/-, CD14-/-, and TLR4-/- mice. Stimulation of TLR2-/- BMDMs with MICs induced production of TNF-α and IL-10 (**Figures 2F, G**, blue bars) at levels close to those produced by WT BMDMs; in both cell types, levels were typically superior to those released by unstimulated cells (medium). This observation indicates that TLR2 is not critical for microneme protein-induced signaling resulting in TNF-α or IL-10 production. CD14-/- BMDMs produced levels of TNF-α similar to levels produced by WT BMDMs (**Figure 2H**), but reduced levels of IL-10 (**Figure 2I**) in response to MIC1 and MIC4. In the absence of TLR4, BMDMs' release of IL-10 and TNF-α became unresponsive to MIC exposure (**Figures 2G, H**). Of note, there was a significant production of TNF-α by TLR4-/- and CD14-/- BMDMs in response to LPS (**Figures 2H, J**). The LPS used in this study was not an ultrapure LPS, thus traces of TLR2-agonist might be triggering proinflammatory cytokine release. BMDMs of all assayed phenotypes produced no IL-10 in response to MIC1, MIC4, or LPS when pretreated with Dynasore (**Figures 2E, G, I, K**), while TNF-α levels were mostly preserved.

Taken together, the results presented in this section reveal that TLR4 endocytosis plays a crucial role in MIC1 or MIC4 induced IL-10 production. Absence of TLR4, or blockade of endocytosis in BMDMs completely quenches IL-10 production.

MIC1 or MIC4 Stimulation Prompts TLR4/CD14-Dependent IRF3 Phosphorylation

LPS stimulation of innate immune cells initiates TLR4 internalization, TRIF activation, and IRF3 phosphorylation. In addition to other effects, IRF3 phosphorylation results in IFN-β and IL-10 secretion (34). Under assayed conditions, we did not verify IFN-β release by BMDMs in response to MICs (**Figure S1**). Because MIC1- or MIC4-stimulated BMDMs vigorously released IL-10 (**Figure 2**), we evaluated whether cell stimulation with MIC1 or MIC4 is implicated in IRF3 phosphorylation.

As expected, stimulation with MIC1 or MIC4 together with LPS activated p38 phosphorylation independently of the background of the assayed BMDMs, as demonstrated by western blotting (**Figure 3**). This finding is consistent with the high TNF-α concentrations we detected by ELISA (**Figures 2D, F, H, J**) under similar experimental conditions. MIC-induced IRF3 phosphorylation occurred only in WT and TLR2-/- BMDMs (**Figures 3A, C**), similar to our observations regarding IL-10 production (**Figures 2E, G**). Stimulation with MICs did not induce IRF3 phosphorylation or IL-10 production in BMDMs lacking CD14 or TLR4 (**Figures 3B, D**). The shared CD14 and TLR4 dependence of these events reinforces our initial

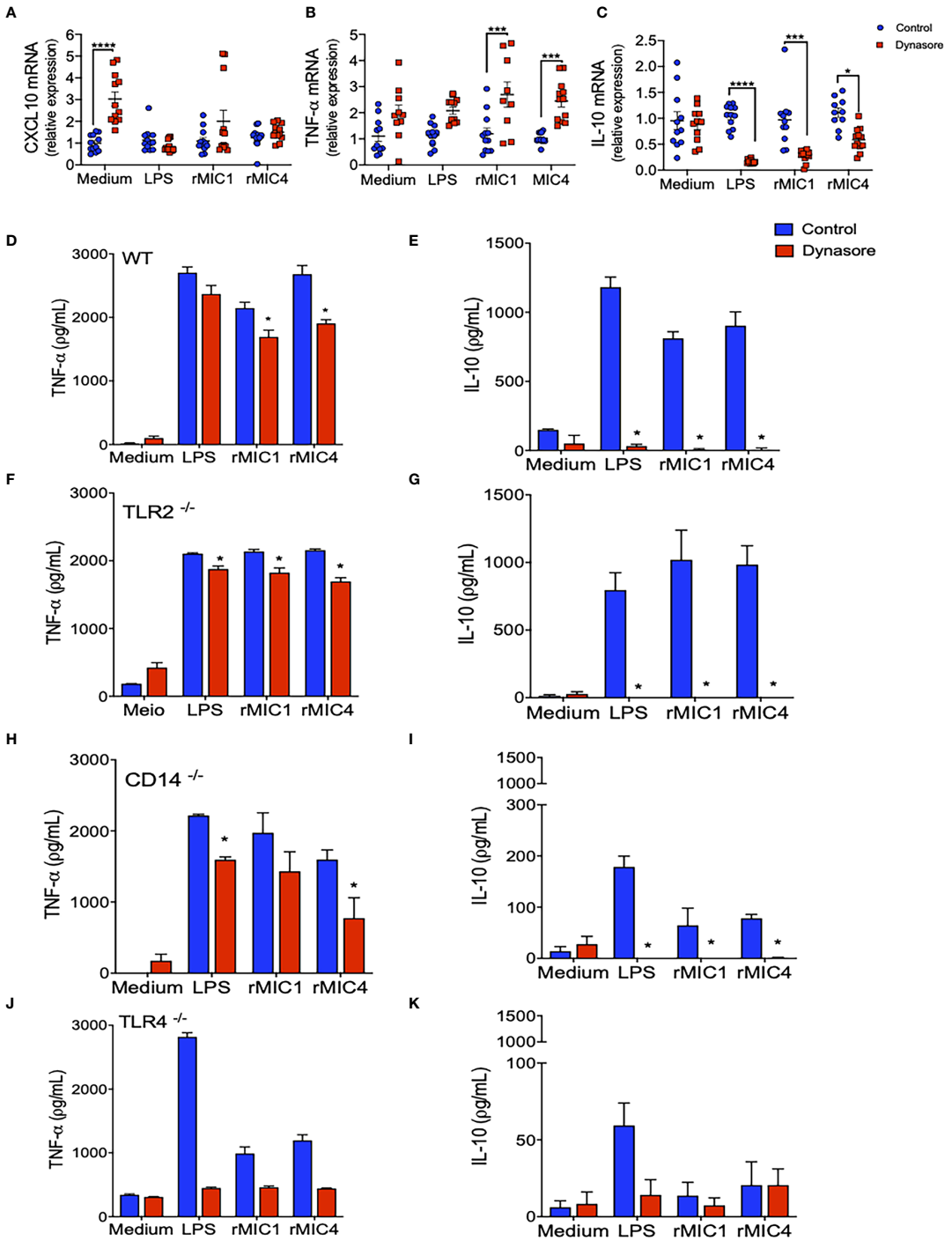

FIGURE 2 | IL-10 production by MIC1- or MIC4-stimulated BMDMs requires TLR4 and a functional endocytic pathway. **(A–C)** WT BMDMs pretreated (red squares) or not (control - blue circles) with Dynasore were stimulated with Medium only, LPS, MIC1, or MIC4 for 5 h. Extracted RNA was reverse transcribed into cDNA, and expression of *Cxcl10* **(A)**, *Tnf-α* **(B)**, and *Il-10* **(C)** was analyzed by real-time PCR. Relative expression was determined as described in "Materials and Methods," and results obtained under Dynasore treatment were compared with control conditions under the same stimulation. Results are expressed as averages + SD of four experiments, each performed in triplicate. Statistical analysis was done by two-way ANOVA followed by Tukey's test (* = $p < 0.05$, *** = $p < 0.001$, **** = $p < 0.0001$). BMDMs from WT **(D, E)**, TLR2$^{-/-}$ **(F, G)**, CD14$^{-/-}$ **(H, I)**, and TLR4$^{-/-}$ **(J, K)** mice were pretreated (red bars) or not (control - blue bars) with Dynasore and then stimulated with medium only, LPS, MIC1, or MIC4. After 24 h, cell supernatants were analyzed by ELISA for TNF-α **(D, F, H, J)** and IL-10 **(E, G, I, K)** levels. Results are expressed as averages + SD of three independent experiments, each performed in triplicate. Statistical analysis was done by two-way ANOVA followed by Tukey's test (* = $p < 0.05$ in comparison with control under same stimulation).

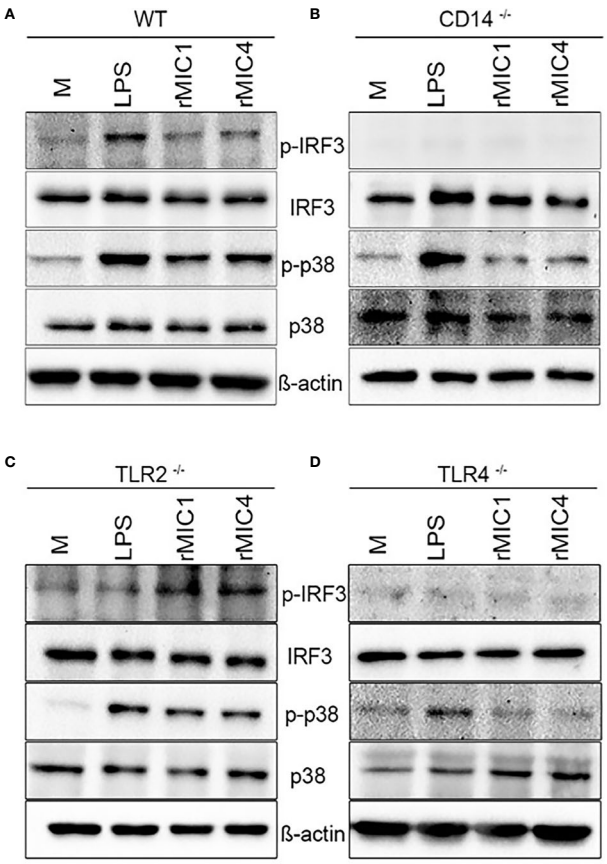

FIGURE 3 | IRF3 phosphorylation in MIC1- or MIC4-stimulated BMDMs depends on CD14 and TLR4. IRF3 and P38 phosphorylation were assessed by western blotting of lysates of WT **(A)**, CD14$^{-/-}$ **(B)**, TLR2$^{-/-}$ **(C)**, and TLR4$^{-/-}$ **(D)** BMDMs, which had been stimulated with medium only (M), LPS, MIC1, or MIC4 for 30 min. Antibodies against phosphorylated and unphosphorylated IRF3 and P38 were used; anti-β-actin was used as a loading control.

hypothesis of an association between these two events (IL-10 production and IRF3 phosphorylation) (**Figures 2I, K**) in MIC1- or MIC4-stimulated cells. BMDM stimulation with MICs triggers IRF3 phosphorylation in a TLR4-and CD14 dependent manner, as does LPS.

Toxoplasma gondii-Infected BMDMs Produce IL-10 in a TLR4 and Endocytosis-Dependent Manner

MIC1 and MIC4 are carbohydrate-binding proteins released by *T. gondii* in the initial steps of host cell invasion. Herein, we have shown that IL-10 production is an early response of host cells to the contact with MICs, mediated by their interaction with TLR4. To apply our observations to a more realistic infection scenario, we quantified levels of cytokines released by BMDMs when incubated with live parasites instead of with recombinant MIC1 or MIC4.

Increased TNF-α and IL-10 production followed *in vitro* infection of BMDMs with whole parasites (**Figures 4A, B**, blue bars). Blockade of the BMDMs endocytic pathway slightly decreased TNF-α secretion, but completely abolished parasite induced IL-10 release (**Figures 4A, B**, red bars). When TLR4-/- BMDMs were infected *in vitro* with the parasite, they barely released IL-10 (**Figure 4D**), but they kept producing TNF-α (**Figure 4C**), in levels even greater than the ones detected in WT BMDMs.

Remarkably, the results we obtained using host cells infected *in vitro* with whole living parasites reproduced those obtained by stimulating cells with recombinant MIC1 or MIC4 (**Figures 2D, E**). This indicates that MIC1 and MIC4 contribute to the early IL-10 production observed *in vivo*, which is an essential component of the host defense. Our observations demonstrate the importance of the endocytic pathway, and dependence on TLR4 for IL-10 secretion by *T. gondii* parasitized host cells.

Endotoxin Tolerance Is Stimulated in BMDMs by MIC1 or MIC4

Exposure of mononuclear phagocytes to LPS induces transient hyporesponsiveness to subsequent LPS stimulus, a state known as endotoxin tolerance (35–37). Its hallmark is the attenuation of TLR4-dependent signaling due to independent mechanisms: TLR4 internalization, and decreased expression of TRIF-dependent genes (38). We found that MIC1 and MIC4 induce IRF3 phosphorylation (**Figure 3**) *via* a cell signaling pathway mediated by TLR4 internalization. To investigate whether MIC mediated TLR4 endocytosis leads to endotoxin tolerance, we first stimulated BMDMs with MIC1, MIC4, or LPS. After 18 h, cells were washed and restimulated for 24 h with LPS.

As expected, we showed that mock-tolerized macrophages ("stimulated" with medium only) produced high concentrations of both TNF-α and IL-10 in response to "restimulation" with MIC1, MIC4, or LPS (**Figures 5A, B**, colored bars compared to Med/Med). We confirmed that in response to LPS restimulation, LPS-stimulated macrophages (LPS/LPS) released 11-fold lower TNF-α levels than mock-tolerized BMDMs (**Figure 5A**, Med/LPS - orange bar). In addition, MIC1- or MIC4-stimulated BMDMs produced 5- and 8-fold lower TNF-α levels, respectively, than mock-tolerized BMDMs when restimulated with LPS (**Figure 5A**). Cells stimulated and restimulated with pairs of MICs (MIC1/MIC1, MIC4/MIC4, MIC1/MIC4, or MIC4/MIC1) allowed us to conclude that homo-and hetero-tolerance to MIC1 and MIC4 have occurred. In these cases, tolerance was manifested by abolishment of TNF-α production, whereas IL-10 levels were mostly preserved (**Table S1**).

Figure 5B shows that cells that were restimulated with LPS after initial stimulation with LPS (LPS/LPS), MIC1 (MIC1/LPS), or MIC4 (MIC4/LPS) displayed diminished IL-10 production compared to mock-tolerized macrophages (Med/LPS - orange bar). IL-10 production in response to LPS restimulation was twice as high in macrophages exposed first to MIC1, and 1.5 fold higher in MIC4-exposed macrophages than in LPS-tolerized cells (**Figure 5B**).

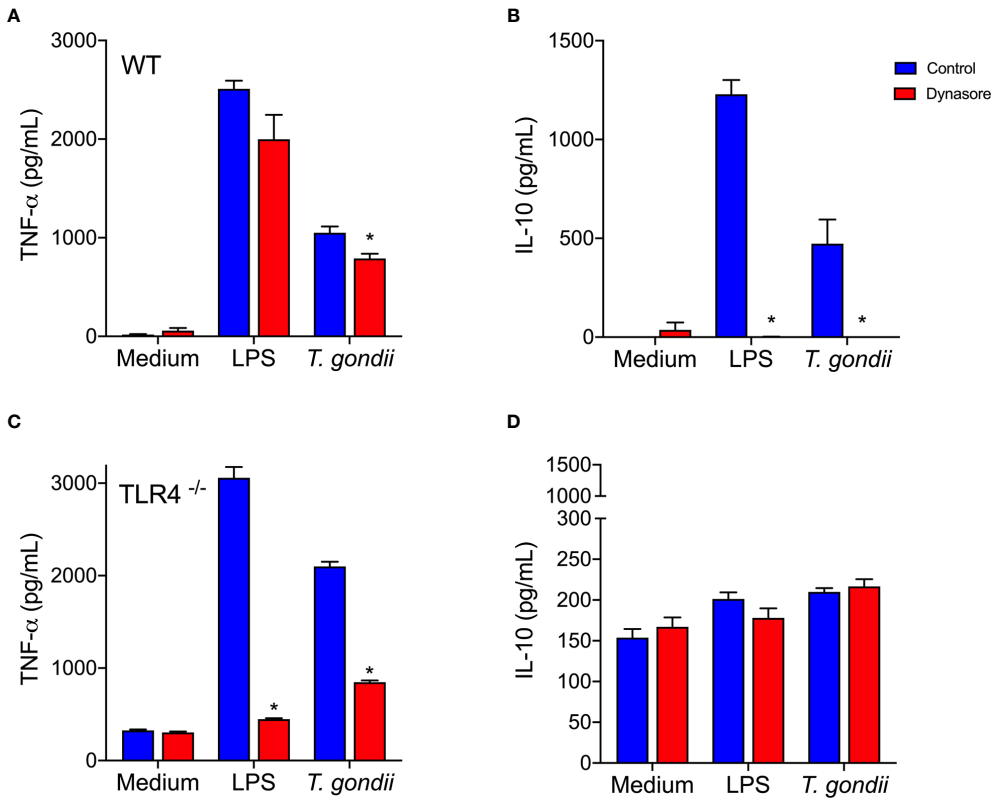

FIGURE 4 | *Toxoplasma gondii*-infected BMDMs produce IL-10 *via* a TLR4 and endocytosis dependent mechanism. WT **(A, B)** and TLR4$^{-/-}$ **(C, D)** BMDMs were pretreated (red bars) or not (control - blue bars) with Dynasore, then stimulated with Medium only or LPS, or infected with *T. gondii* (at a ratio of 3 parasites/BMDM). After 24 h, cell supernatants were analyzed for TNF-α **(A, C)** and IL-10 **(B, D)** levels. Results are expressed as averages + SD of two independent experiments, each performed in triplicate. Two-way ANOVA followed by Tukey's test was performed (* = $p < 0.05$ in comparison with control under same stimulation/infection).

Our results suggest that MIC1 and MIC4 induce cell tolerance to endotoxin, manifested by reduced TNF-α production in response to LPS challenge. This observation, together with the high IL-10 release by MIC1- or MIC4-tolerized BMDMs indicates that tolerized cells are rendered, at least temporarily, anti-inflammatory.

DISCUSSION

This study reports that the *T. gondii* lectins, MIC1 and MIC4, in addition to inducing proinflammatory cytokine release by macrophages, as previously reported (19, 20), stimulate IL-10 production in a TLR4-endocytosis dependent manner. The ability of MIC1 and MIC4 to cause the release of pro-inflammatory cytokines following activation of innate immune cells is attributed to signaling pathways that involve MYD88, TAK-1, and NF-κB nuclear translocation (20). Nonetheless, the mechanisms by which MIC1 and MIC4 induce the anti-inflammatory cytokine IL-10 (19) have not yet been elucidated.

Consistent literature indicates that TLR2 agonists induce IL-10 production by antigen-presenting cells (APCs) (39–41). However, we verified that TLR2-deficient BMDMs produce significant IL-10 levels in response to MIC stimulation (**Figure 2G**), indicating that TLR2 is not crucial for induction of IL-10 release. Indeed, the TLR activation-dependent IL-10-release may change in the different immune cell types. Macrophages and myeloid dendritic cells (DCs), but not plasmacytoid DCs, produce IL-10 in response to TLR activation, with macrophages being the higher producers (42). As reviewed by Saraiva and O'Garra (43), optimal IL-10 production induced by LPS, a classical TLR4 agonist, requires activation of both TRIF- and MYD88-dependent pathways (43). By assaying BMDMs that were pretreated with the dynamin inhibitor Dynasore, we showed that MIC1 and MIC4's ability to induce an anti-inflammatory response requires the integrity of the endocytic pathway. Thus, by interacting with TLR2- and TLR4-associated N-glycans on cell surfaces (19), MIC1 and MIC4 prompt the release of pro-inflammatory cytokines, even by Dynasore-conditioned cells (**Figure 2D**). IL-10 release additionally requires TLR4 endocytosis by MIC1- or MIC4-stimulated macrophages (**Figures 2E** and **6**).

TLR4 endocytosis in response to LPS activates the TRIF-TRAM pathway, leading to IRF3 phosphorylation. This

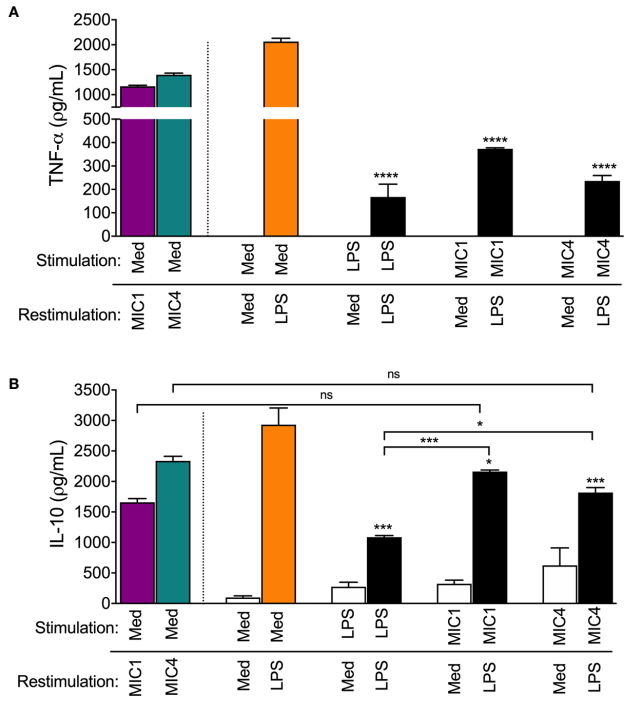

FIGURE 5 | MIC1 and MIC4 induced LPS tolerance in BMDMs. BMDMs were stimulated with Medium only (Med), LPS, MIC1, or MIC4. After 18 h, cells were washed and restimulated for an additional 24 h with medium or LPS. Cell supernatants were assessed for TNF-α **(A)** and IL-10 **(B)** concentrations. Mock-stimulated cells (Med) restimulated with MIC1 or MIC4 (purple and green bars) were used as controls. Results are expressed as averages + SD of three independent experiments, each performed in triplicate. Statistical analysis was performed by two-way ANOVA followed by Tukey's test. * = $p < 0.05$, *** = $p < 0.001$ and **** = $p < 0.0001$, in comparison with cells stimulated with Med and restimulated with LPS (orange bars), or as indicated.

endosomal TLR4 signaling frequently results in IFN-β and CXCL-10 secretion, and negatively regulates inflammation *via* a mechanism referred to as "tolerance" (38). Besides, the up-regulation of type I IFN was shown to enhance the BMDMs release of IL-10 after LPS stimulation (44). Similar to LPS, MIC1 and MIC4 induce TLR4 endocytosis followed by IRF3 phosphorylation (**Figures 1** and **3**). However, their activity diverges from that of LPS in that MIC1 and MIC4 do not cause IFN-β release, as does LPS (**Figure S1**). In addition to IFN-β secretion, IL-10 release was also reported to result from TLR4 endocytosis, *via* a mechanism dependent on the p110δ isoform of the kinase PI(3)K (45). If IL-10 production induced by MIC1 and MIC4 is also dependent in the p110δ isoform of the kinase PI(3)K is still to be investigated. Remarkably, IL-10 secretion induced by LPS, MIC1, and MIC4 is entirely dependent on endocytic pathway integrity, as well as on the presence of TLR4 and CD14 (**Figure 2**).

Although the mechanisms by which MIC1 and MIC4 induce proinflammatory cytokine release have already been explored, questions remain on this issue. For instance, why would *T. gondii* stimulate host cells to mount a potentially lethal response to itself? Indeed, *T. gondii* infections that result in high production of proinflammatory cytokines, including IL-12, TNF, and IFN-γ ultimately control the parasite. Nonetheless, a proinflammatory cytokine storm that would presumably follow *T. gondii* infection does not occur, because it is downregulated by high IL-10 release (46). Therefore, IL-10 is critical for establishing a chronic toxoplasmosis phase, associated with formation of *T. gondii* type II strains (47). Consistently, even when infected with avirulent Type II parasites, IL-10-deficient mice overproduce IFN-γ, TNF-α, and IL-12, leading to exacerbated inflammation, tissue injury, and premature death (29).

To our knowledge, this is the first report describing how *T. gondii* components can induce release of the anti-inflammatory cytokine, IL-10. We therefore highlight two directions in need of further investigation. Firstly, the fact that MIC1- and MIC4-stimulated BMDMs are temporarily LPS-tolerized (**Figure 5**) provides a possible mechanism for evasion of the host inflammatory response by *T. gondii*. Because we already know that MIC1 and MIC4 act on host cells through their carbohydrate recognition domains (CRDs) (19), we hypothesize that during evolution there was a selection for parasites expressing lectin components, favoring host-parasite coexistence. During early infection stage, the balance between inflammatory and anti-inflammatory cytokines produced by the host is controlled, at least partially, by the parasites themselves. During early stages of infection, inflammatory mediators induced by ingested *T. gondii* components activate neutrophil migration, attracting motile parasite reservoirs, whose retrograde transit then spreads *T. gondii* throughout the small intestine (48). Induction of inflammatory mediators thus allows parasites access to different host tissues during early stages of infection. Subsequently, the production of anti-inflammatory mediators can fine-tune host-parasite coexistence during establishment of chronic toxoplasmosis (29, 46, 47). The second aspect to be considered concerns the potential application of recombinant forms of these MICs in immunotherapy against *T. gondii* infection. Administration of either MIC1 or MIC4 confers protection against experimental murine toxoplasmosis, mediated by the Th1 immune response (49). Because MIC1 and MIC4 also induce the anti-inflammatory cytokine IL-10, they are strong candidates for safe vaccines and immunomodulatory agents.

In summary, this study shows that TLR4 but not TLR2 is crucial for IL-10 release induced by the lectins MIC1 and MIC4 from *T. gondii*. Shortly after interacting with TLR4 on BMDMs surface, these lectins are found colocalized with early endosomes. It was also shown that the block of the endocytic pathway strongly impairs the IL-10 secretion while it barely compromises TNF-α release in the cells stimulated with MIC1 and MIC4, suggesting an impairment in endosomal TLR4 signaling pathways, but not the TLR4 signaling triggered on the cell surface. To illustrate the main findings in this study, we propose a graphical model showing the mechanism through which TLR4 endocytosis induced by MIC1 and MIC4 is triggering IRF3 phosphorylation and then IL-10 secretion by BMDMs (**Figure 6**). Lastly, we present evidence

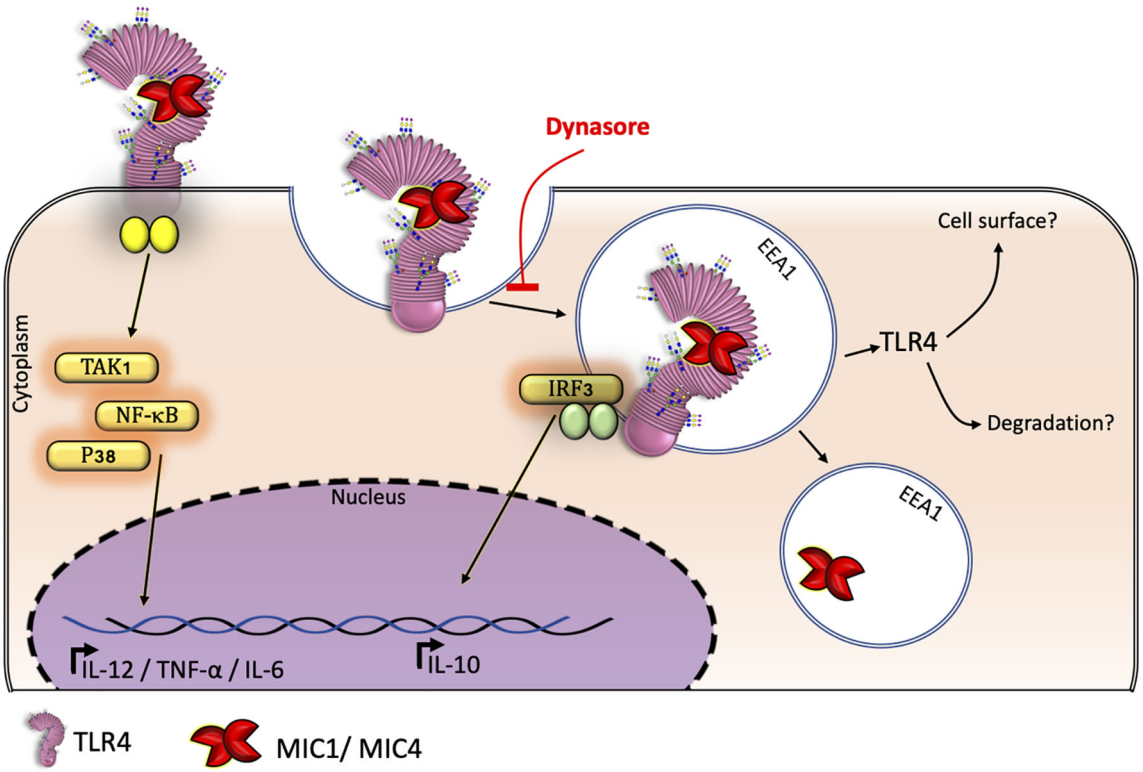

FIGURE 6 | *Tg*MIC1 and *Tg*MIC4 drive TL4 into endosomes inducing BMDM-IL-10 release: a model. BMDMs produce the anti-inflammatory cytokine IL-10 in response to MIC 1 and MIC4 depending on TLR4 internalization from the cell surface. Macrophages subjected to blockage of endocytosis by Dynasore continued to release the proinflammatory cytokine TNF-α but failed to produce IL-10 in response to MIC1 or MIC4 exposure.

suggesting that MIC1 and MIC4, likewise LPS itself, induce BMDMs tolerance to endotoxin.

DATA AVAILABILITY STATEMENT

The original contributions presented in the study are included in the article/**Supplementary Material**. Further inquiries can be directed to the corresponding author.

ETHICS STATEMENT

The animal study was reviewed and approved by Ethics Committee on Animal Experimentation and Research of the Ribeirão Preto Medical School (FMRP) (protocol number 191/2017).

AUTHOR CONTRIBUTIONS

Conceptualization: RR-A, FM-N, MR-B. Experimental design: RR-A, FM-N. Data curation: RR-A, FM-N, AS, JAD. Formal analysis: RR-A, FM-N, AS. Investigation: RR-A, FM-N, AS, JAD. Methodology: RR-A, FM-N, AS, JAD. Project administration: RR-A, FM-N, MR-B. Validation: RR-A, FM-N. Visualization: RR-A, FM-N. Funding acquisition: MR-B. Resources: MR-B. Supervision: MR-B. Writing—original draft. RR-A. Writing—review and editing: RR-A, MR-B. All authors contributed to the article and approved the submitted version.

FUNDING

This study was supported by grants from Conselho Nacional de Desenvolvimento Científico e Tecnológico (CNPq - grant 166166/2014 to AS) and Fundação de Amparo à Pesquisa do Estado de São Paulo (FAPESP - grants #2017/02998-0 to RR-A; #2014/13324-1 to FM-N; #2016/14657-0 to JAD; #2018/21708-5, #2016/10446-4, #2013/04088-0 to MR-B; and 2004/08868-0 to Laboratório Multiusuário de Microscopia Confocal – LMMC-FMRP-USP).

ACKNOWLEDGMENTS

A portion of the experiments described in this manuscript was performed in the Facilities of the Department of Molecular and Cell Biology and Pathogenic Bioagents of the Medical School of Ribeirao Preto. We are thankful to Tânia Defina for technical support with

qPCR experiments, and to Elizabete Rosa Milani for acquisition of confocal images. We are also thankful for the structure and reagents provided by Dr. Angela Kaysel Cruz and Dr. Larissa Dias da Cunha. For laboratory technical support, we thank Sandra Maria de Oliveira Thomaz and Patricia Vendrusculo.

SUPPLEMENTARY MATERIAL

The Supplementary Material for this article can be found online at: https://www.frontiersin.org/articles/10.3389/fimmu.2021.655371/full#supplementary-material

REFERENCES

1. Dubey JP. *Toxoplasmosis of Animals and Humans*. CRC Press (2016). doi: 10.1201/9781420092370.
2. Montoya JG, Liesenfeld O. Toxoplasmosis. *The Lancet* (2004) 363:1965–76. doi: 10.1016/S0140-6736(04)16412-X
3. Hill DE, Dubey JP. Toxoplasma gondii. In: YR Ortega, CR Sterling, editors. *Foodborne Parasites*. Cham: Springer International Publishing (2018) p. 119–38. doi: 10.1007/978-3-319-67664-7_6
4. Wreghitt TG, Joynson DHM. Toxoplasma infection in immunosuppressed (HIV-negative) patients. In: DHM Joynson, TGE Wreghitt, editors. *Toxoplasmosis: A Comprehensive Clinical Guide*. Cambridge University Press, Cambridge (2001) p. 178–92. doi: 10.1017/CBO9780511527005.008
5. Carruthers VB, Sibley LD. Sequential protein secretion from three distinct organelles of Toxoplasma gondii accompanies invasion of human fibroblasts. *Eur J Cell Biol* (1997) 73:114–23.
6. Hunter CA, Sibley LD. Modulation of innate immunity by Toxoplasma gondii virulence effectors. *Nat Rev Microbiol* (2012) 10:766–78. doi: 10.1038/nrmicro2858
7. Reiss M, Viebig N, Brecht S, Fourmaux MN, Soete M, Di Cristina M, et al. Identification and characterization of an escorter for two secretory adhesins in Toxoplasma gondii. *J Cell Biol* (2001) 153:563–78. doi: 10.1083/jcb.152.3.563
8. Xing M, Yang N, Jiang N, Wang D, Sang X, Feng Y, et al. A sialic acid-binding protein SABP1 of toxoplasma gondii mediates host cell attachment and invasion. *J Infect Dis* (2020) 222:126–35. doi: 10.1093/infdis/jiaa072
9. Buzoni-Gatel D, Werts C. Toxoplasma gondii and subversion of the immune system. *Trends Parasitol* (2006) 22(10):448–52. doi: 10.1016/j.pt.2006.08.002
10. Yarovinsky F, Zhang D, Andersen JF, Bannenberg GL, Serhan CN, Hayden MS, et al. Immunology: TLR11 activation of dendritic cells by a protozoan profilin-like protein. *Science (80)* (2005) 308(5728):1629. doi: 10.1126/science.1109893
11. Koblansky AA, Jankovic D, Oh H, Hieny S, Sungnak W, Mathur R, et al. Recognition of Profilin by Toll-like Receptor 12 Is Critical for Host Resistance to Toxoplasma gondii. *Immunity* (2013) 11:541–47. doi: 10.1016/j.immuni.2012.09.016
12. Yarovinsky F. Innate immunity to Toxoplasma gondii infection. *Nat Rev Immunol* (2014) 14:109–21. doi: 10.1038/nri3598
13. Debierre-Grockiego F, Campos MA, Azzouz N, Schmidt J, Bieker U, Resende MG, et al. Activation of TLR2 and TLR4 by Glycosylphosphatidylinositols Derived from Toxoplasma gondii. *J Immunol* (2007) 179(2):1129–37. doi: 10.4049/jimmunol.179.2.1129
14. Kang HK, Lee HY, Lee YN, Jo EJ, Kim JI, Aosai F, et al. Toxoplasma gondii-derived heat shock protein 70 stimulates the maturation of human monocyte-derived dendritic cells. *Biochem Biophys Res Commun* (2004) 322(3):899–904. doi: 10.1016/j.bbrc.2004.07.205
15. Braun L, Brenier-Pinchart MP, Yogavel M, Curt-Varesano A, Curt-Bertini RL, Hussain T, et al. A Toxoplasma dense granule protein, GRA24, modulates the early immune response to infection by promoting a direct and sustained host p38 MAPK activation. *J Exp Med* (2013) 210(10):2071–86. doi: 10.1084/jem.20130103
16. Mercer HL, Snyder LM, Doherty CM, Fox BA, Bzik DJ, Denkers EY. Toxoplasma gondii dense granule protein GRA24 drives MyD88-independent p38 MAPK activation, IL-12 production and induction of protective immunity. *PloS Pathog* (2020). doi: 10.1371/journal.ppat.1008572
17. Lourenço EV, Pereira SR, Faça VM, Coelho-Castelo AAM, Mineo JR, Roque-Barreira MC, et al. Toxoplasma gondii micronemal protein MIC1 is a lactose-binding lectin. *Glycobiology* (2001) 11:541–7. doi: 10.1093/glycob/11.7.541
18. Lourenço EV, Bernardes ES, Silva NM, Mineo JR, Panunto-Castelo A, Roque-Barreira MC. Immunization with MIC1 and MIC4 induces protective immunity against Toxoplasma gondii. *Microbes Infect* (2006) 8:1244–51. doi: 10.1016/j.micinf.2005.11.013
19. Sardinha-Silva A, Mendonça-Natividade FC, Pinzan CF, Lopes CD, Costa DL, Jacot D, et al. The lectin-specific activity of Toxoplasma gondii microneme proteins 1 and 4 binds Toll-like receptor 2 and 4 N-glycans to regulate innate immune priming. *PloS Pathog* (2019) 15:e1007871. doi: 10.1371/journal.ppat.1007871
20. Mendonça-Natividade FC, Lopes CD, Ricci-Azevedo R, Sardinha-Silva A, Pinzan CF, Alegre-Maller ACP, et al. Receptor heterodimerization and co-receptor engagement in TLR2 activation induced by MIC1 and MIC4 from Toxoplasma gondii. *Int J Mol Sci* (2019) 20:5001. doi: 10.3390/ijms20205001
21. Paing MM, Tolia NH. Multimeric Assembly of Host-Pathogen Adhesion Complexes Involved in Apicomplexan Invasion. *PloS Pathog* (2014) 10:e1004120. doi: 10.1371/journal.ppat.1004120
22. Brecht S, Carruthers VB, Ferguson DJP, Giddings OK, Wang G, Jakle U, et al. The Toxoplasma Micronemal Protein MIC4 Is an Adhesin Composed of Six Conserved Apple Domains. *J Biol Chem* (2001) 276:4119–27. doi: 10.1074/jbc.M008294200
23. Marchant J, Cowper B, Liu Y, Lai L, Pinzan C, Marq JB, et al. Galactose recognition by the apicomplexan parasite Toxoplasma gondii. *J Biol Chem* (2012) 287:16720–33. doi: 10.1074/jbc.M111.325928
24. Ricci-Azevedo R, Roque-Barreira M-C, Gay NJ. Targeting and recognition of toll-like receptors by plant and pathogen lectins. *Front Immunol* (2017) 8:1820. doi: 10.3389/fimmu.2017.01820
25. Suzuki Y, Orellana MA, Schreiber RD, Remington JS. Interferon-γ: The major mediator of resistance against Toxoplasma gondii. *Science (80)* (1988) 240:516–8. doi: 10.1126/science.3128869
26. Yarovinsky F. Toll-like receptors and their role in host resistance to Toxoplasma gondii. *Immunol Lett* (2008) 119(1–2):17–21. doi: 10.1016/j.imlet.2008.05.007
27. Jankovic D, Kugler DG, Sher A. IL-10 production by CD4+ effector T cells: A mechanism for self-regulation. *Mucosal Immunol* (2010) 3:239–46. doi: 10.1038/mi.2010.8
28. Couper KN, Blount DG, Riley EM. IL-10: The Master Regulator of Immunity to Infection. *J Immunol* (2008) 180:5771–7. doi: 10.4049/jimmunol.180.9.5771
29. Gazzinelli RT, Wysocka M, Hieny S, Scharton-Kersten T, Cheever A, Kühn R, et al. In the absence of endogenous IL-10, mice acutely infected with Toxoplasma gondii succumb to a lethal immune response dependent on CD4+ T cells and accompanied by overproduction of IL-12, IFN-gamma and TNF-alpha. *J Immunol* (1996) 157:798–805.
30. Costa Mendonça-Natividade F, Ricci-Azevedo R, de Oliveira Thomaz SM, Roque-Barreira MC. Production and characterization of MIC1: A lectin from toxoplasma gondii. In: J Hirabayashi. (ed) *LecQn PurificaQon and Analysis. Methods in Molecular Biology*. New York: Humana (2020) 2132. doi: 10.1007/978-1-0716-0430-4_38
31. Khan A, Grigg ME. Toxoplasma gondii: Laboratory maintenance and growth. *Curr Protoc Microbiol* (2017) 44:20c.1.1. doi: 10.1002/cpmc.26
32. Marim FM, Silveira TN, Lima DSJr, Zamboni DS. A Method for Generation of Bone Marrow-Derived Macrophages from Cryopreserved Mouse Bone Marrow Cells. *PloS One* (2010) 5:e15263. doi: 10.1371/journal.pone.0015263
33. Schindelin J, Arganda-Carreras I, Frise E, Kaynig V, Longair M, Pietzsch T, et al. Fiji: An open-source platform for biological-image analysis. *Nat Methods* (2012) 9:672–82. doi: 10.1038/nmeth.2019
34. Li J, Lee DSW, Madrenas J. Evolving Bacterial Envelopes and Plasticity of TLR2-Dependent Responses: Basic Research and Translational Opportunities. *Front Immunol* (2013). doi: 10.3389/fimmu.2013.00347
35. Henricson BE, Benjamin WR, Vogel SN. Differential cytokine induction by doses of lipopolysaccharide and monophosphoryl lipid A that result in equivalent early endotoxin tolerance. *Infect Immun* (1990). doi: 10.1128/iai.58.8.2429-2437.1990

36. Rajaiah R, Perkins DJ, Polumuri SK, Zhao A, Keegan AD, Vogel SN. Dissociation of Endotoxin Tolerance and Differentiation of Alternatively Activated Macrophages. *J Immunol* (2013) 190(9):4763–72. doi: 10.4049/jimmunol.1202407
37. Foster SL, Hargreaves DC, Medzhitov R. Gene-specific control of inflammation by TLR-induced chromatin modifications. *Nature* (2007) 447:972–8. doi: 10.1038/nature05836
38. Rajaiah R, Perkins DJ, Ireland DDC, Vogel SN, Kagan JC. CD14 dependence of TLR4 endocytosis and TRIF signaling displays ligand specificity and is dissociable in endotoxin tolerance. *Proc Natl Acad Sci USA* (2015) 112 (27):8391–6. doi: 10.1073/pnas.1424980112
39. Netea MG, Sutmuller R, Hermann C, Van der Graaf CAA, Van der Meer JWM, van Krieken JH, et al. Toll-Like Receptor 2 Suppresses Immunity against Candida albicans through Induction of IL-10 and Regulatory T Cells. *J Immunol* (2004) 172(6):3712–8. doi: 10.4049/jimmunol.172.6.3712
40. Dillon S, Agrawal A, Van Dyke T, Landreth G, McCauley L, Koh A, et al. A Toll-Like Receptor 2 Ligand Stimulates Th2 Responses In Vivo, via Induction of Extracellular Signal-Regulated Kinase Mitogen-Activated Protein Kinase and c-Fos in Dendritic Cells. *J Immunol* (2004) 172(8):4733–43. doi: 10.4049/jimmunol.172.8.4733
41. Hu X, Paik PK, Chen J, Yarilina A, Kockeritz L, Lu TT, et al. IFN-γ Suppresses IL-10 Production and Synergizes with TLR2 by Regulating GSK3 and CREB/AP-1 Proteins. *Immunity* (2006) 24(5):563–74. doi: 10.1016/j.immuni.2006.02.014
42. Boonstra A, Rajsbaum R, Holman M, Marques R, Asselin-Paturel C, Pereira JP, et al. Macrophages and Myeloid Dendritic Cells, but Not Plasmacytoid Dendritic Cells, Produce IL-10 in Response to MyD88- and TRIF-Dependent TLR Signals, and TLR-Independent Signals. *J Immunol* (2006) 177(11):7551–8. doi: 10.4049/jimmunol.177.11.7551
43. Saraiva M, O'Garra A. The regulation of IL-10 production by immune cells. *Nat Rev Immunol* (2010) 10:170–81. doi: 10.1038/nri2711
44. Chang EY, Guo B, Doyle SE, Cheng G. Cutting Edge: Involvement of the Type I IFN Production and Signaling Pathway in Lipopolysaccharide-Induced IL-10 Production. *J Immunol* (2007) 178(11):6705–9. doi: 10.4049/jimmunol.178.11.6705
45. Aksoy E, Taboubi S, Torres D, Delbauve S, Hachani A, Whitehead MA, et al. The p110δ isoform of the kinase PI(3)K controls the subcellular compartmentalization of TLR4 signaling and protects from endotoxic shock. *Nat Immunol* (2012) 13:1045–54. doi: 10.1038/ni.2426
46. Wilson EH, Wille-Reece U, Dzierszinski F, Hunter CA. A critical role for IL-10 in limiting inflammation during toxoplasmic encephalitis. *J Neuroimmunol* (2005) 165(1–2):63–74. doi: 10.1016/j.jneuroim.2005.04.018
47. Jeong YI, Hong SH, Cho SH, Park MY, Lee SE. Induction of IL-10-producing regulatory B cells following Toxoplasma gondii infection is important to the cyst formation. *Biochem Biophys Rep* (2016) 7:91–7. doi: 10.1016/j.bbrep.2016.05.008
48. Coombes JL, Charsar BA, Han SJ, Halkias J, Chan SW, Koshy AA, et al. Motile invaded neutrophils in the small intestine of Toxoplasma gondii-infected mice reveal a potential mechanism for parasite spread. *Proc Natl Acad Sci USA* (2013) 10:E1913–22. doi: 10.1073/pnas.1220272110
49. Pinzan CF, Sardinha-Silva A, Almeida F, Lai L, Lopes CD, Lourenço EV, et al. Vaccination with recombinant microneme proteins confers protection against experimental toxoplasmosis in mice. *PloS One* (2015) 10:e0143087. doi: 10.1371/journal.pone.0143087

Conflict of Interest: The authors declare that the research was conducted in the absence of any commercial or financial relationships that could be construed as a potential conflict of interest.

frontiers in Microbiology

ORIGINAL RESEARCH
published: 30 June 2021
doi: 10.3389/fmicb.2021.657726

Effect of Protein O-Mannosyltransferase (MSMEG_5447) on *M. smegmatis* and Its Survival in Macrophages

*Liqiu Jia[1], Shanshan Sha[1], Shufeng Yang[2], Ayaz Taj[1] and Yufang Ma[1,2]**

[1] Department of Biochemistry and Molecular Biology, College of Basic Medical Sciences, Dalian Medical University, Dalian, China, [2] Department of Microbiology, College of Basic Medical Sciences, Dalian Medical University, Dalian, China

Protein O-mannosyltransferase (PMT) catalyzes an initial step of protein O-mannosylation of *Mycobacterium tuberculosis* (Mtb) and plays a crucial role for Mtb survival in the host. To better understand the role of PMT in the host innate immune response during mycobacterial infection, in this study, we utilized *Mycobacterium smegmatis* pmt (*MSMEG_5447*) gene knockout strain, ΔM5447, to infect THP-1 cells. Our results revealed that the lack of *MSMEG_5447* not only impaired the growth of *M. smegmatis* in 7H9 medium but also reduced the resistance of *M. smegmatis* against lysozyme and acidic stress *in vitro*. Macrophage infection assay showed that ΔM5447 displayed attenuated growth in macrophages at 24 h post-infection. The production of TNF-α and IL-6 and the activation of transcription factor NF-κB were decreased in ΔM5447-infected macrophages, which were further confirmed by transcriptomic analysis. Moreover, ΔM5447 failed to inhibit phagosome–lysosome fusion in macrophages. These findings revealed that PMT played a role in modulating the innate immune responses of the host, which broaden our understanding for functions of protein O-mannosylation in mycobacterium–host interaction.

Keywords: host-pathogen interaction, O-mannosylation, protein O-mannosyltransferase, *Mycobacterium smegmatis*, phagosome–lysosome fusion

OPEN ACCESS

Edited by:
Hector Mora Montes, University of Guanajuato, Mexico

Reviewed by:
Jianping Xie, Southwest University, China
Chang-Hwa Song, Chungnam National University, South Korea
Christopher Ealand, University of the Witwatersrand, Johannesburg, South Africa

***Correspondence:**
Yufang Ma
yufangma@dmu.edu.cn

Specialty section:
This article was submitted to Infectious Diseases, a section of the journal Frontiers in Microbiology

Received: *23 January 2021*
Accepted: *31 May 2021*
Published: *30 June 2021*

Citation:
Jia L, Sha S, Yang S, Taj A and Ma Y (2021) Effect of Protein O-Mannosyltransferase (MSMEG_5447) on M. smegmatis and Its Survival in Macrophages. Front. Microbiol. 12:657726. doi: 10.3389/fmicb.2021.657726

INTRODUCTION

Tuberculosis (TB), caused by *Mycobacterium tuberculosis* (Mtb), is one of the top 10 causes of death and the leading cause of death from a single infectious agent. Today, the burden of TB is still in a phase of high level, largely due to the TB/HIV coinfection and emergence of high drug-resistant Mtb strains (WHO, 2020). Under this situation, efforts for understanding pathogenicity of Mtb become eagerly important.

The unique cell envelope of Mtb is composed of peptidoglycan, arabinogalactan, mycolic acids, phosphatidylinositol mannosides, lipomannans, lipoarabinomannans, and proteins. It not only

Abbreviations: ConA, concanavalin A; CW, cell wall; WCL, whole-cell lysate; CM, cell membrane; SOL, soluble fraction; CFU, colony-forming units; MOI, multiplicity of infection; PMA, phorbol 12-myristate 13-acetate; LBT, LB medium supplemented with 0.05% Tween 80; ADC, albumin–dextrose–catalase; LAMP-1, lysosome-associated membrane protein 1; DEGs, differentially expressed genes; PMT, protein O-mannosyltransferase; PSP-A, pulmonary C-type lectin surfactant protein A; Apa, alanine and proline-rich secreted antigen.

provides an impermeable barrier for antimicrobial drugs resistance but also is crucial for Mtb pathogenicity and survival in infected host (Abrahams and Besra, 2016; Turner and Torrelles, 2018). Recent studies showed that many cell envelope proteins and secreted proteins of Mtb were frequently O-mannosylated (Espitia et al., 2010; Mehaffy et al., 2019). For example, 41 putative O-mannosylated proteins in Mtb culture filtrate were identified *via* concanavalin A (ConA) lectin-specific two-dimensional gel electrophoresis (Gonzalez-Zamorano et al., 2009). Tucci et al. (2020) identified 46 O-glycoproteins from culture filtrate of Mtb by LC-MS/MS, and most of those proteins are involved in intermediary metabolism and respiration, as well as cell wall (CW) and cell process according to the Mtb database. The biological roles of Mtb glycoproteins also have been investigated currently. It has been reported that O-mannosylation of protein Mtb had closely linked with protein properties including the activity, subcellular localization, and stability of proteins and the permeability of the CW (Herrmann et al., 1996; Sartain and Belisle, 2009; Arya et al., 2013; Rolain et al., 2013). Additionally, O-mannosylation of protein displayed a profound impact on host–pathogen interaction, such as receptor recognition, immunomodulation, antigenicity, and Mtb pathogenicity (Loke et al., 2016; Vinod et al., 2020). For example, O-mannosylated proteins Apa, LpqH, and PstS1 as adhesins bound with c-type lectins to achieve cell adhesion, facilitating subsequent establishment of infection (Diaz-Silvestre et al., 2005; Ragas et al., 2007; Esparza et al., 2015). Further studies revealed that natural O-mannosylation of Apa is crucial for stimulating the T cell antigenicity and dendritic cell-mediated T cell polarization (Horn et al., 1999; Pitarque et al., 2005; Nandakumar et al., 2013). Recently, the protective capacity of *Mycobacterium bovis* BCG was also improved by boosting with the O-mannosylated protein of BCG (Deng et al., 2020).

Protein O-mannosyltransferase (PMT) catalyzes the initial step of protein mannosylation by transferring the mannosyl residue to serine or threonine residue of proteins. VanderVen et al. (2005) first identified Rv1002c as Mtb PMT because overexpression of Rv1002c in *Mycobacterium smegmatis* increased the PMT activity of membrane fractions *in vitro*. Increased interest in O-mannosylation stemmed from the fact that the absence of Rv1002c had greatly reduced the Mtb survival in mice (Liu et al., 2013). Recent studies showed that PMT related to the release of lipoarabinomannan (LAM) and affected host inflammatory responses (Alonso et al., 2017). Even though these findings endow PMT with potential as a drug-targetable virulence factor in host–pathogen interactions, its physiological role in Mtb and its biological role in innate immunity of the host are still poorly characterized.

Mycobacterium smegmatis is a convenient model for the study of PMT due to its ability to produce glycosylated Mtb recombinant proteins (Bashiri and Baker, 2015). It is also an important tool as a vaccine vector in expressing heterologous proteins (Triccas and Ryan, 2009). Additionally, *MSMEG_5447*, a gene that encodes PMT in *M. smegmatis*, is homologous with Rv1002c and conserved among mycobacteria (**Figure 1**). In our previous work, an *M. smegmatis* mutant strain with *MSMEG_5447* gene disruption, ΔM5447, was constructed and confirmed by obtaining non-mannosylated protein Rv0431 which is a mannosylated protein in Mtb (Deng et al., 2016). In this study, MSMEG_5447 complementary strain was generated by transforming the pMind-MSMEG_5447 plasmid to the ΔM5447 strain. The impact of PMT on *M. smegmatis* viability under stress conditions was measured, and the invasion and survival of ΔM5447 in the human macrophage cell line THP-1 were evaluated. The level of inflammatory cytokines and phagosome–lysosome fusion as well as the transcriptome of macrophages infected by ΔM5447 were analyzed to explore the role of PMT in host–pathogen interaction.

MATERIALS AND METHODS

Bacterial Strains, Culture Media, and Plasmids

The wild-type *M. smegmatis* mc^2155 strain (Wt), the *MSMEG_*5447 gene knockout strain (ΔM5447), and the *MSMEG_*5447 gene complemented strain (Comp) were cultured in liquid Middlebrook 7H9 broth containing 10% albumin–dextrose–catalase (ADC), 0.05% Tween 80, and 0.5% glycerol or in Middlebrook 7H11 solid medium supplemented with 10% ADC and 0.5% glycerol. These bacterial strains were also grown in LBT medium (LB broth containing 0.05% Tween 80) or LB agar. Kanamycin (25 μg/ml) and hygromycin (50 μg/ml) were used for the selection of appropriate strains. The *Escherichia coli–Mycobacterium* shuttle plasmid pMind (Blokpoel et al., 2005) was used to overexpress MSMEG_5447 protein in the ΔM5447 strain. The pCG76-GFP plasmid (Deng et al., 2016) was used to express green fluorescent protein (GFP) in different *M. smegmatis* strains.

Construction of MSMEG_5447 Gene Complemented Strain (Comp)

The *M. smegmatis* mutant with *MSMEG_5447* disruption, ΔM5447, was constructed by using DNA homologous recombination in our previous studies (Deng et al., 2016). For constructing *MSMEG_*5447 gene-complemented strain (Comp), the *MSMEG_5447* gene (1551 bp) was amplified by PCR from *M. smegmatis* mc2155 genomic DNA using a forward primer (5′AGCATATGACCGCCCTCGACACCGATAC3′, underlined is the NdeI site) and a reverse primer (5′GTACTAGTCTAGTGATGATGGTGATGGTGGCGCCA-GCTCGGCAACC3′, underlined is the SpeI site). The PCR product of the *MSMEG_5447* gene was cloned to the pJET1.2/blunt vector, yielding a pJET-*MSMEG_5447* plasmid. After confirmation by DNA sequencing, the *MSMEG_5447* gene was inserted into expression vector pMind, thereby generating pMind-*MSMEG_5447* plasmid. The pMind-*MSMEG_5447* plasmid was transformed into ΔM5447 electro-competent cells, generating a *MSMEG_5447* gene complementary strain, Comp. The expression of His-tagged MSMEG_5447 protein was induced by tetracycline (20 ng/ml) for 24 h and detected by Western blot with α(anti)-polyhistidine clone HIS-1 (Sigma) followed by AP-conjugated goat anti-mouse IgG (Proteintech,

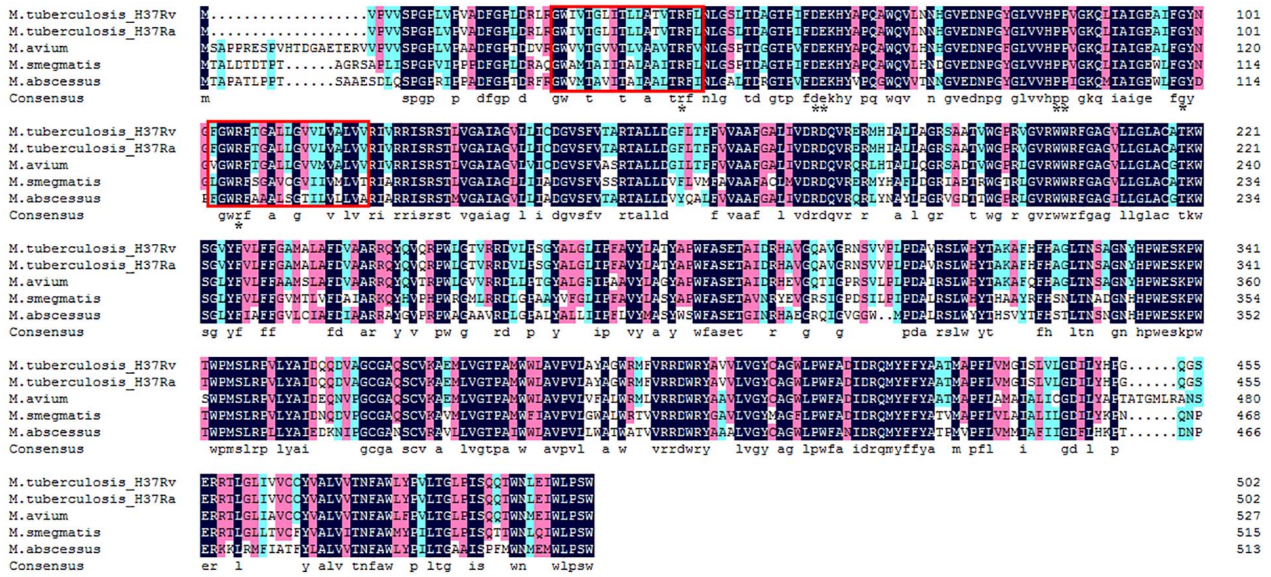

FIGURE 1 | Amino acid multiple-sequence alignment of O-mannosyltransferase in mycobacterium species. GenBank accession numbers: *M. tuberculosis* H37Rv: CCP43752; *M. tuberculosis* H37Ra: ABQ72745; *Mycobacterium avium*: ANR90417; *M. smegmatis*: AFP41739; and *M. abscessus*: WP_005059031. The dark blue box indicates 100% identical of amino acid sequence among five mycobacterium strains. The pink and sky blue colors indicate >75 and >50% similarity of amino acid sequence among five mycobacterium strains, respectively. Two functional transmembrane domains of PMT were framed by the red box, and the conserved PMT active site residues were marked with the black star based on the VanderVen study in 2005. Alignment was conducted using DNAMAN software.

Rosemont, IL, United States) and finally visualized by using NBT/BCIP solution.

ConA Lectin Blot of Bacterial Proteins

Whole-cell lysate (WCL), CW, cell membrane (CM), and soluble (SOL) fractions were separated by differential ultracentrifugation as described previously (Gibbons et al., 2007). Briefly, 100 ml of bacterial cultures was harvested by centrifugation. The bacterial cells were resuspended in 5 ml of lysis buffer (PBS pH 7.4, 1 mM phenylmethylsulfonyl fluoride) and lysed by sonication. Lysates were centrifuged at 3,000 × *g* for 30 min to get WCL, which was centrifuged at 27,000 × *g* for 30 min to obtain the supernatant and CW pellet. The supernatant was then centrifuged at 100,000 × *g* for 2 h to acquire the CM pellet and SOL fraction. CW and CM fractions were resuspended in 0.5 ml of lysis buffer. The concentration of proteins was determined by BCA Protein Quantification kit (Vazyme, Nanjing, China). After separation by SDS-PAGE, the gels was stained with Coomassie Brilliant Blue R250 or transferred onto a nitrocellulose (NC) membrane for 1 h. The NC membrane was blocked with 3% BSA in TBST buffer for 2 h at room temperature and incubated with biotinylated ConA lectin (Vector Laboratories, Burlingame, CA, United States) at 1:10,000 dilution at 4°C overnight. After three times washing with TBST buffer, the NC membrane was incubated with streptavidin-HRP (Beyotime Biotechnology, Shanghai, China) at 1:20,000 dilutions for 1 h at room temperature. Finally, the protein bands were visualized by adding WesternBright ECL detection reagents (Advansta, Menlo Park, CA, United States).

Macrophage Infection and Colony-Forming Units (CFU) Determination

THP-1 macrophage, a suspension cell line, was cultured in RPMI 1640 (Gibco) medium supplemented with 10% fetal bovine serum (FBS) (Lonsera) and penicillin–streptomycin (HyClone) solution in a 37°C incubator with 5% CO_2. THP-1 cells were seeded into 12-well plates at a density of 5 × 10^5 cells/well and differentiated into macrophages by inducing with 100 ng/ml phorbol 12-myristate 13-acetate (PMA) for 24 h. Prior to infection, the bacterial cultures of Wt, ΔM5447, and Comp were centrifuged at 3000 × *g* for 5 min and the pellets were resuspended in RPMI 1640 medium without antibiotic and FBS. The THP-1 cells were washed with PBS and infected by Wt, ΔM5447, or Comp at a multiplicity of infection (MOI) of 10 for 3 h. The THP-1 cells were washed with PBS three times to remove extracellular bacteria and then cultured in RPMI 1640 medium with 10% FBS and 50 μg/ml gentamicin for 1 h to completely remove the extracellular bacteria. This time point was regarded as 0 h of post-infection. After that, the cells were washed with PBS for three times and then cultured in RPMI 1640 medium with 10% FBS and penicillin–streptomycin for an additional 24 h. For the colony-forming unit (CFU) assay, the cells were lysed with 200 μl 0.03% SDS for 5 min. The lysates with 10-fold serial dilutions were plated on the LB agar plates, and the number of colonies was counted 2–3 days later. For cytokine detections, the cell culture was collected at 24 h post-infection and the production of cytokines was analyzed by ELISA.

Immunofluorescence Assay

The pCG76-GFP vector was electro-transformed to Wt, ΔM5447, and Comp strains generating GFP-expressing Wt, ΔM5447, and Comp strains, respectively. THP-1 cells were seeded on glass slide in 24-well plates and stimulated with PMA (100 ng/ml) for 24 h. The THP-1 cells were infected with GFP-expressing Wt, ΔM5447, or Comp at an MOI of 10 for 3 h. The infected cells were cultured in RPMI 1640 medium with 10% FBS and 5 μg/ml gentamicin for 2 and 24 h. The cells were washed with PBS and fixed in 4% paraformaldehyde (PFA) for 20 min at room temperature. The cells were permeabilized in 0.2% Triton-X 100 for 5 min. For visualizing intracellular bacteria, F-actin of cells was stained with rhodamine phalloidin for 30 min in the dark. For detecting the expression of lysosomal-associated membrane protein 1 (LAMP-1) and NF-kB p65, cells were fixed in 4% PFA and incubated with blocking buffer (3% BSA) for 30 min. Then, the cells were incubated with anti-LAMP-1 (Abgent, San Diego, CA, United States) or anti-p65 (Proteintech, United States) antibody overnight at 4°C. Finally, the coverslids were incubated with secondary anti-rabbit antibodies conjugated to Alexa or FITC for 1 h at room temperature. For observing the co-localization of intracellular bacteria with lysosome, cells were incubated with 500 nM LysoTracker Red (Invitrogen) in RPMI 1640 medium for 30 min and fixed in 4% PFA for 20 min. Fluoroshield with DAPI (Abcam, Cambridge, MA, United States) was used for staining nucleic acid. The co-localization of LAMP-1 or lysosome with GFP-expressing bacteria was analyzed in more than 100 cells. Images were visualized with a fluorescence microscope (Olympus). Experiments were performed in two independent experiments.

Resazurin Assay

Lysozyme resistance of bacteria was examined according to the published method (Palomino et al., 2002). The mycobacterial cell suspension was prepared by diluting the bacterial culture in LBT broth at 1:5,000, and its accurate density was confirmed by CFU counting on LB agar plates. The mycobacterial cell suspension of 50 μl was added into 96-well plates followed by adding 50 μl of lysozyme with two-fold serial dilutions. The well containing bacteria without lysozyme were regarded as control. After incubation for 24 h in a 37°C incubator, 100 μl resazurin solution (1:1 mixture of 125 μg/ml resazurin and 10% Tween 80) was added to each well and the plate was incubated for an additional 5–12 h for color development. The blue color of resazurin dye changes to pink in the reducing environment of living cells.

The Acidic Stress Assay

The LBT medium was prepared and adjusted to pH 5.0 by adding HCl before sterilization by filtration using a 0.22-μm filter. The bacterial cultures were diluted to an $OD_{600\ nm}$ of 0.5 in LBT medium and added into acidic broth at 1:100 dilutions. After incubation for 0, 12, 24, and 36 h, the viability of bacteria was determined by plating bacteria at 10-fold serial dilutions on LB agar plates and counting bacterial CFU 2–3 days later. The growth of bacteria was also monitored by measuring $OD_{600\ nm}$ at an interval of 12 h after exposure to acidic broth.

Ethidium Bromide Accumulation Assay

Strains of Wt, ΔM5447, and Comp were grown in LBT medium to an $OD_{600\ nm}$ of 1.0. Cultures were washed and resuspended with PBS containing 0.05% Tween 80. The $OD_{600\ nm}$ of bacterial suspension was adjusted to 0.5 with PBST, and 200 μl suspension was added to a 96-well black fluoroplate with three replicates. Ethidium bromide (EB) at concentrations of 2 μg/ml was added. The EB accumulation of strains was measured in the BioTek Synergy NEO with an excitation of 544 nm and emission of 590 nm. Fluorescence data was acquired for 1 h at an interval of 5 min. All data from each well were normalized to the time of zero reading. All experiments were repeated two times, and similar results were obtained.

Quantitative Real-Time PCR (qPCR)

THP-1 cells were infected with Wt, ΔM5447, or Comp strain for 3 h and cultured for an additional 24 h. The infected cells were harvested, and their total RNA was extracted using RNAiso Plus (Takara, Mountain View, CA, United States) reagent according to the manufacturer's protocol. The cDNA was synthesized with reverse-transcription of RNA (1 μg) by using the PrimeScript RT Reagent Kit with genomic DNA Eraser (Takara). The cDNA of 20 ng served as a template for quantitative real-time PCR (qPCR). The reaction was performed in StepOnePlus Real-Time PCR System (Applied Biosystems, Foster City, CA, United States) using SYBR Green Premix Ex Taq II (Takara) and gene-specific primers (**Table 1**). The amplification condition was as follows: 30 s at 95°C for initial denaturation, and 5 s at 95°C and 30 s at 60°C for 40 cycles. The melting curve was used to confirm the specificity of primers. All qPCR reactions were performed for three independent experiments, and the relative expression of specific genes was evaluated using the $2^{-\Delta\Delta CT}$ method.

Cytokine Measurement

The culture supernatant of infected cells was collected at 24 h post-infection. The concentrations of tumor necrosis factor α (TNF-α), interleukins (IL)-6, IL-12, and IL-10 were measured by ELISA kits (Xinfan Biological Company, Shanghai, China) following the manufacturer's instructions.

TABLE 1 | Primers used in qPCR reactions.

Genes	Primer sequences (5′–3′)
TNF-α	Forward: GCTGCACTTTGGAGTGATCG
	Reverse: ACATGGGCTACAGGCTTGTC
IL-6	Forward: ACTCACCTCTTCAGAACGAATTG
	Reverse: CCATCTTTGGAAGGTTCAGGTTG
NF-κB	Forward: ATGGAGAGTTGCTACAACCCA
	Reverse: CTGTTCCACGATCACCAGGTA
GAPDH	Forward: AGCCTCAAGATCATCAGCAATG
	Reverse: TGTGGTCATGAGTCCTTCCACG

Protein Preparation and Western Blot Analysis

The total proteins of THP-1 cells infected with Wt, ΔM5447, or Comp strain were prepared at 24 h post-infection, and the concentration of proteins was determined by a BCA Protein Quantification kit (Vazyme). After separation of proteins by SDS-PAGE, the proteins were transferred onto an NC membrane. The membrane was blocked with 5% (w/v) non-fat milk in TBST buffer for 2 h at room temperature and incubated with primary antibodies, NF-κB p65 (Cell Signal Technology, Danvers, MA, United States), pSer536-NF-κB p65 (Cell Signal Technology), or GAPDH (Proteintech), at 4°C overnight. After washing three times with TBST buffer, the membrane was incubated with appropriate HRP-conjugated secondary antibody (Beyotime Biotechnology) for 1 h at room temperature. Finally, the protein bands were visualized by Western Bright ECL detection reagents (Advansta) and quantified using ImageJ software.

Transcriptomic Analysis of Infected THP-1 Cells by RNA Sequencing

For RNA sequencing, total RNA was extracted from THP-1 cells infected with Wt and ΔM5447 strain at 24 h post-infection. Each group was performed in duplicate. The RNA quantity and quality were evaluated using the Agilent 2100 bioanalyzer and agarose gel electrophoresis. The cDNA libraries were constructed using NEB Next Ultra^{TM} RNA Library Prep Kit for Illumina (NEB, Ipswich, MA, United States), and the libraries were sequenced on the Illumina HiSeq platform by Novogene Bioinformatics Technology (Beijing, China). Clean data were obtained by removing linker sequences and low-quality bases from raw data. The clean reads were evaluated by Q20, Q30, and GC contents and mapped to the human transcriptome (RefSeq transcriptome index hg19). For analyzing gene expression profiles, differentially expressed genes (DEGs) of two groups were identified by using the DESeq2 R package and an adjusted p-value < 0.05 as the threshold criteria. For functional annotation, gene ontology (GO) enrichment analysis of DEGs was implemented by the cluster Profiler R package and the GO terms with corrected p-value less than 0.05 were considered significantly enriched. Kyoto Encyclopedia of Genes and Genomes (KEGG) pathway analysis of DEGs was done in the KEGG database[1]. Interactions of key genes that presented in two enriched pathways were analyzed by STRING and shown by Cytoscape software. The raw data of RNA-Seq with accession number GSE128970 are available at the NCBI GEO database (Edgar et al., 2002).

Statistical Analysis

The statistical analysis of data was performed by using GraphPad Prism 8.0. Comparisons between groups were conducted by the method of Student's unpaired t-test or two-way ANOVA. Data were shown as means ± SD. $p < 0.05$ was considered as statistical significance.

[1]http://www.genome.jp/kegg/

RESULTS

Inactivation of MSMEG_5447 Impaired *M. smegmatis* Growth and Its Protein O-Mannosylation

To characterize the impact of PMT on physiology of the role of *M. smegmatis*, *MSMEG_5447* gene-complemented strain, Comp, was constructed (**Supplementary Figure 1**). The growth of Wt, ΔM5447, and Comp strain was measured in Middlebrook 7H9 broth and LBT medium. Our data showed that the growth rate of the ΔM5447 strain was significantly reduced in 7H9 broth (**Figure 2A**) and the colonies of ΔM5447 were small and loose as compared to that of Wt (**Supplementary Figure 2**). Interestingly, ΔM5447 had a similar growth rate to the Wt and Comp strains in LBT medium (**Figure 2B**). Subsequently, O-mannosylation of proteins in different subcellular fractions was evaluated by differential centrifugation followed by ConA lectin blot. As shown in **Figure 2C**, the level of O-mannosylation of protein at 25–40 kD in CW and CM fractions of ΔM5447 was reduced as compared to that of the Wt strain when the same amount of samples was observed in Coomassie brilliant blue staining gel. We also found that the level of O-mannosylation of proteins around 70 kD had no differences in all fractions except CM of the Wt and ΔM5447 strains. One possible explanation is that the bands around 70 kD might derive from recognition of α-glucose as ConA can recognize both α-mannose and α-glucose. Furthermore, analysis of O-mannosylation in the supernatant and pellet also indicated that O-mannosylation of proteins in the ΔM5447 strain was decreased as compared to that of the Wt and Comp strains (**Supplementary Figure 3**).

The Lysosomal Resistance of ΔM5447 Strain was Impaired

Exposure of bacteria in an acidic condition, *in vitro*, has been specifically used to mimic the bacteria in acidic phagolysosome, which was considered as a key strategy for the host to clear bacteria during infection (Vandal et al., 2009). Therefore, the effect of PMT deficiency on bacterial resistance to lysosome-related stress was assessed *in vitro* in the LBT medium. The growth of Wt, ΔM5447, and Comp strains in acidic LBT medium (pH 5.0) was examined by monitoring OD_{600} and counting bacterial CFU. As shown in **Figure 3A**, the growth of ΔM5447 in acidic LBT medium was significantly reduced compared to that of Wt and Comp strains after 24 and 36 h of incubation. The CFU results showed that the ΔM5447 strain had a lower rate of viability in acidic culture than those of Wt and Comp strains after 36 h of incubation (**Figure 3B**). The viability of Wt, ΔM5447, and Comp strains under lysozyme stress was also determined by resazurin microplate assay. *M. smegmatis* ΔM5447 showed lower resistance to lysozyme (MIC = 313 μg/ml) as compared to that of the Wt strain and Comp strain (MIC = 625 μg/ml) (**Figure 3C**). The CW permeability was evaluated by measuring the EB accumulation in Wt, ΔM5447, and Comp strains. The results showed that EB accumulation was significantly increased in ΔM5447 as compared with Wt strain, and that increase in ΔM5447 was reversed in Comp strain (**Figure 3D**).

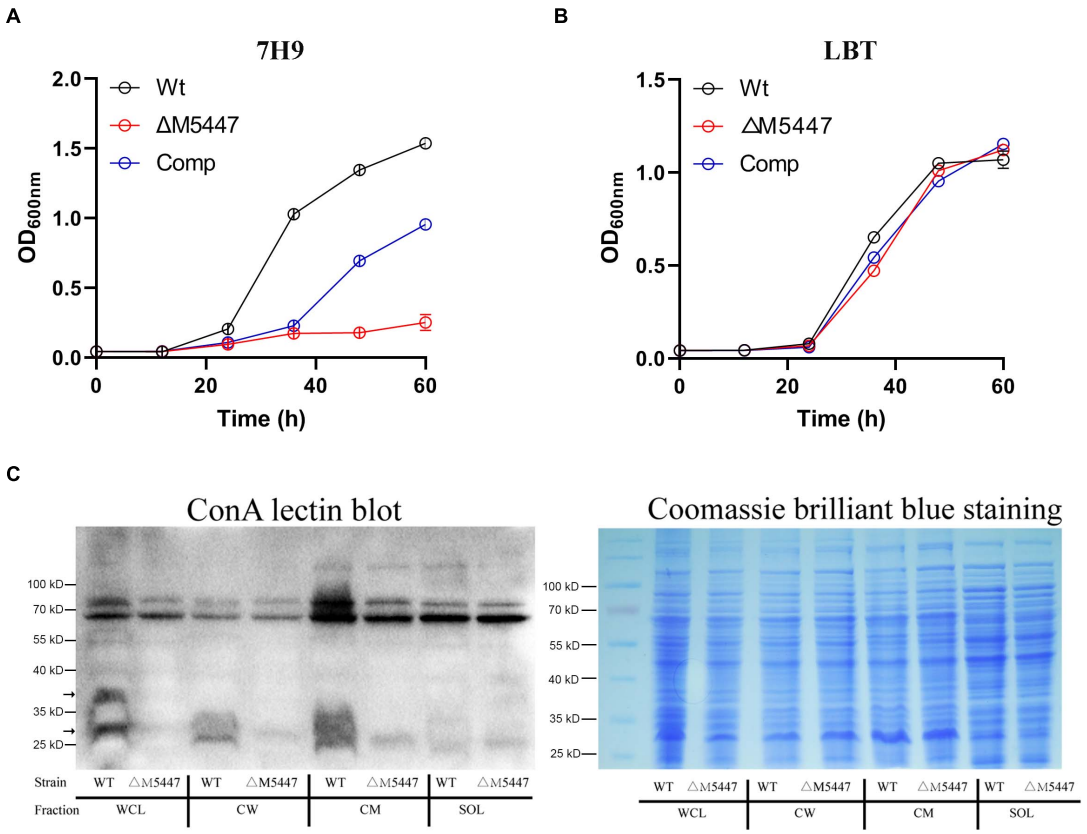

FIGURE 2 | Protein O-mannosyltransferase (PMT) deficiency impaired the growth of *M. smegmatis* and reduced its level of O-mannosylation. Wild-type *M. smegmatis* mc^{2}155 (Wt) strain and MSMEG_5447 gene knockout strain (ΔM5447) and Comp strain were grown in LBT medium **(A)** or Middlebrook 7H9 medium supplemented with 10% ADC and 0.05% Tween 80 **(B)**; the growth rate of bacteria was evaluated by measuring OD_{600} at an interval of 12 h. **(C)** Wt and ΔM5447 strains were grown in LBT broth. After the bacterial pellet was lysed by sonication, whole-cell lysate (WCL), CW, CM, and soluble (SOL) fractions were separated by differential centrifugation. The level of O-mannosylation of proteins in each subcellular fraction was analyzed by ConA lectin blotting (Left). The gels stained with Coomassie brilliant blue showed the same loading amount between different samples (Right). The black arrows for the band indicate the different levels of O-mannosylation in fractions of Wt and ΔM5447 strains.

The Viability of ΔM5447 in THP-1 Macrophages Was Reduced

To evaluate the impact of PMT deficiency on host–pathogen interaction, THP-1 macrophage cells were infected with Wt, ΔM5447, or Comp strain for 3 h and the invasion rate and subsequent intracellular survival of bacteria at 24 h post-infection was examined by CFU assay. As shown in **Figure 4A**, the invasion rate of ΔM5447 strain exhibited a slight but not significant reduction as compared to that of the Wt strain at 0 h post-infection. However, inside THP-1 cells, the survival of ΔM5447 was significantly reduced as compared to that of the Wt strain at 24 h post-infection, and this decline was reversed in the Comp strain (**Figure 4B**). To further confirm the above results, GFP-expressing bacteria and F-actin of macrophages were visualized by fluorescence microscopy. As shown in **Figure 4C** and **Supplementary Figure 4**, the percentage of infected THP-1 cells had no significant difference among Wt, ΔM5447, and Comp strains at 0 h post-infection. However, 24 h after infection, the relative fluorescence intensity of GFP was significantly reduced in ΔM5447-infected THP-1 cells as compared to the Wt- and Comp-infected cells (**Figure 4D**). These data indicated that PMT inactivation decreased the survival of *M. smegmatis* in macrophages.

ΔM5447 Infection Impaired the Production of TNF-α and IL-6 of Macrophage

To explore whether PMT deficiency in mycobacteria could affect the inflammatory response of infected macrophages, the production of cytokines was evaluated by qPCR and ELISA. We found that the expression of TNF-α (**Figure 5A**) and IL-6 (**Figure 5B**) was significantly reduced in ΔM5447-infected THP-1 cells as compared to Wt-infected THP-1 cells at the transcriptional level. Consistently, ELISA results showed that the secretion of TNF-α and IL-6 was significantly decreased in ΔM5447-infected THP-1 cells (**Figures 5E,F**). There was no difference on the transcription and secretion of IL-10 and IL-12 when THP-1 cells were infected with Wt, ΔM5447, or Comp strain (**Figures 5C,D,G,H**).

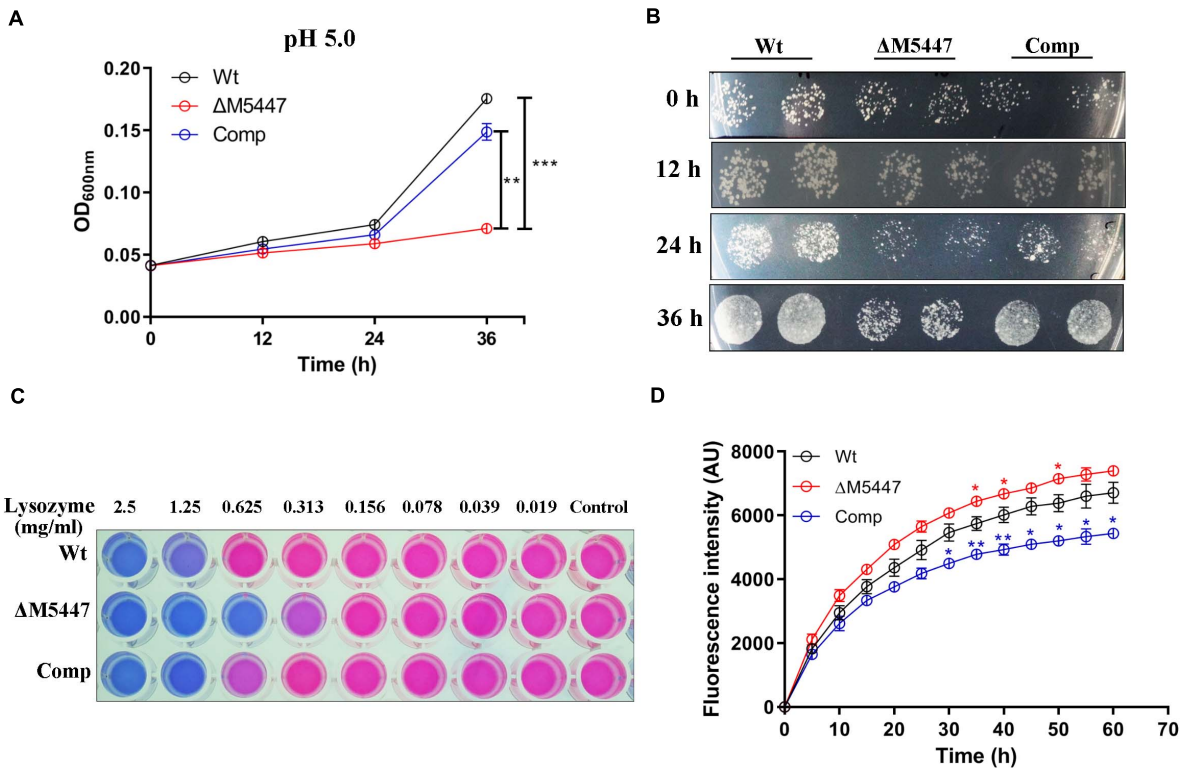

FIGURE 3 | The tolerance of ΔM5447 to lysosome-related stress was reduced. **(A)** Wt, ΔM5447, and Comp strains were cultured in LBT acidic medium (pH 5.0); the growth of bacteria was determined by measuring OD_{600} at an interval of 12 h. **(B)** The corresponding cultures from acidic medium were plated on LB agar plates with a 100-fold dilution at an interval of 12 h. **(C)** Wt, ΔM5447, and Comp strains were treated with lysozyme in a two-fold serial dilution for 24 h. Resazurin dye was added and incubated for 5–12 h for color development. The changed color from original blue to pink indicated that the living cells existed. The well contained bacterial culture only as control. A representative result was shown from three independent experiments. **(D)** Mid-log phage cultures of Wt, ΔM5447, and Comp strains were incubated in PBST with 2 μg/ml EB. The EB accumulation of strains was observed for 1 h at an interval of 5 min. The value at each point is normalized to the time of zero value. Data were shown as mean ± SD of triplicate wells. Statistical analyses were performed by the method of two-way ANOVA (*$p < 0.05$, **$p < 0.01$, ***$p < 0.001$).

ΔM5447 Infection Reduced the Expression and Activation of NF-κB in Macrophage

As a downstream executor of the signal transduction pathway, nuclear factor NF-κB can be activated and thus increase the expression of inflammatory-related genes (Pahl, 1999). To determine whether NF-κB was affected in ΔM5447-infected macrophages, the expression and activation of NF-κB were evaluated in macrophages at 24 h after infection with Wt, ΔM5447, or Comp strain. The qPCR result showed that NF-κB was down-regulated by 35% in ΔM5447-infected macrophages as compared to Wt-infected macrophages, which was partially reversed in Comp-infected macrophages (**Figure 6A**). Western blot results showed that the phosphorylation of p65 (p-p65) was reduced in ΔM5447-infected macrophages as compared to the Wt-infected macrophages (**Figure 6B**). Furthermore, the activation of NF-κB was evaluated by detecting the translocation of the p65 subunit to the nucleus. At 24 h infection, the nuclear translocation of the p65 subunit was reduced in ΔM5447-infected macrophages as compared to the Wt or Comp-infected macrophages (**Figure 6C**). Taken together, our data indicated that PMT deficiency impaired the inflammatory response of macrophages stimulated by mycobacteria.

ΔM5447 Strain Enhanced the Phagolysosomal Fusion in Macrophages

Inhibition of phagosome–lysosome fusion is another effective strategy used by Mtb to evade microbicidal activity of macrophages (Carranza and Chavez-Galan, 2018). We proposed that the reduced survival of ΔM5447 in macrophages was due to the failure of blocking phagosome–lysosome fusion. To test this possibility, THP-1 macrophages were infected with GFP-expressing Wt, ΔM5447, or Comp strain and then stained with LysoTracker Red which is a red-fluorescent dye to label acidic lysosomes. The phagosome–lysosome fusion was assessed by co-localization of lysosome with intracellular GFP-expressing bacterial strains. As shown in **Figure 7A** and **Supplementary Figure 5A**, Wt displayed 30% co-localization with LysoTracker Red whereas ΔM5447 showed 77% co-localization ($p < 0.05$). Comp showed 36% co-localization with lysosome which was similar with Wt. To further assess the effect of MSMEG_5447 on phagosome–lysosome fusion, co-localization of intracellular

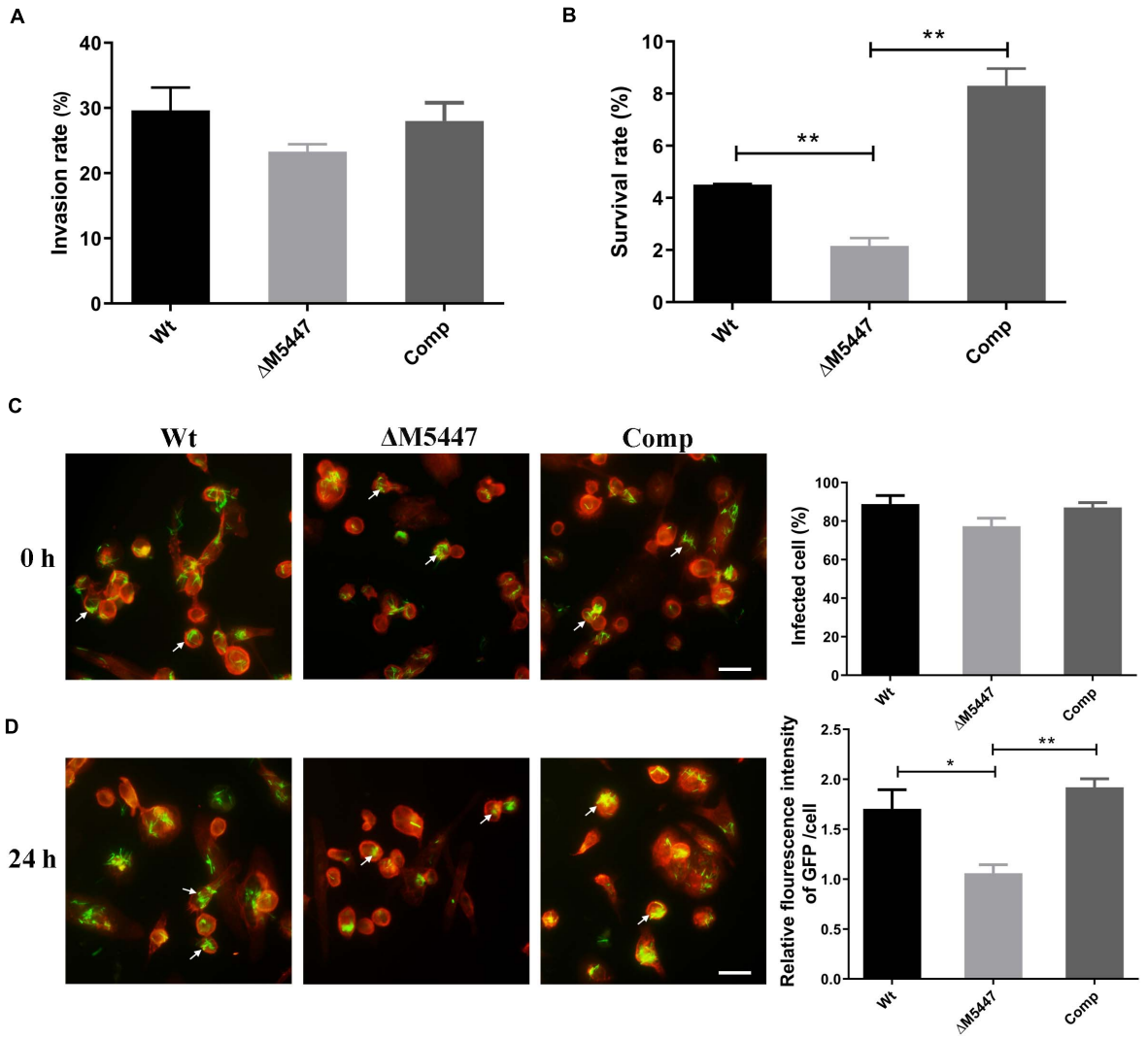

FIGURE 4 | ΔM5447 displayed impairment in survival ability in THP-1 cells. The invasion ability **(A)** and intracellular survival **(B)** of different *M. smegmatis* strains in THP-1 macrophage were evaluated. Macrophage cells were infected with Wt, ΔM5447, and Comp strains at an MOI of 10. The infected cells were lysed by 0.03% SDS at the indicated time, and the colonies were counted by CFU assay. The invasion rate of bacteria was calculated by the number of intracellular bacteria at 0 h post-infection to the number of initial bacteria for infection. The percentage of intracellular survival of bacteria was evaluated by the intracellular bacteria at 24 h post-infection to the number of 0 h of post-infection. The invasion and survival ability of bacteria in THP-1 macrophages were also determined by fluorescence microscopy. Green fluorescence protein (GFP)-expressing plasmid and rhodamine-phalloidin dye were used to visualize the bacteria and macrophage F-actin individually. **(C)** The bacterial invasion rate was evaluated by the percentage of cells containing GFP at 0 h post-infection. **(D)** The bacterial survival rate was evaluated by the relative fluorescence intensity of GFP per cell at 24 h post-infection. The white arrows indicate a representative number of intracellular bacteria. Scale bars, 20 μm. A representative field was shown from two independent experiments. Data were shown as mean ± SD of replicate wells; statistical analyses were performed by the method of two-tailed *t*-test (*$p < 0.05$, **$p < 0.01$).

GFP-expressing bacteria with LAMP-1 was observed under a fluorescence microscope. LAMP-1 is delivered to phagosomes during the phagosome maturation process and considered as a late endosomal-lysosomal marker. As shown in **Figure 7B** and **Supplementary Figure 5B**, Wt showed 17% co-localization with LAMP-1 whereas ΔM5447 showed 58% co-localization ($p < 0.05$). Comp showed 27% co-localization with LAMP-1, which was not significantly different from Wt. In addition, the expression of MR was observed in mycobacteria-infected cells at 0 h of post-infection by flow cytometry in our preliminary expreiment, showing that the expression of MR in ΔM5447-infected cells was decreased as compared to that of the Wt and Comp strains (**Supplementary Figure 6**). These data indicated that PMT deficiency enhanced phagosomal maturation in macrophages.

Transcriptome of ΔM5447-Infected Macrophages Was Analyzed

RNA sequencing is a powerful tool in analyzing the gene expression pattern of cells under specific physiological conditions

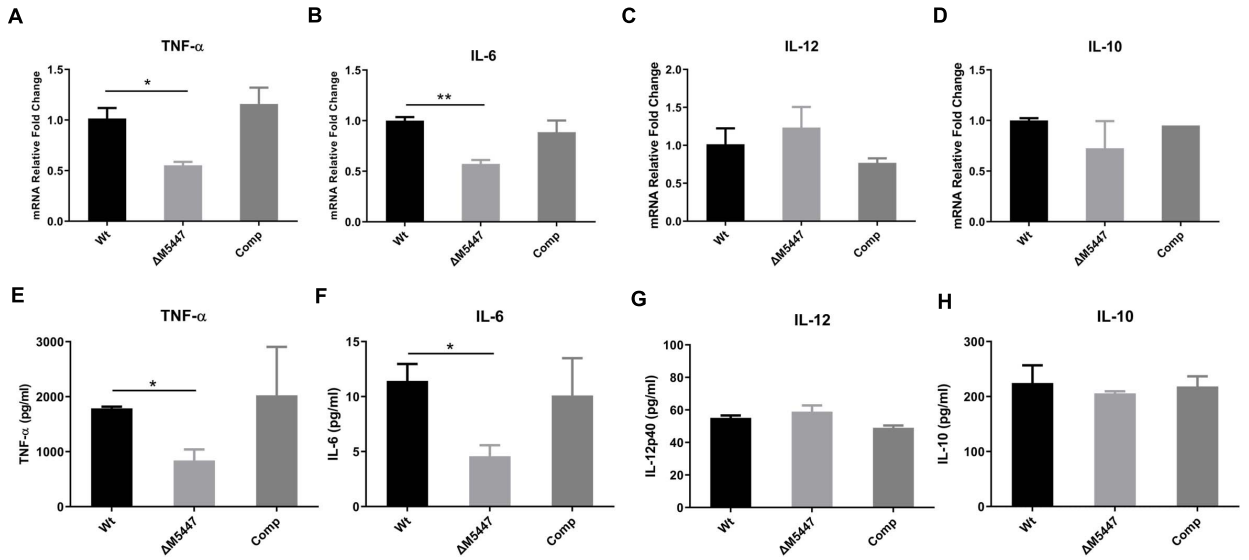

FIGURE 5 | ΔM5447 strain decreased the production of pro-inflammatory cytokines in macrophage. THP-1 macrophages were infected with Wt, ΔM5447, and Comp strains for 3 h at a MOI of 10. Total RNA of infected cells was extracted at 24 h post-infection, and the transcription levels of TNF-α **(A)**, IL-6 **(B)**, IL-12p40 **(C)**, and IL-10 **(D)** were measured by qPCR. Their mRNA levels were normalized by GAPDH mRNA. Culture supernatants were collected, and the production of TNF-α **(E)**, IL-6 **(F)** IL-12p40 **(G)**, and IL-10 **(H)** was evaluated by ELISA. Data were shown as mean ± SD of triplicate wells. Statistical analyses were performed by the method of two-tailed *t*-test (*$p < 0.05$, **$p < 0.01$).

(Nalpas et al., 2015). To further confirm the effect of PMT deficiency of *M. smegmatis* on macrophage infection, the transcriptome of THP-1 cells infected with ΔM5447 or Wt strain was analyzed by RNA sequencing at 24 h post-infection. As shown in a Volcano plot, in total, 497 DEGs were identified in ΔM5447-infected THP-1 cells using adjusted *p*-value < 0.05 as the threshold criteria as compared to the Wt-infected THP-1 cells (**Figure 8A** and **Supplementary Table 1**). Among them, 173 genes were up-regulated and 324 genes were down-regulated. ACOO4057 and EIF3C involved in transcription and translation processes were most significantly up-regulated. The expressions of TNF-α, NF-κB (NF-κB 1, NF-κB 2, NF-κB IA), and IFN-β were down-regulated in ΔM5447-infected THP-1 cells. TNF-α was most significantly down-regulated in all down-regulated genes. In addition, chemokines CXCL1, 2, 3, 8, 10, 11, and 12 were also significantly down-regulated. To better understand the effect of the ΔM5447 strain on macrophages, all DEGs were further mapped to GO and KEGG databases. Totally, 464 out of 497 DEGs were assigned to 841 GO terms, including 788 biological processes (BP), 25 cellular components (CC), and 28 molecular function (MF) terms. Typical GO terms are shown in **Figure 8B**. Most of the BP categories were related to "response to bacterium" and "positive regulation of CC movement." The two highest percentages of GO terms under the CC category were "anchoring junction" and "adherens junction." The mainly enriched MF categories were "Transcription factor binding" and "transcriptional activator activity." The top 20 enriched KEGG pathways are shown in **Figure 8C**, and some of them were involved in inflammatory response such as NF-κB pathway, TNF signaling pathway, NOD-like receptor signaling pathway, IL-17 signaling pathway, and Toll-like receptor signaling pathway. The interaction of proteins that were enriched in at least two pathways was analyzed using STRING. As shown in **Figure 8D**, among 23 genes, NF-κB, JUN, and CXCL8 played a core role in enriched pathways.

Overall, these results demonstrated that PMT deficiency reduced the intracellular survival of *M. smegmatis*, which was associated with failure of inhibiting the phagosome–lysosome fusion in macrophages. Meanwhile, lacking PMT also impaired the capability of *M. smegmatis* to stimulate inflammatory response in macrophages.

DISCUSSION

Protein O-mannosylation in Mtb is frequently found in virulence-related secreted and cell-wall lipoproteins, which plays a crucial role in Mtb pathogenicity (Birhanu et al., 2019). Despite identification of Rv1002c as PMT in Mtb and demonstration of its vital importance for the Mtb interaction with the host, the current knowledge about this enzyme remains limited and its characteristics in the process of infection have not been fully elucidated so far. Previously, we found that the *M. smegmatis MSMEG_5447* gene knockout strain (ΔM5447) failed to produce mannosylated protein Rv0431 (Deng et al., 2016). We supposed that the lack of PMT would exert profound impacts on mycobacterial interaction with host innate immune responses by regulating the O-mannosylation of proteins. In this study, the ΔM5447 strain was utilized and its complementary stain (Comp) was generated. We found that the ΔM5447 strain displayed a lower level of O-mannosylation of proteins and decreased resistance to lysozyme and acidic medium. We also

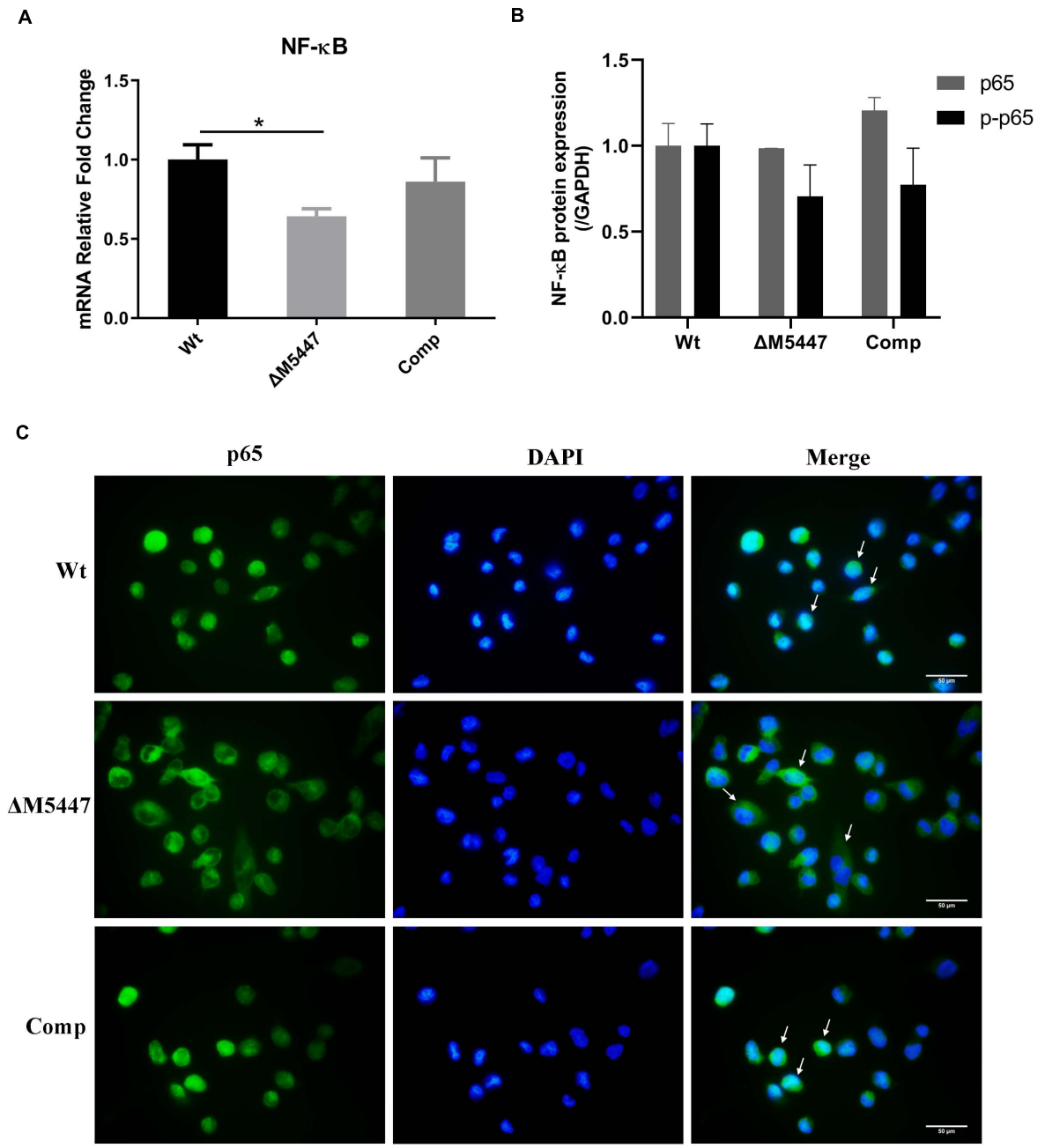

FIGURE 6 | The expression and activation of NF-κB were decreased in ΔM5447-infected macrophages. THP-1 macrophage cells were infected with Wt, ΔM5447, and Comp strains for 3 h. **(A)** The total RNA was extracted from infected THP-1 cells at 24 h post-infection, and the transcriptional level of the p65 subunit of NF-κB was evaluated by qPCR. **(B)** The total protein was extracted from infected THP-1 cells at 24 h post-infection, and the protein levels of p65 and p-p65 were determined by western blot. Densitometric analyses of images of WB have been presented. **(C)** The translocation of the p65 subunit of NF-κB from cytosol to nucleus was evaluated by fluorescence microscopy at 24 h post-infection. The cells were fixed and stained with p65 antibody and DAPI. The white arrows indicate the translocation of the p65 subunit of NF-κB. Scale bars, 50 μm. Data were shown in representative results from three independent experiments. Statistical analyses were performed by the method of two-tailed *t*-test (*$p < 0.05$).

found that the survival of ΔM5447 in THP-1 macrophage cells was impaired and its mechanism related to the failure of inhibition for phagosome–lysosome fusion.

Mycobacterium smegmatis, a non-pathogenic mycobacterium, has been widely used as a tool for the study of many aspects of mycobacterial infections. To clarify the function of proteins, it is often used as an alternative host to express proteins of pathogenic mycobacteria (Bashiri and Baker, 2015). Additionally, the results from Diaz-Silvestre et al. (2005) had shown that *M. smegmatis* could express Mtb 19-kDa antigen which was a

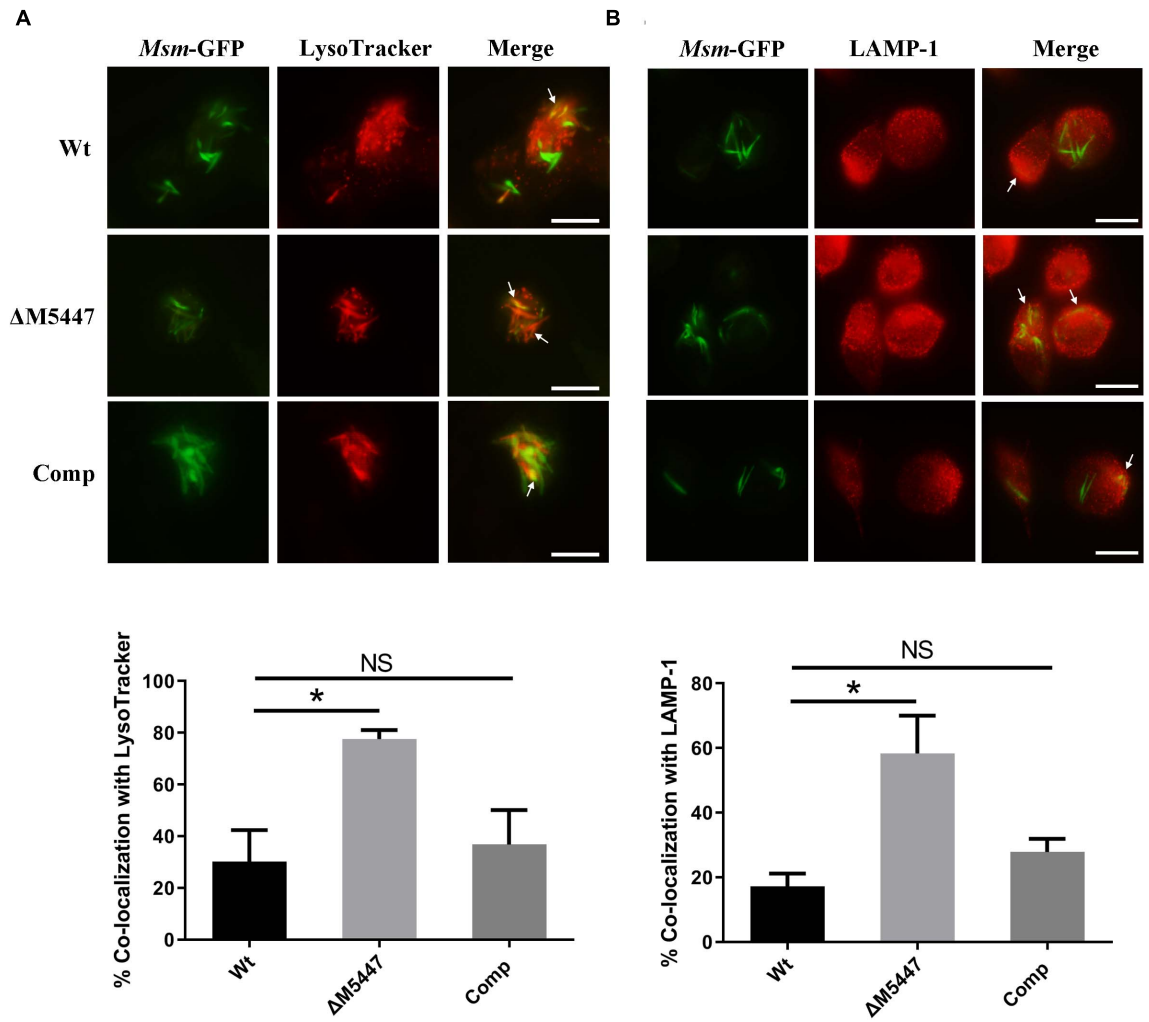

FIGURE 7 | ΔM5447 stain failed to arrest the phagosome–lysosome fusion in infected macrophages. THP-1 macrophages were infected with green fluorescence protein (GFP)-expressing Wt, ΔM5447, and Comp strains for 3 h at an MOI of 10. After 24 h of infection, cells were stained with LysoTracker Red for 30 min before fixation **(A)** or incubated with a LAMP-1 antibody **(B)**. The cells were visualized by fluorescence microscopy. The yellow color represented the co-localization of green and red fluorescence, as shown in images. The white arrows indicate the co-localization of green and red fluorescence. Scale bars, 25 μm. Quantitation of co-localization was shown as mean ± SD in at least 100 random infected cells. NS, there was no statistically significant difference between groups. Statistical analyses were performed by the method of two-tailed *t*-test (*$p < 0.05$).

glycoprotein with O-mannosylation modification and promoted bacterial adhesion to the macrophage *via* mannosyl residues. It indicated that *M. smegmatis* has the same glycosylation system as Mtb and can also be used to investigate recognition and interaction with the host cells. Furthermore, PMT in *M. smegmatis* shared 75% similarity with Mtb and have conserved residues in active sites. In our study, we found that the growth of ΔM5447 was different in LBT and 7H9 broth. We speculated that different growth patterns of the ΔM5447 strain may be due to different nutritional components. As Liu et al. reported, the Rv1002c mutant was almost completely unable to grow in 7H9 medium supplemented with dextrose only but just displayed a slight growth delay in ADC-enriched 7H9 medium. In order to eliminate the difference of the growth rate, the Wt, ΔM5447, and Comp strains were cultured in LBT medium in the following investigations. Previous studies have reported that many glycoproteins and lipoglycoproteins are either CW-associated or surface-exported proteins and depend on sec-translocation. Indeed, in our study, the loss of PMT dramatically reduced the level of O-mannosylation of proteins with 25–40 kD in CW and CM fractions of *M. smegmatis* (Birhanu et al., 2019). Next, we demonstrated that O-mannosyltransferase is dispensable for *M. smegmatis* survival during infection of macrophages since the intracellular survival of ΔM5447 was impaired during THP-1 infection. This finding is consistent with the reports that inactivation of Rv1002c largely reduced the intracellular survival of Mtb in THP-1 macrophage cells (Liu et al., 2013). In our study, the phagocytosis rate between WT and PMT-deficient *M. smegmatis* was similar. We speculated that it was due to the combined effect of pathogen-associated molecular

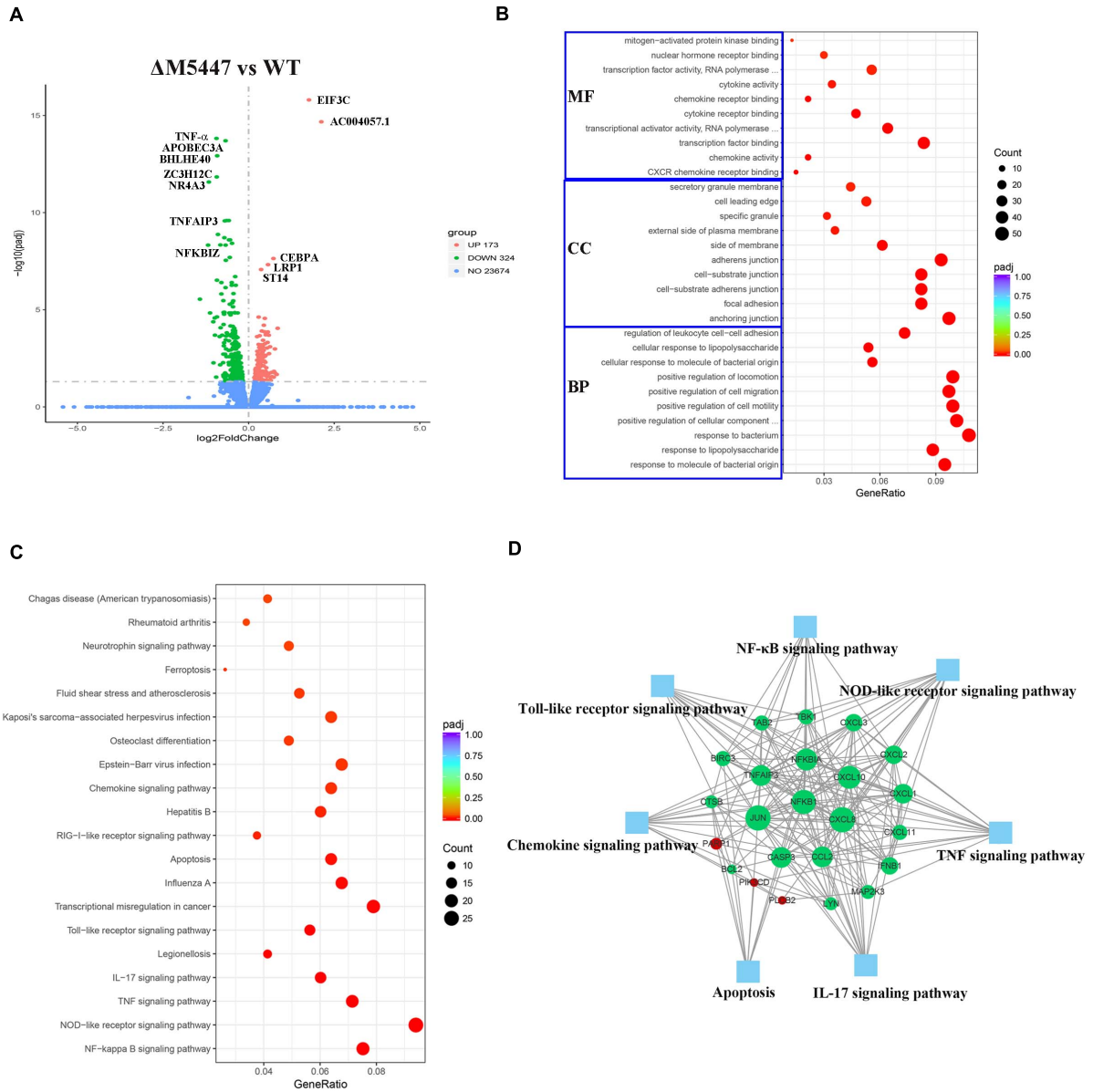

FIGURE 8 | Transcriptional profiles of macrophages during mycobacterial infection. THP-1 macrophage cells were infected with Wt and ΔM5447 strains for 3 h, and the total RNA of THP-1 cells was extracted at 24 h post-infection. **(A)** Volcano plots of differentially expressed genes (DEGs) in ΔM5447-infected THP-1 cells as compared to the Wt-infected THP-1 cells. The name of DEGs was annotated next to the dots. Blue, green, and red splashes represent genes without significant change, significant down-regulation, and significant up-regulation, respectively. **(B)** Scatter plot of GO functional classification of the DEGS. The distributions are summarized in three main categories: biological process (BP), molecular function (MF), and cellular component (CC). GeneRatio is the ratio of the DEG number to the total gene number in each category. The color and size of the dot represent the range of the adjusted *p*-value and the number of DEGs mapped to the categories. The top 10 functions in each category are shown in the figure. **(C)** Scatter plot of enriched KEGG pathways. GeneRatio is the ratio of the DEG number to the total gene number in a certain pathway. The color and size of the dot represent the range of the adjusted *p*-value and the number of DEGs mapped to the indicated pathways, respectively. The top 20 enriched pathways are shown in the data. **(D)** Interaction of key genes that presented in two pathways at least were analyzed by STRING and shown by Cytoscape software. Green and red nodes represent the down- and up-regulated genes, respectively. The size of the node indicated the core role of the gene. Blue squares represent the KEGG pathways.

pattern recognition receptors. The lack of O-mannosylation in mycobacteria affects not only the recognition between O-mannose residues with MR but also the recognition between glycoproteins and their corresponding receptors. Several studies revealed that some glycoproteins recognize TLR2 which also influenced the phagocytosis (Jung et al., 2006; Pecora et al., 2006; Drage et al., 2010). Additionally, it has been reported that the lack of O-mannosylation can affect the localization of proteins, and thus the change of localization of proteins will affect the phagocytosis (VanderVen et al., 2005; Arya et al., 2013).

Generally, as soon as Mtb enters into host cells, it will be exposed to various environmental or physiological stresses such as reactive oxygen or nitrogen intermediates, low pH, hypoxia, and alveolar surfactant (Manganelli et al., 2004). Here, our results demonstrated that the tolerance of ΔM5447 to lysozyme and acidic condition was significantly reduced. It has been reported that PMT deficiency increased CW permeability of *Mycobacterium abscessus* leading to the reduction in anti-tuberculosis drugs and lysozyme tolerance (Becker et al., 2017). Consistently, CW permeability of ΔM5447 was also increased in our study, indicating that the tolerant impairment of ΔM5447 might due to the increased CW permeability.

Macrophages play an essential role in the recognition, digestion, and degradation of invading pathogens (Queval et al., 2017). Mtb could utilize multiple strategies to survive and replicate within macrophages such as evasion of recognition and phagocytosis, attenuation of macrophage antigen presentation, interference with vesicular membrane trafficking, and manipulation of innate immune responses (Liu et al., 2017). By arresting the phagosome–lysosome fusion, Mtb could evade degradation and survive in macrophages, interfering cell immune defense (Carranza and Chavez-Galan, 2018). For example, protein tyrosine phosphatase PtpA secreted by Mtb could dephosphorylate the protein VPS33B of infected macrophages, leading to an inhibition of phagosome–lysosome fusion (Bach et al., 2008). In our study, we found that PMT could inhibit phagosome maturation as the phagosome containing ΔM5447 increased the co-localization with lysosome and LAMP-1. Our preliminary data showed that the expression of MR was reduced in ΔM5447-infected cells. Previous studies reported that glycolipoproteins Pst-S1 and LpqH as adhesin bound to the MR receptor promoting phagocytosis (Diaz-Silvestre et al., 2005; Esparza et al., 2015). Additionally, MR activation by glycopeptidolipids and ManLAM of Mtb was associated with arresting phagosome–lysosome fusion (Kang et al., 2005; Sweet et al., 2010). Therefore, we speculate that PMT inhibits phagosome–lysosome fusion in a mannose receptor (MR)-dependent manner.

Alonso et al. (2017) proposed that induction of pro-inflammatory response was partially responsible for the impaired survival of the Mtb PMT mutant in macrophages. Interestingly, our qPCR and ELISA data showed that inactivation of PMT in *M. smegmatis* decreased the production of IL-6 and TNF-α in macrophages. Our data also showed that ΔM5447 decreased the translocation of the p65 subunit to the nucleus and reduced the activation of NF-κB in macrophages. Consistently, our transcriptomic analyses revealed that inflammatory response-related pathways were significantly down-regulated in ΔM5447-infected macrophages. NF-κB plays a crucial role in inflammatory responses, immunity, apoptosis, and host defense, and its activation can induce a large number of inflammatory genes such as iNOS, TNF-α, and IL-6 (Pahl, 1999; Chen et al., 2017). We considered that production of pro-inflammatory cytokines was reduced in an NF-κB-dependent manner in ΔM5447-infected macrophages. The reduction of pro-inflammatory cytokines may be because of loss of protein O-mannosylation, affecting the TLR2-mediated pro-inflammatory response. It was reported that many glycolipoproteins were ligands of TLR2, such as LpqH, LprG, PstS-1, MPT83, and LprA (Noss et al., 2001; Gehring et al., 2004; Pecora et al., 2006; Sanchez et al., 2009; Wang et al., 2017). Based on the data we got so far, we are not clear whether the reduced pro-inflammatory response caused impairment of intracellular survival or not. The role of NF-κB in host defense may depend on both microbial features and host species. For example, Bai et al. (2013) have reported that inhibition of NF-κB activation decreased the intracellular survival of the mycobacterium in macrophage by promoting the apoptosis and autophagy in THP-1 cells.

In summary, our studies revealed that PMT was necessary for *M. smegmatis* survival within the macrophage and played a key role in arresting the phagosome maturation. We also found that the ΔM5447 mutant failed to activate the NF-κB pathway and subsequent pro-inflammatory response in macrophages. It is worth mentioning that PMT increased the tolerance of *M. smegmatis* to acidic stress *in vitro*. It makes us speculate that the protein O-mannosylation may also contribute to the survival of *M. smegmatis* in acidic phagolysosome pH. More detailed studies to clarify this mechanism are still needed. Since PMT is a PMT controlling the level of protein O-mannosylation, our study provides a new perspective to understand the impact of O-mannosylation of proteins in host–pathogen interaction.

DATA AVAILABILITY STATEMENT

The datasets presented in this study can be found in online repositories. The names of the repository/repositories and accession number(s) can be found below: https://www.ncbi.nlm.nih.gov/geo/, GSE128970.

AUTHOR CONTRIBUTIONS

YM, LJ, and SS designed the experiments, interpreted the results, and wrote the manuscript. LJ, SY, and AT performed the experiments and acquired and analyzed the data. All authors reviewed and discussed the manuscript.

FUNDING

This study was supported by the National Natural Science Foundation of China (81930112 and 81573469) and the Liaoning Provincial Program for Top Discipline of Basic Medical Sciences.

ACKNOWLEDGMENTS

We thank Wenzhe Li for his assistance with ConA lectin blot.

SUPPLEMENTARY MATERIAL

The Supplementary Material for this article can be found online at: https://www.frontiersin.org/articles/10.3389/fmicb.2021.657726/full#supplementary-material

REFERENCES

Abrahams, K. A., and Besra, G. S. (2016). Mycobacterial cell wall biosynthesis: a multifaceted antibiotic target. *Parasitology* 145, 116–133. doi: 10.1017/S0031182016002377

Alonso, H., Parra, J., Malaga, W., Payros, D., Liu, C. F., Berrone, C., et al. (2017). Protein O-mannosylation deficiency increases LprG-associated lipoarabinomannan release by *Mycobacterium tuberculosis* and enhances the TLR2-associated inflammatory response. *Sci. Rep.* 7:7913. doi: 10.1038/s41598-017-08489-7

Arya, S., Sethi, D., Singh, S., Hade, M. D., Singh, V., Raju, P., et al. (2013). Truncated hemoglobin, HbN, is post-translationally modified in *Mycobacterium tuberculosis* and modulates host-pathogen interactions during intracellular infection. *J. Biol. Chem.* 288, 29987–29999. doi: 10.1074/jbc.M113.507301

Bach, H., Papavinasasundaram, K. G., Wong, D., Hmama, Z., and Av-Gay, Y. (2008). *Mycobacterium tuberculosis* virulence is mediated by PtpA dephosphorylation of human vacuolar protein sorting 33B. *Cell Host Microbe* 3, 316–322. doi: 10.1016/j.chom.2008.03.008

Bai, X., Feldman, N. E., Chmura, K., Ovrutsky, A. R., Su, W. L., Griffin, L., et al. (2013). Inhibition of nuclear factor-kappa B activation decreases survival of *Mycobacterium tuberculosis* in human macrophages. *PLoS One* 8:e61925. doi: 10.1371/journal.pone.0061925

Bashiri, G., and Baker, E. N. (2015). Production of recombinant proteins in Mycobacterium smegmatis for structural and functional studies. *Protein Soc.* 24, 1–10. doi: 10.1002/pro.2584

Becker, K., Haldimann, K., Selchow, P., Reinau, L. M., Dal Molin, M., and Sander, P. (2017). Lipoprotein glycosylation by protein-O-mannosyltransferase (MAB_1122c) contributes to low cell envelope permeability and antibiotic resistance of Mycobacterium abscessus. *Front. Microbiol.* 8:2123. doi: 10.3389/fmicb.2017.02123

Birhanu, A. G., Yimer, S. A., Kalayou, S., Riaz, T., Zegeye, E. D., Holm-Hansen, C., et al. (2019). Ample glycosylation in membrane and cell envelope proteins may explain the phenotypic diversity and virulence in the *Mycobacterium tuberculosis* complex. *Sci. Rep.* 9:2927. doi: 10.1038/s41598-019-39654-9

Blokpoel, M. C., Murphy, H. N., O'Toole, R., Wiles, S., Runn, E. S., Stewart, G. R., et al. (2005). Tetracycline-inducible gene regulation in mycobacteria. *Nucleic Acids Res.* 33:e22. doi: 10.1093/nar/gni023

Carranza, C., and Chavez-Galan, L. (2018). Several routes to the same destination: inhibition of phagosome-lysosome fusion by *Mycobacterium tuberculosis*. *Am. J. Med. Sci.* 357, 184–194. doi: 10.1016/j.amjms.2018.12.003

Chen, Y., Ji, N., Pan, S., Zhang, Z., Wang, R., Qiu, Y., et al. (2017). Roburic acid suppresses NO and IL-6 production via targeting NF-kappaB and MAPK pathway in RAW264.7 cells. *Inflammation* 40, 1959–1966. doi: 10.1007/s10753-017-0636-z

Deng, G., Zhang, F., Yang, S., Kang, J., Sha, S., and Ma, Y. (2016). *Mycobacterium tuberculosis* Rv0431 expressed in Mycobacterium smegmatis, a potentially mannosylated protein, mediated the immune evasion of RAW 264.7 macrophages. *Microb. Pathog.* 100, 285–292. doi: 10.1016/j.micpath.2016.10.013

Deng, G., Zhang, W., Ji, N., Zhai, Y., Shi, X., Liu, X., et al. (2020). Identification of secreted O-Mannosylated proteins from BCG and characterization of immunodominant antigens BCG_0470 and BCG_0980. *Front. Microbiol.* 11:407. doi: 10.3389/fmicb.2020.00407

Diaz-Silvestre, H., Espinosa-Cueto, P., Sanchez-Gonzalez, A., Esparza-Ceron, M. A., Pereira-Suarez, A. L., Bernal-Fernandez, G., et al. (2005). The 19-kDa antigen of *Mycobacterium tuberculosis* is a major adhesin that binds the mannose receptor of THP-1 monocytic cells and promotes phagocytosis of mycobacteria. *Microb. Pathog.* 39, 97–107. doi: 10.1016/j.micpath.2005.06.002

Drage, M. G., Tsai, H. C., Pecora, N. D., Cheng, T. Y., Arida, A. R., Shukla, S., et al. (2010). *Mycobacterium tuberculosis* lipoprotein LprG (Rv1411c) binds triacylated glycolipid agonists of Toll-like receptor 2. *Nat. Struct. Mol. Biol.* 17, 1088–1095. doi: 10.1038/nsmb.1869

Edgar, R., Domrachev, M., and Lash, A. E. (2002). Gene Expression Omnibus: NCBI gene expression and hybridization array data repository. *Nucleic Acids Res.* 30, 207–210.

Esparza, M., Palomares, B., Garcia, T., Espinosa, P., Zenteno, E., and Mancilla, R. (2015). PstS-1, the 38-kDa *Mycobacterium tuberculosis* glycoprotein, is an adhesin, which binds the macrophage mannose receptor and promotes phagocytosis. *Scand. J. Immunol.* 81, 46–55. doi: 10.1111/sji.12249

Espitia, C., Servin-Gonzalez, L., and Mancilla, R. (2010). New insights into protein O-mannosylation in actinomycetes. *Mol. Biosyst.* 6, 775–781. doi: 10.1039/b916394h

Gehring, A. J., Dobos, K. M., Belisle, J. T., Harding, C. V., and Boom, W. H. (2004). *Mycobacterium tuberculosis* LprG (Rv1411c): a novel TLR-2 ligand that inhibits human macrophage class II MHC antigen processing. *J. Immunol.* 173, 2660–2668. doi: 10.4049/jimmunol.173.4.2660

Gibbons, H. S., Wolschendorf, F., Abshire, M., Niederweis, M., and Braunstein, M. (2007). Identification of two *Mycobacterium smegmatis* lipoproteins exported by a SecA2-dependent pathway. *J. Bacteriol.* 189, 5090–5100. doi: 10.1128/JB.00163-07

Gonzalez-Zamorano, M., Mendoza-Hernandez, G., Xolalpa, W., Parada, C., Vallecillo, A. J., Bigi, F., et al. (2009). *Mycobacterium tuberculosis* glycoproteomics based on ConA-lectin affinity capture of mannosylated proteins. *J. Proteome Res.* 8, 721–733. doi: 10.1021/pr800756a

Herrmann, J. L., O'Gaora, P., Gallagher, A., Thole, J. E., and Young, D. B. (1996). Bacterial glycoproteins: a link between glycosylation and proteolytic cleavage of a 19 kDa antigen from *Mycobacterium tuberculosis*. *EMBO J.* 15, 3547–3554.

Horn, C., Namane, A., Pescher, P., Riviere, M., Romain, F., Puzo, G., et al. (1999). Decreased capacity of recombinant 45/47-kDa molecules (Apa) of *Mycobacterium tuberculosis* to stimulate T lymphocyte responses related to changes in their mannosylation pattern. *J. Biol. Chem.* 274, 32023–32030.

Jung, S. B., Yang, C. S., Lee, J. S., Shin, A. R., Jung, S. S., Son, J. W., et al. (2006). The mycobacterial 38-kilodalton glycolipoprotein antigen activates the mitogen-activated protein kinase pathway and release of proinflammatory cytokines through Toll-like receptors 2 and 4 in human monocytes. *Infect. Immun.* 74, 2686–2696. doi: 10.1128/IAI.74.5.2686-2696.2006

Kang, P. B., Azad, A. K., Torrelles, J. B., Kaufman, T. M., Beharka, A., Tibesar, E., et al. (2005). The human macrophage mannose receptor directs *Mycobacterium tuberculosis* lipoarabinomannan-mediated phagosome biogenesis. *J. Exp. Med.* 202, 987–999. doi: 10.1084/jem.20051239

Liu, C. F., Tonini, L., Malaga, W., Beau, M., Stella, A., Bouyssie, D., et al. (2013). Bacterial protein-O-mannosylating enzyme is crucial for virulence of *Mycobacterium tuberculosis*. *Proc. Natl. Acad. Sci.U.S.A.* 110, 6560–6565. doi: 10.1073/pnas.1219704110

Liu, C. H., Liu, H., and Ge, B. (2017). Innate immunity in tuberculosis: host defense vs pathogen evasion. *Cell. Mol. Immunol.* 14, 963–975. doi: 10.1038/cmi.2017.88

Loke, I., Kolarich, D., Packer, N. H., and Thaysen-Andersen, M. (2016). Emerging roles of protein mannosylation in inflammation and infection. *Mol. Aspects Med.* 51, 31–55. doi: 10.1016/j.mam.2016.04.004

Manganelli, R., Proveddi, R., Rodrigue, S., Beaucher, J., Gaudreau, L., and Smith, I. (2004). Factors and global gene regulation in *Mycobacterium tuberculosis*. *J. Bacteriol.* 186, 895–902. doi: 10.1128/jb.186.4.895-902.2004

Mehaffy, C., Belisle, J. T., and Dobos, K. M. (2019). Mycobacteria and their sweet proteins: an overview of protein glycosylation and lipoglycosylation in *M. tuberculosis*. *Tuberculosis* 115, 1–13. doi: 10.1016/j.tube.2019.01.001

Nalpas, N. C., Magee, D. A., Conlon, K. M., Browne, J. A., Healy, C., McLoughlin, K. E., et al. (2015). RNA sequencing provides exquisite insight into the manipulation of the alveolar macrophage by tubercle *Bacilli*. *Sci. Rep.* 5:13629. doi: 10.1038/srep13629

Nandakumar, S., Kannanganat, S., Dobos, K. M., Lucas, M., Spencer, J. S., Fang, S. N., et al. (2013). O-mannosylation of the *Mycobacterium tuberculosis* adhesin apa is crucial for T cell antigenicity during infection but is expendable for protection. *PLoS Pathog.* 9:e1003705. doi: 10.1371/journal.ppat.1003705

Noss, E. H., Pai, R. K., Sellati, T. J., Radolf, J. D., Belisle, J., Golenbock, D. T., et al. (2001). Toll-like receptor 2-dependent inhibition of macrophage class II MHC expression and antigen processing by 19-kDa lipoprotein of *Mycobacterium tuberculosis*. *J. Immunol.* 167, 910–918. doi: 10.4049/jimmunol.167.2.910

Pahl, H. L. (1999). Activators and target genes of Rel/NF-kappaB transcription factors. *Oncogene* 18, 6853–6866. doi: 10.1038/sj.onc.1203239

Palomino, J. C., Martin, A., Camacho, M., Guerra, H., Swings, J., and Portaels, F. (2002). Resazurin microtiter assay plate: simple and inexpensive method for detection of drug resistance in *Mycobacterium tuberculosis*. *Antimicrobial. Agents Chemother.* 46, 2720–2722.

Pecora, N. D., Gehring, A. J., Canaday, D. H., Boom, W. H., and Harding, C. V. (2006). *Mycobacterium tuberculosis* LprA Is a lipoprotein agonist of TLR2 that regulates innate immunity and APC function. *J. Immunol.* 177, 422–429. doi: 10.4049/jimmunol.177.1.422

Pitarque, S., Herrmann, J. L., Duteyrat, J. L., Jackson, M., Stewart, G. R., Lecointe, F., et al. (2005). Deciphering the molecular bases of *Mycobacterium tuberculosis* binding to the lectin DC-SIGN reveals an underestimated complexity. *Biochem. J.* 392(Pt 3), 615–624. doi: 10.1042/BJ20050709

Queval, C. J., Brosch, R., and Simeone, R. (2017). The macrophage: a disputed fortress in the battle against *Mycobacterium tuberculosis*. *Front. Microbiol.* 8:2284. doi: 10.3389/fmicb.2017.02284

Ragas, A., Roussel, L., Puzo, G., and Riviere, M. (2007). The *Mycobacterium tuberculosis* cell-surface glycoprotein apa as a potential adhesin to colonize target cells via the innate immune system pulmonary C-type lectin surfactant protein A. *J. Biol. Chem.* 282, 5133–5142. doi: 10.1074/jbc.M610183200

Rolain, T., Bernard, E., Beaussart, A., Degand, H., Courtin, P., Egge-Jacobsen, W., et al. (2013). O-Glycosylation as a novel control mechanism of peptidoglycan hydrolase activity. *J. Biol. Chem.* 288, 22233–22247. doi: 10.1074/jbc.M113.470716

Sanchez, A., Espinosa, P., Esparza, M. A., Colon, M., Bernal, G., and Mancilla, R. (2009). *Mycobacterium tuberculosis* 38-kDa lipoprotein is apoptogenic for human monocyte-derived macrophages. *Scand. J. Immunol.* 69, 20–28. doi: 10.1111/j.1365-3083.2008.02193.x

Sartain, M. J., and Belisle, J. T. (2009). N-Terminal clustering of the O-glycosylation sites in the *Mycobacterium tuberculosis* lipoprotein SodC. *Glycobiology* 19, 38–51. doi: 10.1093/glycob/cwn102

Sweet, L., Singh, P. P., Azad, A. K., Rajaram, M. V., Schlesinger, L. S., and Schorey, J. S. (2010). Mannose receptor-dependent delay in phagosome maturation by Mycobacterium avium glycopeptidolipids. *Infect. Immun.* 78, 518–526. doi: 10.1128/IAI.00257-09

Triccas, J. A., and Ryan, A. A. (2009). Heterologous expression of genes in mycobacteria. *Methods Mol. Biol.* 465, 243–253. doi: 10.1007/978-1-59745-207-6_16

Tucci, P., Portela, M., Chetto, C. R., Gonzalez-Sapienza, G., and Marin, M. (2020). Integrative proteomic and glycoproteomic profiling of *Mycobacterium tuberculosis* culture filtrate. *PLoS One* 15:e0221837. doi: 10.1371/journal.pone.0221837

Turner, J., and Torrelles, J. B. (2018). Mannose-capped lipoarabinomannan in *Mycobacterium tuberculosis* pathogenesis. *Pathog. Dis.* 76:fty026. doi: 10.1093/femspd/fty026

Vandal, O. H., Roberts, J. A., Odaira, T., Schnappinger, D., Nathan, C. F., and Ehrt, S. (2009). Acid-susceptible mutants of *Mycobacterium tuberculosis* share hypersusceptibility to cell wall and oxidative stress and to the host environment. *J. Bacteriol.* 191, 625–631. doi: 10.1128/JB.00932-08

VanderVen, B. C., Harder, J. D., Crick, D. C., and Belisle, J. T. (2005). Export-mediated assembly of mycobacterial glycoproteins parallels eukaryotic pathways. *Science* 309, 941–943. doi: 10.1126/science.1114347

Vinod, V., Vijayrajratnam, S., Vasudevan, A. K., and Biswas, R. (2020). The cell surface adhesins of *Mycobacterium tuberculosis*. *Microbiol. Res.* 232:126392. doi: 10.1016/j.micres.2019.126392

Wang, L., Zuo, M., Chen, H., Liu, S., Wu, X., Cui, Z., et al. (2017). *Mycobacterium tuberculosis* lipoprotein MPT83 induces apoptosis of infected macrophages by activating the TLR2/p38/COX-2 signaling pathway. *J. Immunol.* 198, 4772–4780. doi: 10.4049/jimmunol.1700030

WHO (2020). *Global Tuberculosis Report 2020*. Geneva: WHO.

Conflict of Interest: The authors declare that the research was conducted in the absence of any commercial or financial relationships that could be construed as a potential conflict of interest.

frontiers in Microbiology

REVIEW
published: 16 July 2021
doi: 10.3389/fmicb.2021.712538

Unveiling the Sugary Secrets of *Plasmodium* Parasites

Felix Goerdeler[1,2], *Peter H. Seeberger*[1,2] *and Oren Moscovitz*[1]*

[1] Department of Biomolecular Systems, Max Planck Institute of Colloids and Interfaces, Potsdam, Germany, [2] Institute of Chemistry and Biochemistry, Freie Universität Berlin, Berlin, Germany

Plasmodium parasites cause malaria disease, one of the leading global health burdens for humanity, infecting hundreds of millions of people each year. Different glycans on the parasite and the host cell surface play significant roles in both malaria pathogenesis and host defense mechanisms. So far, only small, truncated *N*- and *O*-glycans have been identified in *Plasmodium* species. In contrast, complex glycosylphosphatidylinositol (GPI) glycolipids are highly abundant on the parasite's cell membrane and are essential for its survival. Moreover, the parasites express lectins that bind and exploit the host cell surface glycans for different aspects of the parasite life cycle, such as adherence, invasion, and evasion of the host immune system. In parallel, the host cell glycocalyx and lectin expression serve as the first line of defense against *Plasmodium* parasites and directly dictate susceptibility to Plasmodium infection. This review provides an overview of the glycobiology involved in *Plasmodium*-host interactions and its contribution to malaria pathogenesis. Recent findings are presented and evaluated in the context of potential therapeutic exploitation.

Keywords: *Plasmodium*, glycans, glycobiology, glycosylphosphatidylinositol (GPI), O-glycans, malaria, glycocalyx, host defense

OPEN ACCESS

Edited by:
Fabrizio Chiodo, National Research Council, Consiglio Nazionale delle Ricerche, Italy

Reviewed by:
Marcin Czerwiński, Hirszfeld Institute of Immunology and Experimental Therapy, Polish Academy of Sciences, Poland
Rafael B. Polidoro, Indiana University Bloomington, United States

***Correspondence:**
Oren Moscovitz
oren.moscovitz@mpikg.mpg.de

Specialty section:
This article was submitted to Infectious Diseases, a section of the journal Frontiers in Microbiology

Received: *20 May 2021*
Accepted: *18 June 2021*
Published: *16 July 2021*

Citation:
Goerdeler F, Seeberger PH and Moscovitz O (2021) Unveiling the Sugary Secrets of Plasmodium Parasites. Front. Microbiol. 12:712538. doi: 10.3389/fmicb.2021.712538

INTRODUCTION

Malaria, the disease caused by the parasite *Plasmodium*, kills approximately 400,000 people each year, the majority of which are children under the age of five (World Health Organization [WHO], 2020). While the number of cases declined for many years, a result of effective prevention and therapy, recent years have witnessed a surge in case numbers due to increasing drug resistance of the parasite and rapid population growth in the most severely affected countries (World Health Organization [WHO], 2020). *Plasmodium* species generally display high specificity for their respective host and among the five *Plasmodium* species that infect humans, *Plasmodium falciparum* and *Plasmodium vivax* are by far the most common and lethal for humans (World Health Organization [WHO], 2020). Other *Plasmodium* species infest non-human hosts, including primates, rodents, birds and even reptiles with varying degrees of host specificity. For instance, *Plasmodium knowlesi* infects both macaques and humans, showing an unusual degree of host promiscuity, while *Plasmodium reichenowi* only infects chimpanzees. In mice, *Plasmodium berghei, Plasmodium yoelii,* and *Plasmodium chabaudi* are the most relevant species that have been extensively used as model organisms in malaria research (De Niz and Heussler, 2018).

Plasmodium parasites have a complex life cycle involving transmission by an insect vector to the human host where parasites at the so-called sporozoite stage first infect the liver and then develop into the blood stages of the parasite (Maier et al., 2019). Inside the red blood cells (RBCs), parasites mature from ring to trophozoite to schizont stage. At this stage, the RBC ruptures, and merozoites emerge to start the next round of RBC infection. A small number of parasites leave the cycle to form gametocytes that are taken up by the insect vector during a blood meal. Inside the vector, sexual reproduction of the parasite takes place, and ookinetes develop into oocysts, while traversing the mosquito midgut. Upon oocyst rupture, sporozoites are released again and invade the mosquito salivary glands to infect the next host (Maier et al., 2019).

Glycans denote the carbohydrate part of a glycoprotein or glycolipid and consist of monosaccharides linked via glycosidic bonds (Varki et al., 2017). At various life stages of the parasite, glycans present on the surface of parasites and host cells engage in host-parasite interactions (summarized in **Table 1**). Glycosylphosphatidylinositol (GPI) glycolipids, produced by the parasite in large quantities, contribute to severe anemia and hyperinflammation in the host (Boutlis et al., 2005; Nebl et al., 2005). *Plasmodium* also expresses small, truncated *N/O*-glycosylations on its surface proteins (Bushkin et al., 2010; Kupferschmid et al., 2017). However, the function of GPIs and *N/O*-glycosylations for the parasite is still being debated. At the host surface, sialic acid-containing *N/O*-glycans and glycosaminoglycans (GAGs) studied in detail because they are used by *Plasmodium* as docking sites for invasion and cytoadherence (Orlandi et al., 1992; Pancake et al., 1992; Frevert et al., 1993; Rogerson et al., 1995). In addition, the host glycocalyx and several glycan-binding host proteins, so-called lectins, play a critical role in host defense and malaria susceptibility (Barragan et al., 2000; Hempel et al., 2014; Introini et al., 2018).

The complexity of glycan–protein interactions at the *Plasmodium*-host interface is further increased by the large number of different *Plasmodium* and host species and most previous work examed the glycobiology of a few selected *Plasmodium* species such as *P. falciparum* or *P. berghei,* further hampering general conclusions. In this article, we mostly focus on *Plasmodium* species that infest humans and rodents. We review recent publications on the glycobiology aspects of the *Plasmodium* life cycle with the aim to disentangle the glycan interactions at the *Plasmodium*-host interface and to point out possible intervention sites for malaria therapy.

Plasmodium GLYCOSYLATIONS

Biosynthesis and Metabolism

The common precursors for glycan biosynthesis are sugar nucleotides from which monosaccharides are transferred to nascent glycan chains, proteins or lipids by glycosyltransferases (Varki et al., 2017). Sugar nucleotides generally consist of a nucleotide, such as UDP, GDP, CMP, or CDP connected to a monosaccharide. Metabolic labeling and liquid-chromatography mass-spectrometry helped to identify pools of UDP-GlcNAc, UDP-Glc, UDP-Gal, GDP-Man and GDP-Fuc in *Plasmodium*. The size of these pools increased from ring to schizont stage (Sanz et al., 2013; López-Gutiérrez et al., 2017; **Figure 1**). Interestingly, UDP-Glc, UDP-GlcNAc and GDP-Man amounts were significantly higher in the sexual stages of the parasite compared to the asexual blood stages (**Figure 1**), suggesting that certain glycosylations are required for sexual reproduction (López-Gutiérrez et al., 2017).

GDP-Fuc is mostly formed through bioconversion of GDP-Man but is not essential for parasite growth (Sanz et al., 2013; Sanz et al., 2016). In contrast, UDP-GlcNAc is essential because a gene knockout of *Pf* GNA1 (*P. falciparum* glucosamine-phosphate *N*-acetyltransferase), involved in the pathway of UDP-GlcNAc production, causes growth arrest of *Plasmodium* at the late trophozoite stage (Chi et al., 2020). Parasite growth is rescued by supplementing GlcNAc, implying that free GlcNAc can be taken up from external sources (Chi et al., 2020).

Compared to mammals, *P. falciparum* evolved a more promiscuous hexose transporter that imports both glucose and fructose for glycan biosynthesis (Qureshi et al., 2020). This observation is especially interesting considering that glucose uptake is a rate-limiting step during glycolysis, the main energy source for *P. falciparum* (Van Niekerk et al., 2016).

Sugar nucleotide trafficking and hexosamine biosynthesis also play important roles in drug targeting and resistance. For instance, a mutation in the UDP-Gal transporter gene protects *P. falciparum* against imidazolopiperazines, a new class of antimalarial compounds currently examined in clinical trials (Lim et al., 2016). However, this resistance mechanism causes a decrease in parasite fitness as mutants grow more slowly than the wildtype in the absence of the drug (Lim et al., 2016).

On the other hand, inhibition of glucosamine-6-phosphate production in the UDP-GlcNAc synthesis pathway with the drug 6-diazo-5-oxo-L-norleucine (DON) leads to growth arrest at ring or late trophozoite stages, depending on the drug's concentration. *P. berghei*-infected mice survived longer when treated with DON compared to untreated mice, thus indicating an essential role of the sugar nucleotide for *Plasmodium* viability. Notably, the protection was lost in mice co-injected with GlcN as GlcN is taken up by the parasite directly and converted to GlcNAc, thereby bypassing the DON-inhibited UDP-GlcNAc synthesis pathway (Gomes et al., 2019).

Glycosylphosphatidylinositols

It was discovered more than 20 years ago that GPI glycolipids are the most abundant glycans on the *P. falciparum* surface, and many GPI-anchored proteins were identified as essential for *P. falciparum* survival (Gerold et al., 1994; Gowda et al., 1997). In addition to their protein-bound form, a major portion of *Plasmodium* GPIs remains devoid of protein (Gerold et al., 1994; **Figure 1**). These free GPIs contribute to the severity of malaria symptoms and act as proinflammatory toxins, e.g., by inducing TNFα production in macrophages (Schofield and Hackett, 1993). *Plasmodium* GPIs have a conserved core, consisting of a phosphatidylinositol, whose fatty acid chains integrate into the plasma membrane, and an oligosaccharide, composed of one glucosamine (GlcN) followed by three or four mannose (Man)

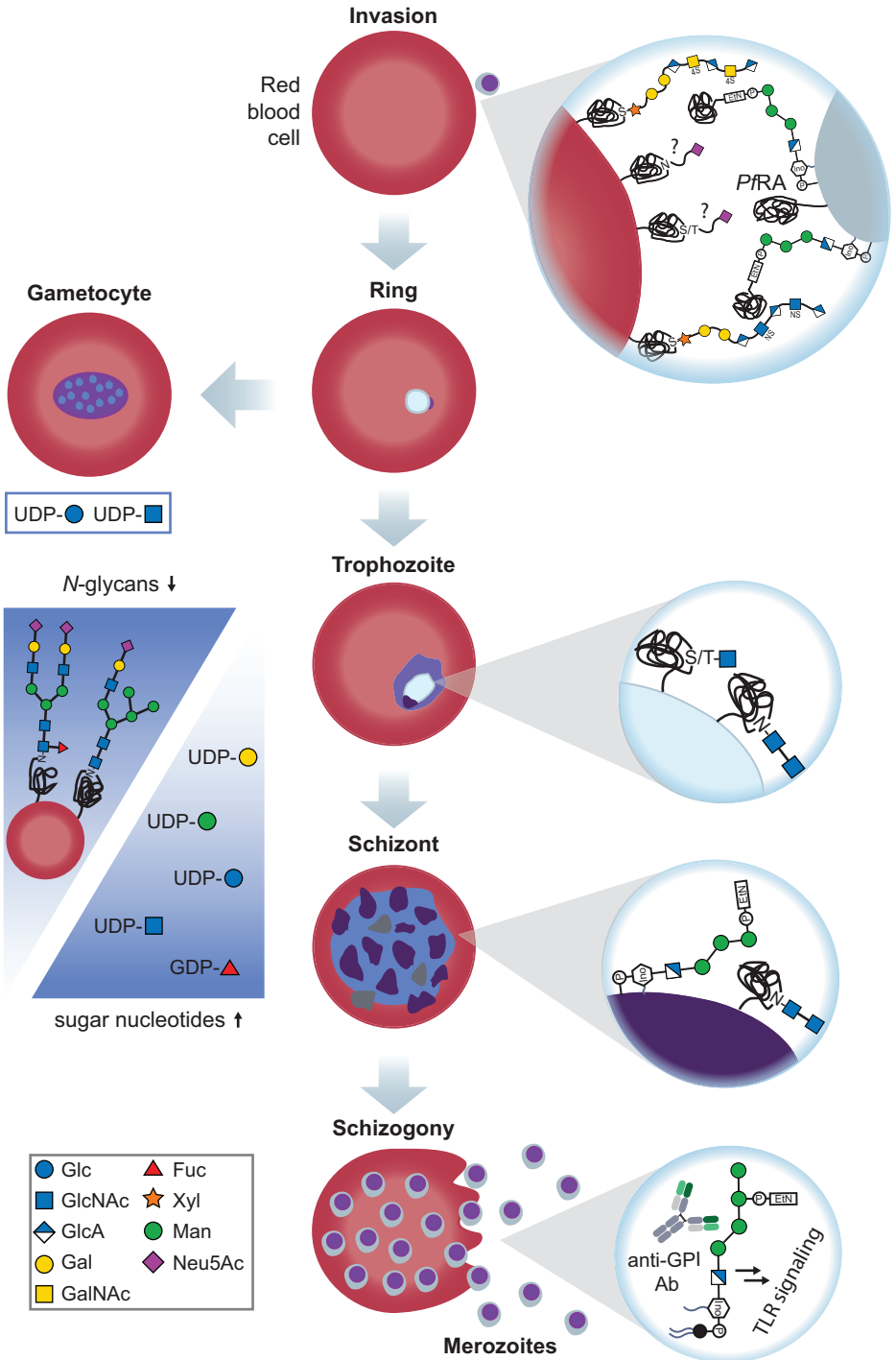

FIGURE 1 | Glycans at the sexual and asexual blood stages of *Plasmodium.* Merozoites recognize RBC GAGs via *Pf*EMP1 and *Pf*BAEBL, an essential interaction for invasion. In addition to GAGs, *Plasmodium* binds to sialylated glycophorin A and C on the RBC surface in the sialic acid-dependent pathway of invasion. Sialic acids are recognized by *Pf*BAEBL and *Pf*EBL-175 on the merozoite surface. After invasion, *Plasmodium* rings either proceed to the trophozoite stage or the gametocyte stage for sexual reproduction (left). Possible gametocyte glycosylation remains to be investigated, but it is known that the levels of UDP-Glc and UDP-GlcNAc are significantly increased at this stage, suggesting a high demand for these building blocks at the sexual life stages. Trophozoite surface glycoproteins possess truncated *O*- and *N*-glycans with 1–2 GlcNAc moieties of unknown function. When progressing to the schizont stage, *Plasmodium* maintains these short *N*-glycans and heavily expresses GPIs, with and without anchored proteins. In addition, *N*-glycans on the infected RBC's surface decline, and sugar nucleotide levels rise (blue arrows), suggesting that *Plasmodium* increasingly utilizes scavenging pathways to build up the required glycosylations. Upon rupture of the schizont, protein-free GPIs are released together with the merozoites. These GPIs are recognized by macrophages and induce a proinflammatory, toxic response, thereby contributing to anemia.

TABLE 1 | List of all glycans with a role in *Plasmodium* infection.

Glycan	Structure	Location	Function	References
A antigen	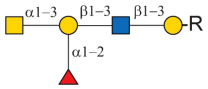	Host RBCs	Blood group antigens, co-receptors for rosette formation of infected RBCs	Barragan et al., 2000; Fry et al., 2008; Pathak et al., 2016; Vagianou et al., 2018
B antigen	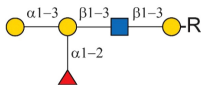			
H antigen	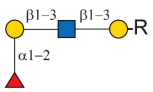			
αGal	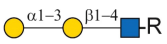	*Plasmodium* sporozoites	Recognized by human Abs	Ramasamy and Field, 2012; Yilmaz et al., 2014
C-manno-sylation		*Plasmodium* TRAP	Unknown	Swearingen et al., 2016; Hoppe et al., 2018
Chondroitin sulfate	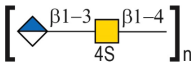	Host cells and *Anopheles* salivary gland	Recognized by *Plasmodium* CSP, BAEBL and EMP1; involved in invasion, rosette formation and cytoadherence of infected RBCs; function in *Anopheles* unknown	Frevert et al., 1993; Fry et al., 2008; Bushkin et al., 2010; Goel et al., 2015; Pathak et al., 2016; Kupferschmid et al., 2017; Vagianou et al., 2018
Heparan sulfate	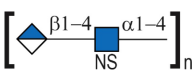			
High-mannose *N-glycan*	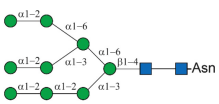	*Plasmodium*-infected RBCs with sickle-cell trait	Exposure due to parasite-induced oxidative stress leads to macrophage phagocytosis	Cao et al., 2021
O-fuco-sylation	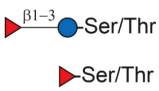	*Plasmodium* CSP, TRAP	Quality control during protein trafficking	Swearingen et al., 2016; Lopaticki et al., 2017
Protein-free GPI	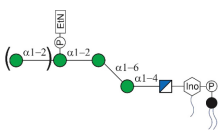	*Plasmodium* schizonts, in the blood after schizogony	Proinflammatory, immunogenic toxin, recognized by human Abs and TLR2/4	Gerold et al., 1994; Gowda et al., 1997
Sialylated glycans		Glycophorin A/C on RBCs	*Plasmodium* invasion via EBL-175/BAEBL	Vogt et al., 2003; Kobayashi et al., 2010; Cao et al., 2021
Truncated *N-glycan*	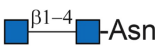	*Plasmodium* trophozoites/schizonts	Unknown	Bushkin et al., 2010
Truncated *O-glycan*		*Plasmodium* trophozoites	Unknown	Kupferschmid et al., 2017

For each glycan, the table contains the structure, location, function and references. In case of heterogeneous glycans (e.g., GAGs), example structures are depicted.

residues. The third mannose carries a phosphoethanolamine (PEtN) moiety that can covalently link the C-terminus of a protein to the GPI.

Database mining recently identified a number of genes involved in biosynthesis of the GPI anchor in *Plasmodium*. The expression of the corresponding enzymes PIG-A, PIG-B, PIG-O, GAA-1, and DPM-1 was validated by immunofluorescence and most proteins were found to localize to the endoplasmic reticulum (ER) (Delorenzi et al., 2002). Another study focused on the addition of the fourth Man to the GPI anchor in *Plasmodium*.

Since this step is catalyzed by the enzyme PIG-Z in mammals that is absent in *Plasmodium,* the authors designed PIG-Z-deficient lethal yeast mutants and examined which *Plasmodium* genes can compensate for this knockout (Cortes et al., 2014). In *Plasmodium*, the catalysis task of PIG-Z is undertaken by PIG-B that is responsible for adding only the third Man in mammals, indicating that *Plasmodium* evolved this additional PIG-B functionality to preserve the fourth Man on its GPI.

Further downstream, the GPI transamidase complex can link proteins to the GPI anchor. Notably, mice infected with *P. berghei* carrying a knockout of the *Pb*GPI16 subunit of the GPI transamidase showed less inflammation, and fewer mice challenged with this knockout developed cerebral malaria compared to the wildtype strain (Liu et al., 2018). These findings corroborate the crucial role of *Plasmodium* GPIs in inflammation and the development of severe malaria.

In recent years, the immunogenicity of different parts of the GPI core structure was examined in more detail. Immunizing rabbits with synthetic GPI glycoconjugates yielded polyclonal sera capable of binding to native *Plasmodium* GPIs (Gurale et al., 2016). Vaccinating mice with glycoconjugates composed of synthetic GPI substructures conjugated to a carrier protein revealed the Man_3-PEtN fragment to be highly immunogenic, while the presence of the fourth Man reduces immunogenicity (Malik et al., 2019). However, only the complete GPI core, also containing GlcN and inositol phosphate (InoP), induced neutralizing antibodies that conveyed protection against *P. berghei* infection. Mice immunized with PEtN-Man_4-GlcN-InoP showed increased survival, and their TNFα levels stayed low (Malik et al., 2019).

These observations corroborate results obtained from analyzing the naturally elicited antibodies in humans from malaria-endemic regions (Naik et al., 2006; Kamena et al., 2008). Antibodies (Abs) from human serum required the Man_3-GlcN-InoP substructure as minimal antigen, as binding was lost when shortening the Man chain (Kamena et al., 2008). Similar to mice, the fourth Man did not contribute to antigenicity (Naik et al., 2006). While serum Abs were found to be predominantly directed against the Man core glycan, complete binding was only achieved with the full structure, containing both glycan and lipid moieties (Naik et al., 2006). Comparing serum samples taken at the end of the wet and dry season revealed that Ab titers against *Plasmodium* GPIs were generally increased after the wet season, indicating a correlation with malaria incidence (Kamena et al., 2008).

Since the majority of malaria-caused deaths occur in children below 5 years of age (World Health Organization [WHO], 2020), several studies also examined the anti-GPI Ab titer in serum obtained from young children. Abs targeting *Plasmodium* proteins can be already found in serum from children $<$12 months, but anti-GPI Abs are only acquired at $>$18 months of age (Tamborrini et al., 2010). Ab titer correlated with severity of malaria as children with only mild symptoms had Abs even against truncated GPIs but showed less response against the full structure. In contrast, Abs from children with severe symptoms did not recognize truncated GPIs but showed a stronger response against the full structure (Tamborrini et al., 2010). Confirming these observations, high IgG titers against *Plasmodium* GPIs were found in children with enlarged spleens and a recent episode of severe malaria, but low titers in asymptomatic or uninfected children (França et al., 2017).

Abs in the serum of humans from malaria-endemic regions may be used to neutralize GPIs. GPI-induced TNFα production and CD40 upregulation in macrophages were efficiently inhibited by purified GPI-targeting IgGs from individuals with a high anti-GPI Ab titer (De Souza et al., 2010). However, the neutralization capacity of these Abs was reduced when activating macrophages with schizont extract instead of pure GPIs, suggesting that GPIs are not the only proinflammatory toxin present in schizonts (De Souza et al., 2010).

A number of host proteins have been identified as interaction partners of *Plasmodium* GPIs. One major GPI-induced signaling pathway involves Toll-like receptor 2 (TLR2) as GPIs almost completely fail to activate TLR2-deficient macrophages (Krishnegowda et al., 2005). To a lesser extent, GPIs can also induce signaling via TLR4. Supporting evidence comes from competition assays with anti-TLR2 and anti-TLR4 antibodies, that successfully inhibited GPI-induced cytokine secretion (Krishnegowda et al., 2005). In addition, recent molecular docking and dynamics simulations unveiled that both Man and lipid moieties engage with TLR2, thereby inducing and stabilizing the formation of TLR2-TLR1 heterodimers (Durai et al., 2013). To downregulate GPI-induced signaling, the host can degrade free GPIs with phospholipases in the serum or on the macrophage surface (Krishnegowda et al., 2005).

These observations are validated by the finding that also CD36, a TLR2-cooperating receptor, plays an important role in GPI-induced inflammation (Patel et al., 2007). Upon stimulation with GPIs, CD36-deficient macrophages showed reduced phosphorylation of MAPK effectors, reduced TNFα secretion and reduced phagocytosis of *Plasmodium*-infected RBCs compared to the CD36-expressing control cells (Patel et al., 2007). CD36 knockout mice were more susceptible to severe malaria with earlier spikes in parasitemia and increased mortality, highlighting the importance of this signaling pathway for host defense against malaria (Patel et al., 2007). *Plasmodium* GPIs also interact with the host protein moesin *in vitro.* However, moesin-deficient mice were not protected against cerebral malaria and still showed *Plasmodium*-induced cytokine secretion (Dunst et al., 2017).

In the field of vaccine development, a recent study investigated a GPI-conjugate vaccine for malaria transmission blocking. The protein Pfs25, a *Plasmodium* surface antigen and initially promising candidate for a transmission blocking vaccine, lacked potency in clinical trials. To improve its efficacy, Pfs25 was conjugated to a synthetic GPI fragment, comprised of PEtN, the Man_3-GlcN-glycan core and the inositol moiety without lipids (Kapoor et al., 2018). The PEtN moiety was functionalized with dibenzocyclooctyne, enabling conjugation to Pfs25 via click chemistry. The authors demonstrated that Pfs25-GPI induces higher Ab titers in the serum than unconjugated Pfs25. Abs induced by Pfs25-GPI were able to almost completely abolish *Plasmodium* transmission in membrane-feeding assays with mosquitoes, where Abs raised against unconjugated Pfs25 failed.

Plasmodium GPIs thus hold great potential for the enhancement of existing protein-based vaccine candidates against malaria (Kapoor et al., 2018).

N-Glycans

N-Glycans are linked to proteins via an *N*-glycosidic bond to asparagine. In eukaryotes, *N*-glycosylation starts with a GlcNAc moiety that is extended in a conserved, multi-step pathway in the ER and Golgi to complex, branched carbohydrate structures (Varki et al., 2017).

The presence of *N*-glycans in *Plasmodium* has been under debate for several decades. While evidence from metabolic labeling and enzymatic glycan cleavage experiments indicated the absence of *N*-glycans in *P. falciparum* (Dieckmann-Schuppert et al., 1992), the presence of long *N*-glycans as $GlcNAc_2$, $Man_3GlcNAc_2$, and $Man_9GlcNAc_2$ at the ring and trophozoite stage of *Plasmodium* was reported (Kimura et al., 1996). A recent analysis of the *Plasmodium* genome suggested that *Plasmodium* can express most subunits of the oligosaccharyl transferase complex (OST; Tamana and Promponas, 2019), needed to link *N*-glycans to the asparagine of a protein, but evidence for OST expression has not been provided so far. Based on the *Plasmodium* genome, Bushkin et al. (2010) predicted that the parasites are only able to produce short *N*-glycans of two GlcNAc moieties at most (**Figure 1**). Indeed, metabolic labeling with tritiated GlcN confirmed that GlcNAc and $GlcNAc_2$ are produced by *Plasmodium,* and the GlcNAc-recognizing lectin GSL-II showed binding to numerous *P. falciparum* glycoproteins which was lost after *N* glycosidase treatment (Bushkin et al., 2010). GSL-II preferentially localizes to the rhoptry organelle of *Plasmodium* and, to a lesser extent, to the ER and cell surface, but does not recognize the apicoplast, food vacuole or parasitophorous vacuole. These findings indicate that *N*-glycosylation in *P. falciparum* is mostly found on the rhoptry, ER and cell surface, but its respective biological function remains a mystery.

O-Glycans

O-Glycans are attached to serine or threonine residues of proteins via an *O*-glycosidic bond. *O*-Glycosylation generally takes place in the Golgi apparatus and begins with a GalNAc moiety. Early glycomics experiments revealed the presence of *O*-glycans in *Plasmodium*-infected RBCs (Dieckmann-Schuppert et al., 1993). Instead of the canonical GalNAc, the reducing end of *Plasmodium O*-glycans is composed of a GlcNAc moiety. GlcNAcylation in *P. falciparum* was confirmed by the discovery of a *Plasmodium O*-GlcNAc transferase (Dieckmann-Schuppert et al., 1993) and by successful purification of *O*-GlcNAcylated proteins from isolated *P. falciparum* parasites (Kupferschmid et al., 2017). At least 13 glycosylated proteins were identified, including Hsp70 and α-tubulin.

O-Fucosylation

A proteome-wide mass spectrometry screen of sporozoite surface proteins revealed that *Plasmodium* is also capable of *O*-fucosylation (Lopaticki et al., 2017), as this modification was identified on the two *Plasmodium* proteins circumsporozoite protein (CSP) and thrombospondin-related anonymous protein (TRAP; see **Figure 2**). *O*-Fucosylation is a non-canonical modification carried out by *O*-fucosyltransferases at special consensus sequences, including the thrombospondin type 1 repeats found in CSP and TRAP (Holdener and Haltiwanger, 2019).

While CSP appeared both with and without fucosylation, TRAP was only present in glycosylated form, modified either with a single fucose or a glucosylfucose dimer. These observations were validated by the discovery of an *O*-fucosyltransferase in *P. falciparum* (POFUT2), that is responsible for CSP and TRAP glycosylations and essential for mosquito midgut colonization of *P. falciparum* sporozoites (Lopaticki et al., 2017).

C-Mannosylation

Interestingly, TRAP was also found to be *C*-mannosylated (Swearingen et al., 2016; Hoppe et al., 2018), a rare glycosylation form where a mannose moiety is attached to the indole ring of a tryptophan (**Figure 2**). This modification is catalyzed in *Plasmodium* by the *C*-mannosyltransferase DPY19 but is not essential for parasite survival as depletion of DPY19 does not impair proliferation and development during the asexual blood stages (Hoppe et al., 2018; López-Gutiérrez et al., 2019). Since both proteins are important vaccine targets, it has been hypothesized that their glycosylations may impact the antigenicity of CSP and TRAP (Swearingen et al., 2016).

α-Gal Antigen

The trisaccharide α-gal (Galα1–3Galβ1–4GlcNAc-R, also known as Galili antigen) was found on *Plasmodium* sporozoites (Yilmaz et al., 2014; **Figure 2**). While humans have lost the ability to synthesize this glycan due to inactivation of the *α1,3GT* gene, many organisms express this glycan, including bacteria found in the human gut microbiota. Therefore, human serum contains large quantities of naturally occurring α-gal Abs. Interestingly, the presence of α-gal Abs in humans from malaria-endemic regions correlated with a lower risk for *Plasmodium* infection (Yilmaz et al., 2014). Anti-α-gal Abs activate complement-dependent cytotoxicity against *Plasmodium* sporozoites and inhibit hepatocyte invasion *in vitro*. Vaccination of *α1,3GT*-depleted mice with α-gal conveyed protection against malaria transmission *in vivo* (Yilmaz et al., 2014). α-Gal surface expression is lost on the later, asexual blood stages of *Plasmodium* (Ramasamy and Field, 2012), rendering α-gal an attractive candidate for a transmission blocking vaccine, possibly in combination with other *Plasmodium* antigens.

HOST GLYCANS

ABO Antigens

The ABO antigens are carbohydrate portions of glycoproteins and glycolipids that terminate with different monosaccharides. Terminal *N*-acetylgalactosamine or galactose determine the A or B blood group, respectively. These sugars cap the core structure Fuc(α1–2)Gal(β1–3)GlcNAc(β1–3)Gal called the H

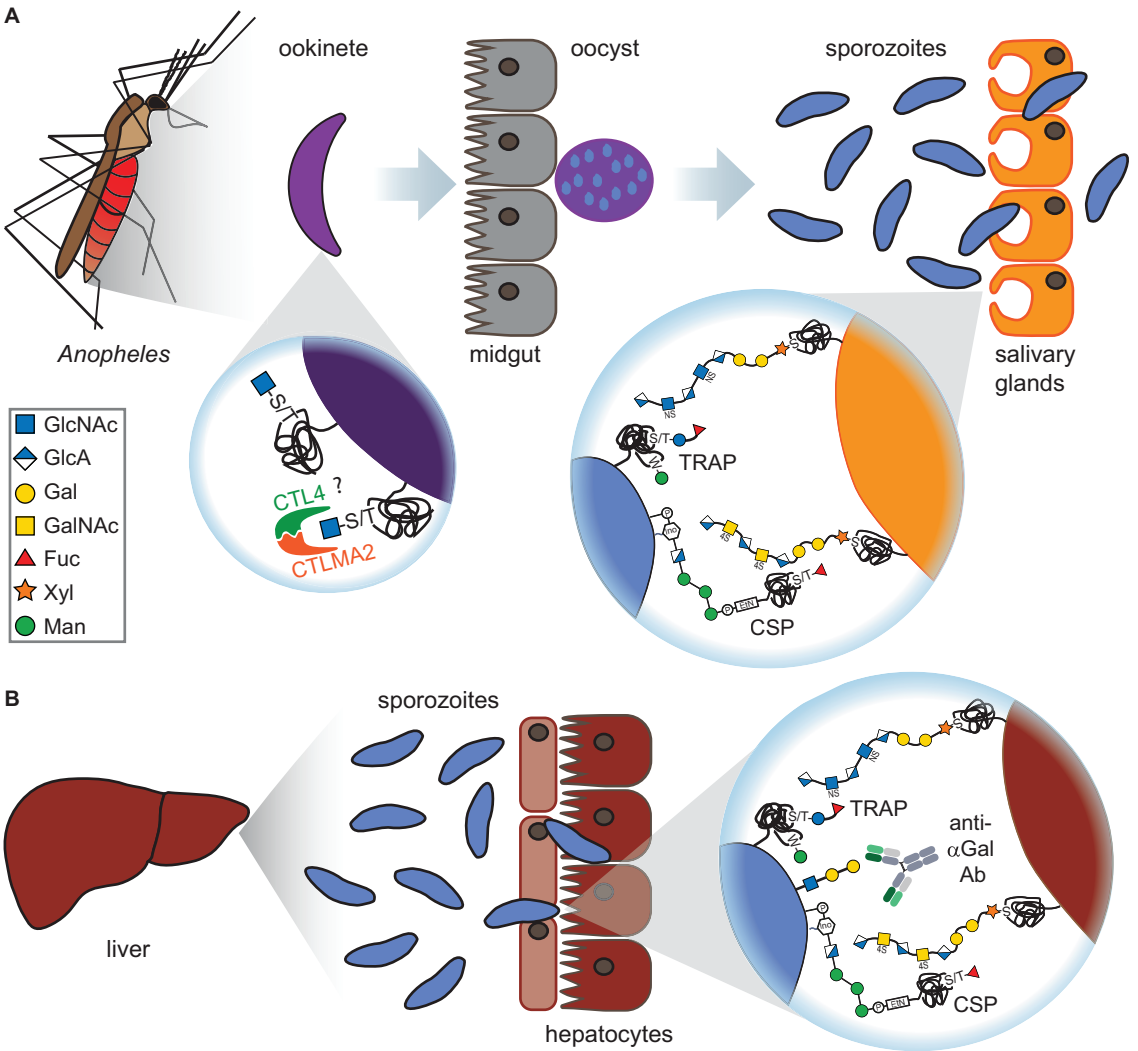

FIGURE 2 | Glycans at the mosquito and liver stages of *Plasmodium*. **(A)** Ookinetes carry short *O*-GlcNAcylations on glycoproteins on their surface which presumably bind to the C-type lectins CTL4 and CTLMA2, thereby preventing melanization through the mosquito's immune system. After oocyst rupture at the mosquito midgut, released sporozoites express the glycoproteins TRAP and CSP. Both proteins are *O*-fucosylated and can interact with GAGs on the surface of *Anopheles* salivary gland cells, although this interaction is dispensable for salivary gland penetration. **(B)** Upon arrival at the liver, CSP and TRAP bind to the GAGs on hepatocytes which is a prerequisite for hepatocyte invasion. Sporozoites have been found to express the αGal antigen that elicits a high Ab titer in humans. This is particularly interesting as vaccination of mice with αGal conveyed protection against malaria transmission.

antigen (**Table 1**). The A and B antigens are produced by human ABO transferase, which transfers GalNac or Gal onto the core structure, depending on missense single nucleotide polymorphisms in the ABO gene. Inheriting two null copies of the ABO gene results in the O blood group (the H antigen remains uncapped). Glycoproteins and glycolipids carrying the ABO antigens are present on the surface of RBCs, endothelial, and epithelial cells (only in secretors) (Yamamoto et al., 1990).

Decades ago, epidemiological data from malaria-endemic regions suggested that the severity of malaria depends to some extent on the blood group [reviewed in Cserti and Dzik (2007) and Uneke (2007)]. However, different serological studies produced ambiguous results, requiring a more precise examination method. Genotyping almost 10,000 individuals found that individuals with blood groups A, B, and AB are more susceptible to severe malaria than blood group O (Fry et al., 2008), validating previous conclusions (Cserti and Dzik, 2007; Uneke, 2007).

The molecular basis for blood-group-dependent differences was investigated as well (**Figure 3A**). Rosetting, the ability of *P. falciparum*-infected RBCs to build clusters with uninfected RBCs, is one determinant for severe malaria and has been suggested to involve blood group antigens (Barragan et al., 2000). When examining rosette formation of multiple clinical isolates of *P. falciparum*, the majority of isolates preferred blood group A or B, but none preferred blood group O (Barragan et al., 2000). Rosette formation in the preferred blood group was inhibited by

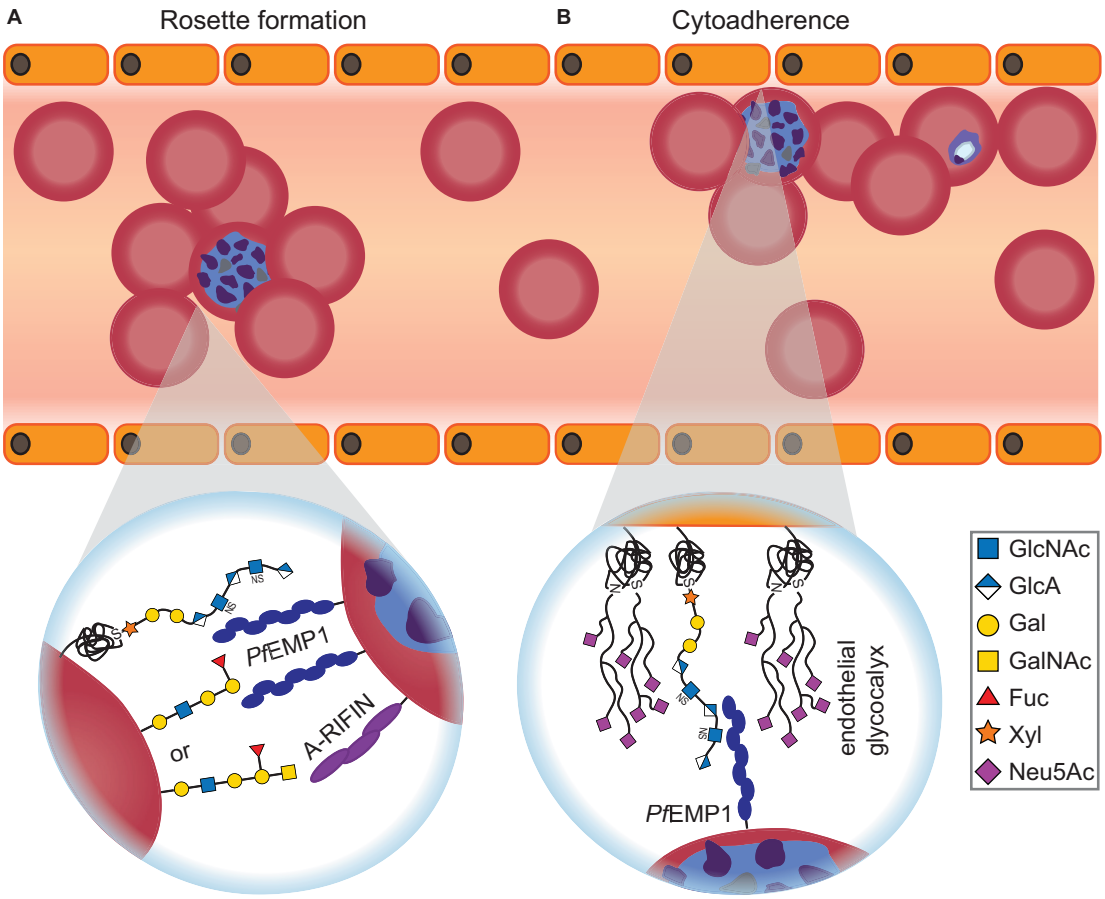

FIGURE 3 | Glycan-dependent interactions between *Plasmodium*-infected RBCs and uninfected host cells. **(A)** Infected RBCs form rosettes with uninfected RBCs, thereby becoming invisible for the host's immune system. Depending on the blood group, *Plasmodium* uses different surface proteins for rosetting. *Pf*EMP1 recognizes O-type RBCs, while A-RIFIN binds to A antigen. Independent of the blood group, *Pf*EMP1 also interacts with RBC GAGs for rosette formation that can be efficiently inhibited by adding soluble GAGs *in vitro* and *in vivo*. **(B)** Infected RBCs adhere to endothelial cells to avoid blood clearance. The interaction between *Pf*EMP1 and GAGs, predominantly heparan sulfate, is crucial for cytoadherence of infected RBCs. On the other hand, it was shown that an intact endothelial glycocalyx conveys protection against *Plasmodium* cytoadherence as severe malaria symptoms are preceded by degradation of the endothelial glycocalyx.

addition of the respective soluble blood group antigen, and the blood group preference was lost after treatment of RBCs with glycosidases (Barragan et al., 2000). Blood group antigens A and B thus appear to be important co-receptors for rosette formation of infected RBCs.

ABO-decorated giant unilamellar vesicles (GUVs) were used as RBC mimetics to examine rosette formation (Vagianou et al., 2018). A- and O-type GUVs participated in rosettes, but not B-type GUVs, and rosetting of O-type GUVs was inhibited with anti-*Pf*EMP1 Abs. Therefore, the different blood groups involve at least two distinct pathways for rosette formation: *Pf*EMP1-dependent for O-type RBCs or *Pf*EMP1-independent for A-type RBCs, respectively (Vagianou et al., 2018; **Figure 3A**). The *Pf*EMP1-independent rosetting pathway involves the *Plasmodium* protein A-RIFIN (repetitive interspersed families of polypeptides) instead (Goel et al., 2015). Indeed, CHO cells that overexpress A-RIFIN from *Plasmodium* sequester A-type RBCs but do not bind to B- or O-type RBCs (Goel et al., 2015).

In vitro invasion experiments with blood from the rare Bombay type O^h that lacks the H antigen of blood group O revealed that O^h-type RBCs, i.e., without any blood group antigens, are more resistant to *Plasmodium* than blood group O (Pathak et al., 2016). This resistance was emulated in O-type RBCs by the addition of lectins against H antigen, suggesting that the presence of a blood group antigen is essential for *P. falciparum* invasion (Pathak et al., 2016).

Glycosaminoglycans

Glycosaminoglycans (GAGs) are extracellular matrix components of mammalian cells, consisting of acidic disaccharide repeating units which show varying degress of sulfation. GAGs have many crucial functions in humans, including cell–cell adhesion and tissue integrity but also tissue hydration and elasticity (Varki et al., 2017).

During *Plasmodium* infection, CSP recognizes the GAGs heparan sulfate and chondroitin sulfate on the surface of human hepatocytes and RBCs (Pancake et al., 1992; Frevert et al.,

1993; Rogerson et al., 1995; **Figures 1**, **2B**). The addition of soluble GAGs *in vitro* and *in vivo* can inhibit this interaction and thereby prevent sporozoite invasion in human cells, raising hopes for the therapeutic exploitation of GAGs (Pancake et al., 1992). Interestingly, heparan sulfate and chondroitin sulfate are also present in the salivary glands of *Anopheles gambiae* but seem dispensable for sporozoite invasion in the mosquito (**Figure 2A**). Silencing of the GAG synthesis enzyme *Ag*OXT1 only marginally reduced sporozoite invasion, indicating that additional interactions contribute to *Plasmodium* invasion in the mosquito midgut (Armistead et al., 2011).

At the blood stages of the *Plasmodium* life cycle, GAGs have been implicated in rosette formation (**Figure 3A**) and adherence of infected RBCs to the human placenta during pregnancy, as soluble GAGs disrupt both processes (Fried and Duffy, 1996; Barragan et al., 1999; Chotivanich et al., 2012). The inhibitory effect of GAGs on rosetting strongly depends on the sulfation state of the glycans (Barragan et al., 1999). Adherence of infected RBCs to placental cells involves the unsulfated GAG hyaluronic acid (HA; Beeson et al., 2000). Since CD44 on RBCs is a known HA receptor, whose recognition of HA can be manipulated by differential glycosylation (Katoh et al., 1995), it is conceivable that CD44 might also be involved in placental adherence of infected RBCs. Furthermore, CD44 mediates adherence of infected RBCs to brain endothelial cells in cerebral malaria via the GAG chondroitin sulfate (Jurzynski et al., 2007). Notably, a knockout of CD44 in RBCs inhibited *Plasmodium* invasion as well, suggesting a broader role of CD44 in the life cycle of the parasite (Kanjee et al., 2017). In addition to GAGs, adherence to placental cells might also involve interaction with Lewis glycan antigens, further complicating the matter (Hromatka et al., 2013).

In order to gain insights on the localization and identity of heparin-binding *Plasmodium* proteins, the heparin interactome has been examined by mass spectrometry and immunoblots (Kobayashi et al., 2013; Zhang et al., 2013, 2014). All identified proteins were part of the Duffy and reticulocyte binding-like families (Kobayashi et al., 2013). Staining of merozoites with biotinylated heparin for confocal microscopy revealed that heparin localized mostly to the apical tip and the rhoptry organelle of the parasite which causes invasion inhibition (Kobayashi et al., 2013; Zhang et al., 2013). Heparin also inhibits merozoite egress during schizogony, by blocking *Plasmodium*-induced RBC membrane pores through simultaneous binding to the inner RBC membrane and the merozoite surface (Glushakova et al., 2017).

Two *Plasmodium* proteins highlight the crucial importance of GAG interactions for the parasite: *Pf*EMP1, found on infected RBCs, plays an essential role in GAG-dependent cytoadherence (Vogt et al., 2003; **Figure 3B**) and rosette formation (Vagianou et al., 2018; also see previous section) as its DBL1α domain can recognize heparan sulfate on the surface of epithelial cells and anti-*Pf*EMP1 Abs disrupt rosetting. Heparan sulfate on the RBC surface is recognized by the protein *Pf*BAEBL that also binds sialic acids on RBCs (see next section), suggesting an alternative recognition pathway independent of sialic acid (Kobayashi et al., 2010).

Considering that heparin is a widely used drug, the inhibitory effect of soluble GAGs against *Plasmodium* invasion and cytoadherence raised hopes for a potential therapeutic exploitation. However, the strong anticoagulating activity of heparin poses a risk for possible antimalarial use because it can cause undesired bleeding. Recent studies examined heparin-like alternatives, in search for compounds without anticoagulating activity but an inhibitory effect on *Plasmodium* invasion. Heparin-like polysaccharides isolated from the capsule of the *E. coli* K5 strain were tested for anti-invasive effects (Boyle et al., 2010). The compound repertoire was expanded by chemical modification of the K5 polysaccharides and heparin, and the key properties of a suitable drug were identified (Boyle et al., 2017). For optimal antimalarial activity, heparin-like molecules (HLMs) should contain at least six monosaccharides and two sulfations per repeating unit with disulfation of a HexA or GlcNAc moiety (Boyle et al., 2010, 2017). Chemical modification (e.g., hypersulfation) can improve invasion inhibition and lower the anticoagulating effect (Boyle et al., 2017).

Based on these results, semi-synthetic non-GAG HLMs with antimalarial activity but little anticoagulating activity were successfully developed (Skidmore et al., 2017). The antimalarial activity of such non-GAG HLMs apparently depends on sulfation as the non-GAG HLMs showing the highest inhibition of *Plasmodium* cytoadherence, glycogen type 2 sulfate and phenoxyacetylcellulose sulfate, are both heavily sulfated (Skidmore et al., 2017).

Heparin-like molecules also proved beneficial against blood–brain barrier (BBB) breakdown in an *in vitro* model of cerebral malaria (Moxon et al., 2020). Accumulation of parasite and RBC histones at the brain endothelium, likely released during schizont rupture, leads to BBB disruption. HLMs prevent histone-induced BBB breakdown, suggesting yet another pathway for therapeutic application of HLMs (Moxon et al., 2020).

Naturally derived HLMs from marine organisms were examined for their antimalarial efficacy. Heparan sulfate isolated from lion's paw scallops and fucosylated chondroitin sulfate isolated from sea cucumbers efficiently inhibit merozoite invasion and cytoadherence *in vitro* (Bastos et al., 2014, 2019). Both GAGs can be readily obtained from natural sources and showed less anticoagulating activity than heparin. Additional HLMs were purified from other types of sea cucumber, red algae and marine sponges, with the majority of marine HLMs exhibiting antimalarial activity on a similar level as heparin but with less anticoagulating side effects (Marques et al., 2016). HLM injection also conveyed protection against *P. yoelii in vivo* as infected mice showed increased survival and decreased parasitaemia in the serum when injected with marine HLMs. Interestingly, surviving, HLM-treated mice displayed high Ab titers against *P. yoelii* antigens and survived re-challenge with the parasite after several months without any HLM treatment. It is thus conceivable that because HLMs disrupt merozoite invasion, the parasites become more exposed to the immune system (Marques et al., 2016).

Sialic-Acid-Containing Glycans

Sialic acids are a group of sugars that commonly cap the termini of *N*- and *O*-glycan chains. The predominant sialic acids in mammals are *N*-acetylneuraminic acid (Neu5Ac) and *N*-glycolylneuraminic acid (Neu5Gc). While most mammals synthesize Neu5Gc from Neu5Ac, humans lack the respective hydroxylase due to a mutation in their *CMAH* gene and thus do not possess sialic acid in the Neu5Gc form (Chou et al., 1998).

Starting from the mid-1980s, evidence for an interaction between the *P. falciparum* erythrocyte-binding antigen 175 (EBA-175) and sialic acid on the host protein glycophorin A (Camus and Hadley, 1985; Orlandi et al., 1992; Sim et al., 1994) was unearthed. This interaction is crucial for RBC invasion in the so-called sialic-acid-dependent pathway (**Figure 1**) and was validated by structural data, showing that Neu5Ac(α2–3)Gal is making essential contacts to EBA-175 (Tolia et al., 2005). Data derived from glycosylation mutants of glycophorin A revealed that an *O*-glycosylation motif encoded by exon 3 is critical for invasion via the sialic-acid-dependent pathway (Salinas et al., 2014).

The interaction between the polymorphic EBA-140 and glycophorin C also contributes to invasion via the sialic-acid-dependent pathway (Lobo et al., 2003), and a structure of EBA-140 in complex with sialic acid confirms this interaction (Malpede et al., 2013). An *N*-glycan on glycophorin C that was subsequently identified, is recognized by one variant of EBA-140, suggesting that not only *O*-glycans are involved in the sialic-acid-dependent pathway of invasion (Mayer et al., 2006). When both glycophorin A and C are enzymatically cleaved, *P. falciparum* binds to glycophorin B for invasion (Dolan et al., 1994). Although glycophorin B shows a high degree of sequence similarity to glycophorin A, it is not recognized by EBA-175 but by the *Plasmodium* protein EBL-1 instead (Li et al., 2012).

Some strains of *P. falciparum* are capable of invading RBCs after enzymatic cleavage of sialic acid with neuraminidase, proving the existence of an alternative, sialic-acid-independent pathway (Hadley et al., 1987). Even strains that usually depend on sialic acid for invasion can switch to the independent pathway when EBA-175 is depleted (Duraisingh et al., 2003).

Both pathways can be efficiently targeted by Abs against EBA-175 and RH5, a protein involved in the sialic-acid-independent pathway (Rodriguez et al., 2008). Ord et al. (2012) raised Abs in mice against both proteins and found that these Abs can block invasion. However, only the anti-RH5 Ab inhibited invasion of neuraminidase-treated RBCs, demonstrating that the sialic-acid-independent pathway needs to be disabled as well to hamper invasion. Recent evidence suggests another protein to participate in the sialic-acid-dependent pathway: *P. falciparum* rhoptry associated adhesin (*Pf*RA), that is only expressed at the schizont stage and localizes to the apical merozoite surface during RBC invasion (Anand et al., 2016). *Pf*RA fails to bind neuraminidase-treated RBCs, and RBC invasion can be inhibited by anti-*Pf*RA Abs (Anand et al., 2016).

Plasmodium knowlesi can transmit from Neu5Gc-producing macaques to humans, raising questions about the sialic-acid-dependent invasion pathway of this *Plasmodium* species (Dankwa et al., 2016). When reconstituting the CMAH enzyme in human RBCs, CMAH+ RBCs become more susceptible to *P. knowlesi* invasion, and Neu5Gc-containing receptors are specifically recognized by the *P. knowlesi* proteins DBPβ and γ (Dankwa et al., 2016). A human-adapted strain of *P. knowlesi* did not require Neu5Gc and lost DBPγ expression, suggesting a shift toward sialic-acid-independent invasion due to selection pressure (Dankwa et al., 2016). Other *Plasmodium* species show a more exclusive preference for one of the two sialoforms. While *P. reichenowi* and *P. falciparum* are genetically very similar, they only infect chimpanzees or humans, respectively (Martin et al., 2005). This difference in host specificity is attributed to preferential binding of *Pf*EBA-175 to Neu5Ac and *Pr*EBA-175 to Neu5Gc. Furthermore, *P. reichenowi* and other ape-specific *Plasmodium* species express EBA-165 that also preferentially recognizes Neu5Gc (Proto et al., 2019). In contrast, *P. falciparum* does not express EBA-165 due to a frame-shift mutation and actively silenced EBA-165 when the frame-shift was corrected by CRISPR-Cas9 editing (Proto et al., 2019). The identity of the recognized sialoprotein also differs between *P. reichenowi* and *P. falciparum*. While *Pf*EBA-140 binds to glycophorin C as described above, the *P. reichenowi* homolog interacts with glycophorin D (Zerka et al., 2017). These observations favor a model in which humans and *P. falciparum* co-evolved and *P. falciparum's* ability to preferentially recognize Neu5Ac-containing proteins led to its emergence as the most deadly human parasite (Martin et al., 2005; Proto et al., 2019).

Sialylation of *N*- and *O*-glycans as well as sulfation of GAGs are both critical for *Plasmodium* cytoadherence and invasion. Both glycan modifications introduce charge to the carbohydrate structure. Thus, it seems likely that ionic interactions are required for the interplay between host and parasite when these carbohydrate moieties are involved. Detailed structural data will be needed to examine this hypothesis.

N-Glycans

Sickle-cell disease conveys resistance against severe malaria. However, *Plasmodium* infects healthy and sickle-cell RBCs equally well with no apparent differences in invasion or release (Friedman, 1978), suggesting that resistance arises from more efficient immune clearance of infected RBCs. RBCs with sickle-cell trait were recently found to express high-mannose *N*-glycans on their surface that are recognized by the macrophage receptor CD206 followed by phagocytosis (Cao et al., 2021). High-mannose *N*-glycan surface levels in sickle-cell RBCs correlated with the parasite's life stage, being elevated at trophozoite and schizont stage (see **Table 1**). Phagocytosis through macrophages can be inhibited by the addition of mannan, a yeast-derived high-mannose glycan, and oxidative stress can induce expression of high-mannose surface *N*-glycans in healthy RBCs (Cao et al., 2021). Improved immune clearance presumably arises from the increased susceptibility of sickle-cell RBCs to oxidative stress caused by the parasite, mediated through an elevated high-mannose *N-glycan* level recognized by macrophages (Cao et al., 2021).

Plasmodium also alters the *N*-glycosylation pattern of infected RBCs without sickle-cell trait. Extensive posttranslational modification-omics screens with infected RBCs at the different

asexual life stages of *Plasmodium* (Wang et al., 2021) revealed that *Plasmodium* downregulates *N*-glycosylation of a variety of RBC proteins (**Figure 1**), including several cluster of differentiation (CD) proteins with known roles in cell adhesion and rosette formation. For the majority of RBC membrane proteins, *N*-glycosylation decreased over the course of the *Plasmodium* life cycle with the lowest glycosylation level at the late schizont stage (Wang et al., 2021). For instance, *N*-glycosylation of the C3 complement protein recedes, suggesting a parasitic strategy to dampen the host immune response. In contrast, *N*-glycosylation of selected RBC proteins is upregulated during parasite development inside the RBC (Wang et al., 2021). Notably, CD55 displays higher levels of *N*-glycosylation which is especially interesting because it has been shown to be an essential receptor in *Plasmodium* invasion (Egan et al., 2015). The exact mechanism behind the observed global changes in RBC glycosylation or their biological purpose is still a mystery. However, the simultaneous increase in *Plasmodium* sugar nucleotide levels (Sanz et al., 2013; López-Gutiérrez et al., 2017; see above) suggests that *Plasmodium* utilizes host glycans for purposes yet to be discovered.

BIOLOGICAL FUNCTIONS

Vector Colonization

First evidence for a crucial role of *Plasmodium* glycans in mosquito midgut invasion came from the observation that ookinetes lose their ability to invade the midgut upon treatment with the GlcNAc-binding lectin wheat germ agglutinin, suggesting that carbohydrate binding is required at this step (Basseri et al., 2016). Since the lectin concanavalin A that predominantly binds mannose structures did not inhibit invasion, the involved carbohydrate likely contains GlcNAc or sialic acid but not mannose or glucose (**Figure 2A**). This notion is confirmed by the finding that a number of *O*-GlcNAcylated proteins have been identified in *Plasmodium* (Kupferschmid et al., 2017). In addition, the *O*-fucosylation on the sporozoite proteins CSP and TRAP is essential for midgut colonization (Lopaticki et al., 2017).

Interestingly, it has been described that after infection with *P. falciparum*, the probing activity of *Anopheles* mosquitoes increases, coinciding with a higher sugar uptake of the mosquito at the *Plasmodium* oocyst stage. Sugar uptake decreases subsequently when parasites reach the sporozoite stage. This argues in favor of a model in which the parasite controls and manipulates the behavior of its vector to increase its sugar supply (Nyasembe et al., 2014).

Investigating potential vector-sided interaction partners of *Plasmodium* glycans, two C-type lectins in *Anopheles* were identified, CTL4 and CTLMA2 (Osta et al., 2004; **Figure 2A**). Both lectins can form heterodimers for a cooperative binding mode and recognize specific glycosaminoglycan motifs, including β1–3- and β1–4-connected Glc, Gal, GlcNAc and GalNAc moieties (Bishnoi et al., 2019). Depletion of the two proteins in *Anopheles* enables a strong immune response against *Plasmodium* followed by melanization, an innate defense mechanism of *Anopheles* leading to sequestration and melanin coating of the parasite. Therefore, parasite binding to these lectins conveys protection against the mosquito's immune response (Osta et al., 2004).

Host Cell Invasion and Immune Defense

We have already touched on various glycans involved in *Plasmodium* invasion above. At the host cell surface, the sialic-acid-dependent pathway as well as the crucial roles of GAGs and blood group antigens were discussed in detail.

These glycans are part of the host cell glycocalyx that was found to be one of the main determinants of malaria resilience. For instance, loss of the glycocalyx on brain endothelial cells is one event preceding cerebral malaria. Transmission electron microscopy revealed that the brain endothelial glycocalyx of mice challenged with uncomplicated *P. chabaudi* was only partially disrupted, whereas it was completely degraded in mice with *P. berghei*-induced cerebral malaria (Hempel et al., 2014). Glycocalyx degradation coincided with an increase in circulating GAGs and was already present before other symptoms of cerebral malaria occurred (Hempel et al., 2014). In a later study, the same group investigated how an intact glycocalyx can convey protection against severe malaria symptoms. The ability of *Plasmodium* to bind to the surface receptor CD36 was examined on CHO cells which develop a thick glycocalyx within 4 days *in vitro* (Hempel et al., 2017). *Plasmodium* binding to CD36 was lost with the maturation of the glycocalyx over time, suggesting that the glycocalyx serves as a shield that can prevent *Plasmodium* cytoadhesion to the endothelium (Hempel et al., 2017; **Figure 3B**). These findings are corroborated by microfluidics experiments examining the interaction between infected RBCs and the glycocalyx (Introini et al., 2018). After artificial disruption of the glycocalyx with sialidases, cytoadhesion of infected RBCs is significantly increased (Introini et al., 2018; **Figure 3B**). Disruption of the glycocalyx caused by *Plasmodium* in cerebral malaria can be prevented *in vivo:* when treating infected mice with corticosteroids or antithrombin-3, the glycocalyx stays intact, and cerebral malaria symptoms as well as mortality are markedly reduced, suggesting glycocalyx integrity as a promising leverage point for enhanced host resilience (Hempel et al., 2019).

Depletion of GlcNAc-transferase V, which adds β1–6-connected GlcNAc to *N*-glycans, renders mice more susceptible to malaria, as marked by higher parasitemia, loss in body weight and more severe pathology in the liver and lung (Shibui et al., 2011). GlcNAc-containing *N*-glycans may convey some degree of protection against severe malaria, but the mechanistic details of this putative protection remain unclear (Shibui et al., 2011).

Lectins are another group of important modulators in the host defense against *Plasmodium*. Mannose-binding lectin (MBL) that triggers the lectin pathway of the complement system is crucial for the host's defense against malaria. It is especially important for resilience to placental malaria as the adaptive immune system has not yet formed in the fetus. Recently, a correlation between susceptibility to placental and

non-placental malaria and single nucleotide polymorphisms in the *MBL* gene was established (Holmberg et al., 2012; Jha et al., 2014). Some variants caused an increased risk for severe malaria while others conferred protection. Counterintuitively, variants with decreased susceptibility to placental malaria dampened complement activation. However, it is conceivable that the protective effect of a reduced complement response lies in the prevention of hyperinflammation at the placenta (Holmberg et al., 2012).

Galectins constitute another lectin type that specifically recognizes β-galactosides as part of *N*- and *O*-glycans. Interestingly, host galectins also seem to be involved in controlling *Plasmodium* infection. Inhibition of galectins through lactose injection led to increased mortality of *Plasmodium*-infected mice (Liu et al., 2016). Lactose-treated mice exhibited increased parasitaemia, lung pathology and expression of interferon α/β/γ and interleukines 4/10 in the lung (Liu et al., 2016). These data suggest that galectins can protect from *Plasmodium* infection. This hypothesis is supported by the observation that galectin-9 expression was significantly upregulated on macrophages in the lungs of infected mice (Liu et al., 2016). In contrast, galectin-3 apparently increases the susceptibility to infection with some *Plasmodium* species as galectin-3-deficient mice show reduced parasitaemia compared to wildtype mice when challenged with *P. yoelii or P. chabaudi* but not *P. berghei.* The galectin-3 knockout mice infected with *P. yoelii* were also able to raise higher Ab titers against *Plasmodium* antigens than the wildtype, suggesting that galectin-3 modulates the immune response against *Plasmodium* in a non-beneficial way (Toscano et al., 2012). The precise role of galectins in malaria host defense remains to be elucidated, but it seems likely that their modulatory effect on the immune response is *Plasmodium* species-dependent and involves additional factors.

In some cases, *Plasmodium* proteins can also prevent immunomodulatory host glycan–protein interactions. It has been reported that *Plasmodium* merozoite surface protein 7 (MSP7) binds to the host's C-type lectin P-selectin (Perrin et al., 2015). P-selectin plays a crucial role in leukocyte recruitment to inflamed endothelial tissue by binding to the glycan sialyl-Lewis X on leukocytes. Binding of MSP7 inhibits the interaction between P-selectin and sialyl-Lewis X (Perrin et al., 2015). It seems conceivable that the proinflammatory, immune-system-recruiting function of P-selectin is abrogated by MSP7, indicating a novel pathway for host immune system attenuation by *Plasmodium.*

DISCUSSION AND OUTLOOK

One of the major challenges in the global fight against malaria is the paucity of an effective malaria vaccine, with the only EMA-approved vaccine RTS,S lacking efficacy in the most vulnerable groups of infants and young children (Agnandji et al., 2014). Recently, a new vaccine candidate named R21 was examined in a phase III clinical trial and found to be more effective than RTS,S with approx. 77% efficacy (Datoo et al., 2021). Since both RTS,S and R21 are based on the glycoprotein CSP, a potential effect of CSP glycosylation on vaccine efficacy should be examined. CSP is *O*-fucosylated in *P. falciparum* but not in yeast where CSP for the vaccines is recombinantly expressed (Agnandji et al., 2014; Swearingen et al., 2016; Lopaticki et al., 2017; Datoo et al., 2021). Therefore, alternative expression systems might be considered for malaria vaccine design to obtain bona fide *Plasmodium* glycosylation.

The *Plasmodium* GPI glycan itself is another promising vaccine candidate, as it is highly immunogenic and a critical proinflammatory toxin contributing to severe malaria. GPI vaccine candidates have been examined, but the feasibility and efficacy of a potential GPI vaccine remains controversial due to inconsistent data, most probably caused by using different glycans, immunization regimes and infection models. Detailed immunogenicity studies in mice determined that a minimal antigen for vaccination should at least comprise the mannose glycan core and the phosphoethanolamine moiety of the GPI structure (Malik et al., 2019; see also GPI section). The combination of protein antigens and GPIs proved particularly effective as transmission-blocking vaccine in mice (Kapoor et al., 2018), suggesting the use of *Plasmodium* GPIs as vaccine adjuvants.

Glycosaminoglycans represent yet another attractive pharmaceutical target. With heparin as an approved and widely used anticoagulant, one prominent GAG is already marketed. The finding that heparin and HLMs can prevent *Plasmodium* invasion renders GAGs attractive antimalarial compounds, and HLMs can avoid the anticoagulating activity of heparin that is undesired for malaria treatment. Indeed, the HLM Sevuparin was found to be non-toxic and well-tolerated in phase I/II human clinical trials (Leitgeb et al., 2017). GAG interactions are also the focus of transmission-blocking vaccines. For instance, *Plasmodium* proteins bind to placental chondroitin sulfate A for invasion, causing placental malaria in pregnant women. Abs inhibiting *Plasmodium* binding to placental GAGs were successfully induced in a phase I clinical trial with the PAMVAC vaccine candidate (Mordmüller et al., 2019).

Another challenge arises from the variability of the *Plasmodium* ssp. While some lectins and glycans, such as GPIs, are conserved across different *Plasmodium* species, it seems likely that their respective interaction partners at the host level vary between distinct host species. For instance, *P. knowlesi* shifts to the sialic acid-independent pathway when infecting humans instead of macaques due to the absence of Neu5Gc on human cells (Dankwa et al., 2016). It is therefore crucial to examine the species-specific differences in *Plasmodium*-host interplay in more detail.

Recent work revealed that *Plasmodium* parasites employ extracellular vesicles (EVs) for cell–cell communication and host cell modulation. Infected RBCs release EVs with diverse cargo, ranging from functional miRNA that changes the barrier properties of host endothelial cells (Mantel et al., 2016) to DNA that promotes sexual differentiation of neighboring parasites

(Regev-Rudzki et al., 2013). EVs can also carry 20S proteasomes that change the cytoskeletal architecture of naïve RBCs, thereby priming them for subsequent *Plasmodium* infection (Dekel et al., 2021). While nucleic acid and protein cargo of *Plasmodium*-derived EVs are intensively studied, the presence, role or origin of glycans carried on the cell membrane of secreted EVs remains to be elucidated.

While recent work has provided important insights about *Plasmodium* glycans, many open questions remain, mostly due to the lack of tools targeting specific glycans. Monoclonal anti-glycan antibodies are scarce and lectins, though often used to examine the terminal moieties of glycans, are not specific enough. Novel glycan-targeting probes will allow for a more in-depth characterization of the *Plasmodium* glycome and facilitate therapeutic applications against drug-resistant parasites.

AUTHOR CONTRIBUTIONS

FG and OM designed and wrote the review. PS revised the manuscript. All authors contributed to the article and approved the submitted version.

FUNDING

Financial support was provided by the Max Planck Society to FG, PS, and OM, Alexander von Humboldt Foundation to OM, and the Deutsche Forschungsgemeinschaft (RTG2046) to FG.

ACKNOWLEDGMENTS

The authors thank Lindsey Young for reviewing the manuscript.

REFERENCES

Agnandji, S. T., Lell, B., Fernandes, J. F., Abossolo, B. P., Kabwende, A. L., Adegnika, A. A., et al. (2014). Efficacy and safety of the RTS,S/AS01 Malaria vaccine during 18 months after vaccination: a phase 3 randomized, controlled trial in children and young infants at 11 African Sites. . *PLoS Med.* 11:e1001685. doi: 10.1371/journal.pmed.1001685

Anand, G., Reddy, K. S., Pandey, A. K., Mian, S. Y., Singh, H., Mittal, S. A., et al. (2016). A novel Plasmodium falciparum rhoptry associated adhesin mediates erythrocyte invasion through the sialic-acid dependent pathway. *Sci. Rep.* 6:29185. doi: 10.1038/srep29185

Armistead, J. S., Wilson, I. B. H., Van Kuppevelt, T. H., and Dinglasan, R. R. (2011). A role for heparan sulfate proteoglycans in Plasmodium falciparum sporozoite invasion of anopheline mosquito salivary glands. *Biochem. J.* 438, 475–483. doi: 10.1042/BJ20110694

Barragan, A., Kremsner, P. G., Wahlgren, M., and Carlson, J. (2000). Blood group A antigen is a coreceptor in Plasmodium falciparum rosetting. *Infect. Immun.* 68, 2971–2975. doi: 10.1128/IAI.68.5.2971-2975.2000

Barragan, A., Spillmann, D., Kremsner, P. G., Wahlgren, M., and Carlson, J. (1999). Plasmodium falciparum: molecular background to strain-specific rosette disruption by glycosaminoglycans and sulfated glycoconjugates. *Exp. Parasitol.* 91, 133–143. doi: 10.1006/expr.1998.4349

Basseri, H. R., Javazm, M. S., Farivar, L., and Abai, M. R. (2016). Lectin-carbohydrate recognition mechanism of Plasmodium berghei in the midgut of malaria vector Anopheles stephensi using quantum dot as a new approach. *Acta Trop.* 156, 37–42. doi: 10.1016/j.actatropica.2016.01.003

Bastos, M. F., Albrecht, L., Gomes, A. M., Lopes, S. C. P., Vicente, C. P., de Almeida, R. P. M., et al. (2019). A new heparan sulfate from the mollusk nodipecten nodosus inhibits merozoite invasion and disrupts rosetting and cytoadherence of plasmodium falciparum. *Mem. Inst. Oswaldo Cruz* 114:e190088. doi: 10.1590/0074-02760190088

Bastos, M. F., Albrecht, L., Kozlowski, E. O., Lopes, S. C. P., Blanco, Y. C., Carlos, B. C., et al. (2014). Fucosylated chondroitin sulfate inhibits Plasmodium falciparum cytoadhesion and merozoite invasion. *Antimicrob. Agents Chemother.* 58, 1862–1871. doi: 10.1128/AAC.00686-13

Beeson, J. G., Rogerson, S. J., Cooke, B. M., Reeder, J. C., Chai, W., Lawson, A. M., et al. (2000). Adhesion of Plasmodium falciparum-infected erythrocytes to hyaluronic acid in placental malaria. *Nat. Med.* 6, 86–90. doi: 10.1038/71582

Bishnoi, R., Sousa, G. L., Contet, A., Day, C. J., Hou, C. F. D., Profitt, L. A., et al. (2019). Solution structure, glycan specificity and of phenol oxidase inhibitory activity of Anopheles C-type lectins CTL4 and CTLMA2. *Sci. Rep.* 9:15191. doi: 10.1038/s41598-019-51353-z

Boutlis, C. S., Riley, E. M., Anstey, N. M., and De Souza, J. B. (2005). Glycosylphosphatidylinositols in malaria pathogenesis and immunity: potential for therapeutic inhibition and vaccination. *Curr. Top. Microbiol. Immunol.* 297, 145–185. doi: 10.1007/3-540-29967-x_5

Boyle, M. J., Richards, J. S., Gilson, P. R., Chai, W., and Beeson, J. G. (2010). Interactions with heparin-like molecules during erythrocyte invasion by Plasmodium falciparum merozoites. *Blood* 115, 4559–4568. doi: 10.1182/blood-2009-09-243725

Boyle, M. J., Skidmore, M., Dickerman, B., Cooper, L., Devlin, A., Yates, E., et al. (2017). Identification of heparin modifications and polysaccharide inhibitors of plasmodium falciparum merozoite invasion that have potential for novel drug development. *Antimicrob. Agents Chemother.* 61, e00709–e00717. doi: 10.1128/AAC.00709-17

Bushkin, G. G., Ratner, D. M., Cui, J., Banerjee, S., Duraisingh, M. T., Jennings, C. V., et al. (2010). Suggestive evidence for Darwinian selection against asparagine-linked glycans of Plasmodium falciparum and Toxoplasma gondii. *Eukaryot Cell* 9, 228–241. doi: 10.1128/EC.00197-09

Camus, D., and Hadley, T. J. A. (1985). Plasmodium falciparum antigen that binds to host erythrocytes and merozoites. *Science (80-)* 230, 553–556. doi: 10.1126/science.3901257

Cao, H., Antonopoulos, A., Henderson, S., Wassall, H., Brewin, J., Masson, A., et al. (2021). Red blood cell mannoses as phagocytic ligands mediating both sickle cell anaemia and malaria resistance. *Nat. Commun.* 12:1792. doi: 10.1038/s41467-021-21814-z

Chi, J., Cova, M., De Las Rivas, M., Medina, A., Junqueira Borges, R., Leivar, P., et al. (2020). Plasmodium falciparum apicomplexan-specific glucosamine-6-phosphate n-acetyltransferase is key for amino sugar metabolism and asexual blood stage development. *MBio* 11, 1–15. doi: 10.1128/mBio.02045-20

Chotivanich, K., Udomsangpetch, R., Suwanarusk, R., Pukrittayakamee, S., Wilairatana, P., Beeson, J. G., et al. (2012). Plasmodium vivax adherence to placental glycosaminoglycans. *PLoS One* 7:e34509. doi: 10.1371/journal.pone.0034509

Chou, H. H., Takematsu, H., Diaz, S., Iber, J., Nickerson, E., Wright, K. L., et al. (1998). A mutation in human CMP-sialic acid hydroxylase occurred after the Homo-Pan divergence. *Proc. Natl. Acad. Sci. U.S.A.* 95, 11751–11756. doi: 10.1073/pnas.95.20.11751

Cortes, L. K., Scarcelli, J. J., and Taron, C. H. (2014). Complementation of essential yeast GPI mannosyltransferase mutations suggests a novel specificity for certain Trypanosoma and Plasmodium pigB proteins. *PLoS One* 9:e87673. doi: 10.1371/journal.pone.0087673

Cserti, C. M., and Dzik, W. H. (2007). The ABO blood group system and Plasmodium falciparum malaria. *Blood* 110, 2250–2258. doi: 10.1182/blood-2007-03-077602

Dankwa, S., Lim, C., Bei, A. K., Jiang, R. H. Y., Abshire, J. R., Patel, S. D., et al. (2016). Ancient human sialic acid variant restricts an emerging zoonotic malaria parasite. *Nat. Commun.* 7:11187. doi: 10.1038/ncomms11187

Datoo, M. S., Magloire Natama, H., Somé, A., Traoré, O., Rouamba, T., Bellamy, D., et al. (2021). High efficacy of a low dose candidate Malaria vaccine, R21 in 1 adjuvant Matrix-M^{TM}, with seasonal administration to children in burkina faso. *SSRN* Preprint. doi: 10.2139/ssrn.3830681

De Niz, M., and Heussler, V. T. (2018). Rodent malaria models: insights into human disease and parasite biology. *Curr. Opin. Microbiol.* 46, 93–101. doi: 10.1016/j.mib.2018.09.003

De Souza, J. B., Runglall, M., Corran, P. H., Okell, L. C., Kumar, S., Gowda, D. C., et al. (2010). Neutralization of malaria glycosylphosphatidylinositol in vitro by serum IgG from malaria-exposed individuals. *Infect. Immun.* 78, 3920–3929. doi: 10.1128/IAI.00359-10

Dekel, E., Yaffe, D., Rosenhek-Goldian, I., Ben-Nissan, G., Ofir-Birin, Y., Morandi, M. I., et al. (2021). 20S proteasomes secreted by the malaria parasite promote its growth. *Nat. Commun.* 12:1172. doi: 10.1038/s41467-021-21344-8

Delorenzi, M., Sexton, A., Shams-Eldin, H., Schwarz, R. T., Speed, T., and Schofield, L. (2002). Genes for glycosylphosphatidylinositol toxin biosynthesis in Plasmodium falciparum. *Infect. Immun.* 70, 4510–4522. doi: 10.1128/IAI.70.8.4510-4522.2002

Dieckmann-Schuppert, A., Bause, E., and Schwarz, R. T. (1993). Studies on O−glycans of Plasmodium−falciparum−infected human erythrocytes Evidence for O−GlcNAc and O−GlcNAc−transferase in malaria parasites. *Eur. J. Biochem.* 216, 779–788. doi: 10.1111/j.1432-1033.1993.tb18198.x

Dieckmann-Schuppert, A., Hensel, J., and Schwartz, R. T. (1992). Studies on the effect of Tunicamycin on erythrocytic stages of Plasmodium falciparum. *Biochem. Soc. Trans.* 20:184S. doi: 10.1042/bst020184s

Dolan, S. A., Proctor, J. L., Alling, D. W., Okubo, Y., Wellems, T. E., and Miller, L. H. (1994). Glycophorin B as an EBA-175 independent Plasmodium falciparum receptor of human erythrocytes. *Mol. Biochem. Parasitol.* 64, 55–63. doi: 10.1016/0166-6851(94)90134-1

Dunst, J., Azzouz, N., Liu, X., Tsukita, S., Seeberger, P. H., and Kamena, F. (2017). Interaction between Plasmodium glycosylphosphatidylinositol and the host protein moesin has no implication in malaria pathology. *Front. Cell Infect. Microbiol.* 7:183. doi: 10.3389/fcimb.2017.00183

Durai, P., Govindaraj, R. G., and Choi, S. (2013). Structure and dynamic behavior of Toll-like receptor 2 subfamily triggered by malarial glycosylphosphatidylinositols of Plasmodium falciparum. *FEBS J.* 280, 6196–6212. doi: 10.1111/febs.12541

Duraisingh, M. T., Maier, A. G., Triglia, T., and Cowman, A. F. (2003). Erythrocyte-binding antigen 175 mediates invasion in Plasmodium falciparum utilizing sialic acid-dependent and -independent pathways. *Proc. Natl. Acad. Sci. U.S.A.* 100, 4796–4801. doi: 10.1073/pnas.0730883100

Egan, E. S., Jiang, R. H. Y., Moechtar, M. A., Barteneva, N. S., Weekes, M. P., Nobre, L. V., et al. (2015). A forward genetic screen identifies erythrocyte CD55 as essential for Plasmodium falciparum invasion. *Science (80-)* 348, 711–714. doi: 10.1126/science.aaa3526

França, C. T., Li Wai Suen, C. S. N., Carmagnac, A., Lin, E., Kiniboro, B., Siba, P. (2017). IgG antibodies to synthetic GPI are biomarkers of immune-status to both Plasmodium falciparum and Plasmodium vivax malaria in young children. *Malar J.* 16, 1–10. doi: 10.1186/s12936-017-2042-2

Frevert, U., Sinnis, P., Cerami, C., Shreffler, W., Takacs, B., and Nussenzweig, V. (1993). Malaria circumsporozoite protein binds to heparan sulfate proteoglycans associated with the surface membrane of hepatocytes. *J. Exp. Med.* 177, 1287–1298. doi: 10.1084/jem.177.5.1287

Fried, M., and Duffy, P. E. (1996). Adherence of Plasmodium falciparum to chondroitin sulfate A in the human placenta. *Science (80-)* 272, 1502–1504. doi: 10.1126/science.272.5267.1502

Friedman, M. J. (1978). Erythrocytic mechanism of sickle cell resistance to malaria. *Proc. Natl. Acad. Sci. U.S.A.* 75, 1994–1997. doi: 10.1073/pnas.75.4.1994

Fry, A. E., Griffiths, M. J., Auburn, S., Diakite, M., Forton, J. T., Green, A., et al. (2008). Common variation in the ABO glycosyltransferase is associated with susceptibility to severe Plasmodium falciparum malaria. *Hum. Mol. Genet.* 17, 567–576. doi: 10.1093/hmg/ddm331

Gerold, P., Dieckmann-Schuppert, A., and Schwarz, R. T. (1994). Glycosylphosphatidylinositols synthesized by asexual erythrocytic stages of the malarial parasite, Plasmodium falciparum. Candidates for plasmodial glycosylphosphatidylinositol membrane anchor precursors and pathogenicity factors. *J. Biol. Chem.* 269, 2597–2606. doi: 10.1016/s0021-9258(17)41986-7

Glushakova, S., Busse, B. L., Garten, M., Beck, J. R., Fairhurst, R. M., Goldberg, D. E., et al. (2017). Exploitation of a newly-identified entry pathway into the malaria parasite-infected erythrocyte to inhibit parasite egress. *Sci. Rep.* 7, 1–13. doi: 10.1038/s41598-017-12258-x

Goel, S., Palmkvist, M., Moll, K., Joannin, N., Lara, P., Akhouri, R., et al. (2015). RIFINs are adhesins implicated in severe Plasmodium falciparum malaria. *Nat. Med.* 21, 314–321. doi: 10.1038/nm.3812

Gomes, P. S., Tanghe, S., Gallego-Delgado, J., Conde, L., Freire-de-Lima, L., Lima, A. C., et al. (2019). Targeting the hexosamine biosynthetic pathway prevents plasmodium developmental cycle and disease pathology in vertebrate host. *Front. Microbiol.* 10:305. doi: 10.3389/fmicb.2019.00305

Gowda, D. C., Gupta, P., and Davidson, E. A. (1997). Glycosylphosphatidylinositol anchors represent the major carbohydrate modification in proteins of intraerythrocytic stage Plasmodium falciparum. *J. Biol. Chem.* 272, 6428–6439. doi: 10.1074/jbc.272.10.6428

Gurale, B. P., He, Y., Cui, X., Dinh, H., Dhawane, A. N., Lucchi, N. W., et al. (2016). Toward the development of the next generation of a rapid diagnostic test: synthesis of glycophosphatidylinositol (GPI) analogues of plasmodium falciparum and immunological characterization. *Bioconjug Chem.* 27, 2886–2899. doi: 10.1021/acs.bioconjchem.6b00542

Hadley, T. J., Klotz, F. W., Pasvol, G., Haynes, J. D., McGinniss, M. H., Okubo, Y., et al. (1987). Falciparum malaria parasites invade erythrocytes that lack glycophorin A and B (M(k)M(k)). Strain differences indicate receptor heterogeneity and two pathways for invasion. *J. Clin. Invest.* 80, 1190–1193. doi: 10.1172/JCI113178

Hempel, C., Hyttel, P., and Kurtzhals, J. A. L. (2014). Endothelial glycocalyx on brain endothelial cells is lost in experimental cerebral malaria. *J. Cereb. Blood Flow. Metab.* 34, 1107–1110. doi: 10.1038/jcbfm.2014.79

Hempel, C., Sporring, J., and Kurtzhals, J. A. L. (2019). Experimental cerebral malaria is associated with profound loss of both glycan and protein components of the endothelial glycocalyx. *FASEB J.* 33, 2058–2071. doi: 10.1096/fj.201800657R

Hempel, C., Wang, C. W., Kurtzhals, J. A. L., and Staalsø, T. (2017). Binding of Plasmodium falciparum to CD36 can be shielded by the glycocalyx. *Malar J.* 16:193. doi: 10.1186/s12936-017-1844-6

Holdener, B. C., and Haltiwanger, R. S. (2019). Protein O-fucosylation: structure and function. *Curr. Opin. Struct. Biol.* 56, 78–86. doi: 10.1016/j.sbi.2018.12.005

Holmberg, V., Onkamo, P., Lahtela, E., Lahermo, P., Bedu-Addo, G., Mockenhaupt, F. P., et al. (2012). Mutations of complement lectin pathway genes MBL2 and MASP2 associated with placental malaria. *Malar J.* 11:61. doi: 10.1186/1475-2875-11-61

Hoppe, C. M., Albuquerque-Wendt, A., Bandini, G., Leon, D. R., Shcherbakova, A., Buettner, F. F. R., et al. (2018). Apicomplexan C-mannosyltransferases modify thrombospondin Type I-containing Adhesins of the TRAP Family. *Glycobiology* 28, 333–343. doi: 10.1093/glycob/cwy013

Hromatka, B. S., Ngeleza, S., Adibi, J. J., Niles, R. K., Tshefu, A. K., and Fisher, S. J. (2013). Histopathologies, immunolocalization, and a glycan binding screen provide insights into plasmodium falciparum interactions with the human placenta. *Biol. Reprod.* 88, 1–14. doi: 10.1095/biolreprod.112.106195

Introini, V., Carciati, A., Tomaiuolo, G., Cicuta, P., and Guido, S. (2018). Endothelial glycocalyx regulates cytoadherence in Plasmodium falciparum malaria. *J. R. Soc. Interface* 15:20180773. doi: 10.1098/rsif.2018.0773

Jha, A. N., Sundaravadivel, P., Singh, V. K., Pati, S. S., Patra, P. K., Kremsner, P. G., et al. (2014). MBL2 variations and malaria susceptibility in Indian populations. *Infect. Immun.* 82, 52–61. doi: 10.1128/IAI.01041-13

Jurzynski, C., Gysin, J., and Pouvelle, B. (2007). CD44, a signal receptor for the inhibition of the cytoadhesion of CD36-binding Plasmodium falciparum-infected erythrocytes by CSA-binding infected erythrocytes. *Microbes Infect.* 9, 1463–1470. doi: 10.1016/j.micinf.2007.07.011

Kamena, F., Tamborrini, M., Liu, X., Kwon, Y. U., Thompson, F., Pluschke, G., et al. (2008). Synthetic GPI array to study antitoxic malaria response. *Nat. Chem. Biol.* 4, 238–240. doi: 10.1038/nchembio.75

Kanjee, U., Grüring, C., Chaand, M., Lin, K. M., Egan, E., Manzo, J., et al. (2017). CRISPR/Cas9 knockouts reveal genetic interaction between strain-transcendent erythrocyte determinants of Plasmodium falciparum invasion. *Proc. Natl. Acad. Sci. U.S.A.* 114, E9356–E9365. 10.1073/pnas.1711310114

Kapoor, N., Vanjak, I., Rozzelle, J., Berges, A., Chan, W., Yin, G., et al. (2018). Malaria derived glycosylphosphatidylinositol anchor enhances Anti-Pfs25 functional antibodies that block malaria transmission. *Biochemistry* 57, 516–519. doi: 10.1021/acs.biochem.7b01099

Katoh, S., Zheng, Z., Oritani, K., Shimozato, T., and Kincade, P. W. (1995). Glycosylation of CD44 negatively regulates its recognition of hyaluronan. *J. Exp. Med.* 182, 419–429. doi: 10.1084/jem.182.2.419

Kimura, E. A., Couto, A. S., Peres, V. J., Casal, O. L., and Katzin, A. M. (1996). N-linked glycoproteins are related to schizogony of the intraerythrocytic stage in Plasmodium falciparum. *J. Biol. Chem.* 271, 14452–14461. doi: 10.1074/jbc.271.24.14452

Kobayashi, K., Kato, K., Sugi, T., Takemae, H., Pandey, K., Gong, H., et al. (2010). Plasmodium falciparum BAEBL binds to heparan sulfate proteoglycans on the human erythrocyte surface. *J. Biol. Chem.* 285, 1716–1725. doi: 10.1074/jbc.M109.021576

Kobayashi, K., Takano, R., Takemae, H., Sugi, T., Ishiwa, A., Gong, H., et al. (2013). Analyses of interactions between heparin and the apical surface proteins of plasmodium falciparum. *Sci. Rep.* 3:3178. doi: 10.1038/srep03178

Krishnegowda, G., Hajjar, A. M., Zhu, J., Douglass, E. J., Uematsu, S., Akira, S., et al. (2005). Induction of proinflammatory responses in macrophages by the glycosylphosphatidylinositols of plasmodium falciparum. *J. Biol. Chem.* 280, 8606–8616. doi: 10.1074/jbc.m413541200

Kupferschmid, M., Aquino-Gil, M. O., Shams-Eldin, H., Schmidt, J., Yamakawa, N., Krzewinski, F., et al. (2017). Identification of O-GlcNAcylated proteins in Plasmodium falciparum. *Malar J.* 16:485. doi: 10.1186/s12936-017-2131-2

Leitgeb, A. M., Charunwatthana, P., Rueangveerayut, R., Uthaisin, C., Silamut, K., Chotivanich, K., et al. (2017). Inhibition of merozoite invasion and transient de-sequestration by sevuparin in humans with Plasmodium falciparum malaria. *PLoS One* 12:e0188754. doi: 10.1371/journal.pone.0188754

Li, X., Marinkovic, M., Russo, C., McKnight, C. J., Coetzer, T. L., and Chishti, A. H. (2012). Identification of a specific region of Plasmodium falciparum EBL-1 that binds to host receptor glycophorin B and inhibits merozoite invasion in human red blood cells. *Mol. Biochem. Parasitol.* 183, 23–31. doi: 10.1016/j.molbiopara.2012.01.002

Lim, M. Y. X., LaMonte, G., Lee, M. C. S., Reimer, C., Tan, B. H., Corey, V., et al. (2016). UDP-galactose and acetyl-CoA transporters as Plasmodium multidrug resistance genes. *Nat. Microbiol.* 1, 1–12. doi: 10.1038/nmicrobiol.2016.166

Liu, J., Huang, S., Su, X. Z., Song, J., and Lu, F. (2016). Blockage of galectin-receptor interactions by α-lactose exacerbates plasmodium berghei-induced pulmonary immunopathology. *Sci. Rep.* 6:32024. doi: 10.1038/srep32024

Liu, Q., Zhao, Y., Zheng, L., Zhu, X., Cui, L., and Cao, Y. (2018). The glycosylphosphatidylinositol transamidase complex subunit PbGPI16 of Plasmodium berghei is important for inducing experimental cerebral malaria. *Infect. Immun.* 86, e929–e917. doi: 10.1128/IAI.00929-17

Lobo, C. A., Rodriguez, M., Reid, M., and Lustigman, S. (2003). Glycophorin C is the receptor for the Plasmodium falciparum erythrocyte binding ligand PfEBP-2 (baebl). *Blood* 101, 4628–4631. doi: 10.1182/blood-2002-10-3076

Lopaticki, S., Yang, A. S. P., John, A., Scott, N. E., Lingford, J. P., O'Neill, M. T., et al. (2017). Protein O-fucosylation in Plasmodium falciparum ensures efficient infection of mosquito and vertebrate hosts. *Nat. Commun.* 8:561. doi: 10.1038/s41467-017-00571-y

López-Gutiérrez, B., Cova, M., and Izquierdo, L. A. (2019). Plasmodium falciparum C-mannosyltransferase is dispensable for parasite asexual blood stage development. *Parasitology* 146, 1767–1772. doi: 10.1017/S0031182019001380

López-Gutiérrez, B., Dinglasan, R. R., and Izquierdo, L. (2017). Sugar nucleotide quantification by liquid chromatography tandem mass spectrometry reveals a distinct profile in Plasmodium falciparum sexual stage parasites. *Biochem. J.* 474, 897–905. doi: 10.1042/BCJ20161030

Maier, A. G., Matuschewski, K., Zhang, M., and Rug, M. (2019). Plasmodium falciparum. *Trends Parasitol.* 35, 481–482. doi: 10.1016/j.pt.2018.11.010

Malik, A., Steinbeis, F., Carillo, M. A., Seeberger, P. H., Lepenies, B., Varón Silva, D., et al. (2019). Immunological evaluation of synthetic glycosylphosphatidylinositol glycoconjugates as vaccine candidates against Malaria. *ACS Chem. Biol.* 15, 171–178. doi: 10.1021/acschembio.9b00739

Malpede, B. M., Lin, D. H., and Tolia, N. H. (2013). Molecular basis for sialic acid-dependent receptor recognition by the Plasmodium falciparum invasion protein erythrocyte-binding antigen-140/baebl. *J. Biol. Chem.* 288, 12406–12415. doi: 10.1074/jbc.M113.450643

Mantel, P. Y., Hjelmqvist, D., Walch, M., Kharoubi-Hess, S., Nilsson, S., Ravel, D., et al. (2016). Infected erythrocyte-derived extracellular vesicles alter vascular function via regulatory Ago2-miRNA complexes in malaria. *Nat. Commun.* 7:12727. doi: 10.1038/ncomms12727

Marques, J., Vilanova, E., Mourão, P. A. S., and Fernàndez-Busquets, X. (2016). Marine organism sulfated polysaccharides exhibiting significant antimalarial activity and inhibition of red blood cell invasion by Plasmodium. *Sci. Rep.* 6:24368. doi: 10.1038/srep24368

Martin, M. J., Rayner, J. C., Gagneux, P., Barnwell, J. W., and Varki, A. (2005). Evolution of human-chimpanzee differences in malaria susceptibility: relationship to human genetic loss of N-glycolylneuraminic acid. *Proc. Natl. Acad. Sci. U.S.A.* 102, 12819–12824. doi: 10.1073/PNAS.0503819102

Mayer, D. C. G., Jiang, L., Achur, R. N., Kakizaki, I., Gowda, D. C., and Miller, L. H. (2006). The glycophorin C N-linked glycan is a critical component of the ligand for the Plasmodium falciparum erythrocyte receptor BAEBL. *Proc. Natl. Acad. Sci. U.S.A.* 103, 2358–2362. doi: 10.1073/pnas.0510648103

Mordmüller, B., Sulyok, M., Egger-Adam, D., Resende, M., De Jongh, W. A., Jensen, M. H., et al. (2019). First-in-human, randomized, double-blind clinical trial of differentially adjuvanted PAMVAC, a vaccine candidate to prevent pregnancy-associated Malaria. *Clin. Infect. Dis.* 69, 1509–1516. doi: 10.1093/cid/ciy1140

Moxon, C. A., Alhamdi, Y., Storm, J., Toh, J. M. H., McGuinness, D., Ko, J. Y., et al. (2020). Parasite histones are toxic to brain endothelium and link blood barrier breakdown and thrombosis in cerebral malaria. *Blood Adv.* 4, 2851–2864. doi: 10.1182/bloodadvances.2019001258

Naik, R. S., Krishnegowda, G., Ockenhouse, C. F., and Gowda, D. C. (2006). Naturally elicited antibodies to glycosylphosphatidylinositols (GPIs) of Plasmodium falciparum require intact GPI structures for binding and are directed primarily against the conserved glycan moiety. *Infect. Immun.* 74, 1412–1415. doi: 10.1128/IAI.74.2.1412-1415.2006

Nebl, T., De Veer, M. J., and Schofield, L. (2005). Stimulation of innate immune responses by malarial glycosylphosphatidylinositol via pattern recognition receptors. *Parasitology* 130, S45–S62. doi: 10.1017/S0031182005008152

Nyasembe, V. O., Teal, P. E. A., Sawa, P., Tumlinson, J. H., Borgemeister, C., and Torto, B. (2014). Plasmodium falciparum infection increases Anopheles gambiae attraction to nectar sources and sugar uptake. *Curr. Biol.* 24, 217–221. doi: 10.1016/j.cub.2013.12.022

Ord, R. L., Rodriguez, M., Yamasaki, T., Takeo, S., Tsuboi, T., and Lobo, C. A. (2012). Targeting sialic acid dependent and independent pathways of invasion in Plasmodium falciparum. *PLoS One* 7:e30251. doi: 10.1371/journal.pone.0030251

Orlandi, P. A., Klotz, F. W., and Haynes, J. D. (1992). A malaria invasion receptor, the 175-kilodalton erythrocyte binding antigen of Plasmodium falciparum recognizes the terminal Neu5Ac(α2-3)Gal- sequences of glycophorin A. *J. Cell Biol.* 116, 901–909. doi: 10.1083/jcb.116.4.901

Osta, M. A., Christophides, G. K., and Kafatos, F. C. (2004). Effects of mosquito genes on plasmodium development. *Science (80-)* 303, 2030–2032. doi: 10.1126/science.1091789

Pancake, S. J., Holt, G. D., Mellouk, S., and Hoffman, S. L. (1992). Malaria sporozoites and circumsporozoite proteins bind specifically to sulfated glycoconjugates. *J. Cell Biol.* 117, 1351–1357. doi: 10.1083/jcb.117.6.1351

Patel, S. N., Lu, Z., Ayi, K., Serghides, L., Gowda, D. C., and Kain, K. C. (2007). Disruption of CD36 impairs cytokine response to plasmodium falciparum glycosylphosphatidylinositol and confers susceptibility to severe and fatal malaria in vivo. *J. Immunol.* 178, 3954–3961. doi: 10.4049/jimmunol.178.6.3954

Pathak, V., Colah, R., and Ghosh, K. (2016). Correlation between 'H' blood group antigen and Plasmodium falciparum invasion. *Ann. Hematol.* 95, 1067–1075. doi: 10.1007/s00277-016-2663-5

Perrin, A. J., Bartholdson, S. J., and Wright, G. J. (2015). P-selectin is a host receptor for Plasmodium MSP7 ligands. *Malar J.* 14:238. doi: 10.1186/s12936-015-0750-z

Proto, W. R., Siegel, S. V., Dankwa, S., Liu, W., Kemp, A., Marsden, S., et al. (2019). Adaptation of Plasmodium falciparum to humans involved the loss of an ape-specific erythrocyte invasion ligand. *Nat. Commun.* 10:4512. doi: 10.1038/s41467-019-12294-3

Qureshi, A. A., Suades, A., Matsuoka, R., Brock, J., McComas, S. E., Nji, E., et al. (2020). The molecular basis for sugar import in malaria parasites. *Nature* 578, 321–325. doi: 10.1038/s41586-020-1963-z

Ramasamy, R., and Field, M. C. (2012). Terminal galactosylation of glycoconjugates in Plasmodium falciparum asexual blood stages and Trypanosoma brucei bloodstream trypomastigotes. *Exp. Parasitol.* 130, 314–320. doi: 10.1016/j.exppara.2012.02.017

Regev-Rudzki, N., Wilson, D. W., Carvalho, T. G., Sisquella, X., Coleman, B. M., Rug, M., et al. (2013). Cell-cell communication between malaria-infected red blood cells via exosome-like vesicles. *Cell* 153, 1120–1133. doi: 10.1016/j.cell.2013.04.029

Rodriguez, M., Lustigman, S., Montero, E., Oksov, Y., and Lobo, C. A. (2008). PfRH5: a novel reticulocyte-binding family homolog of Plasmodium falciparum that binds to the erythrocyte, and an investigation of its receptor. *PLoS One* 3:e3300. doi: 10.1371/journal.pone.0003300

Rogerson, S. J., Chaiyaroj, S. C., Ng, K., Reeder, J. C., and Brown, G. V. (1995). Chondroitin sulfate a is a cell surface receptor for Plasmodium falciparum-infected erythrocytes. *J. Exp. Med.* 182, 15–20. doi: 10.1084/jem.182.1.15

Salinas, N. D., Paing, M. M., and Tolia, N. H. (2014). Critical glycosylated residues in exon three of erythrocyte glycophorin A engage Plasmodium falciparum EBA-175 and define receptor specificity. *MBio* 5, e01606–e01614. doi: 10.1128/mBio.01606-14

Sanz, S., Bandini, G., Ospina, D., Bernabeu, M., Mariño, K., Fernández-Becerra, C., et al. (2013). Biosynthesis of GDP-fucose and other sugar nucleotides in the blood stages of Plasmodium falciparum. *J. Biol. Chem.* 288, 16506–16517. doi: 10.1074/jbc.M112.439828

Sanz, S., López-Gutiérrez, B., Bandini, G., Damerow, S., Absalon, S., Dinglasan, R. R., et al. (2016). The disruption of GDP-fucose de novo biosynthesis suggests the presence of a novel fucose-containing glycoconjugate in Plasmodium asexual blood stages. *Sci. Rep.* 6:37230. doi: 10.1038/srep37230

Schofield, L., and Hackett, F. (1993). Signal transduction in host cells by a glycosylphosphatidyllnositol toxin of malaria parasites. *J. Exp. Med.* 177, 145–153. doi: 10.1084/jem.177.1.145

Shibui, A., Doi, J., Tolba, M. E. M., Shiraishi, C., Sato, Y., Ishikawa, S., et al. (2011). N-acetylglucosaminyltransferase V-deficiency increases susceptibility to murine malaria. *Exp. Parasitol.* 129, 318–321. doi: 10.1016/j.exppara.2011.07.003

Sim, B., Chitnis, C., Wasniowska, K., Hadley, T., and Miller, L. (1994). Receptor and ligand domains for invasion of erythrocytes by Plasmodium falciparum. *Science (80-)* 264, 1941–1944. doi: 10.1126/science.8009226

Skidmore, M. A., Mustaffa, K. M. F., Cooper, L. C., Guimond, S. E., Yates, E. A., and Craig, A. G. (2017). A semi-synthetic glycosaminoglycan analogue inhibits and reverses Plasmodium falciparum cytoadherence. *PLoS One* 12:e186276. doi: 10.1371/journal.pone.0186276

Swearingen, K. E., Lindner, S. E., Shi, L., Shears, M. J., Harupa, A., Hopp, C. S., et al. (2016). Interrogating the plasmodium sporozoite surface: identification of surface-exposed proteins and demonstration of glycosylation on CSP and TRAP by mass spectrometry-based proteomics. *PLoS Pathog.* 12:e1005606. doi: 10.1371/journal.ppat.1005606

Tamana, S., and Promponas, V. J. (2019). An updated view of the oligosaccharyltransferase complex in Plasmodium. *Glycobiology* 29, 385–396. doi: 10.1093/glycob/cwz011

Tamborrini, M., Liu, X., Mugasa, J. P., Kwon, Y. U., Kamena, F., Seeberger, P. H., et al. (2010). Synthetic glycosylphosphatidylinositol microarray reveals differential antibody levels and fine specificities in children with mild and severe malaria. *Bioorganic Med. Chem.* 18, 3747–3752. doi: 10.1016/j.bmc.2010.04.059

Tolia, N. H., Enemark, E. J., Sim, B. K. L., and Joshua-Tor, L. (2005). Structural basis for the EBA-175 erythrocyte invasion pathway of the malaria parasite Plasmodium falciparum. *Cell* 122, 183–193. doi: 10.1016/j.cell.2005.05.033

Toscano, M. A., Tongren, J. E., De Souza, J. B., Liu, F. T., Riley, E. M., and Rabinovich, G. A. (2012). Endogenous galectin-3 controls experimental malaria in a species-specific manner. *Parasite Immunol.* 34, 383–387. doi: 10.1111/j.1365-3024.2012.01366.x

Uneke, C. J. (2007). Plasmodium falciparum malaria and ABO blood group: is there any relationship? *Parasitol. Res.* 100, 759–765. doi: 10.1007/s00436-006-0342-5

Vagianou, C. D., Stuhr-Hansen, N., Moll, K., Bovin, N., Wahlgren, M., and Blixt, O. (2018). ABO blood group antigen decorated giant unilamellar vesicles exhibit distinct interactions with plasmodium falciparum infected red blood cells. *ACS Chem. Biol.* 13, 2421–2426. doi: 10.1021/acschembio.8b00635

Van Niekerk, D. D., Penkler, G. P., Du Toit, F., and Snoep, J. L. (2016). Targeting glycolysis in the malaria parasite Plasmodium falciparum. *FEBS J.* 283, 634–646. doi: 10.1111/febs.13615

Varki, A., Cummings, R. D., Esko, J. D., Stanley, P., Hart, G. W., Aebi, M., et al. (2017). *Essentials of Glycobiology*, 3rd Edn. New York, NY: Cold Spring Harbor Laboratory Press.

Vogt, A. M., Barragan, A., Chen, Q., Kironde, F., Spillmann, D., and Wahlgren, M. (2003). Heparan sulfate on endothelial cells mediates the binding of Plasmodium falciparum-infected erythrocytes via the DBL1α domain of PfEMP1. *Blood* 101, 2405–2411. doi: 10.1182/blood-2002-07-2016

Wang, J., Jiang, N., Sang, X., Yang, N., Feng, Y., Chen, R., et al. (2021). Protein modification characteristics of the malaria parasite plasmodium falciparum and the infected erythrocytes. *Mol. Cell Proteomics* 20:100001. doi: 10.1074/MCP.RA120.002375

World Health Organization [WHO] (2020). *World Malaria Report: 20 Years of Global Progress and Challenges*. Geneva: World Health Organization.

Yamamoto, F. I., Clausen, H., White, T., Marken, J., and Hakomori, S. I. (1990). Molecular genetic basis of the histo-blood group ABO system. *Nature* 345, 229–233. doi: 10.1038/345229a0

Yilmaz, B., Portugal, S., Tran, T. M., Gozzelino, R., Ramos, S., Gomes, J., et al. (2014). Gut microbiota elicits a protective immune response against malaria transmission. *Cell* 159, 1277–1289. doi: 10.1016/j.cell.2014.10.053

Zerka, A., Kaczmarek, R., Czerwinski, M., and Jaskiewicz, E. (2017). Plasmodium reichenowi EBA-140 merozoite ligand binds to glycophorin D on chimpanzee red blood cells, shedding new light on origins of Plasmodium falciparum. *Parasites Vectors* 10:554. doi: 10.1186/s13071-017-2507-8

Zhang, Y., Jiang, N., Jia, B., Chang, Z., Zhang, Y., Wei, X., et al. (2014). A comparative study on the heparin-binding proteomes of Toxoplasma gondii and Plasmodium falciparum. *Proteomics* 14, 1737–1745. doi: 10.1002/pmic.201400003

Zhang, Y., Jiang, N., Lu, H., Hou, N., Piao, X., Cai, P., et al. (2013). Proteomic analysis of Plasmodium falciparum schizonts reveals heparin-binding merozoite proteins. *J. Proteome Res.* 12, 2185–2193. doi: 10.1021/pr400038j

Conflict of Interest: The authors declare that the research was conducted in the absence of any commercial or financial relationships that could be construed as a potential conflict of interest.

frontiers in Immunology

MINI REVIEW
published: 23 August 2021
doi: 10.3389/fimmu.2021.729260

The Epithelial Cell Glycocalyx in Ocular Surface Infection

*Pablo Argüeso**, *Ashley M. Woodward* and *Dina B. AbuSamra*

Department of Ophthalmology, Schepens Eye Research Institute of Massachusetts Eye and Ear, Harvard Medical School, Boston, MA, United States

The glycocalyx is the main component of the transcellular barrier located at the interface between the ocular surface epithelia and the external environment. This barrier extends up to 500 nm from the plasma membrane and projects into the tear fluid bathing the surface of the eye. Under homeostatic conditions, defense molecules in the glycocalyx, such as transmembrane mucins, resist infection. However, many pathogenic microorganisms have evolved to exploit components of the glycocalyx in order to gain access to epithelial cells and consequently exert deleterious effects. This manuscript reviews the implications of the ocular surface epithelial glycocalyx to bacterial, viral, fungal and parasitic infection. Moreover, it presents some ongoing controversies surrounding the functional relevance of the epithelial glycocalyx to ocular infectious disease.

Keywords: epithelium, glycocalyx, mucins, infection, ocular surface

OPEN ACCESS

Edited by:
Hector Mora Montes, University of Guanajuato, Mexico

Reviewed by:
Gordon Laurie, University of Virginia, United States
Sharvan Sehrawat, Indian Institute of Science Education and Research Mohali, India

****Correspondence:***
Pablo Argüeso
pablo_argueso@meei.harvard.edu

Specialty section:
This article was submitted to Microbial Immunology, a section of the journal Frontiers in Immunology

Received: *22 June 2021*
Accepted: *09 August 2021*
Published: *23 August 2021*

Citation:
Argüeso P, Woodward AM and AbuSamra DB (2021) The Epithelial Cell Glycocalyx in Ocular Surface Infection. Front. Immunol. 12:729260. doi: 10.3389/fimmu.2021.729260

INTRODUCTION

The glycocalyx is a carbohydrate-rich coating present on the external surface of plasma membranes. It serves as a barrier against pathogens but, at the same time, can be utilized by such pathogens for attachment and entry. The major components of the glycocalyx are glycans composed of monosaccharides linked to each other with various degrees of structural complexity. Glycans can be classified according to the internal organization of monosaccharides and the nature of the linkage established with protein and lipid moieties on plasma membranes. O-glycans are commonly attached to the hydroxyl group of serine or threonine residues on proteins, whereas N-glycans are linked *via* an amide linkage to asparagine. Glycosaminoglycans contain repeating disaccharide units that are either free or covalently attached to core proteins to form proteoglycans. Glycosphingolipids and glycosylphosphatidylinositols consist of a hydrophobic lipid tail attached to a glycan moiety, with the glycan moiety of glycosylphosphatidylinositols covalently linked to a variety of proteins (1).

The transparent cornea together with the associated tear film is the primary refractive surface of the visual system that allows the passage of light onto the retina for clear vision. It is surrounded and maintained by the adjacent corneoscleral limbus and the connective tissue of the conjunctiva with its adnexa. The outermost layer of the cornea and conjunctiva is composed of a non-keratinized stratified squamous epithelium and constitutes the first cellular barrier against pathogen penetrance. Apical membranes on the most apical cell layer exhibit folds or ridges, termed microplicae, containing a prominent glycocalyx rich in transmembrane mucins, proteoglycans and glycosphingolipids. Components of this glycocalyx extend hundreds of nanometers above the

plasma membrane and interface with the external environment (2). Apical cells also exhibit tight junctions that regulate the paracellular movement of molecules and microorganisms across the epithelium. The surface of the eye, like other mucosal tissues in the human body, represents a route of transmission for many bacteria, viruses, fungi and parasites. Here, we provide a brief review of major components of the ocular surface epithelial glycocalyx and their involvement in resisting or facilitating infection.

THE GLYCOCALYX IN OCULAR SURFACE INFECTION

Bacterial Infection

Bacterial keratitis is a sight-threatening infectious disease of the cornea caused by different types of bacteria, including *Staphylococcus aureus, Streptococcus pneumoniae* and *Pseudomonas aeruginosa* (3). One of the first steps during bacterial infection is the adhesion of the pathogen to glycoproteins and glycolipids on the epithelial cell glycocalyx through specific glycan recognition mechanisms (4, 5). Notably, this adhesive interaction does not take place unless the epithelia are damaged (6). Mucins stand out among the multiple protective components of the healthy glycocalyx because of their ability to limit infectious disease while accommodating resident microbiota (7). Transmembrane mucins have large and rigid extracellular domains that extend 500 nm or more above the cell surface. They can prevent microbial colonization by several mechanisms that include forming a physical barrier, acting as adhesion decoys and, in certain cases, exposing specific glycans that attenuate pathogen virulence.

The presence of the transmembrane mucin MUC16 at the ocular surface is a major restrain to the passage of bacteria. Reports using a human cell culture model of stratified corneal epithelium have evidenced that MUC16 and mucin O-glycans protect the epithelial surface against *S. aureus* adhesion (8, 9). It has been established that transmembrane mucins in cornea play a crucial role in the early response against pathogens by suppressing Toll-like receptor signaling and the expression of the proinflammatory cytokines (10). Therefore, in the absence of pre-existing defects or wounding, non-opportunistic bacteria must rely on the enzymatic removal of transmembrane mucins to access epithelial cells and cause disease. This is the case with epidemic disease-causing *S. pneumoniae* species, which secrete a metalloproteinase, ZmpC, that selectively induces ectodomain shedding of MUC16, leading to loss of glycocalyx barrier function and enhanced bacterial internalization (11, 12). Under homeostatic conditions, the barrier function of MUC16 in the epithelial glycocalyx is reinforced by galectin-3, a multimerizing lectin that causes carbohydrate-dependent crosslinking of transmembrane mucins (13–15). Intriguingly, galectin-3 is highly expressed in the human cornea and serves as a ligand for *P. aeruginosa* lipopolysaccharide (16). A potential explanation for the scarcity of adhesive events leading to *P. aeruginosa* infection in the healthy eye is that the strong, high-affinity association between mucins and galectin-3 on the glycocalyx provides steric hindrance, therefore interfering with the ability of the bacterium to interact with the lectin.

Some bacteria exploit proteoglycans present on the ocular surface epithelia and underlying extracellular matrix to promote infection. Syndecan-1 and perlecan are two proteoglycans containing chains of heparan sulfate and chondroitin sulfate—major glycosaminoglycans found in the human cornea (17). Syndecan-1 is known to enhance the attachment of *S. aureus* to the plasma membrane of several cell types but fails to do so in corneal epithelial cells. Instead, *S. aureus* induces shedding of syndecan-1 from the glycocalyx of corneal epithelial cells to produce ectodomains that interfere with the capacity of neutrophils to kill the bacteria (18). Similarly, the ability of *P. aeruginosa* and *S. pneumoniae* to infect the cornea is not associated with direct adhesion to proteoglycans present on the epithelial glycocalyx. *P. aeruginosa* preferably binds to perlecan exposed in the basement membrane after corneal injury (19, 20), whereas *S. pneumoniae* adhesion relies on the ability of syndecan-1 to promote the assembly of fibronectin fibrils in the basement membrane (21).

The clearance of bacteria can be enhanced by glycans and glycoconjugates present in the tear fluid bathing the ocular surface epithelia. For example, it has been shown that binding of *P. aeruginosa* to N-glycans on tear glycoproteins functions as a protective mechanism that reduces bacterial adhesion and infection, most likely by facilitating the removal of the bacteria through the tear drainage system (22). Similarly, studies have shown that surfactant protein D, a collagen-containing calcium-dependent lectin with ability to bind lipopolysaccharide from Gram-negative bacteria, is present in the tear fluid and protects against *P. aeruginosa* invasion (23, 24).

Viral Infection

Like bacteria, many viruses causing infectious disease employ glycans on cell surface glycoproteins and glycolipids to access cells. These viruses often recognize unique glycan signatures on the glycocalyx, which frequently leads to specific tissue and species tropisms (25). An example is human adenoviruses (HAdV), one of the most common causes of ocular infection. Dozens of HAdVs, classified into seven species, A to G, have been identified on mucosal surfaces, but only a limited number of them cause epidemic keratoconjunctivitis in the eye (26). It appears that some of these viruses, primarily those belonging to species D, use sialic acid-containing glycans to establish infections at the ocular surface (27). One of them, the corneatropic HAdV-D37, specifically binds a branched oligosaccharide present in glycoproteins containing the GD1a glycan motif and featuring two terminal sialic acids (28). Coxsackievirus A24 variant (CVA24v) is another highly contagious infective agent that causes acute hemorrhagic conjunctivitis. Binding and infection experiments using corneal cells indicate that the cell surface receptor used by CVA24v is composed of a sialylated disaccharide (Neu5Acα2,3Gal) on O-glycosylated proteins (29). Consequently, derivatives based on sialic acid have been developed and shown to be effective in preventing HAdV-D37 and CVA24v binding and infection of human corneal epithelial cells (30, 31).

Efforts have been made to establish how these viruses bypass the transmembrane mucin-rich glycocalyx of the ocular surface epithelium to trigger infection and inflammation. The data suggest that, for successful infection, HAdVs need to degrade components of the mucin barrier. This is exemplified by HAdV-D37, which in contrast to HAdV-D19p, a virus that does not cause epidemic keratoconjunctivitis, releases the MUC16 ectodomain from corneal and conjunctival epithelial cells, causing a decrease in glycocalyx barrier function (32). On other occasions, transmembrane mucins contribute to masking viral entry mediators on the epithelial glycocalyx. Affinity assays have shown that herpes simplex virus type 1 (HSV-1), but not HSV-2, binds galectin-3, a component of the human corneal epithelial glycocalyx. Exposure of epithelial cell cultures to transmembrane mucin isolates decreases HSV-1 infectivity, suggesting that the strong association between transmembrane mucins and galectin-3 in the glycocalyx functions to mask the lectin and to provide protection against viral infection (33).

Many pathogens use glycosaminoglycans on the glycocalyx of host cells to initiate infection, and viruses are no exception. Heparan sulfate serves as a main HSV-1 entry receptor in the cornea and facilitates the development of herpetic keratitis (34, 35). Important to infection is the release of the viral progeny from the infected cells so that infection can disseminate into new target cells. Opposing this process are heparan sulfate chains on parent cells, which trap the exiting viral progenies and inhibit their release. Heparanase, a heparan sulfate-degrading enzyme, plays an essential role in facilitating viral egress. Following herpes infection of human corneal epithelial cells, heparanase promotes a continuous loss of heparan sulfate from the cell surface, leading to virus exit and subsequent tissue damage (36). This mechanism involves the upregulation of corneal epithelial heparanase by herpesvirus to promote enzymatic activity at the cell surface, as well as translocation of the enzyme to the nucleus, where it regulates downstream signaling pathways (37). The interaction of HAdV-D37 with sulfated glycosaminoglycans has also been recently reported. In these experiments, removal of heparan sulfate by heparinase III reduced HAdV-D37 binding to corneal epithelial cells but, at the same time, enhanced viral infection, leading the authors to hypothesize that glycosaminoglycans act as decoy receptors (38). Consequently, efforts have been made in the drug development field to use glycosaminoglycan mimetics as artificial decoy receptors that can inhibit HAdV-D37 cell attachment and infection (39).

Fungal and Parasitic Infections

Fungal infections of the cornea can have devastating consequences if not treated promptly. They are frequently caused by species of *Fusarium*, *Aspergillus*, *Curvularia*, and *Candida*, with trauma being the most important predisposing cause (40). The first step for a successful infection is the presence of cell wall components and parasitic adhesins that mediate adhesion to host cells and components of the extracellular matrix. A number of interactions with host cells are known to lead to pathogen internalization, but the studies describing this invasion process remain scarce (41). Studies in corneal epithelium have revealed that *Cephalosporium curvulum* and *Aspergillus oryzae* use fucose-specific lectins to gain access to the host cell surface and, subsequently, promote infection and disease (42). It is worth noting here that a significant number of terminal and core fucose structures are present in the differentiated corneal epithelial glycocalyx, which could facilitate this type of interaction (43). In addition to immune cells, the corneal epithelium expresses lectins that also interact with polysaccharides on the fungal cell wall. An example is the C-type lectin dectin-1, which recognizes β-glucan. Binding of dectin-1 to *Candida albicans* initiates protective responses in the epithelium that include the regulation of the innate immune response through the dectin-1/NF-κB signaling pathway (44).

Acanthamoeba keratitis is a rare but serious parasitic infection of the cornea that can cause permanent vision loss. As previously stated for other microbes, adhesion to the surface of the host is one of the first steps in the pathogenesis of infection. Adhesion of *Acanthamoeba* is followed by lysis of corneal epithelial cells, degradation of extracellular matrix and penetration into the deeper layers of the cornea (45). A major virulence factor of this parasite is a mannose-binding protein that recognizes mannose-containing glycoproteins on the surface of the cornea and plays a role in promoting cytopathic effects (46). The presence of antibodies against the mannose-binding protein in tear fluid is thought to provide protection by inhibiting the adhesion of the parasite. Importantly, oral immunization with recombinant mannose-binding protein in an animal model has been shown to increase the levels of antibodies against this protein in tears and provide protection against *Acanthamoeba* keratitis (47).

CONTROVERSIES

The role of the epithelial glycocalyx in resisting or facilitating ocular infection is not free of controversy. As mentioned previously, the presence of highly glycosylated transmembrane mucins is thought to provide steric hindrance and limit *P. aeruginosa* adhesion to the host. On the other hand, using an azido GalNAc analog to label mucin-type O-linked glycoproteins, Jolly et al. observed that *P. aeruginosa* preferentially associated with GalNAc labeled-regions in the mouse cornea, leading the authors to conclude that surface glycosylation was not sufficient to prevent bacterial binding (48). It should be noted, however, that the metabolism of these azido sugars could pose significant drawbacks, including low specificity and the perturbation of the natural glycosylation process (49, 50). If this is the case, one could draw the opposite conclusion, i.e., that naturally occurring surface glycosylation is sufficient to maintain barrier function since perturbation of glycans physiologically present on the corneal surface, by using chemically modified monosaccharides, leads to bacterial binding.

MUC1 is one of the most extensively studied transmembrane mucins since it is known to regulate both pathogen invasion and the inflammatory response to infection. Assessment of the ocular surface of mice deficient in Muc1 revealed a marked propensity toward the development of irritation and inflammation (51). These mice were also more susceptible to bacterial infections based on the prevalence of *Staphylococcus*, *Streptococcus* and *Corynebacterium* species in infected eyes. Conversely, a parallel

study using Muc1 null mice of a different genetic background found no particular ocular surface phenotype (52). Mouse eyes in the latter study had a normal appearance with no signs of ocular surface infection. Indeed, the authors could not find definitive evidence indicating that Muc1 null mice were more susceptible to *P. aeruginosa* adherence to the cornea. The differences in these studies were attributed to housing conditions of the animals, mouse strain variation, strain variation of pathogens or other environmental or epigenetic differences.

The roles of the different transmembrane mucins in protecting the human ocular surface epithelium have been the subject of intense study. While it was assumed for many years that they play a redundant function in protecting the underlying tissue against environmental insult, new evidence appears to challenge this concept. Experiments *in vitro* have evidenced that MUC16 in human corneal epithelial cells prevents bacterial adherence and invasion, while the smaller MUC1 does not (53). Surprisingly, abrogation of MUC1 in these experiments enhanced the barrier with respect to bacterial adherence and invasion, leading the authors to hypothesize that MUC16 alone produces a more uniform, glycan-rich barrier on the epithelial glycocalyx.

CONCLUDING REMARKS

Multiple studies have evidenced over time the extent of glycosylation at the ocular surface epithelia and its relevance to infection (**Figure 1**). Both corneal and conjunctival epithelial cells contain a complex glycocalyx rich in transmembrane mucins, proteoglycans and glycosphingolipids. Adhesion of pathogens to glycans present in some of these molecules is one of the first steps leading to the successful colonization of the eye. At the same time, the ocular surface exhibits protective glycoconjugates that actively prevent pathogen invasion. One of them is transmembrane mucins that extend high above other molecules present on the glycocalyx, thereby providing a physical barrier and masking receptors by steric hindrance. In addition, the ocular surface fights infection by exposing host molecules that act as decoy receptors, impeding pathogen adhesion and the initiation of signaling cascades.

Contact lens wear, trauma, and ocular surface disease constitute common risk factors that predispose patients to infections. Interestingly, most of these factors have been associated with alterations in glycosylation. Carbohydrate moieties on cell surface glycoproteins change in response to corneal wounding and contact

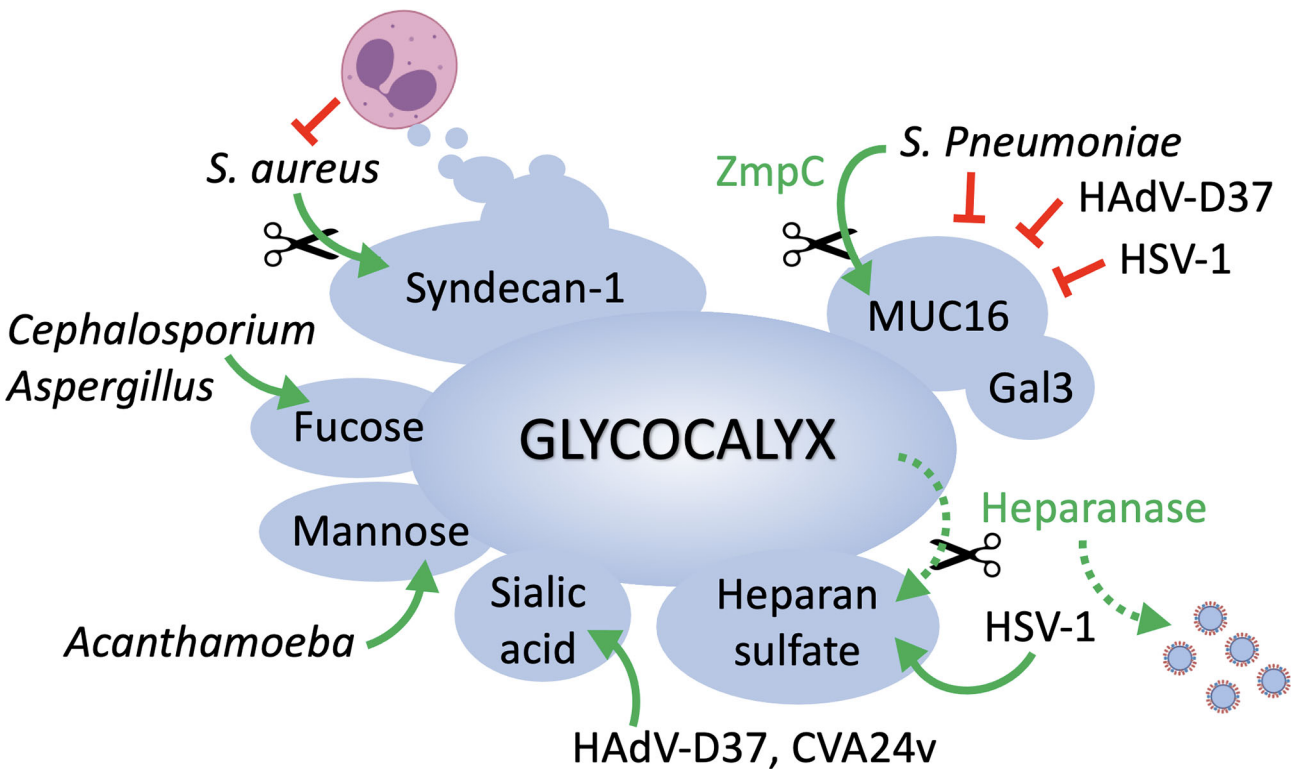

FIGURE 1 | The epithelial cell glycocalyx in ocular surface infection. MUC16 represents one of the first barriers to the passage of bacteria and viruses at the ocular surface, and its function is reinforced by galectin-3. Pathogens must rely on the enzymatic removal of mucins (e.g., ZmpC) to access epithelial cells and cause disease. Pathogens such as *S. aureus* circumvent immune cell destruction by inducing shedding of syndecan-1 from the cell surface. HSV-1 uses heparan sulfate as a main entry receptor but also promotes heparanase biosynthesis in host cells to facilitate the release of viral progenies. Cell surface glycans containing sialic acid, mannose or fucose serve as receptors for viral, fungal and parasitic organisms.

lens wear, and inflammatory stimuli of the ocular surface epithelia induce alterations in mucin-type O-glycosylation and N-glycan processing (43, 54–56). It would be noteworthy to determine if these changes in glycosylation contribute to the higher risk of ocular infection. Other exciting areas that remain understudied in the eye include the influence of genetic factors (e.g., secretor status) on disease susceptibility and the role of ocular surface glycans in controlling microbial stability or virulence (57, 58). This information may be useful for designing effective prophylactic and therapeutic agents targeting the microbe–host interface.

AUTHOR CONTRIBUTIONS

All authors listed have made a substantial, direct, and intellectual contribution to the work and approved it for publication.

FUNDING

We acknowledge the funding support from the National Institutes of Health, NEI Grants R01EY026147 and R01EY030928.

REFERENCES

1. Rodriguez Benavente MC, Argueso P. Glycosylation Pathways at the Ocular Surface. *Biochem Soc Trans* (2018) 46(2):343–50. doi: 10.1042/BST20170408
2. Argueso P. Disrupted Glycocalyx as a Source of Ocular Surface Biomarkers. *Eye Contact Lens* (2020) 46 Suppl 2:S53–6. doi: 10.1097/ICL.0000000000000653
3. Ormerod LD, Hertzmark E, Gomez DS, Stabiner RG, Schanzlin DJ, Smith RE. Epidemiology of Microbial Keratitis in Southern California. A Multivariate Analysis. *Ophthalmology* (1987) 94(10):1322–33. doi: 10.1016/s0161-6420(87)80019-2
4. Poole J, Day CJ, von Itzstein M, Paton JC, Jennings MP. Glycointeractions in Bacterial Pathogenesis. *Nat Rev Microbiol* (2018) 16(7):440–52. doi: 10.1038/s41579-018-0007-2
5. Formosa-Dague C, Castelain M, Martin-Yken H, Dunker K, Dague E, Sletmoen M. The Role of Glycans in Bacterial Adhesion to Mucosal Surfaces: How Can Single-Molecule Techniques Advance Our Understanding? *Microorganisms* (2018) 6(2):1–26. doi: 10.3390/microorganisms6020039
6. Spurr-Michaud SJ, Barza M, Gipson IK. An Organ Culture System for Study of Adherence of Pseudomonas Aeruginosa to Normal and Wounded Corneas. *Invest Ophthalmol Vis Sci* (1988) 29(3):379–86.
7. Linden SK, Sutton P, Karlsson NG, Korolik V, McGuckin MA. Mucins in the Mucosal Barrier to Infection. *Mucosal Immunol* (2008) 1(3):183–97. doi: 10.1038/mi.2008.5
8. Blalock TD, Spurr-Michaud SJ, Tisdale AS, Heimer SR, Gilmore MS, Ramesh V, et al. Functions of MUC16 in Corneal Epithelial Cells. *Invest Ophthalmol Vis Sci* (2007) 48(10):4509–18. doi: 10.1167/iovs.07-0430
9. Ricciuto J, Heimer SR, Gilmore MS, Argueso P. Cell Surface O-Glycans Limit Staphylococcus Aureus Adherence to Corneal Epithelial Cells. *Infect Immun* (2008) 76(11):5215–20. doi: 10.1128/IAI.00708-08
10. Menon BB, Kaiser-Marko C, Spurr-Michaud S, Tisdale AS, Gipson IK. Suppression of Toll-Like Receptor-Mediated Innate Immune Responses at the Ocular Surface by the Membrane-Associated Mucins MUC1 and MUC16. *Mucosal Immunol* (2015) 8(5):1000–8. doi: 10.1038/mi.2014.127
11. Govindarajan B, Menon BB, Spurr-Michaud S, Rastogi K, Gilmore MS, Argueso P, et al. A Metalloproteinase Secreted by Streptococcus Pneumoniae Removes Membrane Mucin MUC16 From the Epithelial Glycocalyx Barrier. *PloS One* (2012) 7(3):e32418. doi: 10.1371/journal.pone.0032418
12. Menon BB, Govindarajan B. Identification of an Atypical Zinc Metalloproteinase, ZmpC, From an Epidemic Conjunctivitis-Causing Strain of Streptococcus Pneumoniae. *Microb Pathog* (2013) 56:40–6. doi: 10.1016/j.micpath.2012.11.006
13. Mauris J, Mantelli F, Woodward AM, Cao Z, Bertozzi CR, Panjwani N, et al. Modulation of Ocular Surface Glycocalyx Barrier Function by a Galectin-3 N-Terminal Deletion Mutant and Membrane-Anchored Synthetic Glycopolymers. *PloS One* (2013) 8(8):e72304. doi: 10.1371/journal.pone.0072304
14. Argueso P, Guzman-Aranguez A, Mantelli F, Cao Z, Ricciuto J, Panjwani N. Association of Cell Surface Mucins With Galectin-3 Contributes to the Ocular Surface Epithelial Barrier. *J Biol Chem* (2009) 284(34):23037–45. doi: 10.1074/jbc.M109.033332
15. Taniguchi T, Woodward AM, Magnelli P, McColgan NM, Lehoux S, Jacobo SMP, et al. N-Glycosylation Affects the Stability and Barrier Function of the MUC16 Mucin. *J Biol Chem* (2017) 292(26):11079–90. doi: 10.1074/jbc.M116.770123
16. Gupta SK, Masinick S, Garrett M, Hazlett LD. Pseudomonas Aeruginosa Lipopolysaccharide Binds Galectin-3 and Other Human Corneal Epithelial Proteins. *Infect Immun* (1997) 65(7):2747–53. doi: 10.1128/IAI.65.7.2747-2753.1997
17. Bairaktaris G, Lewis D, Fullwood NJ, Nieduszynski IA, Marcyniuk B, Quantock AJ, et al. An Ultrastructural Investigation Into Proteoglycan Distribution in Human Corneas. *Cornea* (1998) 17(4):396–402. doi: 10.1097/00003226-199807000-00010
18. Hayashida A, Amano S, Park PW. Syndecan-1 Promotes Staphylococcus Aureus Corneal Infection by Counteracting Neutrophil-Mediated Host Defense. *J Biol Chem* (2011) 286(5):3288–97. doi: 10.1074/jbc.M110.185165
19. Chen L, Hazlett LD. Human Corneal Epithelial Extracellular Matrix Perlecan Serves as a Site for Pseudomonas Aeruginosa Binding. *Curr Eye Res* (2001) 22(1):19–27. doi: 10.1076/ceyr.22.1.19.6973
20. Chen LD, Hazlett LD. Perlecan in the Basement Membrane of Corneal Epithelium Serves as a Site for P. Aeruginosa Binding. *Curr Eye Res* (2000) 20(4):260–7. doi: 10.1076/0271-3683(200004)2041-5FT260
21. Jinno A, Hayashida A, Jenkinson HF, Park PW. Syndecan-1 Promotes Streptococcus Pneumoniae Corneal Infection by Facilitating the Assembly of Adhesive Fibronectin Fibrils. *mBio* (2020) 11(6):1–15. doi: 10.1128/mBio.01907-20
22. Kautto L, Nguyen-Khuong T, Everest-Dass A, Leong A, Zhao Z, Willcox MDP, et al. Glycan Involvement in the Adhesion of Pseudomonas Aeruginosa to Tears. *Exp Eye Res* (2016) 145:278–88. doi: 10.1016/j.exer.2016.01.013
23. Ni M, Evans DJ, Hawgood S, Anders EM, Sack RA, Fleiszig SM. Surfactant Protein D is Present in Human Tear Fluid and the Cornea and Inhibits Epithelial Cell Invasion by Pseudomonas Aeruginosa. *Infect Immun* (2005) 73(4):2147–56. doi: 10.1128/IAI.73.4.2147-2156.2005
24. Ni M, Tam C, Verma A, Ramphal R, Hawgood S, Evans DJ, et al. Expression of Surfactant Protein D in Human Corneal Epithelial Cells is Upregulated by Pseudomonas Aeruginosa. *FEMS Immunol Med Microbiol* (2008) 54(2):177–84. doi: 10.1111/j.1574-695X.2008.00461.x
25. Thompson AJ, de Vries RP, Paulson JC. Virus Recognition of Glycan Receptors. *Curr Opin Virol* (2019) 34:117–29. doi: 10.1016/j.coviro.2019.01.004
26. Rajaiya J, Saha A, Ismail AM, Zhou X, Su T, Chodosh J. Adenovirus and the Cornea: More Than Meets the Eye. *Viruses* (2021) 13(2):1–9. doi: 10.3390/v13020293
27. Chandra N, Frangsmyr L, Imhof S, Caraballo R, Elofsson M, Arnberg N. Sialic Acid-Containing Glycans as Cellular Receptors for Ocular Human Adenoviruses: Implications for Tropism and Treatment. *Viruses* (2019) 11(5):1–12. doi: 10.3390/v11050395
28. Nilsson EC, Storm RJ, Bauer J, Johansson SM, Lookene A, Angstrom J, et al. The GD1a Glycan is a Cellular Receptor for Adenoviruses Causing Epidemic Keratoconjunctivitis. *Nat Med* (2011) 17(1):105–9. doi: 10.1038/nm.2267
29. Mistry N, Inoue H, Jamshidi F, Storm RJ, Oberste MS, Arnberg N. Coxsackievirus A24 Variant Uses Sialic Acid-Containing O-Linked Glycoconjugates as Cellular Receptors on Human Ocular Cells. *J Virol* (2011) 85(21):11283–90. doi: 10.1128/JVI.05597-11
30. Johansson E, Caraballo R, Mistry N, Zocher G, Qian W, Andersson CD, et al. Pentavalent Sialic Acid Conjugates Block Coxsackievirus A24 Variant and Human Adenovirus Type 37-Viruses That Cause Highly Contagious Eye Infections. *ACS Chem Biol* (2020) 15(10):2683–91. doi: 10.1021/acschembio.0c00446
31. Johansson SM, Nilsson EC, Elofsson M, Ahlskog N, Kihlberg J, Arnberg N. Multivalent Sialic Acid Conjugates Inhibit Adenovirus Type 37 From Binding

to and Infecting Human Corneal Epithelial Cells. *Antiviral Res* (2007) 73 (2):92–100. doi: 10.1016/j.antiviral.2006.08.004
32. Menon BB, Zhou X, Spurr-Michaud S, Rajaiya J, Chodosh J, Gipson IK. Epidemic Keratoconjunctivitis-Causing Adenoviruses Induce MUC16 Ectodomain Release To Infect Ocular Surface Epithelial Cells. *mSphere* (2016) 1(1):1–8. doi: 10.1128/mSphere.00112-15
33. Woodward AM, Mauris J, Argueso P. Binding of Transmembrane Mucins to Galectin-3 Limits Herpesvirus 1 Infection of Human Corneal Keratinocytes. *J Virol* (2013) 87(10):5841–7. doi: 10.1128/JVI.00166-13
34. Park PJ, Shukla D. Role of Heparan Sulfate in Ocular Diseases. *Exp Eye Res* (2013) 110:1–9. doi: 10.1016/j.exer.2013.01.015
35. Shukla D, Liu J, Blaiklock P, Shworak NW, Bai X, Esko JD, et al. A Novel Role for 3-O-Sulfated Heparan Sulfate in Herpes Simplex Virus 1 Entry. *Cell* (1999) 99(1):13–22. doi: 10.1016/s0092-8674(00)80058-6
36. Hadigal SR, Agelidis AM, Karasneh GA, Antoine TE, Yakoub AM, Ramani VC, et al. Heparanase Is a Host Enzyme Required for Herpes Simplex Virus-1 Release From Cells. *Nat Commun* (2015) 6:6985. doi: 10.1038/ncomms7985
37. Agelidis A, Shukla D. Heparanase, Heparan Sulfate and Viral Infection. *Adv Exp Med Biol* (2020) 1221:759–70. doi: 10.1007/978-3-030-34521-1_32
38. Chandra N, Liu Y, Liu JX, Frangsmyr L, Wu N, Silva LM, et al. Sulfated Glycosaminoglycans as Viral Decoy Receptors for Human Adenovirus Type 37. *Viruses* (2019) 11(3):1–20. doi: 10.3390/v11030247
39. Chandra N, Frangsmyr L, Arnberg N. Decoy Receptor Interactions as Novel Drug Targets Against EKC-Causing Human Adenovirus. *Viruses* (2019) 11 (3):1–11. doi: 10.3390/v11030242
40. Thomas PA. Fungal Infections of the Cornea. *Eye (Lond)* (2003) 17(8):852–62. doi: 10.1038/sj.eye.6700557
41. Mendes-Giannini MJ, Soares CP, da Silva JL, Andreotti PF. Interaction of Pathogenic Fungi With Host Cells: Molecular and Cellular Approaches. *FEMS Immunol Med Microbiol* (2005) 45(3):383–94. doi: 10.1016/j.femsim.2005.05.014
42. Ballal S, Belur S, Laha P, Roy S, Swamy BM, Inamdar SR. Mitogenic Lectins From Cephalosporium Curvulum (CSL) and Aspergillus Oryzae (AOL) Mediate Host-Pathogen Interactions Leading to Mycotic Keratitis. *Mol Cell Biochem* (2017) 434(1-2):209–19. doi: 10.1007/s11010-017-3050-9
43. Woodward AM, Lehoux S, Mantelli F, Di Zazzo A, Brockhausen I, Bonini S, et al. Inflammatory Stress Causes N-Glycan Processing Deficiency in Ocular Autoimmune Disease. *Am J Pathol* (2019) 189(2):283–94. doi: 10.1016/j.ajpath.2018.10.012
44. Hua X, Yuan X, Li Z, Coursey TG, Pflugfelder SC, Li DQ. A Novel Innate Response of Human Corneal Epithelium to Heat-Killed Candida Albicans by Producing Peptidoglycan Recognition Proteins. *PloS One* (2015) 10(6): e0128039. doi: 10.1371/journal.pone.0128039
45. Niederkorn JY, Alizadeh H, Leher H, McCulley JP. The Pathogenesis of Acanthamoeba Keratitis. *Microbes Infect* (1999) 1(6):437–43. doi: 10.1016/s1286-4579(99)80047-1
46. Panjwani N. Pathogenesis of Acanthamoeba Keratitis. *Ocul Surf* (2010) 8 (2):70–9. doi: 10.1016/s1542-0124(12)70071-x
47. Garate M, Alizadeh H, Neelam S, Niederkorn JY, Panjwani N. Oral Immunization With Acanthamoeba Castellanii Mannose-Binding Protein Ameliorates Amoebic Keratitis. *Infect Immun* (2006) 74(12):7032–4. doi: 10.1128/IAI.00828-06
48. Jolly AL, Agarwal P, Metruccio MME, Spiciarich DR, Evans DJ, Bertozzi CR, et al. Corneal Surface Glycosylation is Modulated by IL-1R and Pseudomonas Aeruginosa Challenge But is Insufficient for Inhibiting Bacterial Binding. *FASEB J* (2017) 31(6):2393–404. doi: 10.1096/fj.201601198R
49. Shajahan A, Supekar NT, Wu H, Wands AM, Bhat G, Kalimurthy A, et al. Mass Spectrometric Method for the Unambiguous Profiling of Cellular Dynamic Glycosylation. *ACS Chem Biol* (2020) 15(10):2692–701. doi: 10.1021/acschembio.0c00453
50. Boyce M, Carrico IS, Ganguli AS, Yu SH, Hangauer MJ, Hubbard SC, et al. Metabolic Cross-Talk Allows Labeling of O-Linked Beta-N-Acetylglucosamine-Modified Proteins *via* the N-Acetylgalactosamine Salvage Pathway. *Proc Natl Acad Sci U.S.A.* (2011) 108(8):3141–6. doi: 10.1073/pnas.1010045108
51. Kardon R, Price RE, Julian J, Lagow E, Tseng SC, Gendler SJ, et al. Bacterial Conjunctivitis in Muc1 Null Mice. *Invest Ophthalmol Vis Sci* (1999) 40 (7):1328–35.
52. Danjo Y, Hazlett LD, Gipson IK. C57BL/6 Mice Lacking Muc1 Show No Ocular Surface Phenotype. *Invest Ophthalmol Vis Sci* (2000) 41(13):4080–4.
53. Gipson IK, Spurr-Michaud S, Tisdale A, Menon BB. Comparison of the Transmembrane Mucins MUC1 and MUC16 in Epithelial Barrier Function. *PloS One* (2014) 9(6):e100393. doi: 10.1371/journal.pone.0100393
54. Brockhausen I, Elimova E, Woodward AM, Argueso P. Glycosylation Pathways of Human Corneal and Conjunctival Epithelial Cell Mucins. *Carbohydr Res* (2018) 470:50–6. doi: 10.1016/j.carres.2018.10.004
55. Zieske JD, Higashijima SC, Gipson IK. Con A- and WGA-Binding Glycoproteins of Stationary and Migratory Corneal Epithelium. *Invest Ophthalmol Vis Sci* (1986) 27(8):1205–10.
56. Versura P, Maltarello MC, Cellini M, Marinelli F, Caramazza R, Laschi R. Detection of Mucus Glycoconjugates in Human Conjunctiva by Using the Lectin-Colloidal Gold Technique in TEM. III. A Quantitative Study in Asymptomatic Contact Lens Wearers. *Acta Ophthalmol (Copenh)* (1987) 65 (6):661–7. doi: 10.1111/j.1755-3768.1987.tb07060.x
57. Taylor SL, McGuckin MA, Wesselingh S, Rogers GB. Infection's Sweet Tooth: How Glycans Mediate Infection and Disease Susceptibility. *Trends Microbiol* (2018) 26(2):92–101. doi: 10.1016/j.tim.2017.09.011
58. Wheeler KM, Carcamo-Oyarce G, Turner BS, Dellos-Nolan S, Co JY, Lehoux S, et al. Mucin Glycans Attenuate the Virulence of Pseudomonas Aeruginosa in Infection. *Nat Microbiol* (2019) 4(12):2146–54. doi: 10.1038/s41564-019-0581-8

Conflict of Interest: The authors declare that the research was conducted in the absence of any commercial or financial relationships that could be construed as a potential conflict of interest.

Publisher's Note: All claims expressed in this article are solely those of the authors and do not necessarily represent those of their affiliated organizations, or those of the publisher, the editors and the reviewers. Any product that may be evaluated in this article, or claim that may be made by its manufacturer, is not guaranteed or endorsed by the publisher.

frontiers in Microbiology

REVIEW
published: 25 August 2021
doi: 10.3389/fmicb.2021.730543

The Role of Arabinogalactan Type II Degradation in Plant-Microbe Interactions

*Maria Guadalupe Villa-Rivera[1], Horacio Cano-Camacho[2], Everardo López-Romero[3] and María Guadalupe Zavala-Páramo[2]**

[1] Departamento de Ingeniería Genética, Centro de Investigación y de Estudios Avanzados del Instituto Politécnico Nacional, Irapuato, Mexico, [2] Centro Multidisciplinario de Estudios en Biotecnología, FMVZ, Universidad Michoacana de San Nicolás de Hidalgo, Tarímbaro, Mexico, [3] División de Ciencias Naturales y Exactas, Departamento de Biología, Universidad de Guanajuato, Guanajuato, Mexico

OPEN ACCESS

Edited by:
Ivan Martinez Duncker, Universidad Autónoma del Estado de Morelos, Mexico

Reviewed by:
Agata Leszczuk, Institute of Agrophysics (PAN), Poland
Ann G. Matthysse, University of North Carolina at Chapel Hill, United States

***Correspondence:**
María Guadalupe Zavala-Páramo
gzavpar@hotmail.com;
maria.zavala.paramo@umich.mx

Specialty section:
This article was submitted to Infectious Diseases, a section of the journal Frontiers in Microbiology

Received: 25 June 2021
Accepted: 04 August 2021
Published: 25 August 2021

Citation:
Villa-Rivera MG, Cano-Camacho H, López-Romero E and Zavala-Páramo MG (2021) The Role of Arabinogalactan Type II Degradation in Plant-Microbe Interactions. Front. Microbiol. 12:730543. doi: 10.3389/fmicb.2021.730543

Arabinogalactans (AGs) are structural polysaccharides of the plant cell wall. A small proportion of the AGs are associated with hemicellulose and pectin. Furthermore, AGs are associated with proteins forming the so-called arabinogalactan proteins (AGPs), which can be found in the plant cell wall or attached through a glycosylphosphatidylinositol (GPI) anchor to the plasma membrane. AGPs are a family of highly glycosylated proteins grouped with cell wall proteins rich in hydroxyproline. These glycoproteins have important and diverse functions in plants, such as growth, cellular differentiation, signaling, and microbe-plant interactions, and several reports suggest that carbohydrate components are crucial for AGP functions. In beneficial plant-microbe interactions, AGPs attract symbiotic species of fungi or bacteria, promote the development of infectious structures and the colonization of root tips, and furthermore, these interactions can activate plant defense mechanisms. On the other hand, plants secrete and accumulate AGPs at infection sites, creating cross-links with pectin. As part of the plant cell wall degradation machinery, beneficial and pathogenic fungi and bacteria can produce the enzymes necessary for the complete depolymerization of AGs including endo-β-(1,3), β-(1,4) and β-(1,6)-galactanases, β-(1,3/1,6) galactanases, α-L-arabinofuranosidases, β-L-arabinopyranosidases, and β-D-glucuronidases. These hydrolytic enzymes are secreted during plant-pathogen interactions and could have implications for the function of AGPs. It has been proposed that AGPs could prevent infection by pathogenic microorganisms because their degradation products generated by hydrolytic enzymes of pathogens function as damage-associated molecular patterns (DAMPs) eliciting the plant defense response. In this review, we describe the structure and function of AGs and AGPs as components of the plant cell wall. Additionally, we describe the set of enzymes secreted by microorganisms to degrade AGs from AGPs and its possible implication for plant-microbe interactions.

Keywords: arabinogalactan proteins, plant cell wall, hydrolytic enzymes, plant-microbe interaction, infection

INTRODUCTION

Cell wall is an essential component of plant cells; they confer flexibility and mechanical support to the cell and perform important functions such as the maintenance of cell, preservation of osmotic pressure, movement of water and nutrients, management of intercellular communication between adjacent cells and prominent involvement in plant-microbe interactions, constituting the main barrier against potential pathogens (Burton et al., 2010; Keegstra, 2010).

Chemically, a plant cell wall (PCW) is composed of cellulosic polysaccharides (cellulose microfibrils from 40.6–51.2% of dry weight), non-cellulosic polysaccharides, lignin, and proteins. Non-cellulosic polysaccharides form a gel-like matrix with remarkable heterogeneity and structural complexity (Burton et al., 2010). The principal non-cellulosic polysaccharides are hemicelluloses (28.5–37.2% of dry weight), which comprise a complex of heteropolysaccharides (the second most abundant type of polysaccharide in nature) assembled into laterally branched and generally amorphous structures on a xylose backbone (xylan) or mannose and glucose backbones (mannan and glucomannan) with galactose, arabinose, and acetic/glucuronic acid ramifications. Depending on their structure, hemicelluloses are classified as xyloglucan, glucuronoxylan, glucuronoarabinoxylan, glucomannan, galactomannan, and β-(1,3; 1,4)-glucan (Pauly and Keegstra, 2008, 2016; Scheller and Ulvskov, 2010). On the other hand, pectin (30–35% of dry weight) constitutes a complex family of polysaccharides that are rich in galacturonic acid, including homogalacturonan, rhamnogalacturonan I and II (the substituted galacturonans), and xylogalacturonan (Mohnen, 2008; Chen, 2014). Finally, lignin (27–32% in woody plants and 15–30% in herbaceous plants) is a complex polymer composed of aromatic residues (coumaroyl alcohol, coniferyl alcohol, and synapyl alcohol) (Chen, 2014).

Plant cell wall proteins (CWPs) constitute ∼5–10% of dry weight of the PCW mass. Analysis of the *Arabidopsis thaliana* proteome has provided important information regarding the diversity of these proteins. CWPs are classified into nine functional classes according to their predicted domains, and their possible partners have been proposed. The nine CWPs classes are proteins that act on carbohydrates; oxide reductases, proteases, proteins with interaction domains, proteins potentially involved in signaling, structural proteins, proteins related to lipid metabolism, miscellaneous proteins, and proteins with unknown function (Jamet et al., 2008; Albenne et al., 2013). An alternative classification of non-enzymatic proteins associated with the PCW into two groups has been proposed: hydroxyproline-rich glycoproteins (HRGPs), also known as the HRGP superfamily; glycine-rich proteins (GRPs) or the GRP superfamily. HRGPs are classified according to their hydroxyproline/proline proportion into different subfamilies such as extensins, proline-rich proteins (PRPs), arabinogalactan proteins (AGPs), solanaceous lectins, and subcellular PELPK proteins (Pro-Glu-Leu/Ile/Val-Pro-Lys). Alternately, GRPs have been classified into five classes based on their Gly-rich repeats (Class I to V) (Rashid, 2016).

Due to its composition, the PCW represents a recalcitrant and complex structure that must be overcome during plant-microbe interactions. Microorganisms, mainly bacteria and fungi, are capable of producing and secreting a plethora of cell wall-degrading enzymes (CWDEs), which carry out a coordinated and synergistic deconstruction of the main structural polysaccharides of the PCW, producing soluble sugars that constitute an abundant source of organic carbon to guarantee their nutrition and survival (Gibson et al., 2011; Kubicek et al., 2014). The set of CWDEs includes cellulases, hemicellulases, pectinases, ligninases and accessory enzymes such as monooxygenases, which significantly increase the action of other polysaccharidases. These CWDEs have been described in several species of fungi and bacteria because they have great biotechnological potential (Malgas et al., 2017; Matias de Oliveira et al., 2018). Although it has not been precisely established whether all polysaccharidases constitute virulence factors, at least some such as endo-β-(1,4)-xylanases (Brito et al., 2006), pectin methyl esterases (Sella et al., 2016), arabinofuranosidases (Wu et al., 2016), and polygalacturonases, among others (Nakajima and Akutsu, 2013; Villa-Rivera et al., 2017a), are known to be essential for the establishment of the infection. Several studies have shown that plant pathogenic bacteria and fungi secrete a set of enzymes that degrade arabinogalactans from AGPs, however, little attention has been paid to their role in infection processes. Although there is evidence that AGPs play important functions in plant-microbe interactions, most studies on this topic have focused on the responses of plants to beneficial or pathogenic microorganisms. In this review, we describe the structure and function of AGs and AGPs as components of the PCW. Additionally, we describe the set of enzymes secreted by microorganisms to degrade AGs from AGPs and what is known regarding its role in plant-microbe interactions.

AGs AND AGPs STRUCTURE

AGs are structural components of the PCW; they are mainly composed of galactose and arabinose and are ubiquitously distributed in the plant kingdom (Seifert and Roberts, 2007; Tan et al., 2012). Depending on their structure, AGs are grouped into three main types.

Arabinogalactan type I (AG type I), also designated arabino-4-galactan, is composed of a linear galactopyranose backbone linked by β-1,4 anchors and substituted with α<(1,5) arabinofuranosyl residues (**Figure 1A**; Clarke et al., 1979). Nevertheless, type I arabinogalactans from potato, soybean, onion and citrus also contain galactopyranose residues linked by β-(1,3) bonds as part of their main backbone (Hinz et al., 2005). AG type I have been shown to be a component of pectic complexes in seeds, bulbs, leaves, and coniferous wood (Clarke et al., 1979).

Arabinogalactan type II (AG type II) also known as arabino-3-6-galactan, consists of a main chain of D-galactopyranose linked by β-(1,3) bonds and branches of C(O)6 with β-(1,6)-galactosyl chains linked by β-(1,6) bonds. Non-reducing ends of

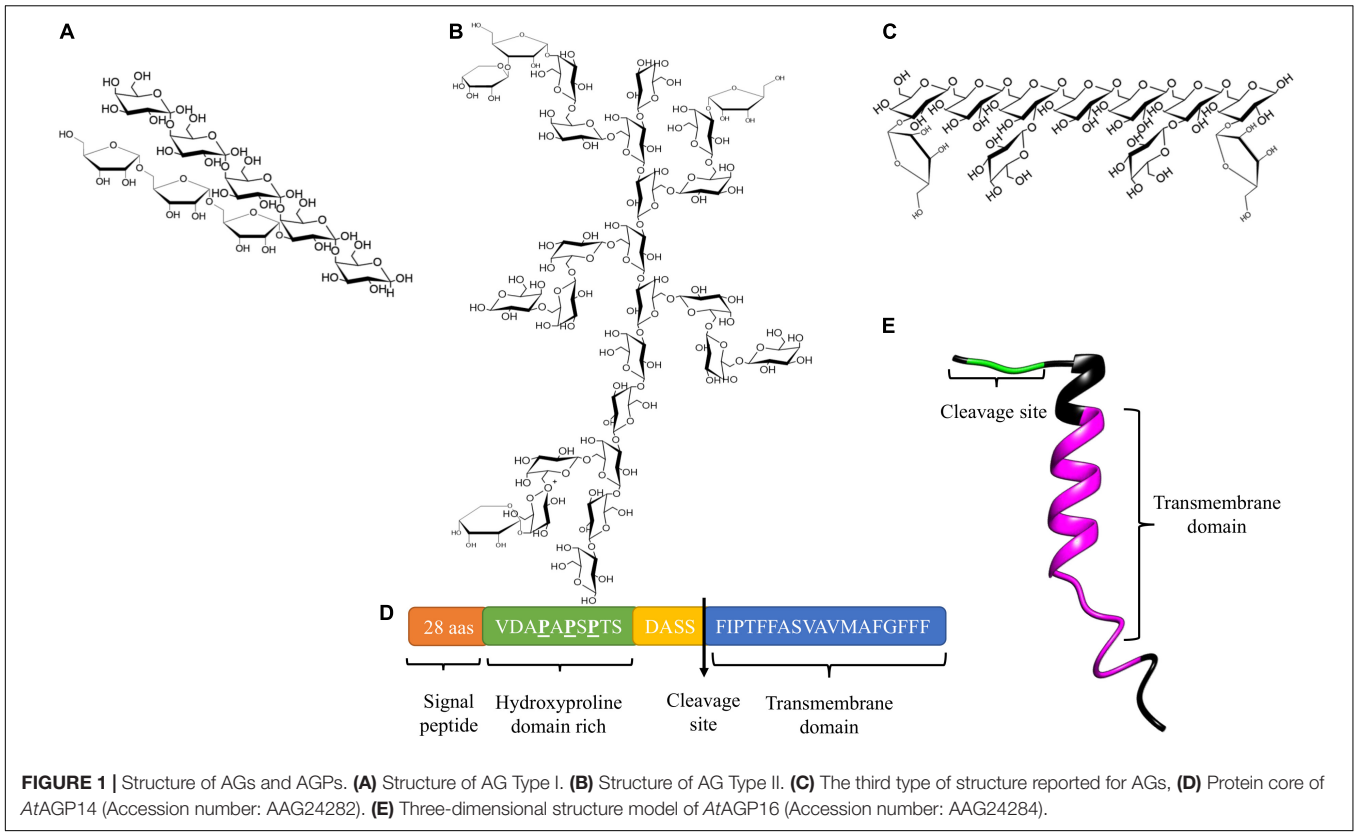

FIGURE 1 | Structure of AGs and AGPs. **(A)** Structure of AG Type I. **(B)** Structure of AG Type II. **(C)** The third type of structure reported for AGs, **(D)** Protein core of *At*AGP14 (Accession number: AAG24282). **(E)** Three-dimensional structure model of *At*AGP16 (Accession number: AAG24284).

the branches may present L-arabinopyranose, L-arabinofuranose, L-rhamnose, D-mannose, D-xylose, D-glucose, L-fucose, D-glucosamine, and D-glucuronic acid (**Figure 1B**; Clarke et al., 1979; Gaspar et al., 2001; Showalter, 2001; Seifert and Roberts, 2007). AG type II is found in mosses, coniferous woods, gums, saps, and exudates of angiosperms, organs such as seeds, leaves, roots, and fruits, as well as the media of various tissues in culture, particularly in polysaccharides with arabinogalactan side chains and pectic complexes such as rhamnogalacturonans (Clarke et al., 1979; Leivas et al., 2016).

Nuclear magnetic resonance (NMR) spectroscopy analyzes performed in different models have demonstrated substantial variability in the structure of AG type II; however, three common characteristics have been observed: first, a main backbone composed of two blocks of three galactopyranose residues linked by β-(1,3) bonds, with the junction between the three galactosyl blocks being a β-(1,6) bond; second, bifurcated branches of arabinose, rhamnose, glucuronic acid, and galactose anchored in the main chain at residues one and two of galactopyranoses; third, a common branch consisting of six residues of α-L-(1,5)-arabinofuranose and two α-L-(1,3)-arabinofuranoses grouped into one unit, with α-L-(1,4)-rhamnose, β-D-(1-6)-glucuronic acid forming a second unit. Both units are anchored to the main chain of β-(1,3)-galactopyranoses (Tan et al., 2010, 2012).

A third structure of AGs has been described, which is mainly associated with pectic polysaccharides in several plant species, consisting of a main backbone of D-galactopyranose residues linked by β-(1,6) bonds with side chains at position O-3 composed of L-arabinoses, arabinans, or individual D-galactopyranose units (**Figure 1C**; Raju and Davidson, 1994; Dong and Fang, 2001; Capek et al., 2009; de Oliveira et al., 2013).

AG type II are commonly anchored to a protein core, and these glycoproteins are denominated arabinogalactan proteins (AGPs). The protein core of AGPs (10% of AGPs) is a short backbone composed of 10 to 20 amino acids. The peptide undergoes posttranslational modifications: conversions of proline residues to hydroxyproline (forming the hydroxyproline domain) and the *O*-glycosylation of hydroxyproline and possibly serine and threonine residues with AG type II (90% of AGPs). In some cases, the protein core of AGPs contains within its structure a small sequence consisting of basic amino acids, and has a hydrophobic transmembrane domain located at the C-terminal end (**Figures 1D,E**; Gaspar et al., 2001; Showalter, 2001; Schultz et al., 2002; Showalter and Basu, 2016b). AGPs are found in the PCW, the apoplastic space, and some secretions such as exudates, and some adhere to the plasma membrane through a glycosylphosphatidylinositol (GPI) anchor in the hydrophobic domain. GPI binds to AGPs through a phosphoethanolamine linked to an oligosaccharide composed of D-mannose-(1-2)-α-D-mannose-(1,6)-α-D-mannose (1-4)-α-D-*N*-acetylglucosamine bound to a lipid residue of inositylphosphoceramide (Oxley and Bacic, 1999; Seifert and Roberts, 2007; Ellis et al., 2010). A consensus cleavage site has been identified in the classic AGP-deduced amino acid sequences, which constitutes a GPI-anchored recognition signal and is located before the transmembrane domain (Schultz et al., 2002).

AGPs are members of the HRGP superfamily, and based on their polypeptide core and the presence/absence of particular motifs/domains, they are classified into classic and non-classic AGPs (Showalter, 2001; Showalter et al., 2010). Classical AGPs are characterized by an *N*-terminal signal peptide, a central domain of variable length enriched in proline, alanine, serine, and threonine (PAST) (**Figure 1D**), and the C-terminal GPI anchor. Other classic AGPs are AG peptides, the structure of which contains 10–13 amino acids (Schultz et al., 2000). Conversely, non-classic AGPs have a low content of hydroxyproline and are enriched in cysteine and asparagine. Analyses of different plant tissues have revealed a high heterogeneity in the structure and composition of AGPs (both core proteins and carbohydrate moieties) (Gaspar et al., 2001; Showalter, 2001). Non-classical or chimeric AGPs have different conserved domains by which they are classified into subfamilies: lysine-rich AGPs with PAST domains separated by Lys-rich regions (Yang and Showalter, 2007), fasciclin-like arabinogalactan proteins (FLAs), with a fasciclin domain possibly involved in cell adhesion (Johnson et al., 2003), phytocyanin-like AGPs (PAGs) (Mashiguchi et al., 2009; Ma et al., 2017), and xylogen-like AGPs (XYLPs) with non-specific lipid transfer protein (nsLTP) domains (Kobayashi et al., 2011). AGPs-extensin hybrids (HAEs) have also been identified (Showalter et al., 2010).

Typical assays for the detection and/or functional analysis of AGPs use the dye β-glucosyl Yariv reagent (β-Glc Yariv), which binds to the β-(1,3)-galactose backbone (Yariv et al., 1967; Kitazawa et al., 2013) and/or specific antibodies against AGP-glycans (LM2, LM6, MAC207, JIM8, JIM13, and JM14). For example, these analyses have been conducted in suspension culture cells (Maurer et al., 2010) and different plant tissues, such as roots and seeds (van Hengel and Roberts, 2003), stems and wood (Zhang et al., 2003), leaves (Kremer et al., 2004), gametophytes and sporophytes (Lee et al., 2005), and flowers and embryos (Hu et al., 2006), among others. In addition, studies focused on the protein components of AGPs have used biochemical and molecular tools such as protein purification (Hu et al., 2006), isolation of genes and heterologous expression (Zhang et al., 2003), genetic expression (Pereira et al., 2006), genetic disruption of the core proteins (van Hengel and Roberts, 2003; Acosta-Garcia and Vielle-Calzada, 2004; Gaspar et al., 2004; Lee et al., 2005), overexpression (Park et al., 2003; Motose et al., 2004; Zhang et al., 2011), suppression (Li et al., 2010), and GFP labeling of genetic promotor sequences (Coimbra et al., 2008), among others. Furthermore, bioinformatics analyses of genomes and transcriptomes from several plant species have allowed the identification of thousands of candidate AGPs genes (Ma and Zhao, 2010; Showalter et al., 2010; Han et al., 2017; Johnson et al., 2017; Ma et al., 2017; Pfeifer et al., 2020). Therefore, AGPs are conserved in the plant kingdom and are expressed in different tissues and stages of plant development.

Regarding how AGPs work, it has also been proposed that soluble AGPs could be involved in cell-cell signaling (Schultz et al., 1998; Motose et al., 2004; Pereira et al., 2014), and GPI-AGPs in lipid rafts/nanodomains in eudicots could be involved in cell-cell communication, signal transduction, immune response, and transport (Borner et al., 2005; Grennan, 2007; Johnson et al., 2017). In support of these hypotheses, some studies have shown that classic AGPs bind reversibly to Ca^{2+} in a pH-dependent manner, suggesting that AGP- Ca^{2+} oscillators might integrate most signaling pathways downstream of the initial Ca^{2+} signal, which would explain the participation of AGPs in many biological process (Lamport and Varnai, 2013; Lamport et al., 2014). On the other hand, there is evidence in *Arabidopsis* that the mechanism responsible for clathrin-mediated endocytosis of extracellular lanthanum cargoes, requires extracellular AGPs anchored to the plasma membrane (Wang et al., 2019), and classic lysine-rich AtAGP18 could function as a coreceptor that binds to signaling molecules and interacts with transmembrane proteins, possibly receptor-like-kinases (RLKs) (Zhang et al., 2011). Specifically, it has been proposed that FLA AGPs are involved in cell-to-cell adhesion and cell signaling (Shi et al., 2003; Showalter and Basu, 2016a).

Currently, despite many studies on AGPs, it remains unclear whether their function resides in the protein backbones, in the glycan epitopes or both. However, given that the mass of AGPs constitutes more than 90% of sugars and that the oligosaccharides play a role in signal transduction in plants, it seems logical to consider these sugars as representatives of the interactive molecular surface defining their function in multiple plant processes. In this sense, heterologous expression studies, *in vitro* enzyme assay and analyses of knockout mutants of genes encoding Hyp-galactosyltransferases (GALTs and HPGTs) that specifically add galactose to AGPs in *A. thaliana*, have shown that glycosylation is essential for plant growth and development (Showalter and Basu, 2016b). On the other hand, enzymatic degradation of the AG type II of AGPs is a strategy that it utilized by microorganisms during their interactions with plants.

DEGRADATION OF AGs BY ENZYMES OF MICROORGANISMS

Fungi and bacteria are capable of synthesizing and secreting the enzymes necessary for complete hydrolysis of AG type II, and these enzymes are listed in **Table 1** and schematized in **Figure 2**.

Exo and Endo Galactanases

Endo and exo-β-(1,3)-D-galactanases degrade the main β-(1,3)-D-galactose backbone of AG type II. Exo-β-(1,3)-D-galactanases (exo1,3 GAL) (EC 3.2.1.145) catalyze the sequential hydrolysis of β-(1,3) linkages at non-reducing ends, releasing galactose and, occasionally, β-(1,6)-galacto-oligosaccharides (Tsumuraya et al., 1990; Pellerin and Brillouet, 1994). Native and recombinant enzymes have been analyzed (heterologous expression in *Escherichia coli* and *Pichia pastoris*), and genes encoding the exo1,3GAL have also been characterized (**Table 1**). Analysis of the crystallized enzyme and deduced amino acid sequences of these enzymes have classified them into subfamily 24 of family 43 of glycosyl hydrolases (GH43) (Jiang et al., 2012; Matsuyama et al., 2020). The topology of exo1,3GAL consists of a catalytic domain structured in a five-blade propeller fold, with each blade including four-stranded antiparallel β-sheets to form a closed propeller ring

with the putative catalytic site located in a central hole (**Figure 2E**; Jiang et al., 2012).

In addition, a C-terminal carbohydrate binding module (CBM) has been described as part of the three-dimensional structure of exo1,3GAL, classified as CBM13 in *Clostridium thermocellum* (symmetric β-trefoil fold topology) (Jiang et al., 2012) and CBM35 in *Phanerochaete chrysosporium* (β-jellyroll fold with a single calcium ion-binding site) (**Figure 2E**; Matsuyama et al., 2020). Interestingly, several studies have shown that typical side chains of AG type II do not interfere with the exo1,3Gal activity, and the enzyme structure contains a space capable of accommodating the β-(1,6)-galactose residues, which allows the protein to surpass the branches of the AG structure (Matsuyama et al., 2020). Nevertheless, the activity of exo1,3GAL has been shown to increase significantly in response to the action of β-(1,6)-D-galactanase, β-L-arabinopyranosidase and α-L-arabinofuranosidase (Okawa et al., 2013).

β-(1,3)-D-galactose chains are also depolymerized by endo-β-(1,3)-D-galactanases (Endo1,3GAL) (EC 3.2.1.145). The action of these enzymes releases β-(1,3)-D-galacto-oligosaccharides

TABLE 1 | Microorganisms that produce AG type II-degrading enzymes and the families of glycosyl hydrolases (GH) to which they belong.

Microorganism species	Enzyme	EC	GH	References
Irpex lacteus[a,b,c]	*Exo-β-(1,3)-galactanase* (exo1,3GAL)	3.2.1.181	43	Tsumuraya et al., 1990; Kiyohara et al., 1997; Kotake et al., 2009
Aspergillus niger[b]				Pellerin and Brillouet, 1994
Phanerochaete chrysosporium[a,c,d]				Ichinose et al., 2005; Ishida et al., 2009; Matsuyama et al., 2020
Streptomyces avermitilis[a,c]				Ichinose et al., 2006a
Clostridium thermocellum[a,c,d]				Ichinose et al., 2006b; Jiang et al., 2012
Sphingomonas sp. [b]				Sakamoto et al., 2011
Streptomyces sp. [a,b,c]				Ling et al., 2012
Fusarium oxysporum[a,b,c]				Okawa et al., 2013
Bifidobacterium longum subsp. longum[a,c]				Fujita et al., 2014
Flammulina velutipes[a,b]	*Endo-β-(1,3)-galactanase* (endo1,3GAL)	3.2.1.145	16	Kotake et al., 2011
Aspergillus flavus[a,c]				Yoshimi et al., 2017
Neurospora crassa[a,c]				Yoshimi et al., 2017
Aspergillus niger[b]	*Endo -β-(1,6)-galactanase* (endo1,6GAL)	3.2.1.164	30	Brillouet et al., 1991
Trichoderma viride[a,b,c]				Okemoto et al., 2003; Kotake et al., 2004
Streptomyces avermitilis[a,c]				Ichinose et al., 2008
Neurospora crassa[a,c]				Takata et al., 2010
Colletotrichum lindemuthianum[a]				Villa-Rivera et al., 2017b
Aspergillus sp[a]	*β-(1,6)-galactanase* (1,6GAL)	3.2.1.164	5	Luonteri et al., 2003
Fusarium oxysporum[a,b,c]				Sakamoto et al., 2007
Hypocrea jecorina[b]	*β-1,3/1,6-galactosidase* (βGAL)	3.2.1.23	35	Gamauf et al., 2007
Aspergillus terreus[a]	*α-L-arabinofuranosidase* (ABF)	3.2.1.55	ND	Luonteri, 1998
Aspergillus awamori[a]			ND	Wood and McCrae, 1996
Streptomyces chartreusis[a]			43 51	Matsuo et al., 2000
Penicillium chrysogenum[a,b,c]			43 51	Sakamoto and Kawasaki, 2003; Sakamoto et al., 2013
Bacillus pumilus[a]			51	Degrassi et al., 2003
Aspergillus oryzae[a]			ND	Hashimoto and Nakata, 2003
Bacillus subtilis			51	Inacio et al., 2008
Neurospora crassa[b,c]			54	Takata et al., 2010
Streptomyces avermitilis[a,b,c,d]	*β-L-arabinopiranosidase* (ABP)	3.2.1.88	27	Ichinose et al., 2009
Fusarium oxysporum[a,c]				Sakamoto et al., 2010
Geobacillus stearothermophilus[a,b,d]				Salama et al., 2012; Lansky et al., 2014
Chitinophaga pinensis[a,b,c]				McKee and Brumer, 2015
Aspergillus niger[b]	*β-D-glucuronidase* (GLUC)	3.2.1.31	79	Kuroyama et al., 2001; Haque et al., 2005; Konishi et al., 2008
Neurospora crassa[b]				Konishi et al., 2008

[a]*Gene characterization.*
[b]*Native protein characterization.*
[c]*Recombinant protein characterization.*
[d]*Crystallized structure.*
ND, Not determined.

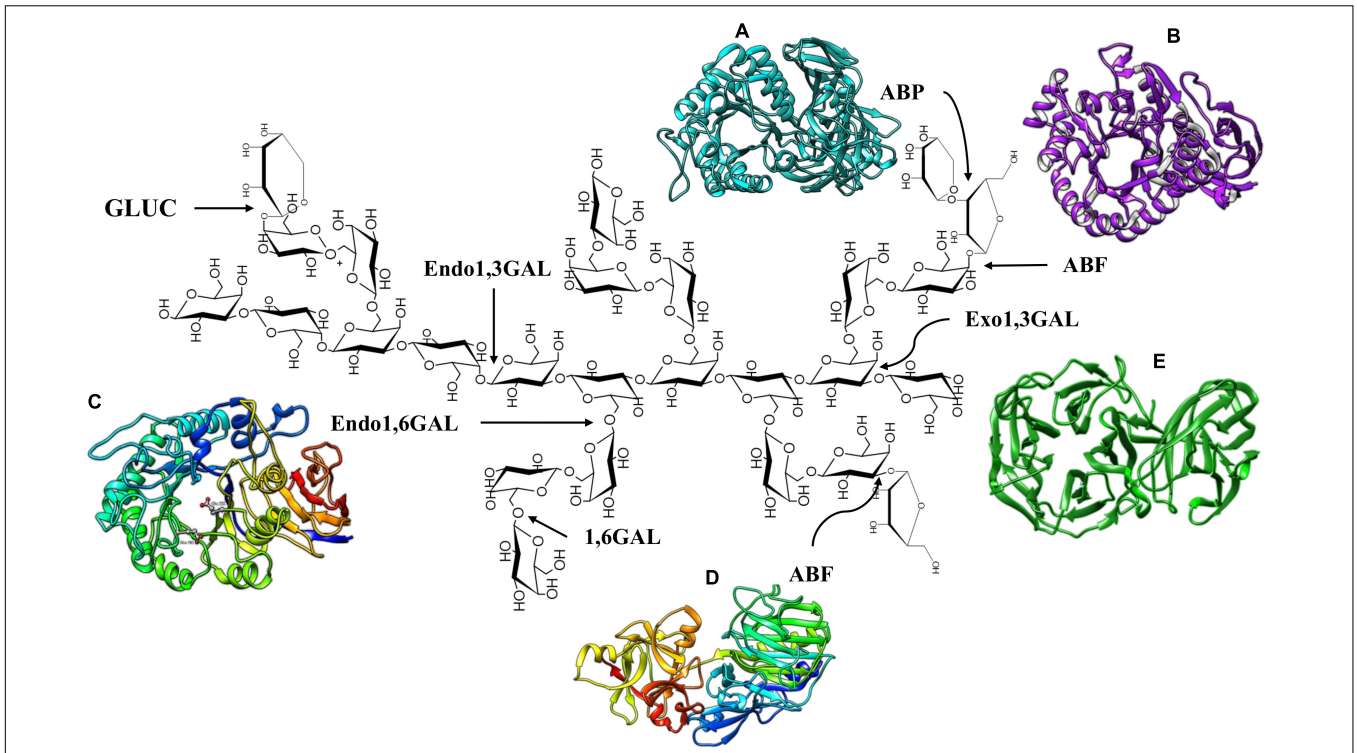

FIGURE 2 | Enzymes that degrade AG Type II. **(A)** *S. avermitilis* ABP, PDB code: 3A21. **(B)** *Thermobacillus xylanolyticus* ABF GH51, PDB code: 2VRQ. **(C)** Endo1,6GAL modeling of *Colletotrichum lindemuthianum* (Villa-Rivera et al., 2017b). **(D)** *Aspergillus luchuensis* ABF GH 54, PDB code: 1WD3. **(E)** *Phanerochaete chrysosporium* Exo1,3 GAL, PDB code: 7BYS.

(galacto-hexoses at early steps) and sometimes galactose in an endo-manner (Kotake et al., 2011). Characterizations of the endo1,3GAL gene and protein have been conducted using only fungal species as a study model (**Table 1**). The synergistic activity of exo and endo1,3GAL has been suggested; apparently, endo1,3GAL creates internal breakpoints in the main chains of AG type II, increasing the number of attack sites for exo1,3GAL (Yoshimi et al., 2017).

The side chains of β-(1,6)-D-galactoses in AG type II are hydrolyzed by endo-β-(1,6)-galactanase (endo1,6GAL) (EC 3.2.1.164) and β-(1,6)-galactanase (1,6GAL). They catalyze the hydrolysis of the β-(1,6) anchors releasing galactobiose, galactooligosaccharides or galactose (Brillouet et al., 1991; Okemoto et al., 2003). The main difference between endo1,6GAL and 1,6GAL is that the former acts on chains with a degree of polymerization greater than or equal to three residues and releases galactooligosaccharides of 2 to 5 residues (Okemoto et al., 2003), while 1,6GAL catalyzes the hydrolysis of galactobiose to release monomers of galactose (Sakamoto et al., 2007; Sakamoto and Ishimaru, 2013). Endo1,6GAL and 1,6GAL are active only on dearabinosylated substrates (Brillouet et al., 1991; Luonteri et al., 2003); therefore, prior action of arabinofuranosidases is required and efficient removal of the side chains of AGP type II depends on the combined action of galactanases and arabinofuranosidases (Takata et al., 2010).

There are no crystallized structures of endo1,6GAL and 1,6GAL; however, a prediction of the three-dimensional structure of *Colletotrichum lindemuthianum* endo1,6GAL has been reported. The endo1,6GAL model adopts a (β/α)8 TIM barrel fold topology (eight-stranded parallel β-strand, forming a central barrel surrounded by eight α-helices) with a putative active site located at the C-terminus, which is consistent with the characteristic structure of GH30 family enzymes (**Figure 2C**; Villa-Rivera et al., 2017b). These enzymes have been characterized from fungi and bacteria and have also been expressed in heterologous models (**Table 1**).

Other enzymes involved in the depolymerization of AG type II are β-galactosidases (βGAL) (EC 3.2.1.23). Although these enzymes have mainly been characterized in plants (Gunter et al., 2009), *Hypocrea jecorina* β-GAL has been purified. The enzyme breaks β-D-galactose bonds at non-reducing ends; however, it is inhibited by its degradation product (β-D-galactose) (Gamauf et al., 2007).

Accessory Proteins

The α-L-arabinofuranosidases (ABFs) (EC 3.2.1.55) are exo-type enzymes that remove the α-L-arabinosyl side chains linked through α-L-(1,2), α-L-(1,3), α-L-(1,5) *O*-glycosidic bonds at the non-reducing ends of arabinoxylans, arabinoxylo-oligosaccharides, arabinan, arabinogalactans and arabino-oligosaccharides of the PCW (Lagaert et al., 2014). According to the Carbohydrate-Active enZYmes database (CAZY), and based on their amino acid sequences, ABFs are classified into families 2, 3, 5, 10, 39, 43, 51, 54, and 62 of

glycoside hydrolases [1](Lombard et al., 2014). ABFs have been purified and characterized from bacteria, fungi and plants (Numan and Bhosle, 2006). Despite many reports on ABFs, only a few have measured the activity of native and recombinant ABFs using AGs as substrates (**Table 1**). Thus, traces of ABF activity in the presence of AGs have been reported in *Aspergillus sojae* and *Aspergillus nidulans* (Kimura et al., 1995; Wilkens et al., 2016), and additionally, AGs have been successfully evaluated as inducers of ABF activity in cultures of *Aspergillus niger*, *Aureobasidium pullulans* and *Penicillium purpurogenum* (vd Veen et al., 1991; Saha and Bothast, 1998; De Ioannes, 2000).

Based on the specificity of the substrate, ABFs are classified into three types: arabinofuranosidase A is capable of hydrolyzing α-(1,5)-L-arabinofuranosyl bonds of arabino-xylooligosaccharides but does not act on polysaccharides; arabinofuranosidase B acts on linear and branched arabino-oligosaccharides and polymers; and the third type of arabinofuranosidase shows a high specificity for complex natural substrates and is known generically as an arabinofuranohydrolase (Numan and Bhosle, 2006; Lagaert et al., 2014; Poria et al., 2020). The regional selectivity of ABFs has also been evaluated. Accordingly, ABFs belonging to GH51 and GH54 are capable of removing arabinosyl residues from the internal and terminal non-reducing ends of xylopyranosyl residues with mono- and disubstitutions. However, the ABFs of the GH54 family show weak activity on internal di-substitutions compared with GH51, which are more versatile in terms of substrate specificity (Koutaniemi and Tenkanen, 2016; Dos Santos et al., 2018). On the other hand, ABFs of the GH62 family show selectivity toward α-(1,2) and α-(1,3) anchors in arabinoxylans mono-substituted with arabinofuranosyl residues (Sarch et al., 2019). Interestingly, bifunctional enzymes with α-L-arabinofuranosidase/xylobiohydrolase (Ravanal et al., 2010) or α-L-arabinofuranosidase/β-xylosidase activities have also been described (Huy et al., 2013).

Several crystallized and characterized ABFs, which present a diversity of structures generally consisting of two domains: the catalytic domain and the arabinose binding module (ABD). The structure of the *Streptomyces avermitilis* ABF belonging to the GH43 family, presents a core catalytic domain composed of a five blanched β-propeller with an ABD similar to CBM42 located at the C-terminus adopting a β-trefoil fold (three similar subdomains assembled against one another around a pseudo3-fold axis) topology (Fujimoto et al., 2010). With respect to ABFs of the GH51 family, the enzymes from *Geobacillus stearethermophilus* (Hovel et al., 2003), *Clostridium thermocellum* (Taylor et al., 2006), and *Thermobacillus xylanilyticus* (Paes et al., 2008) have been crystallized. The catalytic domain of the GH51 family ABFs has a (β/α)8 TIM-barrel fold topology and a C-terminal ABD domain with a jellyroll topology (**Figure 2B**; Hovel et al., 2003; Paes et al., 2008). The structure of *Aspergillus luchuensis* ABFs (formerly known as *A. kawachii*), belonging to the GH54 family, is composed of a catalytic domain (β-sandwich fold topology) similar to clan B of GH54 and an arabinose binding module (β-trefoil fold topology) similar to CBM13 (**Figure 2D**; Miyanaga et al., 2004).

Regarding other accessory enzymes for the deconstruction of AG type II, β-L-arabinopyranosidases (ABPs) (EC3.2.1.88) have also been reported. ABP hydrolyzes β-arabinopyranose from the non-reducing end of AG side chains (Ichinose et al., 2009). Two bifunctional proteins (Fo/AP1 and Fo/AP2) with β-L-arabinopiranosidase/α-D-galactopyranosidase activity have been purified from *Fusarium oxysporum*, both of which are active toward larch wood arabinogalactan (LWAG), releasing only arabinopyranose (Sakamoto et al., 2010). ABPs have been purified and characterized from bacteria and fungi, and they have also been expressed in heterologous systems (**Table 1**). The three-dimensional structure of ABP consists in a catalytic domain (antiparallel β-domain) characteristic of the GH27 family and a CMB13 (antiparallel β-domain adopting a jellyroll structure) at the C-terminal end (Ichinose et al., 2009; Lansky et al., 2014; **Figure 2A**).

In bacteria, ABF and ABP enzymes are non-cellulosomal hydrolases; however, a synergy between cellulosomal and non-cellulosomal hydrolases has been detected during hydrolysis of the PCW by *Clostridium cellulovorans* (Kosugi et al., 2002). Finally, β-glucuronidase (EC3.2.1.31) hydrolyzes the non-reducing ends of 4-*O*-methyl glucuronic acid of the β-1,6 galactosyl side chains of AG type II (**Table 1**; Haque et al., 2005).

It is important to mention that the combined action of exo1,3GAL, 1,6GAL, ABF, and ABP is more efficient than the sum of the independent activities in the depolymerization of AG type II (Okawa et al., 2013). Efficient hydrolysis of this polymer depends of the removal of β-(1,6)-galactose branches (Sakamoto and Ishimaru, 2013).

AGs HYDROLYSIS AND PLANT-MICROBE INTERACTIONS

AGPs play an interesting role in the response pathways of plants to abiotic stress (caused by low and high temperatures, drought, high salinity, excessive light, and floods) and biotic stress (caused by bacteria, fungi, nematodes, and viruses) (Mareri et al., 2018). Particularly, they are important for plant-microbe interactions, whether beneficial or pathogenic.

During beneficial plant-microbe interactions, plant roots produce a complex mucilage that constitutes an important carbon source for rhizosphere microorganisms. Root mucilage from pea, cowpea, wheat, maize, and rice has been reported to contain high levels of galactose and arabinose, the main components of AGs (Knee et al., 2001). Moreover, root tips and border-like cells (BLC) of *A. thaliana* can secrete pectic polysaccharides and AGPs to the rhizosphere (Vicre et al., 2005). Additionally, AGPs have been located in several root structures: epidermal, cortical, and endodermal cells, pericycle, apical meristem, and root infection structures (Nguema-Ona et al., 2013). In this sense, AGPs can act as attractants for symbiotic species of fungi and bacteria, promoting the development of infection structures and, therefore, root tip colonization. It has been observed that the induced alterations in the structure of

[1]http://www.cazy.org/

AGPs trigger an inhibition in the attachment of *Rhizobium* to BLC and the root tip of *A. thaliana* (Vicre et al., 2005; Cannesan et al., 2012; Xie et al., 2012).

Furthermore, AGPs are found at the physical interface between root cells and the infecting structures of microorganisms, allowing for the root-symbiont nutrient exchange necessary for microbe survival. For this purpose, soil microbes such as *Trichoderma viride* and *S. avermitilis*, among other, produce polysaccharidases (**Table 1**) that allow them to access and obtain monosaccharides or disaccharides derived from the hydrolysis of AGs, useful as a carbon source (Knee et al., 2001). On the other hand, it has been suggested that AGPs can prevent infection by pathogenic microorganisms or inhibit their development because the degradation products (oligosaccharides or glycopeptides) generated by hydrolytic enzymes of pathogens can act as damage-associated molecular patterns (DAMPs) and promote the plant defense response. Moreover, the colonization of the rhizosphere by beneficial microbes supported by AGPs, would also activate plant defense mechanisms such as induced systemic resistance (ISR), protecting the plant against pathogen attack, while symbiotic microorganisms could act as antagonists of pathogens and avoid infections. Finally, AGPs have been proposed to be modulators of the plant immune system, favoring the colonization of beneficial microbes (Nguema-Ona et al., 2013).

Regarding the pathogen microbe-plant interaction, an accumulation of HRGPs has been detected as a result of the contact between the pathogen and PCW. For instance, during the infection of tomato roots with *F. oxysporum*, late accumulation of HRGPs has been observed in susceptible plants (Benhamou, 1990). Along the same lines, in response to *F. oxysporum* a consistent increase in the abundance of AGPs was observed, particularly in the roots of resistant cultivars of wax gourd (*Benicasa hispida* Cong.) but not in susceptible ones (Xie et al., 2011). Furthermore, immunohistochemical analysis of *Sesbania exaltata* tissues infected by *Colletotrichum gloeosporioides* has revealed a rapid accumulation of AGPs at the border between the vascular tissue and the necrotic lesion (Bowling et al., 2010). This evidence suggests that HRGP enhancement is a prerequisite for an efficient and localized plant defense response (Benhamou, 1990; Nguema-Ona et al., 2013). At the transcriptomic level, seven extensin genes and 23 genes encoding AGPs were differentially expressed in banana cultivars before and after infection with *F. oxysporum*. These data revealed that extensins and AGPs were dynamic components of the plant cell wall (Wu et al., 2017). In addition, 38 NbFLAs from *Nicotiana benthamiana* were significantly downregulated by infection with turnip mosaic virus (TuMV) or by infection with *Pseudomonas syringae* pv tomato strain DC3000 (*Pst* DC3000), suggesting a relationship between FLAs and immunity (Wu et al., 2017).

The accumulation of HRGPs at the infection sites can be explained because the PCW is not just a physical and passive barrier against pathogens; recently, this complex structure has emerged as a dynamic defense structure involved in sensing and monitoring stressing conditions that result in compensatory responses essential for the maintenance of cell integrity and stability. Abiotic and biotic factors, such as the disruption of the PCW during infection by pathogens, trigger molecular mechanisms of the signaling pathways that sense and maintain cell wall integrity, including sensors that detect changes in the cell surface and signals originating from the wall that transduce downstream signals (Bacete et al., 2018; Rui and Dinneny, 2020). Additionally, CWPs have an important role in defense against pathogens; this proteins carry out (a) a reinforcement of the plant cell wall through insolubilization and oxidative cross-linking of extensins and sensors resident in the plasma membrane (PRPs) through H_2O_2 and peroxidases, (b) AGP secretion and accumulation at sites of infection by pathogens (**Figure 3A**), (c) binding of GRPs to pathogenic RNA to degrade its genetic material and, (d) transcription of genes that encode pathogen-related proteins (PRs) using AGPs as a soluble molecular signal (**Figure 3B**; Rashid, 2016; Bacete et al., 2018).

Thus, the role of AGPs in the defense responses of plants against pathogens comprises the secretion and clumping of AGPs at the infection sites and the creation of cross-links with cell wall polysaccharides such as pectin. Covalent bonds have been described between the AGP At3g4530 from *A. thaliana*, arabinoxylan and rhamnogalacturonan I/homogalacturonan, which form an APAP1 structure (Tan et al., 2013); therefore, the action of enzymes that degrade AGs is necessary to allow the pathogen to surpass the PCW and penetrate the protoplast.

On the other hand, AGPs and other proteins attached to the plasma membrane by GPI anchoring, are involved in connecting the intracellular and extracellular space, and are good candidates for transducing signals from the extracellular space to the cytoplasm. In this sense, the receptor like kinase (RLK) family, AGPs, the mitogen-activated protein kinase (MAPK) pathway, and the target of rapamycin (TOR) pathway could be potential components of perceptual mechanisms of cell wall integrity (Pogorelko et al., 2013). It has been reported that some AGPs contain a domain of six cysteine residues designated the proline-AGP-cysteine domain (PAC) (like that identified in Cys-rich LAT52); this domain can interact with RLK receptors (Tang et al., 2002). In this way, it has been suggested that PAC domain might mediate the binding between some AGPs and RLKs (**Figure 3B**; Seifert and Roberts, 2007). Moreover, the fasciclin-like AGP SOS 5, has been reported as a GPI anchored protein that acts in a pathway involving two cell wall RLKs (FEI1 and FEI2) (Showalter and Basu, 2016a).

Evidence for the role of AGPs in cell signaling during plant-microbe interactions shows that AGP17 from *A. thaliana* is necessary for the activation of systemic acquired resistance (SAR). This glycoprotein seems to be involved in the transduction pathway of intracellular changes in salicylic acid levels and genetic expression of the gene encoding PR1 (Gaspar et al., 2004). Furthermore, binding of β-GlcYariv to plant surface AGPs, triggers wound-like defense responses that include PCW reinforcement and callose synthesis (Guan and Nothnagel, 2004). In addition, treatment with β-Glc Yariv suppresses the expression of genes involved in gibberellin signaling, an effect similar to that caused by elicitors such as chitin (Mashiguchi et al., 2008).

As mentioned above, AG type II are essential components for the function of AGPs. *In vitro* assays using exo1,3GAL have shown that complete hydrolysis of arabinogalactan terminated

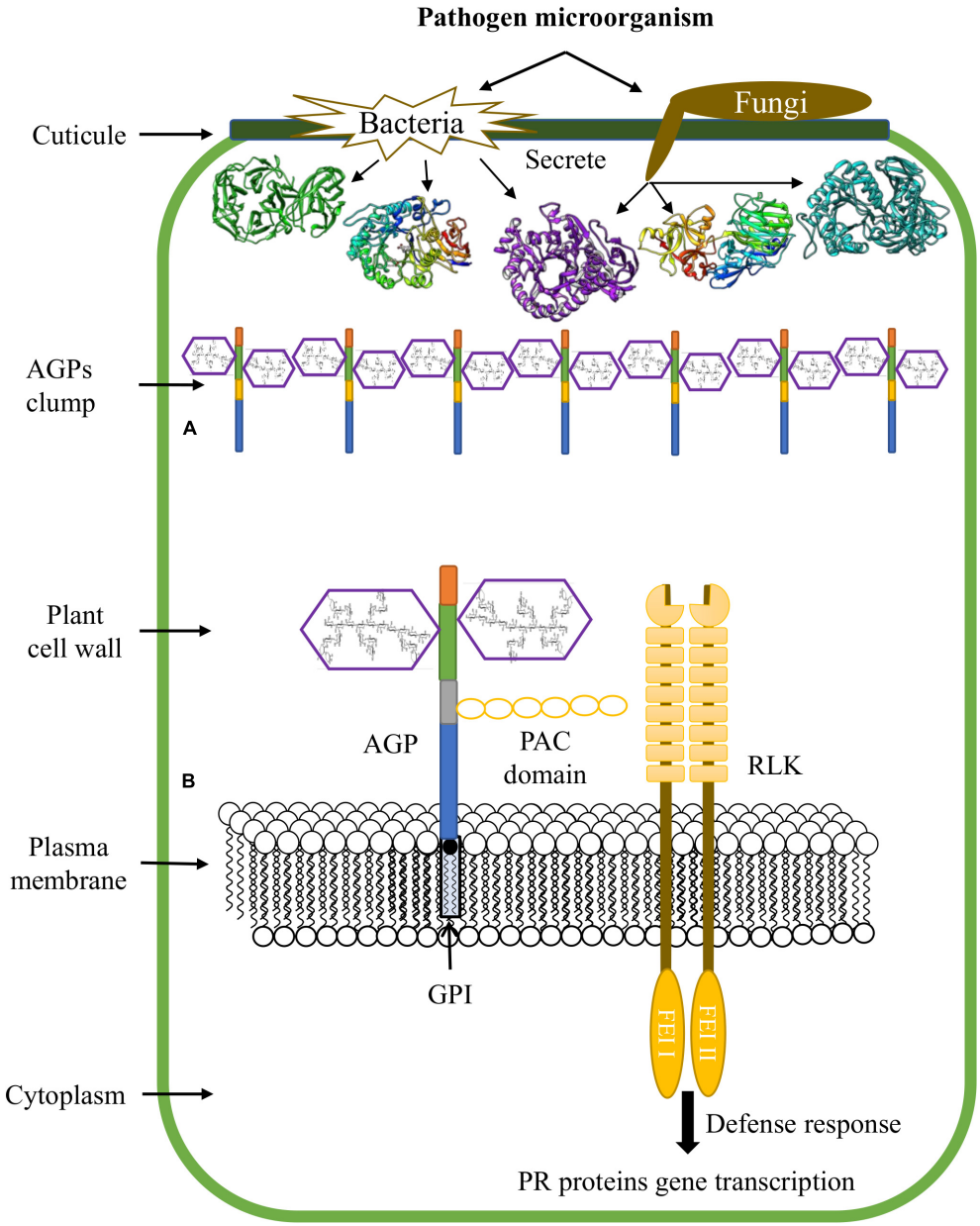

FIGURE 3 | Functions of AGPs during plant-microbe interactions. **(A)** Accumulation of AGPs at sites of pathogen infection. **(B)** AGPs are involved in transduction pathways and promote plant defense responses.

its reactivity with β-Glc Yariv reagent, confirming that the AGP side chains are responsible for its activity (Kiyohara et al., 1997). On the other hand, the expression of a fungal exo1,3GAL in *A. thaliana* leads to a decrease in AGPs reactive to β-Glc Yariv and a severe tissue disorganization in hypocotyl and cotyledons. Furthermore, oligosaccharides released from AG type II were detected in the soluble fraction of transgenic plants (Yoshimi et al., 2020). Thus, hydrolysis of the carbohydrate component of AGPs by hydrolytic enzymes secreted by fungi and bacteria during penetration of the PCW would have consequences for the mechanisms of detection and monitoring of the integrity of the cell wall, favoring infection by pathogens. Damage to the PCW caused by the combination of cellulase and pectinase activities is responsible for the accumulation of jasmonic and salicylic acids in plants, and RLK (FEI2), and mechanosensitive Ca^{+2} channels localized in the plasma membrane (MCA1) are responsible for the activation of responses to damage (osmosensitive responses) (Engelsdorf et al., 2018).

Therefore, the secretion of AG type II-degrading enzymes by phytopathogens appears to be crucial for the establishment of host infection. Deletion of the *MoAbfB* gene encoding an α-*N*-arabinofuranosidase B from *Magnaporthe oryzae* resulted in a

reduction in disease severity in rice (Wu et al., 2016). Likewise, comparison of the genetic expression of an endo1,6GAL between pathogenic and non-pathogenic strains of *C. lindemuthianum*, showed that compared with most of the evaluated conditions, the levels of genetic expression were higher in pathogenic than non-pathogenic strains, supporting a role for this enzyme in the PCW degradation during the establishment of the infection (Villa-Rivera et al., 2017b). Finally, the inactivation of *Malus domestica* AGPs with β-Glc Yariv reagent, which exhibit an effect similar to that of degradation by enzymes, causes a more rapid progress of *Penicillium spinulosum* infection, thus reinforcing the notion that the inactivation of AG type II has an impact on the PCW integrity and the activation of plant defense responses (Leszczuk et al., 2019).

CONCLUSION AND PERSPECTIVES

Several lines of evidence support the proposal that AGPs play different and crucial roles in plant-microorganism interactions. In general, most studies on the role of AGPs in plant-microorganism interactions have focused on the response of plants. Evidence shown that in plant root tips AGPs are attractants of symbiotic species of fungi or bacteria and promoters of the development of infectious structures and colonization, as well, these interactions can activate plant defense mechanisms such as ISR. Furthermore, plants secrete and accumulate AGPs at infection sites, creating cross-links with pectin and probably other PCW polymers. In this sense, it is proposed that AGPs could prevent infection by pathogenic microorganisms because oligosaccharides or glycopeptides generated by hydrolytic enzymes of pathogens act as DAMPs and elicits the plant defense response. But then the question arises why the degradation of AGPs by successful pathogens is crucial for the establishment of the host infection. Moreover, the binding of β-Glc Yariv to AGPs on the plant surface elicits wound-like defense responses, yet, in contrast it can also promote a more rapid progress of fungal infections, similar to the action of the polysaccharidases. On the other hand, although it is well established that phytopathogenic and beneficial fungi and bacteria secrete a set of glycosyl hydrolases that degrade AG type II of AGPs, most of the reports available on these enzymes have focused on their biotechnological applications. Clearly, it is necessary to develop studies on the expression and secretion of AG type II-degrading enzymes, and on their degradation products and their role during the establishment of host infection.

AUTHOR CONTRIBUTIONS

MV-R and MZ-P wrote the first version of the manuscript and figures. MZ-P, HC-C, and EL-R corrected and improved the manuscript. All authors read and approved the submitted version of the manuscript.

FUNDING

Consejo Nacional de Ciencia y Tecnología (CONACYT, research project FONSEC-CB2017-2018-A1-S-27298 to MZ-P), and by Coordinación de la Investigación Científica de la Universidad Michoacana de San Nicolás de Hidalgo, (CIC-UMSNH, research project 2020–2021 to HC-C).

REFERENCES

Acosta-Garcia, G., and Vielle-Calzada, J. P. (2004). A classical arabinogalactan protein is essential for the initiation of female gametogenesis in *Arabidopsis*. *Plant Cell* 16, 2614–2628. doi: 10.1105/tpc.104.024588

Albenne, C., Canut, H., and Jamet, E. (2013). Plant cell wall proteomics: the leadership of *Arabidopsis thaliana*. *Front. Plant Sci.* 4:111. doi: 10.3389/fpls.2013.00111

Bacete, L., Melida, H., Miedes, E., and Molina, A. (2018). Plant cell wall-mediated immunity: cell wall changes trigger disease resistance responses. *Plant J.* 93, 614–636. doi: 10.1111/tpj.13807

Benhamou, N. (1990). Immunocytochemical localization of hydroxyproline-rich glycoproteins in tomato root cells infected by *Fusarium oxysporum* f. sp. *radicis-lycopersici*: study of a compatible interaction. *Phytopathology* 80, 163–173. doi: 10.1094/Phyto-80-163

Borner, G. H. H., Sherrier, D. J., Weimar, T., Michaelson, L. V., Hawkins, N. D., Macaskill, A., et al. (2005). Analysis of detergent-resistant membranes in *Arabidopsis*. *Evidence for plasma membrane lipid rafts*. *Plant Physiol.* 137, 104–116. doi: 10.1104/pp.104.053041

Bowling, A. J., Vaughn, K. C., Hoagland, R. E., Stetina, K., and Boyette, C. D. (2010). Immunohistochemical investigation of the necrotrophic phase of the fungus *Colletotrichum gloeosporioides* in the biocontrol of hemp sesbania (*Sesbania exaltata*. *Papilionaceae*). *Am. J. Bot.* 97, 1915–1925. doi: 10.3732/ajb.1000099

Brillouet, J.-M., Williams, P., and Moutounet, M. (1991). Purification and some properties of a novel endo-β-(1 → 6)-d-galactanase from *Aspergillus niger*. *Agric. Biol. Chem.* 55, 1565–1571. doi: 10.1080/00021369.1991.10870802

Brito, N., Espino, J. J., and Gonzalez, C. (2006). The endo-beta-1,4-xylanase xyn11A is required for virulence in *Botrytis cinerea*. *Mol. Plant Microbe. Interact.* 19, 25–32. doi: 10.1094/MPMI-19-0025

Burton, R. A., Gidley, M. J., and Fincher, G. B. (2010). Heterogeneity in the chemistry, structure and function of plant cell walls. *Nat. Chem. Biol.* 6, 724–732. doi: 10.1038/nchembio.439

Cannesan, M. A., Durand, C., Burel, C., Gangneux, C., Lerouge, P., Ishii, T., et al. (2012). Effect of arabinogalactan proteins from the root caps of pea and *Brassica napus* on *Aphanomyces euteiches* zoospore chemotaxis and germination. *Plant Physiol.* 159, 1658–1670. doi: 10.1104/pp.112.198507

Capek, P., Matulova, M., Navarini, L., and Liverani, F. S. (2009). A comparative study of arabinogalactan-protein isolates from instant coffee powder of *Coffea arabica* beans. *J. Food Nutr. Res.* 48, 80–86. doi: 10.1016/j.carbpol.2009.11.016

Chen, H. (2014). *Chemical composition and structure of natural lignocellulose in Biotechnology of Lignocellulose*. Dordrecht: Springer, 25–71.

Clarke, A. E., Anderson, R. L., and Stone, B. A. (1979). Form and function of arabinogalactans and arabinogalactan-proteins. *Phytochemistry* 18, 521–540. doi: 10.1016/s0031-9422(00)84255-7

Coimbra, S., Jones, B., and Pereira, L. G. (2008). Arabinogalactan proteins (AGPs) related to pollen tube guidance into the embryo sac in *Arabidopsis*. *Plant Signal Behav.* 3, 455–456. doi: 10.4161/psb.3.7.5601

De Ioannes, P. (2000). An α-L-arabinofuranosidase from *Penicillium purpurogenum*: production, purification and properties. *J. Biotechnol.* 76, 253–258. doi: 10.1016/s0168-1656(99)00190-x

de Oliveira, A. J., Cordeiro, L. M., Goncalves, R. A., Ceole, L. F., Ueda-Nakamura, T., and Iacomini, M. (2013). Structure and antiviral activity of arabinogalactan

with (1–>6)-beta-D-galactan core from *Stevia rebaudiana* leaves. *Carbohydr. Polym.* 94, 179–184. doi: 10.1016/j.carbpol.2012.12.068

Degrassi, G., Vindigni, A., and Venturi, V. (2003). A thermostable α-arabinofuranosidase from xylanolytic *Bacillus pumilus*: purification and characterisation. *J. Biotechnol.* 101, 69–79. doi: 10.1016/s0168-1656(02)00304-8

Dong, Q., and Fang, J. N. (2001). Structural elucidation of a new arabinogalactan from the leaves of *Nerium indicum*. *Carbohydr. Res.* 332, 109–114. doi: 10.1016/s0008-6215(01)00073-8

Dos Santos, C. R., de Giuseppe, P. O., de Souza, F. H. M., Zanphorlin, L. M., Domingues, M. N., Pirolla, R. A. S., et al. (2018). The mechanism by which a distinguishing arabinofuranosidase can cope with internal di-substitutions in arabinoxylans. *Biotechnol. Biofuels* 11:223. doi: 10.1186/s13068-018-1212-y

Ellis, M., Egelund, J., Schultz, C. J., and Bacic, A. (2010). Arabinogalactan-proteins: key regulators at the cell surface? *Plant Physiol.* 153, 403–419. doi: 10.1104/pp.110.156000

Engelsdorf, T., Gigli-Bisceglia, N., Veerabagu, M., McKenna, J. F., Vaahtera, L., Augstein, F., et al. (2018). The plant cell wall integrity maintenance and immune signaling systems cooperate to control stress responses in *Arabidopsis thaliana*. *Sci. Signal* 11:aao3070. doi: 10.1126/scisignal.aao3070

Fujimoto, Z., Ichinose, H., Maehara, T., Honda, M., Kitaoka, M., and Kaneko, S. (2010). Crystal structure of an exo-1,5-α-L-arabinofuranosidase from *Streptomyces avermitilis* provides insights into the mechanism of substrate discrimination between exo- and endo-type enzymes in glycoside hydrolase family 43. *J. Biol. Chem.* 285, 34134–34143. doi: 10.1074/jbc.M110.164251

Fujita, K., Sakaguchi, T., Sakamoto, A., Shimokawa, M., and Kitahara, K. (2014). *Bifidobacterium longum* subsp. *longum* exo-beta-1,3-galactanase, an enzyme for the degradation of type II arabinogalactan. *Appl. Environ. Microbiol.* 80, 4577–4584. doi: 10.1128/AEM.00802-14

Gamauf, C., Marchetti, M., Kallio, J., Puranen, T., Vehmaanpera, J., Allmaier, G., et al. (2007). Characterization of the bga1-encoded glycoside hydrolase family 35 beta-galactosidase of *Hypocrea jecorina* with galacto-beta-D-galactanase activity. *FEBS J.* 274, 1691–1700. doi: 10.1111/j.1742-4658.2007.05714.x

Gaspar, Y., Johnson, K. L., McKenna, J. A., Bacic, A., and Schultz, C. J. (2001). "The complex structures of arabinogalactan-proteins and the journey towards understanding function." in *Plant Cell and Walls*. eds *N. C. Carpita, M. Campbell and M. Tierney*. (Dordrecht: Springer), 161–176.

Gaspar, Y. M., Nam, J., Schultz, C. J., Lee, L. Y., Gilson, P. R., Gelvin, S. B., et al. (2004). Characterization of the *Arabidopsis* lysine-rich arabinogalactan-protein AtAGP17 mutant (rat1) that results in a decreased efficiency of *Agrobacterium* transformation. *Plant Physiol.* 135, 2162–2171. doi: 10.1104/pp.104.045542

Gibson, D. M., King, B. C., Hayes, M. L., and Bergstrom, G. C. (2011). Plant pathogens as a source of diverse enzymes for lignocellulose digestion. *Curr. Opin. Microbiol.* 14, 264–270. doi: 10.1016/j.mib.2011.04.002

Grennan, A. K. (2007). Lipid rafts in plants. *Plant Physiol.* 143, 1083–1085. doi: 10.1104/pp.104.900218

Guan, Y., and Nothnagel, E. A. (2004). Binding of arabinogalactan proteins by Yariv phenylglycoside triggers wound-like responses in *Arabidopsis* cell cultures. *Plant Physiol.* 135, 1346–1366. doi: 10.1104/pp.104.039370

Gunter, E. A., Popeyko, O. V., and Ovodov, Y. S. (2009). Action of beta-galactosidase in medium on the *Lemna minor* (L.) callus polysaccharides. *Carbohydr. Res.* 344, 2602–2605. doi: 10.1016/j.carres.2009.08.031

Han, T., Dong, H., Cui, J., Li, M., Lin, S., Cao, J., et al. (2017). Genomic, molecular evolution, and expression analysis of genes encoding putative classical AGPs, lysine-rich AGPs, and AG peptides in *Brassica rapa*. *Front. Plant Sci.* 8:397. doi: 10.3389/fpls.2017.00397

Haque, M., Kotake, T., and Tsumuraya, Y. (2005). Mode of action of beta-glucuronidase from *Aspergillus niger* on the sugar chains of arabinogalactan-protein. *Biosci. Biotechnol. Biochem.* 69, 2170–2177. doi: 10.1271/bbb.69.2170

Hashimoto, T., and Nakata, Y. (2003). Synergistic degradation of arabinoxylan with alpha-L-arabinofuranosidase, xylanase and beta-xylosidase from soy sauce koji mold. Aspergillus oryzae, in high salt condition. *J. Biosci. Bioeng.* 95, 164–169. doi: 10.1016/s1389-1723(03)80123-8

Hinz, S. W., Verhoef, R., Schols, H. A., Vincken, J. P., and Voragen, A. G. (2005). Type I arabinogalactan contains beta-D-Galp-(1–>3)-beta-D-Galp structural elements. *Carbohydr. Res.* 340, 2135–2143. doi: 10.1016/j.carres.2005.07.003

Hovel, K., Shallom, D., Niefind, K., Belakhov, V., Shoham, G., Baasov, T., et al. (2003). Crystal structure and snapshots along the reaction pathway of a family 51 alpha-L-arabinofuranosidase. *EMBO J.* 22, 4922–4932. doi: 10.1093/emboj/cdg494

Hu, Y., Qin, Y., and Zhao, J. (2006). Localization of an arabinogalactan protein epitope and the effects of Yariv phenylglycoside during zygotic embryo development of *Arabidopsis thaliana*. *Protoplasma* 229, 21–31. doi: 10.1007/s00709-006-0185-z

Huy, N. D., Thayumanavan, P., Kwon, T. H., and Park, S. M. (2013). Characterization of a recombinant bifunctional xylosidase/arabinofuranosidase from *Phanerochaete chrysosporium*. *J. Biosci. Bioeng.* 116, 152–159. doi: 10.1016/j.jbiosc.2013.02.004

Ichinose, H., Fujimoto, Z., Honda, M., Harazono, K., Nishimoto, Y., Uzura, A., et al. (2009). A beta-L-Arabinopyranosidase from *Streptomyces avermitilis* is a novel member of glycoside hydrolase family 27. *J. Biol. Chem.* 284, 25097–25106. doi: 10.1074/jbc.M109.022723

Ichinose, H., Kotake, T., Tsumuraya, Y., and Kaneko, S. (2006a). Characterization of an exo-beta-1,3-D-galactanase from *Streptomyces avermitilis* NBRC14893 acting on arabinogalactan-proteins. *Biosci. Biotechnol. Biochem.* 70, 2745–2750. doi: 10.1271/bbb.60365

Ichinose, H., Kotake, T., Tsumuraya, Y., and Kaneko, S. (2008). Characterization of an endo-beta-1,6-Galactanase from *Streptomyces avermitilis* NBRC14893. *Appl. Environ. Microbiol.* 74, 2379–2383. doi: 10.1128/AEM.01733-07

Ichinose, H., Kuno, A., Kotake, T., Yoshida, M., Sakka, K., Hirabayashi, J., et al. (2006b). Characterization of an exo-beta-1,3-galactanase from *Clostridium thermocellum*. *Appl. Environ. Microbiol.* 72, 3515–3523. doi: 10.1128/AEM.72.5.3515-3523.2006

Ichinose, H., Yoshida, M., Kotake, T., Kuno, A., Igarashi, K., Tsumuraya, Y., et al. (2005). An exo-beta-1,3-galactanase having a novel beta-1,3-galactan-binding module from *Phanerochaete chrysosporium*. *J. Biol. Chem.* 280, 25820–25829. doi: 10.1074/jbc.M501024200

Inacio, J. M., Correia, I. L., and de Sa-Nogueira, I. (2008). Two distinct arabinofuranosidases contribute to arabino-oligosaccharide degradation in *Bacillus subtilis*. *Microbiology* 154, 2719–2729. doi: 10.1099/mic.0.2008/018978-0

Ishida, T., Fujimoto, Z., Ichinose, H., Igarashi, K., Kaneko, S., and Samejima, M. (2009). Crystallization of selenomethionyl exo-beta-1,3-galactanase from the basidiomycete *Phanerochaete chrysosporium*. *Acta Crystallogr. Sect. F Struct. Biol. Cryst. Commun.* 65, 1274–1276. doi: 10.1107/S1744309109043395

Jamet, E., Albenne, C., Boudart, G., Irshad, M., Canut, H., and Pont-Lezica, R. (2008). Recent advances in plant cell wall proteomics. *Proteomics* 8, 893–908. doi: 10.1002/pmic.200700938

Jiang, D., Fan, J., Wang, X., Zhao, Y., Huang, B., Liu, J., et al. (2012). Crystal structure of 1,3Gal43A, an exo-beta-1,3-galactanase from *Clostridium thermocellum*. *J. Struct. Biol.* 180, 447–457. doi: 10.1016/j.jsb.2012.08.005

Johnson, K. L., Cassin, A. M., Lonsdale, A., Wong, G. K.-S., Soltis, D. E., Miles, N. W., et al. (2017). Insights into the evolution of hydroxyproline-rich glycoproteins from 1000 plant transcriptomes. *Plant Physiol.* 174, 904–921. doi: 10.1104/pp.17.00295

Johnson, K. L., Jones, B. J., Bacic, A., and Schultz, C. J. (2003). The fasciclin-like arabinogalactan proteins of *Arab*idopsis. A multigene family of putative cell adhesion molecules. *Plant Physiol.* 133, 1911–1925. doi: 10.1104/pp.103.031237

Keegstra, K. (2010). Plant cell walls. *Plant Physiol.* 154, 483–486. doi: 10.1104/pp.110.161240

Kimura, I., Sasahara, H., and Tajima, S. (1995). Purification and characterization of two xylanases and an arabinofuranosidase from *Aspergillus sojae*. *J. Ferment. Bioeng.* 80, 334–339. doi: 10.1016/0922-338x(95)94200-b

Kitazawa, K., Tryfona, T., Yoshimi, Y., Hayashi, Y., Kawauchi, S., Antonov, L., et al. (2013). beta-galactosyl Yariv reagent binds to the beta-1,3-galactan of arabinogalactan proteins. *Plant Physiol.* 161, 1117–1126. doi: 10.1104/pp.112.211722

Kiyohara, H., Zhang, Y., and Yamada, H. (1997). Effect of exo-β-D-(1→3)-galactanase digestion on complement activating activity of neutral arabinogalactan unit in a pectic arabinogalactan from roots of *Angelica acutiloba* Kitagawa. *Carbohydr. Polym.* 32, 249–253. doi: 10.1016/s0144-8617(97)00004-0

Knee, E. M., Gong, F. C., Gao, M., Teplitski, M., Jones, A. R., Foxworthy, A., et al. (2001). Root mucilage from pea and its utilization by rhizosphere bacteria as a sole carbon source. *Mol. Plant Microbe. Interact.* 14, 775–784. doi: 10.1094/MPMI.2001.14.6.775

Kobayashi, Y., Motose, H., Iwamoto, K., and Fukuda, H. (2011). Expression and genome-wide analysis of the xylogen-type gene family. *Plant Cell Physiol.* 52, 1095–1106. doi: 10.1093/pcp/pcr060

Konishi, T., Kotake, T., Soraya, D., Matsuoka, K., Koyama, T., Kaneko, S., et al. (2008). Properties of family 79 beta-glucuronidases that hydrolyze beta-glucuronosyl and 4-O-methyl-beta-glucuronosyl residues of arabinogalactan-protein. *Carbohydr. Res.* 343, 1191–1201. doi: 10.1016/j.carres.2008.03.004

Kosugi, A., Murashima, K., and Doi, R. H. (2002). Characterization of two noncellulosomal subunits. *ArfA and BgaA, from Clostridium cellulovorans* that cooperate with the cellulosome in plant cell wall degradation. *J. Bacteriol.* 184, 6859–6865. doi: 10.1128/jb.184.24.6859-6865.2002

Kotake, T., Hirata, N., Degi, Y., Ishiguro, M., Kitazawa, K., Takata, R., et al. (2011). Endo-beta-1,3-galactanase from winter mushroom *Flammulina velutipes*. *J. Biol. Chem.* 286, 27848–27854. doi: 10.1074/jbc.M111.251736

Kotake, T., Kaneko, S., Kubomoto, A., Haque, M. A., Kobayashi, H., and Tsumuraya, Y. (2004). Molecular cloning and expression in *Escherichia coli* of a *Trichoderma viride* endo-beta-(1–>6)-galactanase gene. *Biochem. J.* 377, 749–755. doi: 10.1042/BJ20031145

Kotake, T., Kitazawa, K., Takata, R., Okabe, K., Ichinose, H., Kaneko, S., et al. (2009). Molecular cloning and expression in *Pichia pastoris* of a *Irpex lacteus* exo-beta-(1–>3)-galactanase gene. *Biosci. Biotechnol. Biochem.* 73, 2303–2309. doi: 10.1271/bbb.90433

Koutaniemi, S., and Tenkanen, M. (2016). Action of three GH51 and one GH54 alpha-arabinofuranosidases on internally and terminally located arabinofuranosyl branches. *J. Biotechnol.* 229, 22–30. doi: 10.1016/j.jbiotec.2016.04.050

Kremer, C., Pettolino, F., Bacic, A., and Drinnan, A. (2004). Distribution of cell wall components in *Sphagnum hyaline* cells and in liverwort and hornwort elaters. *Planta* 219, 1023–1035. doi: 10.1007/s00425-004-1308-4

Kubicek, C. P., Starr, T. L., and Glass, N. L. (2014). Plant cell wall-degrading enzymes and their secretion in plant-pathogenic fungi. *Annu. Rev. Phytopathol.* 52, 427–451. doi: 10.1146/annurev-phyto-102313-045831

Kuroyama, H., Tsutsui, N., Hashimoto, Y., and Tsumuraya, Y. (2001). Purification and characterization of a β-glucuronidase from *Aspergillus niger*. *Carbohydr. Res.* 333, 27–39. doi: 10.1016/s0008-6215(01)00114-8

Lagaert, S., Pollet, A., Courtin, C. M., and Volckaert, G. (2014). beta-xylosidases and alpha-L-arabinofuranosidases: accessory enzymes for arabinoxylan degradation. *Biotechnol. Adv.* 32, 316–332. doi: 10.1016/j.biotechadv.2013.11.005

Lamport, D. T., and Varnai, P. (2013). Periplasmic arabinogalactan glycoproteins act as a calcium capacitor that regulates plant growth and development. *New Phytol.* 197, 58–64. doi: 10.1111/nph.12005

Lamport, D. T. A., Varnai, P., and Seal, C. E. (2014). Back to the future with the AGP-Ca2+ flux capacitor. *Ann. Bot.* 114, 1069–1085. doi: 10.1093/aob/mcu161

Lansky, S., Salama, R., Solomon, H. V., Feinberg, H., Belrhali, H., Shoham, Y., et al. (2014). Structure-specificity relationships in Abp, a GH27 beta-L-arabinopyranosidase from *Geobacillus stearothermophilus* T6. *Acta Crystallogr. Sect. D Biol. Crystallogr.* 70, 2994–3012. doi: 10.1107/S139900471401863X

Lee, K. J. D., Sakata, Y., Mau, S.-L., Pettolino, F., Bacic, A., Quatrano, R. S., et al. (2005). Arabinogalactan proteins are required for apical cell extension in the moss *Physcomitrella patens*. *Plant Cell* 17, 3051–3065. doi: 10.1105/tpc.105.034413

Leivas, C. L., Iacomini, M., and Cordeiro, L. M. (2016). Pectic type II arabinogalactans from starfruit (*Averrhoa carambola* L.). *Food Chem.* 199, 252–257. doi: 10.1016/j.foodchem.2015.12.020

Leszczuk, A., Pieczywek, P. M., Gryta, A., Frac, M., and Zdunek, A. (2019). Immunocytochemical studies on the distribution of arabinogalactan proteins (AGPs) as a response to fungal infection in *Malus* x *domestica* fruit. *Sci. Rep.* 9:17428. doi: 10.1038/s41598-019-54022-3

Li, Y., Liu, D., Tu, L., Zhang, X., Wang, L., Zhu, L., et al. (2010). Suppression of GhAGP4 gene expression repressed the initiation and elongation of cotton fiber. *Plant Cell Rep.* 29, 193–202. doi: 10.1007/s00299-009-0812-1

Ling, N. X., Lee, J., Ellis, M., Liao, M. L., Mau, S. L., Guest, D., et al. (2012). An exo-beta-(1–>3)-D-galactanase from *Streptomyces* sp. provides insights into type II arabinogalactan structure. *Carbohydr. Res.* 352, 70–81. doi: 10.1016/j.carres.2012.02.033

Lombard, V., Golaconda Ramulu, H., Drula, E., Coutinho, P. M., and Henrissat, B. (2014). The carbohydrate-active enzymes database (CAZy) in 2013. *Nucleic Acids Res.* 42, D490–D495. doi: 10.1093/nar/gkt1178

Luonteri, E. (1998). Substrate specificities of *Aspergillus terreus* α-arabinofuranosidases. *Carbohydr. Polym.* 37, 131–141. doi: 10.1016/s0144-8617(98)00052-6

Luonteri, E., Laine, C., Uusitalo, S., Teleman, A., Siika-aho, M., and Tenkanen, M. (2003). Purification and characterization of *Aspergillus* β-D-galactanases acting on β-1,4- and β-1,3/6-linked arabinogalactans. *Carbohydr. Polym.* 53, 155–168. doi: 10.1016/s0144-8617(02)00303-x

Ma, H., and Zhao, J. (2010). Genome-wide identification, classification, and expression analysis of the arabinogalactan protein gene family in rice (*Oryza sativa* L.). *J. Exp. Bot.* 61, 2647–2668. doi: 10.1093/jxb/erq104

Ma, Y., Yan, C., Li, H., Wu, W., Liu, Y., Wang, Y., et al. (2017). Bioinformatics prediction and evolution analysis of arabinogalactan proteins in the plant kingdom. *Front. Plant Sci.* 8:66. doi: 10.3389/fpls.2017.00066

Malgas, S., Thoresen, M., van Dyk, J. S., and Pletschke, B. I. (2017). Time dependence of enzyme synergism during the degradation of model and natural lignocellulosic substrates. *Enzyme Microb. Technol.* 103, 1–11. doi: 10.1016/j.enzmictec.2017.04.007

Mareri, L., Romi, M., and Cai, G. (2018). Arabinogalactan proteins: actors or spectators during abiotic and biotic stress in plants? *Plant Biosyst.* 153, 173–185. doi: 10.1080/11263504.2018.1473525

Mashiguchi, K., Asami, T., and Suzuki, Y. (2009). Genome-wide identification, structure and expression studies, and mutant collection of 22 early nodulin-like protein genes in *Arabidopsis*. *Biosci. Biotechnol. Biochem.* 73, 2452–2459. doi: 10.1271/bbb.90407

Mashiguchi, K., Urakami, E., Hasegawa, M., Sanmiya, K., Matsumoto, I., Yamaguchi, I., et al. (2008). Defense-related signaling by interaction of arabinogalactan proteins and beta-glucosyl Yariv reagent inhibits gibberellin signaling in barley aleurone cells. *Plant Cell Physiol.* 49, 178–190. doi: 10.1093/pcp/pcm175

Matias de Oliveira, D., Rodrigues Mota, T., Marchiosi, R., Ferrarese-Filho, O., Dantas, et al. (2018). Plant cell wall composition and enzymatic deconstruction. *AIMS Bioeng.* 5, 63–77. doi: 10.3934/bioeng.2018.1.63

Matsuo, N., Kaneko, S., Kuno, A., Kobayashi, H., and Kusakabe, I. (2000). Purification, characterization and gene cloning of two alpha-L-arabinofuranosidases from *Streptomyces chartreusis* GS901. *Biochem. J.* 346, 9–15.

Matsuyama, K., Kishine, N., Fujimoto, Z., Sunagawa, N., Kotake, T., Tsumuraya, Y., et al. (2020). Unique active-site and subsite features in the arabinogalactan-degrading GH43 exo-beta-1,3-galactanase from *Phanerochaete chrysosporium*. *J. Biol. Chem.* 295, 18539–18552. doi: 10.1074/jbc.RA120.016149

Maurer, J. B. B., Bacic, A., Pereira-Netto, A. B., Donatti, L., Zawadzki-Baggio, S. F., and Pettolino, F. A. (2010). Arabinogalactan-proteins from cell suspension cultures of *Araucaria angustifolia*. *Phytochemistry* 71, 1400–1409. doi: 10.1016/j.phytochem.2010.04.021

McKee, L. S., and Brumer, H. (2015). Growth of *Chitinophaga pinensis* on plant cell wall glycans and characterisation of a glycoside hydrolase family 27 beta-L-arabinopyranosidase implicated in arabinogalactan utilisation. *PLoS One* 10:e0139932. doi: 10.1371/journal.pone.0139932

Miyanaga, A., Koseki, T., Matsuzawa, H., Wakagi, T., Shoun, H., and Fushinobu, S. (2004). Crystal structure of a family 54 alpha-L-arabinofuranosidase reveals a novel carbohydrate-binding module that can bind arabinose. *J. Biol. Chem.* 279, 44907–44914. doi: 10.1074/jbc.M405390200

Mohnen, D. (2008). Pectin structure and biosynthesis. *Curr. Opin. Plant Biol.* 11, 266–277. doi: 10.1016/j.pbi.2008.03.006

Motose, H., Sugiyama, M., and Fukuda, H. (2004). A proteoglycan mediates inductive interaction during plant vascular development. *Nature* 429, 873–878. doi: 10.1038/nature02613

Nakajima, M., and Akutsu, K. (2013). Virulence factors of *Botrytis cinerea*. *J. Gen. Plant Pathol.* 80, 15–23. doi: 10.1007/s10327-013-0492-0

Nguema-Ona, E., Vicre-Gibouin, M., Cannesan, M. A., and Driouich, A. (2013). Arabinogalactan proteins in root-microbe interactions. *Trends Plant Sci.* 18, 440–449. doi: 10.1016/j.tplants.2013.03.006

Numan, M. T., and Bhosle, N. B. (2006). Alpha-L-arabinofuranosidases: the potential applications in biotechnology. *J. Ind. Microbiol. Biotechnol.* 33, 247–260. doi: 10.1007/s10295-005-0072-1

Okawa, M., Fukamachi, K., Tanaka, H., and Sakamoto, T. (2013). Identification of an exo-β-1,3-D-galactanase from *Fusarium oxysporum* and the synergistic effect with related enzymes on degradation of type II arabinogalactan. *Appl. Microbiol. Biotechnol.* 97, 9685–9694. doi: 10.1007/s00253-013-4759-3

Okemoto, K., Uekita, T., Tsumuraya, Y., Hashimoto, Y., and Kasama, T. (2003). Purification and characterization of an endo-β-(1→6)-galactanase from *Trichoderma viride*. *Carbohydr. Res.* 338, 219–230. doi: 10.1016/s0008-6215(02)00405-6

Oxley, D., and Bacic, A. (1999). Structure of the glycosylphosphatidylinositol anchor of an arabinogalactan protein from *Pyrus communis* suspension-cultured cells. *Proc. Natl. Acad. Sci. USA* 96, 14246–14251. doi: 10.1073/pnas.96.25.14246

Paes, G., Skov, L. K., O'Donohue, M. J., Remond, C., Kastrup, J. S., Gajhede, M., et al. (2008). The structure of the complex between a branched pentasaccharide and *Thermobacillus xylanilyticus* GH-51 arabinofuranosidase reveals xylan-binding determinants and induced fit. *Biochemistry* 47, 7441–7451. doi: 10.1021/bi800424e

Park, M. H., Suzuki, Y., Chono, M., Knox, J. P., and Yamaguchi, I. (2003). CsAGP1, a gibberellin-responsive gene from cucumber hypocotyls, encodes a classical arabinogalactan protein and is involved in stem elongation. *Plant Physiol.* 131, 1450–1459. doi: 10.1104/pp.015628

Pauly, M., and Keegstra, K. (2008). Cell-wall carbohydrates and their modification as a resource for biofuels. *Plant J.* 54, 559–568. doi: 10.1111/j.1365-313X.2008.03463.x

Pauly, M., and Keegstra, K. (2016). Biosynthesis of the plant cell wall matrix polysaccharide xyloglucan. *Annu. Rev. Plant. Biol.* 67, 235–259. doi: 10.1146/annurev-arplant-043015-112222

Pellerin, P., and Brillouet, J.-M. (1994). Purification and properties of an exo-(1→3)-β-d-galactanase from *Aspergillus niger*. *Carbohydr. Res.* 264, 281–291. doi: 10.1016/S0008-6215(05)80012-6

Pereira, A. M., Masiero, S., Nobre, M. S., Costa, M. L., Solis, M. T., Testillano, P. S., et al. (2014). Differential expression patterns of arabinogalactan proteins in *Arabidopsis thaliana* reproductive tissues. *J. Exp. Bot.* 65, 5459–5471. doi: 10.1093/jxb/eru300

Pereira, L. G., Coimbra, S., Oliveira, H., Monteiro, L., and Sottomayor, M. (2006). Expression of arabinogalactan protein genes in pollen tubes of *Arabidopsis thaliana*. *Planta* 223, 374–380. doi: 10.1007/s00425-005-0137-4

Pfeifer, L., Shafee, T., Johnson, K. L., Bacic, A., and Classen, B. (2020). Arabinogalactan-proteins of *Zostera marina* L. contain unique glycan structures and provide insight into adaption processes to saline environments. *Sci. Rep.* 10:8232. doi: 10.1038/s41598-020-65135-5

Pogorelko, G., Lionetti, V., Bellincampi, D., and Zabotina, O. (2013). Cell wall integrity: targeted post-synthetic modifications to reveal its role in plant growth and defense against pathogens. *Plant Signal. Behav.* 8:25435. doi: 10.4161/psb.25435

Poria, V., Saini, J. K., Singh, S., Nain, L., and Kuhad, R. C. (2020). Arabinofuranosidases: Characteristics, microbial production, and potential in waste valorization and industrial applications. *Bioresour. Technol.* 304:123019. doi: 10.1016/j.biortech.2020.123019

Raju, T. S., and Davidson, E. A. (1994). Structural features of water-soluble novel polysaccharide components from the leaves of *Tridax procumbens* Linn. *Carbohydr. Res.* 258, 243–254. doi: 10.1016/0008-6215(94)84090-3

Rashid, A. (2016). Defense responses of plant cell wall non-catalytic proteins against pathogens. *Physiol. Mol. Plant Pathol.* 94, 38–46. doi: 10.1016/j.pmpp.2016.03.009

Ravanal, M. C., Callegari, E., and Eyzaguirre, J. (2010). Novel bifunctional alpha-L-arabinofuranosidase/xylobiohydrolase (ABF3) from *Penicillium purpurogenum*. *Appl. Environ. Microbiol.* 76, 5247–5253. doi: 10.1128/AEM.00214-10

Rui, Y., and Dinneny, J. R. (2020). A wall with integrity: surveillance and maintenance of the plant cell wall under stress. *New Phytol.* 225, 1428–1439. doi: 10.1111/nph.16166

Saha, B. C., and Bothast, R. J. (1998). Effect of carbon source on production of alpha-L-arabinofuranosidase by *Aureobasidium pullulans*. *Curr. Microbiol.* 37, 337–340. doi: 10.1007/s002849900388

Sakamoto, T., Inui, M., Yasui, K., Hosokawa, S., and Ihara, H. (2013). Substrate specificity and gene expression of two *Penicillium chrysogenum* alpha-L-arabinofuranosidases (AFQ1 and AFS1) belonging to glycoside hydrolase families 51 and 54. *Appl. Microbiol. Biotechnol.* 97, 1121–1130. doi: 10.1007/s00253-012-3978-3

Sakamoto, T., and Ishimaru, M. (2013). Peculiarities and applications of galactanolytic enzymes that act on type I and II arabinogalactans. *Appl. Microbiol. Biotechnol.* 97, 5201–5213. doi: 10.1007/s00253-013-4946-2

Sakamoto, T., and Kawasaki, H. (2003). Purification and properties of two type-B α-l-arabinofuranosidases produced by *Penicillium chrysogenum*. *Biochim. Biophys. Acta* 1621, 204–210. doi: 10.1016/s0304-4165(03)00058-8

Sakamoto, T., Tanaka, H., Nishimura, Y., Ishimaru, M., and Kasai, N. (2011). Characterization of an exo-beta-1,3-D: -galactanase from *Sphingomonas* sp. 24T and its application to structural analysis of larch wood arabinogalactan. *Appl. Microbiol. Biotechnol.* 90, 1701–1710. doi: 10.1007/s00253-011-3219-1

Sakamoto, T., Taniguchi, Y., Suzuki, S., Ihara, H., and Kawasaki, H. (2007). Characterization of *Fusarium oxysporum* beta-1,6-galactanase, an enzyme that hydrolyzes larch wood arabinogalactan. *Appl. Environ. Microbiol.* 73, 3109–3112. doi: 10.1128/AEM.02101-06

Sakamoto, T., Tsujitani, Y., Fukamachi, K., Taniguchi, Y., and Ihara, H. (2010). Identification of two GH27 bifunctional proteins with beta-L-arabinopyranosidase/alpha-D-galactopyranosidase activities from *Fusarium oxysporum*. *Appl. Microbiol. Biotechnol.* 86, 1115–1124. doi: 10.1007/s00253-009-2344-6

Salama, R., Alalouf, O., Tabachnikov, O., Zolotnitsky, G., Shoham, G., and Shoham, Y. (2012). The abp gene in *Geobacillus stearothermophilus* T-6 encodes a GH27 beta-L-arabinopyranosidase. *FEBS Lett.* 586, 2436–2442. doi: 10.1016/j.febslet.2012.05.062

Sarch, C., Suzuki, H., Master, E. R., and Wang, W. (2019). Kinetics and regioselectivity of three GH62 alpha-L-arabinofuranosidases from plant pathogenic fungi. *Biochim. Biophys. Acta Gen. Subj.* 1863, 1070–1078. doi: 10.1016/j.bbagen.2019.03.020

Scheller, H. V., and Ulvskov, P. (2010). Hemicelluloses. *Annu. Rev. Plant. Biol.* 61, 263–289. doi: 10.1146/annurev-arplant-042809-112315

Schultz, C., Gilson, P., Oxley, D., Youl, J., and Bacic, A. (1998). GPI-anchors on arabinogalactan-proteins: implications for signalling in plants. *Trends Plant Sci.* 3, 426–431. doi: 10.1016/S1360-1385(98)01328-4

Schultz, C. J., Johnson, K. L., Currie, G., and Bacic, A. (2000). The classical arabinogalactan protein gene family of *Arabidopsis*. *Plant Cell* 12, 1751–1768. doi: 10.1105/tpc.12.9.1751

Schultz, C. J., Rumsewicz, M. P., Johnson, K. L., Jones, B. J., Gaspar, Y. M., and Bacic, A. (2002). Using genomic resources to guide research directions. The arabinogalactan protein gene family as a test case. *Plant Physiol.* 129, 1448–1463. doi: 10.1104/pp.003459

Seifert, G. J., and Roberts, K. (2007). The biology of arabinogalactan proteins. *Annu. Rev. Plant Biol.* 58, 137–161. doi: 10.1146/annurev.arplant.58.032806.103801

Sella, L., Castiglioni, C., Paccanaro, M. C., Janni, M., Schafer, W., D'Ovidio, R., et al. (2016). Involvement of fungal pectin methylesterase activity in the interaction between *Fusarium graminearum* and wheat. *Mol. Plant. Microbe Interact.* 29, 258–267. doi: 10.1094/MPMI-07-15-0174-R

Shi, H., Kim, Y., Guo, Y., Stevenson, B., and Zhu, J. K. (2003). The *Arabidopsis* SOS5 locus encodes a putative cell surface adhesion protein and is required for normal cell expansion. *Plant Cell* 15, 19–32. doi: 10.1105/tpc.007872

Showalter, A. M. (2001). Arabinogalactan-proteins: structure, expression and function. *Cell Mol. Life Sci.* 58, 1399–1417. doi: 10.1007/PL00000784

Showalter, A. M., and Basu, D. (2016a). Extensin and arabinogalactan-protein biosynthesis: glycosyltransferases, research challenges, and biosensors. *Front. Plant Sci.* 7:814. doi: 10.3389/fpls.2016.00814

Showalter, A. M., and Basu, D. (2016b). Glycosylation of arabinogalactan-proteins essential for development in Arabidopsis. *Commun. Integr. Biol.* 9:e1177687. doi: 10.1080/19420889.2016.1177687

Showalter, A. M., Keppler, B., Lichtenberg, J., Gu, D., and Welch, L. R. (2010). A bioinformatics approach to the identification, classification, and analysis of hydroxyproline-rich glycoproteins. *Plant Physiol.* 153, 485–513. doi: 10.1104/pp.110.156554

Takata, R., Tokita, K., Mori, S., Shimoda, R., Harada, N., Ichinose, H., et al. (2010). Degradation of carbohydrate moieties of arabinogalactan-proteins by

glycoside hydrolases from *Neurospora crassa*. *Carbohydr. Res.* 345, 2516–2522. doi: 10.1016/j.carres.2010.09.006

Tan, L., Eberhard, S., Pattathil, S., Warder, C., Glushka, J., Yuan, C., et al. (2013). An *Arabidopsis* cell wall proteoglycan consists of pectin and arabinoxylan covalently linked to an arabinogalactan protein. *Plant Cell* 25, 270–287. doi: 10.1105/tpc.112.107334

Tan, L., Showalter, A. M., Egelund, J., Hernandez-Sanchez, A., Doblin, M. S., and Bacic, A. (2012). Arabinogalactan-proteins and the research challenges for these enigmatic plant cell surface proteoglycans. *Front. Plant Sci.* 3:140. doi: 10.3389/fpls.2012.00140

Tan, L., Varnai, P., Lamport, D. T., Yuan, C., Xu, J., Qiu, F., et al. (2010). Plant O-hydroxyproline arabinogalactans are composed of repeating trigalactosyl subunits with short bifurcated side chains. *J. Biol. Chem.* 285, 24575–24583. doi: 10.1074/jbc.M109.100149

Tang, W., Ezcurra, I., Muschietti, J., and McCormick, S. (2002). A cysteine-rich extracellular protein. LAT52, interacts with the extracellular domain of the pollen receptor kinase LePRK2. *Plant Cell* 14, 2277–2287. doi: 10.1105/tpc.003103

Taylor, E. J., Smith, N. L., Turkenburg, J. P., D'Souza, S., Gilbert, H. J., and Davies, G. J. (2006). Structural insight into the ligand specificity of a thermostable family 51 arabinofuranosidase. Araf51, from Clostridium thermocellum. *Biochem. J.* 395, 31–37. doi: 10.1042/BJ20051780

Tsumuraya, Y., Mochizuki, N., Hashimoto, Y., and Kovac, P. (1990). Purification of an exo-beta-(1—-3)-D-galactanase of *Irpex lacteus* (*Polyporus tulipiferae*) and its action on arabinogalactan-proteins. *J. Biol. Chem.* 265, 7207–7215.

van Hengel, A. J., and Roberts, K. (2003). AtAGP30, an arabinogalactan-protein in the cell walls of the primary root, plays a role in root regeneration and seed germination. *Plant J.* 36, 256–270. doi: 10.1046/j.1365-313x.2003.01874.x

vd Veen, P., Flipphi, M. J., Voragen, A. G., and Visser, J. (1991). Induction, purification and characterisation of arabinases produced by *Aspergillus niger*. *Arch. Microbiol.* 157, 23–28. doi: 10.1007/BF00245330

Vicre, M., Santaella, C., Blanchet, S., Gateau, A., and Driouich, A. (2005). Root border-like cells of Arabidopsis. Microscopical characterization and role in the interaction with rhizobacteria. *Plant Physiol.* 138, 998–1008. doi: 10.1104/pp.104.051813

Villa-Rivera, M. G., Conejo-Saucedo, U., Lara-Marquez, A., Cano-Camacho, H., Lopez-Romero, E., and Zavala-Paramo, M. G. (2017a). The role of virulence factors in the pathogenicity of *Colletotrichum* sp. *Curr. Protein. Pept. Sci.* 18, 1005–1018. doi: 10.2174/1389203717666160813160727

Villa-Rivera, M. G., Zavala-Páramo, M. G., Conejo-Saucedo, U., López-Romero, E., Lara-Márquez, A., and Cano-Camacho, H. (2017b). Differences in the expression profile of endo-β-(1,6)-D-galactanase in pathogenic and non-pathogenic races of *Colletotrichum lindemuthianum* grown in the presence of arabinogalactan, xylan or *Phaseolus vulgaris* cell walls. *Physiol. Mol. Plant Pathol.* 99, 75–86. doi: 10.1016/j.pmpp.2016.10.002

Wang, L., Cheng, M., Yang, Q., Li, J., Wang, X., Zhou, Q., et al. (2019). Arabinogalactan protein-rare earth element complexes activate plant endocytosis. *Proc. Natl. Acad. Sci. USA* 116, 14349–14357. doi: 10.1073/pnas.1902532116

Wilkens, C., Andersen, S., Petersen, B. O., Li, A., Busse-Wicher, M., Birch, J., et al. (2016). An efficient arabinoxylan-debranching alpha-L-arabinofuranosidase of family GH62 from *Aspergillus nidulans* contains a secondary carbohydrate binding site. *Appl. Microbiol. Biotechnol.* 100, 6265–6277. doi: 10.1007/s00253-016-7417-8

Wood, T. M., and McCrae, S. I. (1996). Arabinoxylan-degrading enzyme system of the fungus *Aspergillus awamori:* purification and properties of an alpha-L-arabinofuranosidase. *Appl. Microbiol. Biotechnol.* 45, 538–545. doi: 10.1007/BF00578468

Wu, J., Wang, Y., Park, S. Y., Kim, S. G., Yoo, J. S., Park, S., et al. (2016). Secreted alpha-N-arabinofuranosidase B protein is required for the full virulence of *Magnaporthe oryzae* and triggers host defences. *PLoS One* 11:e0165149. doi: 10.1371/journal.pone.0165149

Wu, Y., Fan, W., Li, X., Chen, H., Takac, T., Samajova, O., et al. (2017). Expression and distribution of extensins and AGPs in susceptible and resistant banana cultivars in response to wounding and *Fusarium oxysporum*. *Sci. Rep.* 7:42400. doi: 10.1038/srep42400

Xie, D., Ma, L., Samaj, J., and Xu, C. (2011). Immunohistochemical analysis of cell wall hydroxyproline-rich glycoproteins in the roots of resistant and susceptible wax gourd cultivars in response to *Fusarium oxysporum* f. sp. Benincasae infection and fusaric acid treatment. *Plant Cell Rep.* 30, 1555–1569. doi: 10.1007/s00299-011-1069-z

Xie, F., Williams, A., Edwards, A., and Downie, J. A. (2012). A plant arabinogalactan-like glycoprotein promotes a novel type of polar surface attachment by *Rhizobium leguminosarum*. *Mol. Plant Microbe. Interact.* 25, 250–258. doi: 10.1094/MPMI-08-11-0211

Yang, J., and Showalter, A. M. (2007). Expression and localization of AtAGP18, a lysine-rich arabinogalactan-protein in *Arabidopsis*. *Planta* 226, 169–179. doi: 10.1007/s00425-007-0478-2

Yariv, J., Lis, H., and Katchalski, E. (1967). Precipitation of arabic acid and some seed polysaccharides by glycosylphenylazo dyes. *Biochem. J.* 105, 1C–2C. doi: 10.1042/bj1050001c

Yoshimi, Y., Hara, K., Yoshimura, M., Tanaka, N., Higaki, T., Tsumuraya, Y., et al. (2020). Expression of a fungal exo-beta-1,3-galactanase in *Arabidopsis* reveals a role of type II arabinogalactans in the regulation of cell shape. *J. Exp. Bot.* 71, 5414–5424. doi: 10.1093/jxb/eraa236

Yoshimi, Y., Yaguchi, K., Kaneko, S., Tsumuraya, Y., and Kotake, T. (2017). Properties of two fungal endo-beta-1,3-galactanases and their synergistic action with an exo-beta-1,3-galactanase in degrading arabinogalactan-proteins. *Carbohydr. Res.* 45, 26–35. doi: 10.1016/j.carres.2017.10.013

Zhang, Y., Brown, G., Whetten, R., Loopstra, C. A., Neale, D., Kieliszewski, M. J., et al. (2003). An arabinogalactan protein associated with secondary cell wall formation in differentiating xylem of loblolly pine. *Plant Mol. Biol.* 52, 91–102. doi: 10.1023/A:1023978210001

Zhang, Y., Yang, J., and Showalter, A. M. (2011). AtAGP18 is localized at the plasma membrane and functions in plant growth and development. *Planta* 233, 675–683. doi: 10.1007/s00425-010-1331-6

Conflict of Interest: The authors declare that the research was conducted in the absence of any commercial or financial relationships that could be construed as a potential conflict of interest.

Publisher's Note: All claims expressed in this article are solely those of the authors and do not necessarily represent those of their affiliated organizations, or those of the publisher, the editors and the reviewers. Any product that may be evaluated in this article, or claim that may be made by its manufacturer, is not guaranteed or endorsed by the publisher.

frontiers in Microbiology

ORIGINAL RESEARCH
published: 20 September 2021
doi: 10.3389/fmicb.2021.726958

Comparison of Cell Wall Polysaccharide Composition and Structure Between Strains of *Sporothrix schenckii* and *Sporothrix brasiliensis*

*Héctor L. Villalobos-Duno[1], Laura A. Barreto[2], Álvaro Alvarez-Aular[3], Héctor M. Mora-Montes[4], Nancy E. Lozoya-Pérez[4], Bernardo Franco[4], Leila M. Lopes-Bezerra[5] and Gustavo A. Niño-Vega[4]**

[1]Laboratorio de Micología, Centro de Microbiología y Biología Celular, Instituto Venezolano de Investigaciones Científicas, Caracas, Venezuela, [2]Instituto Superior de Formación Docente Salome Ureña, Santo Domingo, Dominican Republic, [3]Laboratorio de Síntesis Orgánica y Productos Naturales, Centro de Química, Instituto Venezolano de Investigaciones Científicas, Caracas, Venezuela, [4]División de Ciencias Naturales y Exactas, Departamento de Biología, Universidad de Guanajuato, Guanajuato, Mexico, [5]Biomedical Institute, University of São Paulo, São Paulo, Brazil

OPEN ACCESS

Edited by:
Leonardo Nimrichter, Federal University of Rio de Janeiro, Brazil

Reviewed by:
Max Carlos Ramírez-Soto, Universidad Peruana Cayetano Heredia, Peru
Javier Capilla, University of Rovira i Virgili, Spain

***Correspondence:**
Gustavo A. Niño-Vega
gustavo.nino@ugto.mx

Specialty section:
This article was submitted to Infectious Diseases, a section of the journal Frontiers in Microbiology

Received: 17 June 2021
Accepted: 24 August 2021
Published: 20 September 2021

Citation:
Villalobos-Duno HL, Barreto LA, Alvarez-Aular Á, Mora-Montes HM, Lozoya-Pérez NE, Franco B, Lopes-Bezerra LM and Niño-Vega GA (2021) Comparison of Cell Wall Polysaccharide Composition and Structure Between Strains of Sporothrix schenckii and Sporothrix brasiliensis. Front. Microbiol. 12:726958. doi: 10.3389/fmicb.2021.726958

Sporothrix schenckii, *Sporothrix brasiliensis*, and *Sporothrix globosa* are the main causative agents of sporotrichosis, a human subcutaneous mycosis. Differences in virulence patterns are associated with each species but remain largely uncharacterized. The *S. schenckii* and *S. brasiliensis* cell wall composition and virulence are influenced by the culturing media, with little or no influence on *S. globosa*. By keeping constant the culturing media, we compared the cell wall composition of three *S. schenckii* and two *S. brasiliensis* strains, previously described as presenting different virulence levels on a murine model of infection. The cell wall composition of the five *Sporothrix* spp. strains correlated with the biochemical composition of the cell wall previously reported for the species. However, the rhamnose-to-β-glucan ratio exhibits differences among strains, with an increase in cell wall rhamnose-to-β-glucan ratio as their virulence increased. This relationship can be expressed mathematically, which could be an important tool for the determination of virulence in *Sporothrix* spp. Also, structural differences in rhamnomannan were found, with longer side chains present in strains with lower virulence reported for both species here studied, adding insight to the importance of this polysaccharide in the pathogenic process of these fungi.

Keywords: *Sporothrix* spp., fungal cell wall, beta-gucan, fungal virulence, Rhamnose, Rhamnomannan

INTRODUCTION

Sporotrichosis, a cutaneous and subcutaneous mycosis of humans and other mammals, is caused by species described within the pathogenic clade of the *Sporothrix* genus, of which *S. brasiliensis*, *S. schenckii*, and *S. globosa* are the three species of major clinical importance (de Beer et al., 2016). All species of the *Sporothrix* genus are thermo-dimorphic fungi, presenting

a saprophytic sporulating mycelial phase at 25–28°C and a yeast-like pathogenic phase at 36–37°C. In humans, the disease is characterized by cutaneous and subcutaneous lesions with regional lymphocutaneous dissemination, although some pulmonary and systemic infections have been reported (Callens et al., 2006). It is a neglected infectious disease with a worldwide distribution, and a higher incidence in tropical and subtropical countries (Barros et al., 2011; Chakrabarti et al., 2014). The cutaneous disease begins with a traumatic inoculation of the fungus by contaminated soil or plant debris or through bites and scratches from infected cats (Barros et al., 2011; Chakrabarti et al., 2014). Multiple infections might arise from a single source, which can lead to outbreaks (Chakrabarti et al., 2014).

Sporothrix schenckii is the most widespread species of the pathogenic clade present in the Americas, Europe, Africa, and Asia and is mainly associated with a sapronosis (Zhang et al., 2015), similarly to *S. globosa*, which is predominant in Asia. Furthermore, *S. brasiliensis* is an emerging species related to cat-transmitted sporotrichosis, mainly described in Brazil but now, also, present in other South American countries (Chakrabarti et al., 2014; Etchecopaz et al., 2020; Rossow et al., 2020).

Differences in the virulence profiles in experimental models of infection have been reported within the pathogenic clade. *Sporothrix brasiliensis* is reported as the most virulent species, followed by *S. schenckii*, and *S. globosa*, with the latter been reported as the species with the lowest virulence of the three (Arrillaga-Moncrieff et al., 2009; Almeida-Paes et al., 2015; Clavijo-Giraldo et al., 2016; Lozoya-Pérez et al., 2020). However, differences within *S. schenckii* clinical isolates have also been reported, ranging from highly virulent to non-virulent isolates (Fernandes et al., 2013; Almeida-Paes et al., 2015). Some factors, such as melanization, thermotolerance, protein secretion, and immunogenicity have been related to the differences in virulence patterns between the *Sporothrix* spp. and within clinical isolates (Fernandes et al., 2013; Almeida-Paes et al., 2015).

The fungal cell wall protects the fungus, acting as an initial barrier against hostile environments while preserving the cell's integrity against internal turgor pressure. It is a dynamic structure, presenting continuous changes in composition and structural organization as the cell grows or undergoes morphological changes (Latgé, 2007). These changes are strongly regulated during the cell cycle, or in response to environmental conditions, stress, and mutations in the cell wall biosynthetic processes (Klis et al., 2006; Ruiz-Herrera et al., 2006).

In general, fungal cell walls are bilayered structures, with the innermost layer comprising a core of covalently attached and branched β-(1,3) glucan, forming intrachain hydrogen bonds with chitin assembled into fibrous microfibrils, and all together forming a scaffold around the cell (Gow et al., 2017). The β-(1,3) glucan is a highly immunogenic molecule and is one of the main fungal pathogen-associated molecular patterns (PAMP) that bind to a very specific pathogen recognition receptor (PRR) present on the surface of the host's immune cells, the C-type lectin dectin-1 (Hernández-Chávez et al., 2017). Chitin, is an important immunoreactive polysaccharide, that interacts with different PRRs in a size-dependent mechanism, where big (70–100 μm) or very small (<2 μm) chitin particles do not trigger immune reactions, while medium-sized chitin particles (40–70 μm) induce a proinflammatory response, whereas small-sized chitin particles (2–10 μm) trigger an anti-inflammatory response (Hernández-Chávez et al., 2017). In general, these two polysaccharides are often masked by the components of the cell wall outer layer, which differs from the inner scaffold layer (Erwig and Gow, 2016). The *S. schenckii* and *S. brasiliensis* cell wall is mainly composed of structural polysaccharides, β-glucans, and chitin and has a peptide-rhamnomannan (PRM) outermost layer (Lopes-Bezerra et al., 2018). More recently, it has been reported that the culture media have an influence on changes in the cell wall composition and structure, as well as on the virulence of *S. schenckii* and *S. brasiliensis* but not on *S. globosa* (Lozoya-Pérez et al., 2020).

Within the frame of all the previous bodies of evidence, in the present work, we examine and compare the *S. schenckii* and *S. brasiliensis* cell wall composition in different strains. The isolates studied here, showed distinct virulence profiles (Nascimento et al., 2008; Castro et al., 2013), and the analysis of possible differences in the composition and/or the relative content of cell wall components may add new important aspects that correlate with their difference in virulence profiles.

MATERIALS AND METHODS

Strains and Growth Conditions

Fungal strains used in this study are listed in **Table 1**. The yeast morphology was obtained by growing cells on Brain Heart Infusion (BHI, Oxoid, Hampshire, United Kingdom) liquid medium, with continuous shaking at 100 rpm for 4 days at 37°C. Cells were inspected under a phase-contrast microscope (Nikon Optiphot, Japan) before being used to check for contamination or partial differentiation.

Cell Wall Fractionation

Yeast cells from cultures in exponential phase were collected by centrifugation at 8,000 x *g* for 1 h at 10°C. Briefly, the fungal pellets were suspended in distilled water with an equal volume of glass beads (0.45–0.50 mm diameter) and shaken five times in a Braun homogenizer (Braun, Melsungen, Germany) for 1 min, followed by 1 min cooling on ice between shakings. Cell disruption was followed by light microscopy. Cell homogenates were washed out of glass beads with distilled water and centrifuged at 480 × *g* for 5 min at 4°C. The pellet was freeze-dried, weighted, and

TABLE 1 | Strains used in this work.

Organism	Strain	Virulence reported in the mouse model	Reference
S. brasiliensis	5110 (ATCC MYA 4823)	High	Castro et al., 2013
S. brasiliensis	IPEC 17943 (ATCC MYA 4824)	Low	
S. schenckii	15,383 (ATCC MYA 4820)	Mild	
S. schenckii	1,099-18 (ATCC MYA 4821)	Low	
S. schenckii	M-64 (ATCC MYA 4822)	Non-virulent	Nascimento et al., 2008

fractionated by alkaline separation (Previato et al., 1979; San-Blas and San-Blas, 1994; Lopes-Bezerra et al., 2018). Briefly, the freeze-dried material was re-suspended in 1 M NaOH for 16 h, and the suspension was centrifuged to separate the alkali-insoluble material from the supernatant (fraction 1). The supernatant was neutralized with 1 N HCl, centrifuged and the pellet (alkali-soluble and acid-insoluble, fraction 2) separated from the supernatant (alkali and acid-soluble, fraction 3), which was further analyzed as described previously (Lopes-Bezerra et al., 2018). Rhamnomannan was obtained by treating fraction 3 with Fehling's reagent at 4°C as reported previously (Previato et al., 1979). The insoluble copper complexes generated, were centrifuged, washed three times with 3% KOH, twice with neat ethanol, and collected. The resulting residue was suspended in distilled water and cations removed with Dowex 50 W-X4 (H^+ form; Sigma-Aldrich, St. Louis, MO, United States) for 1 h at room temperature; the supernatant was precipitated by the addition of four volumes of neat ethanol. The residue was collected by centrifugation at 8,000 × *g* for 10 min (fraction 4, rhamnomannan). The mother liquor of the copper complexes was neutralized with acetic acid and centrifuged. The supernatant was dialyzed for 72 h against distilled water and deionized with a mixture of Dowex 1 (HCO_3^- form; Sigma-Aldrich, St. Louis, MO, United States) and Dowex 50W-X4 (H^+ form), the filtrate was concentrated, and the polysaccharides present were precipitated by the addition of three volumes of neat ethanol (fraction 5). All fractions obtained were freeze-dried.

Chemical Analyses of Cell Wall Fractions

Sugar and total amino acid content of cell wall fractions were determined as follows: for hexose content, 10 mg of each cell wall fraction was resuspended in 1 ml of 1 M HCl, sealed in a 2 ml Wheaton 176,776 ampoule, and heated for 3 h at 100°C. Hydrolyzed samples were diluted 1/10 or 1/100. Sugar quantification was accomplished by the Anthrone method for hexose content quantification in concentrated H_2SO_4. To determine amino acid and amino sugar contents, 10 mg of each sample was resuspended in 1 ml 6 M HCl, sealed in a 2 ml Wheaton 176,776 ampoule, and heated for 16 h at 100°C. Amino acid and amino sugar content were determined employing alanine and glucosamine solutions as standards, as described previously (Rondle and Morgan, 1955; Yemm et al., 1955). For rhamnose quantification, 10 mg of fraction 3 was resuspended in 1 ml of 1 M HCl, sealed in a 2 ml Wheaton 176,776 ampoule, and heated for 3 h at 100°C. Hydrolyzed samples were diluted 1/10 or 1/100. Quantification of methyl pentoses was conducted (Dische and Shettles, 1948) using 85.7% H_2SO_4 and 3% cysteine in the reaction mixtures and rhamnose to construct a standard curve.

Infrared Spectroscopy

Samples were prepared as KBr pellets. IR spectra were recorded from 3,500 to 500 cm^{-1}, using a Nicolet iS10 IR spectrometer (Thermo Fisher Scientific, Waltham, MA, United States), coupled to the OMNIC 8.0 software, following the indications of the

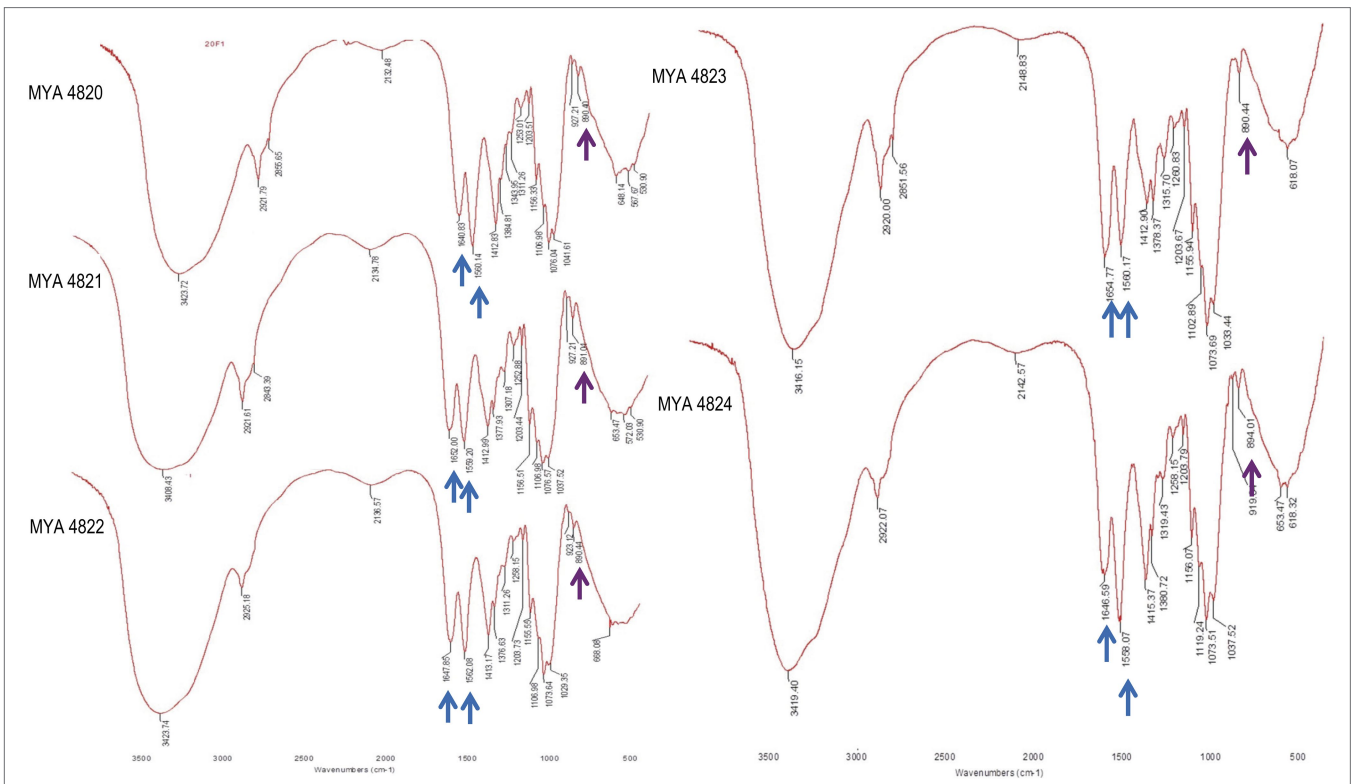

FIGURE 1 | *Sporothrix schenckii* strains IR spectra of alkali-insoluble polysaccharides. Here, the signals corresponding to all strains are shown. Chitin and β-glucan signals are indicated with blue and purple arrows respectively, also are present signals of β-glucans (1,3 and 1,6 evidenced by peaks at 1156, 1076, and 1,041 cm^{-1}).

Infrared Spectroscopy Service, Center of Chemistry, IVIC, Caracas, Venezuela.

Nuclear Magnetic Resonance Analysis

To obtain the structural data, ^{13}C and ^{1}H NMR were employed, briefly, samples of the polysaccharide fraction to be analyzed and standards (ca. 20 mg) were solubilized in D_2O or 2% NaOD and the spectra obtained at 75 MHz with a recollecting time of 16 h and 70°C using a Bruker 300 Ultrashield spectrometer, according to the indication of the Nuclear Magnetic Resonance Service, Center of Chemistry, IVIC, Caracas, Venezuela.

Analysis of Chitin Exposure on the Cell Wall Surface Using Flow Cytometry Analysis

For chitin exposure analysis, cells were stained with 1 mg/ml wheat germ agglutinin-fluorescein isothiocyanate (Sigma-Aldrich, St. Louis, MO, United States), for 60 min at room temperature. Flow cytometry was performed in a MoFlo XDP apparatus (Beckman Coulter), collecting 50,000 singlet events. Fluorescence of positive events was recovered from the compensated FL3 (green) channel using unlabeled yeast cells. Total population densities were gated and analyzed using FlowJo (version 10.0.7) software.

The heat-killed (HK) cells were prepared by incubating at 60°C for 2 h. The cellular death was confirmed by incubating aliquots of the preparations in YPD plates at 37°C for 5 days.

Statistical Analysis

Quantifications of cell wall components were made by triplicate. Statistical analyses were done by the Tukey Honestly Significant Difference (HSD) *post hoc* test. Differences were considered statistically significant at $p < 0.05$.

RESULTS

Cell Wall Composition and Structure of Sporothrix Strains Under Study

Structural and chemical analyses of polysaccharides from yeast walls of *S. schenckii* strains MYA 4820, MYA 4821, MYA 4822,

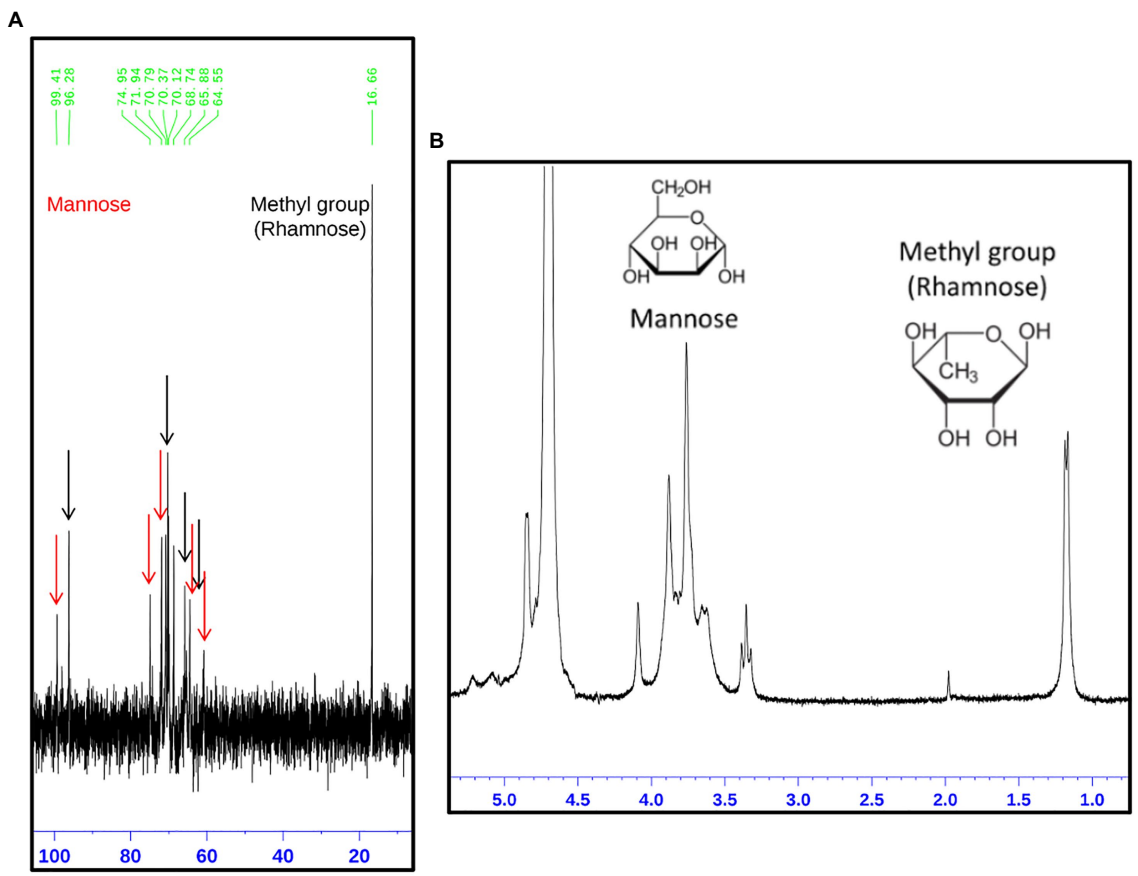

FIGURE 2 | Structural analysis of the rhamnomannan present in the *Sporothrix* strains employing ^{13}C-NMR and ^{1}H-NMR (**A,B**, respectively). On the image, the spectrum corresponding to the rhamnomannan fraction of *S. schenckii* strain MYA 4820 is presented as a representative spectrum of both, *S. schenckii* and *S. brasiliensis* strains under study. **(A)** The signals corresponding to the carbon atoms in the mannose and rhamnose residues are shown as arrows, red for mannose and black for rhamnose. The corresponding signals are shown in **Table 1**. **(B)** Show the presence of the methyl group belonging to rhamnose (1.18 and 1.17 p.p.m.) and the signals correspond to the proton bound to carbon 5 next to the methylene group for carbon 6 in the mannose ring (3.32, 3.35, and 3.39 p.p.m.).

and *S. brasiliensis* strains MYA 4823 and MYA 4824 were analyzed (**Table 1**). Cell walls from BHI-grown cells were purified and fractioned by the acid and alkali solubility and insolubility methods, as previously reported for *Sporothrix* cell wall analyses (Previato et al., 1979; Lopes-Bezerra et al., 2018). For polysaccharide structural characterization, IR spectroscopies, as well as proton and ^{13}C nuclear magnetic resonance (^{1}H-NMR and ^{13}C-NMR respectively) were used, and the generated spectra compared with IR, ^{1}H-NMR, and ^{13}C-NMR spectra previously reported for *S. schenckii* (Travassos et al., 1973; Gorin et al., 1977; Gow et al., 1987; Lopes-Alves et al., 1992; Lopes-Bezerra et al., 2018). For the five strains analyzed, IR spectra of the alkali-insoluble cell wall fraction showed characteristic polysaccharide absorption signals (**Figure 1**), showing a strong and wideband around 3,400 cm^{1} and additional bands around 2,921, 1,641, and 1,412 cm^{-1} (Rodríguez-Brito et al., 2010). Absorption bands around 1,557 and 1,662 cm^{-1} evidenced the presence of chitin, while β-glucan is evidenced by absorption bands at around 897 and 1,378 cm^{-1} (Rodríguez-Brito et al., 2010). Also, the presence of absorption peaks belonging to β-(1,3)-(1,6)-glucan (1,160, 1,078, and 1,044 cm^{-1}; Synytsya and Novak, 2014), is present in all the IR spectra obtained from all the strains.

The rhamnomannan characterization was followed by ^{1}H-NMR and ^{13}C-NMR. For all the cases, ^{1}H-NMR spectra showed the presence of the methyl group that belongs to rhamnose (1.18–1.17 ppm) and the signals corresponding to the proton linked to carbon 5 (3.32–4.10 ppm) next to the methylene group from carbon six in the mannose ring (**Figure 2B**). The H1 region of the ^{1}H-NMR spectra for all the strains under study is shown in **Figure 3**, presenting proton signals 5.21–5.26, 5.08–5.13, and 4.84–4.88 ppm, which are characteristic of *Sporothrix* rhamnomannan, as previously reported (Travassos et al., 1973, 1974). Signals 5.08–5.12 and 5.21–5.25 ppm are related to the presence of Rha(α1-4)GlcA(α1,2)Man(α1,2)Man-ol, as previously reported (Lopes-Alves et al., 1992). Also, the presence of a proton signal 4.97 ppm previously reported as present in *S. brasiliensis* strain MYA 4823 (Lopes-Bezerra et al., 2018) is

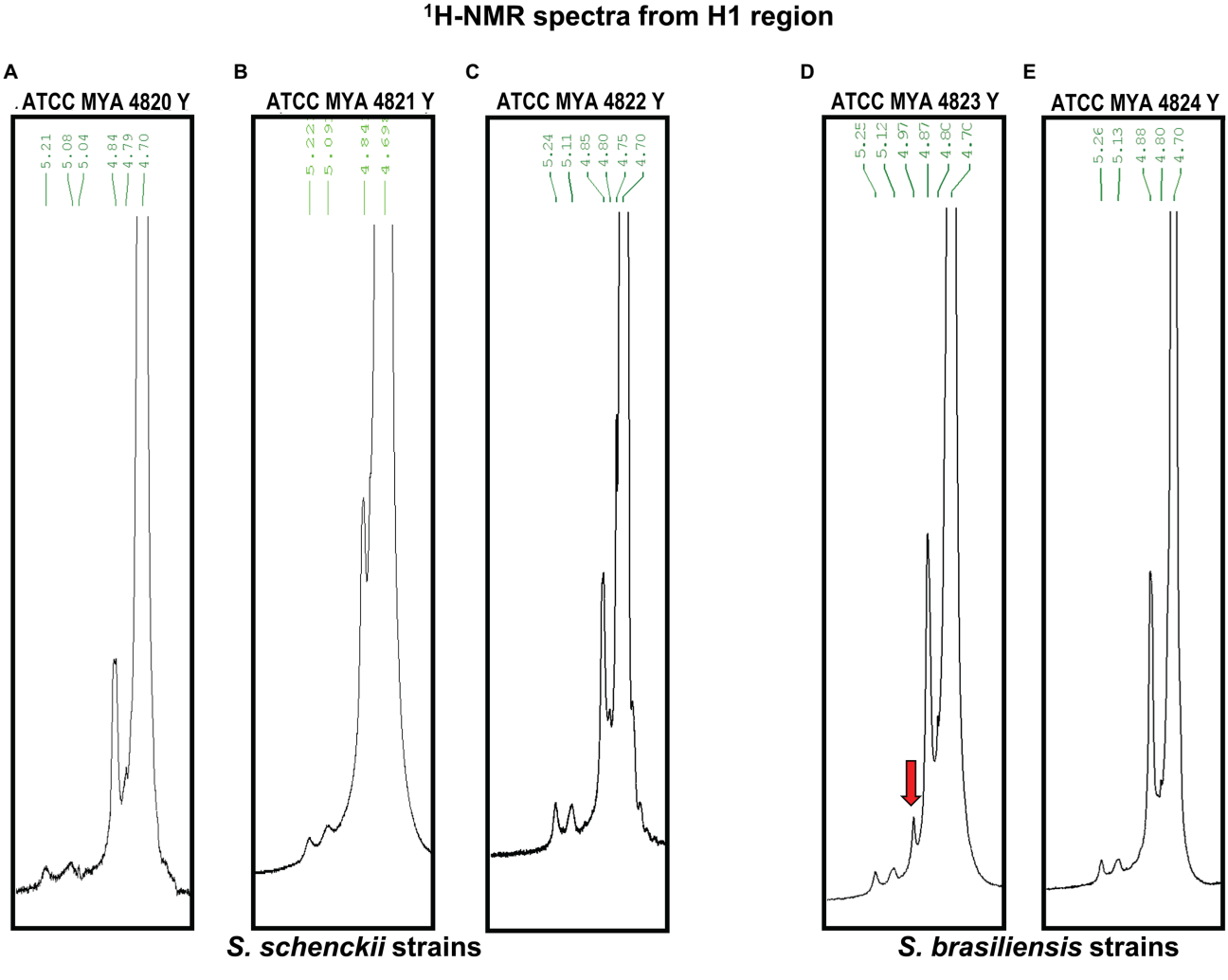

FIGURE 3 | ^{1}H-NMR of the rhamnomannan fraction isolated from *S. schenckii* and *S. brasiliensis* yeast cells. The H1 region of the rhamnomannans of *S. schenckii* **(A–C)** and *S. brasiliensis* **(D,E)** is enlarged. The red arrow shows a unique signal for *S. brasiliensis* strain 4823 as was described recently (Lopes-Bezerra et al., 2018).

TABLE 2 | ^{13}C-NMR signals of *S. schenckii* and *S. brasiliensis* rhamnomannan, yeast phase.

Isolate	Structure	^{13}CNMR – Signal, δ_c (70°C; ppm)						
		C1	C2	C3	C4	C5	C6	CH_3
S. schenckii MYA-4820	α-L-Rhamnopyranose non-reducing end units	96.28	70.37	**N.R.**	71.94	68.74	-------	16.7
	3,6-di-O-substituted α-D-mannopyranose units	99.4	65.88	74.95	64.55	70.79	65.40	-------
S. schenckii MYA-4821	α-L-Rhamnopyranose non-reducing end units	96.28	70.36	**N.R.**	71.93	68.74	-------	16.7
	3,6-di-O-substituted α-D-mannopyranose units	99.44	65.88	74.92	64.55	70.82	65.397	-------
S. schenckii MYA-4822	α-L-Rhamnopyranose non-reducing end units	N.O.	70.13	**N.R.**	71.97	68.72	-------	16.7
	3,6-di-O-substituted α-D-mannopyranose units	99.4	65.91	74.98	64.57	70.72	65.44	-------
S. brasiliensis MYA-4823	α-L-Rhamnopyranose nonreducing end units	96.39	70.17	**N.R.**	72.05	68.8	-------	16.7
	3,6-di-O-substituted α-D-mannopyranose units	99.54	66.04	75.08	64.65	70.92	65.57	-------
S. brasiliensis MYA-4824	α-L-Rhamnopyranose non-reducing end units	96.31	70.11	**N.R.**	71.96	68.7	-------	16.7
	3,6-di-O-substituted α-D-mannopyranose units	99.43	65.9	74.94	64.58	70.8	65.48	-------
Gorin et al., 1977	α-L-Rhamnopyranose non-reducing end units	**98.3**	**72–71.9**	**N.R.**	**73.6**	**70.8**	-------	**18.4**
	3,6-di-O-substituted α-D-mannopyranose units	**101.1**	**67.6**	**76.6**	**66.3**	**72.4**	**67.3**	-------

N.O., not observed; N.R., no registered. Bold values correspond to values previously reported.

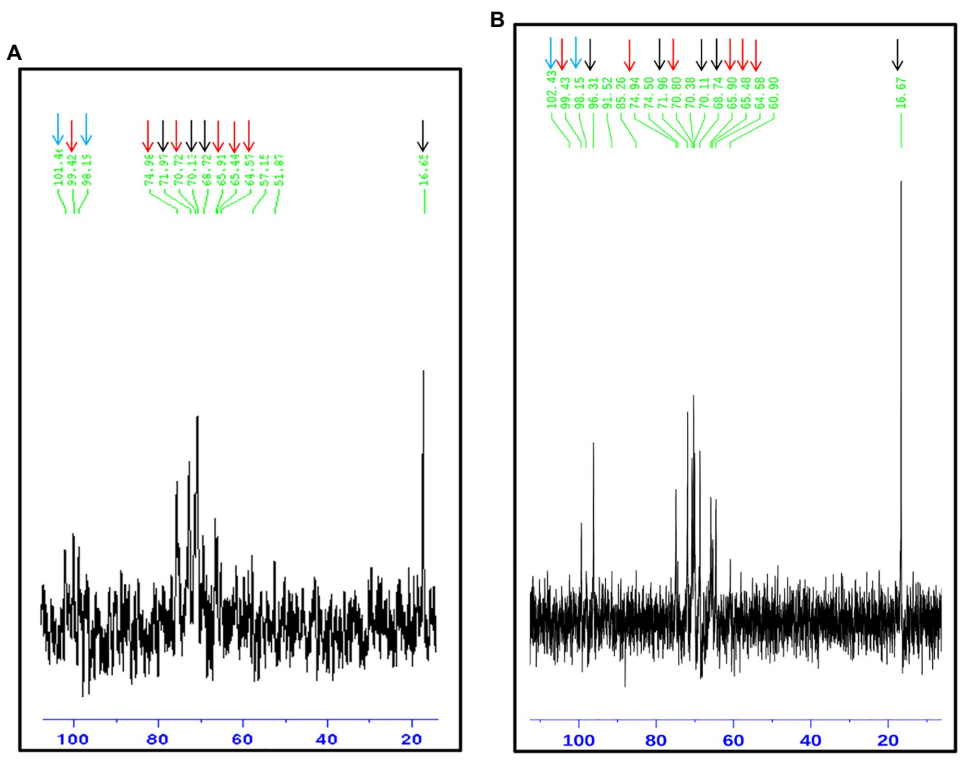

FIGURE 4 | ^{13}C-NMR of the rhamnomannan fraction isolated from the strains presenting less virulence in yeast phase. *Sporothrix schenckii* 4822 **(A)** and *S. brasiliensis* 4824 **(B)** show the signals associated to type I rhamnomannan (red and black arrows), but also a signal corresponding to C-1 of α-L-Rhap nonreducing end unit of α-L-Rhap-(l, 2)-α—Rhap and 2,4-di-0-substituted α-D-mannopyranose units (Cian arrows; Travassos, 1985), which suggest longer side chains in the cell wall for these two strains.

notoriously absent from the rhamnomannan of all the other strains (**Figure 3D**). The pattern of the ^{13}C-NMR spectrum (**Figure 2A**) allowed us to determine how the rhamnose and mannan are linked in the rhamnomannan polymer. The rhamnomannan backbone is composed of mannose linked by α-1,6-glycosidic bonds and single units of rhamnose as side chains, which has been reported as characteristic of rhamnomannans isolated at 37°C from the *S. schenckii* yeast phase, first described as rhamnomannan type I (**Figure 2A**; **Table 2**; Travassos et al., 1973, 1974; Gorin et al., 1977). It is worth mentioning that the ^{13}C-NMR spectra for the cell wall of *S. schenckii*, strain MYA4822, and *S. brasiliensis* MYA4824, showed unique signals at 98.15, 101.4, and 102.4 ppm, associated with the C-1 of α-L-Rhap nonreducing end unit of α-L-Rhap-(l,2)-α-Rhap and 2,4-di-0-substituted α-D-mannopyranose units, which suggest longer side chains in the cell wall rhamnomannan for these two strains when compared to the other strains under study (**Figure 4**).

Polysaccharide Quantification in the Cell Wall Fractions

For polysaccharide quantification, the fractions obtained by alkali and acid fractionation were further analyzed by colorimetric techniques as described in the methods section. **Table 3** shows the relative cell wall polysaccharides content for *S. schenckii* and *S. brasiliensis* strains. The polysaccharide analysis for the cell walls of all strains in the yeast phase, showed a higher chitin content (around 27%) for the two *S. brasiliensis* strains,

TABLE 3 | Cell wall polysaccharide content comparison of the *Y* phase of the *S. schenckii* and *S. brasiliensis* strains under study.

Strain	*S. schenckii* MYA 4820	*S. schenckii* MYA 4821	*S. schenckii* MYA 4822	*S. brasiliensis* MYA 4823	*S. brasiliensis* MYA 4824
Beta glucan	16.7 ± 1.7	20.2 ± 1.4	27.8 ± 1.0	19.9 ± 1.6	28.5 ± 1.9
Rhamnomannan	9.6 ± 0.3	7.3 ± 0.7	6.0 ± 0.8	15.4 ± 0.6	13.1 ± 0.3
Rhamnose	6.5 ± 0.6	5.4 ± 0.1	3.7 ± 0.1	10.8 ± 0.1	10.8 ± 0.2
Chitin	7.6 ± 0.1	7.8 ± 0.2	7.8 ± 0.2	10.7 ± 0.4	10.3 ± 0.1

Tukey Honestly Significant Difference (HSD) post hoc test was used for intra and inter species comparative analyses. Value of $p < 0.05$. Quantification of cell wall components were made by triplicate. SEM is shown.

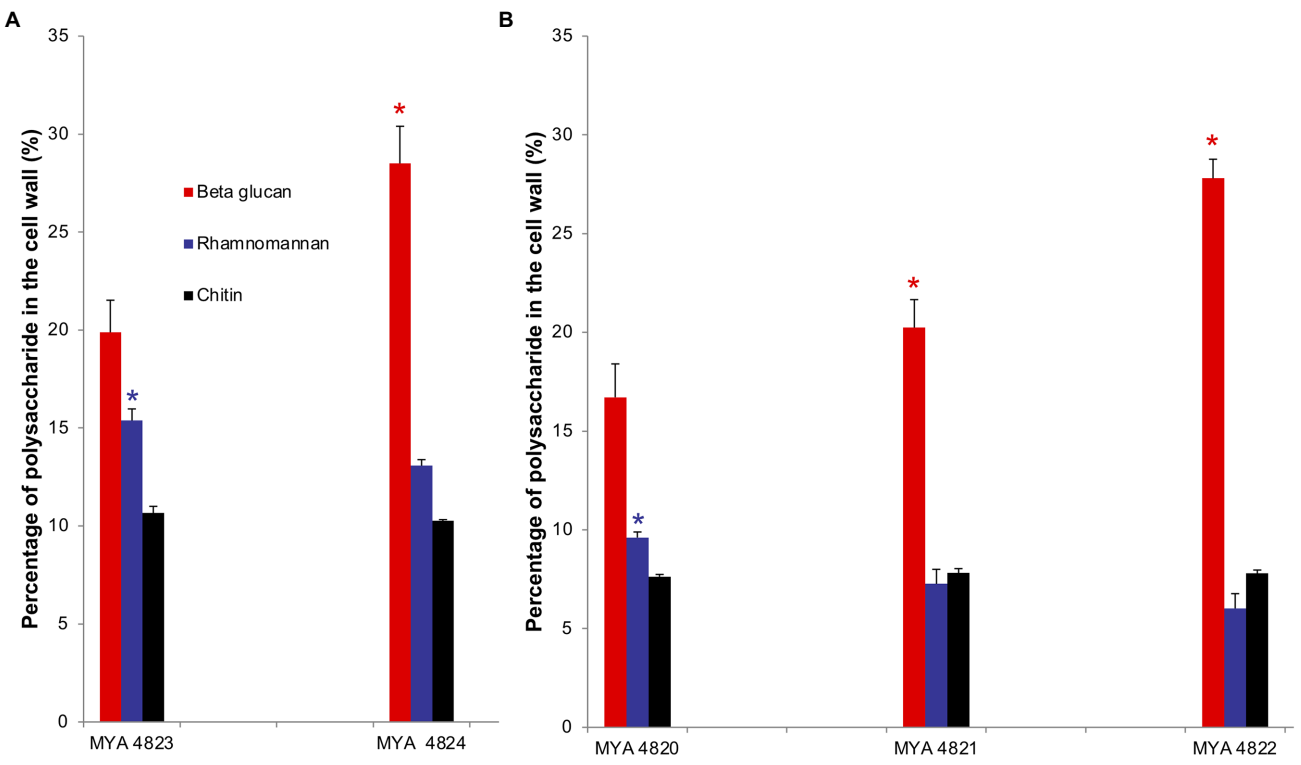

FIGURE 5 | Comparison of polysaccharides represented as percentage in the cell wall of *S. brasiliensis* **(A)** and *S. schenckii* **(B)** strains, yeast phase. Percentage of polysaccharides are represented in colored bars: β glucan (red), rhamnomannan (blue) and chitin (black). *Tukey Honestly Significant Difference (HSD) *post hoc* test was used for intra and inter species comparative analyses. Value of $p < 0.05$. Quantification of cell wall components was made by triplicate.

when compared to the *S. schenckii* strains (**Table 3**; **Figure 5**), as previously reported (Lopes-Bezerra et al., 2018). A difference was evident for the cell wall β-glucan relative content (around 28% more β-glucan) of the lower virulent *S. schenckii* MYA 4822 and *S. brasiliensis* MYA 4824 strains when compared to the higher virulent strains (**Table 3**; **Figure 5**). Rhamnomannan relative contents were higher for both *S. brasiliensis* strains analyzed, when compared to the *S. schenckii* strains (up to 38% more rhamnomannan). Also, a higher rhamnomannan relative content could be observed in the more virulent *S. schenckii* MYA 4820 strain, when compared with the non-virulent *S. schenckii* MYA 4822 strain (over 30% higher; **Table 3**; **Figure 5**). The relationship between the level of virulence reported and the β-glucan/rhamnomannan cell wall ratio can be represented mathematically by an ascendant curve, with an $R^2 = 1$ for the polynomial function $y = 0.0388x^4 - 0.3608x^3 + 1.1913x^2 - 1.1792x + 1.6$ (**Figure 6**), which shows an inverse relationship between the reported virulence and a higher ratio of cell wall β-glucans/rhamnomannan content.

Rhamnose residues from PRM are known to be the main antigenic epitopes found on the *S. schenckii* cell surface (Fernandes et al., 1999). Here, the rhamnose content in *S. brasiliensis* strains was 40% higher compared to *S. schenckii* strains (**Table 3**). When comparing only the *S. schenckii* strains, the cell wall rhamnose content shows differences from high-to-low virulence for strains MYA 4820, MYA 4821, and MYA 4822 (**Table 3**; **Figure 5**). This observation fits the exponential curve: $y = 14.722e^{-0.049x}$, with an $R^2 = 1$, that can be mathematically expressed as the linear equation: $\rho = -0.049\ (\beta) + 2.7$, where β represents the cell wall β-glucan content expressed as percentage and ρ represent the $Ln_{(Rha)}$, where Rha is the rhamnose cell wall content represented as a percentage (**Figure 7**). No significant differences were observed for the cell wall β-glucans among strains, except for *S. schenckii* MYA 4821, which had 20% more β-glucans than the rest of the analyzed strains.

Chitin Exposure on the Yeast Cell Wall

Chitin exposure on the cell wall for the five strains under study was determined in BHI-grown yeast cells. The highest chitin exposure on the cell wall was found for *S. schenckii* strain MYA 4822 (**Figure 8**), followed by *S. schenckii* strain MYA 4820. The lowest cell wall chitin exposure was observed for *S. schenckii* MYA 4821, and the two *S. brasiliensis* strains

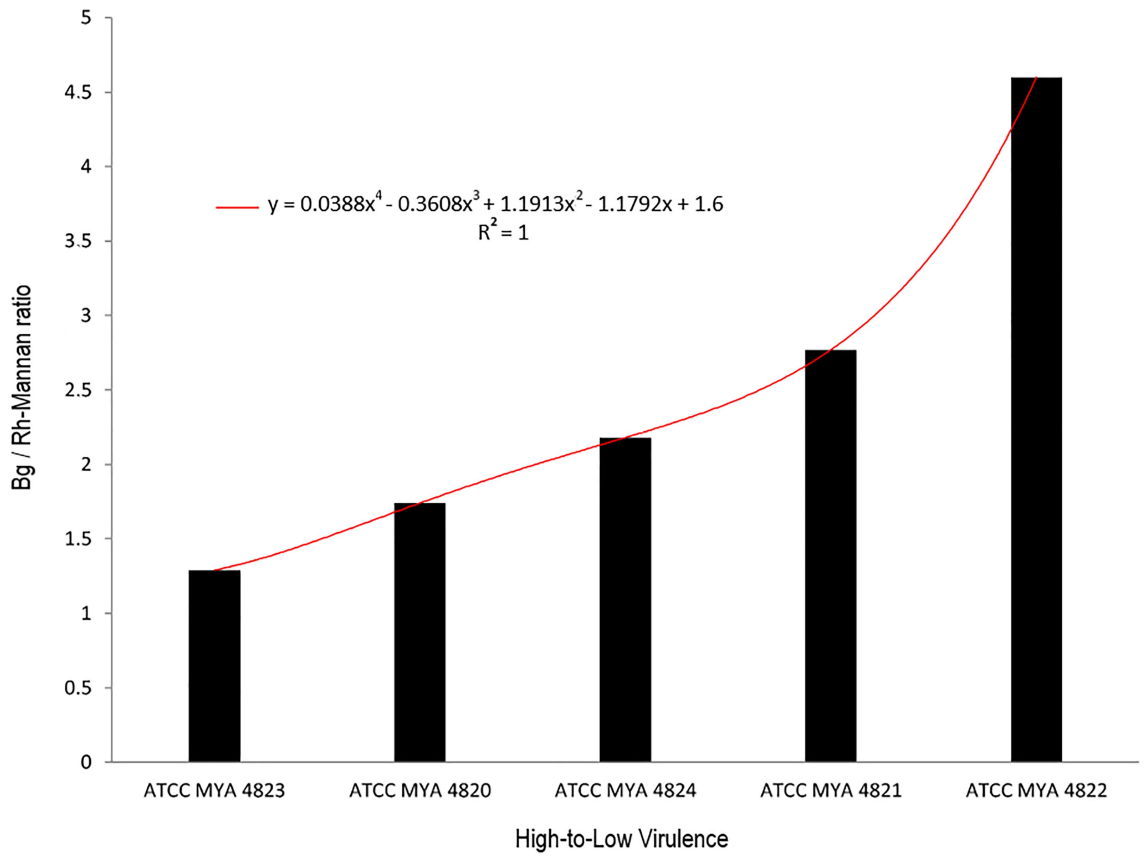

FIGURE 6 | Relation between β glucan vs. rhamnomannan ratio with strain virulence. Black columns represent the ratio of β glucan to rhamnomannan present in the cell wall. Strains are arranged from higher to the lower virulence reported. The red curve represents the polynomial curve of relationship, mathematically represented by an ascendant curve with an $R^2 = 1$ with the polynomial function $y = 0.0388x^4 - 0.3608x^3 + 1.1913x^2 - 1.1792x + 1.6$. Bg, β-glucan; Rh-Mannan, rhamnomannan.

MYA 4823 and MYA 4824, all of them reported as presenting higher virulence patterns (Nascimento et al., 2008; Castro et al., 2013).

DISCUSSION

The cell wall is the first point of contact with the host upon infection and colonization; understanding its composition allow unveiling specific mechanisms triggered by PAMPs and their corresponding PRRs (Gow et al., 2017). Recently, it was reported that carbon or nitrogen limitation during growth of yeast cells of *S. brasiliensis* and *S. schenckii* resulted in a reduced virulence, and the mechanism is related to affect the cell wall composition, where an increase in cell wall β-glucan, and a reduction of rhamnose and mannose was observed (Lozoya-Pérez et al., 2020). Also, the virulence-reduced strains showed a higher exposure of β-glucan, leading to an increase in the uptake of the fungus by hemocytes of *Galleria mellonella* (Lozoya-Pérez et al., 2020).

In the present work, we compared the cell relative composition of the polysaccharides of the pathogenic yeast morphotype of five *Sporothrix* strains, of which three were *S. schenckii* and two *S. brasiliensis* strains, with differences in virulence levels reported in a murine model (**Table 1**; Nascimento et al., 2008; Castro et al., 2013). To normalize the comparison, all the strains were grown under identical conditions in BHI broth, a widely used culture medium for *Sporothrix* spp. (Kong et al., 2006; Brito et al., 2007; Teixeira et al., 2009; Della Terra et al., 2017; De Almeida et al., 2018).

As previously reported, the main polysaccharides present in the cell wall of both *S. schenckii* and *S. brasiliensis* strains were: β-glucan, as major cell wall polysaccharide, followed by rhamnomannan and chitin (**Table 3**; **Figure 5**; Lopes-Bezerra et al., 2018; Lozoya-Pérez et al., 2020). A higher cell wall chitin content was observed in the cell wall of *S. brasiliensis* strains compared to *S. schenckii* strains, which also have been previously reported (Lopes-Bezerra et al., 2018). However, when comparing the cell wall polysaccharide composition of the five *Sporothrix* spp. strains, a pattern appeared to emerge, with higher β-glucans and lower rhamnomannan levels in cell wall contents present in the previously reported non-virulent or low virulent strains (*S. schenckii* MYA 4822 and MYA 4821 and *S. brasiliensis* MYA 4824). In contrast, lower β-glucan and higher rhamnomannan levels in cell wall content were shown in those strains for which higher virulence have been reported, regardless of the species (*S. brasiliensis* MYA 4823 and *S. schenckii* MYA 4820; **Table 3**; **Figure 5**). Therefore, the β-glucan/rhamnomannan cell wall ratio can be mathematically represented by a polynomial function showing an inverse relationship to the virulence increase (**Figure 6**). Then, we focused on *S. schenckii*, for which we had strains with three different levels of virulence

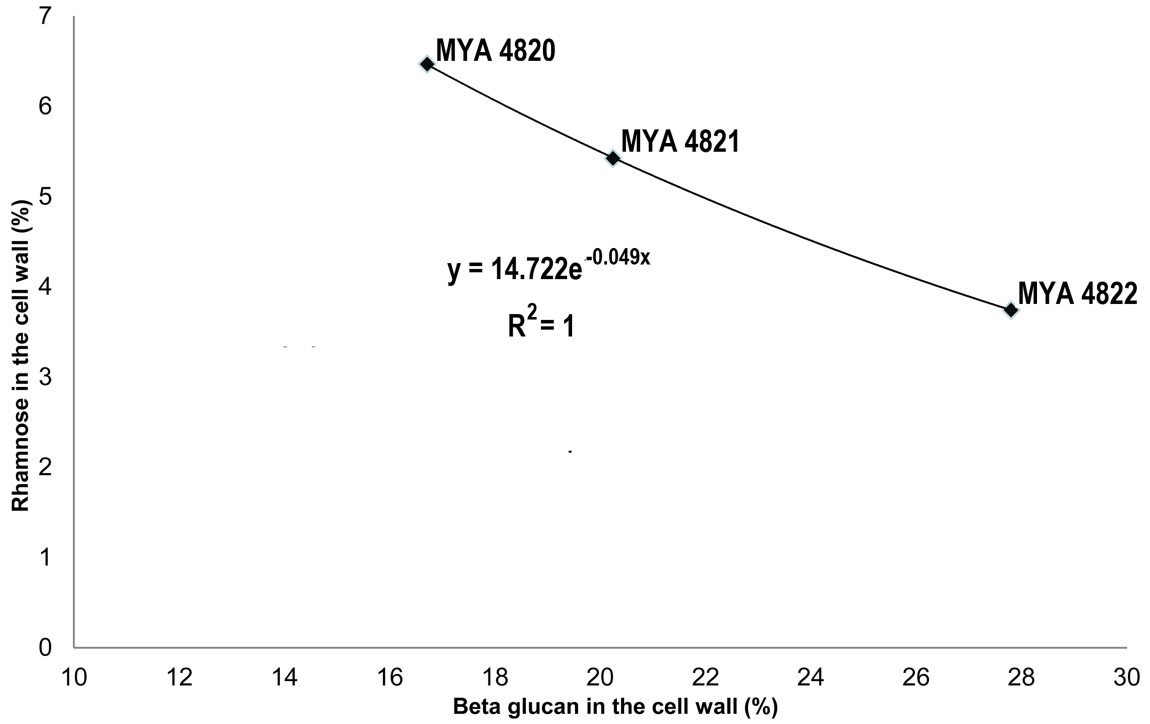

FIGURE 7 | A mathematical model for the Rhamnose/β-glucan composition as expression of virulence. With an increase in reported virulence, the rhamnose proportion rise and β-glucan decreases. This observation fit to an exponential curve with an $R^2 = 1$, that could be expressed as a linear equation: $\rho = -0.049(\beta) + 2.7$, where β represents the β-glucan composition and $\rho = \text{Ln(Rha)}$, where Rha is the rhamnose cell wall percentage. This model might be useful to predict the virulence level employing the β-glucan and rhamnose percentage ratio. This mathematical expression infers the highest rhamnose percentage to 15% ($\beta = 0$) and for the lowest rhamnose percentage (1%) $\beta = 55.1\%$.

reported (**Table 1**) and noticed that cell wall rhamnose content increased, while the cell wall β-glucan content decreased when compared from the less to the highest reported virulence phenotype (**Table 3**; **Figure 5**). This observation can be mathematically expressed as a linear equation (**Figure 7**), which extrapolates the highest virulence for *S. schenckii* strains when the rhamnose percentage in the cell wall reaches 15% and the β-glucans cell wall content is 0%, and the lowest virulence when the rhamnose percentage is 1% and the β-glucan content is 55.1% (intersection points on the *y* and *x* axis of the linear curve, respectively, **Figure 7**).

Recently, a bilayered cell wall model based on experimental data was proposed for *S. schenckii* and *S. brasiliensis* yeast cells (Lopes-Bezerra et al., 2018), which positioned the structural and more immunogenic chitin and β-glucans at the inner-most layer, and the PRM as an outermost layer covering the former.

The structural cell wall glycoconjugates, β-1-3 and β-1-6-glucans, as well as chitin, are found in pathogenic fungal species as involved in the innate immune response as PAMPs, so the exposure of β-glucans and chitin on the fungal surface favors their binding to their corresponding PRRs presented on the host cells surface, allowing the uptake of the microorganism and/or triggering the secretion of specific cytokines (Hernández-Chávez et al., 2017). A *Sporothrix* spp. strain with a higher β-glucans/rhamnomannan ratio might favor the exposition of the immunogenic β-glucans to the host immune system, triggering its response before the infection can be established, therefore presenting a lower level of virulence. Indeed, Lozoya-Pérez et al. (2020) recently reported that a higher β-glucan exposure is in close relation with a lower virulence phenotype in *Sporothrix* spp. To determine whether chitin also might be playing a role in the differences in virulence levels, chitin exposition was measured in the Y pathogenic phase for the five *Sporothrix* strains. Only the non-virulent *S. schenckii* MYA 4822 presented a high chitin exposition on its cell surface under the growth conditions used in the present study (**Figure 8**), which together with the high β-glucans/rhamnomannan ratio, builds up evidence for the involvement in the non-virulence phenotype reported, and by triggering the host immune system more efficiently.

A conserved general structure of the cell wall polysaccharides for all *Sporothrix* strains in their yeast phase was evidenced by the IR spectra analyzed. However, some differences were observed when the rhamnomannans from the cell walls of the five *Sporothrix* strains were characterized by ^{1}H-NMR and ^{13}C-NMR. Although a general pattern for both spectra was apparent for all the five strains studied (**Figure 2**), a closer inspection of the ^{13}C-NMR spectra allowed us to identify unique signals for the cell wall rhamnomannan of the non-virulent and low virulent *S. schenckii* MYA 4822 and *S. brasiliensis* MYA 4824, respectively at 98.15, 101.4, and 102.4, associated

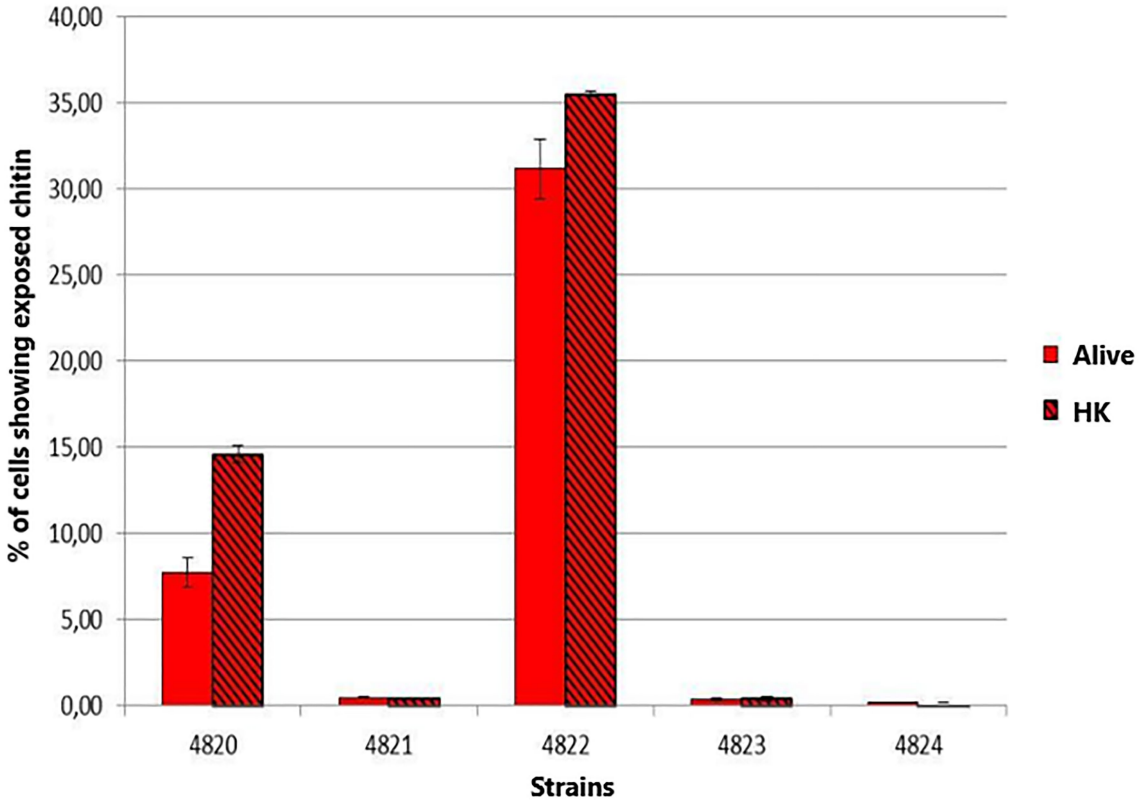

FIGURE 8 | Comparison of the chitin exposure on the yeast cells of *S. schenckii* and *S. brasiliensis* grown in Brain Heart Infusion (BHI) broth. The smooth bars represent the exposure of chitin under normal and live cell (Alive). The bars with frames represent the percentage of exposed chitin after the cells were heat inactivated (HK).

with the C-1 of α-L-Rhap non-reducing end unit of α-L-Rhap-(l,2)-α-Rhap and 2,4-di-0-substituted α-D-mannopyranose units, suggesting longer side chains in the cell wall rhamnomannan for these two strains. Methylation analyses of the rhamnomannan present in the reportedly least virulent strains and comparison with the higher virulent strains would provide further insight into such differences. Also, the comparison of the ^{1}H-NMR spectra for the rhamnomannan of all the strains studied, confirmed a previous report, showing the presence of a 4.97 ppm signal only for the *S. brasiliensis* MYA 4823, which has been reported as a high virulent strain (Castro et al., 2013). The analysis of virulent and non-virulent strains of the *Sporothrix* genus, suggests that the rhamnomannans of the cell wall determines the exposure of chitin and β-glucans, which ultimately triggers a strong immune response that explains the resulting virulence phenotype. To overcome the limitations of the present work and to either strengthen or discard the mathematical model of virulence here proposed, a broader study including more strains, testing their virulence in a single mathematical model of virulence for sporotrichosis, and exploring the alterations in cell wall composition from strains cultured in different media and their possible impacts on virulence would be necessary, and will definitely either reinforce or discard this model to assess virulence, specifically for the *Sporthrix* genus.

DATA AVAILABILITY STATEMENT

The original contributions presented in the study are included in the article/supplementary material, further inquiries can be directed to the corresponding author.

AUTHOR CONTRIBUTIONS

HV-D, LL-B, and GN-V conceived and designed the experiments. HV-D, LB, ÁA-A, BF, and NL-P performed the experiments. HV-D, GN-V, LL-B, and HM-M analyzed the data. HV-D and GN-V wrote the paper. All authors contributed to the article and approved the submitted version.

FUNDING

HV-D was supported by Instituto Venezolano de Investigaciones Cientificas, Venezuela (Project 112). GN-V was supported by CONACYT-Mexico (Ref. CF-2019-170701). HM-M was supported by CONACYT-Mexico (Ref. FC 2015-02-834). Flow cytometry analysis was supported by CONACYT (grants 3013–205744 and 2019–300286).

REFERENCES

Almeida-Paes, R., De Oliveira, L. C., Oliveira, M. M. E., Gutierrez-Galhardo, M. C., Nosanchuk, J. D., and Zancopé-Oliveira, R. M. (2015). Phenotypic characteristics associated with virulence of clinical isolates from the sporothrix complex. *Biomed. Res. Int.* 2015:212308. doi: 10.1155/2015/212308

Arrillaga-Moncrieff, I., Capilla, J., Mayayo, E., Marimon, R., Mariné, M., Gené, J., et al. (2009). Different virulence levels of the species of Sporothrix in a murine model. *Clin. Microbiol. Infect.* 15, 651–655. doi: 10.1111/j.1469-0691.2009.02824.x

Barros, M. B., de Almeida Paes, R., and Oliveira Schubach, A. (2011). *Sporothrix schenckii* and Sporotrichosis. *Clin. Microbiol. Rev.* 24, 633–654. doi: 10.1128/CMR.00007-11

Brito, M. M. S., Conceição-Silva, F., Morgado, F. N., Raibolt, P. S., Schubach, A., Schubach, T. P., et al. (2007). Comparison of virulence of different *Sporothrix schenckii* clinical isolates using experimental murine model. *Med. Mycol.* 45, 721–729. doi: 10.1080/13693780701625131

Callens, S. F. J., Kitetele, F., Lukun, P., Lelo, P., Van Rie, A., Behets, F., et al. (2006). Pulmonary *Sporothrix schenckii* infection in a HIV positive child. *J. Trop. Pediatr.* 52, 144–146. doi: 10.1093/tropej/fmi101

Castro, R. A., Kubitschek-Barreira, P. H., Teixeira, P. A. C., Sanches, G. F., Teixeira, M. M., Quintella, L. P., et al. (2013). Differences in cell morphometry, cell wall topography and Gp70 expression correlate with the virulence of *Sporothrix brasiliensis* clinical isolates. *PLoS One* 8:e75656. doi: 10.1371/journal.pone.0075656

Chakrabarti, A., Bonifaz, A., Gutierrez-Galhardo, M. C., Mochizuki, T., and Li, S. (2014). Global epidemiology of sporotrichosis. *Med. Mycol.* 53, 3–14. doi: 10.1093/mmy/myu062

Clavijo-Giraldo, D. M., Matínez-Alvarez, J. A., Lopes-Bezerra, L. M., Ponce-Noyola, P., Franco, B., Almeida, R. S., et al. (2016). Analysis of *Sporothrix schenckii* sensu stricto and *Sporothrix brasiliensis* virulence in *Galleria mellonella*. *J. Microbiol. Methods* 122, 73–77. doi: 10.1016/j.mimet.2016.01.014

De Almeida, J. R. F., Jannuzzi, G. P., Kaihami, G. H., Breda, L. C. D., Ferreira, K. S., and De Almeida, S. R. (2018). An immunoproteomic approach revealing peptides from *Sporothrix brasiliensis* that induce a cellular immune response in subcutaneous sporotrichosis. *Sci. Rep.* 8:4192. doi: 10.1038/s41598-018-22709-8

de Beer, Z. W., Duong, T. A., and Wingfield, M. J. (2016). The divorce of Sporothrix and Ophiostoma: solution to a problematic relationship. *Stud. Mycol.* 83, 165–191. doi: 10.1016/j.simyco.2016.07.001

Della Terra, P. P., Rodrigues, A. M., Fernandes, G. F., Nishikaku, A. S., Burger, E., and de Camargo, Z. P. (2017). Exploring virulence and immunogenicity in the emerging pathogen *Sporothrix brasiliensis*. *PLoS Negl. Trop. Dis.* 11:e0005903. doi: 10.1371/journal.pntd.0005903

Dische, Z., and Shettles, L. B. (1948). A specific color reaction of methylpentoses and a spectrophotometric micromethod for their determination. *J. Biol. Chem.* 175, 595–603. doi: 10.1016/S0021-9258(18)57178-7

Erwig, L. P., and Gow, N. A. R. (2016). Interactions of fungal pathogens with phagocytes. *Nat. Rev. Microbiol.* 14, 163–176. doi: 10.1038/nrmicro.2015.21

Etchecopaz, A. N., Lanza, N., Toscanini, M. A., Devoto, T. B., Pola, S. J., Daneri, G. L., et al. (2020). Sporotrichosis caused by *Sporothrix brasiliensis* in Argentina: case report, molecular identification and in vitro susceptibility pattern to antifungal drugs. *J. Mycol. Med.* 30:100908. doi: 10.1016/j.mycmed.2019.100908

Fernandes, G. F., dos Santos, P. O., Rodrigues, A. M., Sasaki, A. A., Burger, E., and de Camargo, Z. P. (2013). Characterization of virulence profile, protein secretion and immunogenicity of different *Sporothrix schenckii* sensu stricto isolates compared with *S. globosa* and *S. brasiliensis* species. *Virulence* 4, 241–249. doi: 10.4161/viru.23112

Fernandes, K. S. S., Mathews, H. L., and Bezerra, L. M. L. (1999). Differences in virulence of *Sporothrix schenckii* conidia related to culture conditions and cell-wall components. *J. Med. Microbiol.* 48, 195–203. doi: 10.1099/00222615-48-2-195

Gorin, P. A. J., Haskins, R. H., Travassos, L. R., and Mendonca-Previato, L. (1977). Further studies on the rhamnomannans and acidic rhamnomannans of *Sporothrix schenckii* and *Ceratocystis stenoceras*. *Carbohydr. Res.* 55, 21–33. doi: 10.1016/S0008-6215(00)84440-7

Gow, N. A. R., Gooday, G. W., Russell, J. D., and Wilson, M. J. (1987). Infrared and X-ray diffraction data on chitins of variable structure. *Carbohydr. Res.* 165, 1–160.

Gow, N. A. R., Latge, J., and Munro, C. A. (2017). The fungal cell wall: structure, biosynthesis, and function. *Microbiol. Spectr.* 5, 1–25. doi: 10.1128/microbiolspec.FUNK-0035-2016

Hernández-Chávez, M. J., Pérez-García, L. A., Niño-Vega, G. A., and Mora-Montes, H. M. (2017). Fungal strategies to evade the host immune recognition. *J. Fungi* 3, 1–28. doi: 10.3390/jof3040051

Klis, F. M., Boorsma, A., and De Groot, P. W. J. (2006). Cell wall construction in *Saccharomyces cerevisiae*. *Yeast* 23, 185–202. doi: 10.1002/yea.1349

Kong, X., Xiao, T., Lin, J., Wang, Y., and Chen, H. D. (2006). Relationships among genotypes, virulence and clinical forms of *Sporothrix schenckii* infection. *Clin. Microbiol. Infect.* 12, 1077–1081. doi: 10.1111/j.1469-0691.2006.01519.x

Latgé, J. P. (2007). The cell wall: a carbohydrate armour for the fungal cell. *Mol. Microbiol.* 66, 279–290. doi: 10.1111/j.1365-2958.2007.05872.x

Lopes-Alves, L. M., Mendonça-Previato, L., Fournet, B., Degand, P., and Previato, J. O. (1992). O-Glycosidically linked oligosaccharides from peptidorhamnomannans of *Sporothrix schenckii*. *Glycoconj. J.* 9, 75–81. doi: 10.1007/BF00731702

Lopes-Bezerra, L. M., Walker, L. A., Niño-Vega, G., Mora-Montes, H. M., Neves, G. W. P., Villalobos-Duno, H., et al. (2018). Cell walls of the dimorphic fungal pathogens *Sporothrix schenckii* and *Sporothrix brasiliensis* exhibit bilaminate structures and sloughing of extensive and intact layers. *PLoS Negl. Trop. Dis.* 12, 1–25. doi: 10.1371/journal.pntd.0006169

Lozoya-Pérez, N. E., Clavijo-Giraldo, D. M., Martínez-Duncker, I., García-Carnero, L. C., López-Ramírez, L. A., Niño-Vega, G. A., et al. (2020). Influences of the culturing media in the virulence and cell wall of *Sporothrix schenckii*, *Sporothrix brasiliensis*, and *Sporothrix globosa*. *J. Fungi* 6:323. doi: 10.3390/jof6040323

Nascimento, R. C., Espíndola, N. M., Castro, R. A., Teixeira, P. A. C., Penha, C. V. L., Lopes-Bezerra, L. M., et al. (2008). Passive immunization with monoclonal antibody against a 70-kDa putative adhesin of *Sporothrix schenckii* induces protection in murine sporotrichosis. *Eur. J. Immunol.* 38, 3080–3089. doi: 10.1002/eji.200838513

Previato, J., Gorin, P., Haskins, R., and Travassos, L. (1979). Soluble and insoluble glucans from different cell types of the human pathogen *Sporothrix schenckii*. *Exp. Mycol.* 3, 92–105. doi: 10.1016/S0147-5975(79)80021-3

Rodríguez-Brito, S., Niño-Vega, G., and San-Blas, G. (2010). Caspofungin affects growth of *Paracoccidioides brasiliensis* in both morphological phases. *Antimicrob. Agents Chemother.* 54, 5391–5394. doi: 10.1128/AAC.00617-10

Rondle, C. J. M., and Morgan, W. T. J. (1955). The determination of glucosamine and galactosamine. *Biochem. J.* 61, 586–589. doi: 10.1042/bj0610586

Rossow, J. A., Queiroz-Telles, F., Caceres, D. H., Beer, K. D., Jackson, B. R., Pereira, J. G., et al. (2020). A one health approach to combatting *Sporothrix brasiliensis*: narrative review of an emerging zoonotic fungal pathogen in South America. *J. Fungi* 6, 1–27. doi: 10.3390/jof6040247

Ruiz-Herrera, J., Victoria Elorza, M., Valentín, E., and Sentandreu, R. (2006). Molecular organization of the cell wall of Candida albicans and its relation to pathogenicity. *FEMS Yeast Res.* 6, 14–29. doi: 10.1111/j.1567-1364.2005.00017.x

San-Blas, G., and San-Blas, F. (1994). "Preparation and analysis of purified cell walls of the mycelial and yeast phase of *Paracoccidioides brasiliensis,*" in *Molecular Biology of Pathogenic Fungi: A Laboratory Manual*. eds. B. Maresca and G. Kobayashi (New York: Telos Press), 489–498.

Synytsya, A., and Novak, M. (2014). Structural analysis of glucans. *Ann. Transl. Med.* 2, 1–14. doi: 10.3978/j.issn.2305-5839.2014.02.07

Teixeira, P. A. C., de Castro, R. A., Nascimento, R. C., Tronchin, G., Torres, A. P., Lazéra, M., et al. (2009). Cell surface expression of adhesins for fibronectin correlates with virulence in *Sporothrix schenckii*. *Microbiology* 155, 3730–3738. doi: 10.1099/mic.0.029439-0

Travassos, L. R. (1985). "Sporothrix schenckii," in *Fungal Dimorphism*. eds. P. J. Szaniszlo and J. L. Harris (New York, London: Plenum Press), 121–163.

Travassos, L. R., Gorin, P. A. J., and Lloyd, K. O. (1973). Comparison of the rhamnomannans from the human pathogen *Sporothrix schenckii* with those from the *Ceratocystis* species. *Infect. Immun.* 8, 685–693. doi: 10.1128/iai.8.5.685-693.1973

Travassos, L. R., Gorin, P. A. J., and Lloyd, K. O. (1974). Discrimination between *Sporothrix schenckii* and *Ceratocystis stenoceras* rhamnomannans by proton and carbon-13 magnetic resonance spectroscopy. *Infect. Immun.* 9, 674–680. doi: 10.1128/iai.9.4.674-680.1974

Yemm, E. W., Cocking, E. C., and Ricketts, R. E. (1955). The determination of amino-acids with ninhydrin. *Analyst* 80, 209–214. doi: 10.1039/an9558000209

Zhang, Y., Hagen, F., Stielow, B., Rodrigues, A. M., Samerpitak, K., Zhou, X., et al. (2015). Phylogeography and evolutionary patterns in Sporothrix spanning more than 14 000 human and animal case reports. *Pers. Mol. Phylogeny Evol. Fungi* 35, 1–20. doi: 10.3767/003158515X687416

Conflict of Interest: The authors declare that the research was conducted in the absence of any commercial or financial relationships that could be construed as a potential conflict of interest.

Publisher's Note: All claims expressed in this article are solely those of the authors and do not necessarily represent those of their affiliated organizations, or those of the publisher, the editors and the reviewers. Any product that may be evaluated in this article, or claim that may be made by its manufacturer, is not guaranteed or endorsed by the publisher.

frontiers in Microbiology

REVIEW
published: 24 September 2021
doi: 10.3389/fmicb.2021.745702

Opportunities and Challenges of Bacterial Glycosylation for the Development of Novel Antibacterial Strategies

*Liubov Yakovlieva, Julius A. Fülleborn and Marthe T. C. Walvoort**

Faculty of Science and Engineering, Stratingh Institute for Chemistry, University of Groningen, Groningen, Netherlands

Glycosylation is a ubiquitous process that is universally conserved in nature. The various products of glycosylation, such as polysaccharides, glycoproteins, and glycolipids, perform a myriad of intra- and extracellular functions. The multitude of roles performed by these molecules is reflected in the significant diversity of glycan structures and linkages found in eukaryotes and prokaryotes. Importantly, glycosylation is highly relevant for the virulence of many bacterial pathogens. Various surface-associated glycoconjugates have been identified in bacteria that promote infectious behavior and survival in the host through motility, adhesion, molecular mimicry, and immune system manipulation. Interestingly, bacterial glycosylation systems that produce these virulence factors frequently feature rare monosaccharides and unusual glycosylation mechanisms. Owing to their marked difference from human glycosylation, bacterial glycosylation systems constitute promising antibacterial targets. With the rise of antibiotic resistance and depletion of the antibiotic pipeline, novel drug targets are urgently needed. Bacteria-specific glycosylation systems are especially promising for antivirulence therapies that do not eliminate a bacterial population, but rather alleviate its pathogenesis. In this review, we describe a selection of unique glycosylation systems in bacterial pathogens and their role in bacterial homeostasis and infection, with a focus on virulence factors. In addition, recent advances to inhibit the enzymes involved in these glycosylation systems and target the bacterial glycan structures directly will be highlighted. Together, this review provides an overview of the current status and promise for the future of using bacterial glycosylation to develop novel antibacterial strategies.

Keywords: pathogenic bacteria, glycosylation, antivirulence, antibacterial strategies, metabolic oligosaccharide engineering

OPEN ACCESS

Edited by:
Hector Mora Montes, University of Guanajuato, Mexico

Reviewed by:
Roberto Adamo, GlaxoSmithKline, Italy
Francesco Berti, GlaxoSmithKline, Italy

***Correspondence:**
Marthe T. C. Walvoort
m.t.c.walvoort@rug.nl

Specialty section:
This article was submitted to Infectious Diseases, a section of the journal Frontiers in Microbiology

Received: *22 July 2021*
Accepted: *27 August 2021*
Published: *24 September 2021*

Citation:
Yakovlieva L, Fülleborn JA and Walvoort MTC (2021) Opportunities and Challenges of Bacterial Glycosylation for the Development of Novel Antibacterial Strategies. Front. Microbiol. 12:745702. doi: 10.3389/fmicb.2021.745702

INTRODUCTION

Bacterial pathogens have evolved an extensive arsenal of strategies to persist and thrive in the host. These strategies are referred to as "virulence factors," and in the process of host infection, they directly or indirectly contribute to enhanced survival of the bacterium (Clatworthy et al., 2007). Interestingly, many of the virulence factors are glycosylation products, in the form of

either oligo- and polysaccharides (capsule and LPS) or glycoproteins (pili, flagella, adhesins, autotransporters, and efflux pumps). Additionally, bacterial glycosyltransferases themselves can act as exotoxins, manipulating the host immune response *via* glycosylation of the host proteins.

In bacteria, the synthesis of glycoconjugates takes place in the series of glycosylation reactions, in which carbohydrates are polymerized or attached to the proteins or lipids, by the action of glycosyltransferase enzymes (GTs). Interestingly, bacterial glycans frequently contain unique monosaccharides such as pseudaminic acid (Pse; Schirm et al., 2003), bacillosamine (Bac; Morrison and Imperiali, 2014), 2,4-diacetamido-2,4,6-trideoxygalactose (DATDG; Hartley et al., 2011), *N*-acetylfucosamine (FucNAc; Horzempa et al., 2008), legionaminic acid (Leg; Morrison and Imperiali, 2014), 3-deoxy-D-manno-octulosonic acid (Kdo; Lodowska et al., 2013), rhamnose (Rha; Mistou et al., 2016), and others (Chatterjee and Chaudhuri, 2003; Meeks et al., 2004; Tytgat and Lebeer, 2014; **Figure 1A**). These carbohydrates are presented in the glycan structures of several clinically relevant pathogens (for instance, *Helicobacter pylori, Neisseria meningitidis, Pseudomonas aeruginosa, Campylobacter jejuni, Escherichia coli,* among others) and are often important for their virulence (Schirm et al., 2003; Horzempa et al., 2008; Hartley et al., 2011; Hopf et al., 2011; Clark et al., 2016).

Given the importance of glycans as bacterial virulence factors, the biosynthetic machineries that work on these unusual carbohydrates are interesting targets for novel antibacterial therapeutics (Bhat et al., 2019). To date, prominent antibiotics that target bacterial glycans are small-molecule inhibitors of peptidoglycan production (Tra and Dube, 2014). Among those, the best known are broad-spectrum antibiotics such as penicillin (Park and Strominger, 1957) or vancomycin (Perkins, 1969). Although the use of these drugs has met large success in the clinic, significant drawbacks are associated with these therapeutics. Firstly, the misuse of antibiotics has led to a rapid development of multi-resistant bacteria that are now unsusceptible to most antibacterial treatments (World Health Organization, 2014). Secondly, antibiotics do not act strain specifically and thus cause damage to the commensal gut microbiome leading to side effects and further health complications such as infections with opportunistic pathogens like *Clostridium difficile* (Keeney et al., 2014). Therefore, there is a high demand for novel bacteria-specific therapeutics.

Alternative strategies, in which the virulence factors of pathogenic bacteria are therapeutically targeted, have gained more attention over the years (Clatworthy et al., 2007; Dickey et al., 2017). Drugs targeting virulence factors are collectively called antivirulence drugs or pathoblockers (Calvert et al., 2018). Because virulence factors are not essential for the survival of most bacterial pathogens, their inhibition puts little selective pressure on the organisms for the development of resistance (Calvert et al., 2018). Furthermore, many virulence factors are pathogen-specific, and antivirulence drugs hold the promise to act in a strain-specific way and thereby do not exhibit harmful effects of broad-spectrum antibiotics on the gut microbiome (Dickey et al., 2017). Importantly, a multitude of bacterial virulence factors are glycosylation products, including oligo- and polysaccharides, glycoproteins, and glycosyltransferase effector proteins. They feature bacterial species-specific monosaccharides

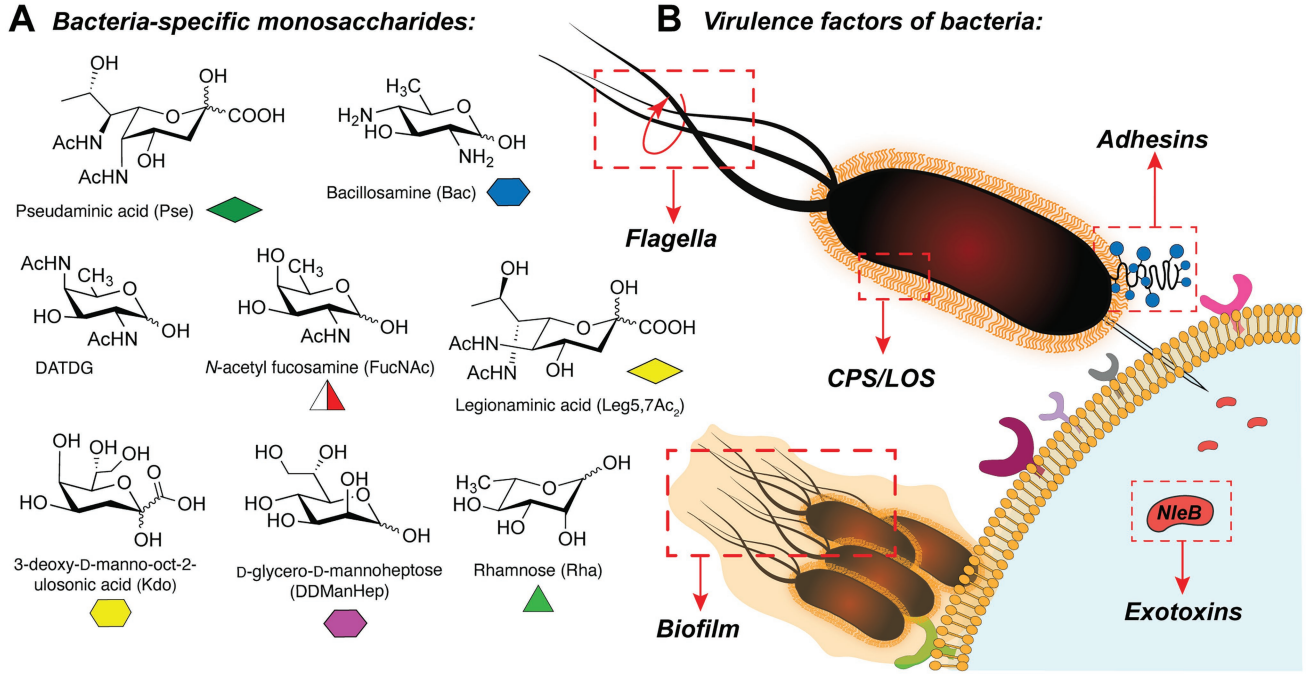

FIGURE 1 | (A) Selection of bacteria-specific monosaccharides featured in infectious glycan structures; **(B)** Schematic overview of the bacterial glyco-virulence factors discussed in this review.

and have unique structures which make them promising candidates for the antivirulence therapies. Although to date no antivirulence drugs are widely used in the clinic, there are already Food and Drug Administration (FDA)-approved antivirulence therapeutics available and many more in the stage of clinical or preclinical development (Dickey et al., 2017). Several experimental approaches have been developed that target bacterial GTs, biosynthetic enzymes of rare bacterial carbohydrates, and metabolic inhibitors of glycosylation (Ménard et al., 2014; El Qaidi et al., 2018; Williams et al., 2020). Together, these methods may provide future directions for the treatment of bacterial infections by targeting the bacterial glycosylation machinery.

In this review, the idea of targeting bacterial glycosylation systems for the development of novel antibacterial therapeutics is explored. Several important classes of bacterial virulence factors are discussed, alongside the strategies developed for their inhibition. Finally, we discuss the potential new glycosylation targets for inhibitors and provide the outlook and future perspectives.

PART 1: GLYCOSYLATION OF BACTERIAL VIRULENCE FACTORS AND INHIBITION STRATEGIES

Motility

Flagellar Glycosylation of *C. jejuni* and *H. pylori*

Many pathogenic bacteria rely on motility during different stages of their infection process (**Figure 1B**). Especially, flagellar motility has been shown to play a critical role in successful infection in many organisms, as it contributes to bacterial movement, adhesion, and biofilm formation. In addition, the glycosylation of flagella is crucial for the proper assembly of flagellar structures and their motility function (Logan, 2006; Merino and Tomás, 2014).

Flagellar glycans feature diverse structures and often incorporate bacteria-specific monosaccharides. For instance, in the gastric pathogens *H. pylori* and *C. jejuni* the unique bacterial carbohydrates pseudaminic acid (Pse), legionaminic acid (Leg), and derivatives containing acetamidino and methylglycerol moieties are required for the proper assembly of flagella (Ud-Din and Roujeinikova, 2018). Biosynthesis of Pse is a multi-step process that relies on several enzymes (PseB-PseI), as shown in **Figure 2A** (Ud-Din and Roujeinikova, 2018). *H. pylori* and *C. jejuni* strains expressing non-functional Pse biosynthesis genes show defects in the formation of flagella and are thus non-motile and less virulent (Linton et al., 2000; Goon et al., 2003; Schirm et al., 2003; Guerry et al., 2006; Schoenhofen et al., 2006; Hopf et al., 2011; Javed et al., 2015a). Consequently, the inhibition of the Pse biosynthesis in these bacterial species is a promising antibacterial strategy.

Small-molecule inhibitors of Pse biosynthesis enzymes of *H. pylori* were identified using high-throughput screening (HTS) and virtual screening (VS) approaches in combination with kinetic studies and structure–activity relationship (SAR) analysis (Ménard et al., 2014). Ultimately, three PseB inhibitors were identified with a conserved *N*-phenyl-2-pyrrolidone core featuring

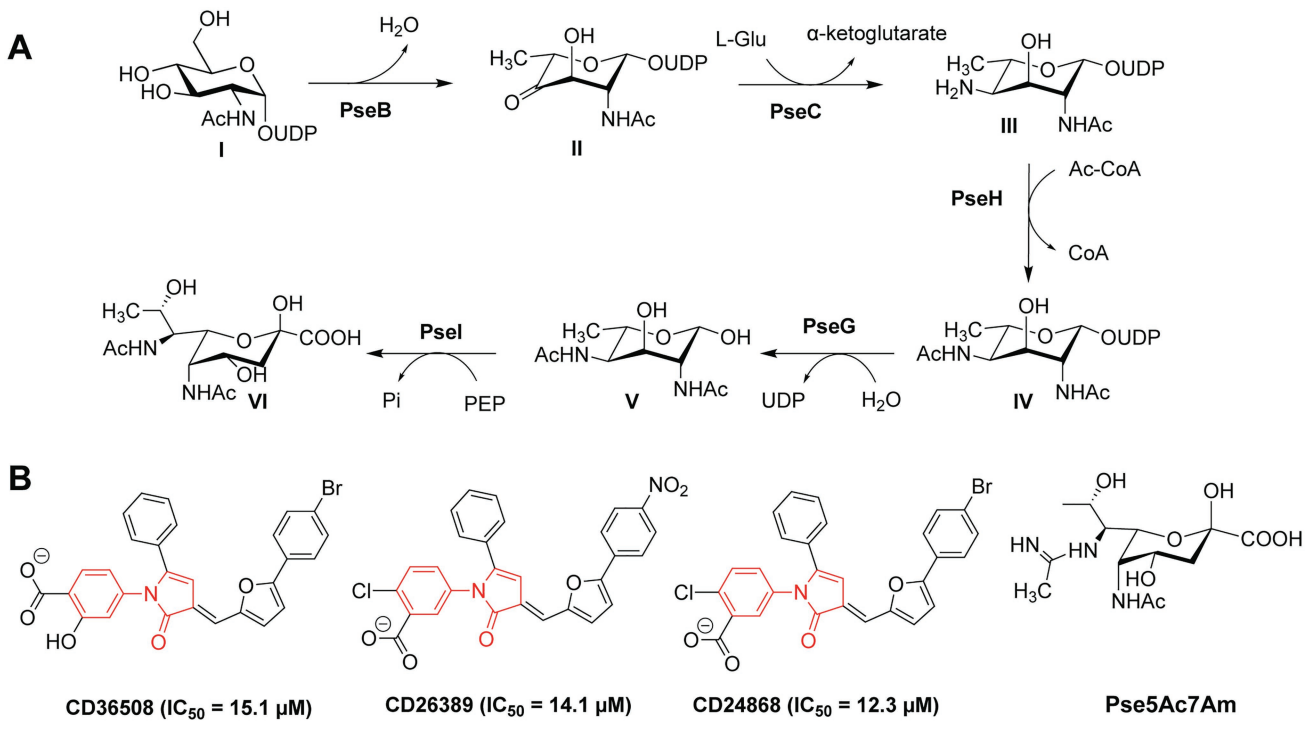

FIGURE 2 | (A) Biosynthetic pathway of Pse in *Campylobacter jejuni* and *Helicobacter pylori*; **(B)** Structures of the PseB inhibitors CD36508, CD26389, and CD24868 with their respective IC_{50} values in μM (Ménard et al., 2014).

different substitution patterns on the phenyl groups (**Figure 2B**). These three PseB inhibitors exhibited IC_{50} values of ~14 μM *in vitro* on purified PseB enzymes. Importantly, the inhibitors were also able to penetrate the bacterial cell wall and inhibit flagellin production in *C. jejuni* in a dose-dependent manner as determined by whole cell ELISA. The relatively low IC_{50} and the ability to cross the bacterial cell wall make these compounds interesting molecules for further development into clinical antibacterial drugs.

In addition to the *O*-linked flagellin glycosylation with unmodified Pse, *C. jejuni* also decorates its flagellin with Pse variants, mainly Pse derivative 7-acetamidino-Pse (Pse5Ac7Am; **Figure 2B**) in which an acetamido group has been substituted for an acetamidino moiety (Thibault et al., 2001; Schirm et al., 2005; Logan et al., 2009). Interestingly, the phage protein FlaGrab [previously called Gp047 (Sacher et al., 2020)] of the *Campylobacter* phage NCTC 12673 specifically binds to Pse5Ac7Am-modified flagellins of *C. jejuni*, resulting in reduced motility and partially inhibition of cell growth (Javed et al., 2015a,b). The C-terminal flagellin binding domain of FlaGrab has only been used for the detection of *C. jejuni* and *C. coli* so far (Singh et al., 2011, 2012; Javed et al., 2013). While a therapeutic use of FlaGrab against *C. jejuni* infections remains attractive, it has not yet been further explored. Notably, the *C. jejuni* strains 12661 and 12664 show reduced binding by FlaGrab due to strain-specific glycan remodeling mechanisms (Sacher et al., 2020). Still, the example of FlaGrab points out the promises of phage proteins as potential therapeutic agents against pathogenic bacteria specifically targeting glycans or other (glycosylated) bacterial structures.

Flagellar Glycosylation of *C. difficile*

The motility of *C. difficile*, an opportunistic Gram-positive pathogen, is dependent on *O*-glycosylation of its flagellum protein FliC. *C. difficile* strains display two different glycan structures (Twine et al., 2009; Faulds-Pain et al., 2014), with the core *N*-acetyl-β-glucosamine (β-GlcNAc) as the only conserved residue (**Figure 3**). NMR studies revealed that the type A *O*-glycan of the *C. difficile* 630 (**Figure 3A**) is composed of the core β-GlcNAc residue modified with an *N*-methylated Thr *via* a phosphate at the C3 position (Faulds-Pain et al., 2014). The more complex type B flagellar glycosylation (in strains BI-I, NAP-I, and ribotype 027) is composed of a Ser/Thr-linked β-GlcNAc, elongated with two rhamnose residues (*O*-methylated at the C3 position, **Figure 3B**; Bouché et al., 2016). An alternative structure featured an additional 3-amino-3-deoxy-D-fucose (Fuc3N in **Figure 3B**) modified with a sulfopeptide (Gly-Ala-taurine) at the C3-amino group (Bouché et al., 2016). The glycosyltransferases involved in the synthesis of the type B glycan include GT1 (core GlcNAc transfer onto Ser/Thr), bifunctional GT2 (Rha transfer and Rha methylation), and GT3 (partially involved in the synthesis of the sulfopeptide; Valiente et al., 2016). *C. difficile* knockout strains of GT1 and GT2 both resulted in decreased motility of the bacterium, whereas a GT1 deletion mutant showed only reduced adherence. These enzymes are interesting targets for antivirulence strategies, as the type B glycan is increasingly associated with the emerging hypervirulent and more aggressive strains of *C. difficile* (*e.g.* RT027, RT023).

Immune Evasion

Capsular Polysaccharides

Capsular polysaccharides (CPS; **Figure 1B**) of Gram-negative and Gram-positive bacteria are constituents of the bacterial glycocalyx, providing protection to immune system recognition. Interestingly, the CPS of bacterial pathogens are often found to contain carbohydrate epitopes that mimic those of human cells which help to evade the immune system and promote infection (Cress et al., 2014). Consequently, encapsulated bacterial pathogens tend to be more virulent as they are less susceptible to immune system recognition and penetration of the antibiotics. Rendering bacterial pathogens non-encapsulated is an attractive prospect, as it would make the bacteria vulnerable to the innate immune response or resensitize the resistant strains to antibacterial treatments.

The CPS of pathogenic *E. coli* (so-called K capsules or K antigens) display highly diverse glycan structures, and ~80 different CPS are reported and classified into four groups depending on their assembly and export machinery (Whitfield, 2006). An interactive overview of the *E. coli* K antigens, their structures, and 3D modeling can be found in the *E. coli* K antigen 3D structure Database (EK3D; Kunduru et al., 2016).[1]

[1]www.iith.ac.in/EK3D/

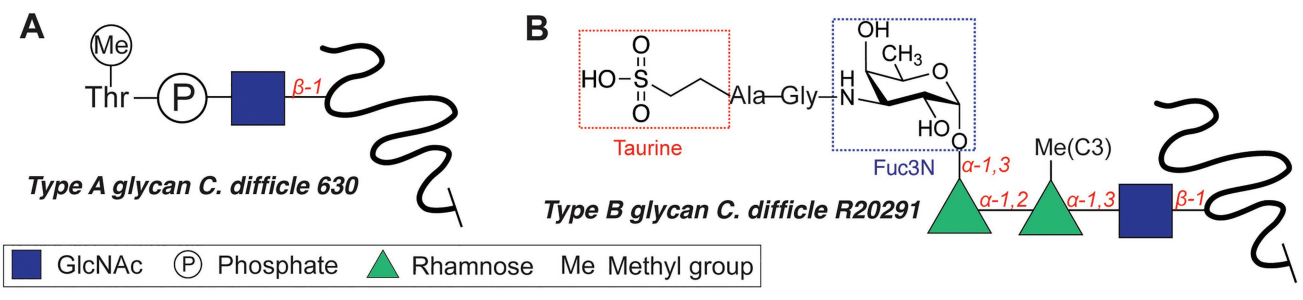

FIGURE 3 | Flagellar glycan structures of *Clostridium difficile*. **(A)** Type A glycan. **(B)** Type B glycan.

For example, the K15 antigen (**Figure 4A**) of enterotoxigenic *E. coli* O6:K15 is a polymer containing α-GlcNAc(1➔5)-α-Kdo(2➔4) disaccharide repeating units (Azurmendi et al., 2020), the K1 capsule (**Figure 4A**) of uropathogenic *E. coli* (UPEC) is composed of α-2,8-Neu5Ac repeats, and the K5 capsule is a polymer of α-GlcNAc(1➔4)-β-GlcA(1➔4) repeats (**Figure 4A**). The highly acidic capsule polysaccharides enhance bacterial survival by sequestering the antimicrobial peptides produced by the host immune system. A capsule-specific phage screen was used to identify inhibitors of CPS synthesis of UPEC K1 and K5 capsules (Goller and Seed, 2010). The most potent compound was 2-(4-phenylphenyl)benzo[g]quionoline-4-carboxylic acid (also called "C7," **Figure 4A**), which showed an IC_{50} value of 12.5–25 μM with UPEC K1 UTI89. C7 was evaluated in a variety of biochemical studies and was shown to specifically disrupt the oligomerization of the *E. coli* K1 antigen leading to its absence on the outside of the cell. Importantly, upon treatment with C7, the *E. coli* cells were more susceptible to human serum and the compound proved to be active also on clinical *E. coli* isolates. In a follow-up study, compounds DU003 and DU011 (**Figure 4A**) were identified from a structurally diverse set of small-molecule inhibitors, because they improved pharmacological properties (IC_{50}, solubility, toxicity, permeability and plasma stability; Goller et al., 2014). Compound DU011 was later shown to attenuate CPS production in *E. coli via* interaction with the multi-drug efflux pump transcriptional regulator MprA (Arshad et al., 2016). Notably, this mode of inhibition was found to be antivirulent in nature, as it did not lead to the development of antibiotic resistance (Arshad et al., 2016).

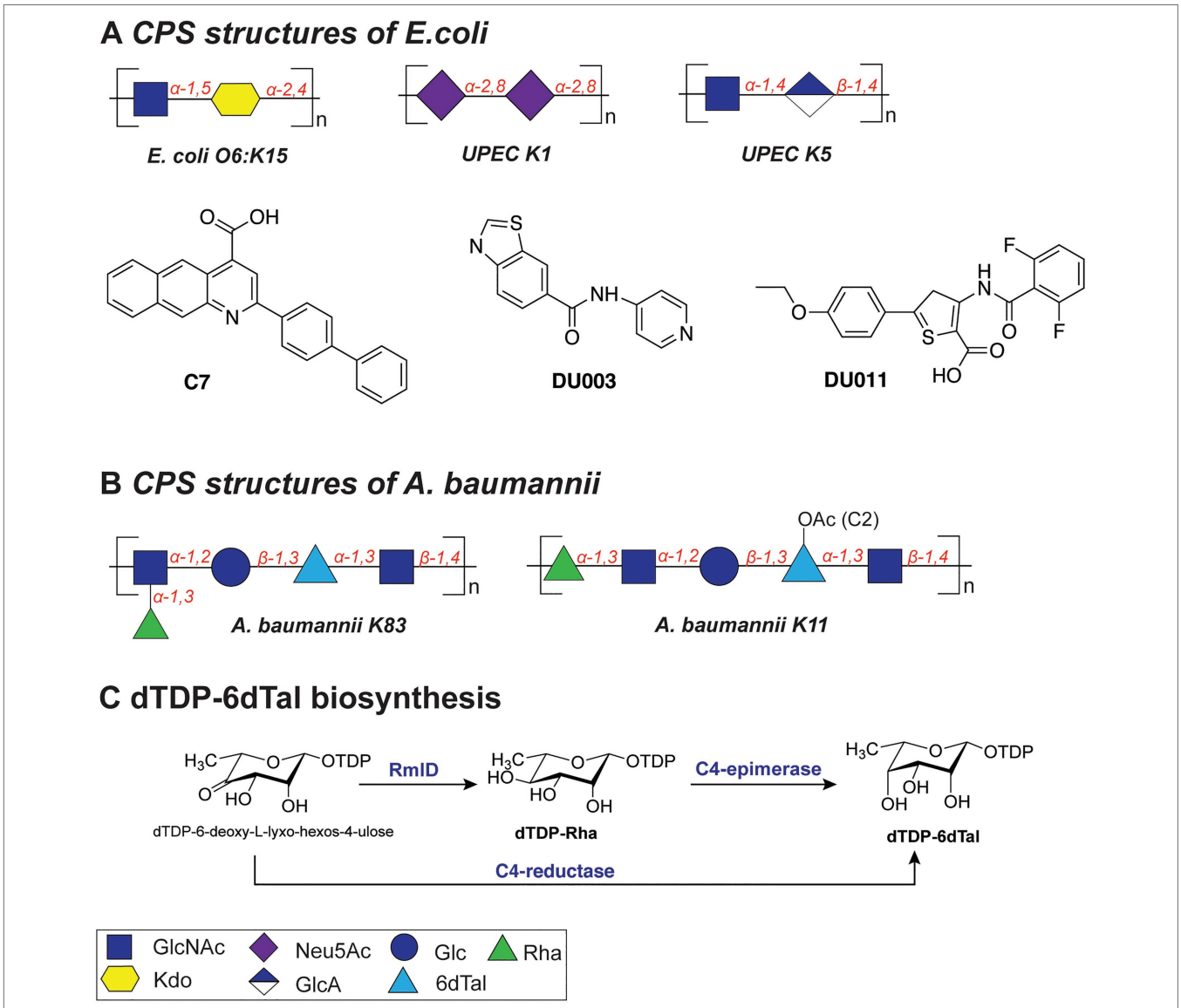

FIGURE 4 | (A) Structures of the capsular polysaccharides of *Escherichia coli* and inhibitors described in this section. **(B)** Structures of the capsular polysaccharides of *Acinetobacter baumannii*. **(C)** Biosynthesis of dTDP-6dTal.

A different strategy to de-encapsulate *E. coli* is based on phage-derived polysaccharide depolymerases (Lin et al., 2017). Several depolymerases were tested for their *in vitro* and *in vivo* (mouse models) activity with depolymerase enzyme K5 displaying the highest efficacy and consequent survival of mice. Importantly, the enzymes tested in this study (K1E, K1F, K1H, K5, and K30) were not toxic when injected in animals (based on survival, behavior and body weight monitoring for 5 days). Furthermore, when *E. coli* was tested in a serum sensitivity assay, in the presence of depolymerases, the viability of the cells was reduced significantly, with K5 depolymerase displaying the most pronounced effect. The high specificity of depolymerases toward certain CPS structures represents a potential novel narrow-spectrum treatment.

The capsules of *Acinetobacter baumannii* are the main virulence factor of these bacterial species (Harding et al., 2017). Their CPS structures feature an impressive diversity of monosaccharides in repeating units and linkages, all of which complicate the development of treatments, especially vaccines (Singh et al., 2019). For example, a study of the association of different *A. baumannii* capsule types with carbapenem resistance revealed four main serotypes that contribute to resistance (KL2, KL10, KL22, and KL52), indicative of the importance of capsule structure in infection (Hsieh et al., 2020).

The repeating K units of *A. baumannii* CPS typically consist of 2–6 monosaccharide units and feature glucose, galactose, glucuronic acid, and nonulosonic acid, among others, also with acetyl or acyl modifications (K83 and K11; **Figure 4B**; Singh et al., 2019). Interestingly, several clinical isolates of *A. baumannii* (strains KL106, KL112, 48-1789, MAR24) were found to contain the bacterial monosaccharides 6-deoxy-L-talose and L-rhamnose (Kenyon et al., 2017; Kasimova et al., 2021). Importantly, dTDP-6-deoxy-L-talose is produced either from dTDP-L-Rha by the action of C4-epimerase or from dTDP-6-deoxy-L-lyxo-hexos-4-ulose by C4-reductase (**Figure 4C**; Kenyon et al., 2017). Consequently, the disruption of the dTDP-L-Rha biosynthesis pathway (*rmlABCD* cluster) can potentially abolish the synthesis of both rare monosaccharides in *A. baumannii*.

Lipooligosaccharides of *Neisseria gonorrhoeae* and *C. jejuni*

Lipooligosaccharides (LOS) are a major family of glycolipids presented on the outer membrane of the Gram-negative bacteria, and they play central roles in the virulence of many pathogens such as *Neisseria gonorrhoeae* and *C. jejuni*. Among other functions, LOS may aid pathogens in evading the host immune system or conferring immune resistance (Preston et al., 1996; Harvey et al., 2000; Song et al., 2000).

Several *N. gonorrhoeae* strains express the tetrasaccharide lacto-*N*-neotetraose (LNnT) at their LOS termini which mimics the terminal glycan structure of the human glycosphingolipid precursor paragloboside (Mandrell et al., 1988; Tsai and Civin, 1991). The LNnT termini of LOS can be sialylated with *N*-acetylneuraminic acid (Neu5Ac) by the *N. gonorrhoeae* sialyltransferase LsT (**Figure 5Aa**; Mandrell et al., 1990, 1993; Gulati et al., 2005; Packiam et al., 2006). The sialylated LNnT motif confers resistance to the bactericidal effect of the complement system, a trait also denoted as "serum resistance," and enables immune evasion (Mandrell et al., 1990; Wetzler et al., 1992; Ram et al., 1998, 2017; Gulati et al., 2005; Ricklin et al., 2010). Due to its key role in the establishment and maintenance of an infection by immune evasion, LsT of *N. gonorrhoeae* is therefore an attractive target for antivirulence intervention. In recent studies (Gulati et al., 2015), several CMP-nonulosonate analogues were identified which partly inhibited serum resistance and relieved the burden of gonococcal infection in mice models. Of the identified CMP-nonulosonate analogues, CMP-Leg5,7Ac_2 and CMP-ketodeoxynonulosonate (CMP-Kdn; **Figure 5B**) were found to be most promising as future therapeutics (Gulati et al., 2020). Both compounds were stable in an acidic environment mimicking the human vaginal site of infection. Furthermore, they effectively treated infection with multi-drug-resistant gonococci in mice models presenting a humanized sialome or expressing a humanized complement system. Thus, CMP-Leg5,7Ac_2 and CMP-Kdn are promising candidates for future therapeutics against multi-drug resistant *N. gonorrhoeae* strains. Interestingly, their mode of action follows the mechanism of metabolic oligosaccharide engineering (MOE), as will be discussed in section "Promising Strategies to Abolish Bacterial Glycosylation Systems". Interestingly, a recent study identified an alternative terminal epitope of LNnT, featuring a Kdo residue that was transferred by the sialyltransLsT (Jen et al., 2021). This specific LOS structure was identified in the clinical isolates of *N. gonorrhoeae* and shown to be recognized by anti-Kdo monoclonal antibody 6E4 with potential for the future vaccine development.

Biosynthesis of the LOS core of *Campylobacter jejuni* is performed by a series of carbohydrate biosynthesis and glycosyltransferase enzymes. Whereas the inner LOS core of *C. jejuni* (which contains two heptose and two glucose moieties) is conserved (Klena et al., 1998; Gilbert et al., 2002; Kanipes et al., 2004, 2006), the outer core LOS is highly variable among *C. jejuni* strains. For example, the outer LOS core of *C. jejuni* strains CCUG 10938 and 10,950 contains the monosaccharides Gal, GalNAc, and Neu5Ac, which together resemble the terminal saccharides of host gangliosides GM1 or GD1a (**Figures 5Ab-e**; Yuki et al., 2004; Goodfellow et al., 2005; Godschalk et al., 2007; Janssen et al., 2008; Jasti et al., 2016). Bacterial strains that express the enzymes to produce these host-mimicking epitopes have been linked to the development of the autoimmune Guillain-Barré syndrome (GBS) wherein autoantibodies induce damage to nerve gangliosides (Nachamkin et al., 2002; Godschalk et al., 2004; Mortensen et al., 2009; Poole et al., 2018). Counteracting the molecular mimicry of *C. jejuni* is therefore of interest for reducing immune evasion and severity of GBS following a *C. jejuni* infection. Inhibition of the glycosyltransferases that are required to build the core LOS glycans of *C. jejuni* would be an effective way to preclude the immune evasion caused by molecular mimicry of *C. jejuni*.

Lipopolysaccharides of *P. aeruginosa*

The Gram-negative bacterial pathogen *P. aeruginosa* produces two main types of the lipopolysaccharides: common polysaccharide antigen (CPA) with D-Rha repeats as an outer core (**Figure 5Af**) and O-specific antigen (OSA) with varied structures across 20 serotypes (heteropolymer of 2–4

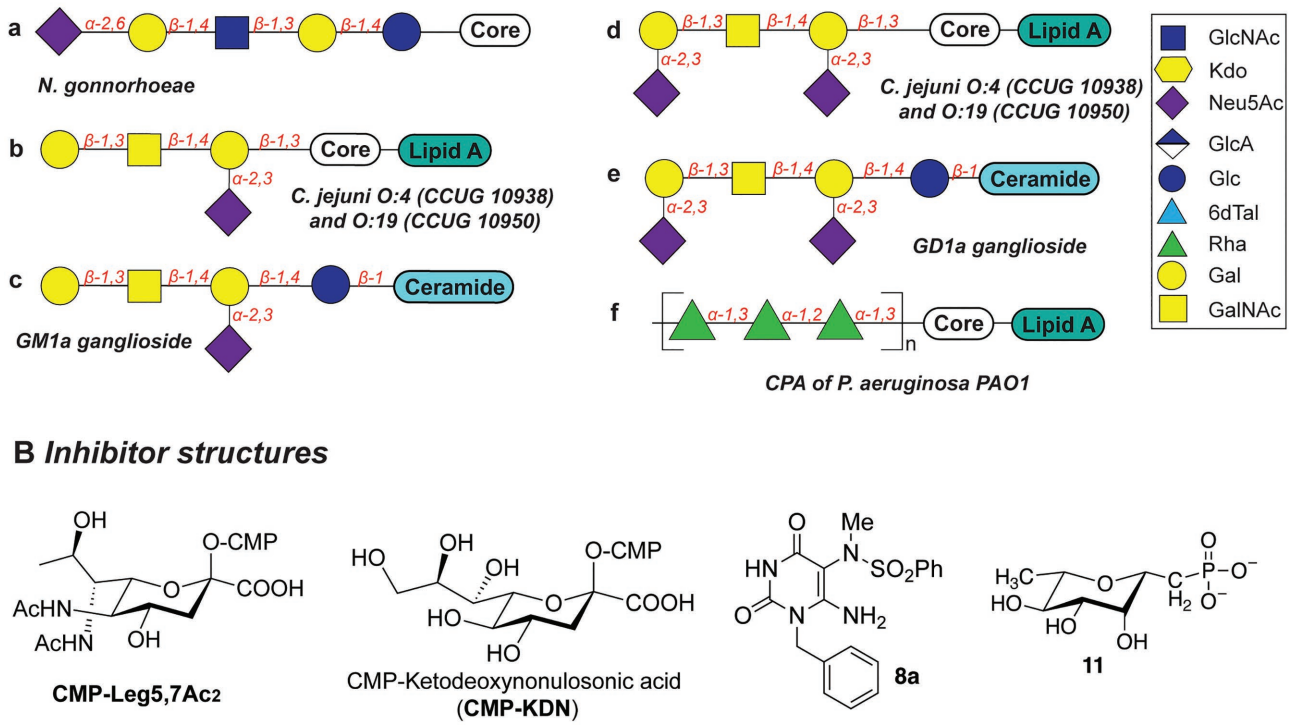

FIGURE 5 | (A) Structures of LOS described in this section. **(B)** Structures of inhibitors discussed in this section.

monosaccharides: GalNAc, GlcNAc, ManNAc, QuiNAc, GulNAc, FucNAc, L-Rha, Xyl, among others; Lam et al., 2011). Both types of LPS are important for the pathogenesis and survival of *P. aeruginosa*, as they confer serum resistance, prevent phagocytosis, and promote swimming and swarming motility and biofilm formation (Huszczynski et al., 2020).

Due to the importance of rhamnose in the infection strategies of *P. aeruginosa*, the dTDP-L-Rha donor synthesis pathway is an attractive antibiotic target. Several studies explored substrate mimics as inhibitors of the TDP-L-Rha biosynthesis. For example, thymidine-based allosteric inhibitors have been developed for RmlA, the first enzyme in the TDP-Rha synthesis that performs condensation of the glucose-1-phosphate (G1P) with thymidine triphosphate (dTTP; Alphey et al., 2013). The library screen and subsequent optimization of the lead compounds yielded a potent inhibitor (called "8a," **Figure 5B**) with IC_{50} of 0.073 μM, as determined *in vitro*. Importantly, *via* X-ray structure determination and SPR analyses, the authors deduced that 8a acts as a competitive allosteric inhibitor of glucose-1-phosphate binding. The allosteric site of the RmlA plays a role of inducing a negative feedback loop of the TDP-Rha synthesis upon binding the TDP-Rha. It is hypothesized that binding of 8a locks the tetrameric enzyme in a fixed conformation, which prevents G1P binding in the active site.

In a different study, a panel of L-rhamnose 1C-phosphonate and (fluorinated) ketosephosphonate compounds was prepared and evaluated as inhibitors of the TDP-L-Rha biosynthesis enzymes from *P. aeruginosa* and *Streptococcus pneumoniae* (Loranger et al., 2013). L-rhamnose 1C-phosphonate (called "11," **Figure 5B**) was determined to be the best with an IC_{50} of 5.7 mM. Compound 11 is expected to behave as a competitive inhibitor of the G1P binding in the active site of Cps2L of *S. pneumoniae* (RmlA in *P. aeruginosa*), and addition of a thymidine moiety may improve the potency of the inhibitor.

Biofilms

Bacterial biofilms are complex entities comprised of aggregated bacterial cells enclosed in a secreted matrix that contains polysaccharides, proteins, lipids, and extracellular DNA and typically attached to the (a)biotic surfaces. Biofilms are characterized by increased resistance to antimicrobials and subsequent enhanced survival of bacteria in the biofilm and feature a distinct metabolic and genetic makeup (Flemming et al., 2016). Microbial biofilms are of great concern in the context of hospital infections (especially *via* medical devices), and multiple methods have been developed to study and mimic biofilm formation (Azeredo et al., 2017). Antibiotic resistance conferred by biofilms results in recurring or chronic infections which are responsible for a great personal and healthcare burden (Sharma et al., 2019). Therefore, methods to prevent or disrupt the biofilms are of great importance. A plethora of small-molecule therapeutics, enzymes and physical methods for biofilm prevention, inhibition, and dissemination have been developed (Verderosa et al., 2019; Ghosh et al., 2020; Pinto et al., 2020).

Whereas bacterial capsules generally confer enhanced survival for encapsulated pathogens (as described above), they also display inhibitory properties toward competing microbial species. For instance, a soluble polysaccharide (K2 capsule, **Figure 6**) secreted by UPEC was found to have anti-adhesive properties that preclude biofilm formation of both Gram-negative (*E. coli*, *K. pneumoniae*, and *P. aeruginosa*) and Gram-positive species (*Staphylococcus aureus*, *Staphylococcus epidermidis*, and *Enterococcus faecalis*; Valle et al., 2006). The released CPS of UPEC tested in the study were shown to reduce the initial cell surface contacts and interfere with the cell–cell aggregation, both processes necessary for the biofilm formation. Importantly, a full-length polysaccharide was required to confer the inhibitory properties, as hydrolyzed polymer did not exert the same effect.

Similarly, the alginate oligomer OligoG [α-GulA(1➔4)-β-ManA(1➔4), **Figure 6**], currently in stage 2b clinical trials for cystic fibrosis treatment, was found to dissolve the biofilms of mucoid *P. aeruginosa* (Hengzhuang et al., 2016). The low-molecular weight OligoG *CF*-5/20 (purified from seaweed *Laminaria hyperborea*, 85% GulA, and 15% ManA content, ~3,200 Da, DP = 16) showed synergistic effects when combined with the antibiotic colistin in a murine lung infection model. A follow-up study revealed that OligoG interacts with components of the *P. aeruginosa* EPS, penetrating into the biofilm and disrupting the Ca^{2+}-eDNA complexes involved in the biofilm maturation process (Powell et al., 2018).

Interestingly, biofilms frequently feature multi-species communities which complicate the development of effective antibacterial therapies. Consequently, combination therapies and drug adjuvants are a promising strategy to target and eradicate several (bacterial) pathogens simultaneously. For instance, the joint use of antifungal and antibacterial compounds was recently reported to effectively disperse a *Candida albicans-S. aureus* biofilm (Rogiers et al., 2018). These species are postulated to have a mutualistic relationship, specifically in the context of intra-abdominal infections (IAIs). In addition, a combination therapy of anidulafungin (against *C. albicans*; **Figure 6**) and tigecycline (against *S. aureus*; **Figure 6**) on a dual-species biofilm in the IAI murine model showed a synergistic effect, eradicating *S. aureus* more effectively compared to the treatment with tigecycline alone. Increased administration of anidulafungin resulted in the reduced presence of poly-β-1,6-*N*-acetylglucosamine (PNAG) which is a major polysaccharide constituent of the *S. aureus* biofilm EPS. It was hypothesized that the mode of action of anidulafungin parallels the action of caspofungin, which was previously reported to disrupt the function of the PNAG-synthesizing *N*-acetylglucosamine transferase IcA (Siala et al., 2016). When used as an adjuvant with fluoroquinolones, which are typically used to treat *S. aureus* infections, anidulafungin showed a marked synergistic effect, resulting in enhanced penetration of fluoroquinolones into the biofilm, possibly due to the decreased PNAG presence.

Exotoxins

Bacterial pathogens actively modulate host immune and tissue cells processes to evade recognition and promote survival and spread in the host (Sastalla et al., 2016). This is achieved, for instance, *via* the secretion of bacterial exotoxins with glycosyltransferase activity which alters or disrupt specific host processes (Sastalla et al., 2016). For example, NleB1 of enterohaemorrhagic *E. coli* (EHEC), enteropathogenic *E. coli* (EPEC), and *Citrobacter rodentum*, and SseK of *Salmonella enterica* are conserved glycosyltransferase effectors, that are

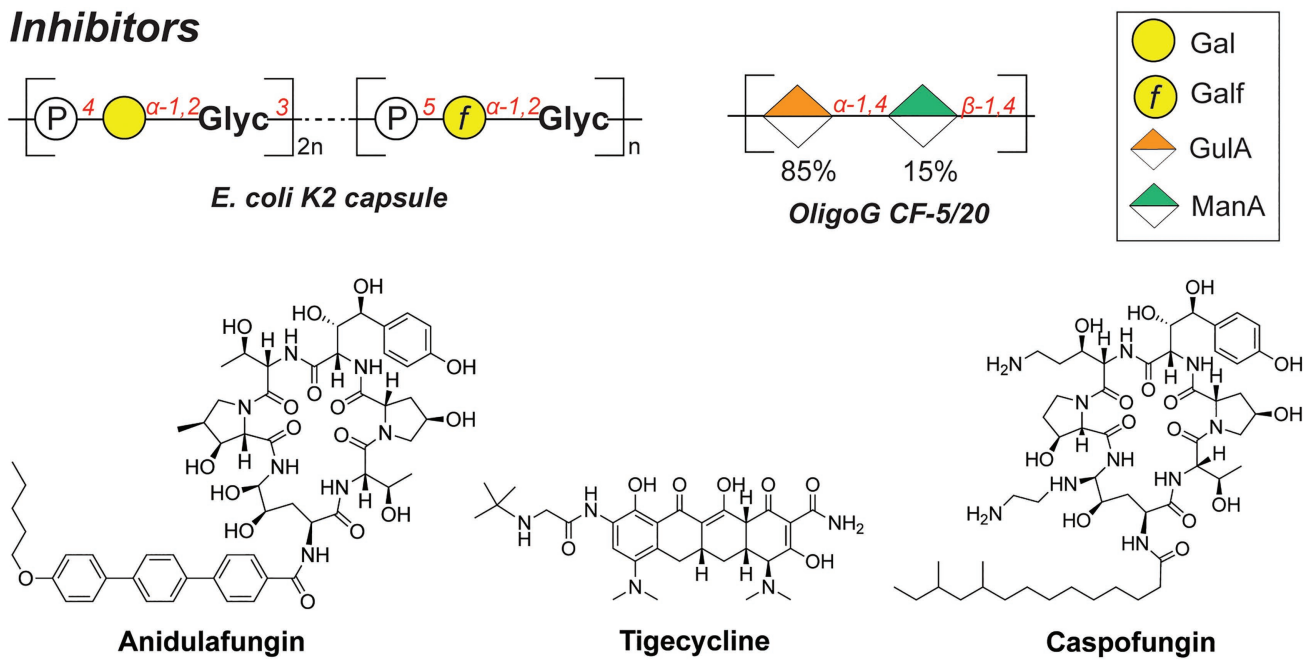

FIGURE 6 | Structures of biofilm inhibitors described in this section.

injected into the host cells by a type III secretion system (**Figure 7A**). These exotoxins transfer β-GlcNAc to arginine residues on host cell proteins, such as serine/threonine-protein kinase 1 (RIPK1), tumor necrosis factor receptor (TNFR) type 1-associated DEATH domain protein (TRADD), the Fas-associated protein with death domain (FADD), and the mammalian glycolysis enzyme glyceraldehyde 3-phosphate dehydrogenase (GAPDH). Glycosylation of these target proteins results in the inhibition of innate host immune responses facilitating spread and host cell infection (Gao et al., 2013; Li et al., 2013; Pearson et al., 2013; Esposito et al., 2018; Park et al., 2018).

Inhibitors directed against NleB1, as well as the *S. enterica* analogues Ssek1 and Ssek2, have been identified and showed promising results as new antivirulence agents. In a recent study, a small-scale high-throughput screen for inhibitors of NleB1 of EPEC and EHEC was performed using a library of 5,160 small-molecule compounds (El Qaidi et al., 2018). Using this setup, two compounds, 100066N and 102644N (**Figure 7B**), were found to inhibit Nleb1 and SseK1/SseK2 activity *in vitro*, as well as NleB1 activity on mammalian HEK293 cells. The compounds inhibited replication of *S. enterica* strain ATCC 14028 in mouse macrophage-like cell infection assays, while they were not cross-reactive toward mammalian *O*-linked *N*-acetylglucosaminyltransferases (OGT) and did not inhibit growth of *S. enterica* bacterial cultures indicating that they are not bactericidal (El Qaidi et al., 2018). Since compounds 100066N and 102644N have relatively low solubilities and are not commercially available, a library screen of 42,498 compounds, containing more diverse chemical scaffolds with favorable characteristics for future chemical optimization, was performed. In this new screen, the commercially available compound sepantronium bromide (YM155, **Figure 7B**) was found to robustly inhibit NleB/SseK glycosyltransferases. YM155 was previously described as a small-molecule inhibitor of survivin, which belongs to the inhibitor of apoptosis (IAP) protein family (Ambrosini et al., 1997; Nakahara et al., 2007). While the inhibition of NleB/SseK is concentration-dependent, YM155 did not cross-react with the human OGT enzyme, supporting its specificity to NleB/SseK glycosyltransferases. In addition, YM155 did not exhibit toxicity in RAW264.7 cells (Zhu et al., 2021). However, the effect of YM155-mediated inhibition on survivin has not been characterized in the study. The growth of *C. rodentium,* EHEC, or *S. enterica* cultures was not significantly altered at maximum concentrations of YM155 (125 μM). Furthermore, treatment of macrophage RAW264.7 cells with YM155 reduced the amount of infected, intracellular bacteria as quantified by *Salmonella* infection assays. Compared to 100066N and 102644N, YM155 is less potent, but showed higher solubility and is easier to chemically modify for future structural improvements. Together with its commercial availability, YM155 poses an interesting candidate for further characterization and chemical modification and development into a future antivirulence drug.

TcdA/B Toxins of *C. difficile*

One of the best-studied examples of bacterial cytotoxins is TcdA and TcdB of the opportunistic pathogen *C. difficile*, with TcdB expressed predominantly in hypervirulent

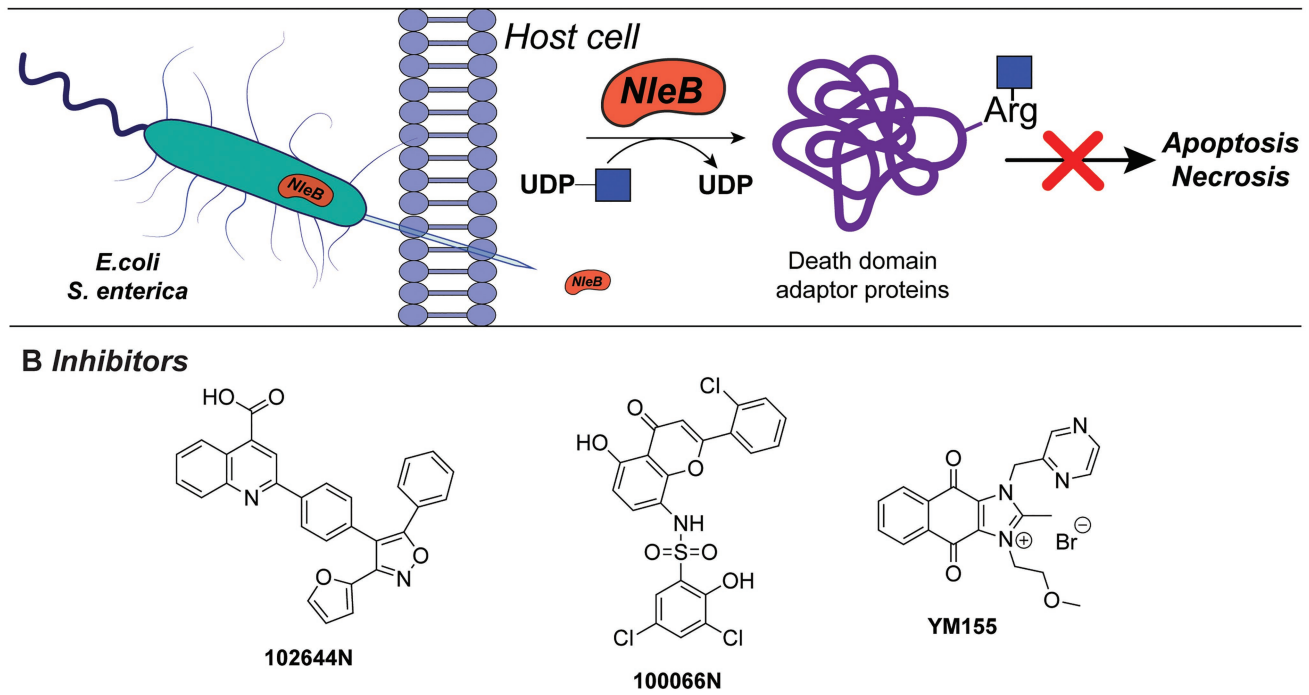

FIGURE 7 | (A) NleB/Ssek exotoxin system. **(B)** Developed inhibitors against NleB/Ssek discussed in this section.

strains (**Figure 8A**). These clostridial toxins are the main determinants of bacterial pathogenesis, as they form pores in the host cells and modulate cell death, thereby spreading the infection. TcdA/TcdB toxins are composed of four domains, namely, transporter domain, receptor-binding domain, cysteine protease domain (CPD), and an N-terminal glycosyltransferase domain (GT; Di Bella et al., 2016; Aktories et al., 2017). Upon acidic endocytosis into the host cell, the toxins are translocated through the membrane where the CDP domain catalyzes cleavage and release of the N-terminal GT domain (**Figure 8A**; Di Bella et al., 2016). Subsequently, the GT domain transfers D-glucose onto threonine residues of host cell Rho-guanosine triphosphatases (Rho-GTPase; Just et al., 1995a,b; Kuehne et al., 2010). This leads to necrosis characterized by cell rounding, membrane blobbing, and finally, cell death (Sehr et al., 1998; Genth et al., 1999; Voth and Ballard, 2005).

Several HTS studies were performed to identify small-molecule inhibitors of *C. difficile* toxins. A screen of six million compounds, followed by extensive optimization of the lead compounds *via* chemical synthesis and SAR analysis, yielded compounds "13j" and "13l" (**Figure 8B**). These compounds share a benzodiazepinedione core and displayed potent inhibitory activity against TcdB (low nM IC_{50} *in vitro*, low μM in a cell assay; Letourneau et al., 2018). Interestingly, the compounds were not bactericidal to *C. difficile* or gut bacteria. However, all potent compounds demonstrated low mouse plasma stability and rapid clearance. The same research group also reported the biological evaluation of compound VB-82252 (**Figure 8B**), which exhibited low plasma stability, but high oral bioavailability (Stroke et al., 2018). Compound VB-82252 was found to be a potent inhibitor (IC_{50} of 32 nM) of UDP-Glc hydrolysis by TcdB (used as a measure of TcdB activity), as determined in an *in vitro* assay (Stroke et al., 2018). The compound was effective in preventing CHO cells rounding in an assay with several strains of *C. difficile*. The therapeutic efficiency of VB-82252 was further evaluated in a mouse and hamster *C. difficile* disease model, where it was effective in sustaining body weight and prolonging the survival of the animals.

In addition, the cell rounding assay was also employed to quantify the effects of various approved therapeutics on TcdB toxins inhibition (Tam et al., 2018). From this library screen assay, the drug niclosamide (**Figure 8B**), originally developed to treat GI parasites, was most potent (EC_{50} ~ 0.5 μM) in protecting the human cells from rounding. Interestingly, niclosamide does not inhibit the TcdB toxin directly, but instead increases the pH of the host endosomes which disrupts the toxin uptake into the cells. Treatment with niclosamide was effective in a murine model of infection while it exhibited no bactericidal effect on *C. difficile* or beneficial gut bacteria (determined with an MIC assay and diversity monitoring, respectively).

In an alternative approach to TcdA/B inhibition, small-molecule inhibitors of the cysteine protease domain (CPD) of the *C. difficile* toxin were identified (Bender et al., 2015).

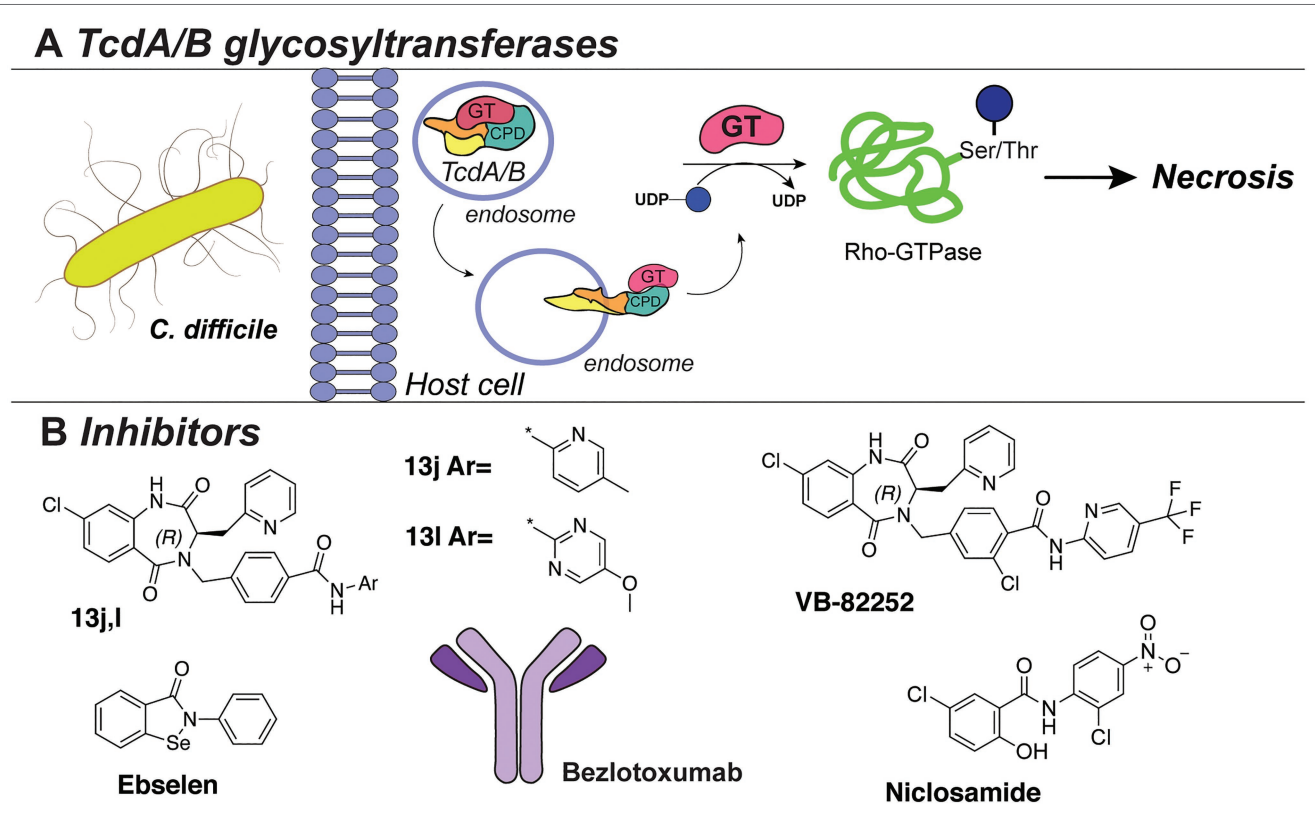

FIGURE 8 | (A) The TcdA/TcdB bacterial exotoxin system. **(B)** Inhibitors against TcdB discussed in this section.

By utilizing fluorescence-polarization HTS of compound libraries with clinically safe drugs (*e.g.*, LOPAC library), multiple inhibitors were identified, with the selenium-containing drug ebselen (**Figure 8B**) exhibiting the highest potency (IC_{50} 6.9 nM). Notably, the drug could preclude the GT domain release and cell rounding. The effects of the drug were confirmed to be due to the prevention of Rho-GTPases glucosylation, and it was shown to be effective in a murine model of *C. difficile* infection. Importantly, ebselen is a developed drug in late clinical trials for the treatment of tinnitus, hearing loss, and bipolar disorder and has been proven safe for use in humans.

Besides conventional antibiotics to treat a *C. difficile* infection, the TcdB-neutralizing antibody bezlotoxumab is an FDA-approved therapy against recurring *C. difficile* (Zinplava, Merck; Navalkele and Chopra, 2018). Bezlotoxumab binds the N-terminal part of the receptor-binding domain of the TcdB toxin, preventing toxin binding and entry into host cells (Orth et al., 2014). It was also effective against hypervirulent *C. difficile* strains (NAP1, BI, 027). Currently, bezlotoxumab is only used in combination with antibiotic treatments and is not a stand-alone therapy against *C. difficile*.

PART 2: FUTURE PERSPECTIVES

Bacterial Protein Glycosylation Systems as Promising Targets

Adhesins and Autotransporters

Adhesion is one of the first step in the bacterial colonization of the host. It is mediated by various adhesion factors presented on the surface of the bacterium that recognize and bind to the host cell receptors (Chagnot et al., 2013; Poole et al., 2018). Adhesin proteins in particular are often (hyper)glycosylated, and the presence of glycans often plays a vital role for their stability and proper function (Lu et al., 2015). Therefore, glycosylation of the adhesion factors is an attractive target for the development of novel anti-adhesive therapies.

O-Heptosylation of the Self-Associating Autotransporters

Diffusely adhering *E. coli* (DAEC), enterotoxigenic *E. coli* (ETEC), and the murine pathogen *Citrobacter rodentium* share a common adhesion mechanism to host cells. These bacteria rely on a type Va secretion system, which is also called a self-associating autotransporter (SAAT) system (Lu et al., 2014). Autotransporter proteins consist of a C-terminal β-barrel domain that forms a transport channel in the outer membrane and a passenger domain which is translocated through this channel and fulfils the effector adhesion function (Leyton et al., 2012). In DAEC, ETEC, and *C. rodentium,* the passenger domains of autotransporters AIDA-I, TibA, and CARC, respectively, are *O*-hyperglycosylated with bacteria-specific D-glycero-D-manno-heptose (DDManHep **Figure 1**) by a cognate GT belonging to the *b*acterial *a*utotransporter *h*eptosyl*t*ransferase (BAHT) family (Lu et al., 2014, 2015). Hyperglycosylation is important for the successful adherence of AIDA-I to HeLa cells (Benz and Schmidt, 2001) and was later found to enhance protein stability (Charbonneau et al., 2007). Similarly, TibA is the SAAT of enterotoxigenic *E. coli* and depends on hyperheptosylation for stability as it was found to mediate its (re)folding and subsequently influence adherence function (Côté et al., 2013). Interestingly, heptose residues also constitute the LPS core of Gram-negative bacteria, and the synthesis pathway of ADP-L-glycero-β-D-manno-heptose (Kneidinger et al., 2002) is considered a promising target for inhibitors. Several studies have already identified inhibitors with IC_{50} values in the milli/micromolar range (De Leon et al., 2006; Kim et al., 2021a,b). It would be interesting to investigate whether these inhibitors indeed abolish SAAT hyperheptosylation and subsequent adherence of the bacterial cells.

N-Glycosylation of HMW Adhesins and Trimeric Autotransporters

Non-typeable *Haemophilus influenzae* (NTHi) utilizes a type Vb secretion system (also called two-partner secretion (TPS) pathway) to transport and present high molecular weight (HMW) adhesin proteins on the surface as a first step in host colonization (St Geme et al., 1993; Grass and St Geme, 2000). Stability and efficient surface tethering of HMW adhesins is dependent on *N*-hyperglycosylation on asparagine with simple mono- and disaccharides of glucose (Glc; Grass et al., 2003). A total of 31 glycosylation sites have been identified at asparagine residues in the Asn-X-Ser/Thr consensus sequence of HMW1A (Grass et al., 2003, 2010; Gross et al., 2008), modified by the action of the associated glycosyltransferase HMW1C (Grass et al., 2010). Interestingly, the glycosylation of HMW1A by HMW1C follows an unconventional OTase-independent *N*-glycosylation pathway, wherein cytoplasmic HMW1C transfers single nucleotide-activated carbohydrates to the acceptor protein HMW1A. Upon deletion of the genes encoding for HMW1C and UDP-Glc biosynthesis, *hmw1c* or *galU,* respectively, HMW1A surface presentation as well as adhesion to epithelial cells was abolished *in vitro* (Grass et al., 2010). Interestingly, we recently revealed that hyperglycosylation is established through a semiprocessive mechanism *in vitro* (Yakovlieva et al., 2021). Homologues of the HMW1C glycosyltransferase have been identified in *Kingella kingae* ($HMW1C_{Kk}$) and *Aggregatibacter aphrophilus* ($HMW1C_{Aa}$) where they perform the glycosylation of cognate trimeric autotransporters Knh and EmaA, respectively (Rempe et al., 2015). Analogously to the *H. influenzae* HMW1A, abolishing glycosylation of Knh and EmaA was shown to inhibit the bacterial aggregation and adherence to the host cells.

O-Glycosylation of Serine-Rich Repeat Proteins of Gram-Positive Bacteria

Multiple members of the serine-rich repeat proteins (SRRPs) of clinically relevant Gram-positive bacteria are found to be (hyper) *O*-glycosylated with carbohydrates that influence stability and adhesive function. Examples include fimbriae-associated protein Fap1 of *Streptococcus parasanguinis*, GspB of *Streptococcus gordonii*, SraP of *S. aureus*, PsrP of *S. pneumoniae,* and others, which are reviewed elsewhere (Zhou and Wu, 2009;

Lizcano et al., 2012). Glycosyltransferases termed Gtf1-Gtf2 (GtfA-GtfB) are responsible for the core GlcNAc modification on the Ser/Thr residues of SRRPs. These enzyme pairs operate in tandem with Gtf1 performing the glycosylation reaction and Gtf2 acting as a chaperone and substrate-binding domain (Wu and Wu, 2011; Chen et al., 2016; Zhao et al., 2018). After attachment of the initial GlcNAc, the character of the glycan modifications varies between different SRRPs and features GlcNAc/Glc (Srr1, GspB; Bensing et al., 2004; Chaze et al., 2014), Glc/GlcNAc/Rha (Fap1; Zhu et al., 2016), and GlcNAc (SraP; Li et al., 2014). The presence of the multiple glycans on the SRRPs is crucial for their function in conferring adhesion and biofilm formation of the Gram-positive pathogens and therefore constitutes an interesting antibacterial target.

Glycosylation of Pili

Neisseria gonorrhoeae produces type IV pili (TFP; Patel et al., 1991) that are required for effective adhesion to epithelial cells in an initial stage of the infection (Swanson, 1973; McGee and Stephens, 1984; Virji and Heckels, 1984; Craig et al., 2004). The glycans of TFP interact with complement receptor 3 (CR3), an innate pattern recognition receptor expressed on human cervical cells. The PilE subunits that make up the TFP feature glycans containing either a *N,N′*-diactetylbacillosamine (diNAcBac) or a galactose-modified diNAcBac (Gal(α1-3) diNAcBac) linked to serine residues (Jennings et al., 1998, 2011; Power et al., 2003; Hegge et al., 2004; Hartley et al., 2011). Only *N. gonorrhoeae* cells carrying the disaccharide Gal(α1-3)diNAcBac on their PilE proteins survive infection of the primary human cervical (Pex) cells, while TFP decorated with a single diNAcBac die within the cervical cells, even though they were found to be hyperinvasive. Glycosylation of PilE follows an OTase-dependent *O*-glycosylation pathway by multiple pilin glycosylation genes (pgl), which encode enzymes for the synthesis and attachment of diNAcBac to an intermediate lipid carrier, as well as GTs that attach galactose or glucose to diBacNAc (Hartley et al., 2011). Considering the importance of PilE glycosylation in the colonization capacity of *N. gonorrhoeae*, inhibitors of the pgl enzymes are attractive antibacterial agents. However, no inhibitors of *N. gonorrhoeae* pgl enzymes have been reported to date. Nonetheless, there are alternative approaches for targeting the interaction between the glycosylated TFP and CR3. Recently, two clinically approved drugs have been identified that inhibit the interaction of glycosylated PilE of *N. gonorrhoeae* with the l-domain of CR3. The drugs carbamazepine and methyldopa act as competitive inhibitors of CR3 binding and thereby efficiently blocked *N. gonorrhoeae* infection in Pex cells. Importantly, both drugs were also effective against multi-drug resistant gonococci and did not lead to development of resistance.

Efflux Pump Glycosylation

Efflux pumps are membrane proteins involved in the transport of various molecules (Alcalde-Rico et al., 2016). In bacterial pathogens, efflux pumps are often responsible for ejecting antibiotics from bacterial cells. They are especially prominent in the multi-drug resistance species and are an attractive drug target, especially in combination therapies (Ferrer-Espada et al., 2019; Marshall et al., 2020; Rodrigues et al., 2020).

In *C. jejuni*, the CmeABC complex is the main multi-drug efflux pump that confers resistance to various antibiotics. Together, CmeA, CmeB, and CmeC form a superstructure that spans the inner membrane, periplasmic space and creates a pore in the outer membrane of the bacterial cell. It was previously reported to be *N*-glycosylated with complex *C. jejuni N*-glycans (Abouelhadid et al., 2020). In a recent study, the importance of *N*-glycosylation for CmeABC efflux pump function was revealed (Dubb et al., 2020). Abolishing glycosylation of CmeA, which spans the periplasmic space, led to the increased accumulation of ethidium bromide and significant increase in antibiotic susceptibility, both indicating the impaired functioning of the efflux pump machinery. Additionally, the loss of CmeA glycosylation resulted in the loss of colonization ability of the chicken ceca.

Promising Strategies to Abolish Bacterial Glycosylation Systems

Inhibition by Metabolic Oligosaccharide Engineering

With the increasing knowledge of bacterial glycosylation systems, a variety of strategies to inhibit the enzymes involved has been developed. For instance, inhibitors of the enzymes involved in production of the carbohydrate-nucleotide donors, such as dTDP-Rha (*vide supra*), have been developed and described elsewhere (Alphey et al., 2013; Loranger et al., 2013; Van Der Beek et al., 2019). In addition, several classes of compounds have been designed as inhibitors for glycosyltransferases (Compain and Martin, 2001; Kajimoto and Node, 2009; Tedaldi and Wagner, 2014; Ema et al., 2018; Conforti and Marra, 2021). For this review, we decided to focus on the technique of MOE, as a promising strategy to interfere with bacterial glycosylation systems in a specific manner.

The technique of MOE, as originally developed by Reutter (Kayser et al., 1992) and Bertozzi (Mahal et al., 1997; Bertozzi and Saxon, 2000), relies on hijacking the cell's own metabolism to introduce carbohydrate variants with altered properties. In this way, carbohydrate precursors carrying bioorthogonal handles can be introduced into the native glycans by permissive enzymes, allowing the subsequent attachment of reporter groups to detect carbohydrate incorporation and glycan production. While the technique was originally developed on eukaryotic cells, the interest in applying MOE to bacterial cells is steeply rising, and several bacterial glycans have now been targeted with unnatural carbohydrates (Tra and Dube, 2014; Clark et al., 2016).

In addition to the promising application of labeling bacterial glycans for visualization, the MOE technique can also be used to introduce monosaccharide analogues that inhibit the proper assembly of bacterial glycans. To this end, both substrate decoys, which act as surrogate glycan acceptor sites (Dimitroff et al., 2003; Metastasis et al., 2009; Gloster and Vocadlo, 2012; Rillahan et al., 2012; Villalobos et al., 2015), and chain-terminating carbohydrate analogues, which lack a specific hydroxyl group for elongation (Li et al., 2016) have been developed for different

bacterial strains. In a recent study, analogues of DiNAcBac, FucNAc, and DATDG were employed both as substrate decoys and inhibitors (**Figure 9**) to perturb glycan synthesis in *H. pylori* (Williams et al., 2020). The benzyl glycoside analogues BnBac, BnFucNAc, and BnDAT were synthesized as decoy substrates, and fluoro analogues F-Bac, F-FucNAc, and F-DAT were designed as chain-terminating inhibitors. Interestingly, treatment of *H. pylori* with BnBac, BnFucNAc, and F-DAT resulted in reduction of glycoprotein synthesis and defects in growth, biofilm formation, and motility. These functional defects could be largely reproduced in an isogenic *H. pylori* ΔGT mutant lacking a functional glycosylation system, proving that the MOE approach indeed has potential to be an antivirulence strategy. In addition, the analogues under study here also revealed bacteria-specific effects. In *C. jejuni*, none of the carbohydrate analogues impacted glycan biosynthesis or fitness, and only subtle changes were observed in the commensal *Bacteroides fragilis*. It will be interesting to test these carbohydrate analogues in animal models of infection and to understand their potential as narrow-spectrum antivirulence compounds.

DISCUSSION

Glycosylation is an intriguing feature of virtually all bacteria, and increasing amounts of evidence indicate that many bacteria rely on glycosylation for fitness and infection. As illustrated by the various examples in this review, especially pathogenic bacteria are often dependent on glycosylation of biomolecules related to virulence factors to successfully establish an infection. Whereas many virulence factors such as adhesins or flagella are glycosylated by internal GTs, exotoxins act as GTs themselves and actively modify molecular structures of the host organism to enable infection (Lu et al., 2015). Given the importance of virulence factors in the establishment of an infection, novel approaches that target glycosylation of virulence factors hold great promise as antibacterial strategy (Clatworthy et al., 2007). Several antivirulence agents have already been developed, and many are in (pre)clinical stages (Dickey et al., 2017); however, only few examples are specifically directed against bacterial glycans or glycosylation processes (*e.g.*, against TcdA/B; Dickey et al., 2017).

In this review, recent progress is highlighted in developing strategies to disturb and inhibit bacterial glycosylation enzymes and products, with a focus on antivirulence factors. While for some strategies the phenotypical effects are already validated on whole cells or infection models, others are still in the stage of proof of inhibition *ex vivo* (*e.g.*, on isolated enzymes). For instance, potent small-molecule inhibitors of diNAcBac biosynthesis in *C. jejuni* and inhibitors of GTs from *Neisseria* and *Haemophilus* have been developed, but they have not yet been tested or did not show a phenotypic effect in cell culture or *in vivo* models (De Schutter et al., 2017; Xu et al., 2017, 2018). A major challenge for small-molecule inhibitors of cytoplasmic targets, such as GTs or carbohydrate biosynthesis enzymes, is to pass the complex bacterial cell wall to gain cell entrance (Tiz et al., 2018). Indeed, most antivirulence drugs in advanced preclinical or clinical developmental stages act on surface-exposed or secreted virulence factors (Dickey et al., 2017). Various approaches have been developed to overcome the problem of cell wall permeability which include altering

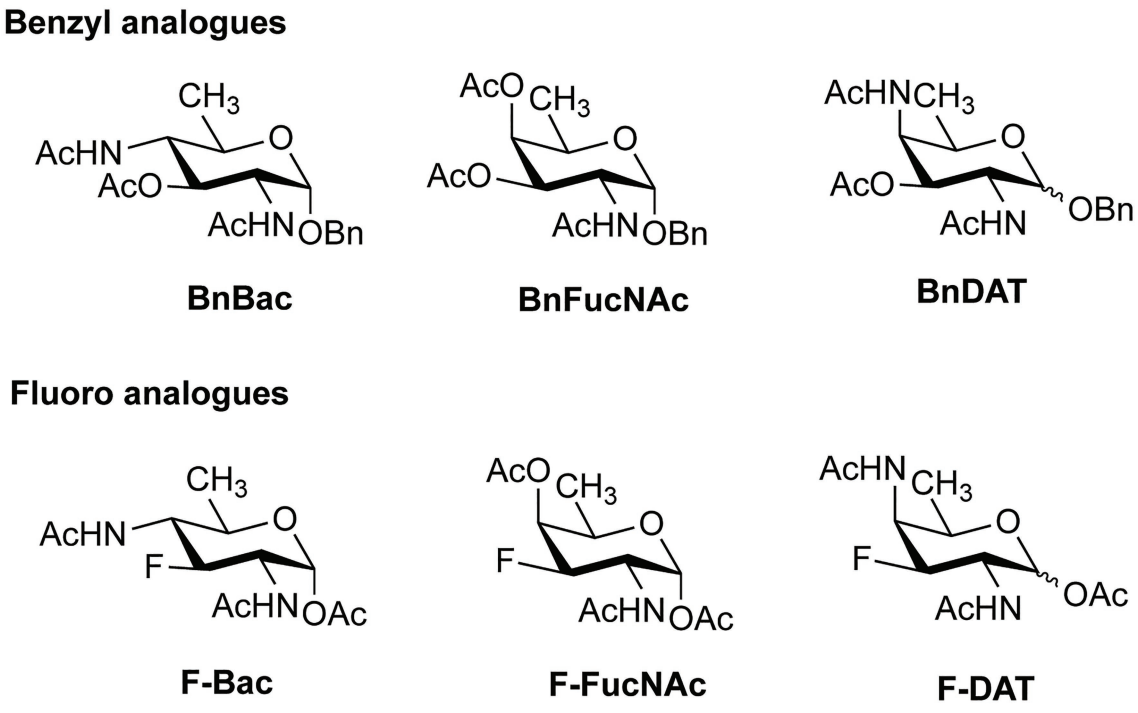

FIGURE 9 | Benzyl and fluoro analogues designed for metabolic inhibition of glycosylation.

of physicochemical properties of the drugs, coupling drugs to siderophores, inhibiting efflux pumps, and using liposomes as drug carriers (Tiz et al., 2018). However, there is not a common consensus about universal rules facilitating drug penetration yet (Tiz et al., 2018). In addition to the challenge of target localization, the generation of inhibitors against carbohydrate-active enzymes is itself a daunting task. The high hydrophilicity of carbohydrate substrates and pyrophosphate moieties in nucleotide sugars warrant a creative approach to generate inhibitors that are also able to arrive at the target location (Merino et al., 2016). In case of glycosyltransferases, also the complex mechanism, in which multiple substrates are involved, complicates this process. The concept of bisubstrate-analogue inhibitors is a promising strategy (Kajimoto and Node, 2009), as is the development of bacteria-specific iminosugars (Conforti and Marra, 2021). Future developments in this area will facilitate the generation of small-molecule inhibitors of glycosylation enzymes with better cell wall penetration properties.

Metabolic inhibitors of bacterial glycan biosynthesis hold a promise to selectively target specific bacteria and their virulence factors (Williams et al., 2020). As the MOE technique relies on the peracetylated monosaccharide analogues, the compounds can successfully pass the bacterial cell membrane. Interestingly, a recent study reveals that these peracetylated carbohydrates may suffer from non-enzymatic *S*-glycosylation in living (eukaryotic) cells (Qin et al., 2018). Additional experiments to further investigate this side effect are needed to profile the occurrence of protein labeling and the impact on both bacterial and eukaryotic cells.

The sheer number of different monosaccharides that are identified in bacteria (Imperiali, 2019), and the certainty that this number will increase over time, makes the development of strategies to target the enzymes involved and their respective products a highly promising strategy to tackle the challenge of antibiotic resistance.

AUTHOR CONTRIBUTIONS

LY and JF contributed to the organization and structure of the review. LY, MW, and JF contributed to the writing and critical evaluation of the article. All authors contributed to the article and approved the submitted version.

FUNDING

This work was financially supported by the Dutch Organization for Scientific Research (VENI 722.016.006) and the European Union through the Rosalind Franklin Fellowship COFUND project 60021 (both to MW).

REFERENCES

Abouelhadid, S., Raynes, J., Bui, T., Cuccui, J., and Wren, B. W. (2020). Characterization of posttranslationally modified multidrug efflux pumps reveals an unexpected link between glycosylation and antimicrobial resistance. *mBio* 11, 1–19. doi: 10.1128/ mBio.02604-20

Aktories, K., Schwan, C., and Jank, T. (2017). *Clostridium difficile* toxin biology. *Annu. Rev. Microbiol.* 71, 281–307. doi: 10.1146/annurev- micro-090816-093458

Alcalde-Rico, M., Hernando-Amado, S., Blanco, P., and Martínez, J. L. (2016). Multidrug efflux pumps at the crossroad between antibiotic resistance and bacterial virulence. *Front. Immunol.* 7:1483. doi: 10.3389/fmicb.2016.01483

Alphey, M. S., Pirrie, L., Torrie, L. S., Boulkeroua, W. A., Gardiner, M., Sarkar, A., et al. (2013). Allosteric competitive inhibitors of the glucose-1-phosphate thymidylyltransferase (RmlA) from *Pseudomonas aeruginosa*. *ACS Chem. Biol.* 8, 387–396. doi: 10.1021/cb300426u

Ambrosini, G., Adida, C., and Altieri, D. C. (1997). A novel anti-apoptosis gene, survivin, expressed in cancer and lymphoma. *Nat. Med.* 3, 917–921. doi: 10.1038/nm0897-917

Arshad, M., Goller, C. C., Pilla, D., Schoenen, F. J., and Seed, P. C. (2016). Threading the needle: small-molecule targeting of a xenobiotic receptor to ablate *Escherichia coli* polysaccharide capsule expression without altering antibiotic resistance. *J. Infect. Dis.* 213, 1330–1339. doi: 10.1093/infdis/jiv584

Azeredo, J., Azevedo, N. F., Briandet, R., Cerca, N., Costa, A. R., Desvaux, M., et al. (2017). Critical review on biofilm methods. *Crit. Rev. Microbiol.* 43, 313–351. doi: 10.1080/1040841X.2016.1208146

Azurmendi, H. F., Veeramachineni, V., Freese, S., Lichaa, F., Freedberg, D. I., and Vann, W. F. (2020). Chemical structure and genetic organization of the *E. coli* O6: K15 capsular polysaccharide. *Sci. Rep.* 10:12608. doi: 10.1038/s41598-020-69476-z

Bender, K. O., Garland, M., Ferreyra, J. A., Hryckowian, A. J., Child, M. A., Puri, A. W., et al. (2015). A small-molecule antivirulence agent for treating *Clostridium difficile* infection. *Sci. Transl. Med.* 7, 1–12. doi: 10.1126/scitranslmed.aac9103

Bensing, B. A., Gibson, B. W., and Sullam, P. M. (2004). The *Streptococcus gordonii* platelet binding protein GspB undergoes glycosylation independently of export. *J. Bacteriol.* 186, 638–645. doi: 10.1128/JB.186.3.638-645.2004

Benz, I., and Schmidt, M. A. (2001). Glycosylation with heptose residues mediated by the aah gene product is essential for adherence of the AIDA-I adhesin. *Mol. Microbiol.* 40, 1403–1413. doi: 10.1046/j.1365-2958.2001.02487.x

Bertozzi, C. R., and Saxon, E. (2000). Cell surface engineering by a modified Staudinger reaction. *Science* 287, 2007–2010. doi: 10.1126/science.287.5460.2007

Bhat, A. H., Maity, S., Giri, K., Ambatipudi, K., Bhat, A. H., Maity, S., et al. (2019). Protein glycosylation: sweet or bitter for bacterial pathogens? *Crit. Rev. Microbiol.* 45, 82–102. doi: 10.1080/1040841X.2018.1547681

Bouché, L., Panico, M., Hitchen, P., Binet, D., Sastre, F., Faulds-pain, A., et al. (2016). The type B flagellin of hypervirulent *Clostridium difficile* is modified with novel sulfonated peptidylamido-glycans. *J. Biol. Chem.* 291, 25439–25449. doi: 10.1074/jbc.M116.749481

Calvert, M. B., Jumde, V. R., and Titz, A. (2018). Pathoblockers or antivirulence drugs as a new option for the treatment of bacterial infections. *Beilstein J. Org. Chem.* 14, 2607–2617. doi: 10.3762/bjoc.14.239

Chagnot, C., Zorgani, M. A., Astruc, T., and Desvaux, M. (2013). Proteinaceous determinants of surface colonization in bacteria: bacterial adhesion and biofilm formation from a protein secretion perspective. *Front. Microbiol.* 4:303. doi: 10.3389/fmicb.2013.00303

Charbonneau, M. È., Girard, V., Nikolakakis, A., Campos, M., Berthiaume, F., Dumas, F., et al. (2007). O-linked glycosylation ensures the normal conformation of the autotransporter adhesin involved in diffuse adherence. *J. Bacteriol.* 189, 8880–8889. doi: 10.1128/JB.00969-07

Chatterjee, S. N., and Chaudhuri, K. (2003). Lipopolysaccharides of Vibrio cholerae I. Physical and chemical characterization. *Biochim. Biophys. Acta* 1639, 65–79. doi: 10.1016/j.bbadis.2003.08.004

Chaze, T., Guillot, A., Valot, B., Langella, O., Chamot-Rooke, J., Di Guilmi, A.-M., et al. (2014). O-glycosylation of the N -terminal region of the serine-rich adhesin Srr1 of Streptococcus agalactiae explored by mass spectrometry. *Mol. Cell. Proteomics* 13, 2168–2182. doi: 10.1074/mcp.M114.038075

Chen, Y., Seepersaud, R., Bensing, B. A., Sullam, P. M., and Rapoport, T. A. (2016). Mechanism of a cytosolic O -glycosyltransferase essential for the synthesis of a bacterial adhesion protein. *Proc. Natl. Acad. Sci. U. S. A.* 113, E1190–E1199. doi: 10.1073/pnas.1600494113

Clark, E. L., Emmadi, M., Krupp, K. L., Podilapu, A. R., Helble, J. D., Kulkarni, S. S., et al. (2016). Development of rare bacterial monosaccharide

analogs for metabolic glycan labeling in pathogenic bacteria. *ACS Chem. Biol.* 11, 3365–3373. doi: 10.1021/acschembio.6b00790

Clatworthy, A. E., Pierson, E., and Hung, D. T. (2007). Targeting virulence: a new paradigm for antimicrobial therapy. *Nat. Chem. Biol.* 3, 541–548. doi: 10.1038/nchembio.2007.24

Compain, P., and Martin, O. R. (2001). Carbohydrate mimetics-based glycosyltransferase inhibitors. *Bioorg. Med. Chem.* 9, 3077–3092. doi: 10.1016/S0968-0896(01)00176-6

Conforti, I., and Marra, A. (2021). Iminosugars as glycosyltransferase inhibitors. *Org. Biomol. Chem.* 19, 5439–5475. doi: 10.1039/D1OB00382H

Côté, J. P., Charbonneau, M. È., and Mourez, M. (2013). Glycosylation of the *Escherichia coli* TibA self-associating autotransporter influences the conformation and the functionality of the protein. *PLoS One* 8:e80739. doi: 10.1371/journal.pone.0080739

Craig, L., Pique, M. E., and Tainer, J. A. (2004). Type IV pilus structure and bacterial pathogenicity. *Nat. Rev. Microbiol.* 2, 363–378. doi: 10.1038/nrmicro885

Cress, B. F., Englaender, J. A., He, W., Kasper, D., Linhardt, R. J., and Koffas, M. A. G. (2014). Masquerading microbial pathogens: capsular polysaccharides mimic host-tissue molecules. *FEMS Microbiol. Rev.* 38, 660–697. doi: 10.1111/1574-6976.12056

De Leon, G. P., Elowe, N. H., Koteva, K. P., Valvano, M. A., and Wright, G. D. (2006). An in vitro screen of bacterial lipopolysaccharide biosynthetic enzymes identifies an inhibitor of ADP-heptose biosynthesis. *Chem. Biol.* 13, 437–441. doi: 10.1016/j.chembiol.2006.02.010

De Schutter, J. W., Morrison, J. P., Morrison, M. J., Ciulli, A., and Imperiali, B. (2017). Targeting bacillosamine biosynthesis in bacterial pathogens: development of inhibitors to a bacterial amino-sugar acetyltransferase from *Campylobacter jejuni*. *J. Med. Chem.* 60, 2099–2118. doi: 10.1021/acs.jmedchem.6b01869

Di Bella, S., Ascenzi, P., Siarakas, S., Petrosillo, N., and Masi, A. (2016). *Clostridium difficile* toxins A and B: insights into pathogenic properties and extraintestinal effects. *Toxins.* 8, 1–25. doi: 10.3390/toxins8050134

Dickey, S. W., Cheung, G. Y. C., and Otto, M. (2017). Different drugs for bad bugs: antivirulence strategies in the age of antibiotic resistance. *Nat. Rev. Drug Discov.* 16, 457–471. doi: 10.1038/nrd.2017.23

Dimitroff, C. J., Kupper, T. S., Sackstein, R., Dimitroff, C. J., Kupper, T. S., and Sackstein, R. (2003). Prevention of leukocyte migration to inflamed skin with a novel fluorosugar modifier of cutaneous lymphocyte-associated antigen. *J. Clin. Invest.* 112, 1008–1018. doi: 10.1172/JCI19220

Dubb, R. K., Nothaft, H., Beadle, B., Richards, M. R., and Szymanski, C. M. (2020). N-glycosylation of the CmeABC multidrug efflux pump is needed for optimal function in *Campylobacter jejuni*. *Glycobiology* 30, 105–119. doi: 10.1093/glycob/cwz082

El Qaidi, S., Zhu, C., McDonald, P., Roy, A., Maity, P. K., Rane, D., et al. (2018). High-throughput screening for bacterial glycosyltransferase inhibitors. *Front. Cell. Infect. Microbiol.* 8:435. doi: 10.3389/fcimb.2018.00435

Ema, M., Xu, Y., Gehrke, S., and Wagner, G. K. (2018). Identification of non-substrate-like glycosyltransferase inhibitors from library screening: pitfalls & hits. *Med. Chem. Commun.* 9, 131–137. doi: 10.1039/C7MD00550D

Esposito, D., Gu, R. A., Martino, L., Omari, K.El, Wagner, A., and Thurston, T. L. M. (2018). Structural basis for the glycosyltransferase activity of the *Salmonella* effector SseK3. *J. Biol. Chem.* 293, 5064–5078. doi: 10.1074/jbc.RA118.001796

Faulds-Pain, A., Twine, S. M., Vinogradov, E., Strong, P. C. R., Dell, A., Buckley, A. M., et al. (2014). The post-translational modification of the *Clostridium difficile* flagellin affects motility, cell surface properties and virulence. *Mol. Microbiol.* 94, 272–289. doi: 10.1111/mmi.12755

Ferrer-Espada, R., Shahrour, H., Pitts, B., Stewart, P. S., Sánchez-Gómez, S., and Martínez-de-Tejada, G. (2019). A permeability-increasing drug synergizes with bacterial efflux pump inhibitors and restores susceptibility to antibiotics in multi-drug resistant *Pseudomonas aeruginosa* strains. *Sci. Rep.* 9, 1–12. doi: 10.1038/s41598-019-39659-4

Flemming, H., Wingender, J., Szewzyk, U., Steinberg, P., and Rice, S. A. (2016). Biofilms: an emergent form of bacterial life. *Nat. Rev. Microbiol.* 14, 563–575. doi: 10.1038/nrmicro.2016.94

Gao, X., Wang, X., Pham, T. H., Feuerbacher, L. A., Lubos, M. L., Huang, M., et al. (2013). NleB, a bacterial effector with glycosyltransferase activity, targets GADPH function to inhibit NF-κB activation. *Cell Host Microbe* 13, 87–99. doi: 10.1016/j.chom.2012.11.010

Genth, H., Aktories, K., and Just, I. (1999). Monoglucosylation of RhoA at threonine 37 blocks cytosol-membrane cycling. *J. Biol. Chem.* 274, 29050–29056. doi: 10.1074/jbc.274.41.29050

Ghosh, A., Jayaraman, N., and Chatterji, D. (2020). Small-molecule inhibition of bacterial biofilm. *ACS Omega* 5, 3108–3115. doi: 10.1021/acsomega.9b03695

Gilbert, M., Karwaski, M. F., Bernatchez, S., Young, N. M., Taboada, E., Michniewicz, J., et al. (2002). The genetic bases for the variation in the lipo-oligosaccharide of the mucosal pathogen, *Campylobacter jejuni*. Biosynthesis of sialylated ganglioside mimics in the core oligosaccharide. *J. Biol. Chem.* 277, 327–337. doi: 10.1074/jbc.M108452200

Gloster, T. M., and Vocadlo, D. J. (2012). Developing inhibitors of glycan processing enzymes as tools for enabling glycobiology. *Nat. Chem. Biol.* 8, 683–694. doi: 10.1038/nchembio.1029

Godschalk, P. C. R., Heikema, A. P., Gilbert, M., Komagamine, T., Ang, C. W., Glerum, J., et al. (2004). The crucial role of *Campylobacter jejuni* genes in anti-ganglioside antibody induction in Guillain-Barré syndrome. *J. Clin. Invest.* 114, 1659–1665. doi: 10.1172/JCI200415707

Godschalk, P. C. R., Kuijf, M. L., Li, J., St. Michael, F., Ang, C. W., Jacobs, B. C., et al. (2007). Structural characterization of *Campylobacter jejuni* lipooligosaccharide outer cores associated with Guillain-Barré and Miller fisher syndromes. *Infect. Immun.* 75, 1245–1254. doi: 10.1128/IAI.00872-06

Goller, C. C., Arshad, M., Noah, J. W., Ananthan, S., Evans, C. W., Nebane, M., et al. (2014). Lifting the mask: identification of new small molecule inhibitors of uropathogenic *Escherichia coli* group 2 capsule biogenesis. *PLoS One* 9:e96054. doi: 10.1371/journal.pone.0096054

Goller, C. C., and Seed, P. C. (2010). High-throughput identification of chemical inhibitors of *E. coli* group 2 capsule biogenesis as anti-virulence agents. *PLoS One* 5:e11642. doi: 10.1371/journal.pone.0011642

Goodfellow, J. A., Bowes, T., Sheikh, K., Odaka, M., Halstead, S. K., Humphreys, P. D., et al. (2005). Overexpression of GD1a ganglioside sensitizes motor nerve terminals to anti-GD1a antibody-mediated injury in a model of acute motor axonal neuropathy. *J. Neurosci.* 25, 1620–1628. doi: 10.1523/JNEUROSCI.4279-04.2005

Goon, S., Kelly, J. F., Logan, S. M., Ewing, C. P., and Guerry, P. (2003). Pseudaminic acid, the major modification on Campylobacter flagellin, is synthesized via the Cj1293 gene. *Mol. Microbiol.* 50, 659–671. doi: 10.1046/j.1365-2958.2003.03725.x

Grass, S., Buscher, A. Z., Swords, W. E., Apicella, M. A., Barenkamp, S. J., Ozchlewski, N., et al. (2003). The haemophilus influenzae HMW1 adhesin is glycosylated in a process that requires HMW1C and phosphoglucomutase, an enzyme involved in lipooligosaccharide biosynthesis. *Mol. Microbiol.* 48, 737–751. doi: 10.1046/j.1365-2958.2003.03450.x

Grass, S., Lichti, C. F., Townsend, R. R., Gross, J., and St. Geme, J. W. (2010). The haemophilus influenzae HMW1c protein is a glycosyltransferase that transfers hexose residues to asparagine sites in the HMW1 adhesin. *PLoS Pathog.* 6:e1000919. doi: 10.1371/journal.ppat.1000919

Grass, S., and St Geme, J. W. (2000). Maturation and secretion of the non-typable haemophilus influenzae HMW1 adhesin: roles of the N-terminal and C-terminal domains. *Mol. Microbiol.* 36, 55–67. doi: 10.1046/j.1365-2958.2000.01812.x

Gross, J., Grass, S., Davis, A. E., Gilmore-erdmann, P., Townsend, R. R., St, J. W., et al. (2008). The haemophilus influenzae HMW1 adhesin is a glycoprotein with an unusual N-linked carbohydrate modification. *J. Biol. Chem.* 283, 26010–26015. doi: 10.1074/jbc.M801819200

Guerry, P., Ewing, C. P., Schirm, M., Lorenzo, M., Kelly, J., Pattarini, D., et al. (2006). Changes in flagellin glycosylation affect Campylobacter autoagglutination and virulence. *Mol. Cell* 60, 299–311. doi: 10.1111/j.1365-2958.2006.05100.x

Gulati, S., Cox, A., Lewis, L. A., St. Michael, F., Li, J., Boden, R., et al. (2005). Enhanced factor H binding to sialylated gonococci is restricted to the sialylated lacto-N-neotetraose lipooligosaccharide species: implications for serum resistance and evidence for a bifunctional lipooligosaccharide sialyltransferase in gonococci. *Infect. Immun.* 73, 7390–7397. doi: 10.1128/IAI.73.11.7390-7397.2005

Gulati, S., Schoenhofen, I. C., Lindhout-Djukic, T., Schur, M. J., Landig, C. S., Saha, S., et al. (2020). Therapeutic CMP-nonulosonates against multidrug-resistant *Neisseria gonorrhoeae*. *J. Immunol.* 204, 3283–3295. doi: 10.4049/jimmunol.1901398

Gulati, S., Schoenhofen, I. C., Whitfield, D. M., Cox, A. D., Li, J., St. Michael, F., et al. (2015). Utilizing CMP-sialic acid analogs to unravel *Neisseria gonorrhoeae* lipooligosaccharide-mediated complement resistance and design novel therapeutics. *PLoS Pathog.* 11:e1005290. doi: 10.1371/journal.ppat.1005290

Harding, C. M., Hennon, S. W., and Feldman, M. F. (2017). Uncovering the mechanisms of *Acinetobacter baumannii* virulence. *Nat. Rev. Microbiol.* 16, 91–102. doi: 10.1038/nrmicro.2017.148

Hartley, M. D., Morrison, M. J., Aas, F. E., Børud, B., Koomey, M., and Imperiali, B. (2011). Biochemical characterization of the O-linked glycosylation pathway in *Neisseria gonorrhoeae* responsible for biosynthesis of protein glycans containing N, N′-diacetylbacillosamine. *Biochemistry* 50, 4936–4948. doi: 10.1021/bi2003372

Harvey, H. A., Porat, N., Campbell, C. A., Jennings, M., Gibson, B. W., Phillips, N. J., et al. (2000). Gonococcal lipooligosaccharide is a ligand for the asialoglycoprotein receptor on human sperm. *Mol. Microbiol.* 36, 1059–1070. doi: 10.1046/j.1365-2958.2000.01938.x

Hegge, F. T., Hitchen, P. G., Aas, F. E., Kristiansen, H., Løvold, C., Egge-Jacobsen, W., et al. (2004). Unique modifications with phosphocholine and phosphoethanolamine define alternate antigenic forms of *Neisseria gonorrhoeae* type IV pili. *Proc. Natl. Acad. Sci. U. S. A.* 101, 10798–10803. doi: 10.1073/pnas.0402397101

Hengzhuang, W., Song, Z., Ciofu, O., Onsøyen, E., Rye, P. D., and Høiby, N. (2016). Biofilm in a murine lung infection model. *Antimicrob. Agents Chemother.* 60, 2620–2626. doi: 10.1128/AAC.01721-15

Hopf, P. S., Ford, R. S., Zebian, N., Merkx-Jacques, A., Vijayakumar, S., Ratnayake, D., et al. (2011). Protein glycosylation in helicobacter pylori: Beyond the flagellins? *PLoS One* 6:e25722. doi: 10.1371/journal.pone.0025722

Horzempa, J., Held, T. K., Cross, A. S., Furst, D., Qutyan, M., Neely, A. N., et al. (2008). Immunization with a *Pseudomonas aeruginosa* 1244 pilin provides O-antigen-specific protection. *Clin. Vaccine Immunol.* 15, 590–597. doi: 10.1128/CVI.00476-07

Hsieh, Y.-C., Wang, S.-H., Chen, Y.-Y., Lin, T.-L., Shie, S.-S., Huang, C.-T., et al. (2020). Association of capsular types with carbapenem resistance, disease severity, and mortality in *Acinetobacter baumannii*. *Emerg. Microbes Infect.* 9, 2094–2104. doi: 10.1080/22221751.2020.1822757

Huszczynski, S. M., Lam, J. S., and Khursigara, C. M. (2020). The role of *Pseudomonas aeruginosa* lipopolysaccharide in bacterial pathogenesis and physiology. *Pathogens* 9:6. doi: 10.3390/pathogens9010006

Imperiali, B. (2019). Bacterial carbohydrate diversity – a brave new world. *Curr. Opin. Chem. Biol.* 53, 1–8. doi: 10.1016/j.cbpa.2019.04.026

Janssen, R., Krogfelt, K. A., Cawthraw, S. A., Van Pelt, W., Wagenaar, J. A., and Owen, R. J. (2008). Host-pathogen interactions in Campylobacter infections: the host perspective. *Clin. Microbiol.* 21, 505–518. doi: 10.1128/CMR.00055-07

Jasti, A. K., Selmi, C., Sarmiento-monroy, J. C., Vega, D. A., Anaya, M., Gershwin, M. E., et al. (2016). Guillain-Barré syndrome: causes, immunopathogenic mechanisms and treatment. *Expert Rev. Clin. Immunol.* 12, 1175–1189. doi: 10.1080/1744666X.2016.1193006

Javed, M. A., Poshtiban, S., Arutyunov, D., Evoy, S., and Szymanski, C. M. (2013). Bacteriophage receptor binding protein based assays for the simultaneous detection of *Campylobacter jejuni* and *Campylobacter coli*. *PLoS One* 8:e69770. doi: 10.1371/journal.pone.0069770

Javed, M. A., Van Alphen, L. B., Sacher, J., Ding, W., Kelly, J., Nargang, C., et al. (2015a). A receptor-binding protein of *Campylobacter jejuni* bacteriophage NCTC 12673 recognizes flagellin glycosylated with acetamidino-modified pseudaminic acid. *Mol. Microbiol.* 95, 101–115. doi: 10.1111/mmi.12849

Javed, M. A., Sacher, J. C., Van Alphen, L. B., Patry, R. T., and Szymanski, C. M. (2015b). A flagellar glycan-specific protein encoded by Campylobacter phages inhibits host cell growth. *Viruses* 7, 6661–6674. doi: 10.3390/v7122964

Jen, F. E.-C., Ketterer, M. R., Semchenko, E. A., Day, C. J., Seib, K. L., Apicella, M. A., et al. (2021). The Lst Sialyltransferase of *Neisseria gonorrhoeae* can transfer Keto-Deoxyoctanoate as the terminal sugar of Lipooligosaccharide: a Glyco-Achilles heel that provides a new strategy for vaccines to prevent gonorrhea. *mBio* 12:e03666-20. doi: 10.1128/mBio.03666-20

Jennings, M. P., Jen, F. E. C., Roddam, L. F., Apicella, M. A., and Edwards, J. L. (2011). *Neisseria gonorrhoeae* pilin glycan contributes to CR3 activation during challenge of primary cervical epithelial cells. *Cell. Microbiol.* 13, 885–896. doi: 10.1111/j.1462-5822.2011.01586.x

Jennings, M. P., Virji, M., Evans, D., Foster, V., Srikhanta, Y. N., Steeghs, L., et al. (1998). Identification of a novel gene involved in pilin glycosylation in *Neisseria meningitidis*. *Mol. Microbiol.* 29, 975–984. doi: 10.1046/j.1365-2958.1998.00962.x

Just, I., Selzer, J., Wilm, M., Eichel-Streiber, C.Von, Mann, M., and Aktories, K. (1995a). Glucosylation of rho proteins by *Clostridium difficile* toxin B. *Nature* 375, 500–503. doi: 10.1038/375500a0

Just, I., Wilm, M., Selzer, J., Rex, G., Von Eichel-Streiber, C., Mann, M., et al. (1995b). The enterotoxin from *Clostridium difficile* (ToxA) monoglucosylates the rho proteins. *J. Biol. Chem.* 270, 13932–13936. doi: 10.1074/jbc.270.23.13932

Kajimoto, T., and Node, M. (2009). Synthesis of glycosyltransferase inhibitors. *Synthesis (Stuttg)* 4, 3179–3210. doi: 10.1055/s-0029-1216976

Kanipes, M. I., Holder, L. C., Corcoran, A. T., Moran, A. P., and Guerry, P. (2004). A deep-rough mutant of *Campylobacter jejuni* 81-176 is noninvasive for intestinal epithelial cells. *Infect. Immun.* 72, 2452–2455. doi: 10.1128/IAI.72.4.2452-2455.2004

Kanipes, M. I., Papp-Szabo, E., Guerry, P., and Monteiro, M. A. (2006). Mutation of waaC, encoding heptosyltransferase I in *Campylobacter jejuni* 81-176, affects the structure of both lipooligosaccharide and capsular carbohydrate. *J. Bacteriol.* 188, 3273–3279. doi: 10.1128/JB.188.9.3273-3279.2006

Kasimova, A. A., Arbatsky, N. P., Tickner, J., Kenyon, J. J., Hall, R. M., Shneider, M. M., et al. (2021). *Acinetobacter baumannii* K106 and K112: two structurally and genetically related 6-Deoxy-l-talose-containing capsular polysaccharides K83 K11. *Int. J. Mol. Sci.* 22, 1–13. doi: 10.3390/ijms22115641

Kayser, H., Zeitler, R., Kannicht, C., Grunow, D., Nuck, R., and Reutter, W. (1992). Biosynthesis of a nonphysiological sialic acid in different rat organs, using N-Propanoyl-D-hexosamines as precursors. *J. Biol. Chem.* 267, 16934–16938. doi: 10.1016/S0021-9258(18)41874-1

Keeney, K. M., Yurist-Doutsch, S., Arrieta, M.-C., and Finlay, B. B. (2014). Effects of antibiotics on human microbiota and subsequent disease. *Annu. Rev. Microbiol.* 68, 217–235. doi: 10.1146/annurev-micro-091313-103456

Kenyon, J. J., Shashkov, A. S., Senchenkova, N., Shneider, M. M., Liu, B., Popova, A. V., et al. (2017). *Acinetobacter baumannii* K11 and K83 capsular polysaccharides have the same 6-deoxy-l-talose-containing pentasaccharide K units but different linkages between the K units. *Int. J. Biol. Macromol.* 103, 648–655. doi: 10.1016/j.ijbiomac.2017.05.082

Kim, S., Jo, S., Kim, M., Kam, H., and Shin, D. H. (2021a). Inhibition of D-glycero-β-D-manno-heptose 1-phosphate adenylyltransferase from *Burkholderia pseudomallei* by epigallocatechin gallate and myricetin. *Biochem. J.* 478, 235–245. doi: 10.1042/BCJ20200677

Kim, S., Jo, S., Kim, M., and Shin, D. H. (2021b). A study of inhibitors of d-glycero-β-d-manno-heptose-1-phosphate adenylyltransferase from *Burkholderia pseudomallei* as a potential antibiotic target. *J. Enzyme Inhib. Med. Chem.* 36, 776–784. doi: 10.1080/14756366.2021.1900166

Klena, J. D., Gray, S. A., and Konkel, M. E. (1998). Cloning, sequencing, and characterization of the lipopolysaccharide biosynthetic enzyme heptosyltransferase I gene (waaC) from *Campylobacter jejuni* and *Campylobacter coli*. *Gene* 222, 177–185. doi: 10.1016/S0378-1119(98)00501-0

Kneidinger, B., Marolda, C., Graninger, M., Zamyatina, A., McArthur, F., Kosma, P., et al. (2002). Biosynthesis pathway of ADP-L-glycero-beta-D-manno-heptose in *Escherichia coli*. *J. Bacteriol.* 184, 363–369. doi: 10.1128/JB.184.2.363-369.2002

Kuehne, S. A., Cartman, S. T., Heap, J. T., Kelly, M. L., Cockayne, A., and Minton, N. P. (2010). The role of toxin A and toxin B in *Clostridium difficile* infection. *Nature* 467, 711–714. doi: 10.1038/nature09397

Kunduru, B. R., Nair, S. A., and Rathinavelan, T. (2016). EK3D: an *E. coli* K antigen 3-dimensional structure database. *Nucleic Acids Res.* 44, 675–681. doi: 10.1093/nar/gkv1313

Lam, J. S., Taylor, V. L., Islam, S. T., Hao, Y., Kocíncová, D., and Ohman, D. (2011). Genetic and functional diversity of *Pseudomonas aeruginosa* lipopolysaccharide. *Front. Microbiol.* 2:118. doi: 10.3389/fmicb.2011.00118

Letourneau, J. J., Stroke, I. L., Hilbert, D. W., Sturzenbecker, L. J., Marinelli, B. A., Quintero, J. G., et al. (2018). Identification and initial optimization of inhibitors of *Clostridium difficile* (C. difficile) toxin B (TcdB). *Bioorg. Med. Chem. Lett.* 28, 756–761. doi: 10.1016/j.bmcl.2018.01.005

Leyton, D. L., Rossiter, A. E., and Henderson, I. R. (2012). From self sufficiency to dependence: mechanisms and factors important for autotransporter biogenesis. *Nat. Rev. Microbiol.* 10, 213–225. doi: 10.1038/nrmicro2733

Li, Y., Huang, X., Li, J., Zeng, L., Zhu, F., and Hu, L. (2014). Both GtfA and GtfB are required for SraP glycosylation in *Staphylococcus aureus*. *Curr. Microbiol.* 69, 121–126. doi: 10.1007/s00284-014-0563-2

Li, J., Wang, J., Wen, L., Zhu, H., Li, S., Huang, K., et al. (2016). An OGA-resistant probe allows specific visualization and accurate identification of O-GlcNAc-modified proteins in cells. *ACS Chem. Biol.* 11, 3002–3006. doi: 10.1021/acschembio.6b00678

Li, S., Zhang, L., Yao, Q., Li, L., Dong, N., Rong, J., et al. (2013). Pathogen blocks host death receptor signalling by arginine GlcNAcylation of death domains. *Nature* 501, 242–246. doi: 10.1038/nature12436

Lin, H., Paff, M. L., Molineux, I. J., and Bull, J. J. (2017). Therapeutic application of phage capsule depolymerases against K1, K5, and K30 capsulated *E. coli* in mice. *Front. Microbiol.* 8:2257. doi: 10.3389/fmicb.2017.02257

Linton, D., Karlyshev, A. V., Hitchen, P. G., Morris, H. R., Dell, A., Gregson, N. A., et al. (2000). Multiple N-acetyl neuraminic acid synthetase (neuB) genes in *Campylobacter jejuni*: identification and characterization of the gene involved in sialylation of lipo-oligosaccharide. *Mol. Microbiol.* 35, 1120–1134. doi: 10.1046/j.1365-2958.2000.01780.x

Lizcano, A., Sanchez, C. J., and Orihuela, C. J. (2012). A role for glycosylated serine-rich repeat proteins in gram-positive bacterial pathogenesis. *Mol Oral Microbiol* 27, 257–269. doi: 10.1111/j.2041-1014.2012.00653.x

Lodowska, J., Wolny, D., and Węglarz, L. (2013). The sugar 3-deoxy-D-manno-oct-2-ulosonic acid (Kdo) as a characteristic component of bacterial endotoxin – a review of its biosynthesis, function, and placement in the lipopolysaccharide core. *Can. J. Microbiol.* 59, 645–655. doi: 10.1139/cjm-2013-0490

Logan, S. M. (2006). Flagellar glycosylation – a new component of the motility repertoire? *Microbiology* 152, 1249–1262. doi: 10.1099/mic.0.28735-0

Logan, S. M., Hui, J. P. M., Vinogradov, E., Aubry, A. J., Melanson, J. E., Kelly, J. F., et al. (2009). Identification of novel carbohydrate modifications on *Campylobacter jejuni* 11168 flagellin using metabolomics-based approaches. *FEBS J.* 276, 1014–1023. doi: 10.1111/j.1742-4658.2008.06840.x

Loranger, M. W., Forget, S. M., McCormick, N. E., Syvitski, R. T., and Jakeman, D. L. (2013). Synthesis and evaluation of L-rhamnose 1C-phosphonates as nucleotidylyltransferase inhibitors. *J. Org. Chem.* 78, 9822–9833. doi: 10.1021/jo401542s

Lu, Q., Li, S., and Shao, F. (2015). Sweet talk: protein glycosylation in bacterial interaction with the host. *Trends Microbiol.* 23, 630–641. doi: 10.1016/j.tim.2015.07.003

Lu, Q., Yao, Q., Xu, Y., Li, L., Li, S., Liu, Y., et al. (2014). An iron-containing dodecameric heptosyltransferase family modifies bacterial autotransporters in pathogenesis. *Cell Host Microbe* 16, 351–363. doi: 10.1016/j.chom.2014.08.008

Mahal, L. K., Yarema, K. J., and Bertozzi, C. R. (1997). Engineering chemical reactivity on cell surfaces through oligosaccharide biosynthesis. *Science* 276, 1–5. doi: 10.1126/science.276.5315.1125

Mandrell, R. E., Griffiss, J. M., and Machers, B. A. (1988). Lipooligosaccharides (LOS) of *Neisseria gonorrhoeae* and *Neisseria meningitidis* have components that are immunochemically similar to precursors of human blood group antigens carbohydrate sequence specificity of the mouse monoclonal antibodies that recogniz. *J. Exp. Med.* 168, 107–126. doi: 10.1084/jem.168.1.107

Mandrell, R. E., Griffiss, J. M., Smith, H., and Cole, J. A. (1993). Distribution of a lipooligosaccharide-specific sialyltransferase in pathogenic and non-pathogenic Neisseria. *Microb. Pathog.* 14, 315–327. doi: 10.1006/mpat.1993.1031

Mandrell, R. E., Lesse, A. J., Sugai, J. V., Shero, M., Griffiss, J. M., Cole, J. A., et al. (1990). In vitro and in vivo modification of *Neisseria gonorrhoeae* lipooligosaccharide epitope structure by sialylation. *J. Exp. Med.* 171, 1649–1664. doi: 10.1084/jem.171.5.1649

Marshall, R. L., Lloyd, G. S., Lawler, A. J., Element, S. J., Kaur, J., Ciusa, L., et al. (2020). New multidrug efflux inhibitors for gram-negative bacteria. *mBio* 11:e01340-20. doi: 10.1128/mBio.01340-20

McGee, Z. A., and Stephens, D. S. (1984). Common pathways of invasion of mucosal barriers by *Neisseria gonorrhoeae* and *Neisseria meningitidis*. *Surv. Synth. Pathol. Res.* 3, 1–10

Meeks, M. D., Saksena, R., Ma, X., Wade, T. K., Taylor, R. K., and Wade, W. F. (2004). Synthetic fragments of Vibrio cholerae O1 Inaba O-specific polysaccharide bound to a protein carrier are immunogenic in mice but do not induce protective antibodies. *Infect. Immun.* 72, 4090–4101. doi: 10.1128/IAI.72.7.4090-4101.2004

Ménard, R., Schoenhofen, I. C., Tao, L., Aubry, A., Bouchard, P., Reid, C. W., et al. (2014). Small-molecule inhibitors of the pseudaminic acid biosynthetic pathway: targeting motility as a key bacterial virulence factor. *Antimicrob. Agents Chemother.* 58, 7430–7440. doi: 10.1128/AAC.03858-14

Merino, P., Delso, I., Tejero, T., Ghirardello, M., and Juste-Navarro, V. (2016). Nucleoside diphosphate sugar analogues that target glycosyltransferases. *Asian J. Org. Chem.* 5, 1413–1427. doi: 10.1002/ajoc.201600396

Merino, S., and Tomás, J. M. (2014). Gram-negative flagella glycosylation. *Int. J. Mol. Sci.* 15, 2840–2857. doi: 10.3390/ijms15022840

Metastasis, T., Brown, J. R., Yang, F., Sinha, A., Ramakrishnan, B., Tor, Y., et al. (2009). Deoxygenated disaccharide analogs as specific inhibitors of 1–4-galactosyltransferase 1 and selectin-mediated. *J. Biol. Chem.* 284, 4952–4959. doi: 10.1074/jbc.M805782200

Mistou, M., Sutcliffe, I. C., and Van Sorge, N. M. (2016). Bacterial glycobiology: rhamnose-containing cell wall polysaccharides in gram-positive bacteria. *FEMS Microbiol. Rev.* 40, 464–479. doi: 10.1093/femsre/fuw006

Morrison, M. J., and Imperiali, B. (2014). The renaissance of bacillosamine and its derivatives: pathway characterization and implications in pathogenicity. *Biochemistry* 53, 624–638. doi: 10.1021/bi401546r

Mortensen, N. P., Kuijf, M. L., Ang, C. W., Schiellerup, P., Krogfelt, K. A., Jacobs, B. C., et al. (2009). Sialylation of *Campylobacter jejuni* lipo-oligosaccharides is associated with severe gastro-enteritis and reactive arthritis. *Microbes Infect.* 11, 988–994. doi: 10.1016/j.micinf.2009.07.004

Nachamkin, I., Liu, J., Li, M., Ung, H., Moran, A. P., Prendergast, M. M., et al. (2002). *Campylobacter jejuni* from patients with Guillain-Barré syndrome preferentially expresses a GD1a -Like epitope. *Infect. Immun.* 70, 5299–5303. doi: 10.1128/IAI.70.9.5299-5303.2002

Nakahara, T., Takeuchi, M., Kinoyama, I., Minematsu, T., Shirasuna, K., Matsuhisa, A., et al. (2007). YM155, a novel small-molecule survivin suppressant, induces regression of established human hormone-refractory prostate tumor xenografts. *Cancer Res.* 67, 8014–8021. doi: 10.1158/0008-5472.CAN-07-1343

Navalkele, B. D., and Chopra, T. (2018). Bezlotoxumab: an emerging monoclonal antibody therapy for prevention of recurrent *Clostridium difficile* infection. *Biol. Targets Ther.* 12, 11–21. doi: 10.2147/BTT.S127099

Orth, P., Xiao, L., Hernandez, L. D., Reichert, P., Sheth, P. R., Beaumont, M., et al. (2014). Mechanism of action and epitopes of *Clostridium difficile* toxin B-neutralizing antibody bezlotoxumab revealed by X-ray crystallography. *J. Biol. Chem.* 289, 18008–18021. doi: 10.1074/jbc.M114.560748

Packiam, M., Shell, D. M., Liu, S. V., Liu, Y., Mcgee, D. J., Srivastava, R., et al. (2006). Differential expression and transcriptional analysis of the alpha-2,3-sialyltransferase gene in pathogenic Neisseria spp. *Infect. Immun.* 74, 2637–2650. doi: 10.1128/IAI.74.5.2637-2650.2006

Park, J. B., Kim, Y. H., Yoo, Y., Kim, J., Jun, S. H., Cho, J. W., et al. (2018). Structural basis for arginine glycosylation of host substrates by bacterial effector proteins. *Nat. Commun.* 9:4283. doi: 10.1038/s41467-018-06680-6

Park, J. T., and Strominger, J. L. (1957). Mode of action of penicillin: biochemical basis for the mechanism of action of penicillin and for its selective toxicity. *Science* 125, 99–101. doi: 10.1126/science.125.3238.99

Patel, P., Marrs, C. F., Mattick, J. S., Ruehl, W. W., Taylor, R. K., and Koomey, M. (1991). Shared antigenicity and immunogenicity of type 4 pilins expressed by *Pseudomonas aeruginosa*, Moraxella bovis, *Neisseria gonorrhoeae*, Dichelobacter nodosus, and Vibrio cholerae. *Infect. Immun.* 59, 4674–4676. doi: 10.1128/iai.59.12.4674-4676.1991

Pearson, J. S., Giogha, C., Ong, S. Y., Kennedy, C. L., Kelly, M., Robinson, K. S., et al. (2013). A type III effector antagonizes death receptor signalling during bacterial gut infection. *Nature* 501, 247–251. doi: 10.1038/nature12524

Perkins, H. R. (1969). Specificity of combination between mucopeptide precursors and vancomycin or ristocetin. *Biochem. J.* 111, 195–205. doi: 10.1042/bj1110195

Pinto, R. M., Soares, F. A., Reis, S., Nunes, C., and Van Dijck, P. (2020). Innovative strategies toward the disassembly of the EPS matrix in bacterial biofilms. *Front. Microbiol.* 11:952. doi: 10.3389/fmicb.2020.00952

Poole, J., Day, C. J., Itzstein, M.Von, Paton, J. C., and Jennings, M. P. (2018). Glycointeractions in bacterial pathogenesis. *Nat. Rev. Microbiol.* 16, 440–452. doi: 10.1038/s41579-018-0007-2

Powell, L. C., Pritchard, M. F., Ferguson, E. L., Powell, K. A., Patel, S. U., Rye, P. D., et al. (2018). Targeted disruption of the extracellular polymeric network of *Pseudomonas aeruginosa* bio fi lms by alginate oligosaccharides. *Biofilms Microbiomes* 4:13. doi: 10.1038/s41522-018-0056-3

Power, P. M., Roddam, L. F., Rutter, K., Fitzpatrick, S. Z., Srikhanta, Y. N., and Jennings, M. P. (2003). Genetic characterization of pilin glycosylation and phase variation in *Neisseria meningitidis*. *Mol. Microbiol.* 49, 833–847. doi: 10.1046/j.1365-2958.2003.03602.x

Preston, A., Mandrell, R. E., Gibson, B. W., and Apicella, M. A. (1996). The lipooligosaccharides of pathogenic gram-negative bacteria. *Crit. Rev. Microbiol.* 22, 139–180. doi: 10.3109/10408419609106458

Qin, W., Qin, K., Fan, X., Peng, L., Hong, W., Zhu, Y., et al. (2018). Artificial cysteine S-glycosylation induced by per-O-acetylated unnatural monosaccharides during metabolic glycan labeling. *Angew. Chem.* 130, 1835–1838. doi: 10.1002/ange.201711710

Ram, B. S., Sharma, A. K., Simpson, S. D., Gulati, S., Mcquillen, D. P., Pangburn, M. K., et al. (1998). A novel sialic acid binding site on factor H mediates serum resistance of sialylated *Neisseria gonorrhoeae*. *J. Exp. Med.* 187, 743–752. doi: 10.1084/jem.187.5.743

Ram, S., Shaughnessy, J., De Oliveira, R. B., Lewis, L. A., Gulati, S., and Rice, P. A. (2017). Gonococcal lipooligosaccharide sialylation: virulence factor and target for novel immunotherapeutics. *Pathog. Dis.* 75, 1–13. doi: 10.1093/femspd/ftx049

Rempe, K. A., Spruce, L. A., Porsch, E. A., Seeholzer, S. H., Nørskov-Lauritsen, N., and St. Geme, J. W. (2015). Unconventional N-linked glycosylation promotes trimeric autotransporter function in Kingella kingae and Aggregatibacter aphrophilus. *mBio* 6:e01206-15. doi: 10.1128/mBio.01206-15

Ricklin, D., Hajishengallis, G., Yang, K., and Lambris, J. D. (2010). Complement: a key system for immune surveillance and homeostasis. *Nat. Immunol.* 11, 785–797. doi: 10.1038/ni.1923

Rillahan, C. D., Antonopoulos, A., Lefort, C. T., Sonon, R., Azadi, P., Ley, K., et al. (2012). Global metabolic inhibitors of sialyl- and fucosyltransferases remodel the glycome. *Nat. Chem. Biol.* 8, 6–13. doi: 10.1038/nchembio.999

Rodrigues, L., Cravo, P., and Viveiros, M. (2020). Efflux pump inhibitors as a promising adjunct therapy against drug resistant tuberculosis: a new strategy to revisit mycobacterial targets and repurpose old drugs. *Expert Rev. Anti-Infect. Ther.* 18, 741–757. doi: 10.1080/14787210.2020.1760845

Rogiers, O., Holtappels, M., Siala, W., Lamkanfi, M., Lagrou, K., Van Dijck, P., et al. (2018). Anidulafungin increases the antibacterial activity of tigecycline in polymicrobial Candida albicans/*Staphylococcus aureus* biofilms on intraperitoneally implanted foreign bodies. *J. Antimicrob. Chemother.* 73, 2806–2814. doi: 10.1093/jac/dky246

Sacher, J. C., Shajahan, A., Butcher, J., Patry, R. T., Flint, A., Hendrixson, D. R., et al. (2020). Binding of phage-encoded FlaGrab to motile *Campylobacter jejuni* flagella inhibits growth, downregulates energy metabolism, and requires specific flagellar glycans. *Front. Microbiol.* 11:397. doi: 10.3389/fmicb.2020.00397

Sastalla, I., Monack, D. M., and Kubatzky, K. F. (2016). Editorial: bacterial exotoxins: how bacteria fight the immune system. *Front. Immunol.* 7:300. doi: 10.3389/fimmu.2016.00300

Schirm, M., Schoenhofen, I. C., Logan, S. M., Waldron, K. C., and Thibault, P. (2005). Identification of unusual bacterial glycosylation by tandem mass spectrometry analyses of intact proteins. *Anal. Chem.* 77, 7774–7782. doi: 10.1021/ac051316y

Schirm, M., Soo, E. C., Aubry, A. J., Austin, J., Thibault, P., and Logan, S. M. (2003). Structural, genetic and functional characterization of the flagellin glycosylation process in *Helicobacter pylori*. *Mol. Microbiol.* 48, 1579–1592. doi: 10.1046/j.1365-2958.2003.03527.x

Schoenhofen, I. C., Lunin, V. V., Julien, J., Li, Y., Ajamian, E., Matte, A., et al. (2006). Structural and functional characterization of PseC, an aminotransferase involved in the biosynthesis of pseudaminic acid, an essential flagellar modification in *Helicobacter pylori*. *J. Biol. Chem.* 281, 8907–8916. doi: 10.1074/jbc.M512987200

Sehr, P., Joseph, G., Genth, H., Just, I., Pick, E., and Aktories, K. (1998). Glucosylation and ADP ribosylation of rho proteins: effects on nucleotide binding, GTPase activity, and effector coupling. *Biochemistry* 37, 5296–5304. doi: 10.1021/bi972592c

Sharma, D., Misba, L., and Khan, A. U. (2019). Antibiotics versus biofilm: an emerging battleground in microbial communities. *Antimicrob. Resist. Infect. Control* 8, 1–10. doi: 10.1186/s13756-019-0533-3

Siala, W., Kucharíková, S., Braem, A., Vleugels, J., Tulkens, P. M., Mingeot-Leclercq, M.-P., et al. (2016). The antifungal caspofungin increases fluoroquinolone activity against staphylococcus. *Nat. Commun.* 7:13286. doi: 10.1038/ncomms13286

Singh, J. K., Adams, F. G., and Brown, M. H. (2019). Diversity and function of capsular polysaccharide in *Acinetobacter baumannii*. *Front. Microbiol.* 9:3301. doi: 10.3389/fmicb.2018.03301

Singh, A., Arutyunov, D., Mcdermott, M. T., Szymanski, C. M., and Evoy, S. (2011). Specific detection of *Campylobacter jejuni* using the bacteriophage NCTC 12673 receptor binding protein as a probe. *Analyst* 136, 4780–4786. doi: 10.1039/c1an15547d

Singh, A., Arutyunov, D., Szymanski, M., and Evoy, S. (2012). Bacteriophage based probes for pathogen detection. *Analyst* 137, 3405–3421. doi: 10.1039/c2an35371g

Song, W., Ma, L., Chen, R., and Stein, D. C. (2000). Role of lipooligosaccharide in Opa-independent invasion of *Neisseria gonorrhoeae* into human epithelial cells. *J. Exp. Med.* 191, 949–959. doi: 10.1084/jem.191.6.949

St Geme, J. W., Falkow, S., and Barenkamp, S. J. (1993). High-molecular-weight proteins of nontypable haemophilus influenzae mediate attachment to human epithelial cells. *Proc. Natl. Acad. Sci. U. S. A.* 90, 2875–2879. doi: 10.1073/pnas.90.7.2875

Stroke, I. L., Letourneau, J. J., Miller, T. E., Xu, Y., Pechik, I., Savoly, D. R., et al. (2018). Treatment of *Clostridium difficile* infection with a small-molecule inhibitor of toxin UDP-glucose hydrolysis activity. *Antimicrob. Agents Chemother.* 62, 1–12. doi: 10.1128/AAC.00107-18

Swanson, J. (1973). Studies on gonococcus infection: IV. Pill: their role in attachment of gonococci to tissue culture cells. *J. Exp. Med.* 137, 571–589. doi: 10.1084/jem.137.3.571

Tam, J., Hamza, T., Ma, B., Chen, K., Beilhartz, G. L., Ravel, J., et al. (2018). Host-targeted niclosamide inhibits *C. difficile* virulence and prevents disease in mice without disrupting the gut microbiota. *Nat. Commun.* 9, 1–11. doi: 10.1038/s41467-018-07705-w

Tedaldi, L., and Wagner, G. K. (2014). Beyond substrate analogues: new inhibitor chemotypes for glycosyltransferases. *Med. Chem. Commun.* 5, 1106–1125. doi: 10.1039/C4MD00086B

Thibault, P., Logan, S. M., Kelly, J. F., Brisson, J. R., Ewing, C. P., Trust, T. J., et al. (2001). Identification of the carbohydrate moieties and glycosylation motifs in *Campylobacter jejuni* flagellin. *J. Biol. Chem.* 276, 34862–34870. doi: 10.1074/jbc.M104529200

Tiz, D. B., Kikelj, D., and Zidar, N. (2018). Overcoming problems of poor drug penetration into bacteria: challenges and strategies for medicinal chemists. *Expert Opin. Drug Discov.* 13, 497–507. doi: 10.1080/17460441.2018.1455660

Tra, V. N., and Dube, D. H. (2014). Glycans in pathogenic bacteria-potential for targeted covalent therapeutics and imaging agents. *Chem. Commun.* 50, 4659–4673. doi: 10.1039/C4CC00660G

Tsai, C.-M., and Civin, C. I. (1991). Eight lipooligosaccharides of *Neisseria meningitidis* react with. *Infect. Immun.* 59, 3604–3609. doi: 10.1128/iai.59.10.3604-3609.1991

Twine, S. M., Reid, C. W., Aubry, A., Mcmullin, D. R., Fulton, K. M., Austin, J., et al. (2009). Motility and flagellar glycosylation in *Clostridium difficile*. *J. Bacteriol.* 191, 7050–7062. doi: 10.1128/JB.00861-09

Tytgat, H. L. P., and Lebeer, S. (2014). The sweet tooth of bacteria: common themes in bacterial glycoconjugates. *Microbiol. Mol. Biol. Rev.* 78, 372–417. doi: 10.1128/MMBR.00007-14

Ud-Din, A. I. S., and Roujeinikova, A. (2018). Flagellin glycosylation with pseudaminic acid in campylobacter and helicobacter: prospects for development of novel therapeutics. *Cell. Mol. Life Sci.* 75, 1163–1178. doi: 10.1007/s00018-017-2696-5

Valiente, E., Bouche, L., Hitchen, P., Faulds-pain, A., Songane, M., Dawson, L. F., et al. (2016). Role of Glycosyltransferases modifying type B flagellin of emerging hypervirulent *Clostridium difficile* lineages and their impact on motility and biofilm formation. *J. Biol. Chem.* 291, 25450–25461. doi: 10.1074/jbc.M116.749523

Valle, J., Da Re, S., Henry, N., Fontaine, T., Balestrino, D., Latour-lambert, P., et al. (2006). Broad-spectrum biofilm inhibition by a secreted bacterial polysaccharide. *Proc. Natl. Acad. Sci. U. S. A.* 103, 12558–12563. doi: 10.1073/pnas.0605399103

Van Der Beek, S. L., Zorzoli, A., Çanak, E., Chapman, R. N., Lucas, K., Meyer, B. H., et al. (2019). Streptococcal dTDP-L-rhamnose biosynthesis enzymes: functional characterization and lead compound identification. *Mol. Microbiol.* 111, 951–964. doi: 10.1111/mmi.14197

Verderosa, A. D., Totsika, M., and Fairfull-Smith, K. E. (2019). Bacterial biofilm eradication agents: A current review. *Front. Chem.* 7:824. doi: 10.3389/fchem.2019.00824

Villalobos, J. A., Yi, B. R., and Wallace, I. S. (2015). 2-Fluoro-L-Fucose is a metabolically incorporated inhibitor of plant cell wall polysaccharide fucosylation. *PLoS One* 10:e0139091. doi: 10.1371/journal.pone.0139091

Virji, M., and Heckels, J. E. (1984). The role of common and type-specific pilus antigenic domains in adhesion and virulence of gonococci for human epithelial cells. *J. Gen. Microbiol.* 130, 1089–1095. doi: 10.1099/00221287-130-5-1089

Voth, D. E., and Ballard, J. D. (2005). Clostridium difficile toxins: mechanism of action and role in disease. *Clin. Microbiol. Rev.* 18, 247–263. doi: 10.1128/CMR.18.2.247-263.2005

Wetzler, L. E. E. M., Barry, K., Blake, M. S., and Gotschlich, E. C. (1992). Gonococcal lipooligosaccharide sialylation prevents complement-dependent killing by immune sera. *Infect. Immun.* 60, 39–43. doi: 10.1128/iai.60.1.39-43.1992

Whitfield, C. (2006). Biosynthesis and assembly of capsular polysaccharides in *Escherichia coli*. *Annu. Rev. Biochem.* 75, 39–68. doi: 10.1146/annurev.biochem.75.103004.142545

World Health Organization (2014). Antimicrobial resistance: global report on surveillance. World Health Organization. Available at: https://apps.who.int/iris/handle/10665/112642

Williams, D. A., Pradhan, K., Paul, A., Olin, I. R., Tuck, O. T., Moulton, K. D., et al. (2020). Metabolic inhibitors of bacterial glycan biosynthesis. *Chem. Sci.* 11, 1761–1774. doi: 10.1039/C9SC05955E

Wu, R., and Wu, H. (2011). A molecular chaperone mediates a two-protein enzyme complex and glycosylation of serine-rich streptococcal adhesins. *J. Biol. Chem.* 286, 34923–34931. doi: 10.1074/jbc.M111.239350

Xu, Y., Cuccui, J., Denman, C., Maharjan, T., Wren, B. W., and Wagner, G. K. (2018). Structure-activity relationships in a new class of non-substrate-like covalent inhibitors of the bacterial glycosyltransferase LgtC. *Bioorg. Med. Chem.* 26, 2973–2983. doi: 10.1016/j.bmc.2018.03.006

Xu, Y., Smith, R., Vivoli, M., Ema, M., Goos, N., Gehrke, S., et al. (2017). Covalent inhibitors of LgtC: A blueprint for the discovery of non-substrate-like inhibitors for bacterial glycosyltransferases. *Bioorg. Med. Chem.* 25, 3182–3194. doi: 10.1016/j.bmc.2017.04.006

Yakovlieva, L., Ramírez-Palacios, C., Marrink, S. J., and Walvoort, M. T. C. (2021). Semiprocessive hyperglycosylation of adhesin by bacterial protein *N*-Glycosyltransferases. *ACS Chem. Biol.* 16, 165–175. doi: 10.1021/acschembio.0c00848

Yuki, N., Susuki, K., Koga, M., Nishimoto, Y., Odaka, M., Hirata, K., et al. (2004). Carbohydrate mimicry between human ganglioside GM1 and *Campylobacter jejuni* lipooligosaccharide causes Guillain-Barré syndrome. *Proc. Natl. Acad. Sci. U. S. A.* 101, 11404–11409. doi: 10.1073/pnas.0402391101

Zhao, J., Zeng, X., Huang, T., and Li, Y. (2018). GtfA interacting with GtfB is required for PsrP glycosylation in *Streptococcus pneumoniae*. *Jundishapur J. Microbiol.* 11:e68982. doi: 10.5812/jjm.68982

Zhou, M., and Wu, H. (2009). Glycosylation and biogenesis of a family of serine- rich bacterial adhesins. *Microbiology* 155, 317–327. doi: 10.1099/mic.0.025221-0

Zhu, C., Qaidi, S.El, McDonald, P., Roy, A., and Hardwidge, P. R. (2021). YM155 inhibits NleB and SseK arginine glycosyltransferase activity. *Pathogens* 10, 1–10. doi: 10.3390/pathogens10020253

Zhu, F., Zhang, H., Yang, T., Haslam, S. M., Dell, A., and Wu, H. (2016). Engineering and dissecting the glycosylation pathway of a streptococcal serine-rich repeat adhesin. *J. Biol. Chem.* 291, 27354–27363. doi: 10.1074/jbc.M116.752998

Conflict of Interest: The authors declare that the research was conducted in the absence of any commercial or financial relationships that could be construed as a potential conflict of interest.

Publisher's Note: All claims expressed in this article are solely those of the authors and do not necessarily represent those of their affiliated organizations, or those of the publisher, the editors and the reviewers. Any product that may be evaluated in this article, or claim that may be made by its manufacturer, is not guaranteed or endorsed by the publisher.

GLOSSARY

Term	Definitions
Ac	acetyl
ADP	adenosine diphosphate
Ala	alanine
Asn	asparagine
Bac	bacillosamine
BAHT	bacterial autotransporter heptosyltransferase
CMP	cytidine monophosphate
CPA	common polysaccharide antigen
CPD	cysteine protease domain
CPS	capsular polysaccharide
DAEC	diffusely adhering *E. coli*
DATDG	2,4-diacetamido-2,4,6-trideoxygalactose
diNAcBac	*N*, *N*'-diacetylbacillosamine
DNA	deoxyribonucleic acid
DP	degree of polymerization
dTDP	deoxythymidine diphosphate
dTDP-L-Rha	deoxythymidine diphosphate-L-rhamnose
EHEC	enterohaemorrhagic *E. coli*
ELISA	enzyme-linked immunosorbent assay
EPEC	enteropathogenic *E. coli*
EPS	extracellular polymeric substances
ETEC	enterotoxigenic *E. coli*
FDA	Food and Drug Administration
Fuc3N	3-amino-3-deoxy-D-fucose
FucNAc	*N*-acetylfucosamine
G1P	glucose-1-phosphate
GAPDH	glyceraldehyde 3-phosphate dehydrogenase
GBS	Guillain-Barré syndrome
GI	gastrointestinal
Glc	glucose
GlcA	glucuronic acid
GlcNAc	*N*-acetylglucosamine
Gly	glycine
GT	glycosyltransferase
GulNAc	*N*-acetylgulosamine
HMW	high molecular weight
HTS	high throughput
IAI	intra-abdominal infection
IAP	inhibitor of apoptosis
IC_{50}	concentration to inhibit 50% enzyme activity
Kdo	3-deoxy-D-manno-octulosonic acid
Leg	legionaminic acid
LNnT	lacto-*N*-neotetraose
LOS	lipooligosaccharides
LPS	lipopolysaccharide
ManA	mannuronic acid
ManNAc	*N*-acetylmannosamine
MDR	multidrug resistance
MIC	minimal inhibitory concentration
MOE	metabolic oligosaccharide engineering
Neu5Ac	neuraminic acid
NTHi	nontypeable *Haemophilus influenzae*
OGT	*O*-GlcNAc transferase
OSA	O-specific antigen
OTase	oligosaccharyltransferase
PNAG	poly-β-1,6-*N*-acetylglucosamine
Pse	pseudaminic acid
QuiNAc	N-acetylquinosamine
Rha	L-rhamnose
Rho-GTPase	Rho-guanosine triphosphatases
RIPK1	serine-threonine protein kinase 1
SAAT	self-associating autotransporter
SAR	structure-activity relationship
Ser	serine

Term	Definitions
SPR	surface plasmon resonance
SRRPs	serine-rich repeat proteins
TFP	type IV pili
Thr	threonine
TNFR	tumor necrosis factor receptor
TPS	two-partner secretion
TRADD	type 1 associated DEATH domain protein
UDP	uridine diphosphate
UDP-GlcNAc	uridine diphosphate *N*-acetylglucosamine
UPEC	uropathogenic *E. coli*
VS	virtual screening
Xyl	xylose

frontiers in Microbiology

PERSPECTIVE
published: 27 September 2021
doi: 10.3389/fmicb.2021.731008

The Crossroads of Glycoscience, Infection, and Immunology

*Tanya R. McKitrick[1], Margaret E. Ackerman[2], Robert M. Anthony[3], Clay S. Bennett[4], Michael Demetriou[5], Gregory A. Hudalla[6], Katharina Ribbeck[7], Stefan Ruhl[8], Christina M. Woo[9], Loretta Yang[10], Seth J. Zost[11], Ronald L. Schnaar[12] and Tamara L. Doering[13]**

[1]National Center for Functional Glycomics, Harvard Medical School, Boston, MA, United States, [2]Thayer School of Engineering, Dartmouth College, Hanover, NH, United States, [3]Center for Immunology and Inflammatory Diseases, Division of Rheumatology, Allergy, and Immunology, Massachusetts General Hospital, Harvard Medical School, Boston, MA, United States, [4]Department of Chemistry, Tufts University, Medford, MA, United States, [5]Department of Neurology, Microbiology, and Molecular Genetics, University of California, Irvine, Irvine, CA, United States, [6]J Crayton Pruitt Family Department of Biomedical Engineering, University of Florida, Gainesville, FL, United States, [7]Department of Biological Engineering, Massachusetts Institute of Technology, Cambridge, MA, United States, [8]Department of Oral Biology, University at Buffalo School of Dental Medicine, Buffalo, NY, United States, [9]Department of Chemistry and Chemical Biology, Harvard University, Cambridge, MA, United States, [10]Lectenz Bio, Athens, GA, United States, [11]Vanderbilt Vaccine Center, Vanderbilt University Medical Center, Nashville, TN, United States, [12]Department of Pharmacology, Johns Hopkins University, Baltimore, MD, United States, [13]Department of Molecular Microbiology, Washington University School of Medicine, St. Louis, MO, United States

OPEN ACCESS

Edited by:
Gerardo R. Vasta, University of Maryland, Baltimore, United States

Reviewed by:
Janice Endsley, University of Texas Medical Branch at Galveston, United States
Shinya Suzu, Kumamoto University, Japan

***Correspondence:**
Tamara L. Doering
doering@wustl.edu

Specialty section:
This article was submitted to Infectious Diseases, a section of the journal Frontiers in Microbiology

Received: *25 June 2021*
Accepted: *12 August 2021*
Published: *27 September 2021*

Citation:
McKitrick TR, Ackerman ME, Anthony RM, Bennett CS, Demetriou M, Hudalla GA, Ribbeck K, Ruhl S, Woo CM, Yang L, Zost SJ, Schnaar RL and Doering TL (2021) The Crossroads of Glycoscience, Infection, and Immunology. Front. Microbiol. 12:731008. doi: 10.3389/fmicb.2021.731008

Advances in experimental capabilities in the glycosciences offer expanding opportunities for discovery in the broad areas of immunology and microbiology. These two disciplines overlap when microbial infection stimulates host immune responses and glycan structures are central in the processes that occur during all such encounters. Microbial glycans mediate host-pathogen interactions by acting as surface receptors or ligands, functioning as virulence factors, impeding host immune responses, or playing other roles in the struggle between host and microbe. In the context of the host, glycosylation drives cell–cell interactions that initiate and regulate the host response and modulates the effects of antibodies and soluble immune mediators. This perspective reports on a workshop organized jointly by the National Institute of Allergy and Infectious Diseases and the National Institute of Dental and Craniofacial Research in May 2020. The conference addressed the use of emerging glycoscience tools and resources to advance investigation of glycans and their roles in microbe-host interactions, immune-mediated diseases, and immune cell recognition and function. Future discoveries in these areas will increase fundamental scientific understanding and have the potential to improve diagnosis and treatment of infections and immune dysregulation.

Keywords: glycobiology, glycomedicine, glycoscience, host response, infection, immunity, microbial glycans

INTRODUCTION

During the early months of the COVID-19 pandemic (May 27–28, 2020), an NIH workshop on "Glycoscience and Immunology at the Crossroads of Biology" was convened on-line. The component topics of the workshop were infection, immunity, and glycobiology. Each of these broad areas is the subject of intense scientific investigation, and resulting discoveries have

advanced human health. Many studies also occur at the intersections of these fields. For example, infection and immunity represent two views of the events that occur during and after encounters between pathogenic microbes and their hosts. Understanding how these events unfold from each vantage point has been critical for the development of modern immunology and microbiology and for the development of strategies to treat immune dysregulation and infectious disease. This perspective, like the NIH workshop on which it is based, focuses on the overlap of glycoscience with each of these two fields (**Figure 1**).

Glycans play key roles in infection and immunity: Pathogen glycans may mediate host interactions and stimulate or inhibit host immune responses, while host glycans may serve as specific targets of microbial adhesion molecules or toxins (Varki and Gagneux, 2015). Glycans also act in mediating the host response to infection and in regulating immunity at multiple levels. In all of these roles, their primary function is molecular recognition, as opposed to their structural and dietary cousins (more often termed sugars, saccharides, or carbohydrates).

This brief perspective will use the topics discussed at the NIH workshop as examples to focus attention on emerging areas of research and opportunities in the many areas of infection and immunity where glycans play key roles. It will also highlight the importance of glycoscience tools for scientific progress on these topics and identify areas where investment in basic research efforts will advance knowledge and practice in glycobiology and glycomedicine.

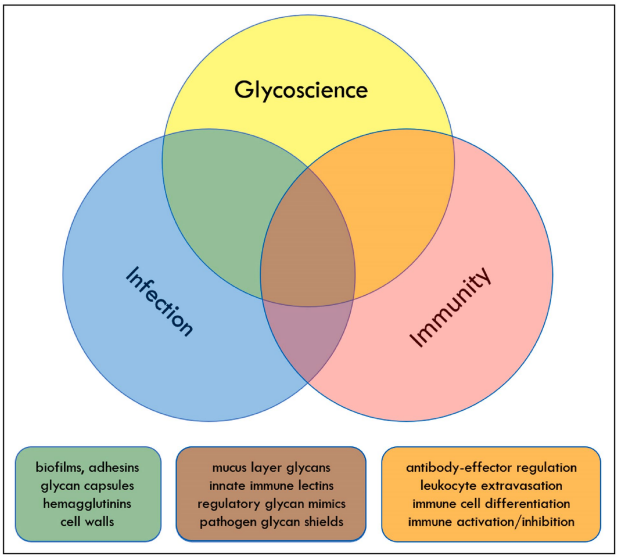

FIGURE 1 | Glycoscience, infection, and immunity overlap in multiple areas that drive pathogen and host function. Color-coded overlap topics mentioned in the text are listed as examples.

GLYCANS IN HOST-PATHOGEN RECOGNITION AND DISEASE

Microbial glycans are incredibly diverse and play critical roles in the interactions between infectious agents and their hosts and in the pathogenesis of resulting infections. These compounds frequently constitute much of the microbial cell surface and therefore mediate the initial encounters between pathogen and host cells. Bacteria, for example, are protected by a peptidoglycan cell wall and often display polysaccharide capsules as well as other glycan-containing moieties. The cell walls of fungi are primarily composed of glycan polymers and highly glycosylated proteins. Many parasites display surface coats that are both anchored by glycolipids and abundantly glycosylated. Study of these glycans has revealed novel biological pathways, elucidated pathogenic processes, and led to the development of vaccines and therapeutics.

Microbial glycan structures contribute to pathogenesis by an array of distinct mechanisms. They may physically protect the invading pathogen, mediate cell adherence or protein interactions, transmit signaling information, serve as decoys, or alter the environment to the benefit of the invader, as when biofilm production reduces the efficacy of antibiotics or efficiency of host clearance. Tamara Doering presented the opportunistic eukaryote *Cryptococcus neoformans* as an example of a pathogen whose glycans are critical for the development of disease (Loza and Doering, 2021). This yeast, which is responsible for roughly 200,000 deaths from meningitis each year, elaborates an extracellular capsule that is composed of large (up to millions of daltons) polysaccharides and can comprise >75% of the pathogen volume. The capsule, made primarily of mannose or galactose chains with appendant glucuronic acid and xylose residues, is required for infection and inhibits host cell phagocytosis (Gaylord et al., 2020). Shed capsule components also perturb host immune responses; this material is also the basis for rapid tests that are valuable for diagnosis of this frequently lethal infection.

In addition to glycans produced by microbes themselves, host glycoconjugates are critical in determining the outcomes of host-pathogen interactions. Influenza virus is a compelling example of this dual association of glycobiology and pathogenesis. This virus exploits host glycans by using sialic acid bearing proteins for cell entry (mediated by hemagglutinin) and a sialidase (neuraminidase) to trigger release of budding virions (Gamblin and Skehel, 2010); as a result, species-specific differences in sialic acid isomers impact the host selectivity of various strains. For example, pathogenic human influenza strains all bear hemagglutinins that bind sialic acid linked to the 6-carbon hydroxyl of galactose whereas bird influenza binds to sialic acid when linked to the 3-carbon hydroxyl of galactose. The molecular switch in human to bird specificity can occur when as few as two amino acids in the sialic acid binding site of influenza hemagglutinin are appropriately mutated.

On the flip side, influenza also illustrates how microbial protein glycosylation can impact host defenses. Seth Zost discussed how antigenic drift in the influenza virus hemagglutinin protein may alter its glycosylation, which in turn can change characteristics of the infection, such as infectivity and viral fitness, as well as the efficacy of host antibody responses that

neutralize the virus (Zost et al., 2017; Altman et al., 2019). Vaccine efficacy may also change in this scenario, both because the new antigen will induce a distinct antibody response and because protection conferred by prior immunization may be less robust.

The exploitation of host glycans by microbial invaders to advance infection and disease occurs frequently across domains of microbiology. For instance, Stefan Ruhl discussed the contributions of host glycan recognition to the physiology of the oral microbiome. The interactions between lectin-like adhesins on bacteria and complementary glycan motifs on glycoproteins adsorbed to tooth enamel play central roles in initial bacterial colonization. Lectin-glycan binding also facilitates bacterial coadhesion that leads to the formation of microbial biofilms. Glycan-driven bacterial-host interactions are key both to establishing the commensal oral microbiota and to oral disease progression (Thamadilok et al., 2016; Cross and Ruhl, 2018). Host glycans can also significantly impact pathogen behavior by modulating the immediate pathogen environment. As a striking example, Katharina Ribbeck presented the effects on epithelial microbes of host mucus, which is often excluded from experiments performed *in vitro* despite its known role in defense against infection. Her group has shown that mucin-associated glycans influence multiple microbial functions that are central to pathogenic processes of yeast and bacteria, including surface attachment, quorum sensing, virulence gene expression, and biofilm formation. Released O-linked glycans from highly glycosylated mucins, such as MUC5B, retain many of these effects.

GLYCANS IN TUNING AND CONTROL OF IMMUNE RESPONSES

As major molecular determinants on cell surfaces, on secreted proteins, and in the extracellular matrix, glycans are well suited to regulate molecular recognition and molecular signaling events. Nowhere is this more evident than in the immune system, where different types of immune cells respond to secreted factors, each other, and molecules in their extracellular milieu to coordinate pathogen clearance while avoiding damage to host cells and tissues. Glycans and glycan recognition drive and regulate immune responses at every level and provide inviting and often untapped opportunities for therapeutic development targeting immune dysregulation.

Among the most exciting recent findings is that humoral immunity is tuned by antibody glycosylation. Robert Anthony and Margaret Ackerman provided clinical and mechanistic insights related to IgE and IgG glycosylation. Allergen-specific IgE is absolutely required for allergic symptoms and disease. Unbiased examination of glycosylation patterns of total IgE from individuals with a peanut allergy and non-atopic individuals revealed altered glycosylation – an increase in sialic acid content – on IgE from allergic subjects (Shade et al., 2020). Selective sialic acid removal from IgE lessened effector-cell degranulation and anaphylaxis in allergic disease models. These findings make IgE glycosylation a promising target for therapeutic modulation.

Human IgG Fc glycans also correlate with disease outcomes, in both infectious and autoimmune diseases (Cobb, 2020). This appears to be due to the ability of various IgG Fc glycoforms to drive distinct Fc-dependent mechanisms and immune outcomes, from activating immunity to supporting tolerance. Intriguingly, glycoform expression may be specific for the antigen eliciting the response. Evidently, B-cell glycan biosynthetic enzymes respond to the antigen and regulate Fc glycosylation to tune the downstream response (Larsen et al., 2021). For both IgE and IgG, the technology has been developed to create designer immunoglobulin glycans, thereby modulating immune responses for therapeutic benefit.

Glycosylation of cell surface molecules on immune cells also regulates immune outcomes. Michael Demetriou described how the patterns of N-glycosylation on cell surface glycoproteins control the distribution, clustering, and surface residency of immune regulatory glycoproteins in a predictable manner. The mechanism involves glycan-binding proteins called galectins that, when N-glycans are sufficiently abundant and branched, form a cell surface lattice of immune regulatory molecules on both T cells and B cells (Mortales et al., 2020). Insufficient branching of N-glycans can result in autoimmune sensitivity, for example, in multiple sclerosis and autoimmune diabetes (Brandt et al., 2021). Remarkably, oral administration of the sugar N-acetylglucosamine in human subjects increases N-glycan branching, raising the hope that dietary supplementation may reduce autoimmunity.

Whereas GlcNAc-induced N-glycan branching regulates cell surface residency on immune cells, the same single sugar is dynamically attached to and removed from specific serine and threonine residues of cytoplasmic, nuclear, and mitochondrial proteins. This modification (O-GlcNAc) modulates protein and cell functions in immunity, cancer, neurodegeneration, and diabetes (among others) and is regulated by a single transferase (OGT) and glycosidase (OGA). Christina Woo shared new technologies to fuse nanobodies to these enzymes to modulate the O-GlcNAc residency of a particular protein or protein site (Ramirez et al., 2020; Ge et al., 2021). These methods promise to allow interrogation of the roles of O-GlcNAc on target proteins and to decode O-GlcNAc regulation.

Once an immune response is elicited, it must be controlled to avoid pathology due to the activated immune cells causing host tissue damage. Glycans play a role in this process as well. Ronald Schnaar described the 14-member family of human glycan-binding proteins (GBPs) called Siglecs, most of which are expressed on the surfaces of overlapping sets of immune cells and most of which dampen immune responses *via* intracellular immunoreceptor tyrosine-based inhibitory motifs (Duan and Paulson, 2020). When inhibitory Siglecs on activated immune cells encounter their native glycan ligands on target tissues, the immune cells apoptose or are otherwise inhibited, halting the ongoing immune event. Based on these findings, Siglecs are being targeted therapeutically as immune checkpoint inhibitors (Youngblood et al., 2020).

TOOLS AND RESOURCES FOR GLYCOBIOLOGY

Despite significant advances in the study of glycosylation, there is much to be learned regarding the biological roles of these highly diverse molecules. For example, the human glycome is predicted to be vast: Some estimates suggest well over 7,500 unique structures, which require more than 700 genes for synthesis (Cummings, 2009). These structures are further diversified with additional modifications, including sulfation, methylation, and acetylation, which can directly impact or alter the function of individual glycans. Progress in the fields of glycomics and glycobiology has been limited by technical challenges in glycan sequencing and glycan synthesis, and insufficient tools to characterize the temporal and spatial expression of glycan determinants at high resolution. These barriers are coming down, providing enhanced opportunities to decode glycosylation function in physiology and pathology.

Determining the sequences of glycan structures remains a highly specialized technique that requires multiple orthogonal approaches, microgram amounts of material isolated from proteins or lipids, and does not capture the spatial and temporal nature of the glycan itself. Glycan synthesis also presents significant challenges. Functional synthetic glycans must retain the correct linkages between sugars in the correct stereochemical orientation. Clay Bennett introduced ways in which the stereochemical outcome of glycosylation can be controlled using methods that are accessible to novice synthetic chemists and scalable (Zhuo et al., 2019; Ling and Bennett, 2020). Democratizing glycan synthesis can advance glycomedicine, as evidenced by the development of synthetic glycans capable of targeting drug resistant pathogens and a potentially new class of antibiotic drugs.

To define the localization of glycans, identify their components, and explore their functions in biological tissues, the most commonly utilized tools in the glycobiologist's toolkit are lectins and monoclonal antibodies (mAbs). Lectins, which are GBPs found in animals and plants, are used extensively, although their broad specificity can limit their utility. For example, three plant lectins are commonly used to distinguish between two biologically important structures: α2-3 linked sialic acid (bound by MAL, *Maackia amurensis* lectin I and II) and α2-6 linked sialic acid (bound by SNA, *Sambucus nigra* agglutinin). However, MAL-I and MAL-II also bind 3-O-sulfated determinants and SNA binding can be inhibited by lactose or galactose. Thus, interpretation of such experiments always requires caveats. Addressing this challenge, Lori Yang presented exciting technology in development to engineer more specific GBPs called Lectenz®. These proteins are engineered from carbohydrate-processing enzymes that exhibit high specificity and affinity for monosaccharides and glycosidic linkages. By eliminating catalytic activity and enhancing affinity using directed evolution informed by computational predictions of known molecular interactions, enhanced GBPs are generated. In theory, this innovative approach could convert any glycoactive enzyme to a binding reagent that is far more specific than traditional lectins, providing valuable reagents to further our understanding of glycobiology (Angel et al., 2021; Büll et al., 2021).

Monoclonal antibodies are another powerful tool to examine glycan localization and function. However, the mAbs available to researchers bind only a small fraction of the predicted glycan epitopes within the human glycome and fewer than a third of them are reliably available from commercial sources (according to a survey of the Database for Anti-Glycan Reagents); the situation is even worse for mAbs that specifically recognize microbial glycans. The paucity of such commercial reagents forces many laboratories to produce their own mAbs, an expensive solution that perpetuates problems of availability. Finally, due to the similarity of the human and mouse glycomes, human glycan structures are often not immunogenic and result in the production of IgM mAbs with broader specificity. To address these obstacles, Tanya McKitrick is developing "smart" anti-glycan reagents (SAGRs) by immunizing the sea lamprey, *Petromyzon marinus*, and then producing recombinant lamprey antibodies with a mouse/rabbit Fc for detection purposes (McKitrick et al., 2020, 2021). Lampreys have evolved an alternative adaptive immune system that occurs only in jawless vertebrates and uses a family of highly diverse, single-chain antibody-like proteins called variable lymphocyte receptors B (VLRBs). The potential diversity of SAGRs exceeds that of antibody production in mice, studies to date have identified over 25 VLRBs which can discriminate between glycosidic linkages, functional groups, and monosaccharides. These VLRB antibody sequences are publicly available in GenBank.

A further exciting area of tool development relates to protein-glycan interactions. Greg Hudalla discussed how galectins recognize glycans of the cell surface and extracellular matrix and thereby modulate biological processes, including those relevant to inflammation and infection. His group has developed peptide-based platforms to engineer multivalent scaffolds to influence galectin interactions at the cellular level (Restuccia et al., 2015; Farhadi et al., 2021). Beyond defining key biological interactions, these approaches have potential application in areas, including signaling, apoptosis, and drug delivery.

DISCUSSION

The workshop presentations briefly reviewed above highlight the importance of research in glycobiology for the advancement of fundamental knowledge and human health. Approaches from glycome profiling to glycan engineering have deepened our understanding of glycan mediated host-pathogen interactions and regulation of host immunity. This understanding in turn increases our ability to develop feasible approaches for diagnosis, treatment, and prevention of infectious disease as well as for control of both protective and dysregulated immune responses.

Further development of tools and resources to help characterize, localize, and engineer glycans and glycan-binding proteins will accelerate discovery and application in both infection and immunity. Studies of infection will benefit from analysis and synthesis of microbial glycans, examination of the host activities and glycoconjugates that modulate events

at the host-pathogen interface, the use of microbe diversity to uncover new processes and cellular interactions, and the expansion and availability of glycan arrays that reflect the diversity of microbes and their host niches. Studies of immunity will benefit from the ability to analyze, create, and regulate specifically glycosylated antibodies to control immune outcomes; therapeutically regulate cell surface glycans to modulate their responsiveness target intercellular glycosylation to modulate signaling pathways; and target native immune inhibitory pathways with glycans. Robust support of these efforts will continue to yield exciting scientific discoveries and improved human health.

AUTHOR CONTRIBUTIONS

RS and TM drafted individual sections and edited the manuscript. TD drafted the remainder of the manuscript and edited the manuscript. All other authors edited the manuscript.

FUNDING

Glycobiology studies in the Doering group are funded by the National Institute of Allergy and Infectious Diseases (NIAID) R01 AI135012 and in the Schnaar group by NIAID U19 AI135443. The May 27–28, 2020, NIH workshop on Glycoscience and Immunology at the Crossroads of Biology was funded by NIAID and the National Institute of Dental and Craniofacial Research (NIDCR), with meeting support from NIAID.

ACKNOWLEDGMENTS

The authors thank Preethi Chander (NIDCR), Dona Love (NIAID), and Mercy PrabhuDas (NIAID) for organizing the workshop and for reviewing this manuscript. They also thank the vibrant community of glycoscientists for their enthusiasm and efforts in this field.

REFERENCES

Altman, M. O., Angel, M., Kosik, I., Trovao, N. S., Zost, S. J., Gibbs, J. S., et al. (2019). Human influenza A virus hemagglutinin glycan evolution follows a temporal pattern to a glycan limit. *mBio* 10:e00204-19. doi: 10.1128/mBio.00204-19

Angel, P. M., Drake, R. R., Park, Y., Clift, C. L., West, C., Berkhiser, S., et al. (2021). Spatial N-glycomics of the human aortic valve in development and pediatric endstage congenital aortic valve stenosis. *J. Mol. Cell. Cardiol.* 154, 6–20. doi: 10.1016/j.yjmcc.2021.01.001

Brandt, A. U., Sy, M., Bellmann-Strobl, J., Newton, B. L., Pawling, J., Zimmermann, H. G., et al. (2021). Association of a marker of N-acetylglucosamine with progressive multiple sclerosis and neurodegeneration. *JAMA Neurol.* 78, 842–852. doi: 10.1001/jamaneurol.2021.1116

Büll, C., Nason, R., Sun, L., Van Coillie, J., Madriz Sørensen, D., Moons, S. J., et al. (2021). Probing the binding specificities of human Siglecs by cell-based glycan arrays. *Proc. Natl. Acad. Sci. U. S. A.* 118:e2026102118. doi: 10.1073/pnas.2026102118

Cobb, B. A. (2020). The history of IgG glycosylation and where we are now. *Glycobiology* 30, 202–213. doi: 10.1093/glycob/cwz065

Cross, B. W., and Ruhl, S. (2018). Glycan recognition at the saliva - oral microbiome interface. *Cell. Immunol.* 333, 19–33. doi: 10.1016/j.cellimm.2018.08.008

Cummings, R. D. (2009). The repertoire of glycan determinants in the human glycome. *Mol. Biosyst.* 5, 1087–1104. doi: 10.1039/b907931a

Duan, S., and Paulson, J. C. (2020). Siglecs as immune cell checkpoints in disease. *Annu. Rev. Immunol.* 38, 365–395. doi: 10.1146/annurev-immunol-102419-035900

Farhadi, S. A., Liu, R., Becker, M. W., Phelps, E. A., and Hudalla, G. A. (2021). Physical tuning of galectin-3 signaling. *Proc. Natl. Acad. Sci. U. S. A.* 118:e2024117118. doi: 10.1073/pnas.2024117118

Gamblin, S. J., and Skehel, J. J. (2010). Influenza hemagglutinin and neuraminidase membrane glycoproteins. *J. Biol. Chem.* 285, 28403–28409. doi: 10.1074/jbc.R110.129809

Gaylord, E. A., Choy, H. L., and Doering, T. L. (2020). Dangerous liaisons: interactions of *Cryptococcus neoformans* with host phagocytes. *Pathogens* 9:891. doi: 10.3390/pathogens9110891

Ge, Y., Ramirez, D. H., Yang, B., D'Souza, A. K., Aonbangkhen, C., Wong, S., et al. (2021). Target protein deglycosylation in living cells by a nanobody-fused split O-GlcNAcase. *Nat. Chem. Biol.* 17, 593–600. doi: 10.1038/s41589-021-00757-y

Larsen, M. D., de Graaf, E. L., Sonneveld, M. E., Plomp, H. R., Nouta, J., Hoepel, W., et al. (2021). Afucosylated IgG characterizes enveloped viral responses and correlates with COVID-19 severity. *Science* 371:eabc8378. doi: 10.1126/science.abc8378

Ling, J., and Bennett, C. S. (2020). Versatile glycosyl sulfonates in beta-selective C-glycosylation. *Angew. Chem. Int. Ed. Engl.* 59, 4304–4308. doi: 10.1002/anie.201914221

Loza, L., and Doering, T. L. (2021). "Glycans of the pathogenic yeast *Cryptococcus neoformans* and related opportunities for therapeutic advances," in *Comprehensive Glycoscience*. ed. J. Barchi (Amsterdam, Netherlands: Elsevier).

McKitrick, T. R., Bernard, S. M., Noll, A. J., Collins, B. C., Goth, C. K., McQuillan, A. M., et al. (2021). Novel lamprey antibody recognizes terminal sulfated galactose epitopes on mammalian glycoproteins. *Commun. Biol.* 4:674. doi: 10.1038/s42003-021-02199-7

McKitrick, T. R., Goth, C. K., Rosenberg, C. S., Nakahara, H., Heimburg-Molinaro, J., McQuillan, A. M., et al. (2020). Development of smart an ti-glycan reagents using immunized lampreys. *Commun. Biol.* 3:91. doi: 10.1038/s42003-020-0819-2

Mortales, C. L., Lee, S. U., Manousadjian, A., Hayama, K. L., and Demetriou, M. (2020). N-glycan branching decouples B cell innate and adaptive immunity to control inflammatory demyelination. *iScience* 23:101380. doi: 10.1016/j.isci.2020.101380

Ramirez, D. H., Aonbangkhen, C., Wu, H. Y., Naftaly, J. A., Tang, S., O'Meara, T. R., et al. (2020). Engineering a proximity-directed O-GlcNAc transferase for selective protein O-GlcNAcylation in cells. *ACS Chem. Biol.* 15, 1059–1066. doi: 10.1021/acschembio.0c00074

Restuccia, A., Tian, Y. F., Collier, J. H., and Hudalla, G. A. (2015). Self-assembled glycopeptide nanofibers as modulators of galectin-1 bioactivity. *Cell. Mol. Bioeng.* 8, 471–487. doi: 10.1007/s12195-015-0399-2

Shade, K. C., Conroy, M. E., Washburn, N., Kitaoka, M., Huynh, D. J., Laprise, E., et al. (2020). Sialylation of immunoglobulin E is a determinant of allergic pathogenicity. *Nature* 582, 265–270. doi: 10.1038/s41586-020-2311-z

Thamadilok, S., Roche-Håkansson, H., Håkansson, A. P., and Ruhl, S. (2016). Absence of capsule reveals glycan-mediated binding and recognition of salivary mucin MUC7 by *Streptococcus pneumoniae*. *Mol. Oral Microbiol.* 31, 175–188. doi: 10.1111/omi.12113

Varki, A., and Gagneux, P. (2015). "Biological functions of glycans," in *Essentials of Glycobiology*. eds. A. Varki, R. D. Cummings, J. D. Esko, P. Stanley, G. W. Hart and M. Aebi et al. (Cold Spring Harbor, NY: Cold Spring Harbor Laboratory Press), 77–88.

Youngblood, B. A., Leung, J., Falahati, R., Williams, J., Schainin, J., Brock, E. C., et al. (2020). Discovery, function, and therapeutic targeting of Siglec-8. *Cell* 10:19. doi: 10.3390/cells10010019

Zhuo, M. H., Wilbur, D. J., Kwan, E. E., and Bennett, C. S. (2019). Matching glycosyl donor reactivity to sulfonate leaving group ability permits SN2 glycosylations. *J. Am. Chem. Soc.* 141, 16743–16754. doi: 10.1021/jacs.9b07022

Zost, S. J., Parkhouse, K., Gumina, M. E., Kim, K., Diaz Perez, S., Wilson, P. C., et al. (2017). Contemporary H3N2 influenza viruses have a glycosylation site that alters binding of antibodies elicited by egg-adapted vaccine strains. *Proc. Natl. Acad. Sci. U. S. A.* 114, 12578–12583. doi: 10.1073/pnas.1712377114

Conflict of Interest: MD is an inventor on a patent for use of GlcNAc in MS and co-founded Glixis Therapeutics, a company that was developing analogs of GlcNAc for MS and other autoimmune diseases. GAH is a founder and stockholder of Anchor Biologics, Inc. and is an inventor on patents filed by and awarded to the University of Florida. Harvard University has filed a patent application on the nanobodies mentioned in conjunction with the work of CMW, who is an inventor of the patent. LY was employed by the company Lectenz Bio, which has joint patents with the University of Georgia Research Foundation, Inc. related to the research discussed. Lectenz Bio has licensed the patents, and LY is a named inventor.

The remaining authors declare that the research was conducted in the absence of any commercial or financial relationships that could be construed as a potential conflict of interest.

Publisher's Note: All claims expressed in this article are solely those of the authors and do not necessarily represent those of their affiliated organizations, or those of the publisher, the editors and the reviewers. Any product that may be evaluated in this article, or claim that may be made by its manufacturer, is not guaranteed or endorsed by the publisher.

frontiers in Microbiology

REVIEW
published: 29 September 2021
doi: 10.3389/fmicb.2021.725741

The Role of L-Selectin in HIV Infection

*Jason Segura†, Biao He†, Joanna Ireland†, Zhongcheng Zou, Thomas Shen, Gwynne Roth and Peter D. Sun**

Laboratory of Immunogenetics, National Institute of Allergy and Infectious Diseases, National Institutes of Health, Rockville, MD, United States

HIV envelope glycoprotein is the most heavily glycosylated viral protein complex identified with over 20 glycans on its surface. This glycan canopy is thought to primarily shield the virus from host immune recognition as glycans are poor immunogens in general, however rare HIV neutralizing antibodies nevertheless potently recognize the glycan epitopes. While CD4 and chemokine receptors have been known as viral entry receptor and coreceptor, for many years the role of viral glycans in HIV entry was controversial. Recently, we showed that HIV envelope glycan binds to L-selectin in solution and on CD4 T lymphocytes. The viral glycan and L-selectin interaction functions to facilitate the viral adhesion and entry. Upon entry, infected CD4 T lymphocytes are stimulated to progressively shed L-selectin and suppressing this lectin receptor shedding greatly reduced HIV viral release and caused aggregation of diminutive virus-like particles within experimental infections and from infected primary T lymphocytes derived from both viremic and aviremic individuals. As shedding of L-selectin is mediated by ADAM metalloproteinases downstream of host-cell stimulation, these findings showed a novel mechanism for HIV viral release and offer a potential new class of anti-HIV compounds.

Keywords: L-selectin (CD62L), HIV-1 infection, envelope gp120, ADAM metalloproteinases, shedding, viral release, viral entry

OPEN ACCESS

Edited by:
Ivan Martinez Duncker, Universidad Autónoma del Estado de Morelos, Mexico

Reviewed by:
Margherita Doria, Bambino Gesù Children Hospital (IRCCS), Italy
Yuntao Wu, George Mason University, United States

***Correspondence:**
Peter D. Sun
psun@nih.gov

Specialty section:
This article was submitted to Infectious Diseases, a section of the journal Frontiers in Microbiology

Received: *15 June 2021*
Accepted: *27 August 2021*
Published: *29 September 2021*

Citation:
Segura J, He B, Ireland J, Zou Z, Shen T, Roth G and Sun PD (2021) The Role of L-Selectin in HIV Infection. Front. Microbiol. 12:725741. doi: 10.3389/fmicb.2021.725741

INTRODUCTION

Many phases of the HIV lifecycle, including the viral entry, reverse transcription and integration, viral gene transcription, translation and replication, and viral release and maturation, have been intensely studied over the years and targeted by the development of highly active antiretroviral therapies (HAART/ART; Deeks et al., 2015). The success of combinatory ART (cART) has ushered in an era searching for a functionally cured state (Saag et al., 2020). To date, there are four classes of FDA-approved antiviral inhibitors targeting distinct phases of the viral lifecycle for frontline and prolonged suppression of infection, with generational advances in efficacy and resistance barrier: entry/fusion inhibitors (Matthews et al., 2004; Tsibris and Kuritzkes, 2007; Emu et al., 2018), nucleoside/non-nucleoside reverse transcriptase inhibitors (NRTI/NNRTI; Holec et al., 2017), integrase inhibitors (INTI; Lusic and Siliciano, 2017), and protease inhibitors (Flexner, 1998; Paton et al., 2015). Notably, while there is a growing development of inhibitors that target viral transcription (Pinto et al., 2019; Yeh et al., 2020), there are no FDA-approved therapeutics targeting viral release. Recent advances towards prolonging suppression of viremia have

revealed late-stage capsid assembly perturbation by a small molecule inhibitor suggesting success is possible with targeting late mechanisms crucial to viral budding (Link et al., 2020).

Investigations into the mechanisms acting on HIV release have revealed a complexing matrix of viral strategies that counter host-cell restriction factors to facilitate the successful trafficking of viral components that assemble and release at the plasma membrane (Ramdas et al., 2020; Rose et al., 2020). For most part, HIV release from either productive infected cells or the latent reservoir is thought to be spontaneous, but can be modulated by various host-cell restrictions, including CD317/BST-2/tetherin (Neil et al., 2008), TIM family membrane proteins (Li et al., 2014), serine incorporator membrane-spanning proteins (SERINC; Usami et al., 2015). While these restriction factors exhibited clear antiviral effect in HIV susceptible cell lines, some of them, including BST-2/tetherin and TIM members are not well expressed in primary CD4 T cells and it is difficult to develop compounds enhancing the expression of these restriction factors. In addition, the viral encoded nef and vpu have been shown to antagonize host restriction factors by actively promoting their degradations (Neil et al., 2008; Jolly et al., 2010). More recently, L-selectin/CD62L has been identified as an HIV adhesion receptor (Kononchik et al., 2018). Like BST-2/tetherin, L-selectin expressions are regulated by interferon-dependent processes during host-cell inflammation for several pathogens and disease states (Wang et al., 2010; Yang et al., 2011; Arias and Evans, 2014). Interestingly, L-selectin shedding appears required for HIV release from infected cells (Kononchik et al., 2018). Unlike tetherin and TIM members, however, L-selectin is abundantly expressed on primary CD4 T cells, and inhibition of L-selectin shedding presents a more efficacious target for suppressing the viral infection. These recent findings also showed that HIV release is not spontaneous and revealed a potential strategy to suppress HIV release from latently infected cellular reservoirs.

HIV envelope gp120 binds many lectins, DC-SIGN, Siglecs, and carbohydrate-binding Cyanovirin-N (CVN; Curtis et al., 1992; Mori et al., 1998; Esser et al., 1999; Snyder et al., 2005; Zou et al., 2011). Binding to DC-SIGN captures HIV by dendritic cells while binding to Siglec-1 facilitates HIV infection of macrophage (Snyder et al., 2005; Zou et al., 2011). Selectin family consists of L-selectin (CD62L), E-selectin and P-selectin and they are named according to their main cell origin with L-selectin present on leukocytes, E-selectin on activated endothelial cells, and P-selectin on activated platelets and endothelial cells (Tedder et al., 1995a). L-selectin (CD62L) functions to provide leukocyte rolling adhesion on endothelial cells (Gallatin et al., 1983; Berg et al., 1993), thus, regulates the migration of leukocytes to peripheral lymph nodes and sites of inflammation (Tedder et al., 1995b). It is one of the earliest surface markers on lymphoid-primed hematopoietic stem cell and is constitutively expressed on most circulating leucocytes (Alon et al., 1997; Ivetic et al., 2019). L-selectin consists of a C-type lectin domain, EGF-like domain, sushi domain, transmembrane domain and cytoplasmic tail (Spencer et al., 2017). The C-type lectin domain interacts with numerous glycans which is involved in rolling adhesion between leucocytes and endothelial cells (Fuhlbrigge et al., 1996). The cleavage of L-selectin can be induced by cell activation agonists such as PMA or infection (Kahn et al., 1994; Kononchik et al., 2018).

For HIV infection, the regulation of L-selectin shedding is especially meaningful. The paradoxical function of L-selectin in HIV biology, the one promotes viral adhesion to facilitate host cell entry vs. and the one hinders viral release through virion tethering, revealed complex roles of L-selectin in HIV lifecycle. Both are based on the same biochemical interaction, the binding of glycosylated envelope protein to cell surface L-selectin on CD4 T cells. As a consequence, a beneficial interaction to facilitate the adhesion step in viral entry of a multi-round infection becomes detrimental to successive viral dissemination that HIV induces the shedding of L-selectin to permit viral dissemination.

Cellular Ligands of L-Selectin

L-selectin was found essential for homing of naive lymphocytes to secondary lymphoid organs in carbohydrate dependent manner (Gesner and Ginsburg, 1964; Butcher and Picker, 1996). The ligand of L-selectin on high endothelial venules (HEV) are often O-linked Sialyl-Lewis X type sulfated glycans that can be blocked by MECA-79, an antibody specific for 6-sulfo sialyl-Lewis X in a sulfation and sialic acid dependent manner (Foxall et al., 1992; Mitsuoka et al., 1998). The O-linked sulfated sialyl-Lewis x was found on peripheral lymph node, CD34, glycosylation-dependent cell adhesion molecule (GlyCAM-1) and mucosal vascular addressin cell adhesion molecule-1 (MAdCAM-1) on HEV and all were identified as L-selectin ligands (Streeter et al., 1988; Baumheter et al., 1993; Berg et al., 1993; Puri et al., 1995). Further, sulfated glycans can be induced on HEV-like blood vessels at the site of inflammation caused by ulcerative colitis, rheumatoid arthritis or Helicobacter pylor infection (Kobayashi et al., 2004). Ligands of L-selectin also include abluminal and extravascular glycoproteins, such as heparin sulfate proteoglycan (Rosen, 2004). In general, the binding of L-selectin to its ligands mediates low affinity rolling adhesion of lymphocytes along HEV prior to high affinity attachment mediated by the interaction between LFA-1 on lymphocytes and ICAMs on HEV (Xu et al., 2003). L-selectin binding initiates the activation of integrins (Lawrence and Springer, 1991), activates chemokine receptors to promote trans-endothelial migration (Ding et al., 2003). However, mice lacking O-linked oligosaccharide still had considerable lymphocyte-homing activity and the remaining L-selectin attachment was abolished after enzymatic removal of N-glycans attached to HEV and CD34 (Mitoma et al., 2007). Therefore, both O- and N-glycans are ligands of L-selectin.

HIV Infections Regulate L-Selectin Expression

As L-selectin plays important roles in lymphocyte and leukocyte adhesion, activation and homing, as well as serves as a marker for central memory T cells, its expression is therefore often used as an indicator for HIV infection caused immune activation

and dysregulation. Early clinical observations from HIV infected individuals showed lower L-selectin expression on T cells and neutrophils compared to healthy controls or individuals on ART therapy, suggesting the viral infection caused protracted immune activation and dysregulated lymphocyte homing (Moore et al., 1998; Gainet et al., 1999; Meddows-Taylor et al., 2001; Schneider-Hohendorf et al., 2014). This is further supported by the observation that antiviral therapy restored L-selectin expression in HIV infected, ART-naïve individuals (Vassena et al., 2016). The soluble L-selectin levels detected in circulation were found to be higher in infected than healthy individuals (Kourtis et al., 2000, 2003; Meddows-Taylor et al., 2001; Schramm et al., 2007; Yang et al., 2014), reminisce to elevated soluble selectin found in autoimmune diseases, including rheumatoid arthritis, systemic sclerosis, and systemic lupus erythematosus (Sfikakis et al., 1999; Shimada et al., 2001; Ates et al., 2004). These early studies established the dynamics of HIV infection in overall T lymphocyte and neutrophil activations and the infection resulted dysregulation in immune functions. Many of these studies, however, did not address any specific mechanism involving L-selectin in HIV biology.

In human T cells, the expression of L-selectin appears to be controlled by members of Forkhead box transcription factors, such as FOXO1 (Fabre et al., 2008). Suppression of FOXO1 has been implicated in HIV infection-mediated downregulation of L-selectin expression in infected CD4 T cells (Trinite et al., 2014). Early mechanistic work showed that mere binding of viral envelope gp120 protein to CD4 and CXCR4 was sufficient to induce down regulation in L-selectin expression (Marschner et al., 1999; Wang et al., 2004). The envelope binding, however, was found insufficient by Trinite et al. (2014) and L-selectin down regulation required HIV infection and was mediated by the suppression of transcription factor Foxo1 and KLF2. Vassena et al. (2015) showed that HIV nef and vpu contributed to the viral induced L-selectin down regulation that was attributed to the retention of the receptor in perinuclear compartments as a result of nef association. Interestingly, HIV encoded vpr appears to induce L-selectin transcription and counter the nef and vpu-mediated receptor downregulation (Giuliani et al., 2018). These publications established specific viral-induced cellular signaling changes in infected cells, thus providing a molecular mechanism for HIV infection regulated host immune functions, including T cell homing to site of inflammation and viral evasion to immune response. Previously, L-selectin shedding during HIV infections was also reported with the assumption that the shedding of L-selectin helps HIV to evade immune detection (Wang et al., 2004; Vassena et al., 2016). In addition, the work of Kononchik et al. (2018) also supports an HIV infection-induced shedding of L-selectin as another mechanism to down regulate the selectin expression on infected cells. Thus, HIV infection induces both L-selectin shedding and intracellular retention. While both shedding and retention are likely connected to cellular signaling apparatus, it is not clear to what extend they overlap, for example, are linked by common cellular signaling pathways, such as PI3K signaling pathway (Trinite et al., 2014).

Binding of gp120 to L-Selectin Enhanced HIV Viral Entry

Compared to its cellular ligands, little is known about L-selectin recognition of viral ligands. HIV-1 envelope is heavily glycosylated with over 20 N-linked glycans on each envelope monomer. In general, L-selectin prefers O-linked glycans with few exceptions in which N-glycans are linked to 6-sulfo sialy Lewis X (Clark et al., 1998; Mitoma et al., 2007). However, the densely populated gp120 glycans may enhance the avidity of L-selectin binding as soluble glycosylated but not deglycosylated gp120 readily bound to L-selectin with 50-300 nM affinities (Kononchik et al., 2018). L-selectin binding to gp120 exhibited typical C-type lectin receptor characteristics and can be inhibited with EDTA and various competing carbohydrates, including heparin, fucoidan and sialyl-Lewis X. In addition, cell surface expressed L-selectin can bind gp120 and capture HIV virions.

The binding of viral envelope glycan to L-selectin provided viral adhesion to target cells. Overexpression of L-selectin in CEM T cells enhanced HIV infection while knockdown of the gene decreased the infection. Consistently, HIV viruses produced in GnTI$^-$ 293 T cells that are deficient in mature complex N-glycans infected CD8-depleted peripheral blood mononuclear cells (PBMC) less than their glycan sufficient counterparts. These results support the notion that binding of gp120 to L-selectin enhanced HIV infection in a glycan dependent way. Mechanistically, the binding of HIV envelope glycan to L-selectin may provide the rolling adhesion for the virion on CD4+ T lymphocytes, thus facilitate the binding of HIV to CD4 and other coreceptors (**Figure 1**). It is also possible that L-selectin binding initiates a conformational change to facilitate the envelope binding to CD4 (Wang et al., 2020).

L-Selectin Shedding Facilitates HIV Viral Release

L-selectin can be cleaved at its membrane proximal region from cell surface by a disintegrin and metalloproteinase domain-containing proteins, ADAM10 and ADAM17, in response to inflammation or apoptotic signals (Wang et al., 2010). Shedding of L-selectin is part of normal host immune response and regulates migration of neutrophils and T cells in and out of the sites of inflammation (Kishimoto et al., 1989; Galkina et al., 2003). Excessive shedding of L-selectin is observed to correlate with the severity of lupus erythematosus (SLE) and type I diabetes (Font et al., 2000; Kretowski et al., 2000).

Early patient studies showed increased soluble L-selectin levels detected in HIV infected serum samples compared to healthy controls (Kourtis et al., 2000, 2003; Meddows-Taylor et al., 2001; Schramm et al., 2007; Yang et al., 2014). This HIV infection associated increase in soluble L-selectin, however, was mechanistically associated with dysregulated cytokine production and immune exhaustion rather than direct viral induced shedding. In experimental HIV infections, the loss of the CD4$^+$/CD62L$^+$ and the gain of the CD4$^-$/CD62L$^-$ lymphocytes are apparent (Kononchik et al., 2018). The progressive loss of L-selectin expression in infected CD4$^+$ T

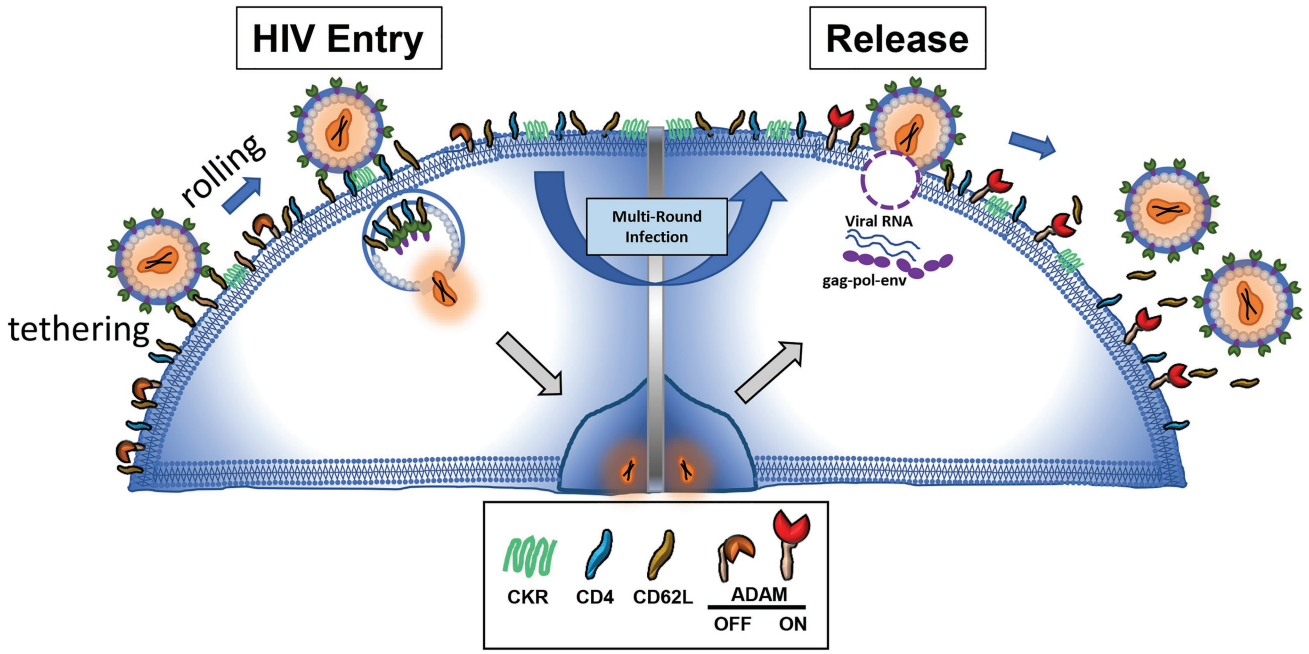

FIGURE 1 | HIV envelope binding to L-selectin facilitates HIV adhesion and infection to CD4 T cells (left). The same envelope and L-selectin interaction hinders the release of budding virions (right).

cells correlated with the viral infection suggesting that the shedding of L-selectin is viral infection-induced. HIV infection induced down regulation of entry receptors (Garcia and Miller, 1991; Alkhatib, 2009). The downregulation of CD4 expression through envelope gp120-mediated internalization on infected cells was thought to prevent superinfection, more than one virus entering the same host cell, a strategy to maximize viral transmission, while the down regulation of L-selectin may be part of viral evasion to immune response. Since L-selectin facilitates HIV adhesion and infection of CD4 T cells, inhibition of its shedding was predicted to enhance the viral infection, presumably increasing the mode of superinfection (Garcia and Miller, 1991; Michel et al., 2005). When metalloproteinase activity was inhibited, infected lymphocytes retained L-selectin expressions. HIV infection, however, was suppressed in the presence of metalloproteinase inhibitors. Further experiments showed that the metalloproteinase inhibitors did not affect the viral entry but hampered the viral release, resulting in tethering of budding virions on cell surface. These cell surface tethered infectious virions can be recovered by trypsinization (Kononchik et al., 2018). Strikingly, many tethered virion-like particles exhibit diminutive morphology in electron microscopy images in the presence of L-selectin shedding inhibitors. These data support the notion that HIV viral release from infected CD4 T cells requires shedding of L-selectin (**Figure 2**). Consistently, inhibition of L-selectin shedding also suppressed HIV release from viral reservoir CD4 T cells derived from infected individuals (Kononchik et al., 2018). While new to HIV infection, the concept of shedding of viral attachment receptor to facilitate viral release is known to influenza infections, in which the viral attachment receptor, sialic acid, is cleaved by viral neuraminidase to facilitate the viral release. Notably, most FDA approved drugs for influenza infections are neuraminidase inhibitors, suggesting viral release is a good target for developing antiviral compounds.

Viral Regulation of L-Selectin Shedding

The cellular signaling pathways controlling L-selectin expression and shedding has not been fully characterized. The shedding of L-selectin has been linked to inflammation and apoptotic activations (Wang et al., 2010). It involves caspase activation of ADAM10,17 metalloproteinases through phosphatidylserine exposure (Sommer et al., 2016). The mechanism of HIV induced L-selectin shedding is less clear. Earlier work showed that ligation of CD4 and chemokine receptor CXCR4 by HIV envelope gp120 induced L-selectin shedding (Marschner et al., 1999; Wang et al., 2004). Nef and vpu are likely the viral genes to regulate L-selectin shedding as they have been implicated in previous studies investigating viral induced inflammatory dysregulation of cell surface markers. Nef is an accessory protein required for viral transmission in primary cells and for disease progression in humans and animal models (Sodroski et al., 1986; Strebel et al., 1987; Kestler et al., 1991; Gulizia et al., 1997; Rhodes et al., 2000; Chakrabarti et al., 2003). Further, nef has been shown to activate host cellular signaling pathways, such as PKC complex, resulting in downregulation of CD4 expressions (Smith et al., 1996; Rasola et al., 2001; Wolf et al., 2008; Dikeakos et al., 2012; Pereira and daSilva, 2016; Jacob et al., 2017). Nef has also been linked to cellular apoptosis (Jacob et al., 2017), and the activation of ADAM10 and 17

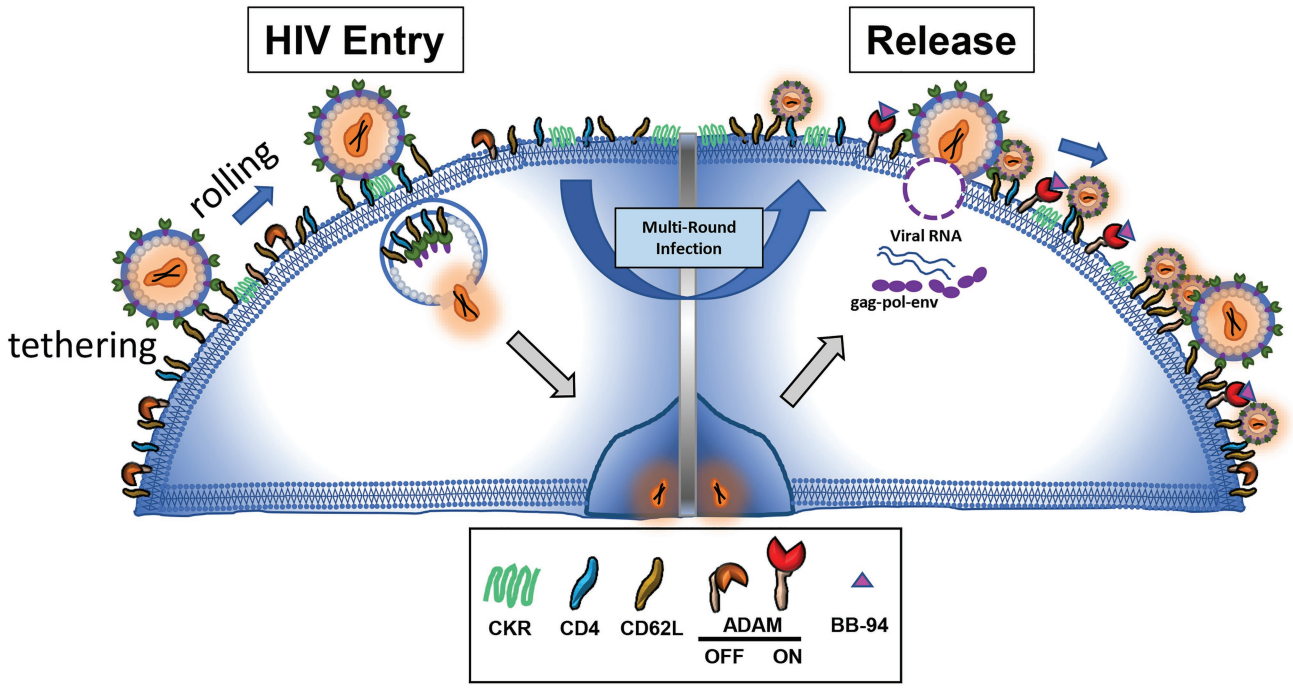

FIGURE 2 | L-selectin shedding is inhibited by metalloproteinase inhibitor BB-94, resulting in tethered and defective virions on infected cells.

through paxillin (Lee et al., 2013). Vpu is linked to HIV release through antagonizing tetherin (Neil et al., 2008). It is likely that these known viral-host interactions somehow form a coordinated signaling pathway leading to the activation of L-selectin shedding and viral release.

Interestingly, both P-selectin glycoprotein ligand 1 (PSGL-1) and CD43, have been recently reported to be incorporated into HIV virion and inhibit the virion attachment to CD4 T cells (Liu et al., 2019; Murakami et al., 2020). Both PSGL-1 and CD43 were found associated with virions and are thought to interfere viral envelope binding to CD4 and chemokine receptors due to a non-specific size preclusion (Fu et al., 2020; Murakami et al., 2020). PSGL-1 exists in a glycosylated mucin-like homodimer of 240kD protein, approximately half the size of an HIV envelope trimer. CD43, also known as sialophorin, is also heavily glycosylated with an apparent molecular weight of ~140kD. Both PSGL-1 and CD43 appear to be smaller than HIV envelope gp160. However, both are heavily glycosylated. In fact, PSGL-1 is a known ligand of L-, E- and P-selectin. This brings a possibility, in addition to the proposed interference by the size of PSGL-1, that the binding between virion-expressed PSGL-1 and host L-selectin prevents the dissemination of virus. It is conceivable that the virion-expressed PSGL-1 competitively inhibits HIV envelope binding to L-selectin on CD4 T cells, resulting in none-productive viral adhesion but not entry. If so, gp120 binding to L-selectin not only functions to promote viral adhesion, it is also a prerequisite for the viral envelope binding to CD4 and chemokine receptor. It is worth noting that both L-selectin and PSGL-1 are markers of inflammation, and both expressions are downregulated during acute infections (Kononchik et al., 2018; Fu et al., 2020). It is conceivable that the viral infection-induced downregulation of both L-selectin and PSGL-1 expressions on infected cells facilitates viral dissemination. While L-selectin downregulation is through shedding, the downregulation of PSGL-1 involved Vpu-induced ubiquitination and degradation pathway that may be targeted for antiviral development (Liu et al., 2019; Fu et al., 2020). Taken together, the growing role of selectins in viral pathogenesis and host cell defense requires further investigation into the transcriptomic state of infected cells that regulate upstream pathways leading to the currently identified viral restriction mechanisms.

Conclusion and Future Perspective

L-selectin not only regulates the migration of leucocytes but also functions as a receptor for HIV adhesion to CD4 T lymphocytes and facilitates the viral entry. Upon viral entry, infected T cells loose L-selectin expression through both receptor internalization and shedding by ADAM metalloproteinases and the inhibition of L-selectin shedding resulted in budding virions aggregation, impaired the viral release in experimental infections and reduced viral RNA released from ART-suppressed viral reservoirs (Kononchik et al., 2018). It is likely that both L-selectin internalization and shedding occur at different stages of HIV infections. For example, attachment of HIV virus may induce internalization of viral envelope bound L-selectin to endosomal compartments during viral entry. Such internalization serves to initiate cellular signaling through interaction with nef and

other viral proteins, leading to the activation of kinases and transcription machinery for viral replication. The infection induced cellular activation is not only required for viral replication, but also needed for the shedding of remaining L-selectin on infected T cells to facilitate the viral release. These recent findings suggest that the regulation of L-selectin is a promising target for developing anti-HIV therapies. While the expression and shedding of L-selectin play important roles in HIV biology, many questions remain to be addressed. The structural recognition of L-selectin to HIV gp120 glycans remains unresolved. As the intrinsic carbohydrate binding affinity of L-selectin is low (Klopocki et al., 2008), it is likely that L-selectin and gp120 binding is enhanced by the avidity of multiple glycans distributed on the envelope protein. Secondly, L-selectin is also expressed on macrophages, a known viral reservoir. Like T cells, macrophages also regulate L-selectin shedding by host cell metalloproteinases (Tedder et al., 1995a; Link et al., 2017; Wong et al., 2019). It remains to be seen if HIV release from infected macrophages also requires shedding of L-selectin. Third, L-selectin, as a member of C-type lectin receptor, presumably recognize viral glycans independent of their peptide sequences. Namely, the effect of L-selectin on HIV entry and release may be generalized to other lectin receptors interacting with viruses with heavily glycosylated envelopes.

AUTHOR CONTRIBUTIONS

JS, JI, and ZZ did the experiments for the original publications. JS, BH, and PS wrote the manuscript. TS and GR contributed to the write-up. All authors contributed to the article and approved the submitted version.

FUNDING

This work was supported in part by the National Institutes of Health Strategic Fund in HIV/AIDS research from Office of AIDS Research, and by the Intramural Research Program of National Institute of Allergy and Infectious Diseases, National Institutes of Health.

REFERENCES

Alkhatib, G. (2009). The biology of CCR5 and CXCR4. *Curr. Opin. HIV AIDS* 4, 96–103. doi: 10.1097/COH.0b013e328324bbec

Alon, R., Chen, S., Puri, K., Finger, E., and Springer, T. (1997). The kinetics of L-selectin tethers and the mechanics of selectin-mediated rolling. *J. Cell Biol.* 138, 1169–1180. doi: 10.1083/jcb.138.5.1169

Arias, J. F., and Evans, D. T. (2014). Tethering viral restriction to signal transduction. *Cell Host Microbe* 16, 267–269. doi: 10.1016/j.chom.2014.08.013

Ates, A., Kinikli, G., Turgay, M., and Duman, M. (2004). Serum-soluble selectin levels in patients with rheumatoid arthritis and systemic sclerosis. *Scand. J. Immunol.* 59, 315–320. doi: 10.1111/j.0300-9475.2004.01389.x

Baumheter, S., Singer, M. S., Henzel, W., Hemmerich, S., Renz, M., Rosen, S. D., et al. (1993). Binding of L-selectin to the vascular sialomucin CD34. *Science* 262, 436–438. doi: 10.1126/science.7692600

Berg, E. L., McEvoy, L. M., Berlin, C., Bargatze, R. F., and Butcher, E. C. (1993). L-selectin-mediated lymphocyte rolling on MAdCAM-1. *Nature* 366, 695–698. doi: 10.1038/366695a0

Butcher, E. C., and Picker, L. J. (1996). Lymphocyte homing and homeostasis. *Science* 272, 60–66. doi: 10.1126/science.272.5258.60

Chakrabarti, L. A., Metzner, K. J., Ivanovic, T., Cheng, H., Louis-Virelizier, J., Connor, R. I., et al. (2003). A truncated form of Nef selected during pathogenic reversion of simian immunodeficiency virus SIVmac239Deltanef increases viral replication. *J. Virol.* 77, 1245–1256. doi: 10.1128/JVI.77.2.1245-1256.2003

Clark, R., Fuhlbrigge, R., and Springer, T. (1998). L-Selectin ligands that are O-glycoprotease resistant and distinct from MECA-79 antigen are sufficient for tethering and rolling of lymphocytes on human high endothelial venules. *J. Cell Biol.* 140, 721–731. doi: 10.1083/jcb.140.3.721

Curtis, B. M., Scharnowske, S., and Watson, A. J. (1992). Sequence and expression of a membrane-associated C-type lectin that exhibits CD4-independent binding of human immunodeficiency virus envelope glycoprotein gp120. *Proc. Natl. Acad. Sci. U.S.A.* 89, 8356–8360.

Deeks, S. G., Overbaugh, J., Phillips, A., and Buchbinder, S. (2015). HIV infection. *Nat. Rev. Dis. Primers* 1:15035. doi: 10.1038/nrdp.2015.35

Dikeakos, J. D., Thomas, L., Kwon, G., Elferich, J., Shinde, U., and Thomas, G. (2012). An interdomain binding site on HIV-1 Nef interacts with PACS-1 and PACS-2 on endosomes to down-regulate MHC-I. *Mol. Biol. Cell* 23, 2184–2197. doi: 10.1091/mbc.E11-11-0928

Ding, Z., Issekutz, T., Downey, G., and Waddell, T. (2003). L-selectin stimulation enhances functional expression of surface CXCR4 in lymphocytes: implications for cellular activation during adhesion and migration. *Blood* 101, 4245–4252. doi: 10.1182/blood-2002-06-1782

Emu, B., Fessel, J., Schrader, S., Kumar, P., Richmond, G., Win, S., et al. (2018). Phase 3 study of Ibalizumab for multidrug-resistant HIV-1. *N. Engl. J. Med.* 379, 645–654. doi: 10.1056/NEJMoa1711460

Esser, M., Mori, T., Mondor, I., and Sattentau, Q. (1999). Cyanovirin-N binds to gp120 to interfere with CD4-dependent human immunodeficiency virus type 1 virion binding, fusion, and infectivity but does not affect the CD4 binding site on gp120 or soluble CD4-induced conformational changes in gp120. *J. Virol.* 73, 4360–4371. doi: 10.1128/JVI.73.5.4360-4371.1999

Fabre, S., Carrette, F., Chen, J., Lang, V., Semichon, M., Denoyelle, C., et al. (2008). FOXO1 regulates L-Selectin and a network of human T cell homing molecules downstream of phosphatidylinositol 3-kinase. *J. Immunol.* 181, 2980–2989. doi: 10.4049/jimmunol.181.5.2980

Flexner, C. (1998). HIV-protease inhibitors. *N. Engl. J. Med.* 338, 1281–1292. doi: 10.1056/NEJM199804303381808

Font, J., Pizcueta, P., Ramos-Casals, M., Cervera, R., Garcia-Carrasco, M., Navarro, M., et al. (2000). Increased serum levels of soluble L-selectin (CD62L) in patients with active systemic lupus erythematosus (SLE). *Clin. Exp. Immunol.* 119, 169–174. doi: 10.1046/j.1365-2249.2000.01082.x

Foxall, C., Watson, S., Dowbenko, D., Fennie, C., Lasky, L., Kiso, M., et al. (1992). The three members of the selectin receptor family recognize a common carbohydrate epitope, the sialyl Lewis(x) oligosaccharide. *J. Cell Biol.* 117, 895–902. doi: 10.1083/jcb.117.4.895

Fu, Y., He, S., Waheed, A. A., Dabbagh, D., Zhou, Z., Trinite, B., et al. (2020). PSGL-1 restricts HIV-1 infectivity by blocking virus particle attachment to target cells. *Proc. Natl. Acad. Sci. U. S. A.* 117, 9537–9545. doi: 10.1073/pnas.1916054117

Fuhlbrigge, R., Alon, R., Puri, K., Lowe, J., and Springer, T. (1996). Sialylated, fucosylated ligands for L-selectin expressed on leukocytes mediate tethering and rolling adhesions in physiologic flow conditions. *J. Cell Biol.* 135, 837–848. doi: 10.1083/jcb.135.3.837

Gainet, J., Dang, P. M., Chollet-Martin, S., Brion, M., Sixou, M., Hakim, J., et al. (1999). Neutrophil dysfunctions, IL-8, and soluble L-selectin plasma levels in rapidly progressive versus adult and localized juvenile periodontitis: variations according to disease severity and microbial flora. *J. Immunol.* 163, 5013–5019.

Galkina, E., Tanousis, K., Preece, G., Tolaini, M., Kioussis, D., Florey, O., et al. (2003). L-selectin shedding does not regulate constitutive T cell trafficking but controls the migration pathways of antigen-activated T lymphocytes. *J. Exp. Med.* 198, 1323–1335. doi: 10.1084/jem.20030485

Gallatin, W. M., Weissman, I. L., and Butcher, E. C. (1983). A cell-surface molecule involved in organ-specific homing of lymphocytes. *Nature* 304, 30–34. doi: 10.1038/304030a0

Garcia, J. V., and Miller, A. D. (1991). Serine phosphorylation-independent downregulation of cell-surface CD4 by nef. *Nature* 350, 508–511. doi: 10.1038/350508a0

Gesner, B. M., and Ginsburg, V. (1964). Effect of glycosidases on the fate of transfused lymphocytes. *Proc. Natl. Acad. Sci. U. S. A.* 52, 750–755.

Giuliani, E., Vassena, L., Galardi, S., Michienzi, A., Desimio, M. G., and Doria, M. (2018). Dual regulation of L-selectin (CD62L) by HIV-1: enhanced expression by Vpr in contrast with cell-surface down-modulation by Nef and Vpu. *Virology* 523, 121–128. doi: 10.1016/j.virol.2018.07.031

Gulizia, R. J., Collman, R. G., Levy, J. A., Trono, D., and Mosier, D. E. (1997). Deletion of nef slows but does not prevent CD4-positive T-cell depletion in human immunodeficiency virus type 1-infected human-PBL-SCID mice. *J. Virol.* 71, 4161–4164. doi: 10.1128/jvi.71.5.4161-4164.1997

Holec, A. D., Mandal, S., Prathipati, P. K., and Destache, C. J. (2017). Nucleotide reverse transcriptase inhibitors: a thorough review, present status and future perspective as HIV therapeutics. *Curr. HIV Res.* 15, 411–421. doi: 10.2174/1570162X15666171120110145

Ivetic, A., Hoskins Green, H. L., and Hart, S. J. (2019). L-selectin: a major regulator of leukocyte adhesion, migration and signaling. *Front. Immunol.* 10:1068. doi: 10.3389/fimmu.2019.01068

Jacob, R. A., Johnson, A. L., Pawlak, E. N., Dirk, B. S., Van Nynatten, L. R., Haeryfar, S. M. M., et al. (2017). The interaction between HIV-1 Nef and adaptor protein-2 reduces Nef-mediated CD4(+) T cell apoptosis. *Virology* 509, 1–10. doi: 10.1016/j.virol.2017.05.018

Jolly, C., Booth, N., and Neil, S. (2010). Cell-cell spread of human immunodeficiency virus type 1 overcomes tetherin/BST-2-mediated restriction in T cells. *J. Virol.* 84, 12185–12199. doi: 10.1128/JVI.01447-10

Kahn, J., Ingraham, R. H., Shirley, F., Migaki, G. I., and Kishimoto, T. K. (1994). Membrane proximal cleavage of L-selectin: identification of the cleavage site and a 6-kD transmembrane peptide fragment of L-selectin. *J. Cell Biol.* 125, 461–470. doi: 10.1083/jcb.125.2.461

Kestler, H. W. 3rd., Ringler, D. J., Mori, K., Panicali, D. L., Sehgal, P. K., Daniel, M. D., et al. (1991). Importance of the nef gene for maintenance of high virus loads and for development of AIDS. *Cell* 65, 651–662. doi: 10.1016/0092-8674(91)90097-I

Kishimoto, T. K., Jutila, M. A., Berg, E. L., and Butcher, E. C. (1989). Neutrophil Mac-1 and MEL-14 adhesion proteins inversely regulated by chemotactic factors. *Science* 245, 1238–1241. doi: 10.1126/science.2551036

Klopocki, A. G., Yago, T., Mehta, P., Yang, J., Wu, T., Leppanen, A., et al. (2008). Replacing a lectin domain residue in L-selectin enhances binding to P-selectin glycoprotein ligand-1 but not to 6-sulfo-sialyl Lewis x. *J. Biol. Chem.* 283, 11493–11500. doi: 10.1074/jbc.M709785200

Kobayashi, M., Mitoma, J., Nakamura, N., Katsuyama, T., Nakayama, J., and Fukuda, M. (2004). Induction of peripheral lymph node addressin in human gastric mucosa infected by *Helicobacter pylori*. *Proc. Natl. Acad. Sci. U. S. A.* 101, 17807–17812. doi: 10.1073/pnas.0407503101

Kononchik, J., Ireland, J., Zou, Z., Segura, J., Holzapfel, G., Chastain, A., et al. (2018). HIV-1 targets L-selectin for adhesion and induces its shedding for viral release. *Nat. Commun.* 9:2825. doi: 10.1038/s41467-018-05197-2

Kourtis, A. P., Lee, F. K., and Stoll, B. J. (2003). Soluble L-selectin, a marker of immune activation, in neonatal infection. *Clin. Immunol.* 109, 224–228. doi: 10.1016/S1521-6616(03)00209-2

Kourtis, A. P., Nesheim, S. R., Thea, D., Ibegbu, C., Nahmias, A. J., and Lee, F. K. (2000). Correlation of virus load and soluble L-selectin, a marker of immune activation, in pediatric HIV-1 infection. *AIDS* 14, 2429–2436. doi: 10.1097/00002030-200011100-00003

Kretowski, A., Gillespie, K. M., Bingley, P. J., and Kinalska, I. (2000). Soluble L-selectin levels in type I diabetes mellitus: a surrogate marker for disease activity? *Immunology* 99, 320–325. doi: 10.1046/j.1365-2567.2000.00967.x

Lawrence, M., and Springer, T. (1991). Leukocytes roll on a selectin at physiologic flow rates: distinction from and prerequisite for adhesion through integrins. *Cell* 65, 859–873. doi: 10.1016/0092-8674(91)90393-D

Lee, J. H., Wittki, S., Brau, T., Dreyer, F. S., Kratzel, K., Dindorf, J., et al. (2013). HIV Nef, paxillin, and Pak1/2 regulate activation and secretion of TACE/ADAM10 proteases. *Mol. Cell* 49, 668–679. doi: 10.1016/j.molcel.2012.12.004

Li, M., Ablan, S. D., Miao, C., Zheng, Y. M., Fuller, M. S., Rennert, P. D., et al. (2014). TIM-family proteins inhibit HIV-1 release. *Proc. Natl. Acad. Sci. U. S. A.* 111, E3699–E3707. doi: 10.1073/pnas.1404851111

Link, M. A., Lucke, K., Schmid, J., Schumacher, V., Eden, T., Rose-John, S., et al. (2017). The role of ADAM17 in the T-cell response against bacterial pathogens. *PLoS One* 12:e0184320. doi: 10.1371/journal.pone.0184320

Link, J. O., Rhee, M. S., Tse, W. C., Zheng, J., Somoza, J. R., Rowe, W., et al. (2020). Clinical targeting of HIV capsid protein with a long-acting small molecule. *Nature* 584, 614–618. doi: 10.1038/s41586-020-2443-1

Liu, Y., Fu, Y., Wang, Q., Li, M., Zhou, Z., Dabbagh, D., et al. (2019). Proteomic profiling of HIV-1 infection of human CD4(+) T cells identifies PSGL-1 as an HIV restriction factor. *Nat. Microbiol.* 4, 813–825. doi: 10.1038/s41564-019-0372-2

Lusic, M., and Siliciano, R. F. (2017). Nuclear landscape of HIV-1 infection and integration. *Nat. Rev. Microbiol.* 15, 69–82. doi: 10.1038/nrmicro.2016.162

Marschner, S., Freiberg, B. A., Kupfer, A., Hunig, T., and Finkel, T. H. (1999). Ligation of the CD4 receptor induces activation-independent down-regulation of L-selectin. *Proc. Natl. Acad. Sci. U. S. A.* 96, 9763–9768.

Matthews, T., Salgo, M., Greenberg, M., Chung, J., DeMasi, R., and Bolognesi, D. (2004). Enfuvirtide: the first therapy to inhibit the entry of HIV-1 into host CD4 lymphocytes. *Nat. Rev. Drug Discov.* 3, 215–225. doi: 10.1038/nrd1331

Meddows-Taylor, S., Kuhn, L., Meyers, T. M., and Tiemessen, C. T. (2001). Altered expression of L-selectin (CD62L) on polymorphonuclear neutrophils of children vertically infected with human immunodeficiency virus type 1. *J. Clin. Immunol.* 21, 286–292. doi: 10.1023/A:1010935409997

Michel, N., Allespach, I., Venzke, S., Fackler, O. T., and Keppler, O. T. (2005). The Nef protein of human immunodeficiency virus establishes superinfection immunity by a dual strategy to downregulate cell-surface CCR5 and CD4. *Curr. Biol.* 15, 714–723. doi: 10.1016/j.cub.2005.02.058

Mitoma, J., Bao, X., Petryanik, B., Schaerli, P., Gauguet, J.-M., Yu, S.-Y., et al. (2007). Critical functions of N-glycans in L-selectin-mediated lymphocyte homing and recruitment. *Nat. Immunol.* 8, 409–418. doi: 10.1038/ni1442

Mitsuoka, C., Sawada-Kasugai, M., Ando-Furui, K., Izawa, M., Nakanishi, H., Nakamura, S., et al. (1998). Identification of a major carbohydrate capping group of the L-selectin ligand on high endothelial venules in human lymph nodes as 6-sulfo sialyl Lewis X. *J. Biol. Chem.* 273, 11225–11233. doi: 10.1074/jbc.273.18.11225

Moore, D. A., Henderson, D., and Gazzard, B. G. (1998). Neutrophil adhesion molecules in HIV disease. *Clin. Exp. Immunol.* 114, 73–77. doi: 10.1046/j.1365-2249.1998.00686.x

Mori, T., Gustafson, K. R., Pannell, L. K., Shoemaker, R. H., Wu, L., McMahon, J. B., et al. (1998). Recombinant production of cyanovirin-N, a potent human immunodeficiency virus-inactivating protein derived from a cultured cyanobacterium. *Protein Expr. Purif.* 12, 151–158. doi: 10.1006/prep.1997.0838

Murakami, T., Carmona, N., and Ono, A. (2020). Virion-incorporated PSGL-1 and CD43 inhibit both cell-free infection and transinfection of HIV-1 by preventing virus-cell binding. *Proc. Natl. Acad. Sci. U. S. A.* 117, 8055–8063. doi: 10.1073/pnas.1916055117

Neil, S., Zang, T., and Bieniasz, P. (2008). Tetherin inhibits retrovirus release and is antagonized by HIV-1 Vpu. *Nature* 451, 425–430. doi: 10.1038/nature06553

Paton, N. I., Stohr, W., Arenas-Pinto, A., Fisher, M., Williams, I., Johnson, M., et al. (2015). Protease inhibitor monotherapy for long-term management of HIV infection: a randomised, controlled, open-label, non-inferiority trial. *Lancet HIV* 2, e417–e426. doi: 10.1016/S2352-3018(15)00176-9

Pereira, E. A., and daSilva, L. L. (2016). HIV-1 Nef: taking control of protein trafficking. *Traffic* 17, 976–996. doi: 10.1111/tra.12412

Pinto, D. O., Scott, T. A., DeMarino, C., Pleet, M. L., Vo, T. T., Saifuddin, M., et al. (2019). Effect of transcription inhibition and generation of suppressive viral non-coding RNAs. *Retrovirology* 16:13. doi: 10.1186/s12977-019-0475-0

Puri, K. D., Finger, E. B., Gaudernack, G., and Springer, T. A. (1995). Sialomucin CD34 is the major L-selectin ligand in human tonsil high endothelial venules. *J. Cell Biol.* 131, 261–270. doi: 10.1083/jcb.131.1.261

Ramdas, P., Sahu, A. K., Mishra, T., Bhardwaj, V., and Chande, A. (2020). From entry to egress: strategic exploitation of the cellular processes by HIV-1. *Front. Microbiol.* 11:559792. doi: 10.3389/fmicb.2020.559792

Rasola, A., Gramaglia, D., Boccaccio, C., and Comoglio, P. M. (2001). Apoptosis enhancement by the HIV-1 Nef protein. *J. Immunol.* 166, 81–88. doi: 10.4049/jimmunol.166.1.81

Rhodes, D. I., Ashton, L., Solomon, A., Carr, A., Cooper, D., Kaldor, J., et al. (2000). Characterization of three nef-defective human immunodeficiency virus type 1 strains associated with long-term nonprogression. Australian long-term nonprogressor study group. *J. Virol.* 74, 10581–10588. doi: 10.1128/jvi.74.22.10581-10588.2000

Rose, K. M., Hirsch, V. M., and Bouamr, F. (2020). Budding of a retrovirus: some assemblies required. *Viruses* 12:1188. doi: 10.3390/v12101188

Rosen, S. D. (2004). Ligands for L-selectin: homing, inflammation, and beyond. *Annu. Rev. Immunol.* 22, 129–156. doi: 10.1146/annurev.immunol.21.090501.080131

Saag, M. S., Gandhi, R. T., Hoy, J. F., Landovitz, R. J., Thompson, M. A., Sax, P. E., et al. (2020). Antiretroviral drugs for treatment and prevention of HIV infection in adults: 2020 recommendations of the international antiviral society-USA panel. *JAMA* 324, 1651–1669. doi: 10.1001/jama.2020.17025

Schneider-Hohendorf, T., Philipp, K., Husstedt, I. W., Wiendl, H., and Schwab, N. (2014). Specific loss of cellular L-selectin on CD4(+) T cells is associated with progressive multifocal leukoencephalopathy development during HIV infection. *AIDS* 28, 793–795. doi: 10.1097/QAD.0000000000000201

Schramm, D. B., Meddows-Taylor, S., Gray, G. E., Kuhn, L., and Tiemessen, C. T. (2007). Low maternal viral loads and reduced granulocyte-macrophage colony-stimulating factor levels characterize exposed, uninfected infants who develop protective human immunodeficiency virus type 1-specific responses. *Clin. Vaccine Immunol.* 14, 348–354. doi: 10.1128/CVI.00464-06

Sfikakis, P. P., Charalambopoulos, D., Vaiopoulos, G., and Mavrikakis, M. (1999). Circulating P- and L-selectin and T-lymphocyte activation and patients with autoimmune rheumatic diseases. *Clin. Rheumatol.* 18, 28–32. doi: 10.1007/s100670050047

Shimada, Y., Hasegawa, M., Takehara, K., and Sato, S. (2001). Elevated serum L-selectin levels and decreased L-selectin expression on CD8(+) lymphocytes in systemic sclerosis. *Clin. Exp. Immunol.* 124, 474–479. doi: 10.1046/j.1365-2249.2001.01514.x

Smith, B. L., Krushelnycky, B. W., Mochly-Rosen, D., and Berg, P. (1996). The HIV nef protein associates with protein kinase C theta. *J. Biol. Chem.* 271, 16753–16757. doi: 10.1074/jbc.271.28.16753

Snyder, G. A., Ford, J., Torabi-Parizi, P., Arthos, J. A., Schuck, P., Colonna, M., et al. (2005). Characterization of DC-SIGN/R interaction with human immunodeficiency virus type 1 gp120 and ICAM molecules favors the receptor's role as an antigen-capturing rather than an adhesion receptor. *J. Virol.* 79, 4589–4598. doi: 10.1128/JVI.79.8.4589-4598.2005

Sodroski, J., Goh, W. C., Rosen, C., Tartar, A., Portetelle, D., Burny, A., et al. (1986). Replicative and cytopathic potential of HTLV-III/LAV with sor gene deletions. *Science* 231, 1549–1553. doi: 10.1126/science.3006244

Sommer, A., Kordowski, F., Buch, J., Maretzky, T., Evers, A., Andra, J., et al. (2016). Phosphatidylserine exposure is required for ADAM17 sheddase function. *Nat. Commun.* 7:11523. doi: 10.1038/ncomms11523

Spencer, M., Max, N., Ireland, J., Zou, Z., Wang, R., and Sun, P. (2017). Over-expression of a human CD62L ecto-domain and a potential role of RNA pseudoknot structures in recombinant protein expression. *Protein Expr. Purif.* 140, 65–73. doi: 10.1016/j.pep.2017.08.008

Strebel, K., Daugherty, D., Clouse, K., Cohen, D., Folks, T., and Martin, M. A. (1987). The HIV 'A' (sor) gene product is essential for virus infectivity. *Nature* 328, 728–730. doi: 10.1038/328728a0

Streeter, P. R., Rouse, B. T., and Butcher, E. C. (1988). Immunohistologic and functional characterization of a vascular addressin involved in lymphocyte homing into peripheral lymph nodes. *J. Cell Biol.* 107, 1853–1862. doi: 10.1083/jcb.107.5.1853

Tedder, T. F., Steeber, D. A., Chen, A., and Engel, P. (1995a). The selectins: vascular adhesion molecules. *FASEB J.* 9, 866–873.

Tedder, T. F., Steeber, D. A., and Pizcueta, P. (1995b). L-selectin-deficient mice have impaired leukocyte recruitment into inflammatory sites. *J. Exp. Med.* 181, 2259–2264.

Trinite, B., Chan, C. N., Lee, C. S., Mahajan, S., Luo, Y., Muesing, M. A., et al. (2014). Suppression of Foxo1 activity and down-modulation of CD62L (L-selectin) in HIV-1 infected resting CD4 T cells. *PLoS One* 9:e110719. doi: 10.1371/journal.pone.0110719

Tsibris, A. M., and Kuritzkes, D. R. (2007). Chemokine antagonists as therapeutics: focus on HIV-1. *Annu. Rev. Med.* 58, 445–459. doi: 10.1146/annurev.med.58.080105.102908

Usami, Y., Wu, Y., and Gottlinger, H. G. (2015). SERINC3 and SERINC5 restrict HIV-1 infectivity and are counteracted by Nef. *Nature* 526, 218–223. doi: 10.1038/nature15400

Vassena, L., Giuliani, E., Buonomini, A. R., Malagnino, V., Andreoni, M., and Doria, M. (2016). Brief report: L-selectin (CD62L) is downregulated on CD4+ and CD8+ T lymphocytes of HIV-1-infected individuals naive for ART. *J. Acquir. Immune Defic. Syndr.* 72, 492–497. doi: 10.1097/QAI.0000000000000999

Vassena, L., Giuliani, E., Koppensteiner, H., Bolduan, S., Schindler, M., and Doria, M. (2015). HIV-1 Nef and Vpu interfere with L-selectin (CD62L) cell surface expression to inhibit adhesion and signaling in infected CD4+ T lymphocytes. *J. Virol.* 89, 5687–5700. doi: 10.1128/JVI.00611-15

Wang, Q., Finzi, A., and Sodroski, J. (2020). The conformational states of the HIV-1 envelope glycoproteins. *Trends Microbiol.* 28, 655–667. doi: 10.1016/j.tim.2020.03.007

Wang, J., Marschner, S., and Finkel, T. (2004). CXCR4 engagement is required for HIV-1-induced L-selectin shedding. *Blood* 103, 1218–1221. doi: 10.1182/blood-2003-02-0576

Wang, Y., Zhang, A. C., Ni, Z., Herrera, A., and Walcheck, B. (2010). ADAM17 activity and other mechanisms of soluble L-selectin production during death receptor-induced leukocyte apoptosis. *J. Immunol.* 184, 4447–4454. doi: 10.4049/jimmunol.0902925

Wolf, D., Giese, S. I., Witte, V., Krautkramer, E., Trapp, S., Sass, G., et al. (2008). Novel (n)PKC kinases phosphorylate Nef for increased HIV transcription, replication and perinuclear targeting. *Virology* 370, 45–54. doi: 10.1016/j.virol.2007.08.015

Wong, M. E., Jaworowski, A., and Hearps, A. C. (2019). The HIV reservoir in monocytes and macrophages. *Front. Immunol.* 10:1435. doi: 10.3389/fimmu.2019.02517

Xu, B., Wagner, N., Pham, L. N., Magno, V., Shan, Z., Butcher, E. C., et al. (2003). Lymphocyte homing to bronchus-associated lymphoid tissue (BALT) is mediated by L-selectin/PNAd, alpha4beta1 integrin/VCAM-1, and LFA-1 adhesion pathways. *J. Exp. Med.* 197, 1255–1267. doi: 10.1084/jem.20010685

Yang, S., Liu, F., Wang, Q. J., Rosenberg, S. A., and Morgan, R. A. (2011). The shedding of CD62L (L-selectin) regulates the acquisition of lytic activity in human tumor reactive T lymphocytes. *PLoS One* 6:e22560. doi: 10.1371/journal.pone.0029502

Yang, W., Zhou, J. Y., Chen, L., Ao, M., Sun, S., Aiyetan, P., et al. (2014). Glycoproteomic analysis identifies human glycoproteins secreted from HIV latently infected T cells and reveals their presence in HIV+ plasma. *Clin. Proteomics* 11:9. doi: 10.1186/1559-0275-11-9

Yeh, Y. J., Jenike, K. M., Calvi, R. M., Chiarella, J., Hoh, R., Deeks, S. G., et al. (2020). Filgotinib suppresses HIV-1-driven gene transcription by inhibiting HIV-1 splicing and T cell activation. *J. Clin. Invest.* 130, 4969–4984. doi: 10.1172/JCI137371

Zou, Z., Chastain, A., Moir, S., Ford, J., Trandem, K., Martinelli, E., et al. (2011). Siglecs facilitate HIV-1 infection of macrophages through adhesion with viral sialic acids. *PLoS One* 6:e24559. doi: 10.1371/journal.pone.0024559

Conflict of Interest: The authors declare that the research was conducted in the absence of any commercial or financial relationships that could be construed as a potential conflict of interest.

Publisher's Note: All claims expressed in this article are solely those of the authors and do not necessarily represent those of their affiliated organizations, or those of the publisher, the editors and the reviewers. Any product that may be evaluated in this article, or claim that may be made by its manufacturer, is not guaranteed or endorsed by the publisher.

frontiers in Microbiology

ORIGINAL RESEARCH
published: 08 October 2021
doi: 10.3389/fmicb.2021.731026

Full-Length Galectin-3 Is Required for High Affinity Microbial Interactions and Antimicrobial Activity

*Shang-Chuen Wu[1], Alex D. Ho[1], Nourine A. Kamili[2], Jianmei Wang[2], Kaleb L. Murdock[1], Richard D. Cummings[3], Connie M. Arthur[1]*and Sean R. Stowell[1,2]**

[1]Joint Program in Transfusion Medicine, Department of Pathology, Brigham and Women's Hospital, Harvard Medical School, Boston, MA, United States, [2]Center for Transfusion Medicine and Cellular Therapies, Emory University School of Medicine, Atlanta, GA, United States, [3]Department of Surgery, Beth Israel Deaconess Medical Center, Harvard Medical School, Boston, MA, United States

OPEN ACCESS

Edited by:
Fabrizio Chiodo, National Research Council (CNR), Italy

Reviewed by:
Gabriel Adrián Rabinovich, CONICET Instituto de Biología y Medicina Experimental (IBYME), Argentina
Fu-Tong Liu, Academia Sinica, Taiwan

***Correspondence:**
Connie M. Arthur
cmarthur@bwh.harvard.edu
Sean R. Stowell
srstowell@bwh.harvard.edu

Specialty section:
This article was submitted to Microbial Immunology, a section of the journal Frontiers in Microbiology

Received: *25 June 2021*
Accepted: *30 August 2021*
Published: *08 October 2021*

Citation:
Wu S-C, Ho AD, Kamili NA, Wang J, Murdock KL, Cummings RD, Arthur CM and Stowell SR (2021) Full-Length Galectin-3 Is Required for High Affinity Microbial Interactions and Antimicrobial Activity. Front. Microbiol. 12:731026. doi: 10.3389/fmicb.2021.731026

While adaptive immunity enables the recognition of a wide range of microbial antigens, immunological tolerance limits reactively toward self to reduce autoimmunity. Some bacteria decorate themselves with self-like antigens as a form of molecular mimicry to limit recognition by adaptive immunity. Recent studies suggest that galectin-4 (Gal-4) and galectin-8 (Gal-8) may provide a unique form of innate immunity against molecular mimicry by specifically targeting microbes that decorate themselves in self-like antigens. However, the binding specificity and antimicrobial activity of many human galectins remain incompletely explored. In this study, we defined the binding specificity of galectin-3 (Gal-3), the first galectin shown to engage microbial glycans. Gal-3 exhibited high binding toward mammalian blood group A, B, and αGal antigens in a glycan microarray format. In the absence of the N-terminal domain, the C-terminal domain of Gal-3 (Gal-3C) alone exhibited a similar overall binding pattern, but failed to display the same level of binding for glycans over a range of concentrations. Similar to the recognition of mammalian glycans, Gal-3 and Gal-3C also specifically engaged distinct microbial glycans isolated and printed in a microarray format, with Gal-3 exhibiting higher binding at lower concentrations toward microbial glycans than Gal-3C. Importantly, Gal-3 and Gal-3C interactions on the microbial microarray accurately predicted actual interactions toward intact microbes, with Gal-3 and Gal-3C displaying carbohydrate-dependent binding toward distinct strains of *Providentia alcalifaciens* and *Klebsiella pneumoniae* that express mammalian-like antigens, while failing to recognize similar strains that express unrelated antigens. While both Gal-3 and Gal-3C recognized specific strains of *P. alcalifaciens* and *K. pneumoniae*, only Gal-3 was able to exhibit antimicrobial activity even when evaluated at higher concentrations. These results demonstrate that while Gal-3 and Gal-3C specifically engage distinct mammalian and microbial glycans, Gal-3C alone does not possess antimicrobial activity.

Keywords: galectin, blood group, microbe, antimicrobial, molecular mimicry

INTRODUCTION

Galectins are an ancient and evolutionarily conserved protein family that have a diverse range of functions relevant to a wide variety of diseases (Liu and Rabinovich, 2005, 2010; Vasta, 2009). Among carbohydrate binding proteins, galectins are the most widely expressed in all organisms and primarily engage counter ligands through recognition of β-galactose-containing glycoconjugates (Barondes et al., 1994). Galectins have been classified into three major groups based on their quaternary structural features, prototypical, tandem repeat, and chimeric (Liu and Rabinovich, 2010; Arthur et al., 2015a). Among these, Gal-3 is the only chimeric galectin, possessing a single carbohydrate recognition domain (CRD) and a self-aggregating N-terminal domain rich in proline, glycine, and tyrosine residues which can mediate oligomerization in presence of multivalent ligands (Hsu et al., 1992; Ahmad et al., 2004a; Morris et al., 2004).

In addition to modulating host cell function through engagement of cell surface carbohydrates, galectins can also interact directly with bacterial surface glycans (Vasta, 2009). Gal-3 in particular was the first shown to engage bacterial glycans where early studies demonstrated binding to lipopolysaccharides (LPS) isolated from *Pseudomonas aeruginosa*, *Klebsiella pneumoniae*, *Neisseria gonorrhoeae*, *Neisseria meningitidis,* and *Helicobacter pylori* (Mey et al., 1996; Gupta et al., 1997; John et al., 2002; Fowler et al., 2006; Quattroni et al., 2012; Vasta, 2012). Although interactions between Gal-3 and the LPS of *N. meningitidis* in particular appear to involve carbohydrate recognition through its C-terminal CRD domain (Vinogradov and Perry, 2001), the fine specificity of Gal-3 for microbial glycans, many of which can be quite diverse and distinct in structure, remains incompletely understood.

The ability of galectins to engage bacterial glycans may represent an important element of host immunity. While adaptive immunity can target a nearly infinite range of antigens, the breadth of this ability is tempered by tolerance mechanisms that limit reactivity toward self. Although this may reduce the probability of autoimmunity, this creates a gap in adaptive immunity toward microbes that decorate themselves in self-like antigens as a form of molecular mimicry (Arthur et al., 2015c). Previous studies demonstrated that Gal-4 and Gal-8 in particular can kill strains of *Escherichia coli* through recognition of bacterial surface glycans that mimic blood group antigens (Stowell et al., 2010). However, despite early studies demonstrating that Gal-3 can bind LPS (Mey et al., 1996; Gupta et al., 1997; John et al., 2002; Fowler et al., 2006; Quattroni et al., 2012), the overall antimicrobial activity of Gal-3, including key features of the quaternary structure of Gal-3 responsible for this antimicrobial activity, remains relatively unexplored.

As carbohydrate recognition have been previously shown to reside within the C-terminal domain of Gal-3 (Seetharaman et al., 1998), in this study, we examined the binding specificity of Gal-3 and Gal-3C over a range of concentrations using a series of glycan microarrays populated with mammalian or microbial glycans. While Gal-3 and Gal-3C possess similar overall binding specificity, full-length Gal-3 was required for higher affinity binding toward glycans on each array, suggesting that oligomerization status through the N-terminal domain likely plays a key role in higher affinity glycan recognition. Importantly, the relative affinity of Gal-3 toward glycans on the microbial glycan microarray (MGM) accurately predicted actual antimicrobial activity. However, while Gal-3 and Gal-3C both engaged microbial glycans and intact microbes, only Gal-3 possessed microbicidal activity.

MATERIALS AND METHODS

Protein Expression and Purification of Human Gal-3 by *Escherichia coli*

Expression plasmids encoding human Gal-3 and Gal-3C were transformed into *E.coli* BL21 (DE3), and Gal-3 and Gal-3C were then expressed as outlined previously (Stowell et al., 2010; Wu et al., 2021b). Briefly, transformed bacteria were cultured in LB broth containing 100 μg/ml ampicillin with agitation (250 rpm) at 37°C. When bacteria were grown to the mid-log phase, protein expression was induced by addition of isopropyl 1-thio-β-D-galactopyranoside (IPTG, 1.5 mM). After 20-h induction in 16°C, 6 L cultured bacteria were pelleted and harvested by centrifugation and then resuspended in 60 ml bacterial lysis buffer (PBS with 14 mM 2-mercaptoethanol (2-ME), 60 μl ribonuclease A (RNase A), 60 μl DNase I, 60 μl lysozyme, and 2 protease inhibitor cocktail tablets). The suspension was passed through a cell disruptor, and the lysate was centrifuged at 17,000 rpm at 4°C for 1 h. Supernatant was applied to lactosyl-sepharose affinity chromatography column. For elution, the elution buffer (PBS with 14 mM 2-ME and 100 mM lactose) was added. The desired fractions were pooled and stained with Coomassie blue on SDS-PAGE gel to test purity (**Supplementary Figure 1**). Before derivatization, 2-ME and lactose were removed from Gal-3 using a PD-10 gel filtration column for bacteria killing assay.

Effect of Recombinant Gal-3 on Bacteria Viability

When assaying potential antimicrobial effects of Gal-3 and Gal-3C, each strain was assessed in the mid-logarithmic growth phase (OD_{600} of ~0.1) and grown in LB media as outlined previously (Arthur et al., 2015b). Bacterial cells were incubated with the concentrations of each galectin indicated in the figure legends (0.04–10 μM) at 37°C for 2 h with shaking at 250 rpm. Bacteria were then pipetted and plated on LB agar plate to determine the number of viable bacteria by CFU enumeration.

Bacterial Strains

Providentia alcalifaciens O5 and *P. alcalifaciens* O21 were kindly provided by Y. Knirel (ND Zelinsky Institute of Organic Chemistry, Moscow, Russia). *K. pneumoniae* O1 and *K. pneumoniae* O4 were kindly provided by C. Whitfield (University of Guelph). Each bacteria strain was grown and maintained at 37°C using LB culture medium (Fisher).

Mammalian Glycan Array Analysis

Galectins were labeled with Alexa Fluor™ 488 NHS Ester (succinimidyl ester) by incubating 2 mg/ml galectin with 1 mg Alexa Fluor™ 488 for 1 h at room temperature and avoid from light as outlined previously (Stowell et al., 2004). Unconjugated Alexa Fluor™ 488 and free lactose were separated using a PD-10 gel filtration column (GE Healthcare). Labeled galectin was purified again by lactosyl-sepharose column to remove any inactive protein generated during the labeling process. Bound galectin was eluted with 100 mM lactose in PBS plus 2-ME. While 2-ME is not required for Gal-3 activity, this approach was used to provide a consistent protocol for all galectin purification. Importantly, 2-ME and lactose were then removed using PD-10 gel filtration column. Finally, labeled galectin was applied to CFG glycan microarray (CFG) and MGM prepared as described previously (Blixt et al., 2004; Stowell et al., 2008a, 2014; Song et al., 2009; Wu et al., 2021a). For galectin recognition of glycans on the printed glycan microarray, the slides were blocked with blocking buffer (500 mg of BSA in 50 ml PBST) for 1 h at room temperature. Slides were then incubated with directly labeled Gal-3 or Gal-3C at the indicated concentrations using binding buffer (500 mg of BSA in 50 ml PBST with 14 mM 2-ME) for 1 h at room temperature in a dark humid chamber. As noted previously, while 2-ME is not required for Gal-3 stability, as it is required to maintain the activity of other galectins, we have employed this binding buffer for all galectin assays to provide a uniform approach when assessing galectin binding specificity using glycan microarrays. Slides were then washed by successive immersion in PBST containing 0.5% Tween 20 (four times), PBS (four times), and H_2O (four times). The slide was dried by microcentrifugation, and an image of bound fluorescence was obtained using a microarray scanner (GenePix 4000 B, Molecular devices). Integrated spot intensities were obtained using Imagene software (GenePix Pro 7). The heat map was created by GraphPad Prism 8 (Prism 8) as outlined previously (Verkerke et al., 2021), which was also used to ascertain dissociation constants (K_D). For non-saturated positive glycan interactions, the relative fluorescence units were plotted as a percent of the maximal binding at the highest concentration examined.

Flow Cytometry Analysis

To examine potential binding by each galectin, bacteria were resuspended and washed twice in PBS at 4°C and then incubated with 0.1 μM Alexa Fluor™ 488 labeled Gal-3 or Gal-3C at 4°C for 20 min. In some experiments, Gal-3 or Gal-3C were co-incubated with 20 mM thiodigalactoside (TDG) for 10 min before incubation with the bacteria as a control. After incubation, cells were washed twice and resuspended them in 400 μl PBS for flow cytometry analysis using FACSCanto II flow cytometer (BD Biosciences). The data were processed with FlowJo version 10.

RESULTS

Gal-3 and Gal-3C Display Similar Preferences for Blood Group Antigens

To better understand the binding specificity and affinity of Gal-3, including the influence of the N-terminal domain, for glycan ligands, we first examined its binding specificity using the Consortium for Functional Glycomics (CFG) glycan microarray. To accomplish this, we expressed the Gal-3 and Gal-3C (**Supplementary Figure 1**), followed by the evaluation of both proteins in parallel on the CFG array. As the overall apparent specificity of carbohydrate binding proteins can be influenced by the protein concentration used for array analysis and as the N-terminal domain may enhance overall binding affinity through cross linking of bound glycans, we examined glycan recognition over a range of concentrations as opposed to a single concentration primarily employed in our previous studies using glycan microarray analysis (Stowell et al., 2010). Using this approach, we found that virtually no binding could be detected for either Gal-3 or Gal-3C at or below concentrations of 0.12 μM (data not shown). However, at 0.36 μM, recognition of blood group B was observed by Gal-3, but not by Gal-3C (**Figures 1A**,**B**). Nevertheless, at 1.1 μM, binding toward the same blood group B antigen was observed for Gal-3C (**Figure 1B**). Binding toward additional glycan ligands, primarily polymorphic blood group antigens, became readily apparent following incubation of Gal-3 at higher concentration. However, in contrast to Gal-3, incubation with 3.3 μM Gal-3C was required to achieve a similar level of absolute binding toward the same initial blood group B antigen bound by Gal-3 at 0.36 μM (**Figure 1B**). Similar to Gal-3, at higher concentrations, additional glycan recognition, including a strong preference for blood group antigens, could be detected for Gal-3C, which generally mirrored glycan recognition by Gal-3 at lower concentrations (**Figures 1A**,**B**).

Although overall binding specificity of Gal-3 and Gal-3C appeared to display high level of similarity when adjusted for concentration, the apparent affinity of each protein for individual glycan ligands differed. In order to define the relatively affinity of Gal-3 and Gal-3C for glycan ligands on the CFG microarray in more detail, we next examined binding isotherms generated following incubation of each galectin over a range of concentrations. Given the high affinity interactions observed toward blood group antigens, we specifically evaluated Gal-3 and Gal-3C binding toward distinct blood group antigen types as presented on the CFG array. While very little binding could be observed toward lactose (Galβ1-4Glc) or type 1 or type 2 LacNAc (Galβ1-3GlcNAc or Galβ1-4GlcNAc, respectively; **Figure 2A**), similar high affinity interactions were observed for blood group A and blood group B, although Gal-3 and Gal-3C each displayed a slightly higher affinity for type 2 blood group A and blood group B antigens than type 1 antigens (**Figures 2B**,**C**). In contrast, Gal-3 and Gal-3C appeared to possess a lower affinity for the H antigens regardless of type 1 or type 2 configuration when compared to blood group A or B (**Figure 2D**). However, the fucose modification present in B antigens likely positively influences Gal-3 and Gal-3C blood group recognition, as neither Gal-3 nor Gal-3C displayed similar binding affinity toward αGal containing type 1 or type 2 structures despite the fact that these glycans terminate in the blood group B disaccharide (**Figure 2E**). These results suggest that Gal-3

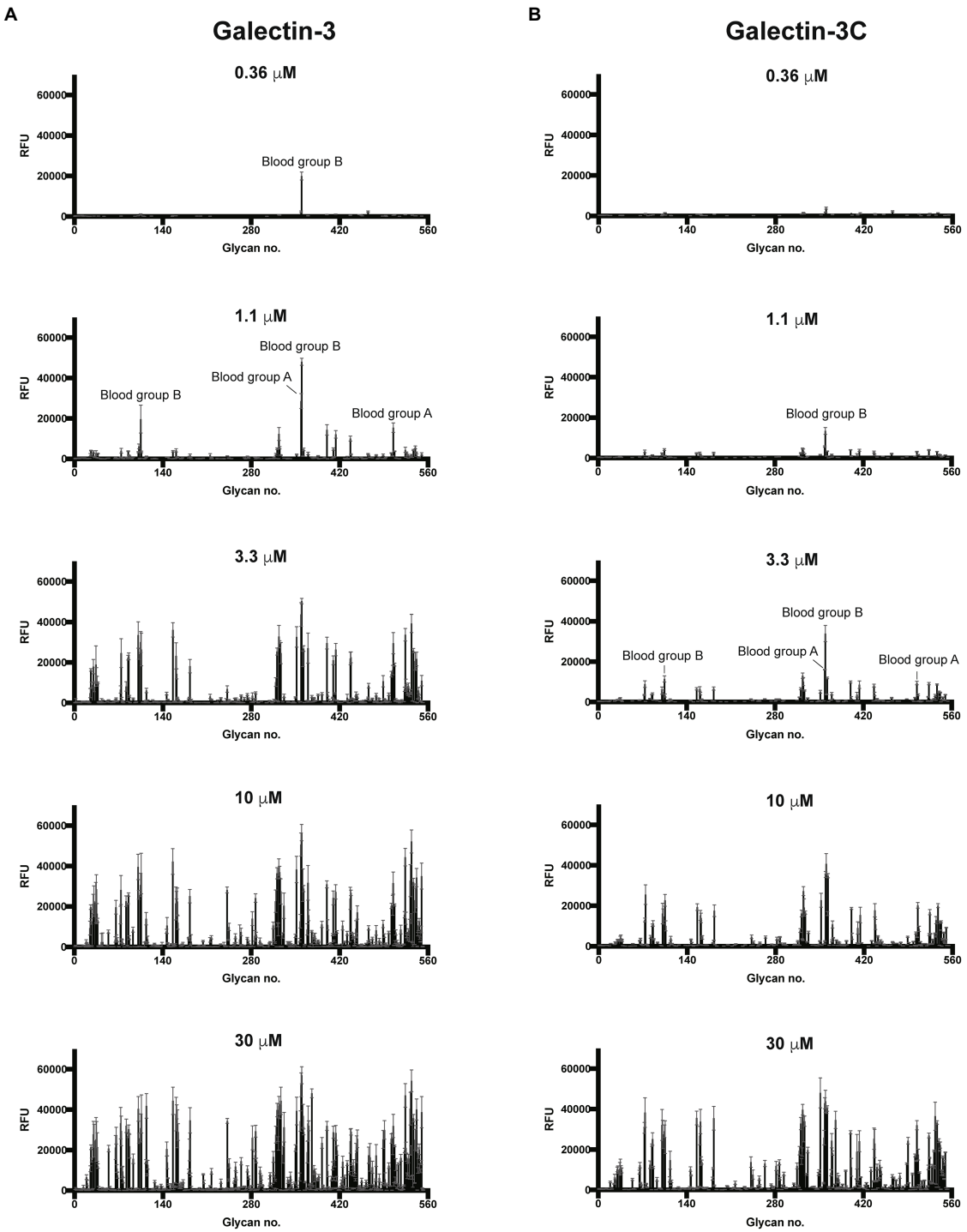

FIGURE 1 | Gal-3 and Gal-3C preferentially recognize blood group antigens at distinct concentrations. Consortium for functional glycomics (CFG) glycan microarray data obtained after incubation with the indicated concentrations of Gal-3 **(A)** and Gal-3C **(B)**. RFU, relative fluorescence units. Error bars represent means ± standard deviation (SD).

has high affinity for blood group antigens and that both terminal glycan modifications (α1-2Fuc and α1-3GalNAc or Gal) present in blood group A and blood group B are likely required to support higher affinity interactions by Gal-3.

In order to compare the relative binding affinities of Gal-3 and Gal-3C toward blood group antigens and other glycan structures present on the array, we calculated the relative K_D generated from binding isotherm data for each galectin toward

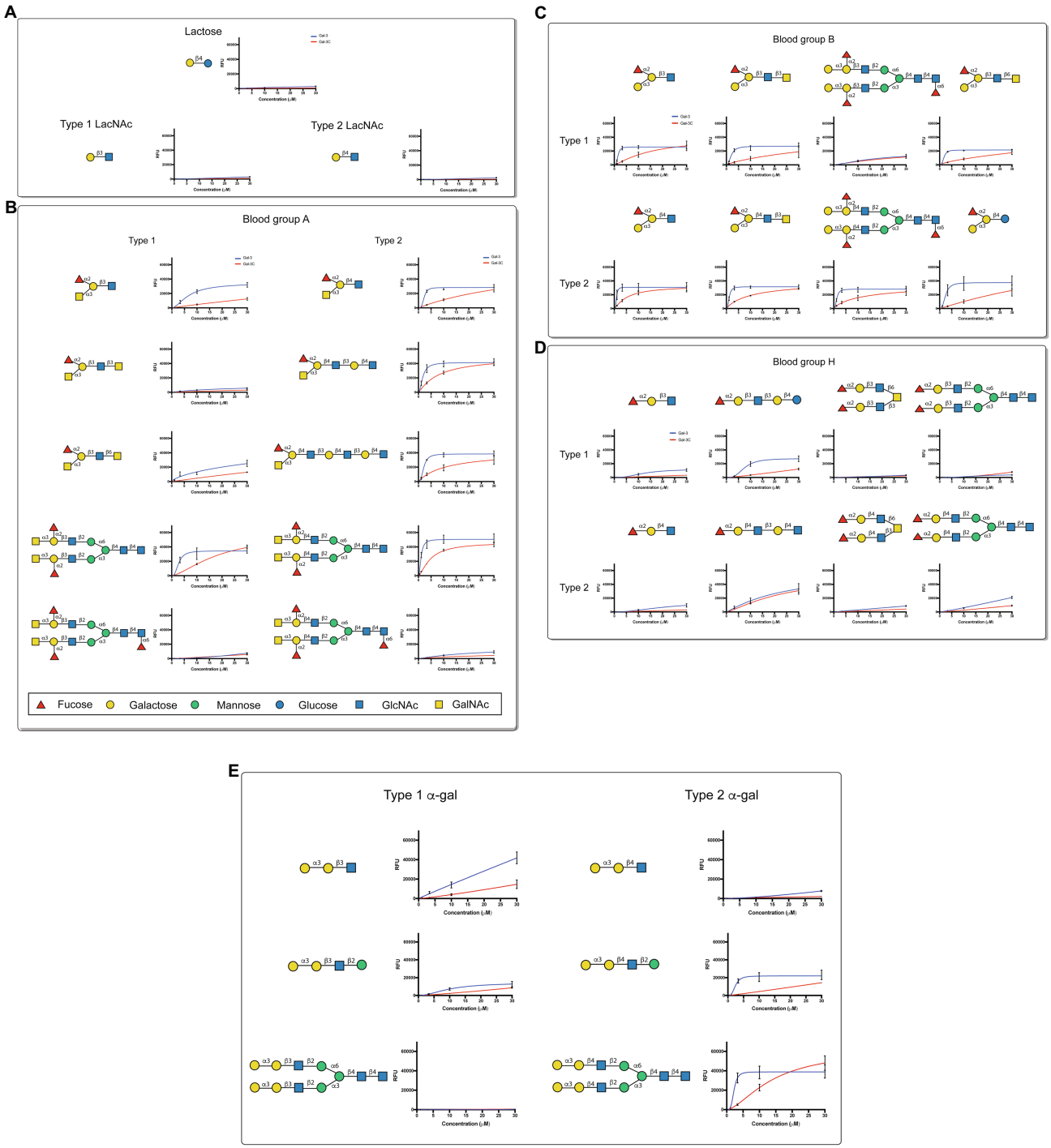

FIGURE 2 | Gal-3 displays high affinity for blood group antigens on a CFG glycan microarray. **(A-E)** Binding isotherms generated following incubation of Gal-3 (blue) and Gal- 3C (red) on the CFG glycan microarray are shown for lactose and *N*-acetyllactosamine (LacNAc) (A), blood group A containing glycan structures **(B)**, blood group B containing glycan structures **(C)**, H antigen (blood group O) containing glycan structures **(D)** and -Gal containing glycan structures **(E)**. Detailed Symbol Nomenclature for Glycans (SNFG) structures are shown. Error bars represent means ± standard deviation (SD). GalNAc: *N*-Acetylgalactosamine; GlcNAc: *N*-Acetylglucosamine.

various blood group antigens, polylactosamine (polyLacNAc), and other common structural modifications previously shown to influence galectin recognition (e.g., α2-6 sialylation). As there are many distinct glycan determinants in this array format, we highlighted K_D values for general classes of glycans; the detailed structural information for each glycan shown is available

in supplemental data (**Supplementary Table 1**). As the binding profile against some glycans did not saturate over the concentrations employed in this analysis (**Figure 1**), we compared the relatively weak, but detectable binding observed toward glycans where saturation did not occur as a percentage of the maximal binding on the array at the highest concentration examined (30 μM). This was done to capture binding that did occur, but that failed to saturate over the concentrations tested. Using this approach, relative differences in weaker binding profiles could be highlighted while clearly separating these binding profiles from higher binding interactions where saturation did occur, and therefore, relative K_D values could be ascertained (**Figure 3A**). Using this approach, blood group antigens are clearly some of the highest affinity ligands for Gal-3, although polyLacNAc structures, such as $(LacNAc)_2$ and $(LacNAc)_3$, were also bound with high affinity as well (**Figure 3B**). In contrast, appreciably K_D values for Gal-3C were only apparent for blood group antigens over the concentrations examined, while binding toward polyLacNAc glycans was certainly detected at the higher concentrations (**Figure 3C**).

Gal-3 and Gal-3C Bind to Microbial Glycans Decorated With Mammalian-Like Structures

Given the proclivity of Gal-3 and Gal-3C for blood group antigens on the CFG arrays, we next sought to determine whether the same level of specificity occurs when similar ligands are instead presented on a microbial glycan. To accomplish this, we examined Gal-3 and Gal-3C binding toward more than 300 microbial glycans isolated from distinct strains of bacteria using a previously characterized MGM (**Supplementary Table 2**; Stowell et al., 2014; Wesener et al., 2015). Similar to binding on the CFG array, appreciable Gal-3 binding was not detected until a concentration of 0.36 μM Gal-3 was employed (**Figure 4A**). The structure recognized at this concentration was the glycan isolated from *Streptococcus pneumoniae* 43. When examining Gal-3 glycan recognition at a slightly higher concentration of 1.1 μM, the O antigen of *Providentia alcalifaciens* O5 was also recognized. At higher concentrations, the glycan antigens of additional microbes were detected, including the O antigen of *Klebsiella pneumoniae* O1. In contrast to Gal-3, detectable binding on the MGM was not observed for Gal-3C until at least 1.1 μM was employed, with appreciable binding toward *S. pneumoniae* type 43 or *P. alcalifaciens* O5 only apparent following incubation with 3.3 μM Gal-3C (**Figure 4B**). However, similar to results obtained following incubation with the CFG array, while differences in the concentrations needed to detect binding were certainly apparent between Gal-3 and Gal-3C, the overall trends in bindings specificity were similar, strongly suggesting that while the N-terminal domain likely facilitates higher affinity binding, the intrinsic specificity for individual glycans appears to be driven by the C-terminal domain.

The ability of Gal-3 and Gal-3C to bind the isolated glycans from *S. pneumoniae* type 43 or *P. alcalifaciens* O5 at concentrations similar to that observed on the CFG array was intriguing in part because the intrinsic structure of each glycan reflects lactose and αGal antigens, respectively (**Figure 5**); Gal-3 exhibited low binding toward these individual structures on the CFG array (**Figures 2A**,**E**). As a result, we next explored in more detail the binding affinity of Gal-3 and Gal-3C toward the microbial glycans present on the MGM using the same approach outlined for evaluating saturated and non-saturated binding toward the CFG arrays. Using this approach, we observed a very high apparent affinity for the glycan antigens of *S. pneumoniae* type 43 or *P. alcalifaciens* O5, with relatively K_D values of 0.24 and 0.68 μM, respectively (**Figure 6**). In contrast, binding to the glycan of *K. pneumoniae* O1 by Gal-3 was apparent, but much weaker, where binding failed to fully saturate and therefore provide a relative K_D over the concentrations tested (**Figure 6**). Importantly, Gal-3 and Gal-3C binding did not appear to reflect indiscriminate engagement of microbial glycans, as neither exhibited appreciable binding toward related strains of microbes, such as *P. alcalifaciens* O21, *Streptococcus pneumoniae* 57, or *K. pneumoniae* O4, which fail to express glycan with mammalian-like structural motifs (**Figure 5**). These results suggest that while Gal-3 can certainly recognize microbial glycans, this recognition exhibits a certain level of specificity, with most microbial glycans not recognized by Gal-3 or Gal-3C.

Gal-3, but Not Gal-3C, Kills *P. alcalifaciens* O5 and *K. pneumoniae* O1

Given the ability of Gal-3 to differentially recognize microbial glycans on the MGM, we next sought to determine whether binding on the microarray accurately predicted actual interactions and overall antimicrobial potency toward intact microbes. Clear interactions between Gal-3 or Gal-3C and *P. alcalifaciens* O5 could be observed by flow cytometric examination (**Figures 7A**,**B**). Engagement of *P. alcalifaciens* O5 by both Gal-3 and Gal-3C also required carbohydrate recognition, as inclusion of TDG, a non-metabolizable inhibitor of galectin-glycan interactions, inhibited recognition (**Figures 7A**,**B**). Recognition by Gal-3 and Gal-3C appeared to be specific to *P. alcalifaciens* O5 as incubation with *P. alcalifaciens* O21 failed to result in any detectable binding when evaluated in parallel (**Figures 7A**,**B**). To determine the impact of Gal-3 and Gal-3C engagement of *P. alcalifaciens* O5 on microbial viability, we next examined the outcome of Gal-3 or Gal-3C incubation with *P. alcalifaciens* O5 over a range of concentrations. Incubation of Gal-3 resulted in reduced viability of *P. alcalifaciens* O5, with an effective concentration 50 (EC50) of around 0.17 μM. In contrast, incubation with the same concentrations of Gal-3 with *P. alcalifaciens* O21 failed to result in any detectable impact on microbial viability (**Figure 7C**). To determine whether Gal-3C can likewise impact microbial viability, we incubated *P. alcalifaciens* O5 with Gal-3C. Unlike Gal-3, Gal-3C failed to influence the viability of *P. alcalifaciens* O5 at all concentrations tested; similar results were observed following incubation of Gal-3C with *P. alcalifaciens* O21 (**Figure 7D**).

While Gal-3 and Gal-3C recognized a variety of glycan determinants isolated from distinct strains of microbes, the apparent affinity differed, suggesting that differential killing activity

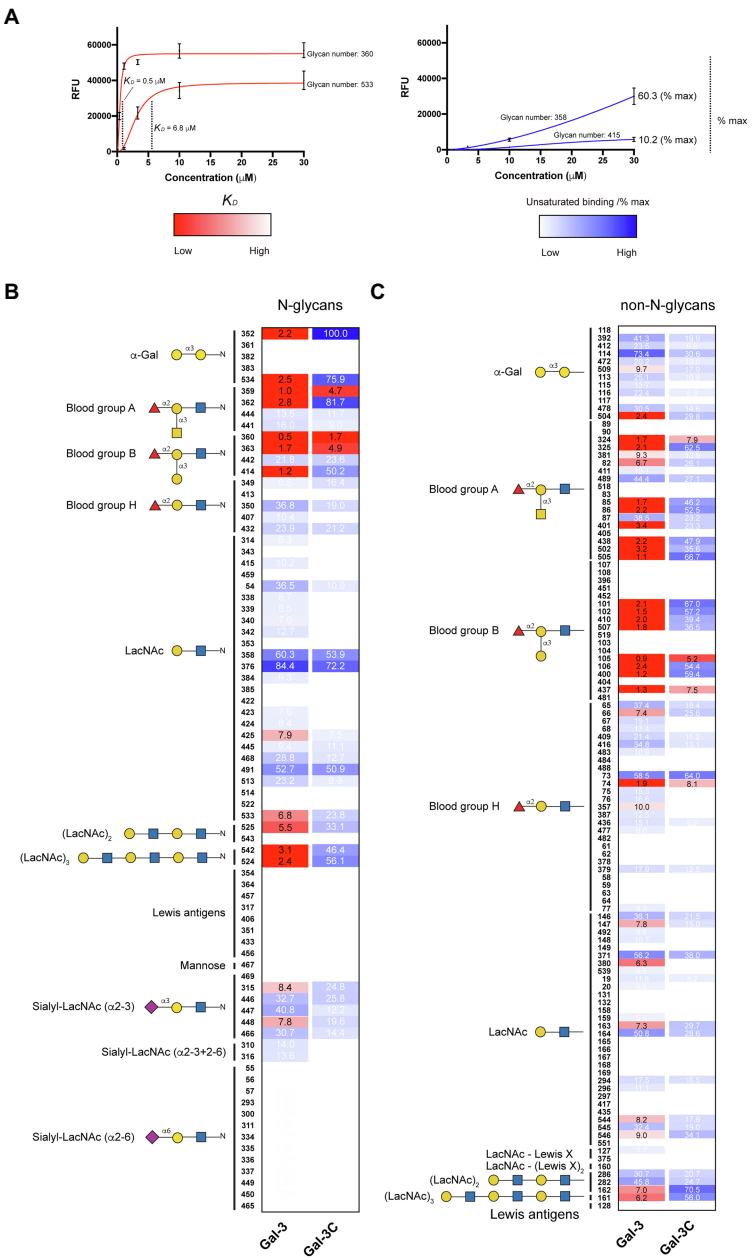

FIGURE 3 | K_D values for Gal-3 and Gal-3C binding toward blood group antigens and other mammalian glycans. **(A)** Representative binding isotherms used to generate K_D values and the % max of the highest concentration tested for unsaturated glycans. **(B,C)** Selected blood group antigens were shown along with heat map representation of K_D values (red) and the % max of the highest concentration tested for unsaturated glycans (blue) for antigens located on N-glycans **(B)** and non-N-glycans **(C)**. The heat map from darker red (low K_D) to light red (high K_D) is shown. For the unsaturated binding, the heat map from light blue (low % max) to darker blue (high % max) is shown. Examples of glycans examined are annotated to the left of each heat map as structures that are present on N-glycans (N-glycans) as shown in **(B)** or as the isolated glycan motifs (non-N-glycans) as shown in **(C)**.

may also occur toward distinct microbial targets. Furthermore, whether the inability of Gal-3C to kill *P. alcalifaciens* O5 is limited to this strain of microbe remained unknown. As a result, we next evaluated the binding of Gal-3 and Gal-3C toward *K. pneumoniae* O1 as both Gal-3 and Gal-3C displayed detectable, albeit lower, binding toward the O antigen isolated from this microbe (**Figure 6**). Similar to Gal-3 and Gal-3C interactions with *P. alcalifaciens* O5, Gal-3 and Gal-3C not only bound *K. pneumoniae* O1, but these interactions likewise depended on carbohydrate recognition as inclusion of TDG prevented binding. Engagement of *K. pneumoniae* O1 also appeared to be specific, as similar binding failed to occur when evaluated against *K. pneumoniae* O4 (**Figures 7E,F**). To determine the sensitivity of *K. pneumoniae* O1 to Gal-3, we next evaluated *K. pneumoniae*

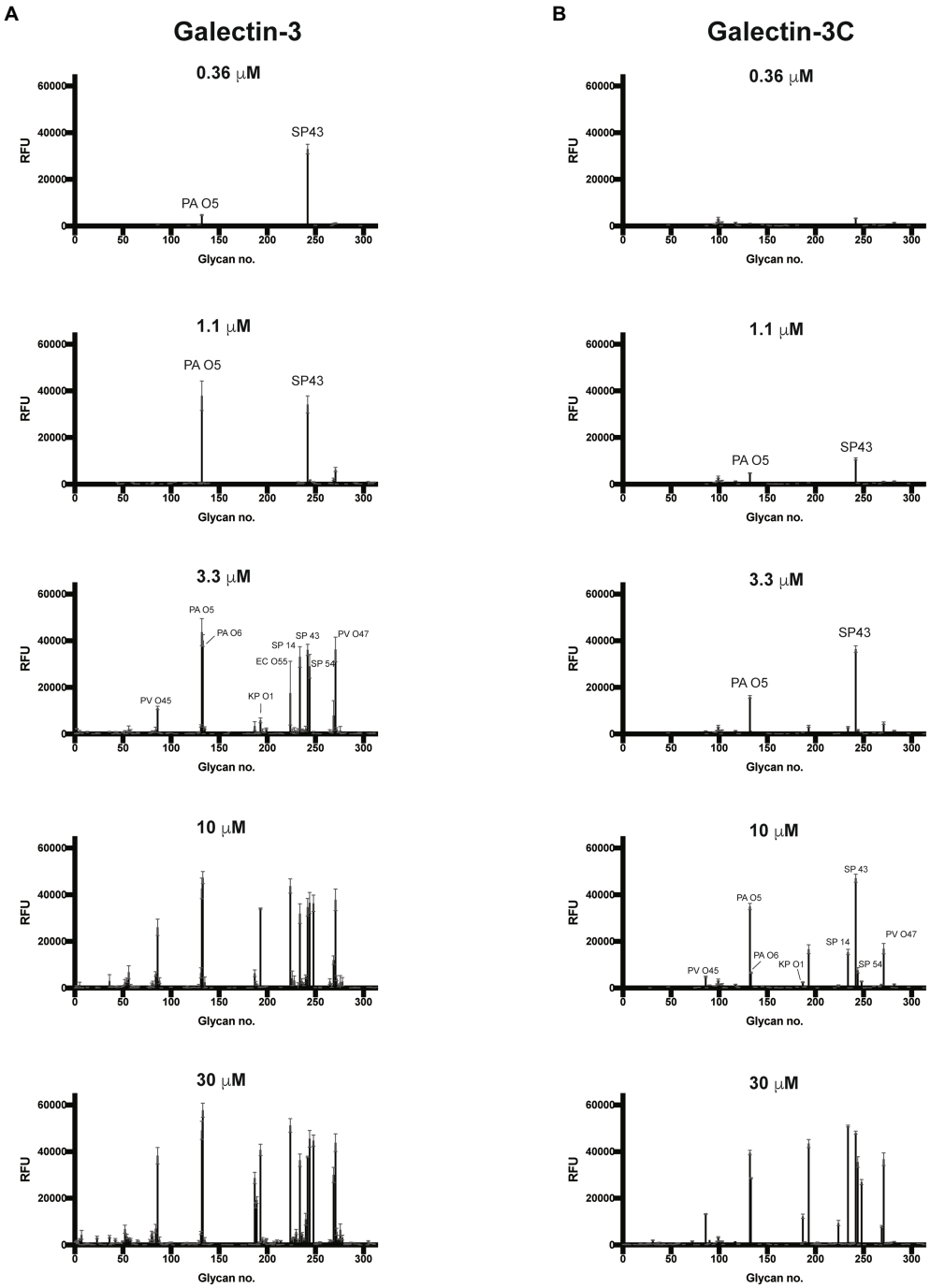

FIGURE 4 | Gal-3 and Gal-3C recognize distinct microbial glycans **(A,B)** Microbial glycan microarray (MGM) data obtained after incubation with the Gal-3 **(A)** or Gal-3C **(B)** at the concentrations indicated. Error bars represent means ± standard deviation (SD). RFU, relative fluorescence units; PA O5, *Providencia alcalifaciens* O5; PA O6, *P. alcalifaciens* O6; KP O1, *Klebsiella pneumoniae* O1; SP 14, *Streptococcus pneumoniae* type 14; SP 43, *S. pneumoniae* type 43; SP54, *S. pneumoniae* type 54; PV O45, *Proteus vulgaris* O45; PV O47, *P. vulgaris* O47; EC O55, *Escherichia coli* O55.

O1 viability following incubation with increasing concentrations of Gal-3. While loss of microbial viability was noted at higher concentrations, the EC50 of Gal-3 toward *K. pneumoniae* O1 was higher (0.75 μM), suggesting that like binding, killing activity toward *K. pneumoniae* O1 required higher concentrations of Gal-3. Also similar to binding, Gal-3 failed to impact the viability of *K. pneumoniae* O4 at all concentrations tested (**Figure 7G**). To determine whether Gal-3C possesses the ability to kill *K. pneumoniae* O1, we next examined *K. pneumoniae* O1 viability following incubation with Gal-3C. Similar to its inability to

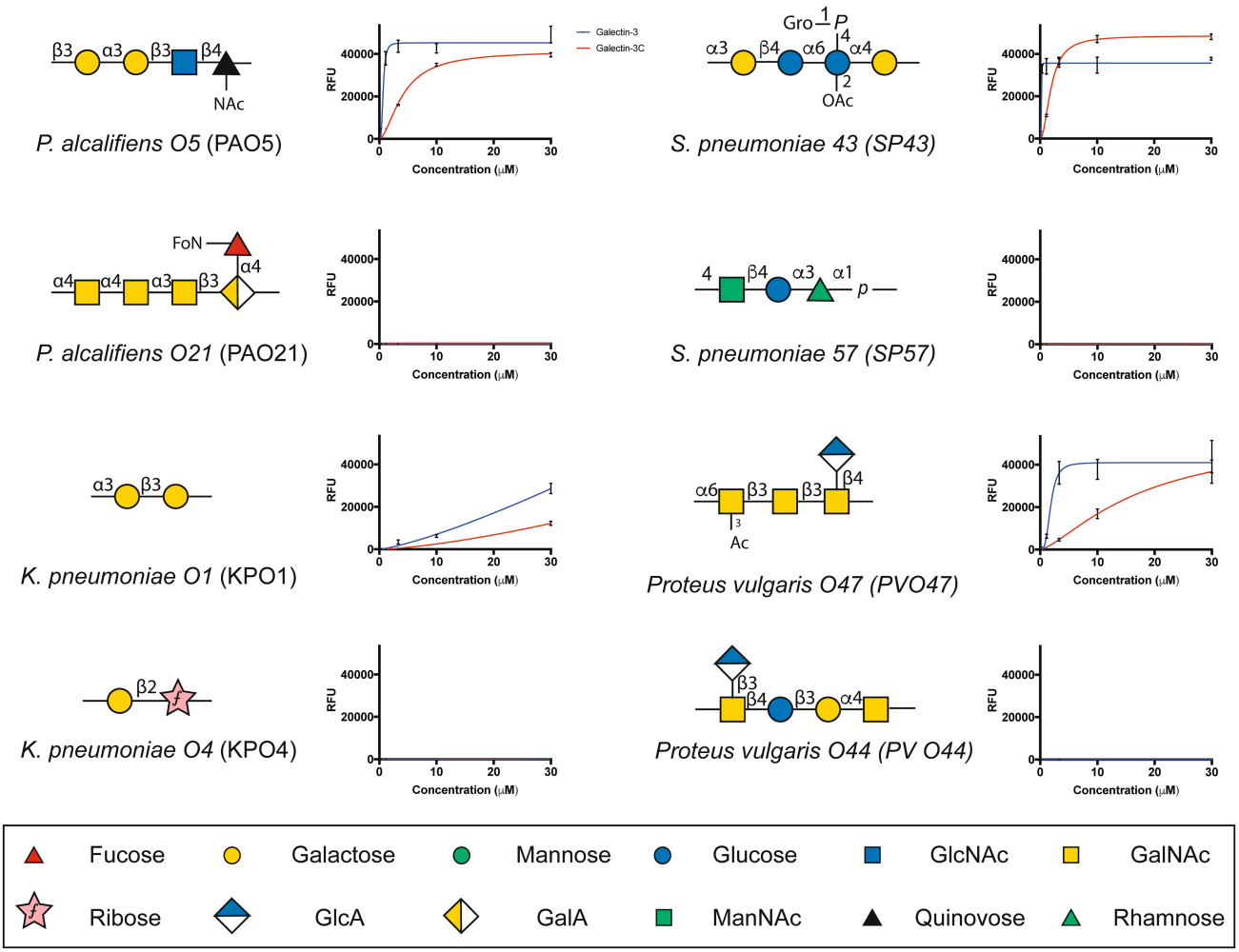

FIGURE 5 | Gal-3 and Gal-3C exhibit high affinity interactions with select microbial glycans. The binding isotherms of Gal-3 (blue) and Gal-3C (red) for microbial glycans are shown. The structure for each corresponding glycan is depicted on the left of each binding isotherm. Symbols used to represent each monosaccharide present in each bacterial glycan are represented in the legend below. Error bars represent means ± standard deviation (SD). GlcA: D-Glucuronic acid, GalA: D-Galacturonic acid and ManNAc: N-Acetyl-D-mannosamine

impact the viability of *P. alcalifaciens* O5, Gal-3C likewise failed to impact the viability of *K. pneumoniae* O1 or *K. pneumoniae* O4 (**Figure 7H**). Taken together, these results suggest that the MGM can ascertain relative affinity and microbicidal potency of Gal-3 toward distinct strains of microbes and that the N-terminal domain is required for both high affinity interactions with microbial glycans and the overall antimicrobial activity of Gal-3.

DISCUSSION

While galectins have long been recognized as carbohydrate binding proteins defined by their ability to engage β-galactose-containing glycans, the fine specificity of many galectins, especially toward microbial glycans, has remained incompletely defined. Gal-3 in particular is intriguing as it is the only galectin that belongs to the chimeric type subfamily, where it possesses a unique N-terminal domain that does not possess critical residues responsible for carbohydrate recognition, but is required for oligomerization (Hsu et al., 1992; Chiu et al., 2020; Zhao et al., 2021). While many studies have examined the binding specificity of the full-length protein (Hirabayashi et al., 2002; Stowell et al., 2008a; Song et al., 2009; Horlacher et al., 2010; Gao et al., 2019), much less is known regarding the intrinsic specificity of Gal-3C toward a wide variety of glycan determinants. The results of the present study suggest that the specificity of Gal-3 for most glycans appears to reside within the C-terminal domain with higher affinity interactions with glycan ligands requiring the full-length protein. The present results also demonstrate that full-length Gal-3 is required for its antimicrobial activity.

Although general binding toward β-galactose containing glycans became a defining feature of galectins, modifications of β-galactose can have a significant impact on overall glycan recognition. The preference for ABO(H) glycans has become

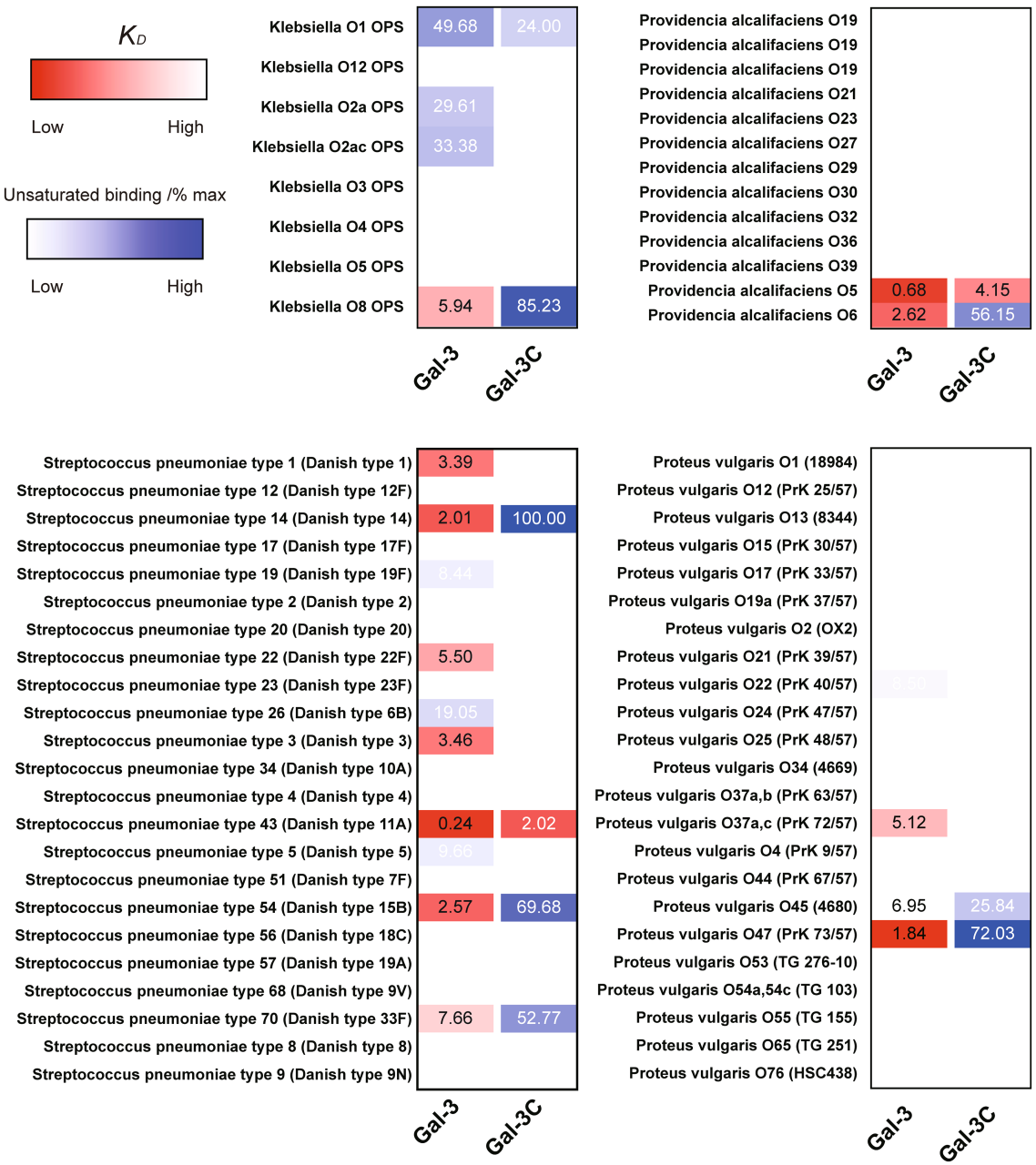

FIGURE 6 | *KD* values of Gal-3 and Gal-3C binding to microbial glycans. Selected bacteria are presented along with heat map representation of *KD* and unsaturated binding (% max). The *KD* and % max values were sorted by red and blue color, respectively. The heat map from darker red (low *KD*) to light red (high *KD*). For the unsaturated binding, the heat map from light blue (low % max) to darker blue (high % max).

an intriguing and almost defining feature of galectins (Feizi et al., 1994; Hirabayashi et al., 2002; Carlsson et al., 2007; Stowell et al., 2008a; Arthur et al., 2015d; Kamili et al., 2016), although the extent to which other galectins likewise possess similar overall binding preferences remains to be defined. The overall binding preferences exhibited by Gal-3 in the present study are largely in agreement with earlier studies, where Gal-3 was observed to exhibit higher binding to blood group A and blood group B than the H antigen (Feizi et al., 1994). More recent studies suggested that galectins may exhibit a slight preference for blood group B over blood group A (Stowell et al., 2010). Consistent with this, microarray analysis in the present study demonstrated that blood group B was the first glycan bound at the lowest concentration of Gal-3 or Gal-3C examined for which any appreciable glycan recognition could be observed. At slightly higher concentrations, binding to blood group A could also be readily detected. However, analysis of galectin binding at a single concentration

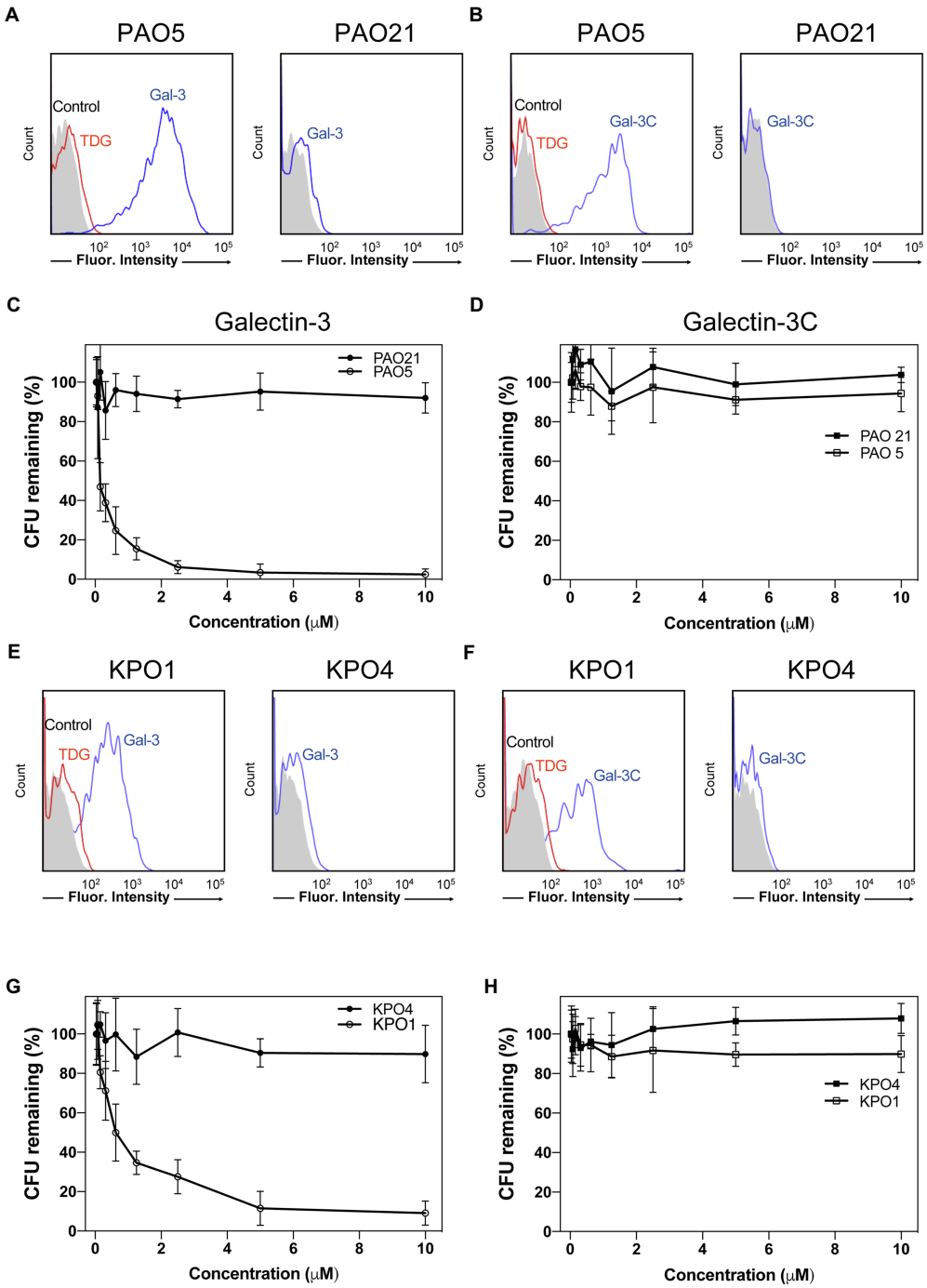

FIGURE 7 | Gal-3 and Gal-3C recognize and kill *Providencia alcalifaciens* O5 (PA O5) and *Klebsiella pneumoniae* O1 (KP O1). **(A,B)** Flow cytometric analysis of Gal-3 **(A)** and Gal-3C **(B)** binding to PA O5 and PA O21 with or without inclusion of 20 mM thiodigalactoside (TDG) as indicated. **(C,D)** Quantification of viable bacteria after incubation with the indicated concentrations Gal-3 **(C)** and Gal-3C **(D)**. **(E,F)** Flow cytometric analysis of Gal-3 **(E)** and Gal-3C **(F)** binding to KP O1 and KP O4 with or without inclusion of 20 mM TDG as indicated. **(G,H)** Quantification of viable bacteria after incubation with the indicated concentrations Gal-3 **(G)** and Gal-3C **(H)**. Error bars represent means ± SD.

on the microarray can be misleading, as such an approach only ascertains relative binding at a given concentration without providing the additional insight obtained when examining galectin binding over a range of concentrations that allows the establishment a binding isotherm capable of providing relative K_D values. Using this approach, the impact of subtle differences in blood group presentation can become more apparent.

The selective forces that facilitated ABO(H) blood group polymorphism evolution within the human population have remained incompletely understood (Cooling, 2015; Stowell and Stowell, 2019a,b). However, several studies suggest that various pathogens may have influenced the selection of ABO(H) polymorphisms (Reid and Bird, 1990; Cooling, 2015), much like other blood group and blood group-like antigens that can likewise be a barrier to blood transfusion and the optimal use of similar therapeutics (Zerra et al., 2017, 2021; Mener et al., 2018; Patel et al., 2018; Arthur et al., 2021). The polymorphic nature of ABO(H) antigens strongly suggests that the high binding affinity of Gal-3 toward these antigens is not due to selective pressures that facilitate the engagement and modulation of host cells. Rather, this preference points to an evolutionary process that likely selected for this binding specificity in the context of host immunity toward microbes. In this way, galectins may provide a unique form of innate immunity against microbes that utilize molecular mimicry to avoid adaptive immunity. As innate immune factors are not subjected to tolerogenic programs that limit adaptive immunity toward self-antigens, galectins and perhaps other lectins may fill this gap in adaptive immunity by targeting microbes that express mammalian-like structures on their surface.

The ability of Gal-3 to recognize a diverse range of microbes that express distinct self-like antigens is intriguing and suggests that the relatively promiscuous binding profile often attributed to this protein family over a range of concentrations may actually reflect an important ability to recognize a variety of microbial glycans with self-like antigen features. However, there are clearly differences in the binding that can be observed toward microbial glycans and similar motifs as presented on mammalian glycans. For example, while Gal-3 failed to exhibit a high level of binding toward lactose, presentation of this motif within the microbial glycan of *S. pneumoniae* type 43 appeared to support high affinity glycans. These results strongly suggest that the presentation of a given glycan motif, possibly due to the polymerizing nature of repeating structures on the microbial surface, may be important glycan feature that facilitates this type of interaction. Consistent with this, while almost no detectable binding was observed for Gal-3 toward LacNAc, polymers of LacNAc in the form of polyLacNAc supported high affinity Gal-3 interactions. However, subtle differences in glycan presentation on the microbial surface can still impact overall Gal-3 binding. For example, while *K. pneumoniae* O1 and *P. alcalifaciens* O5 contain the Galα1-3Gal motif, this structure is polymerized within distinct glycans on each microbe (Galα1-3Galβ1-3Gal-R in *K. pneumoniae* O1 and Galα1-3Galβ1-3GlcNAc-R in *P. alcalifaciens* O5). Unfortunately, a major limitation in the MGM is the lack of availability of most of the microbes represented on the array. While this limited the ability to perform confirmatory tests for all positive events observed, the correlation between binding and the potency of killing activity toward *K. pneumoniae* O1 and *P. alcalifaciens* O5 suggests that this overall approach may be useful when seeking to examine the binding specificity of a given carbohydrate binding protein for microbial glycans. Despite subtle differences in binding affinity unique microbial glycans, Gal-3 and Gal-3C displayed a fairly high level of specificity for distinct microbial glycans when compared to all the microbial glycans present on the array. This stands in stark contrast to most innate immune factors that often recognize microbial motifs that are common to a diverse range of microbes (Janeway and Medzhitov, 2002). This unique specificity for individual strains of microbes places galectins as unique innate immune factors that selectively bind and kill a subset of microbes.

Glycan microarrays have become a powerful way to examine the binding specificity of carbohydrate binding proteins against a wide range of glycan determinants (Rillahan and Paulson, 2011). The construction of microarrays requires less glycan material than many other assay formats and therefore expands the ability to explore a particular glycan library when assessing the binding specificity of a given carbohydrate binding protein. While microarray approaches for assessing carbohydrate binding proteins have improved the overall analysis of carbohydrate binding proteins specificity, the manufacturing and use of glycan microarrays can remain resource intense, and therefore, analysis has primarily focused on a single concentration of a particular carbohydrate binding protein on a given microarray. This approach can uncover important features of glycan binding for a particular carbohydrate binding protein, including glycan modifications that appear to directly inhibit glycan recognition. However, when using this approach, it can be challenging to know *a priori* where the linear range of glycan binding for a particular carbohydrate binding protein resides. Similarly, while the density of glycans printed is relatively similar to discrete glycans, printing can result in subtle differences in glycan concentration that can impact the maximal binding possible for a given carbohydrate binding protein. While these differences can be subtle, they can suggest possible differences in glycan binding affinity that may actually reflect slight differences in printing efficiency between different glycans. The ability to examine Gal-3 and Gal-3C binding over a range of concentrations provided a relative binding affinity that may aid in reducing variability due to slight differences in glycan printing density, while also providing a general framework for assessing the actual affinity for a given glycan as printed in an array format. Using this approach, a number of glycans were bound at higher concentration where saturation was not achieved but where binding was clearly detected. To document these lower affinity interactions, we employed the more commonly ranked analysis as a percentage of maximal binding only at the highest concentration tested. This combined approach of K_D analysis for glycans that clearly saturated coupled with a relative binding assessment of unsaturated glycans builds on recent advances in glycan array analysis with the goal of providing additional insight into carbohydrate binding protein glycan recognition. More definitive K_D values could have been obtained for lower affinity interaction by expanding the concentrations tested. However, as galectin concentrations in excess of 30 μM *in vivo* are unlikely, the relevance of K_D ascertained following escalating test concentrations beyond 30 μM is of uncertain value, and therefore, analysis was limited to the concentration range tested.

A variety of previous studies has examined the requirement of the N-terminal domain in Gal-3 signaling of host cells,

with a primary focus on immune cells (Chen et al., 2005). Through N-terminal domain self-association, Gal-3 can cross link counter receptors and impact the signaling outcomes of many host cells (Horlacher et al., 2010; Guha et al., 2013; Gao et al., 2019). However, less has been known regarding the involvement for the N-terminal domain in Gal-3-mediated antimicrobial activity and overall binding to a wide range of both mammalian and microbial glycans. Given the similarities in overall specificity, despite significant differences in the concentration at which binding was detected on each array, the intrinsic affinity of glycans within the Gal-3 CRD may not differ whether in the context of the full-length protein or as an isolated CRD. Consistent with this, several studies using solution-based isothermal calorimetry demonstrated that Gal-3 and Gal-3C exhibit very similar affinity for various glycan ligands (Ahmad et al., 2004b; Rodriguez et al., 2015). Given the ability of the N-terminal domain to facilitate Gal-3 self-association (Hsu et al., 1992; Chiu et al., 2020; Zhao et al., 2021), initial binding by one CRD within the full-length protein may increase the effective concentration of the second CRD toward glycans immobilized on the same surface, directly increasing the probability that additional binding events occur in the context of the multimeric protein. In this context, the microscopic K_a or binding affinity of each domain within the full-length protein is likely no different than the CRD alone, but the impact of enhanced effective concentration of each CRD within the oligomeric full-length protein following initial binding likely increases the overall avidity of interactions with immobilized glycans; this can be observed as an apparent increase in affinity for mammalian and microbial glycans. Recent studies have demonstrated that the C-terminal domain of Gal-3 can also self-associate (Lepur et al., 2012; Sundqvist et al., 2018), suggesting that higher order Gal-3 structures may form independent of the N-terminal domain. However, while the C-terminal domain may self-associate following engagement of microbial glycans or on the microbial surface in general, this interaction does not appear to be sufficient to convey antimicrobial activity following Gal-3C binding.

Prior studies defining the antimicrobial activity of galectins have primarily focused on the tandem repeat galectins, Gal-4 and Gal-8, which possess two distinct CRDs linked by an intervening peptide (Levy et al., 2001; Rustiguel et al., 2016). Examination of the components of Gal-8 in particular that are required for killing microbes demonstrated that the C-terminal domain (Gal-8C) alone possesses its antimicrobial activity (Stowell et al., 2010). As prior data suggest that Gal-8C is a monomer (Stowell et al., 2008b), the intrinsic ability of Gal-8C to kill microbes suggested that monovalent galectin interactions with microbial glycans alone can alter microbial viability. Given these prior findings, we anticipated that Gal-3C, despite lacking its intrinsic ability to oligomerize, may likewise possess the ability to kill microbes. In contrast, despite being able to engage blood group antigens with similar affinity as Gal-8C (Stowell et al., 2008b), Gal-3C failed to impact microbial viability. It is possible that the requirement of the N-terminal domain for Gal-3-mediated microbial killing reflects an activity that is completely independent of its role in facilitating multimerization. However, as inclusion of hapten inhibitors prevented Gal-3 microbial binding and killing, initial engagement of microbes likely requires recognition of glycan ligands by the Gal-3 CRD. Consistent with this, Gal-3 also failed to recognize or kill microbes that do not express self-like antigens. These results do not rule out the possibility that the N-terminal domain may facilitate Gal-3 interactions with the microbial surface following initial engagement by Gal-3. Examination of the N-terminal domain alone will be required to determine whether this isolated domain possesses the ability to directly interact with microbes. As Gal-4 and Gal-8 do not possess a similar N-terminal domain as Gal-3, yet possess the ability to effectively kill microbes, the requirement of full-length Gal-3 for microbial killing may indeed reflect a need for N-terminal domain-mediated oligomerization. Since oligomerization status is crucial for Gal-3 to mediate many carbohydrate-dependent processes (Horlacher et al., 2010; Gao et al., 2019), proteolytic cleavage on the N-terminal domain may reflect a regulatory circuit that modulates its antimicrobial activity among other regulatory features of the protein (Hsu et al., 1992; Herrmann et al., 1993).

The outcome of Gal-3 binding to bacterial glycans may not be limited to antimicrobial killing. Gal-3 can facilitate LPS detection by neutrophils and directly impact neutrophil activation (Li et al., 2008; Fermino et al., 2011), suggesting that Gal-3 may not only serve as a danger-associated molecular pattern molecule (Sato and Nieminen, 2002), but may also alter the ability of innate immune cells and perhaps other cells, to detect pathogen associated molecular patterns. Some of these interactions may be mediated by direct interactions with lipid A (Mey et al., 1996). However, the present results suggest that the composition of the glycan present on LPS may influence these interactions and attendant consequences. Indeed, the ability of Gal-3 to engage specific microbial glycan determinants may not only play a role in providing direct protection against molecular mimicry, but also may have related consequences on the ability of Gal-3 to detect LPS shed from individual strains of microbes and therefore alert or otherwise alter a host immune response following exposure to a given microbe.

Taken together, these results demonstrate that Gal-3 binds a very diverse range of mammalian glycans, but exhibits a high affinity for polymorphic blood group antigens, a process that appears to require the full-length protein. However, whether Gal-3 can successfully bind and kill similar microbes *in vivo* remains to be tested. Despite the ability of the C-terminal domain of Gal-8 alone to kill bacteria, Gal-3C fails to alter microbial viability, suggesting that some self-association of Gal-3 that occurs independent of the C-terminal domain alone is likely required for the ability of Gal-3 to kill microbes. These results also demonstrate that Gal-3 binding alone is not sufficient to kill bacteria, as examination of Gal-3C at concentrations that achieved similar levels of microbial glycan binding as was observed by Gal-3 failed to kill bacteria. Thus, the N-terminal domain of Gal-3 is required not only for high

affinity microbial glycan interactions, but also for the ability of Gal-3 to kill microbes.

DATA AVAILABILITY STATEMENT

The original contributions presented in the study are included in the article/**Supplementary Material**, and further inquiries can be directed to the corresponding authors.

AUTHOR CONTRIBUTIONS

S-CW, CA, and SS conceived the project, which was facilitated by AH, NK, JW, KM, and RC who provided critical reagents, experimental support, and critical discussion. S-CW and SS wrote the manuscript, which was additionally commented on and edited by the remaining authors. All authors contributed to the article and approved the submitted version.

FUNDING

This work was supported in part by the Burroughs Wellcome Trust Career Award for Medical Scientists, the National Institutes of Health Early Independence grant DP5OD019892, and UO1 CA242109 to SS.

ACKNOWLEDGMENTS

We would like to thank the Emory Cloning Center and Oskar Laur for cloning assistance.

SUPPLEMENTARY MATERIAL

The Supplementary Material for this article can be found online at: https://www.frontiersin.org/articles/10.3389/fmicb.2021.731026/full#supplementary-material

REFERENCES

Ahmad, N., Gabius, H. J., Andre, S., Kaltner, H., Sabesan, S., Roy, R., et al. (2004a). Galectin-3 precipitates as a pentamer with synthetic multivalent carbohydrates and forms heterogeneous cross-linked complexes. *J. Biol. Chem.* 279, 10841–10847. doi: 10.1074/jbc.M312834200

Ahmad, N., Gabius, H. J., Sabesan, S., Oscarson, S., and Brewer, C. F. (2004b). Thermodynamic binding studies of bivalent oligosaccharides to galectin-1, galectin-3, and the carbohydrate recognition domain of galectin-3. *Glycobiology* 14, 817–825. doi: 10.1093/glycob/cwh095

Arthur, C. M., Baruffi, M. D., Cummings, R. D., and Stowell, S. R. (2015a). Evolving mechanistic insights into galectin functions. *Methods Mol. Biol.* 1207, 1–35. doi: 10.1007/978-1-4939-1396-1_1

Arthur, C. M., Cummings, R. D., and Stowell, S. R. (2015b). Evaluation of the bactericidal activity of galectins. *Methods Mol. Biol.* 1207, 421–430. doi: 10.1007/978-1-4939-1396-1_27

Arthur, C. M., Patel, S. R., Mener, A., Kamili, N. A., Fasano, R. M., Meyer, E., et al. (2015c). Innate immunity against molecular mimicry: Examining galectin-mediated antimicrobial activity. *BioEssays* 37, 1327–1337. doi: 10.1002/bies.201500055

Arthur, C. M., Rodrigues, L. C., Baruffi, M. D., Sullivan, H. C., Heimburg-Molinaro, J., Smith, D. F., et al. (2015d). Examining galectin binding specificity using glycan microarrays. *Methods Mol. Biol.* 1207, 115–131. doi: 10.1007/978-1-4939-1396-1_8

Arthur, C. M., Zerra, P. E., Shin, S., Wang, J., Song, X., Doering, C. B., et al. (2021). Non-human glycans can regulate anti-FVIII antibody formation in mice. *Blood*. [Epub ahead of print] doi: 10.1182/blood.2020009210.

Barondes, S. H., Castronovo, V., Cooper, D. N., Cummings, R. D., Drickamer, K., Feizi, T., et al. (1994). Galectins: a family of animal beta-galactoside-binding lectins. *Cell* 76, 597–598. doi: 10.1016/0092-8674(94)90498-7

Blixt, O., Head, S., Mondala, T., Scanlan, C., Huflejt, M. E., Alvarez, R., et al. (2004). Printed covalent glycan array for ligand profiling of diverse glycan binding proteins. *Proc. Natl. Acad. Sci. U. S. A.* 101, 17033–17038. doi: 10.1073/pnas.0407902101

Carlsson, S., Oberg, C. T., Carlsson, M. C., Sundin, A., Nilsson, U. J., Smith, D., et al. (2007). Affinity of galectin-8 and its carbohydrate recognition domains for ligands in solution and at the cell surface. *Glycobiology* 17, 663–676. doi: 10.1093/glycob/cwm026

Chen, H. Y., Liu, F. T., and Yang, R. Y. (2005). Roles of galectin-3 in immune responses. *Arch. Immunol. Ther. Exp.* 53, 497–504.

Chiu, Y. P., Sun, Y. C., Qiu, D. C., Lin, Y. H., Chen, Y. Q., Kuo, J. C., et al. (2020). Liquid-liquid phase separation and extracellular multivalent interactions in the tale of galectin-3. *Nat. Commun.* 11:1229. doi: 10.1038/s41467-020-15007-3

Cooling, L. (2015). Blood groups in infection and host susceptibility. *Clin. Microbiol. Rev.* 28, 801–870. doi: 10.1128/CMR.00109-14

Feizi, T., Solomon, J. C., Yuen, C. T., Jeng, K. C., Frigeri, L. G., Hsu, D. K., et al. (1994). The adhesive specificity of the soluble human lectin, IgE-binding protein, toward lipid-linked oligosaccharides. Presence of the blood group A, B, B-like, and H monosaccharides confers a binding activity to tetrasaccharide (lacto-N-tetraose and lacto-N-neotetraose) backbones. *Biochemistry* 33, 6342–6349. doi: 10.1021/bi00186a038

Fermino, M. L., Polli, C. D., Toledo, K. A., Liu, F. T., Hsu, D. K., Roque-Barreira, M. C., et al. (2011). LPS-induced galectin-3 oligomerization results in enhancement of neutrophil activation. *PLoS One* 6:e26004. doi: 10.1371/journal.pone.0026004

Fowler, M., Thomas, R. J., Atherton, J., Roberts, I. S., and High, N. J. (2006). Galectin-3 binds to *Helicobacter pylori* O-antigen: it is upregulated and rapidly secreted by gastric epithelial cells in response to *H. pylori* adhesion. *Cell. Microbiol.* 8, 44–54. doi: 10.1111/j.1462-5822.2005.00599.x

Gao, C., Wei, M., Mckitrick, T. R., Mcquillan, A. M., Heimburg-Molinaro, J., and Cummings, R. D. (2019). Glycan microarrays as chemical tools for identifying glycan recognition by immune proteins. *Front. Chem.* 7:833. doi: 10.3389/fchem.2019.00833

Guha, P., Kaptan, E., Bandyopadhyaya, G., Kaczanowska, S., Davila, E., Thompson, K., et al. (2013). Cod glycopeptide with picomolar affinity to galectin-3 suppresses T-cell apoptosis and prostate cancer metastasis. *Proc. Natl. Acad. Sci. U. S. A.* 110, 5052–5057. doi: 10.1073/pnas.1202653110

Gupta, S. K., Masinick, S., Garrett, M., and Hazlett, L. D. (1997). *Pseudomonas aeruginosa* lipopolysaccharide binds galectin-3 and other human corneal epithelial proteins. *Infect. Immun.* 65, 2747–2753. doi: 10.1128/iai.65.7.2747-2753.1997

Herrmann, J., Turck, C. W., Atchison, R. E., Huflejt, M. E., Poulter, L., Gitt, M. A., et al. (1993). Primary structure of the soluble lactose binding lectin L-29 from rat and dog and interaction of its non-collagenous proline-, glycine-, tyrosine-rich sequence with bacterial and tissue collagenase. *J. Biol. Chem.* 268, 26704–26711. doi: 10.1016/S0021-9258(19)74370-1

Hirabayashi, J., Hashidate, T., Arata, Y., Nishi, N., Nakamura, T., Hirashima, M., et al. (2002). Oligosaccharide specificity of galectins: a search by frontal affinity chromatography. *Biochim. Biophys. Acta* 1572, 232–254. doi: 10.1016/s0304-4165(02)00311-2

Horlacher, T., Oberli, M. A., Werz, D. B., Krock, L., Bufali, S., Mishra, R., et al. (2010). Determination of carbohydrate-binding preferences of human galectins with carbohydrate microarrays. *Chembiochem* 11, 1563–1573. doi: 10.1002/cbic.201000020

Hsu, D. K., Zuberi, R. I., and Liu, F. T. (1992). Biochemical and biophysical characterization of human recombinant IgE-binding protein, an S-type

animal lectin. *J. Biol. Chem.* 267, 14167–14174. doi: 10.1016/S0021-9258(19)49693-2

Janeway, C. A. Jr., and Medzhitov, R. (2002). Innate immune recognition. *Annu. Rev. Immunol.* 20, 197–216. doi: 10.1146/annurev.immunol.20.083001.084359

John, C. M., Jarvis, G. A., Swanson, K. V., Leffler, H., Cooper, M. D., Huflejt, M. E., et al. (2002). Galectin-3 binds lactosaminylated lipooligosaccharides from *Neisseria gonorrhoeae* and is selectively expressed by mucosal epithelial cells that are infected. *Cell. Microbiol.* 4, 649–662. doi: 10.1046/j.1462-5822.2002.00219.x

Kamili, N. A., Arthur, C. M., Gerner-Smidt, C., Tafesse, E., Blenda, A., Dias-Baruffi, M., et al. (2016). Key regulators of galectin-glycan interactions. *Proteomics* 16, 3111–3125. doi: 10.1002/pmic.201600116

Lepur, A., Salomonsson, E., Nilsson, U. J., and Leffler, H. (2012). Ligand induced galectin-3 protein self-association. *J. Biol. Chem.* 287, 21751–21756. doi: 10.1074/jbc.C112.358002

Levy, Y., Arbel-Goren, R., Hadari, Y. R., Eshhar, S., Ronen, D., Elhanany, E., et al. (2001). Galectin-8 functions as a matricellular modulator of cell adhesion. *J. Biol. Chem.* 276, 31285–31295. doi: 10.1074/jbc.M100340200

Li, Y., Komai-Koma, M., Gilchrist, D. S., Hsu, D. K., Liu, F. T., Springall, T., et al. (2008). Galectin-3 is a negative regulator of lipopolysaccharide-mediated inflammation. *J. Immunol.* 181, 2781–2789. doi: 10.4049/jimmunol.181.4.2781

Liu, F. T., and Rabinovich, G. A. (2005). Galectins as modulators of tumour progression. *Nat. Rev. Cancer* 5, 29–41. doi: 10.1038/nrc1527

Liu, F. T., and Rabinovich, G. A. (2010). Galectins: regulators of acute and chronic inflammation. *Ann. N. Y. Acad. Sci.* 1183, 158–182. doi: 10.1111/j.1749-6632.2009.05131.x

Mener, A., Patel, S. R., Arthur, C. M., Chonat, S., Wieland, A., Santhanakrishnan, M., et al. (2018). Complement serves as a switch between CD4+ T cell-independent and -dependent RBC antibody responses. *JCI Insight* 3:e121631. doi: 10.1172/jci.insight.121631

Mey, A., Leffler, H., Hmama, Z., Normier, G., and Revillard, J. P. (1996). The animal lectin galectin-3 interacts with bacterial lipopolysaccharides via two independent sites. *J. Immunol.* 156, 1572–1577

Morris, S., Ahmad, N., Andre, S., Kaltner, H., Gabius, H. J., Brenowitz, M., et al. (2004). Quaternary solution structures of galectins-1, -3, and -7. *Glycobiology* 14, 293–300. doi: 10.1093/glycob/cwh029

Patel, S. R., Gibb, D. R., Girard-Pierce, K., Zhou, X., Rodrigues, L. C., Arthur, C. M., et al. (2018). Marginal zone B cells induce alloantibody formation following RBC transfusion. *Front. Immunol.* 9:2516. doi: 10.3389/fimmu.2018.02516

Quattroni, P., Li, Y., Lucchesi, D., Lucas, S., Hood, D. W., Herrmann, M., et al. (2012). Galectin-3 binds Neisseria meningitidis and increases interaction with phagocytic cells. *Cell. Microbiol.* 14, 1657–1675. doi: 10.1111/j.1462-5822.2012.01838.x

Reid, M. E., and Bird, G. W. (1990). Associations between human red cell blood group antigens and disease. *Transfus. Med. Rev.* 4, 47–55. doi: 10.1016/S0887-7963(90)70247-7

Rillahan, C. D., and Paulson, J. C. (2011). Glycan microarrays for decoding the glycome. *Annu. Rev. Biochem.* 80, 797–823. doi: 10.1146/annurev-biochem-061809-152236

Rodriguez, M. C., Yegorova, S., Pitteloud, J. P., Chavaroche, A. E., Andre, S., Arda, A., et al. (2015). Thermodynamic switch in binding of adhesion/growth regulatory human galectin-3 to tumor-associated TF antigen (CD176) and MUC1 glycopeptides. *Biochemistry* 54, 4462–4474. doi: 10.1021/acs.biochem.5b00555

Rustiguel, J. K., Soares, R. O., Meisburger, S. P., Davis, K. M., Malzbender, K. L., Ando, N., et al. (2016). Full-length model of the human galectin-4 and insights into dynamics of inter-domain communication. *Sci. Rep.* 6:33633. doi: 10.1038/srep33633

Sato, S., and Nieminen, J. (2002). Seeing strangers or announcing "danger": galectin-3 in two models of innate immunity. *Glycoconj. J.* 19, 583–591. doi: 10.1023/B:GLYC.0000014089.17121.cc

Seetharaman, J., Kanigsberg, A., Slaaby, R., Leffler, H., Barondes, S. H., and Rini, J. M. (1998). X-ray crystal structure of the human galectin-3 carbohydrate recognition domain at 2.1-A resolution. *J. Biol. Chem.* 273, 13047–13052. doi: 10.1074/jbc.273.21.13047

Song, X., Xia, B., Stowell, S. R., Lasanajak, Y., Smith, D. F., and Cummings, R. D. (2009). Novel fluorescent glycan microarray strategy reveals ligands for galectins. *Chem. Biol.* 16, 36–47. doi: 10.1016/j.chembiol.2008.11.004

Stowell, S. R., Arthur, C. M., Dias-Baruffi, M., Rodrigues, L. C., Gourdine, J. P., Heimburg-Molinaro, J., et al. (2010). Innate immune lectins kill bacteria expressing blood group antigen. *Nat. Med.* 16, 295–301. doi: 10.1038/nm.2103

Stowell, S. R., Arthur, C. M., Mcbride, R., Berger, O., Razi, N., Heimburg-Molinaro, J., et al. (2014). Microbial glycan microarrays define key features of host-microbial interactions. *Nat. Chem. Biol.* 10, 470–476. doi: 10.1038/nchembio.1525

Stowell, S. R., Arthur, C. M., Mehta, P., Slanina, K. A., Blixt, O., Leffler, H., et al. (2008a). Galectin-1, -2, and -3 exhibit differential recognition of sialylated glycans and blood group antigens. *J. Biol. Chem.* 283, 10109–10123. doi: 10.1074/jbc.M709545200

Stowell, S. R., Arthur, C. M., Slanina, K. A., Horton, J. R., Smith, D. F., and Cummings, R. D. (2008b). Dimeric Galectin-8 induces phosphatidylserine exposure in leukocytes through polylactosamine recognition by the C-terminal domain. *J. Biol. Chem.* 283, 20547–20559. doi: 10.1074/jbc.M802495200

Stowell, S. R., Dias-Baruffi, M., Penttila, L., Renkonen, O., Nyame, A. K., and Cummings, R. D. (2004). Human galectin-1 recognition of poly-N-acetyllactosamine and chimeric polysaccharides. *Glycobiology* 14, 157–167. doi: 10.1093/glycob/cwh018

Stowell, C. P., and Stowell, S. R. (2019a). Biologic roles of the ABH and Lewis histo-blood group antigens Part I: infection and immunity. *Vox Sang.* 114, 426–442. doi: 10.1111/vox.12787

Stowell, S. R., and Stowell, C. P. (2019b). Biologic roles of the ABH and Lewis histo-blood group antigens part II: thrombosis, cardiovascular disease and metabolism. *Vox Sang.* 114, 535–552. doi: 10.1111/vox.12786

Sundqvist, M., Welin, A., Elmwall, J., Osla, V., Nilsson, U. J., Leffler, H., et al. (2018). Galectin-3 type-C self-association on neutrophil surfaces; The carbohydrate recognition domain regulates cell function. *J. Leukoc. Biol.* 103, 341–353. doi: 10.1002/JLB.3A0317-110R

Vasta, G. R. (2009). Roles of galectins in infection. *Nat. Rev. Microbiol.* 7, 424–438. doi: 10.1038/nrmicro2146

Vasta, G. R. (2012). Galectins as pattern recognition receptors: structure, function, and evolution. *Adv. Exp. Med. Biol.* 946, 21–36. doi: 10.1007/978-1-4614-0106-3_2

Verkerke, H., Horwath, M., Saeedi, B., Boyer, D., Allen, J. W., Owens, J., et al. (2021). Comparison of antibody class specific SARS-CoV-2 serology for the diagnosis of acute COVID-19. *J. Clin. Microbiol.* 59:e02026-20. doi: 10.1128/JCM.02026-20

Vinogradov, E., and Perry, M. B. (2001). Structural analysis of the core region of the lipopolysaccharides from eight serotypes of *Klebsiella pneumoniae*. *Carbohydr. Res.* 335, 291–296. doi: 10.1016/S0008-6215(01)00216-6

Wesener, D. A., Wangkanont, K., Mcbride, R., Song, X., Kraft, M. B., Hodges, H. L., et al. (2015). Recognition of microbial glycans by human intelectin-1. *Nat. Struct. Mol. Biol.* 22, 603–610. doi: 10.1038/nsmb.3053

Wu, S. C., Arthur, C. M., Wang, J., Verkerke, H., Josephson, C. D., Kalman, D., et al. (2021a). The SARS-CoV-2 receptor-binding domain preferentially recognizes blood group A. *Blood Adv.* 5, 1305–1309. doi: 10.1182/bloodadvances.2020003259

Wu, S. C., Paul, A., Ho, A., Patel, K. R., Allen, J. W. L., Verkerke, H., et al. (2021b). Generation and use of recombinant galectins. *Curr. Protoc.* 1:e63. doi: 10.1002/cpz1.63

Zerra, P. E., Cox, C., Baldwin, W. H., Patel, S. R., Arthur, C. M., Lollar, P., et al. (2017). Marginal zone B cells are critical to factor VIII inhibitor formation in mice with hemophilia A. *Blood* 130, 2559–2568. doi: 10.1182/blood-2017-05-782912

Zerra, P. E., Patel, S. R., Jajosky, R. P., Arthur, C. M., Mccoy, J. W., Allen, J. W. L., et al. (2021). Marginal zone B cells mediate a CD4 T cell dependent extrafollicular antibody response following RBC transfusion in mice. *Blood*. doi: 10.1182/blood.2020009376 [Epub ahead of print]

Zhao, Z., Xu, X., Cheng, H., Miller, M. C., He, Z., Gu, H., et al. (2021). Galectin-3 N-terminal tail prolines modulate cell activity and glycan-mediated

oligomerization/phase separation. *Proc. Natl. Acad. Sci. U. S. A.* 118:e2021074118. doi: 10.1073/pnas.2021074118

Conflict of Interest: The authors declare that the research was conducted in the absence of any commercial or financial relationships that could be construed as a potential conflict of interest.

Publisher's Note: All claims expressed in this article are solely those of the authors and do not necessarily represent those of their affiliated organizations, or those of the publisher, the editors and the reviewers. Any product that may be evaluated in this article, or claim that may be made by its manufacturer, is not guaranteed or endorsed by the publisher.

frontiers in Microbiology

REVIEW
published: 03 January 2022
doi: 10.3389/fmicb.2021.794765

Galectins in Chagas Disease: A Missing Link Between *Trypanosoma cruzi* Infection, Inflammation, and Tissue Damage

Carolina V. Poncini[1,2†], Alejandro F. Benatar[3†], Karina A. Gomez[4‡] and Gabriel A. Rabinovich[5,6*‡]*

[1] Laboratorio de Inmunología Celular e Inmunopatología de Infecciones, Instituto de Investigaciones en Microbiología y Parasitología Medica, Universidad de Buenos Aires-Consejo Nacional de Investigaciones Científicas y Técnicas, Buenos Aires, Argentina, [2] Departamento de Microbiología, Parasitología e Inmunología, Facultad de Medicina, Universidad de Buenos Aires, Buenos Aires, Argentina, [3] Servicio de Citometría de Flujo, Instituto de Medicina Experimental (IMEX), Academia Nacional de Medicina, Consejo Nacional de Investigaciones Científicas y Técnicas (CONICET), Buenos Aires, Argentina, [4] Laboratorio de Biología e Inmunología de las Infecciones por Tripanosomátidos, Instituto de Investigaciones en Ingeniería Genética y Biología Molecular, Consejo Nacional de Investigaciones Científicas y Técnicas, Buenos Aires, Argentina, [5] Laboratorio de Glicomedicina, Instituto de Biología y Medicina Experimental, Consejo Nacional de Investigaciones Científicas y Técnicas, Buenos Aires, Argentina, [6] Facultad de Ciencias Exactas y Naturales, Universidad de Buenos Aires, Buenos Aires, Argentina

Trypanosoma cruzi, the protozoan parasite causative agent of Chagas disease, affects about seven million people worldwide, representing a major global public health concern with relevant socioeconomic consequences, particularly in developing countries. In this review, we discuss the multiple roles of galectins, a family of β-galactoside-binding proteins, in modulating both *T. cruzi* infection and immunoregulation. Specifically, we focus on galectin-driven circuits that link parasite invasion and inflammation and reprogram innate and adaptive immune responses. Understanding the dynamics of galectins and their β-galactoside-specific ligands during the pathogenesis of *T. cruzi* infection and elucidating their roles in immunoregulation, inflammation, and tissue damage offer new rational opportunities for treating this devastating neglected disease.

Keywords: galectin, *Trypanosoma cruzi*, galectin-1, galectin-3, Chagas disease

OPEN ACCESS

Edited by:
Gerardo R. Vasta, University of Maryland, Baltimore, United States

Reviewed by:
Debora Decote-Ricardo, Universidade Federal Rural do Rio de Janeiro, Brazil
Tarun Dam, Michigan Technological University, United States

***Correspondence:**
Karina A. Gomez
drkagomez@gmail.com
Gabriel A. Rabinovich
gabyrabi@gmail.com

†These authors share first authorship

‡These authors share senior authorship

Specialty section:
This article was submitted to Microbial Immunology, a section of the journal Frontiers in Microbiology

Received: *14 October 2021*
Accepted: *25 November 2021*
Published: *03 January 2022*

Citation:
Poncini CV, Benatar AF, Gomez KA and Rabinovich GA (2022) Galectins in Chagas Disease: A Missing Link Between Trypanosoma cruzi Infection, Inflammation, and Tissue Damage. Front. Microbiol. 12:794765. doi: 10.3389/fmicb.2021.794765

INTRODUCTION

Chagas disease is a major neglected disease in Latin America, affecting around seven million people worldwide and causing 50,000 deaths per year (WHO, 2014; Lidani et al., 2019). It is an anthropozoonosis affecting humans for more than 4,000 years (Guhl et al., 1999; Aufderheide et al., 2004). Although, in the past, the disease was mainly circumscribed to the American continent, there are an increasing number of cases in non-endemic countries mostly due to the migration of infected people from endemic areas (Schmunis, 2007; Lidani et al., 2019). The infection takes place either by vector-borne, congenital routes, blood-borne, and oral or organ-derived transmission (Bern et al., 2019). Successful strategies used to eliminate vectors in some endemic regions, as well as the exhaustive screening in blood banks, highlight the relevance of congenital mother-to-child transmission as the main actor of Chagas disease's urbanization (Schmunis and Cruz, 2005; Coura and Dias, 2009; De Rissio et al., 2010; Bisio et al., 2011).

The flagellated protozoan *Trypanosoma cruzi* is the etiologic agent of Chagas disease. Glycoproteins and glycolipids play an important role in most of the steps of the complex life cycle of this microorganism, which involves interactions with mammalian hosts and insect vectors from the *Triatominae* subfamily (*Hemiptera*, *Reduviidae*), usually called vinchuca, kissing bug, barbeiro, among others (Tyler and Engman, 2001; De Souza et al., 2010; Garcia et al., 2010). *T. cruzi* has an incredible adaptation capacity that allows infection of more than one hundred mammalian species as well as a great versatility to transmit disease to sylvatic and domiciliary adapted Triatomine vectors (Noireau et al., 2009; Jansen et al., 2020). This flourished life cycle is sharpened by different lineages of *T. cruzi*. Hence, a committee of experts, in 2009, came to the decision to cluster the parasite strains into six discrete typing units (DTU), named TcI to TcVI, and a seventh DTU named TcBat (Zingales et al., 2009), based on biological, biochemical, and genetic diversities. Each DTU exhibits a typical geographic distribution, as well as different predominance in the sylvatic or domestic cycle, variations in their reservoirs, and vectors (Zingales et al., 2012). Until now, it has not been possible to determine a correlation between clinical manifestations and the circulating DTUs in human pathology (Del Puerto et al., 2010; Zingales et al., 2012; Jansen et al., 2020). Thus, despite the usefulness of DTU partition for genetic purposes, the species display a high diversity even in strains present within the same DTU (Roman et al., 2018).

Along its life cycle, *T. cruzi* undergoes biologic, structural, and metabolic transformations to adapt and survive in the different evolving environments. Different forms or parasite stages are epimastigotes and metacyclic trypomastigotes in the vector and amastigotes and blood trypomastigotes in the mammalian host (De Souza et al., 2010; Garcia et al., 2010). Variation in surface mucin glycoconjugates has been described not only in each parasite stage but also in each lineage of the different DTUs (Giorgi and de Lederkremer, 2020). Epimastigotes are rich in mucins that protect them from the action of agglutinins and proteases in the digestive tract (Buscaglia et al., 2006; Villalta et al., 2008). The attachment to peri-microvillar membranes through the interaction of parasite glycoinositolphospholipids with insect-derived glycoconjugates triggers metacyclogenesis and transforms replicative epimastigotes in highly infective metacyclic trypomastigotes that are released by feces and urine during vector feeding (De Souza et al., 2010; Garcia et al., 2010). These forms cannot pass through intact skin but can enter the bloodstream through mucosal tissue or at the biting site after a scratch (Giddings et al., 2010). Once inside the mammalian host, trypomastigotes infect macrophages, fibroblasts, adipocytes, and other cell types, before they reach skeletal, smooth, and cardiac muscle (Landskroner-Eiger et al., 2005; Epting et al., 2010; Ferreira et al., 2011). Invasion is a complex process involving many glycoproteins expressed in metacyclic trypomastigotes, such as gp90, gp82, gp30 y gp35/50 that are differentially expressed in the parasite strains and modulate diverse signaling pathways, which determine efficient internalization of the parasite (Ferreira et al., 2006; Yoshida, 2006; Alves and Colli, 2007; Villalta et al., 2008; Calvet et al., 2012; Romano et al., 2012; Ferri and Edreira, 2021). Other relevant molecules that are implicated in adhesion and invasion processes are mucins, cruzipain, and *trans*-sialidase (TS), a unique protein that reversely transfers sialic acid to β-Gal residues on acceptor molecules present in parasite's or host's cell membranes (Vandekerckhove et al., 1992; Buscaglia et al., 2006; De Souza et al., 2010; Calvet et al., 2012; Bartholomeu et al., 2014). Once inside the cell and independently of the route of entry, the parasite transiently persists into the parasitophorous vacuole (PV), where TS has an important role in the protection and maturation of trypomastigotes. Notably, sialic acid transfer activity of TS avoids parasite membranes degradation, and after differentiation, the parasite escapes from the vacuole to the cytosol using TS and other virulence factors (De Souza et al., 2010; Epting et al., 2010). After several rounds of replication, amastigotes start trypomastigote transformation (De Souza, 2002; Waghabi et al., 2005; Alves and Colli, 2007). Finally, and by a poorly understood mechanism, parasites can lyse the cell gaining access to the extracellular space, infect the neighboring cells, or reach the bloodstream, where the cycle restarts (Barrias et al., 2013).

Infection can be divided into two phases: the acute phase mostly presents symptoms that are difficult to ascribe to Chagas disease in a general clinical examination (Pinto et al., 2008); the only exception is the cutaneous damage caused at the site of inoculation, when it occurs (WHO, 2007; Tanowitz et al., 2009; Hemmige et al., 2012). Some people, especially children, may develop life-threatening alterations in the heart and brain during this phase. This number could be as high as 2–5% of the cases in which acute phase is detected (Pinto et al., 2008; Tanowitz et al., 2009; Hemmige et al., 2012; Healy et al., 2015). After 2–4 months, and although the immune system manages to partially control the infection, the chronic asymptomatic stage ensues. It can last throughout the life of the infected individual; the only clinical manifestation could be a subtle degree of myocardial abnormalities in stress echocardiography and Dopler tests that sometimes may lead to sudden death (Punukollu et al., 2007; Tanowitz et al., 2009). However, approximately 30–40% of infected people show clinical alterations, affecting cardiac tissue with an incidence of 20–30%, the digestive organs such as megaesophagus or megacolon with a frequency of 6–10%, or mixed form (Dutra et al., 2009; Hemmige et al., 2012; Viotti et al., 2014). Chronic chagasic cardiomyopathy (CCC), the most frequent manifestation, is a dilated heart disease with focal or disseminated inflammatory infiltrates, destruction of cardiac muscle, progressive fibrosis, and a high prevalence of conduction abnormalities, sinus node dysfunction, complex ventricular arrhythmias, and apical thrombus (Tanowitz et al., 2009; Esper et al., 2015; Healy et al., 2015).

So far, the events that trigger the transition from the chronic asymptomatic to the symptomatic stage are still unknown, and the paradigm shifted over time now accepting that the direct action of the parasite, as well as the immune response generated by the host, are the main mechanisms responsible for cardiac and digestive pathology (Acevedo et al., 2018). Thus, a strong cellular response with a predominance of $CD4^+$ T and $CD8^+$ T cells producing interferon (IFN)-γ and tumor necrosis factor (TNF)-α has been demonstrated, not only in the heart but also in the blood (Dutra et al., 2009). However, some mechanisms

seem to be independent of the parasite persistence, including the development of an autoimmune process, mainly due to molecular mimicry between parasite and host proteins (Levin et al., 1993; Kaplan et al., 1997; Freedman and Lefkowitz, 2004; Smulski et al., 2006; Labovsky et al., 2007; Medei et al., 2007). The list of cross-reactive antibodies is extensive and is out of the scope of this revision (Acosta and Santos-Buch, 1985; Cunha-Neto et al., 1996; Bilate and Cunha-Neto, 2008; Ribeiro et al., 2009). However, $CD4^+$ T cells with the ability to recognize host-self antigens have been detected in cardiac tissue of experimentally infected animals, as well as in patients with CCC (Silva-Barbosa and Savino, 2000; Cunha-Neto et al., 2011). In addition, neurogenic degeneration due to denervation of the heart (dysautonomia) and alterations in microcirculation, which generate the ischemic foci observed in hearts from patients with CCC, contribute to the development of this pathology (Bonney and Engman, 2008; Machado et al., 2012). Although the pathogenesis of CCC is multifactorial, it is clear that the presence of different lineages of the parasite, as well as different components of the host's immune system, may contribute to the progression from an asymptomatic form of the disease toward chronic heart pathology (Viotti et al., 2014; Healy et al., 2015; Acevedo et al., 2018).

GALECTINS

Galectins are a family of glycan-binding proteins characterized by the presence of at least one carbohydrate recognition domain (CRD) and a common structural fold. They mainly recognize glycoconjugates containing repetitive structures of the disaccharide *N*-acetyl-lactosamine (Galβ1-4GlcNac or LacNac) (Rabinovich et al., 2007, Van Kooyk and Rabinovich, 2008; Rabinovich and Toscano, 2009; Vasta, 2009; Davicino et al., 2011). Although these proteins bind to the same functional group, their carbohydrate specificity and plasticity in the CRDs are different, which in turn confers diverse functional properties (Vasta, 2012). In fact, each galectin recognizes a distinct set of glycosylated proteins or lipids at the cellular surface, extracellular matrix (ECM), or inside the cell (Wiersma et al., 2013). In general, galectin binding to a single ligand has a low affinity, but their multivalence and the complexity of the glycosylated ligands present on cell glycoproteins turn this binding into reversible high-affinity interactions (Thiemann and Baum, 2016). Terminal modifications such as sialylation, sulfation, or fucosylation on galactose affect galectin binding affinities (Hirabayashi et al., 2002; Rabinovich and Toscano, 2009).

There are at least 15 galectins in mammals expressed in different cells and tissues, including 10 galectins in humans, which are classified in prototype, chimera type, and tandem-repeat type. Prototype galectins (galectins-1, -2, -5, -7, -10, -11, -13, -14, and -15) have one CRD per subunit and are able to form non-covalent dimers; the chimera type galectin-3 has an *N*-terminal region responsible for their oligomerization, whereas tandem-repeat galectins (galectins-4, 6, 8, 9, and 12) have two homolog CRD in the same polypeptide chain, separated by a linker peptide of up to 70 amino acids long. Most of them are secreted through a non-classical mechanism (Van Kooyk and Rabinovich, 2008; Vasta, 2012; Schnaar, 2015), which still remains uncertain. In this regard, recent studies revealed that, in response to stress or infection, galectins are secreted through mechanisms involving non-canonical inflammasome activation and pyroptosis (Russo et al., 2021).

Some galectins, such as galectins-1 and 3, are ubiquitously expressed, whereas others present a more restricted distribution (Van Kooyk and Rabinovich, 2008). By interacting with specific glycoconjugates, galectins can trigger different signaling pathways leading to modulation of several cell processes, including activation, differentiation, apoptosis, receptor turnover, and trafficking (Rabinovich et al., 2007, Van Kooyk and Rabinovich, 2008; Ilarregui et al., 2009; Rabinovich and Toscano, 2009). By tempering these processes, galectins can control immune homeostasis, either in normal or pathologic conditions, with beneficial or detrimental effects to host tissues (Rabinovich and Croci, 2012). Moreover, galectins can modulate host–pathogen interactions and serve as mediators of immune evasion mechanisms (Davicino et al., 2011).

Interestingly, galectins have been proposed to bind glycan moieties present on the surface of viruses, fungi, bacteria, and parasites (Vasta, 2009), highlighting the role of these lectins as pattern recognition receptors. Under certain conditions, they can directly interact with receptors in host cells and inhibit the interaction of pathogens or even cross-link and immobilize them at the ECM, ultimately blocking infection (reviewed by Vasta, 2020). Furthermore, galectins are abundant both in the intracellular and the extracellular compartments and can influence infection, dissemination, or pathogen eradication through different mechanisms. Through direct or indirect pathways, pathogens themselves can up- or downregulate expression, concentration, and subcellular distribution of galectins at sites of infection (Levroney et al., 2005; Lujan et al., 2018). Strikingly, galectins may indirectly control pathogen persistence or elimination by positively or negatively shaping antimicrobial immunity (Sato et al., 2014; Nita-Lazar et al., 2015; Davicino et al., 2017; Xue et al., 2017).

GALECTINS AND *Trypanosoma cruzi*

Previous studies described differential binding of human galectins to *T. cruzi*, demonstrating selective recognition of different parasite stages by these glycan-binding proteins. Interestingly, they can display a particular binding profile related to the parasite's genetic background (Pineda et al., 2015a). *T. cruzi* is highly glycosylated, and surface glycoconjugates differ among biological stages of the parasite (de Lederkremer and Agusti, 2009). As described earlier, the parasite surface is enriched in mucins, which are complex glycoproteins displaying a dense array of *O*-linked oligosaccharides that constitute a coat that protects the parasite from the host and mediates interactions with host receptors and glycan-binding proteins. In general, most of the components are mucins-like proteins anchored to the parasite surface by glycosylphosphatidylinositol. Of note, carbohydrates are the major components of these molecules and account for up to 60% of their molecular mass (Buscaglia et al., 2006). Here, we review several interactions that take place between galectins and *T. cruzi* that control parasite invasion and immunity (**Figure 1**).

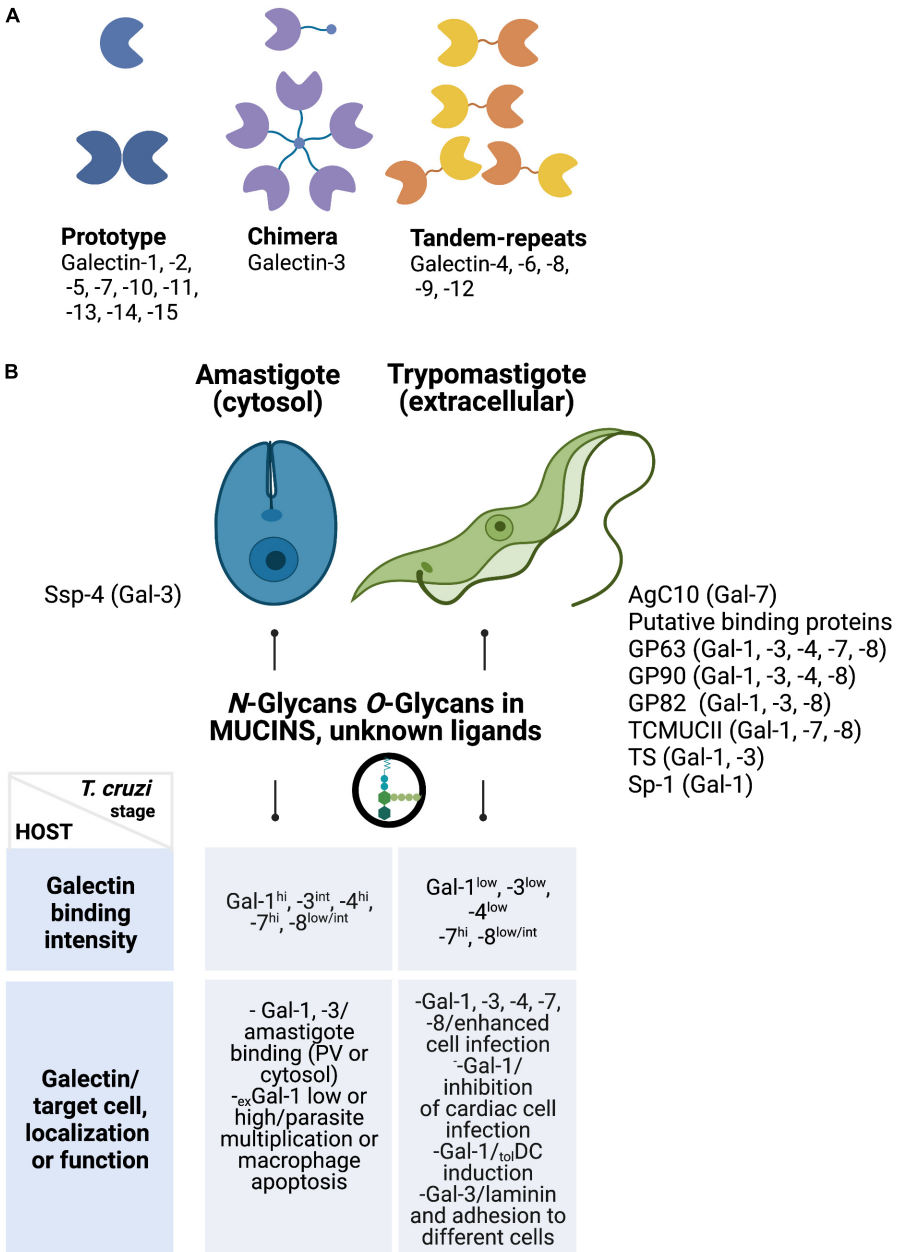

FIGURE 1 | (A) Structural classification of galectins. Some members of the prototype (galectin-1 and -7), chimera-type (galectin-3), and tandem-repeat type (galectins-8 and -9) galectins have been associated with *T. cruzi* recognition. **(B)** Galectins preferentially recognize parasite stages found in the mammalian host (amastigotes and trypomastigotes). Only galectin-7 recognizes epimastigotes (not shown). Potential receptors that bind human galectins (upper panel) and the intensity of some of these interactions reported by Pineda et al. (2015a) and others are summarized here (lower panel). Target cells, cellular localization, and/or properties of endogenous galectins during *T. cruzi* infection are enumerated in the lower panel. Ssp-4, stage-specific protein 4; AgC10, surface mucin AgC10; GP63, surface protease 63; GP82-90, surface glycoprotein (82–90); TcMUCII, *T. cruzi* mucin II; TS, *trans*-sialidase; Sp-1, surface protein 1.

GALECTIN-1 AND *Trypanosoma cruzi* INFECTION

Galectin-1, a prototype member of the galectin family, is highly expressed by different cell types, including immune cells, epithelial cells, endothelial cells, and adipocytes, at sites of infection and inflammation (Toscano et al., 2018). The binding affinity of galectin-1 for LacNAc-expressing glycoconjugates depends on the structure and nature of the glycoconjugate, presented either as a glycoprotein or glycolipid, and on the galactose linkage type and the branches on complex *N*-glycans. In general, galectin-1 binding to a single ligand is a low-affinity interaction, but the complexity of the glycan ligands present on cellular glycoproteins can turn this association into a

reversely high-affinity interaction (Thiemann and Baum, 2016). Of note, this lectin has a high affinity for complex *N*-glycans, and the binding to LacNac is interrupted by α2,6-sialylation on the terminal galactose. In addition, elongated core 2-*O*-glycans, glycosphingolipids, and some gangliosides have been described to bind galectin-1 (Rabinovich and Toscano, 2009). The binding to multivalent glycans on the cell surface promotes galectin-1–glycan interactions (Bourne et al., 1994). This effect favors proximity between two or more cells, adhesion of cells to glycosylated surfaces, and the formation of lattices at the cell surface, which facilitates receptor clustering, signaling, turnover, and endocytosis (Kutzner et al., 2020). Moreover, these effects rely on tissue-specific expression, distribution, and local concentrations of this lectin (Vasta, 2020). In general, galectin-1 displays anti-inflammatory and pro-resolving capacity by targeting multiple immune cells, including lymphoid and myeloid cells. In fact, this lectin influences cellular activation, differentiation, and survival of T cells, B cells, and dendritic cells (DCs) (Sundblad et al., 2017). By virtue of these mechanisms, this lectin has been shown to foster cancer immunosuppression (Rabinovich and Conejo-García, 2016), promote resolution of autoimmune disorders (Rabinovich et al., 1999; Toscano et al., 2006, 2018), and dampen immunity against several pathogens (Davicino et al., 2011; Vasta, 2020). Interestingly, galectin-1 has been proposed to serve as a danger-associated molecular pattern secreted in response to infection inflammation and stress (Sato et al., 2009; Vasta, 2020; Russo et al., 2021).

An early report in Chagas disease demonstrated the upregulation of galectin-1 in cardiac tissues of CCC patients and revealed an increased titer of circulating anti-galectin-1 autoantibodies in sera from these individuals (Giordanengo et al., 2001). More recently, galectin-1 was found to be upregulated in the myenteric plexus ganglia of patients with Chagas disease, suggesting a possible association between this lectin and the ganglionitis in the chagasic megacolon (Beghini et al., 2017). Interestingly, the presence of anti-galectin-1 antibodies has also been documented in patients with autoimmune neurological disorders (Lutomski et al., 1997), systemic lupus erythematosus (Montiel et al., 2010), and rheumatoid arthritis (RA, Xibillé-Friedmann et al., 2013). Of note, not only auto- anti-galectin-1 antibodies but also changes in galectin-1 serum levels have been found in these autoimmune disorders (Montiel et al., 2010; Mendez-Huergo et al., 2018). Likewise, elevated levels of galectin-1 have been detected in sera from *T. cruzi*-infected patients in both the asymptomatic and cardiac phases of this inflammatory disease (Benatar et al., 2015).

Chronic chagasic disease is multifactorial cardiomyopathy, and the mechanisms involved in the progression to severe manifestations have not been fully elucidated. It is well accepted that both the persistence of the parasite and immune effector cells trigger tissue damage (Marin-Neto et al., 2007). An inflammatory microenvironment generated by the infection modifies the expression of metalloproteinases, galectins, and cytokines, including transforming growth factor-β, which contribute to the development of myocarditis, tissue remodeling, and fibrosis, thus influencing the progression of the parasite cycle and stimulation of cardiac tissue alteration (da Costa et al., 2019). As observed in patients with severe CCC (Giordanengo et al., 2001), Seropian et al. (2013) described the upregulation of galectin-1 in human cardiac tissue from patients with end-stage chronic failure (Seropian et al., 2013). Interestingly, galectin-1 was overexpressed in cardiac cells exposed to pro-inflammatory cytokines or hypoxic stimuli. Mice lacking galectin-1 (*Lgals1*$^{-/-}$) presented exacerbated symptoms with more inflammatory cells and fewer regulatory T cells (Tregs) in hearts compared with their wild-type (WT) counterparts (Seropian et al., 2013), suggesting a protective role for this lectin in cardiac tissue homeostasis.

In the early 1980s, Henriquez et al. (1981) documented *in vitro* the effect of pretreatment of three distinct cell types (Vero, MA-103, and chick muscle cells) with different lectins to prevent *T. cruzi* infection. More recently, galectin-1 has been shown to inhibit the infection of cardiac cells exposed to *T. cruzi* in culture, using two strains of the parasite with different genetic backgrounds. Interestingly, a parasite strain-dependent glycophenoytpe of cardiac cells was observed, characterized by a reduction in galectin-1-specific ligands on the surface of cells infected with the most virulent strain (Tulahuen, Tul). Protection against *T. cruzi* infection mediated by galectin-1 was confirmed in the experimental *T. cruzi* infection model, where *Lgals1*$^{-/-}$ animals infected with Tul strain displayed enhanced mortality and parasite load in cardiac tissue compared with WT mice. Thus, modulation of galectin-1–glycan interactions in cardiac cells may influence parasite-driven heart injury (Benatar et al., 2015).

In the past years, an increasing number of reports documented the role of galectin-1 within innate and adaptive immune compartments (Toscano et al., 2018). Through its ability to induce tolerogenic DCs and Tregs (Ilarregui et al., 2009) and promote apoptosis of activated Th1 and Th17 cells (Toscano et al., 2007), galectin-1 promotes tumor-immune escape (Cagnoni et al., 2021), feto-maternal tolerance (Blois et al., 2007), and resolution of autoimmune neuroinflammation (Ilarregui et al., 2009). Interestingly, *T. cruzi* infection upregulates the expression of galectin-1 in different immune cells, including B cells and macrophages (Zúñiga et al., 2001a,b). Of note, galectin-1 produced by activated B cells triggered apoptosis of activated T cells and reduced IFN-γ production by these cells (Zúñiga et al., 2001a). In addition, J774 macrophages responded to *T. cruzi* trypomastigotes by releasing high amounts of galectin-1 (Zúñiga et al., 2001b). Recombinant galectin-1 enhanced microbicidal activity and controlled survival of *T. cruzi*-infected macrophages. Under low concentrations of this lectin, splenic macrophages from infected mice showed active replication of the parasite, low interleukin (IL)-12 production, and inhibition of nitric oxide production, consistent with alternative M2 macrophage activation (Correa et al., 2003). On the other hand, a high concentration of galectin-1 promoted dose-dependent apoptosis of macrophages and inhibition of parasite replication (Zúñiga et al., 2001b).

Compelling evidence shows that *T. cruzi* can directly influence the function of DCs, interfering with the development of adaptive immune responses. Van Overtvelt et al. (1999) reported that human monocyte-derived DCs could be infected by *T. cruzi*, preventing optimal activation and blunting production of pro-inflammatory cytokines. Subsequently, it was demonstrated

that the parasite promotes IL-10-producing bone marrow-derived tolerogenic DCs (Poncini et al., 2008). In this regard, galectin-1 has emerged as a decisive factor instructing DCs to become tolerogenic. *Lgals1*$^{-/-}$ mice are refractory to the regulatory effects of *T. cruzi*, preserving immunogenicity of DCs upon parasite stimulation. Intradermal infection with the high virulent RA strain of *T. cruzi* induced early recruitment of DCs to draining lymph nodes and local upregulation of galectin-1. Of note, this lectin was expressed in the spleen during the acute phase of infection. Surprisingly, and in contrast with the results obtained by Benatar et al. (2015) following the intraperitoneal route of infection, *Lgals1*$^{-/-}$ mice presented enhanced resistance to acute *T. cruzi* infection and low parasite burden in tissue, with a major susceptibility in female compared with male animals. Enhanced susceptibility to *T. cruzi* infection in WT mice and persistence of the parasite in infected tissues were driven by a regulatory circuit initiated by upregulation of galectin-1, which elicited tolerogenic DCs, Tregs, and inhibition of antigen-specific T cell responses (Poncini et al., 2015). The discrepancies described in the experimental models of infection using *Lgals1*$^{-/-}$ mice could be related to distinct parasite administration routes, the presence of different phagocytes at the site of inoculation, and the local immune response triggered by different *T. cruzi* strains (Barbosa et al., 2019). In addition, it was demonstrated that *T. cruzi* could modulate the glycophenotype in some cell types suggesting an exquisite evolutionary condition of this parasite that allows manipulation to persist in host cells. This plasticity would also add complexity to the outcome of the infection that is affected by the parasite strain (Tul, Brazil, or RA), the route of infection (intraperitoneal or intradermoplantar inoculation), and the immune responses triggered by the parasite. In this regard, strain-dependent discrepancies have been previously described in other parasite infection models (Toscano et al., 2012). Thus, galectin-1 emerges as a central component of the infection machinery co-opted by *T. cruzi* to persist in the host, evade immune responses, and promote tissue damage. However, despite considerable progress, the mechanisms leading to upregulation of galectin-1 synthesis by *T. cruzi* and the signaling pathways underlying galectin-1–glycan signaling in response to parasite infection remain largely unexplored.

GALECTIN-3 AND *Trypanosoma cruzi* INFECTION

Galectin-3, the chimera type member of the galectin family, has a high affinity to oligosaccharides bearing 2- or 3-*O*-α-substituents on the outer galactose residue of glycans, such as NeuNAcα2,3 lactosamine or the A-blood group structure GalNAcα1,3 [Fucα1,2] Galβ1,4GlcNAc (Barboni et al., 2000; Krzeminski et al., 2010).

Galectin-3 is the best-studied galectin in the context of *T. cruzi* infection. It has been shown to promote *T. cruzi* adhesion and invasion and modulate interactions between the parasite and the host immune system. An early report came from Moody et al. (2000), who showed that *T. cruzi* adhesion to mammalian cells was favored by interactions between parasite mucins and human laminin *via* galectin-3-mediated bridging. *In vitro* experiments showed that human galectin-3 significantly increased the attachment of trypomastigotes to laminin-coated plates but not to collagen. As this association was blocked by lactose in a dose-dependent manner, it has been proposed that interactions between *T. cruzi* mucins and this lectin involve its conserved CRD. Interestingly, the authors proposed the presence of a parasite-derived galectin-3, although genes encoding this protein have not been reported in *T. cruzi* (Turner et al., 2002). Later, the role of human galectin-3 in favoring the adhesion of the infected forms of *T. cruzi* was confirmed using different types of cells, including human coronary artery smooth muscle (CASM) cells, peritoneal macrophages, DCs, cardiac fibroblasts, and Hela cells (Kleshchenko et al., 2004; Vray et al., 2004; Machado et al., 2014; Souza et al., 2017a,b; Chain et al., 2020). By treating CASM cells with galectin-3 antisense oligonucleotides, the attachment of *T. cruzi* diminished dramatically, and this effect was reverted when recombinant galectin-3 was added to the culture media (Kleshchenko et al., 2004; Chain et al., 2020). Exogenous galectin-3, which is secreted by the same cells, could bind glycans present on the surface of both the parasite and human CASM cells in a lectin-like manner. These data indicate that the autocrine action of galectin-3 is essential for parasite attachment and invasion to host cells. However, a similar experimental approach used in previous studies was not successful at demonstrating that adhesion of trypomastigotes to spleen-derived murine DCs line D2SC-1 requires expression of galectin-3. In fact, D2SC-1 cells stably transfected with galectin-3 antisense revealed no differences in the percentages of infected cells or in the number of amastigotes per cell compared with its WT counterpart. The rationale behind this discrepancy was mainly based on the fact that *de novo* synthesis of galectin-3 might occur during the experimental procedure. The authors then moved forward to show that the expression of galectin-3, as well as galectin-3-specific ligands, was upregulated in splenic DCs isolated from BALB/c mice infected with trypomastigotes (Vray et al., 2004). These findings supported the notion that *T. cruzi* infection can modulate lectin expression using both *in vitro* and *in vivo* experimental models and could have a direct effect on the capacity of parasites to migrate and attach to host cells.

Of note, *T. cruzi* also enhanced the expression of other components of the ECM, such as laminin γ-1 and thrombospondin. By taking advantage of bioinformatics approaches and using these proteins together with galectin-3 as seed nodes, Cardenas et al. (2010) constructed an interactome network highlighting how *T. cruzi* could modulate the human ECM to facilitate cellular infection and trigger disease progression during the early phase of the infection (Nde et al., 2012). However, experimental models of chronicity spilled over the idea that galectin-3 was modulated only during the early stages of infection. In fact, galectin-3 was found to be upregulated in macrophages of the inflammatory infiltrate in hearts from C57Bl/6 mice for a total of 8 months post-infection (Soares et al., 2011). The expression of galectin-3 returned to basal levels of naïve mice when chagasic animals were injected with bone marrow cells or were treated with granulocyte colony-stimulating factor (Soares et al., 2011; Vasconcelos et al., 2013). In both cases,

reduction of this lectin was associated with a recovery of heart tissue, lower inflammatory responses, and attenuated fibrosis.

Accordingly, *T. cruzi* also induced elevated levels of galectin-3 in the thymus and modulated the functionality of thymocytes. Infection of BALB/c mice with the blood-derived *T. cruzi* parasites of the Colombian strain induced upregulation of this lectin in both the cortical and medullary compartments of the thymus. In addition, galectin-3 was also found to be increased in the cytoplasm of the $CD4^+/CD8^+$ thymocytes and fostered the migration of this cell subset to peripheral lymphoid organs secondary to parasite infection (Silva-Monteiro et al., 2007). Similarly, the expression of galectin-3 was upregulated in *T. cruzi*-infected mesenchymal stromal cells, which are multipotent stem cells with the capacity to differentiate into mesoderm-derived cell lineages, such as chondrocytes, osteocytes, and adipocytes (Souza et al., 2017a). In further studies, it would be interesting to investigate whether galectin-3 helps to "hide" the parasite in tissues where immune responses are not fully active.

Remarkably, the role of galectin-3 during *T. cruzi* infection is not restricted to modulation of cellular attachment, as it also extends to invasion and intracellular trafficking of the replicative form of the parasite in mammals (Machado et al., 2014; Chain et al., 2020). Immunofluorescence staining showed recruitment of galectin-3 at sites of parasite entry using different cell types, i.e., peritoneal macrophages from C57BL/6 mice, mouse embryonic fibroblasts, and breast carcinoma cell lines (SKBR) cells. After 6 h post-infection, galectin-3, but not the lysosomal membrane proteins (LAMP)-2, was found to be accumulated around *T. cruzi* amastigotes, supporting the notion that this lectin encloses the parasite that has recently lysed the phagolysosome and escaped to the cytoplasm (Machado et al., 2014). The recruitment of galectin-3 in the lysed vacuoles was first described in cells infected with Gram-negative and Gram-positive bacteria, forming the so-called galectin-3-containing structures (Paz et al., 2010). In both models of infection, galectin-3-containing structures depend on the galectin-3 CRD, but this interaction seemed not to comprise the microorganism but galactose-containing glycoconjugates present in the membrane of the lysed vacuole (Paz et al., 2010; Machado et al., 2014). Mirroring these data, galectin-3, plus LAMP-1 and actin filaments, was found around the PV containing amastigotes and trypomastigotes in murine peritoneal macrophages at early times of infection (Reignault et al., 2014). However, immunofluorescence assays carried out after 96 h post-infection showed a diminished number of parasites in cells in the absence of galectin-3, which did not interfere with *T. cruzi* escape from PV into the cytoplasm. This finding opened a conundrum with respect to the role of galectin-3 in the process of parasite intracellular trafficking. Moreover, recent studies demonstrated that the stage-specific protein 4, a glycoprotein present in the surface of amastigotes, could be involved in galectin-3 recruitment during host cell invasion (Florentino et al., 2018). Recently, it was reported that *T. cruzi* induces the cleavage of galectin-3 through different parasite proteases, including Zn-metalloproteases and collagenases, rendering a truncated form of the lectin, which retains an intact CRD but impedes its oligomerization. This phenomenon raised the question of possible causes and mechanisms through which *T. cruzi* affects lectin structure. Pineda et al. (2020) demonstrated that parasite death induced by long-term interactions between galectin-3 and *T. cruzi* is avoided by cleavage of the lectin *N*-terminal domain. Through this mechanism, the parasite likely counteracts galectin-3-driven immunity and host microbicidal activity, highlighting a possible strategy developed by parasites to survive inside mammalian hosts (Pineda et al., 2020).

There is ample evidence stressing the role of galectin-3 in immune responses mounted during *T. cruzi* infection and the outcome of cardiac alterations. This lectin was found to be highly expressed in B cells isolated from BALB/c mice infected with *T. cruzi* (Acosta-Rodríguez et al., 2004). This elevated expression was also detected when resting B cells were activated *in vitro* with different stimuli, such as lipopolysaccharide and F(ab')2 anti-μ and anti-CD40 antibodies, reaching a maximum effect after a long period of incubation. In both cases, galectin-3 was upregulated in the presence of IL-4, a cytokine that favored B cell survival and the generation of a memory phenotype (Rothstein et al., 2000; Acosta Rodriguez et al., 2003). However, IL-4 activity was abolished when the synthesis of endogenous galectin-3 was interrupted, clearly demonstrating the existence of a mechanism of cross-talk between IL-4 and galectin-3 in the context of acute Chagas disease. Thus, endogenous galectin-3 could serve as a possible mechanism used by the parasite to evade B cell responses. In this regard, inhibition of endogenous galectin-3 during acute *T. cruzi* infection reduced parasitemia by promoting plasma cell formation and secretion of immunoglobulin (Ig)M and IgG (Acosta-Rodríguez et al., 2004).

Interestingly, infected *Lgals3*$^{-/-}$ mice showed a drop in serum levels of Th1 and Th2 cytokines, including IFN-γ, IL-2, IL-5, IL-6, IL-10, and TNF, compared with WT mice; these differences were significantly pronounced at 14 days but ceased at 28 days post-infection. Also, the expression of IL-5, IFN-γ, and TLR4 was also significantly diminished in splenocytes of galectin-3-deficient mice. These data, which correlated with the increase in parasitemia, demonstrated that galectin-3 is involved in the initial anti-*T. cruzi* response that connects innate and adaptive immunity. In line with these findings, this lectin favored the occurrence of cardiac alterations, as hearts from *Lgals3*$^{-/-}$ mice showed fewer inflammatory infiltrates and prominent signs of fibrosis. Of note, this effect was accompanied by increased parasitemia in the absence of parasite load. Delving into antigen-presenting cell functionality, a lower activation state was evidenced by a reduced expression of the co-stimulatory molecule CD80 and decreased IL-1 and TNF-α production after *in vitro* infection with the parasite. As *Tlr1* and *Tlr4* messenger RNA levels were also affected in *Lgals3*$^{-/-}$ DCs, one might speculate that endogenous galectin-3 controls DC responses by interacting with these receptors. Overall, these findings support the notion that galectin-3 is associated with the outcome of heart injury and inflammation in the context of *T. cruzi* infection (Pineda et al., 2015b).

It is important to emphasize that, similar to galectin-1, the parasite strain used is clearly a relevant factor that governs host–parasite interplay and should be clearly specified in all studies performed. Thus, by exploring the development of cardiac alterations in the murine infection and its association with

galectin-3 expression using different human isolates of *T. cruzi* fitting with DTUs I, V, and VI, only animals infected with the former strains developed moderate to severe myocarditis (Ferrer et al., 2014). Immunohistochemical analysis revealed that the myocardial fibrotic areas correlated with higher expression of galectin-3, suggesting a role of this lectin as a putative marker of cardiac progression in Chagas disease (Ferrer et al., 2014). In addition, specific binding of galectin-3 changed among the different life stages of the parasite and also among the six lineages analyzed, probably due to dissimilar glycoconjugates decorating *T. cruzi* cell surface (Pineda et al., 2015a).

A widespread study using animal models and human settings underscored the involvement of galectin-3 in the development of heart disease at the chronic stage of Chagas disease. Souza et al. (2017a) confirmed in an experimental murine model that *T. cruzi* induced galectin-3 expression in the heart and favored the recruitment of infiltrating inflammatory cells at day 30 post-infection, whereas signs of fibrosis appeared after 180 days of the prime infection. Interestingly, the expression of galectin-3 was not limited to $CD3^+$ T cells but was also verified in macrophages and fibroblasts. In the latter, both exogenous addition of galectin-3 and its silencing demonstrated that this lectin promotes cellular proliferation *via* its CRD. Even more, treatment with *N*-acetyl-D-lactosamine in mice chronically infected with *T. cruzi* did not improve their cardiological performance but significantly reduced inflammatory infiltrates and fibrosis (Souza et al., 2017b). These effects were accompanied by a considerable reduction of pro-inflammatory cytokines, such as TNF and IFN-γ, transcription factors associated with development and regulation of adaptive immune responses including T-bet (Th1), GATA-3 (Th2), and FoxP3F (Tregs), and modulation of chemokines including chemokine ligand 8 (CCL8) and the chemokine receptor 5 (CCR5), compared with untreated infected animals. However, *IL-10* messenger RNA levels were not altered when compared with naïve mice. Explants of heart from chronic cardiac patients obtained during transplantation also extended previous observation regarding galectin-3 expression in the inflamed areas of this tissue. This study demonstrated the critical roles of galectin-3 in the progression of Chagas cardiac pathology, highlighting its potential role as a therapeutic target in the management of the disease. In this sense, the use of compounds such as 1,2,3-triazole arylsulfonamide-derived-3-*O*-galactosides, which inhibit galectin-3, diminished *T. cruzi* invasion of LLCMK2 cells, a cell line derived from monkey kidney epithelial cells (Marchiori et al., 2017).

Studies in WT and galectin-3 knockout Swiss mice during the acute infection with *T. cruzi* Y strain contributed to unveiling the effect of galectin-3 in the modulation of serum cytokines. Although IFN-γ and TNF were elevated in the *Lgals-3*$^{-/-}$ animals, upregulation of IL-4, IL-6, IL-10, and IL-17 were also evident at 15 days post-infection, inducing a shift toward Th17 and Th2 responses that could be explained by mechanisms involving galectin-3 modulation of the innate immune response during *T. cruzi* primo-infection (Chain et al., 2020). Noteworthy, the lack of galectin-3 led to a drop in systemic parasitemia and increased mouse survival. This study suggested that murine models of infection involved a higher parasitic Y load when compared with those used by Pineda et al. (2015a), whereas da Silva et al. (2017) used another *T. cruzi* strain. Furthermore, this investigation revealed the role of galectin-3 in cell survival by demonstrating that parasite-infected peritoneal macrophages or Hela cells required this lectin to escape apoptotic cell death. Infected galectin-3-depleted cells showed not only loss of mitochondrial membrane potential but also an increase in caspase-3 activity and elevated proteolytic processing of poly (ADP-ribose) polymerase after 4 and 8 h post-infection (Pineda et al., 2015b; da Silva et al., 2017; Chain et al., 2020). In line with these findings, chronically infected *Parp1*$^{-/-}$ mice showed lower levels of galectin-3, along with additional markers of fibrosis such as transforming growth factor-β and vimentin in heart-resident $CD68^+$ macrophages, compared with their WT counterparts (Choudhuri and Garg, 2020). Hence, a signaling pathway connecting galectin-3 with poly (ADP-ribose) polymerase seems to be involved in the apoptotic and fibrotic processes occurring in cardiac tissue during *T. cruzi* infection. Finally, da Silva et al. (2017) also showed, using an infection model of the *T. cruzi* CL strain, that the absence of galectin-3 increased the replication of intracellular parasites in mouse peritoneal macrophages and cell lysis while augmenting blood parasite levels and reducing mast cell recruitment to the heart (da Silva et al., 2017). The discrepancies found among different reports emphasized the critical relevance of parasite strain and doses, inoculation routes, and acute *versus* chronic murine models of *T. cruzi* infection.

When the impact of galectin-3 on digestive manifestations of chronic *T. cruzi* infection was studied, it was observed that the myenteric plexus ganglia in biopsied fragments of the colon from patients with megacolon presented higher expression of galectin-3 along with galectins-1 and 9 (Beghini et al., 2017). A recent study confirmed this observation revealing an increased number of cells expressing galectin-3 that are associated with major staining of collagen type I and type III in tissue areas, suggesting the occurrence of ganglionitis and myositis, two pathological traits implicated in this process. Although galectin-3 was mainly upregulated in the group of patients presenting megacolon with intact intestinal mucosa but not in those with an ulcerated intestinal mucosa and/or mucosal hypertrophy, it has been proposed that this lectin could be a key factor implicated in the progression of colon pathology in the context of Chagas disease (Garvil et al., 2020). Thus, galectin-3 controls not only parasite infection and immune responses but also cardiac and digestive pathology.

OTHER GALECTINS IMPLICATED IN *Trypanosoma cruzi* INFECTION

Despite significant evidence demonstrating the role of galectins-1 and 3 during *T. cruzi* infection, the role of other members of the galectin family in the context of Chagas disease is still uncertain.

In a comprehensive study focused on the interaction between human galectins and the three forms belonging to the six DTUs of *T. cruzi*, Pineda et al. (2015b) showed, using the Y strain, that galectins-7 and 8 bound mainly to trypomastigotes, whereas

galectins-1 and 4 presented higher affinity for amastigotes. Interestingly, only galectin-7 showed the binding capacity to epimastigotes, the non-infective *T. cruzi* stage (Pineda et al., 2015b). Moreover, these differences were not only observed among the genetic lineages of the parasite but were also evident among the diverse strains within them. Galectin binding to *T. cruzi* was disrupted in the presence of lactose, highlighting the relevance of the CRD in galectin–parasite interaction. These findings demonstrated that the glycan profile exposed on the parasite surface varies during its life cycle, suggesting that it could be one of the mechanisms used by the parasite to survive in invertebrate and vertebrate hosts. Like galectin-3, the majority of tested galectins, mainly galectin-8, fostered adhesion of trypomastigotes to different cells lines, including THP-1 (human monocytic cells), LLC-MK2 (rhesus monkey kidney epithelial cells), CaCo (human colorectal adenocarcinoma cells), and HL-1 (cardiac myocyte cells). Particularly, parasite adhesion induced by galectin-7 was enhanced with higher concentrations of this lectin, suggesting the need for homodimer formation for this effect. These results emphasize the distinct roles of different galectins during *T. cruzi* infection. Thus, galectin-7, which is mostly expressed in stratified epithelia (Advedissian et al., 2017), could be one of the first mediators that favor the entry of the parasite to host cells.

Galectin-8 has recently been studied in WT and C57BL/6J *Lgals8*$^{-/-}$ mice chronically infected with Ac strain, belonging to DTU TcI (Bertelli et al., 2020). Lack of galectin-8 induced higher inflammatory infiltrates, mainly neutrophils and macrophages in heart tissue, and IFN-γ production, but systemic parasitemia and survival rate remained similar. Of note, galectin-8 was increased in the heart of infected WT mice (Bertelli et al., 2020). These findings highlight the anti-inflammatory role of galectin-8 in chronic *T. cruzi* infection.

Finally, galectin-9 was found to be upregulated in biopsy fragments of the colon from patients with chronic Chagas disease presenting megacolon (Beghini et al., 2017).

Thus, despite a major role for galectins-1- and 3 in Chagas disease, galectins-7, 8, and 9 have also been shown to control anti-parasite immunity and modulate tissue damage.

CONCLUSION AND FUTURE DIRECTIONS

Galectins play decisive roles during the life cycle of *T. cruzi*. Whereas most studies have focused on the role of galectins-1 and 3 in parasite adhesion, invasion, immune evasion, and tissue damage, other galectins, including galectins-7, 8, and 9, also play relevant functions in the context of Chagas disease. Future studies should be aimed at examining, in parallel using the same parasite lineages and strains, the unique and distinctive roles of different members of the galectin family in mice lacking galectins in relevant tissues. Moreover, given the preferential recognition of individual members of the galectin family for different glycans, further work using glycan array technologies (Arthur et al., 2014) should be performed to dissect biochemical determinants of *T. cruzi*–galectin interactions. Furthermore, the prognostic value of soluble galectins and anti-galectin autoantibodies in sera from patients with Chagas disease should be confirmed in a larger cohort of patients. Finally, given the design of selective galectin inhibitors (Cagnoni et al., 2016), the therapeutic activity of these antagonists should be evaluated in preclinical models of Chagas disease and further validated in *in vitro* settings of infection of human cells with the ultimate goal of finding new treatments for this neglected disabling disease that affects more than two to three million people worldwide.

AUTHOR CONTRIBUTIONS

CP, AB, and KG contributed to the selection of the manuscript, integration of studies, and writing of the original draft. GR contributed to the conceptualization and integration of the review. All authors approved the submitted version.

FUNDING

Work in authors' laboratories were supported by grants from the Argentinean National Agency for Promotion of Science and Technology (PICT 2014-3687 and 2017-0494 to GR and PICT 2014-1026 to KG), Argentinian National Council for Scientific and Technical Investigations (CONICET-PIP 112- 2015010-0547 to KG), as well as Fundación Sales, Fundación Bunge and Born, and Fundación Williams (to GR).

ACKNOWLEDGMENTS

We apologize to the many authors whose manuscript could not be cited for space limitations. We are grateful to Ramiro Perrotta for his assistance in graphical art. We thank the Ferioli, Ostry, and Caraballo families for their generous support.

REFERENCES

Acevedo, G. R., Girard, M. C., and Gómez, K. A. (2018). The unsolved jigsaw puzzle of the immune response in chagas disease. *Front. Immunol.* 9:1929. doi: 10.3389/fimmu.2018.01929

Acosta, A. M., and Santos-Buch, C. A. (1985). Autoimmune myocarditis induced by *Trypanosoma cruzi*. *Circulation* 71, 1255–1261. doi: 10.1161/01.cir.71.6.1255

Acosta Rodriguez, E. V., Zuñiga, E., Montes, C. L., and Gruppi, A. (2003). Interleukin-4 biases differentiation of B cells from *Trypanosoma cruzi*-infected mice and restrains their fratricide: role of Fas ligand down-regulation and MHC class II-transactivator up-regulation. *J. Leukoc. Biol.* 73, 127–136. doi: 10.1189/jlb.0702353

Acosta-Rodríguez, E. V., Montes, C. L., Motrán, C. C., Zuniga, E. I., Liu, F. T., Rabinovich, G. A., et al. (2004). Galectin-3 mediates IL-4-induced survival and differentiation of B cells: functional cross-talk and implications during *Trypanosoma cruzi* infection. *J. Immunol. 1* 172, 493–502. doi: 10.4049/jimmunol.172.1.493

Advedissian, T., Deshayes, F., and Viguier, M. (2017). Galectin-7 in epithelial homeostasis and carcinomas. *Int. J. Mol. Sci.* 18:2760. doi: 10.3390/ijms18122760

Alves, M. J., and Colli, W. (2007). *Trypanosoma cruzi*: adhesion to the host cell and intracellular survival. *IUBMB Life* 59, 274–279. doi: 10.1080/15216540701200084

Arthur, C. M., Cummings, R. D., and Stowell, S. R. (2014). Using glycan microarrays to understand immunity. *Curr. Opin. Chem. Biol.* 18, 55–61. doi: 10.1016/j.cbpa.2013.12.017

Aufderheide, A. C., Salo, W., Madden, M., Streitz, J., Bulkestra, J., Guhl, F., et al. (2004). A 9,000-years record of Chagas disease. *Proc. Natl. Acad. Sci. U.S.A.* 101, 2034–2039. doi: 10.1073/pnas.0307312101

Barboni, E. A., Bawumia, S., Henrick, K., and Hughes, R. C. (2000). Molecular modeling and mutagenesis studies of the N-terminal domains of galectin-3: evidence for participation with the C-terminal carbohydrate recognition domain in oligosaccharide binding. *Glycobiology* 10, 1201–1208. doi: 10.1093/glycob/10.11.1201

Barbosa, C. G., Carvalho Costa, T. M., Desidério, C. S., Ferreira, P. T. M., Silva, M. O., Hernández, C. G., et al. (2019). *Trypanosoma cruzi* Mexican strains differentially modulate surface markers and cytokine production in bone marrow-derived dendritic cells from C57BL/6 and BALB/c Mice. *Mediators Inflamm.* 2019:7214798. doi: 10.1155/2019/7214798

Barrias, E. S., de Carvalho, T. M., and De Souza, W. (2013). *Trypanosoma cruzi*: entry into mammalian host cells and parasitophorous vacuole formation. *Front. Immunol.* 4:186. doi: 10.3389/fimmu.2013.00186

Bartholomeu, D. C., de Paiva, R. M., Mendes, T. A., DaRocha, W. D., and Teixeira, S. M. (2014). Unveiling the intracellular survival gene kit of trypanosomatid parasites. *PLoS Pathog.* 10:e1004399. doi: 10.1371/journal.ppat.1004399

Beghini, M., de Araújo, M. F., Severino, V. O., Etchebehere, R. M., Rocha Rodrigues, D. B., and de Lima Pereira, S. A. (2017). Evaluation of the immunohistochemical expression of Gal-1, Gal-3 and Gal-9 in the colon of chronic chagasic patients. *Pathol. Res. Pract.* 213, 1207–1214. doi: 10.1016/j.prp.2017.04.014

Benatar, A. F., García, G. A., Bua, J., Cerliani, J. P., Postan, M., Tasso, L. M., et al. (2015). Galectin-1 prevents infection and damage induced by *trypanosoma cruzi* on cardiac cells. *PLoS Negl. Trop. Dis.* 9:e0004148. doi: 10.1371/journal.pntd.0004148

Bern, C., Messenger, L. A., Whitman, J. D., and Maguire, J. H. (2019). Chagas disease in the united states: a public health approach. *Clin. Microbiol. Rev.* 33:e00023-19. doi: 10.1128/CMR.00023-19

Bertelli, A., Sanmarco, L. M., Pascuale, C. A., Postan, M., Aoki, M. P., and Leguizamón, M. S. (2020). Anti-inflammatory role of galectin-8 during *Trypanosoma cruzi* chronic infection. *Front. Cell Infect. Microbiol.* 10:285. doi: 10.3389/fcimb.2020.00285

Bilate, A. M., and Cunha-Neto, E. (2008). Chagas disease cardiomyopathy: current concepts of an old disease. *Rev. Inst. Med. Trop. Sao Paulo.* 50, 67–74. doi: 10.1590/s0036-46652008000200001

Bisio, M., Seidenstein, M. E., Burgos, J. M., Ballering, G., Risso, M., Pontoriero, R., et al. (2011). Urbanization of congenital transmission of *Trypanosoma cruzi*: prospective polymerase chain reaction study in pregnancy. *Trans. R. Soc. Trop. Med. Hyg.* 105, 543–549. doi: 10.1016/j.trstmh.2011.07.003

Blois, S. M., Ilarregui, J. M., Tometten, M., Garcia, M., Orsal, A. S., Cordo-Russo, R., et al. (2007). A pivotal role for galectin-1 in fetomaternal tolerance. *Nat Med.* 2017, 1450–1457. doi: 10.1038/nm1680

Bonney, K. M., and Engman, D. M. (2008). Chagas heart disease pathogenesis: one 280 mechanisms or many? *Curr. Mol. Med.* 8, 510–518. doi: 10.2174/156652408785748004

Bourne, Y., Bolgiano, B., Liao, D. I., Strecker, G., Cantau, P., Herzberg, O., et al. (1994). Crosslinking of mammalian lectin (galectin-1) by complex biantennary saccharides. *Nat. Struct. Biol.* 1, 863–870. doi: 10.1038/nsb1294-863

Buscaglia, C. A., Campo, V. A., Frasch, A. C., and Di Noia, J. M. (2006). *Trypanosoma cruzi* surface mucins: host-dependent coat diversity. *Nat. Rev. Microbiol.* 4, 229–236. doi: 10.1038/nrmicro1351

Cagnoni, A. J., Giribaldi, M. L., Blidner, A. G., Cutine, A. M., Gatto, S. G., Morales, R. M., et al. (2021). Galectin-1 fosters an immunosuppressive microenvironment in colorectal cancer by reprogramming CD8+ regulatory T cells. *Proc. Natl. Acad. Sci. U.S.A.* 118:e2102950118. doi: 10.1073/pnas.2102950118

Cagnoni, A. J., Pérez Sáez, J. M., Rabinovich, G. A., and Mariño, K. V. (2016). Turning-off signaling by siglecs, selectins, and galectins: chemical inhibition of glycan-dependent interactions in cancer. *Front. Oncol.* 6:109. doi: 10.3389/fonc.2016.00109

Calvet, C. M., Melo, T. G., Garzoni, L. R., Oliveira, F. O. Jr., Neto, D. T., Maria, N. S. L. M., et al. (2012). Current understanding of the *Trypanosoma cruzi*-cardiomyocyte interaction. *Front. Immunol.* 3:327. doi: 10.3389/fimmu.2012.00327

Cardenas, T. C., Johnson, C. A., Pratap, S., Nde, P. N., Furtak, V., Kleshchenko, Y. Y., et al. (2010). Regulation of the extracellular matrix interactome by *Trypanosoma cruzi*. *Open Parasitol. J.* 4, 72–76. doi: 10.2174/1874421401004010072

Chain, M. O., Paiva, C. A. M., Maciel, I. O., Neto, A. N., Castro, V. F., Oliveira, C. P., et al. (2020). Galectin-3 mediates survival and apoptosis pathways during *Trypanosoma cruzi*-host cell interplay. *Exp. Parasitol.* 216:107932. doi: 10.1016/j.exppara.2020.107932

Choudhuri, S., and Garg, N. J. (2020). *Trypanosoma cruzi* Induces the PARP1/AP-1 Pathway for upregulation of metalloproteinases and transforming growth factor β in macrophages: role in cardiac fibroblast differentiation and fibrosis in chagas disease. *mBio* 11:e01853-20. doi: 10.1128/mBio.01853-20

Correa, S. G., Sotomayor, C. E., Aoki, M. P., Maldonado, C. A., and Rabinovich, G. A. (2003). Opposite effects of galectin-1 on alternative metabolic pathways of L-arginine in resident, inflammatory, and activated macrophages. *Glycobiology* 13, 119–128. doi: 10.1093/glycob/cwg010

Coura, J. R., and Dias, J. C. P. (2009). Epidemiology, control and surveillance of Chagas disease - 100 years after its discovery. *Mem. Inst. Oswaldo Cruz Rio Janeiro* 104 (Suppl. I), 31–40. doi: 10.1590/s0074-02762009000900060006

Cunha-Neto, E., Coelho, V., Guilherme, L., Fiorelli, A., Stolf, N., and Kalil, J. (1996). Autoimmunity in Chagas' disease. Identification of cardiac myosin-B13 *Trypanosoma cruzi* protein crossreactive T cell clones in heart lesions of a chronic Chagas' cardiomyopathy patient. *J. Clin. Invest.* 98, 1709–1712. doi: 10.1172/JCI118969

Cunha-Neto, E., Teixeira, P. C., Nogueira, L. G., and Kalil, J. (2011). Autoimmunity. *Adv. Parasitol.* 76, 129–152. doi: 10.1016/B978-0-12-385895-5.00006-2

da Costa, A. W. F., do Carmo Neto, J. R., Braga, Y. L. L., Silva, B. A., Lamounier, A. B., Silva, B. O., et al. (2019). Cardiac chagas disease: mmps. timps, galectins, and TGF-β as tissue remodelling players. *Dis. Markers* 25:3632906. doi: 10.1155/2019/3632906

da Silva, A. A., Teixeira, T. L., Teixeira, S. C., Machado, F. C., Dos Santos, M. A., Tomiosso, T. C., et al. (2017). Galectin-3: a friend but not a foe during *Trypanosoma cruzi* experimental infection. *Front. Cell Infect. Microbiol.* 7:463. doi: 10.3389/fcimb.2017.00463

Davicino, R. C., Eliçabe, R. J., Di Genaro, M. S., and Rabinovich, G. A. (2011). Coupling pathogen recognition to innate immunity through glycan-dependent mechanisms. *Int. Immunopharmacol.* 11, 1457–1463. doi: 10.1016/j.intimp.2011.05.002

Davicino, R. C., Méndez-Huergo, S. P., Eliçabe, R. J., Stupirski, J. C., Autenrieth, I., Di Genaro, M. S., et al. (2017). Galectin-1-driven tolerogenic programs aggravate yersinia enterocolitica infection by repressing antibacterial immunity. *J. Immunol.* 199, 1382–1392. doi: 10.4049/jimmunol.1700579

de Lederkremer, R. M., and Agusti, R. (2009). Glycobiology of *Trypanosoma cruzi*. *Adv. Carbohydr. Chem. Biochem.* 62, 311–366. doi: 10.1016/S0065-2318(09)00007-9

De Rissio, A. M., Riarte, A. R., Martín García, M., Esteva, M. I., Quaglino, M., and Ruiz, A. M. (2010). Congenital *Trypanosoma cruzi* infection. Efficacy of its monitoring in an urban reference health center in a non-endemic area of Argentina. *Am. J. Trop. Med. Hyg.* 82, 838–845. doi: 10.4269/ajtmh.2010.08-0383

De Souza, W. (2002). From the cell biology to the development of new chemotherapeutic approaches against trypanosomatids: dreams and reality. *Kinetoplastid Biol. Dis.* 1:3. doi: 10.1186/1475-9292-1-3

De Souza, W., De Carvalho, T. M., and Barrias, E. S. (2010). Review on *Trypanosoma cruzi*: hostcell interaction. *Int. J. Cell Biol.* 2010:295394. doi: 10.1155/2010/295394

Del Puerto, R., Nishizawa, J. E., Kikuchi, M., Iihoshi, N., Roca, Y., Avilas, C., et al. (2010). Lineage analysis of circulating *Trypanosoma cruzi* parasites and their association with clinical forms of Chagas disease in Bolivia. *PLoS Negl. Trop. Dis.* 4:e687. doi: 10.1371/journal.pntd.0000687

Dutra, W. O., Menezes, C. A. S., Villani, F. N. A., Carneiro da Costa, G., Morais da Silveira, A. B., D'Avila Reis, D., et al. (2009). Cellular and genetic mechanisms involved in the generation of protective and pathogenic immune responses in human Chagas disease. *Mem. Inst. Oswaldo Cruz Rio Janeiro* 104(Suppl. I), 208–218. doi: 10.1590/s0074-02762009000900027

Epting, C. L., Coatesa, B. M., and Engmanb, D. E. (2010). Molecular mechanisms of host cell invasion by *Trypanosoma cruzi*. *Exp. Parasitol.* 126, 283–291. doi: 10.1016/j.exppara.2010.06.023

Esper, L., Talvani, A., Pimentel, P., Teixeira, M. M., and Machado, F. S. (2015). Molecular mechanismsof myocarditis caused by *Trypanosoma cruzi*. *Curr. Opin. Infect. Dis.* 28, 246–252. doi: 10.1097/QCO.0000000000000157

Ferreira, A. V., Segatto, M., Menezes, Z., Macedo, A. M., Gelape, C., de Oliveira Andrade, L., et al. (2011). Evidence for *Trypanosoma cruzi* in adipose tissue in human chronic Chagas disease. *Microbes Infect.* 13, 1002–1005. doi: 10.1016/j.micinf.2011.06.002

Ferreira, D., Cortez, M., Atayde, V. D., and Yoshida, N. (2006). Actin cytoskeleton-dependent and -independent host cell invasion by *Trypanosoma cruzi* is mediated by distinct parasite surface molecules. *Infect. Immun.* 74, 5522–5528. doi: 10.1128/IAI.00518-06

Ferrer, M. F., Pascuale, C. A., Gomez, R. M., and Leguizamón, M. S. (2014). DTU I isolates of *Trypanosoma cruzi* induce upregulation of Galectin-3 in murine myocarditis and fibrosis. *Parasitology* 141, 849–858. doi: 10.1017/S0031182013002254

Ferri, G., and Edreira, M. M. (2021). All roads lead to cytosol: *Trypanosoma cruzi* multi-strategic approach to invasion. *Front. Cell Infect. Microbiol.* 11:634793. doi: 10.3389/fcimb.2021.634793

Florentino, P. T. V., Real, F., Orikaza, C. M., da Cunha, J. P. C., Vitorino, F. N. L., Cordero, E. M., et al. (2018). A carbohydrate moiety of secreted stage-specific glycoprotein 4 participates in host cell invasion by *Trypanosoma cruzi* extracellular amastigotes. *Front. Microbiol.* 9:693. doi: 10.3389/fmicb.2018.00693

Freedman, N. J., and Lefkowitz, R. J. (2004). Anti-β1-adrenergic receptor antibodies and heart failure: causation, not just correlation. *J. Clin. Invest.* 113, 1379–1382. doi: 10.1172/JCI21748

Garcia, E. S., Genta, F. A., de Azambuja, P., and Schaub, G. A. (2010). Interactions between intestinal compounds of triatomines and *Trypanosoma cruzi*. *Trends Parasitol.* 26, 499–505. doi: 10.1016/j.pt.2010.07.003

Garvil, M. P., Furtado, T. C. S., Lima, N. B., Marteleto, M. V. M., Faria, J. B., Rodrigues, D. B. R., et al. (2020). Although with intact mucosa at colonoscopy, chagasic megacolons have an overexpression of Gal-3. *Einstein (Sao Paulo).* 18:eAO5105. doi: 10.31744/einstein_journal/2020AO5105

Giddings, O. K., Eickhoff, C. S., Sullivan, N. L., and Hoft, D. F. (2010). Intranasal vaccinations with the *trans*-sialidase antigen plus CpG adjuvant induce mucosal immunity protective against conjunctival *Trypanosoma cruzi* challenges. *Infect. Immun.* 78, 1333–1338. doi: 10.1128/IAI.00278-09

Giordanengo, L., Gea, S., Barbieri, G., and And Rabinovich, G. A. (2001). Anti-galectin-1 autoantibodies in human *Trypanosoma cruzi* infection: diferential expression of this β-galactosidase-binding protein in cardiac Chagas' disease. *Clin. Exp. Immunol.* 124, 266–273. doi: 10.1046/j.1365-2249.2001.01512.x

Giorgi, M. E., and de Lederkremer, R. M. (2020). The Glycan Structure of *T. cruzi* mucins Depends on the Host. Insights on the Chameleonic Galactose. *Molecules* 25:3913. doi: 10.3390/molecules25173913

Guhl, F., Jamillo, C., Vallejo, G. A., Yockteng, R., Cardenas-Arroyo, F., and Forniciari, G. (1999). Isolation of *Trypanosoma cruzi* DNA in 4.000 years old mummified human tissue from morthern Chile. *Am. J. Physiol. Anthropol.* 108, 625–635.

Healy, C., Viles-Gonzalez, J. F., Sáenz, L. C., Soto, M., Ramírez, J. D., and d'Avila, A. (2015). Arrhythmias in chagasic cardiomyopathy. *Card Electrophysiol. Clin.* 7, 251–268. doi: 10.1016/j.ccep.2015.03.016

Hemmige, V., Tanowitz, H., and Sethi, A. (2012). *Trypanosoma cruzi* infection: a review with emphasis on cutaneous manifestations. *Int. J. Dermatol.* 51, 501–508. doi: 10.1111/j.1365-4632.2011.05380.x

Henriquez, D., Piras, R., and Piras, M. M. (1981). The effect of surface membrane modifications of fibroblastic cells on the entry process of *Trypanosoma cruzi* trypomastigotes. *Mol. Biochem. Parasitol.* 2, 359–366. doi: 10.1016/0166-6851(81)90087-6

Hirabayashi, J., Hashidate, T., Arata, Y., Nishi, N., Nakamura, T., Hirashima, M., et al. (2002). Oligosaccharide specificity of galectins: a search by frontal affinity chromatography. *Biochim. Biophys. Acta* 1572, 232–254. doi: 10.1016/s0304-4165(02)00311-2

Ilarregui, J. M., Croci, D. O., Bianco, G. A., Toscano, M. A., Salatino, M., Vermeulen, M. E., et al. (2009). Tolerogenic signals delivered by dendritic cells to T cells through a galectin-1-driven immunoregulatory circuit involving interleukin 27 and interleukin 10. *Nat. Immunol.* 10, 981–991. doi: 10.1038/ni.1772

Jansen, A. M., Xavier, S. C. D. C., and Roque, A. L. R. (2020). Landmarks of the knowledge and *Trypanosoma cruzi* Biology in the Wild Environment. *Front. Cell Infect. Microbiol.* 10:10. doi: 10.3389/fcimb.2020.00010

Kaplan, D., Ferrari, I., Lopez Bergami, P., Mahler, E., Levitus, G., Chiale, P., et al. (1997). Antibodies to ribosomal P proteins of *Trypanosoma cruzi* in Chagas disease possess functional autoreactivity with heart tissue and differ from anti-P autoantibodies in Lupus. *Proc. Natl. Acad. Sci.U.S.A.* 94, 10301–10306. doi: 10.1073/pnas.94.19.10301

Kleshchenko, Y. Y., Moody, T. N., Vyacheslav, A. F., Ochieng, J., Lima, M. F., and Villalta, F. (2004). Human galectin-3 promotes *Trypanosoma cruzi* Adhesión to human coronary artery smooth muscle cells. *Infect. Immun.* 72, 6717–6721. doi: 10.1128/IAI.72.11.6717-6721.2004

Krzeminski, M., Singh, T., André, S., Lensch, M., Wu, A. M., Bonvin, A. M., et al. (2010). Human galectin-3 (Mac-2 antigen): defining molecular switches of affinity to natural glycoproteins, structural and dynamic aspects of glycan binding by flexible ligand docking and putative regulatory sequences in the proximal promoter region. *Biochim. Biophys. Acta* 1810, 150–161. doi: 10.1016/j.bbagen.2010.11.001

Kutzner, T. J., Higuero, A. M., Süßmair, M., Kopitz, J., Hingar, M., Díez-Revuelta, N., et al. (2020). How presence of a signal peptide affects human galectins-1 and -4: Clues to explain common absence of a leader sequence among adhesion/growth-regulatory galectins. *Biochim. Biophys. Acta Gen. Subj.* 1864:129449. doi: 10.1016/j.bbagen.2019.129449

Labovsky, V., Smulski, C. R., Gómez, K., Levy, G., and Levin, M. J. (2007). Anti- β1-adrenergic receptor autoantibodies in patients with chronic Chagas heart disease. *Clin. Exp. Immunol.* 148, 440–449. doi: 10.1111/j.1365-2249.2007.03381.x

Landskroner-Eiger, S., Cordero, A., Factor, S. M., Weiss, L. M., Lisanti, M. P., Tanowitz, H. B., et al. (2005). The adipocyte as an important target cell for *Trypanosoma cruzi* infection. *J. Biol. Chem.* 280, 24085–24094. doi: 10.1074/jbc.M412802200

Levin, M. J., Kaplan, D., Ferrari, I., Arteman, P., Vazquez, M., and Panebra, A. (1993). Humoral autoimmune response in Chagas disease: *Trypanosoma cruzi* ribosomal antigens as immunizing agents. *FEMS Immunol. Med. Microbiol.* 7, 205–210. doi: 10.1111/j.1574-695X.1993.tb00400.x

Levroney, E. L., Aguilar, H. C., Fulcher, J. A., Kohatsu, L., Pace, K. E., Pang, M., et al. (2005). Novel innate immune functions for galectin-1: galectin-1 inhibits cell fusion by Nipah virus envelope glycoproteins and augments dendritic cell secretion of proinflammatory cytokines. *J. Immunol.* 175, 413–420. doi: 10.4049/jimmunol.175.1.413

Lidani, K. C. F., Andrade, F. A., Bavia, L., Damasceno, F. S., Beltrame, M. H., Messias-Reason, I. J., et al. (2019). Chagas disease: from discovery to a worldwide health problem. *Front. Public Health* 7:166. doi: 10.3389/fpubh.2019.00166

Lujan, A. L., Croci, D. O., Gambarte Tudela, J. A., Losinno, A. D., Cagnoni, A. J., Mariño, K. V., et al. (2018). Glycosylation-dependent galectin-receptor interactions promote Chlamydia trachomatis infection. *Proc. Natl. Acad. Sci. U.S.A.* 115, E6000–E6009. doi: 10.1073/pnas.1802188115

Lutomski, D., Joubert-Caron, R., Lefebure, C., Salama, J., Belin, C., Bladier, D., et al. (1997). Anti-galectin-1 autoantibodies in serum of patients with neurological diseases. *Clin. Chim. Acta* 262, 131–138. doi: 10.1016/s0009-8981(97)06544-3

Machado, F. C., Cruz, L., da Silva, A. A., Cruz, M. C., Mortara, R. A., Roque-Barreira, M. C., et al. (2014). Recruitment of galectin-3 during cell invasion and intracellular trafficking of *Trypanosoma cruzi* extracellular amastigotes. *Glycobiology* 24, 179–184. doi: 10.1093/glycob/cwt097

Machado, F. S., Jelicks, L. A., Kirchhoff, L. V., Shirani, J., Nagajyothi, F., Mukherjee, S., et al. (2012). Chagas heart disease: report on recent developments. *Cardiol. Rev.* 20, 53–65. doi: 10.1097/CRD.0b013e31823efde2

Marchiori, M. F., Riul, T. B., Oliveira Bortot, L., Andrade, P., Junqueira, G. G., Foca, G., et al. (2017). Binding of triazole-linked galactosyl arylsulfonamides

to galectin-3 affects *Trypanosoma cruzi* cell invasion. *Bioorg. Med. Chem.* 25, 6049–6059. doi: 10.1016/j.bmc.2017.09.042

Marin-Neto, J. A., Cunha-Neto, E., Maciel, B. C., and Simões, M. V. (2007). Pathogenesis of chronic Chagas heart disease. *Circulation* 115:1109. doi: 10.1161/CIRCULATIONAHA.106.624296

Medei, E., Pedrosa, R. C., Benchimol Barbosa, P. R., Costa, P. C., Hernández, C. C., Chaves, E. A., et al. (2007). Human antibodies with muscarinic activity modulate ventricular repolarization: basis for electrical disturbance. *Int. J. Cardiol.* 115, 373–380. doi: 10.1016/j.ijcard.2006.03.022

Mendez-Huergo, S. P., Hockl, P. F., Stupirski, J. C., Maller, S. M., Morosi, L. G., Pinto, N. A., et al. (2018). Clinical relevance of galectin-1 and galectin-3 in rheumatoid arthritis patients: differential regulation and correlation with disease activity. *Front. Immunol.* 2019:3057. doi: 10.3389/fimmu.2018.03057

Montiel, J. L., Monsiváis-Urenda, A., Figueroa-Vega, N., Moctezuma, J. F., Burgos-Vargas, R., González-Amaro, R., et al. (2010). Anti-CD43 and anti-galectin-1 autoantibodies in patients with systemic lupus erythematosus. *Scand. J. Rheumatol.* 39, 50–57. doi: 10.3109/03009740903013213

Moody, T. N., Ochieng, J., and Villalta, F. (2000). Novel mechanism that *Trypanosoma cruzi* uses to adhere to the extracellular matrix mediated by human galectin-3. *FEBS Lett.* 470, 305–308.

Nde, P. N., Lima, M. F., Johnson, C. A., Pratap, S., and Villalta, F. (2012). Regulation and use of the extracellular matrix by *Trypanosoma cruzi* during early infection. *Front. Immunol.* 3:337. doi: 10.3389/fimmu.2012.00337

Nita-Lazar, M., Banerjee, A., Feng, C., and Vasta, G. R. (2015). Galectins regulate the inflammatory response in airway epithelial cells exposed to microbial neuraminidase by modulating the expression of SOCS1 and RIG1. *Mol. Immunol.* 68, 194–202. doi: 10.1016/j.molimm.2015.08.005

Noireau, F., Diosque, P., and Jansen, A. M. (2009). *Trypanosoma cruzi*: adaptation to its vectors and its hosts. *Vet. Res.* 40:26. doi: 10.1051/vetres/2009009

Paz, I., Sachse, M., Dupont, N., Mounier, J., Cederfur, C., Enninga, J., et al. (2010). Galectin-3, a marker for vacuole lysis by invasive pathogens. *Cell Microbiol.* 12, 530–544. doi: 10.1111/j.1462-5822.2009.01415.x

Pineda, M., Corvo, L., Callejas-Hernández, F., Fresno, M., and Bonay, P. (2020). *Trypanosoma cruzi* cleaves galectin-3 N-terminal domain to suppress its innate microbicidal activity. *Clin. Exp. Immunol.* 199, 216–229. doi: 10.1111/cei.13379

Pineda, M. A., Corvo, L., Soto, M., Fresno, M., and Bonay, P. (2015a). Interactions of human galectins with *Trypanosoma cruzi*: binding profile correlate with genetic clustering of lineages. *Glycobiology* 25, 197–210. doi: 10.1093/glycob/cwu103

Pineda, M. A., Cuervo, H., Fresno, M., Soto, M., and Bonay, P. (2015b). Lack of Galectin-3 prevents cardiac fibrosis and effective immune responses in a murine model of *Trypanosoma cruzi* infection. *J. Infect. Dis.* 212, 1160–1171. doi: 10.1093/infdis/jiv185

Pinto, A. Y., Valente, S. A., Valente, Vda C, Ferreira Junior, A. G., and Coura, J. R. (2008). Fase aguda da doença de Chagas na Amazônia brasileira. Estudo de 233 casos do Pará, Amapá e Maranhão observados entre 1988 e 2005. *Rev. Soc. Bras. Med. Trop.* 41, 602–614. doi: 10.1590/s0037-86822008000600011

Poncini, C. V., Alba Soto, C. D., Batalla, E., Solana, M. E., and González Cappa, S. M. (2008). *Trypanosoma cruzi* induces regulatory dendritic cells *in vitro*. *Infect. Immun.* 76, 2633–2641. doi: 10.1128/IAI.01298-07

Poncini, C. V., Ilarregui, J. M., Batalla, E. I., Engels, S., Cerliani, J. P., Cucher, M. A., et al. (2015). *Trypanosoma cruzi* infection imparts a regulatory program in dendritic cells and T cells *via* galectin-1-dependent mechanisms. *J. Immunol.* 195, 3311–3324. doi: 10.4049/jimmunol.1403019

Punukollu, G., Gowda, R., Khan, I., Navarro, V. S., and Vasavada, B. (2007). Clinical aspects of the Chagas' heart disease. *Int. J. Cardiol.* 115, 279–283. doi: 10.1016/j.ijcard.2006.03.004

Rabinovich, G. A., and Conejo-García, J. R. (2016). Shaping the immune landscape in cancer by galectin-driven regulatory pathways. *J. Mol. Biol.* 428, 3266–3281. doi: 10.1016/j.jmb.2016.03.021

Rabinovich, G. A., and Croci, D. O. (2012). Regulatory circuits mediated by lectin-glycan interactions in autoimmunity and cancer. *Immunity* 36, 322–335. doi: 10.1016/j.immuni.2012.03.004

Rabinovich, G. A., Daly, G., Dreja, H., Tailor, H., Riera, C. M., Hirabayashi, J., et al. (1999). Recombinant galectin-1 and its genetic delivery suppress collagen-induced arthritis *via* T cell apoptosis. *J. Exp. Med.* 190, 385–398. doi: 10.1084/jem.190.3.385

Rabinovich, G. A., and Toscano, M. A. (2009). Turning 'sweet' on immunity: galectin–glycan interactions in immune tolerance and inflammation. *Nat. Rev. Immunol.* 9, 338–352. doi: 10.1038/nri2536

Rabinovich, G. A., Toscano, M. A., Jackson, S. S., and Vasta, G. R. (2007). Functions of cell surface galectin-glycoprotein lattices. *Curr. Opin. Struct. Biol.* 17, 513–520. doi: 10.1016/j.sbi.2007.09.002

Reignault, L. C., Barrias, E. S., Soares Medeiros, L. C., de Souza, W., and de Carvalho, T. M. (2014). Structures containing galectin-3 are recruited to the parasitophorous vacuole containing *Trypanosoma cruzi* in mouse peritoneal macrophages. *Parasitol. Res.* 113, 2323–2333. doi: 10.1007/s00436-014-3887-8

Ribeiro, C. H., López, N. C., Ramírez, G. A., Valck, C. E., Molina, M. C., Aguilar, L., et al. (2009). *Trypanosoma cruzi* calreticulin: a possible role in Chagas' disease autoimmunity. *Mol. Immunol.* 46, 1092–1099. doi: 10.1016/j.molimm.2008.10.034

Roman, F., das Chagas Xavier, S., Messenger, L. A., Pavan, M. G., Miles, M. A., Jansen, A. M., et al. (2018). Dissecting the phyloepidemiology of *Trypanosoma cruzi* I (TcI) in Brazil by the use of high resolution genetic markers. *PLoS Negl. Trop. Dis.* 12:e0006466. doi: 10.1371/journal.pntd.0006466

Romano, P. S., Cueto, J. A., Casassa, A. F., Vanrell, M. C., Gottlieb, R. A., and Colombo, M. I. (2012). Molecular and cellularmechanisms involved in the *Trypanosoma cruzi*/host cell interplay. *IUBMB Life* 64, 387–396. doi: 10.1002/iub.1019

Rothstein, T. L., Zhong, X., Schram, B. R., Negm, R. S., Donohoe, T. J., Cabral, D. S., et al. (2000). Receptor-specific regulation of B-cell susceptibility to Fas-mediated apoptosis and a novel Fas apoptosis inhibitory molecule. *Immunol. Rev.* 176, 116–133. doi: 10.1034/j.1600-065x.2000.00616.x

Russo, A. J., Vasudevan, S. O., Méndez-Huergo, S. P., Kumari, P., Menoret, A., Duduskar, S., et al. (2021). Intracellular immune sensing promotes inflammation *via* gasdermin D-driven release of a lectin alarmin. *Nat. Immunol.* 22, 154–165. doi: 10.1038/s41590-020-00844-7

Sato, S., Bhaumik, P., St-Pierre, G., and Pelletier, I. (2014). Role of galectin-3 in the initial control of Leishmania infection. *Crit. Rev. Immunol.* 34, 147–175. doi: 10.1615/critrevimmunol.2014010154

Sato, S., St-Pierre, C., Bhaumik, P., and Nieminen, J. (2009). Galectins in innate immunity: dual functions of host soluble beta-galactoside-binding lectins as damage-associated molecular patterns (DAMPs) and as receptors for pathogen-associated molecular patterns (PAMPs). *Immunol. Rev.* 230, 172–187. doi: 10.1111/j.1600-065X.2009.00790.x

Schmunis, G. A. (2007). Epidemiology of Chagas disease in non-endemic countries: the role of international migration. *Mem. Inst. Oswaldo Cruz.* 102(Suppl. 1), 75–85. doi: 10.1590/s0074-02762007005000093

Schmunis, G. A., and Cruz, J. R. (2005). Safety of the blood supply in Latin America. *Clin. Microbiol. Rev.* 18, 12–29. doi: 10.1128/CMR.18.1.12-29.2005

Schnaar, R. L. (2015). Glycans and glycan-binding proteins in immune regulation: a concise introduction to glycobiology for the allergist. *J. Allergy Clin. Immunol.* 135, 609–615. doi: 10.1016/j.jaci.2014.10.057

Seropian, I. M., Cerliani, J. P., Toldo, S., Van Tassell, B. W., Ilarregu, J. M., González, G. E., et al. (2013). Galectin-1 controls cardiac inflammation and ventricular remodeling during acute myocardial infarction. *Am. J. Pathol.* 182, 29–40. doi: 10.1016/j.ajpath.2012.09.022

Silva-Barbosa, S. D., and Savino, W. (2000). The involvement of laminin in anti-myocardial cell autoimmune response in murine chagas disease. *Developmental. Immunol.* 7, 293–301. doi: 10.1155/2000/17424

Silva-Monteiro, E., Reis Lorenzato, L., Kenji Nihei, O., Junqueira, M., Rabinovich, G. A., Hsu, D. K., et al. (2007). Altered expression of galectin-3 induces cortical thymocyte depletion and premature exit of immature thymocytes during *Trypanosoma cruzi* infection. *Am. J. Pathol.* 170, 546–556. doi: 10.2353/ajpath.2007.060389

Smulski, C., Labovsky, V., Levy, G., Hontebeyrie, M., Hoebeke, J., and Levin, M. J. (2006). Structural basis of the cross-reaction between an antibody to the *Trypanosoma cruzi* ribosomal P2 β protein and the human β1-adrenergic receptor. *FASEB J.* 20, 1396–1406. doi: 10.1096/fj.05-5699com

Soares, M. B., Lima, R. S., Souza, B. S., Vasconcelos, J. F., Rocha, L. L., Dos Santos, R. R., et al. (2011). Reversion of gene expression alterations in hearts of mice with chronic chagasic cardiomyopathy after transplantation of bone marrow cells. *Cell Cycle* 10, 1448–1455. doi: 10.4161/cc.10.9.15487

Souza, B. S. F., da Silva, K. N., Silva, D. N., Rocha, V. P. C., Paredes, B. D., Azevedo, C. M., et al. (2017a). Galectin-3 knockdown impairs survival, migration, and immunomodulatory actions of mesenchymal stromal cells in a mouse model

of chagas disease cardiomyopathy. *Stem Cells Int.* 2017:3282656. doi: 10.1155/2017/3282656

Souza, B. S. F., Silva, D. N., Carvalho, R. H., Sampaio, G. L. A., Paredes, B. D., Aragão França, L., et al. (2017b). Association of cardiac galectin-3 expression, myocarditis, and fibrosis in chronic chagas disease cardiomyopathy. *Am. J. Pathol.* 187, 1134–1146. doi: 10.1016/j.ajpath.2017.01.016

Sundblad, V., Morosi, L. G., Geffner, J. R., and Rabinovich, G. A. (2017). Galectin-1: a jack-of-all-trades in the resolution of acute and chronic inflammation. *J. Immunol.* 199, 3721–3730. doi: 10.4049/jimmunol.1701172

Tanowitz, H. B., Machado, F. S., Jelicks, L. A., Shirani, J., de Carvalho, A. C., Spray, D. C., et al. (2009). Perspectives on *Trypanosoma cruzi*-induced heart disease (Chagas disease). *Prog. Cardiovasc. Dis.* 51, 524–539. doi: 10.1016/j.pcad.2009.02.001

Thiemann, S., and Baum, L. G. (2016). Galectins and immune responses-just how do they do those things they do? *Annu. Rev. Immunol.* 34, 243–264. doi: 10.1146/annurev-immunol-041015-055402

Toscano, M. A., Bianco, G. A., Ilarregui, J. M., Croci, D. O., Correale, J., Hernandez, J. D., et al. (2007). Differential glycosylation of TH1, TH2 and TH-17 effector cells selectively regulates susceptibility to cell death. *Nat. Immunol.* 8, 825–834. doi: 10.1038/ni1482

Toscano, M. A., Commodaro, A. G., Ilarregui, J. M., Bianco, G. A., Liberman, A., Serra, H. M., et al. (2006). Galectin-1 suppresses autoimmune retinal disease by promoting concomitant Th2 and T regulatory-mediated anti-inflammatory responses. *J. Immunol.* 176, 6323–6332. doi: 10.4049/jimmunol.176.10.6323

Toscano, M. A., Martínez Allo, V. C., Cutine, A. M., Rabinovich, G. A., and Mariño, K. V. (2018). Untangling galectin-driven regulatory circuits in autoimmune inflammation. *Trends Mol. Med.* 24, 348–363.

Toscano, M. A., Tongren, J. E., de Souza, J. B., Liu, F. T., Riley, E. M., and Rabinovich, G. A. (2012). Endogenous galectin-3 controls experimental malaria in a species-specific manner. *Parasite Immunol.* 34, 383–387. doi: 10.1111/j.1365-3024.2012.01366.x

Turner, C. W., Lima, M. F., and Villalta, F. (2002). *Trypanosoma cruzi* uses a 45-kDa mucin for adhesion to mammalian cells. *Biochem. Biophys. Res. Commun.* 290, 29–34. doi: 10.1006/bbrc.2001.6189

Tyler, K. M., and Engman, D. M. (2001). The lifecycle of *Trypanosoma cruzi* revisited. *Int. J. Parasitol.* 31, 472–481. doi: 10.1016/s0020-7519(01)00153-9

Van Kooyk, Y., and Rabinovich, G. A. (2008). Protein-glycan interactions in the control of innate and adaptative immune responses. *Nat. Immunol.* 9, 593–601. doi: 10.1038/ni.f.203

Van Overtvelt, L., Vanderheyde, N., Verhasselt, V., Ismaili, J., De Vos, L., Goldman, M., et al. (1999). *Trypanosoma cruzi* infects human dendritic cells and prevents their maturation: inhibition of cytokines, HLA-DR, and costimulatory molecules. *Infect. Immun.* 67, 4033–4040. doi: 10.1128/IAI.67.8.4033-4040.1999

Vandekerckhove, F., Schenkman, S., Pontes de Carvalho, L., Tomlinson, S., Kiso, M., Yoshida, M., et al. (1992). Substrate specificity of the *Trypanosoma cruzi* trans-sialidase. *Glycobiology* 2, 541–548. doi: 10.1093/glycob/2.6.541

Vasconcelos, J. F., Souza, B. S., Lins, T. F., Garcia, L. M., Kaneto, C. M., Sampaio, G. P., et al. (2013). Administration of granulocyte colony-stimulating factor induces immunomodulation, recruitment of T regulatory cells, reduction of myocarditis and decrease of parasite load in a mouse model of chronic Chagas disease cardiomyopathy. *FASEB J.* 27, 4691–4702.

Vasta, G. R. (2009). Roles of galectins in infection. *Nat. Rev. Microbiol.* 7, 424–438. doi: 10.1038/nrmicro2146

Vasta, G. R. (2012). Galectins as pattern recognition receptors: structure, function, and evolution. *Adv. Exp. Med. Biol.* 946, 21–36. doi: 10.1007/978-1-4614-0106-3_2

Vasta, G. R. (2020). "Galectins in host–pathogen interactions: structural, functional and evolutionary aspects," in *Lectin in Host Defense Against Microbial Infections. Advances in Experimental Medicine and Biology*, Vol. 1204, ed. S. L. Hsieh (Berlin: Springer).

Villalta, F., Madison, M. N., Kleshchenko, Y. Y., Nde, P. N., and Lima, M. F. (2008). Molecular analysis of early host cell infection by *Trypanosoma cruzi*. *Front. Biosci.* 13:3714–3734. doi: 10.2741/2961

Viotti, R., Alarcón de Noya, B., Araujo-Jorge, T., Grijalva, M. J., Guhl, F., López, M. C., et al. (2014). Towards a paradigm shift in the treatment of chronic Chagas disease. *Antimicrob. Agents Chemother.* 58, 635–639. doi: 10.1128/AAC.01662-13

Vray, B., Camby, I., Vercruysse, V., Mijatovic, T., Bovin, N. V., Ricciardi-Castagnoli, P., et al. (2004). Up-regulation of galectin-3 and its ligands by *Trypanosoma cruzi* infection with modulation of adhesion and migration of murine dendritic cells. *Glycobiology* 14, 647–657. doi: 10.1093/glycob/cwh068

Waghabi, M. C., Keramidas, M., Bailly, S., Degrave, W., Mendonça-Lima, L., Soeiro Mde, N., et al. (2005). Uptake of host cell transforming growth factor-beta by *Trypanosoma cruzi* amastigotes in cardiomyocytes: potential role in parasite cycle completion. *Am. J. Pathol.* 167, 993–1003. doi: 10.1016/s0002-9440(10)61189-3

WHO (2007). *World Health Organization, Report of the Scientific Working Group on Chagas Disease. Buenos Aires, Argentina, 17, 20. 2005, Updated in 2007*. Geneva: WHO.

WHO (2014). *WHO Fact Sheet No 340*. Geneva: WHO.

Wiersma, V. R., de Bruyn, M., Helfrich, W., and Bremer, E. (2013). Therapeutic potential of Galectin-9 in human disease. *Med. Res. Rev.* 33(Suppl. 1), E102–E126. doi: 10.1002/med.20249

Xibillé-Friedmann, D., Bustos Rivera-Bahena, C., Rojas-Serrano, J., Burgos-Vargas, R., and Montiel-Hernández, J. L. (2013). A decrease in galectin-1 (Gal-1) levels correlates with an increase in anti-Gal-1 antibodies at the synovial level in patients with rheumatoid arthritis. *Scand. J. Rheumatol.* 42, 102–107. doi: 10.3109/03009742.2012.725769

Xue, J., Fu, C., Cong, Z., Peng, L., Peng, Z., Chen, T., et al. (2017). Galectin-3 promotes caspase-independent cell death of HIV-1-infected macrophages. *FEBS J.* 284, 97–113. doi: 10.1111/febs.13955

Yoshida, N. (2006). Molecular basis of mammalian cell invasion by *Trypanosoma cruzi*. *Ann. Acad. Bras. Ciênc.* 78, 87–111. doi: 10.1590/s0001-37652006000100010

Zingales, B., Andrade, S. G., Briones, M. R. S., Campbell, D. A., Chirai, E., Fernandes, O., et al. (2009). A new consensus for *Trypanosoma cruzi* intraspecific nomenclature: second revision meeting recommends TcI to TcVI. *Mem. Inst. Oswaldo. Cruz Rio Janeiro* 104, 1051–1054. doi: 10.1590/s0074-02762009000700021

Zingales, B., Miles, M. A., Campbell, D. A., Tibayrenc, M., Macedo, A. M., Teixeira, M. M., et al. (2012). The revised *Trypanosoma cruzi* subspecific nomenclature: rationale, epidemiological relevance and research applications. *Infect. Genet. Evol.* 12, 240–253. doi: 10.1016/j.meegid.2011.12.009

Zúñiga, E., Rabinovich, G. A., Iglesias, M. M., and Gruppi, A. (2001a). Regulated expression of galectin-1 during B-cell activation and implications for T-cell apoptosis. *J. Leukoc. Biol.* 70, 73–79. doi: 10.1189/jlb.70.1.73

Zúñiga, E., Gruppi, A., Hirabayashi, J., Kasai, K. I., and Rabinovich, G. A. (2001b). Regulated expression and effect of galectin-1 on *Trypanosoma cruzi*-infected macrophages: modulation of microbicidal activity and survival. *Infect. Immun.* 69, 6804–6812. doi: 10.1128/IAI.69.11.6804-6812.2001

Conflict of Interest: The authors declare that the research was conducted in the absence of any commercial or financial relationships that could be construed as a potential conflict of interest.

The handling editor declared a past co-authorship with one of the authors GR.

Publisher's Note: All claims expressed in this article are solely those of the authors and do not necessarily represent those of their affiliated organizations, or those of the publisher, the editors and the reviewers. Any product that may be evaluated in this article, or claim that may be made by its manufacturer, is not guaranteed or endorsed by the publisher.

frontiers in Microbiology

REVIEW
published: 04 January 2022
doi: 10.3389/fmicb.2021.767038

In vitro Models of the Small Intestine for Studying Intestinal Diseases

Sang-Myung Jung[1] *and Seonghun Kim*[1,2]*

[1]*Jeonbuk Branch Institute, Korea Research Institute of Bioscience and Biotechnology (KRIBB), Jeongeup, South Korea,* [2]*Department of Biosystems and Bioengineering, KRIBB School of Biotechnology, University of Science and Technology (UST), Daejeon, South Korea*

The small intestine is a digestive organ that has a complex and dynamic ecosystem, which is vulnerable to the risk of pathogen infections and disorders or imbalances. Many studies have focused attention on intestinal mechanisms, such as host–microbiome interactions and pathways, which are associated with its healthy and diseased conditions. This review highlights the intestine models currently used for simulating such normal and diseased states. We introduce the typical models used to simulate the intestine along with its cell composition, structure, cellular functions, and external environment and review the current state of the art for *in vitro* cell-based models of the small intestine system to replace animal models, including *ex vivo*, 2D culture, organoid, lab-on-a-chip, and 3D culture models. These models are described in terms of their structure, composition, and co-culture availability with microbiomes. Furthermore, we discuss the potential application for the aforementioned techniques to these *in vitro* models. The review concludes with a summary of intestine models from the viewpoint of current techniques as well as their main features, highlighting potential future developments and applications.

Keywords: small intestine, *in vitro* model, *ex vivo* model, 3D culture, disease model, intestinal glycans, host-microbiome interaction

OPEN ACCESS

Edited by:
Gerardo R. Vasta, University of Maryland, Baltimore, United States

Reviewed by:
Rishi Drolia, Purdue University, United States
Wei Long Ng, Nanyang Technological University, Singapore
Michael Super, Harvard University, United States

***Correspondence:**
Seonghun Kim
seonghun@kribb.re.kr

Specialty section:
This article was submitted to Infectious Agents and Disease, a section of the journal Frontiers in Microbiology

Received: *30 August 2021*
Accepted: *07 December 2021*
Published: *04 January 2022*

Citation:
Jung S-M and Kim S (2022) In vitro Models of the Small Intestine for Studying Intestinal Diseases. Front. Microbiol. 12:767038. doi: 10.3389/fmicb.2021.767038

INTRODUCTION

The small intestine is a key part of the digestive system that has critical roles essential for sustaining life. It plays crucial roles in food digestion and nutrient absorption, as well as homeostasis maintenance *via* host–microbe interactions. The small intestine has a long tubular structure of 6 m–7 m in length and an inner diameter of 3 cm–4 cm. The inner side of the small intestine, called the lumen, is an epithelial cell layer whose microstructure consists of villi and the basal crypt. Moreover, the small intestine has a large surface area around 250 m^2; thus, its vast microstructure area enhances the efficient absorption of a wide range of smaller molecules that result from the digestion of macromolecules in the stomach, i.e., amino acids from proteins, sugars from polysaccharides, glycerol, and short-chain fatty acids from lipids, etc. (Biernat et al., 1999; Sokolis and Sassani, 2013). Gut intestines are complex ecosystems under anaerobic conditions that include a variety of microorganisms and are rich in nutrients. Such human gut microbiota are relevant to human health and pathogenesis (Tuddenham and Sears, 2015; Hillman et al., 2017; Shortt et al., 2018).

Gut microbiomes predominantly consist of bacterial genera, including *Faecalibacterium*, *Roseburia*, and *Bifidobacterium*, even though other main groups of microorganisms, such as archaea, fungi, protozoa, and viruses, can be observed (Bédard et al., 2020). These microbiome

consortia can uptake or metabolize exogenous dietary substrates in the gut and convert them into valuable metabolites; notable examples are bile acids, short-chain fatty acids, branched amino acids, trimethylamine N-oxide, tryptophan, and indole derivatives. These microorganisms can also utilize endogenous host compounds, mucins, and other glyco-conjugates derived from gut intestines.

Mucins are O-linked glycan-attached glycoproteins secreted from goblet cells and anchored to the intestinal epithelial layer. Heavily glycosylated mucins have unique properties, such as viscoelasticity. The gel-forming mucin glycan covers the whole intestinal lumen in a thick mucus layer. They mask the host epithelial cell layers and block pathogenic microorganisms that are potentially responsible infection. Thus, these glycan layers protect epithelial cells from harsh gut conditions as well as many infectious microorganisms. On the other hand, these branched glycoconjugates can also facilitate niches for gut microbiomes. Glycoconjugates on the host cell surfaces are used by a variety of pathogenic microorganisms as infectious mediators for attachment and invasion. Furthermore, bacterial glycosidases and glycosyltransferases can modify the host surface glycans, leading to pathogenicity. Therefore, several types of O-glycan-decorated mucins in gut intestines are considered to be cause of glycan-mediated infection resulting from interactions between the host and microbiomes (Ziegler et al., 2016).

Gut microbiota, in both humans and animals; interact directly with the host by the production of a diverse reservoir of metabolites obtained from exogenous or endogenous substances. Examining intestine homeostasis between the gut microbiota and the host immunity is a key factor in assessing the health status of a body. Moreover, the role of gut microbiota in immune homeostasis and autoimmunity has been intensively studied to evaluate the interaction of microbial communities and the host immune system for understanding pathogenesis and related diseases as well as for developing novel immuno- or microbe-based therapies. However, various exogenous/endogenous conditions would be influent to dramatically alter the profiles of microbes and their metabolites, making their impact on host health status change. Therefore, the interactions between the hosts' cells and microbiomes have been studied using *in vitro* and *ex vivo* models instead of animal models. Nowadays, *in vitro* or *ex vivo* intestinal models are established and utilized to evaluate host–microbiome interactions. In this review, we describe the current emerging technologies of *in vitro* and *ex vivo* intestinal models adopted in place of animal intestinal models (**Figure 1**). We also discuss their benefits and the future perspectives for the development of gut-mimetic models for bacteria–gut epithelium interactions.

ROLES AND CHARACTERISTICS OF THE INTESTINE

The gastrointestinal tract (also referred to as the GI tract, GIT, digestive tract, digestion tract, and alimentary canal) extends from the mouth to the anus, with the intestine being the long, continuous tubular organ responsible for digestion and absorption. It mainly comprises the small and large intestine, where each is divided into three parts, according to their main roles and structures, as duodenum, jejunum, and ileum (Lopez et al., 2020).

Starting at the duodenum and ending at the ileum, dietary substrates are digested by enzymes to obtain nutrients. Proteins are digested by trypsin, chymotrypsin, and additional enzymes to obtain amino acids. Fat is emulsified and transformed into micelles by bile salts and lecithin. Most nutrients are absorbed from the small intestine, which has a large surface area, then transferred to blood vessels and delivered to the liver or other organs. Subsequently, undigested and unabsorbed residues are transferred to the large intestine.

As described above, the intestine is an organ designed to digest food and absorb digested residues, including nutrients and moisture. The intestine is the largest organ in the body, almost 6 m–7 m in length in adults, and is tightly packed into the abdominal cavity. The length plays a role in maximizing the residual time for the whole volume of digested residue passing through the intestine to facilitate the complete absorption of nutrients and moisture. Moreover, the intestine is its ripples, consisting of villi and crypts, which maximize the surface area to increase the absorption efficiency in a limited volume. Crypts are the indented parts of the ripples, composed of stem cells and transit amplifying cells, while the villi are the protruding parts, composed of differentiated cells, including enterocytes, goblet cells, and endocrine cells. In addition, the microvilli are high-density, small hair-like cellular structures on the villi, which increase the surface area (Biernat et al., 1999; Sokolis and Sassani, 2013).

The intestine interacts directly or indirectly with gut microbiota, which can metabolize digested substances catalyzed by secreted bacterial enzymes. These intestinal microbiota and their metabolites can influence to host metabolism through the regulation of various cellular mechanisms in the organ (Martin et al., 2019). On the other hand, for the homeostasis and maintenance of intestinal tissue, a defense system is needed to prevent pathogenicity *via* microbial invasion. Harmful external pathogens are primarily sterilized when passing through the stomach. Nevertheless, the intestinal tissue would be still at risk for infection due to potential pathogens present in the gut organs. To overcome risk, intestinal tissues produce self-defensive substances called mucins, glycoproteins, for the defense system against infectious diseases.

Goblet cells sparsely located among enterocytes secret mucus composed of many different molecules, with mucins forming the basic skeleton (Birchenough et al., 2015; Johansson and Hansson, 2016). Mucin consists of a group of transmembrane and gel-forming proteins with high O-glycosylation. The glycosylation consists of O-linked oligosaccharides (glycans), including mainly N-acetylgalactosamine (GalNAc), N-acetylglucosamine (GlcNAc), galactose (Gal), fucose (Fuc), and a terminal sugar sialic acid (Sia). The polypeptide backbones for mucin have a serine or threonine residue and N-acetylgalactosamine attached to the residue for initiating O-linked oligosaccharide elongation. These O-linked glycoconjugates stretch out in high density and have strong viscoelastic properties (**Figure 2**).

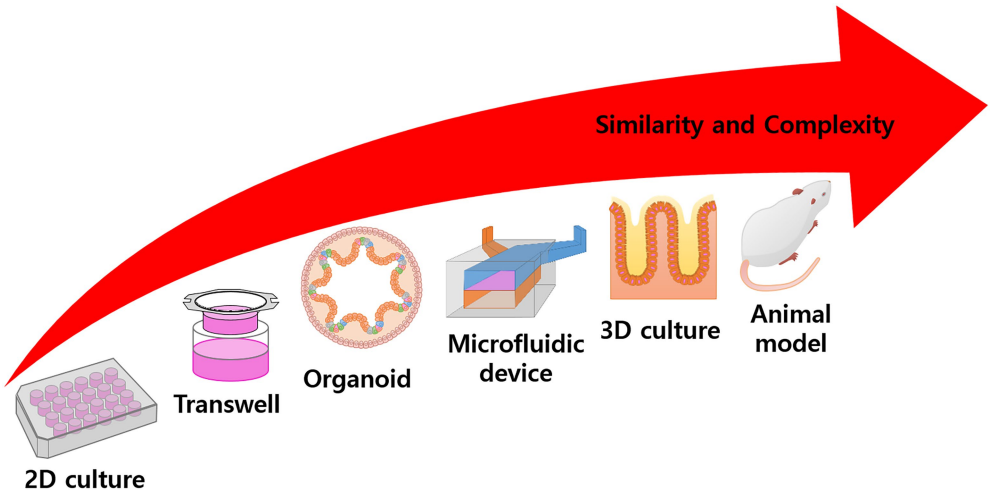

FIGURE 1 | Overall scheme of experimental model. Conventional 2D culturing is rather simple and has high productivity, but application is limited to target treatment experiments. In the Transwell system, the culture area is floated into the media and can simulate mass transfer or other activities. Many models try to simulate specific functions or structures using complex techniques, such as organoid differentiation, microfluidic devices, 3D scaffold fabrication, tissue engineering, etc. In animal models, the body represents a complete model, but there are problems with observation and ethical issues. In general, with increased complexity, the similarity of the model also increases.

Mucin forms a gel-like structure and covers the entire surface of the gastrointestinal tract. More than 20 types of mucins have been observed. Among them, MUC2, MUC5AC, MUC5B, and MUC6 are secreted form for the mucus layer of the intestine. Mucin anchors to the cell surface, is secreted into the lumen, or is taken up through ingestion to sustain its levels and status. Therefore, susceptibility to infection or pathogen invasion depends on the presence of the glycan anchoring site, where pathogens will adhere. Thus, glycans can reduce infection susceptibility by acting as receptor decoys, because they are in contact with but not directly attached to the epithelial tissue. This is one of the main characteristics of the epithelial tissue of the intestine and lung, and the presence of mucin not only secures the robustness of the epithelial tissue but also directly affects the mass transfer (Devine and McKenzie, 1992; Linden et al., 2008; Grondin et al., 2020).

TYPES OF INTESTINE MODELS

In vivo Model

There are several ways in which the intestinal environment status can be altered abnormal for the construction of a disease; this is a physiological approach that is used in conjunction with other methods. While rodent models have been especially important in promoting a mechanistic understanding of human diseases, there are cases where it is scientifically appropriate to use large animals. Various species are used for *in vivo* models, such as murine, other rodents, canids, swine, and monkeys, and each has its own advantageous features as a model (Hugenholtz and de Vos, 2018). Among those species, rodents, especially murine rodents, represent an important species for intestinal modeling, as the human intestine microstructure is almost completed replicated in the rodent intestine, and achieving this degree of replication is difficult using cell cultures.

Even though there are advantages to using animal models, they do not fully simulate the human intestine and there are risks involved. Rodents have similar microbial species to the human intestinal ecosystem, but the proportions of those species are vastly different. For this reason, even though the rodent model is valuable as a primary preclinical model, a direct comparison to the interaction or disease relationships between the intestinal microbiome and intestinal tissues in humans is problematic. The differences between animals and humans are also apparent when considering other aspects; for example, the ecosystem differs between humans and rodents not only in terms of the population but also the composition of the digestive residue, because most digestive residues are used as metabolites of the microbiome and are converted to small molecules or bioactive molecules, such as short-chain fatty acids, glycerol, etc. Therefore, direct comparisons between humans and animal models are not necessarily valid, and an alternative model that can effectively control these factors is required (Xiao et al., 2015; Hugenholtz and de Vos, 2018).

The animal model is a traditional and conventional platform that is used when biological data are needed from specific organs in complex environments. As a model, it has a complete network and structure; however, methods for preparing animal models require more concentration and a longer preparatory period than for *in vitro* models is required to complete and maintain a specific status prior to experiments, as mentioned above.

Models of the intestine are essential for research on enteric pathogens. The mechanism of interaction between foodborne pathogens, mammalian hosts, and intestinal microflora remain

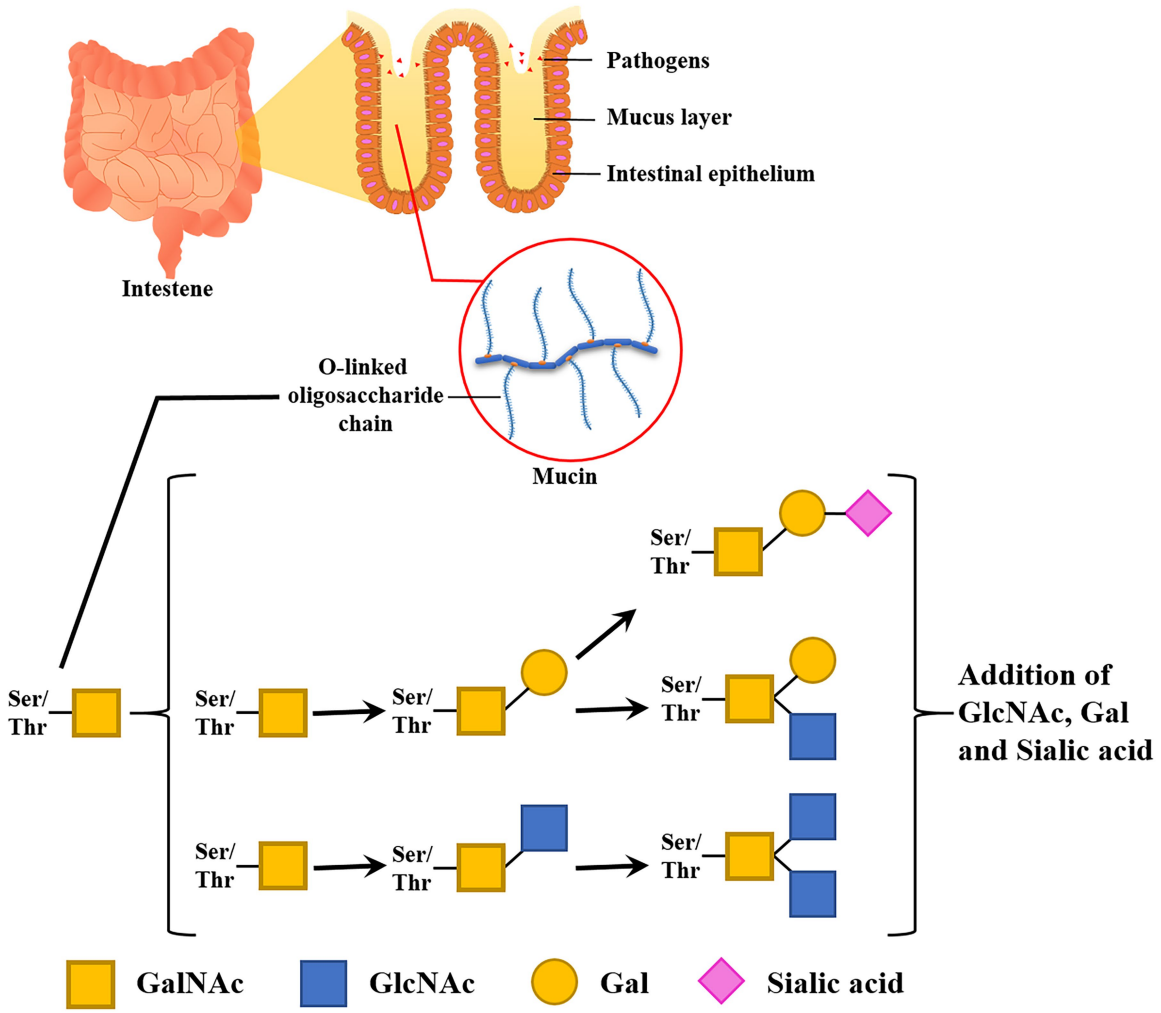

FIGURE 2 | Functions and compositions of intestinal glycan (mucin). A mucus layer covers the intestinal lumen. This thick layer prevents the epithelial cell layer from invading microbes. Glycan entraps pathogens and infectious microbes in its dense O-linked oligosaccharide chain.

largely unknown, including the mechanism of microbial attachment and crosstalk with the host epithelium and the preventive and curative effects of probiotic bacteria.

Various experimental models have been developed for clinical studies and animal models have typically been employed. In those models, germ-free mice were widely used as an *in vivo* model experimental system to understand the underlying mechanisms and estimate human mechanisms.

Although the traditional animal model offers a good standard model for biomedical studies, including studies on cellular signaling pathways, potential drug candidates, and the design of drugs for probiotic healthcare and infectious disease, it has obvious disadvantages. First, the intestines of animals cannot completely mimic the human intestine. For example, Cao et al. (2006) found that a rat model could not completely simulate the drug metabolism and oral bioavailability of humans based on differences in the underlying molecular mechanisms (Stappaerts et al., 2015). Large deviations were observed in the animal models, and it was challenging to reproduce the obtained results. Therefore, it was difficult to determine the relevance of clinical data and any physiological results in the host (Clancy, 2003; Suntharalingam et al., 2006).

There is also criticism among scientists that mechanistic approaches between animal and human models are insufficient. Not only are there differences in metabolism, but physiological differences also occur in incomplete simulations with animal models. For example, some pathogens or viruses only infect certain species or induce symptoms, which is an especially serious limitation for an intestinal model being applied in host–microbiome research. Given these differences, it is not always possible to create a suitable model for the intestinal pathogens and gut environment of humans. The gut microbiome is a complex microbial group, and each species has a unique profile, which applies not only to common and benign microorganisms but also gut pathogens, which can vary in terms of microbiome or species. For example, the gut bacterium *Listeria monocytogenes* cannot infect rodent species, due to metabolic differences between humans and rodents. When

fully simulating *L. monocytogenes* infection, the microbe should mediate cell extrusion of the enterocyte. For cell extrusion, the adherens junction of the enterocyte is targeted by *L. monocytogenes*, with InlA/E-cadherin playing a role in *L. monocytogenes* transcytosis. However, the interaction between InlA and E-cadherin of the non-permissive hosts (i.e., mouse and rat) is not sufficient to simulate the interaction in humans, which is a kind of permissive hosts. It would be necessary to modify transgenic mice with humanized InlA to fully simulate listeriosis in humans including InlA-mediated transcytosis or translocation (Drolia et al., 2018; Drolia and Bhunia, 2019). Therefore, rodent intestinal models are not suitable for studying the infection of listeriosis fully, which is a serious infectious disease in humans. Even though there is another model using oral infection of mice and it showed that *L. monocytogenes* expressing murinized InlA (InlAm) with a high affinity for E-cadherin, but it excludes InlA-mediated transcytosis or translocation. It is a weakness of animal model that it needs additional modifications, and verifications to replace humans. Additionally, in many cases, these animal models show a part of whole mechanisms. In this sense, an organism is an aggregate of complex networks and systems and, if even a single phenomenon occurs differently, it is hard to predict the result and analyze it mechanistically using other species. Indeed, many studies have identified several biological responses that are specific to humans and cannot be simulated in models of other animal (Shanks et al., 2009).

Further, it is expensive and time-consuming to obtain reliable results regarding human responses and physiology using *in vivo* models from other animals. For the development of *in vivo* models, sufficient space and many facilities and materials are needed for breeding experimental animals. An animal is a complete organism with complex networks and systems that maintains its own homeostasis. For this reason, it is impossible to induce an immediate change in its condition for experiments. Ideally, the animal's condition is gradually changed, and limited methods are available for this, which typically involve diet regulation and compound injection over time to finalize a specific animal model. The intestine, in particular, is the organ with the most complex ecosystem and is directly affected by diet. Another method is to use transgenic animal models, but few verified models exist, and they are usually more expensive than wild-type animals. The swine intestine has remarkably close resemblance to that of humans and the results from this model demonstrate good relatability to human intestine. Based on these advantages, swine models are very widely used and considered high quality; however, the animals are too large and take up too much dedicated time to be used in the laboratory. Finally, there are concerns and debates about animal welfare, and the promotion of animal models is not in accordance with the trend of minimizing animal use for research purposes. With the EU leading, many societies are eager to reduce animal experimentation in all biotechnological industries, such as cosmetics, pharmaceuticals, and healthcare (Lunney, 2007).

To overcome the above problems and enhance experimental availability, various models have been developed, including *ex vivo* and *in vitro* models. With *ex vivo* models, we can transfer the complexity of *in vivo* tissue to the laboratory. Researchers can use the complete intestinal structure and cell composition based on intestinal tissue segments. Human tissue is harder to secure than animal tissue, but the advantage is that the model can fully simulate human intestine *in vivo*, and researchers can make feasible predictions for clinical trials using the results. For example, *ex vivo* models are widely used in pharmacological studies on the transport of drugs across intestinal barriers, gastrointestinal hormones, and metabolism (Ripken and Hendriks, 2015). *In vitro* intestine models could potentially solve the problems of animal models, namely the dissimilarity between humans and animals, the burden as a model for laboratory use and ethical issues. First of all, *in vitro* models have good human predictive power; most *in vitro* intestine models are composed of human cell lines, which mean the model can satisfactorily simulate *in vivo* responses. The mechanistic approaches are sufficient to yield data that support the interpretation of the results for *in vivo* states (Cencic and Langerholc, 2010). In addition, *in vitro* models are easier for researchers to use than animal models. Fewer facilities and less equipment are required for cell cultures and they are well standardized for repeating experiments to get reliable data. They can be developed for ready availability and easy handling in high-throughput testing. This is a strong advantage for a model system in the discovery of drug candidates and pathways of signaling and metabolism.

In vitro Model

As already mentioned, the conventional animal intestine model has a few limitations. First of all, it is hard to achieve homogeneity of experimental units (environments and other requirements) because each individual has congenital characteristics, derived from complex networks and ecosystems of the animal. These networks and ecosystems help to achieve valuable results from preclinical trials; on the other hand, these complex elements are intricately related to each other, making it difficult to focus clearly on the target in the experiment (Lu et al., 2014; Ziegler et al., 2016). Therefore, to ensure data reliability, more replications are required for animal experiments than *in vitro* experiments. In particular, as the intestine has the most complex ecosystem in an animal's body, it is hard to perform direct observation, highlighting the limitations. In addition, the cost, time, and ethical issues of animal experiments are always a concern (Knecht et al., 2020; Pilla and Suchodolski, 2020).

Due to these limitations, there has been demand for the development of *in vitro* models. Cell-based models are in the spotlight as an alternative to animal models based on their numerous advantages, including that they allow target-restricted experimentation, direct observation, and continuous analysis. In the case of general *in vitro* experiments, deviations and noise in the experimental results can be minimized, because researchers design the experiments with only the specific elements they want to check. Such well-controlled and restricted experiments can be used to derive more detailed and accurate research results. The various intestinal models are introduced at **Figure 3** and **Table 1**.

Ex vivo INTESTINE MODEL FOR DIRECT EXPERIMENTATION

The *ex vivo* model is a transitional model between *in vivo* and *in vitro* models. The model consists of whole intestine or specific tissues and a designed culture system to prolong its survival and activity. This model is used to obtain selective advantages from both *in vivo* and *in vitro* models. The advantages from *in vivo* models are that it has full cell type composition; suborgans made up of groups of specific cells (glands, vessels, etc.) and complete tissue structure and ecosystem. Direct observation and simple treatment or stimulation of tissues are the advantages of *in vitro* models. The intestinal tissue has a tubular structure and apical cell layer, so the inner and outer environment can be separately controlled. Researchers can circulate and control the inner fluid and its flow to understand the interaction between tissue and microbiome (Westerhout et al., 2015; Pearce et al., 2018).

However, this model requires high-level techniques for successful culture and prolonged intestinal function. The intestine is exposed to contaminants during the extraction process and many microorganisms, including infectious pathogens, are also contained in the lumen. In the case of an *ex vivo* model using animal tissue, another disadvantage is that there are differences in anatomical structure and physiological conditions, including diet and microbiome, derived from differences among species. The disadvantages complicate the extrapolation of data to humans. In addition, the *ex vivo* model does not avoid ethical issues, because the organs and tissue are extracted from animals (Pearce et al., 2018).

TWO-DIMENSIONAL CULTURE MODEL FOR SIMPLE AND FAST SCREENING

The two-dimensional (2D) model is a basic cell-based model of culturing a single cell or multiple cells on a flat surface. To create an intestinal model, cell lines, typically Caco-2, HT-29, T-84, IEC, and other enterocytes, are generally used to construct an apical epithelial layer, and additional cell lines are used to add specific functions to the model, such as mucus secretion and immune response. The cells are attached at the bottom of the culture vessel, which is then filled with a medium on the cell layer such that it is easy to initiate treatment, i.e., with a molecule and continuously observe the system. In this way, the model is simple and easy to construct and conduct experiment with, so it can be used similarly to a conventional model in screening assays (Simon-Assmann et al., 2007; Smetanová et al., 2011).

However, 2D cultures are not suitable for simulating intestinal structure. The culture surface of the model is usually a flat plastic vessel bottom, so it is hard to change the shape. In addition, this intestinal model can be used only in limited situations for interactions between tissue layers and microorganisms. There is only one vessel for the culture medium, so it is impossible to treat living microorganisms, which have higher growth rates than inoculated animal cells, because microorganisms exhaust the nutrients of the medium and secrete various harmful substances into animal cells, such as proteolytic enzymes, pathogens, etc. For this reason, microorganisms are treated for only a few hours or are inactivated by fixing to prevent overgrowth (Co et al., 2019). This 2D model has a rather simple structure and configuration, so it

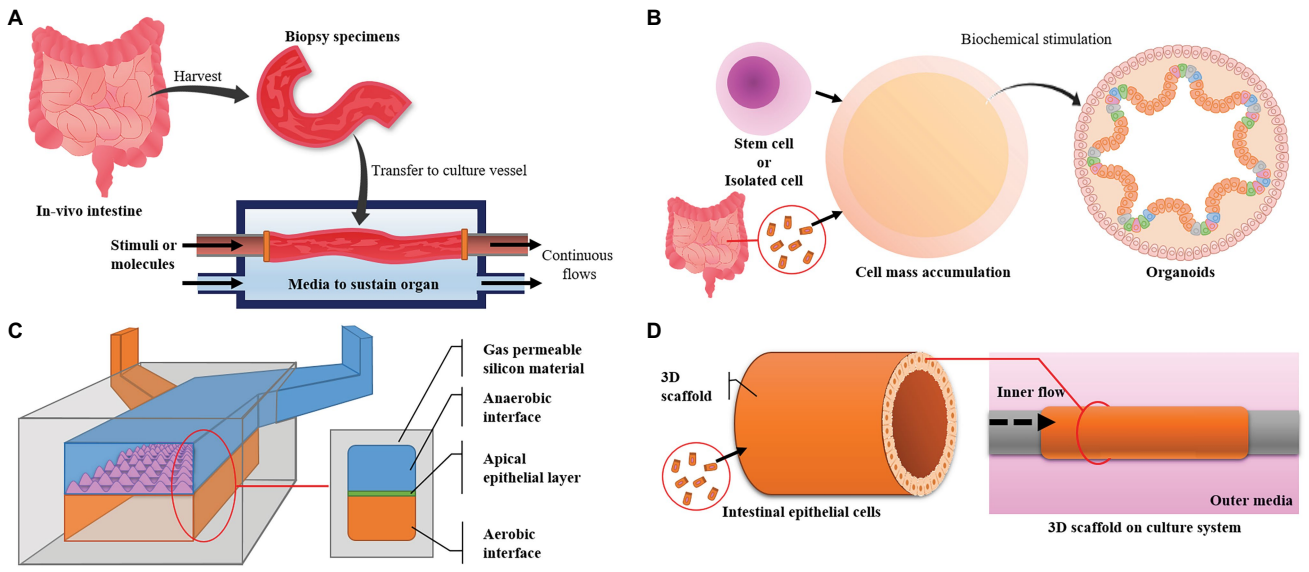

FIGURE 3 | Major intestinal models and their designs. **(A)** The *ex vivo* model uses intestine harvested from experimental animals and maintains its live state. It has high similarity, but the live state is hard to maintain. **(B)** Organoids are derived from pluripotent stem cells or cells harvested from *in vivo* tissue. The model has high similarity in function and cell composition but can only be maintained for a limited time. **(C)** Microfluidic devices can control the environment, are easy to observe and make it easy to focus on targets but have low productivity and a small area for experiments. **(D)** Three-dimensional (3D) cultures can provide large areas for experiments and high productivity but advanced techniques are required to simulate *in vivo* conditions and maintain a high level of uniformity.

TABLE 1 | Types of intestine models and their properties.

Type	Origin	Simulating degree (complexity)	Configuration	Uniformity	Methods	Viability	Applications	Features
Ex vivo	Intestinal tissue from animal	Complete structure, with muscular layer, all component cell types	Epithelial cells, enteroendocrine goblet cells, Paneth cells, blood and lymph vessels, M cells, Peyer's patches, and immune cells	Large deviation among individuals	Intestinal rings, intestinal segments, and everted sac, using system	Under 2 h (over 10 days when using biopsy only)	Regional absorption mechanisms, GI hormone release, and drug transport	Relatively simple, already formed and available for harvest, and hard to maintain
In vitro	Cell line	Low simulation [two-dimensional (2D) culture]	Epithelial cells, immune cells	Low deviation	Cell culture on culture plate	Continuous culture	GI hormone release, transcriptomics, and early immune response	Easy to configure, limited to simulating cell components, structure hard to simulate
3D culture	Cell line	Simulated cell components (co-culture), structure (scaffold), and dimension (size)	Epithelial cells, enteroendocrine goblet cells, and immune cells	Low deviation	Cell culture on Transwell, 3D scaffolds	Continuous culture	Regional absorption mechanisms, transcriptomics, and drug transport	Simulate structure using scaffolds, ability to separate areas
Organoids	Isolated crypt cells, stem cells	Simulated cell components (raw cell from tissue, cell differentiation), parts of lumen and villi	Epithelial cells, enteroendocrine goblet cells, Paneth cells, M cells, Peyer's patches, and immune cells	Large deviation, hard to control	Digested crypt tissue and re-suspension, stem cell differentiation	Continuous culture	GI hormone release, transcriptomics, and early immune response	Requires special skill, simulates detailed structures but not large structures

is easy to use and the model composition can easily be modified, including changing the cell line and medium component. Because of these advantages, *in vitro* 2D models are widely used, and various models have been established and are currently being used to screen the pharmacology and toxicology of new drug candidates.

THREE-DIMENSIONAL CULTURE MODEL WITH TRANSWELL TO SIMULATE *in vivo* STRUCTURE

The Transwell® system is a useful piece of equipment with separate reservoirs for supplying nutrients and treatment substances. The porous membrane housed in the Transwell insert is located in the middle of the culture vessel, and the vessel is divided into two reservoirs by the membrane. Therefore, it is suitable for constructing an apical cell layer such as the intestinal epithelial layer (e.g., intestinal lumen and blood vessel). The Transwell model has the additional advantage of easily simulating the intestinal structure. There is a porous membrane in the Transwell, so cells can be organized into homogeneous layers. From these layers, it is easy to organize models using the Transwell with high standardization, but some characteristics or properties of the original organ or tissue need to be simplified. Typically, it is optimized to construct cellular monolayers and homogeneous environments. However, *in vivo* tissues are composed of three-dimensional (3D) cellular multilayers and exist in heterogeneous or complex environments suitable for each part of the tissue. In general, the Transwell intestine model is used to study mass transfer and barrier functions through cellular layers because it offers the possibility to use on-target screening and construct a high-throughput system by mass production, even if there are some limitations in the representation (Ghaffarian and Muro, 2013; Srinivasan et al., 2015).

To overcome these limitations, the membrane can be modified to mimic the intestinal microstructure (especially crypts and villi). For effective 3D culture on the membrane, several ECM-like substrates (e.g., collagen, hyaluronic acid, hydrogel, or Matrigel®) are often embedded with the cell line to construct the basal cell layer. These substrates are made of a substance composed of a tissue basement layer and have properties that represent multi-cell layers by ensuring area-to-cell dispersion. From the cell dispersion and multi-cell layer formation, cell-to-cell interaction is induced and cellular function is activated in single cells; finally, this helps cells to be organized into tissues and affects the tissue robustness and adaptation to external environments. The basement layer provides an adherent residue to cells and a viscoelastic property to the tissue, finally helping to organize the tissue into a specific structure. If a designed scaffold is used to replace the Transwell membrane, the villus and crypt architecture of the epithelial layer is arranged before cell inoculation, enhancing the level of simulation of the whole model by biofabrication (Sung et al., 2011).

Except for structural development by basal layer construction, the heterogeneous and complex environment is mimicked in a modified model. First, the different kinds of cells to be inoculated are increased in the model. In the simple composition of cells, only those with a single phenotype are inoculated to organize the epithelial layer, such as enterocyte-like Caco-2 or another cell line derived from intestinal epithelium. After this simple model, additional cells are added to enhance the model's degree of simulation. Mucin-secreting cells are a typical additional cell line, such as goblet cells or goblet cell-like cells. The mucin layer is effective in mass transfer tests in the intestinal epithelial model and helps to represent physiological features of *in vivo* intestinal tissue. To more closely mimic cell type diversity, stem cells or precultured organoids are inoculated in the Transwell (Costa and Ahluwalia, 2019).

In order to focus more on physiological and immunological causes, immune cells are used as candidates for additional cell lines. When using the Transwell, immune cells are cultured in a chamber on the side opposite to the apical cell layer. The immune cells, typically dendritic cells, are dispersed into the chamber or cell layer and migrate depending on the immune response. When using this Transwell model, pathogen candidates, microbiome, and various intestinal substrates are treated to assess the susceptibility to infection and stimulation of the immune system. To investigate host–microbe interactions in the advanced model, not only cells of human origin but also microorganisms are used for co-culture in the apical chamber. A semipermeable membrane that mimics the intestinal epithelial layer separates the reservoir, and microbes are inoculated at the apical chamber, thus resulting in an *in vitro* representation of the complex *in vivo* ecosystem.

Apart from cell type diversity, the external environment of the *in vivo* intestine can be simulated by supplying various supplements. ECM components can be supplemented to support the basal layer, such as certain proteoglycans and fibrous proteins (collagen, elastin, fibronectin, and laminin). When stem cells are cultured, growth factors, complements, and small molecules for the niche are supplemented to control differentiation and maturation (Sung et al., 2011). This type of advanced Transwell model was developed to overcome the excessive simplification and reductionism of earlier models, resulting in a more complex system that may recapitulate *in vivo* physiology more accurately but with disadvantages in terms of cost, culturing difficulty and reproducibility.

LAB-ON-A-CHIP FOR SIMULATING INTESTINAL ECOSYSTEM

The purpose of the lab-on-a-chip, a type of microfluidic device, is to simulate the target tissue as closely as possible within a limited area; it was developed to achieve simulation at micro- and nanoscales. The microfluidic device contains a hollow channel less than 1 mm wide with a continuously perfused flow. The microchannel limits the volume to a microliter and supports fine control of the fluid from nano- to microliter scales. With the use of a peristaltic pump, the culture medium is perfused at a constant flow rate into the microwidth channel, forming a laminar flow in the channel, which helps in easily estimating and controlling the fluid hydrodynamics. The microstructure is printed using a fabricated template and a silicon material such as PDMS; it is easy to produce using simple protocols and with secure gas permeability for cell cultures. The cells and media are added in the structure to form a model. It is easy to control the culture environment in the microfluidic device because the volume of the culture is small, and the structure is accordingly designed (Vickerman et al., 2008; Song et al., 2020). In addition, this model can be designed by the researcher using silicon material, i.e., the model has been modified for the advantages of TEER measurement and visualization (Henry et al., 2017).

In the intestine model, this device simulates the intestine microstructure. The channel of the device is used as the lumen of the intestine and the medium flow into the channel is used to represent intestinal flow. This flow rate can be regulated to simulate intestinal flow in the lumen or shear stress on the cell surface located at the intestinal epithelial layer, so the channel can be inhabited by cells arranged to simulate physiological features of a tissue or the whole organ. In the intestinal model developed using a microfluidic device, two chambers are constructed in the device and two air conditions are set in each chamber. In one chamber, intestinal residue is simulated with microorganisms or without microorganisms and just containing metabolites, while, in the other, an environment for animal cells that supplies the proper culture conditions, such as media, gas, etc., is realized. Finally, a cell culture layer is placed between the two chambers to simulate the intestinal structure (Giusti et al., 2014).

Even though there are many advantages, the microfluidic chip is too small and fine and can only deal with a small volume, so it is hard to produce a chip that can be stable and provide fine control during the whole culture period. A microfluidic chip of human intestine has a more complex structure and conditions in terms of intestine-specific microstructure (villi and crypts), so the challenges are more apparent in the model. To overcome these challenges, computer techniques are widely applied in microchip fabrication (e.g., soft lithography) and lumen flow control. This fine control is a typical advantage of the microfluidic chip to manipulate luminal components, such as microbes, nutrients, drugs, or toxins. In response to these challenges, the aim of various studies has been to enhance the complexity of the intestinal simulating microfluidic chip by focusing on the production of mucin, the unidirectional flow, and the cocultivation of mammalian and microbial cells without contamination (Workman et al., 2017; Bein et al., 2018). Accordingly, several designs of the microfluidic chip have been ideated, such as two-channel, *ex-vivo*, multichannel, and gut chip.

Recently, the complexity of microfluidic chips simulating the intestine has increased with the application of tissue engineering techniques. The model has been developed in the direction of including additional neighboring channels for surrounding environments, such as microvessels, immune cells, and pathogenic substrates. In some studies, these subchannels

are used to generate mechanical stress in the cell culture chamber and are applied to mimic peristaltic deformations of the *in vivo* intestine using peristaltic pumps. Recently, Don Ingber's group focused on reproducing intestinal characteristics on a microfluidic chip using the two-channel microfluidic chip, which has two channels parallel to the porous membrane. The intestinal epithelial structure was constructed on the membrane. Based on this model, they developed additional elements, such as the mechanical intensity to applied to the model, cocultivation of mammalian and microbial cells, etc. (Kim et al., 2016).

Based on those studies, the technologies and designs of microfluidic organ-on-a-chip models have undergone dramatic development, making this the most industrialized type of intestinal model. This model is used in scientific discovery, preclinical evaluation, and safety assays. There are many suppliers for these high-simulated microfluidic devices known as microphysiological systems (MPSs). However, many pharmaceutical companies have been worried about the availability and reliability of MPSs compared to conventional proven processes. Recently, there has been a sharp increase in MPS examples, including novel designs and concepts in the literature. Following those studies, companies have been increasing their production of the model slowly but steadily. Among the major suppliers are Emulate, MIMETAS, TissueUse, Wyss, and AIST (Marx et al., 2020).

As mentioned above, the advantages of the microfluidic device are its very high degree of simulation rate and uniformity. Recently, a model was developed to expand on its capabilities with additional functions to mimic the *in vivo* intestine. However, the size of the model is extremely limited, and it is not easy to increase its productivity, so there are limits to its use as an assay model. For these reasons, most of the past microfluidic intestine models had their own standards in individual academic labs, so their results and reliability may be too varied to share and collect as big data. These limitations of the model may be resolved by recently emerged companies that will commercialize the technology through scale-up manufacturing. Nonetheless, trials must be conducted before the microfluidic intestine model becomes a tool commonly used in academic and industrial research laboratories.

ORGANOID

Organoids are cellular aggregates with a spherical shape that include aggregates of stem cells and cell groups with diverse cell types extracted from tissues. Stem cell-derived organoids are formed by embryonic or pluripotent stem cells and construct spheroid-like cell masses. After cell mass formation, various supplements, including complement and signaling molecules for cellular niches, induce the differentiation and maturation of stem cells into intestinal tissues to generate similar tissues. Cell-extracted organoids are recovered from *in vivo* intestinal tissue and single cells are obtained from the tissue through enzymatic digestion. Organoids are formed by inoculating the obtained cells into ECM components, Matrigel®, or a researcher-designed scaffold. The general form of the organoids is a spherical cell mass, and the features of intestinal enterocytes are expressed at the inner wall of the spheroid. An empty space (lumen) is created in the center in a form surrounding the cell layer. The advantage is that intestinal organoids, through self-organization, represent typical features of *in vivo* tissue, such as 3D structures and microstructures. A highly curved epithelium structure is self-organized by crypts and villi, similar to in the *in vivo* intestinal epithelium. Organoids are organized with a central hollow region with a curved structure, similarly to the intestinal lumen. The apex site of a crypt consists of Lgr5+ stem cells and Paneth cells, while the central region of an organoid consists of differentiated cells, not stem cells (Nakamura and Sato, 2017).

The lumen is completely separated from the outside by the cell layer, so it is used to configure and maintain an anaerobic state. At this point, several researchers have constructed an anaerobic state at the lumen and treated microbes by syringe injection to simulate a highly similar intestinal environment (Simian and Bissell, 2017). The advantages of these organoids are that they have high reproducibility of intestinal tissue and can be used to observe interactions with microorganisms, but the model configuration is difficult and the uniformity is poor for repeated experiments, which may cause problems with the reliability of repeated experimental results. In addition, since the size of the cell mass continues to increase according to the culture period of the organoid, there is a limit to how long the structure can be maintained. It is difficult to maintain a constant steady state because the shape and environment change depending on the culture time (Panek et al., 2018). Specifically, self-organization is an advantage of organoids, but quality cannot be controlled by the organoids since they are always organized heterogeneously in terms of shape.

Furthermore, because each organoid forms a closed lumen when cultured within the surrounding ECM gel and the cellular layer of the organoid and the surrounding gel intersects, it can be difficult to sample or manipulate the experimental components (e.g., microbes, nutrients, drugs, or toxins) into the internal lumen. Furthermore, it is hard to mimic the *in vivo* biomechanical stress and lumen flow. For these reasons, the structure of the organoid model also significantly limits its availability to study many critical intestinal functions (e.g., mass transfer, absorption, drug metabolism, or microbiome interaction). Despite these disadvantages and limitations, organoids show fast growth in applications spanning from assays to regenerative medicine. The potential of structural self-organization and cell differentiation make the model available as a "mini-gut," and attempts have been made to engraft them in mice for testing.

THREE-DIMENSIONAL INTESTINE MODELS IN TISSUE ENGINEERING

The models mentioned above simulate the intestinal ecosystem and particular tissue structure. The models are limited in size to increase the simulation degree, so they have disadvantages in terms of narrow observation and producibility. To overcome these disadvantages, typical features of the *in vivo* intestine are selected for simulation in the tissue-engineered model,

namely microstructure, whole structure, and lumen environments. First, the structure is simulated using a tubular scaffold, microstructure is added using additional scaffold or basement substances (collagen and hyaluronic acid). During construction of the cell layer on the scaffold, the lumen environments are controlled by lumen fluid and gas concentration, among other parameters. In this regard, research is being conducted to construct a model in the form of artificial tissue by fabricating a tubular scaffold. For example, in one study, a group constructed a tube with an inner diameter of 2 mm based on silk proteins and inoculated cells with culturing for up to 8 weeks (Yin et al., 2016). Additionally, various techniques for scaffold fabrication are being developed, such as 3D printing, and many researchers are designing their own tubular culture product by applying several materials and structures.

The advantage of this type of model is that it is easy to create and maintain an anaerobic environment on the lumen side because it the culture environment on the inside can be separated from the outside of the tube using the intestine structure itself. In addition, compared to other models (microfluidic chip and organoid), it can provide high productivity with reproducibility, a larger tissue area, and a longer culture period, successfully maintaining tissue structure. In addition, it is possible to simulate the flow in the gut along the tube, so it could be used in new experiments or even transplants.

For example, studies indicate and demonstrate various perspectives on the tissue-engineered model at various scales. A 3D porous silk protein scaffold, including an engineered hollow lumen structure, was constructed (Chen et al., 2015). The hollow lumen of the 3D scaffold was a secure region to inoculate Caco-2 and HT29-MTX cells. At the same time, primary human intestinal myofibroblasts (H-InMyoFibs) were cultured in the porous bulk space, which was embedded in collagen gel. This culture product, including scaffold and cells, induced typical physiological responses based on the tubular architecture and derived features, with a low oxygen level in the lumen. The results showed secretion and accumulation of mucous substrates on the apical epithelium of the lumen, enabling the *in vitro* model to mimic the interaction with the gut microbiome. Moreover, this 3D model demonstrated its robustness in allowing the tissue structure, activity, and cellular phenotype to be maintained over several months.

In other studies, PLGA scaffolds were utilized by Costello et al. (2014) and a novel designed tubular scaffold was used by Shaffiey et al. (2016) to evaluate the activity of intestine-derived cells, such as cellular growth and differentiation. Recently, researchers expanded the scope to test cellular responses *in vitro* and *in vivo* using intestinal stem cells (with engraftment in animal models). They reported that cells differentiated from scaffolds into crypt–villus structures, and their colonization was enhanced by co-culture with myofibroblasts, macrophages, and the gut microbiome. Remarkably, the implanted scaffolds enhanced mucosal regeneration *in vivo*.

Despite these advantages, there are a few disadvantages. It is difficult to proceed with a complete culture and it is almost impossible to observe the culture directly using a microscope due to the thick layer. Similar to a microfluidic chip, the model requires dedicated equipment. Moreover, the model size and area are larger than those of conventional cultures, so there are some difficulties in simulating and representing the intestinal microstructure uniformly throughout the entire culture product. The tissue model usually simulates the dimension of the intestinal cell layer to a high degree, so it requires a thick and dense cell layer. Due to this complexity, adding the surrounding environments of *in vivo* tissue can be relatively difficult compared to other models, such as microvessels, immune cells etc. In addition, when microorganism co-cultures are processed, they could possibly play a role in confining the lumen from external air. Therefore, the required culture period is longer than that of simple cell culture. Nevertheless, while the disadvantages limit expansion of this technique, it is also suitable for studying or mimicking dynamic intestinal tissue with gut microbiome.

DEVELOPMENT OF DISEASE MODELS FROM *in vitro* MODELS

The intestine is characterized by having the most complex ecosystem and dynamic environmental changes of all other organs in the body. Nutrients and substrates are primarily supplied, and their amounts are always dramatically changing. Therefore, the ecosystem does not maintain a steady state, and it is possible that events such as diarrhea, inflammatory bowel disease, and infectious diseases occur. Such symptoms are quite common, but they can become serious and painful (Maloy and Powrie, 2011). For a long time, researchers have tried to address those problems and design rational disease models for effective experiments.

Of the various diseases, one major target of disease modeling is inflammatory bowel disease, which occurs as a result of disrupted homeostasis and inflammation. Bacterial or viral infection of the digestive tract is known to be an initial trigger of this disease (De Hertogh et al., 2008). An infection of the digestive tract directly interacts with the mucus layer; therefore, the mucus layer, as a factor in model simulations of inflammatory bowel disease or other infectious diseases, is more important here than the ordinary intestinal model. Animal models have usually been constructed and used to study intestinal diseases. For the construction of such models (Dosh et al., 2019), there are various methods for causing defects in the mucus layer of animal intestine, including chemical treatment, mucin-related gene defection, specific disruption of intestinal epithelial cells, and immune cell deformation (**Table 2**).

However, these methods also have limitations, including in terms of their reproducibility, observation scope, cost, and level of experimental difficulty. For direct and reliable experiments, a cell culture model with a mucus glycan layer was developed. In the intestinal model, glycan is added to the mucus layer *via* a mucus-secreting cell line [HT29 methotrexate (MTX) cells, LS174T] or goblet cells. For example, HT-29 MTX was cultured with Caco-2 in various ratios (1:9–3:7) or stem cells were differentiated into several intestinal epithelial cell types (enterocytes, goblet cells, and enteroendocrine cells) to mimic the intestinal and colonic mucosa (Dosh et al., 2019). To create

TABLE 2 | Commonly used IBD mouse models.

Categories	Model examples	Prevalent type of response	Details of barrier defect	References
Chemical induction	Dextran sodium sulfate (DSS) colitis	Epithelial damage	Deficiency of Muc2, main gastrointestinal mucin.	Persše and Cerar, 2012; Chassaing et al., 2014
	2,4,6-trinitrobenzene sulfonic acid (TNBS)	Epithelial damage, immune-mediated	Coupled with intestinal proteins eliciting significant immunologic response, such as Th1 inflammatory response.	Loeuillard et al., 2014
	Oxazolone	Epithelial damage, immune-mediated	Direct destruction of colonic mucosa and association with Th2-type inflammatory response.	Heller et al., 2002; Weigmann and Neurath, 2016
Spontaneous mutation	SAMP1/Yit	Immune-mediated	Spontaneous inflammation of terminal ileum and cecum driven by TH1 response and epithelial barrier defect, but TH2 response may develop at later stages of disease.	Pizarro et al., 2011
	C3H/HeJBir	Immune-mediated	Increased B-cell and T-cell reactivity to antigens of enteric bacterial flora causing colitis.	Elson et al., 2000
	Nuclear factor κB (NF-κB) essential modulator (NEMO) colitis	Cytokine release	Reduced paneth cell numbers and increased IEC apoptosis.	Liu et al., 2017
Adoptive T-cell transfer	Systemic T-cell activation	Immune-mediated	Cytokine release (TNF, LIGHT) causing MLCK activation and occludin endocytosis.	Chen and Sundrud, 2016
	CD4 + CD45RBhi	Immune-mediated	CD4+ cells from diseased mice displayed highly polarized Th1 pattern of cytokine synthesis.	Byrne et al., 2005
Genetic engineering	IL-10−/− knockout	Cytokine release, epithelial damage	IL-10 signaling in macrophages and neutrophils is necessary to prevent abnormal regulation of responses to normal microflora.	Scheinin et al., 2003
	FOXP3 mutation	Immune-mediated	Autoimmune enteropathy by excessive T-cell activation.	Bamidele et al., 2018
	Dominant negative N-cadherin transgene expression	Epithelial damage	Defective epithelial maturation, migration, and adherens junctions.	Radice, 2013
	MDR1A-deficient mice	Epithelial damage	Reduced occludin phosphorylation, increased epithelial cell response to LPS.	Wilk et al., 2005
	Constitutively active MLCK transgene expression	Epithelial damage	MLC hyperphosphorylation, barrier dysregulation.	Cunningham and Turner, 2012
	JAM-A-deficient mice	Epithelial damage	Effect on epithelial permeability.	Laukoetter et al., 2007
	Mucin-2-deficient mice	Epithelial damage	Intercellular junction defects, mitochondrial damage, and ATP depletion.	Borisova et al., 2020
Microbiome induction	Enteropathogenic *Escherichia coli* infection	Immune-mediated	Type III secretion (of bacterial proteins), MLCK activation, and occludin endocytosis.	Glotfelty and Hecht, 2012
	Clostridium difficile-induced colitis	Epithelial damage	Actomyosin disruption and glucosylation of Rho proteins, loss of ZO1 and ZO2.	Best et al., 2012
	Enteric microbial transfer to germ-free IL-10−/− mice	Immune-mediated	Resident enteric bacteria are necessary for the development of spontaneous colitis and immune system activation in IL-10-deficient mice.	Keubler et al., 2015

a disease model from an *in vitro* model, various methods are used. One is direct deformation of the mucus layer in the model. Before pathogen treatment, the defensive glycan-rich barrier is removed by a chemical or enzymatic method. Then, researchers can create an obvious disease physiology and observe the interaction and effect of the pathogen in the condition. Another method is to treat with the pathogen over a long time and elicit an inflammatory response from a model with normal physiology and a mucus layer, which can mimic the chronic disease physiology (Zheng et al., 2020).

The simulation degree of this model can be enhanced by increasing the model complexity. In a more complex model, immune cells can be treated, and it is possible to observe immune responses against infectious pathogens. With the use of such a model, immune signaling molecules expressed by infectious stimulation and inflammation were observed. This model can be used effectively to assay the effect of a pathogen or infectious microbe under normal intestinal conditions (Sekirov and Finlay, 2009; Kho and Lal, 2018). The use of gene-modified cells can create a model that more simply simulates congenital disease.

The intestinal culture models introduced in this review for modeling inflammatory or infectious conditions have distinct advantages. First, the cell type (normal cells, transformed cell lines, stem cells, or isolated cells) with the least limitations on physiological conditions can be selected. Many studies have used various cell types for their own purposes. For example, Caco-2 and HT-29 cell lines have been widely used to construct models simulating intestinal layers based on their immortality and accessibility. However, these immortalized cells have

significant differences in their state of differentiation, viability, proliferation, metabolic properties, and immune responses. Consequently, models using immortalized cells may be less representative of the normal colonic epithelium, with high differentiation, which may be a disadvantage in mimicking intestinal disease. To circumvent the disadvantages of the abovementioned models, many studies have shown that a disease model can be organized using cells from biopsy specimens obtained from the intestines of IBD patients. These cells have increased expression of inflammatory cytokines, including IL-1β and TNFα (Yamane and Yamane, 2007).

Second, model cultures are available for direct environmental maintenance and control, such as cellular populations, mucus thickness, etc. Third, the culture conditions allow researchers to create phenotypic and morphologic similarities, including the formation of 3D multilayered epithelial tissue or crypt structures and multi-phenotype cells (enterocytes, goblet cells, or enteroendocrine, and goblet cells). In the latter, *in vitro* models can be modified to inoculate cell types of interest into other systems, for example, immune cells for the immune system or smooth muscle cells and fibroblasts for structural enhancement. Therefore, the complexity of the model can be increased by adding more factors to simulate actual human tissue more closely (Sekirov and Finlay, 2009; Coccia et al., 2012).

Recently, *in vitro* models have experienced rapid development; however, their diversity and specific properties as disease models are insufficient compared to conventional animal disease models that have been developed for a long time. The current intestinal culture models have critical limitations that restrict their application in lab-scale experiments and research. The complex conditions mean that these models cannot easily be used in conventional diagnosis or preclinical trials. The conventional process is already certified by the FDA and is widely used in industries as a suitable high-throughput screening system to search for infectious or therapeutic compounds. It is more difficult than culturing with a simple Transwell or other platforms, so it is emphasized that there may be a need to standardize the model as a novel platform. Several models have bright prospects, with the properties required for an intestinal model, including mucus layer, mucus-secreting cells, and microbe treatment, and further studies are needed to improve their reliability and properties so that they can be used as experimental models after collecting more data and conducting big data analysis to verify their relevance and applicability.

CONCLUSION AND FUTURE PROSPECTS

In the current review, we highlight the structural and functional features of models intended to replace cell-based animal models containing microbiomes and the potential for a disease model derived from infectious inflammation examined with mucin glycan. The gastrointestinal system, which contains the oral cavity–stomach–gut components, is essential for human activity with regard to energy production and complement supply. Because of its importance, homeostasis is tightly regulated, but is surprisingly easy to disrupt, with consequences being diarrhea as well as inflammatory and infectious diseases. For several reasons, food is continuously supplied to the system, whose microbiome is always changing; therefore, pathogens or sources of infection can occasionally invade the system *via* food consumption. The most important underlying reason for this variation is the complexity of the intestinal environment. Even when the same food is supplied, infectious substrates can be produced by microorganisms depending on the conditions in the intestine. The complexity of the intestine is derived from the intestinal tissue and microorganisms. Therefore, it is difficult to construct a rational experimental model, because the structure and environment of the intestine different from those of other tissues. In this context, the model should strike a balance between physiological complexity and experimental simplicity. As a result, from the simplest 2D culture model, various technologies, such as 3D scaffolds, Transwell, microfluidic chips, organoids, and 3D printers, are being used for model construction. With the development of these technologies, the ability to implement physiological complexity in a model that can confirm the interactions between intestinal tissues and microbes is also increasing. Such techniques are applied to create models, with *in vitro* disease models being developed that focus on the glycan-rich layer that protects the tissue from infectious pathogens. The mucin glycan is added to the model by inoculating mucus-secreting cells or differentiating stem cells. In conclusion, novel engineered human intestinal tissue systems that recapitulate normal physiology provide an innovative and attractive approach to modeling inflammatory diseases of the gastrointestinal tract. In future models, a critical issue will be how to ensure uniformity and ease of use while increasing the physiological complexity. Models could provide not only normal physiology but also inflammatory and infectious diseases of the gastrointestinal tract as an attractive approach. Therefore, researchers are focusing on developing a novel platform and standards covering diverse physiological conditions for more reliable data.

AUTHOR CONTRIBUTIONS

S-MJ and SK conceived and designed the review manuscript. S-MJ wrote the manuscript draft. SK evaluated and approved the manuscript. All authors contributed to the article and approved the submitted version.

FUNDING

This work was supported by the basic science research program (NRF-2021R1A2C1005811) to SK, the National Research Council of Science & Technology (NST)-Korea Research Institute of Bioscience and Biotechnology (KRIBB) postdoctoral fellowship program for Young Scientists at KRIBB to S-MJ. It was also partially funded by Korea Institute of Planning and Evaluation for Technology in Food, Agriculture, Forestry and Fisheries (IPET) supported by Ministry of Agriculture, Food and Rural Affairs (1545021966) and KRIBB Research Initiative Program grant.

REFERENCES

Bamidele, A. O., Svingen, P. A., Sagstetter, M. R., Sarmento, O. F., Gonzalez, M., Braga Neto, M. B., et al. (2018). Disruption of FOXP3-EZH2 interaction represents a Pathobiological mechanism in intestinal inflammation. *Cell Mol. Gastroenterol. Hepatol.* 7, 55–71. doi: 10.1016/j.jcmgh.2018.08.009

Bédard, P., Gauvin, S., Ferland, K., Caneparo, C., Pellerin, È., Chabaud, S., et al. (2020). Innovative human three-dimensional tissue-engineered models as an alternative to animal testing. *Bioengineering* 7:115. doi: 10.3390/bioengineering7030115

Bein, A., Shin, W., Jalili-Firoozinezhad, S., Park, M. H., Sontheimer-Phelps, A., Tovaglieri, A., et al. (2018). Microfluidic organ-on-a-Chip models of human intestine. *Cell Mol. Gastroenterol. Hepatol.* 5, 659–668. doi: 10.1016/j.jcmgh.2017.12.010

Best, E. L., Freeman, J., and Wilcox, M. H. (2012). Models for the study of Clostridium difficile infection. *Gut Microbes* 3, 145–167. doi: 10.4161/gmic.19526

Biernat, M., Zabielski, R., Sysa, P., Sosak-Swiderska, B., Le Huërou-Luron, I., and Guilloteau, P. (1999). Small intestinal and pancreatic microstructures are modified by an intraduodenal CCK-A receptor antagonist administration in neonatal calves. *Regul. Pept.* 85, 77–85. doi: 10.1016/s0167-0115(99)00079-8

Birchenough, G., Johansson, M., Gustafsson, J., Bergström, J. H., and Hanssonet, G. C. (2015). New developments in goblet cell mucus secretion and function. *Mucosal Immunol.* 8, 712–719. doi: 10.1038/mi.2015.32

Borisova, M. A., Achasova, K. M., Morozova, K. N., Andreyeva, E. N., Litvinova, E. A., Ogienko, A. A., et al. (2020). Mucin-2 knockout is a model of intercellular junction defects, mitochondrial damage and ATP depletion in the intestinal epithelium. *Sci. Rep.* 10:21135. doi: 10.1038/s41598-020-78141-4

Byrne, F. R., Morony, S., Warmington, K., Geng, Z., Brown, H. L., Flores, S. A., et al. (2005). CD4+CD45RBHi T cell transfer induced colitis in mice is accompanied by osteopenia which is treatable with recombinant human osteoprotegerin. *Gut* 54, 78–86. doi: 10.1136/gut.2003.035113

Cao, X., Gibbs, S. T., Fang, L., Miller, H. A., Landowski, C. P., Shin, H. C., et al. (2006). Why is it challenging to predict intestinal drug absorption and oral bioavailability in human using rat model. *Pharm. Res.* 23, 1675–1686. doi: 10.1007/s11095-006-9041-2

Cencic, A., and Langerholc, T. (2010). Functional cell models of the gut and their applications in food microbiology-a review. *Int. J. Food Microbiol.* 141, S4–S14. doi: 10.1016/j.ijfoodmicro.2010.03.026

Chassaing, B., Aitken, J. D., Malleshappa, M., and Vijay-Kumar, M. (2014). Dextran sulfate sodium (DSS)-induced colitis in mice. *Curr. Protoc. Immunol.* 104, 15.25.1–15.25.14. doi: 10.1002/0471142735.im1525s104

Chen, Y., Lin, Y., Davis, K. M., Wang, Q., Rnjak-Kovacina, J., Li, C., et al. (2015). Robust bioengineered 3D functional human intestinal epithelium. *Sci. Rep.* 5:13708. doi: 10.1038/srep13708

Chen, M. L., and Sundrud, M. S. (2016). Cytokine networks and T-cell subsets in inflammatory bowel diseases. *Inflamm. Bowel Dis.* 22, 1157–1167. doi: 10.1097/MIB.0000000000000714

Clancy, R. (2003). Immunobiotics and the probiotic evolution. *FEMS Immunol. Med. Microbiol.* 38, 9–12. doi: 10.1016/S0928-8244(03)00147-0

Co, J. Y., Margalef-Català, M., Li, X., Mah, A. T., Kuo, C. J., Monack, D. M., et al. (2019). Controlling epithelial polarity: A human enteroid model for host-pathogen interactions. *Cell Rep.* 26, 2509–2520.e4. doi: 10.1016/j.celrep.2019.01.108

Coccia, M., Harrison, O. J., Schiering, C., Asquith, M. J., Becher, B., Powrie, F., et al. (2012). IL-1beta mediates chronic intestinal inflammation by promoting the accumulation of IL-17A secreting innate lymphoid cells and CD4(+) Th17 cells. *J. Exp. Med.* 209, 1595–1609. doi: 10.1084/jem.20111453

Costa, J., and Ahluwalia, A. (2019). Advances and current challenges in intestinal *in vitro* model engineering: a digest. *Front. Bioeng. Biotechnol.* 7:144. doi: 10.3389/fbioe.2019.00144

Costello, C. M., Hongpeng, J., Shaffiey, S., Yu, J., Jain, N. K., Hackam, D., et al. (2014). Synthetic small intestinal scaffolds for improved studies of intestinal differentiation. *Biotechnol. Bioeng.* 111, 1222–1232. doi: 10.1002/bit.25180

Cunningham, K. E., and Turner, J. R. (2012). Myosin light chain kinase: pulling the strings of epithelial tight junction function. *Ann. N. Y. Acad. Sci.* 1258, 34–42. doi: 10.1111/j.1749-6632.2012.06526.x

De Hertogh, G., Aerssens, J., Geboes, K. P., and Geboes, K. (2008). Evidence for the involvement of infectious agents in the pathogenesis of Crohn's disease. *World J. Gastroenterol.* 14, 845–852. doi: 10.3748/wjg.14.845

Devine, P. L., and McKenzie, I. F. C. (1992). Mucins: structure, function, and associations with malignancy. *BioEssays* 14, 619–625. doi: 10.1002/bies.950140909

Dosh, R. H., Jordan-Mahy, N., Sammon, C., and Le Maitre, C. L. (2019). Long-term in vitro 3D hydrogel co-culture model of inflammatory bowel disease. *Sci. Rep.* 9:1812. doi: 10.1038/s41598-019-38524-8

Drolia, R., and Bhunia, A. K. (2019). Crossing the intestinal barrier via listeria adhesion protein and Internalin A. *Trends Microbiol.* 27, 408–425. doi: 10.1016/j.tim.2018.12.007

Drolia, R., Tenguria, S., Durkes, A. C., Turner, J. R., and Bhunia, A. K. (2018). Listeria adhesion protein induces intestinal epithelial barrier dysfunction for bacterial translocation. *Cell Host Microbe* 23, 470–484.e7. doi: 10.1016/j.chom.2018.03.004

Elson, C. O., Cong, Y., and Sundberg, J. (2000). The C3H/HeJBir mouse model: a high susceptibility phenotype for colitis. *Int. Rev. Immunol.* 19, 63–75. doi: 10.3109/08830180009048390

Ghaffarian, R., and Muro, S. (2013). Models and methods to evaluate transport of drug delivery systems across cellular barriers. *J. Vis. Exp.* 80:e50638. doi: 10.3791/50638

Giusti, S., Sbrana, T., La Marca, M., Di Patria, V., Martinucci, V., Tirella, A., et al. (2014). A novel dual-flow bioreactor simulates increased fluorescein permeability in epithelial tissue barriers. *Biotechnol. J.* 9, 1175–1184. doi: 10.1002/biot.201400004

Glotfelty, L. G., and Hecht, G. A. (2012). Enteropathogenic E. coli effectors EspG1/G2 disrupt tight junctions: new roles and mechanisms. *Ann. N. Y. Acad. Sci.* 1258, 149–158. doi: 10.1111/j.1749-6632.2012.06563.x

Grondin, J. A., Kwon, Y. H., Far, P. M., Haq, S., and Khan, W. I. (2020). Mucins in intestinal mucosal defense and inflammation: learning from clinical and experimental studies. *Front. Immunol.* 11:2054. doi: 10.3389/fimmu.2020.02054

Heller, F., Fuss, I. J., Nieuwenhuis, E. E., Blumberg, R. S., and Strober, W. (2002). Oxazolone colitis, a Th2 colitis model resembling ulcerative colitis, is mediated by IL-13-producing NK-T cells. *Immunity* 17, 629–638. doi: 10.1016/s1074-7613(02)00453-3

Henry, O., Villenave, R., Cronce, M. J., Leineweber, W. D., Benz, M. A., and Ingber, D. E. (2017). Organs-on-chips with integrated electrodes for trans-epithelial electrical resistance (TEER) measurements of human epithelial barrier function. *Lab Chip* 17, 2264–2271. doi: 10.1039/c7lc00155j

Hillman, E. T., Lu, H., Yao, T., and Nakatsu, C. H. (2017). Microbial ecology along the gastrointestinal tract. *Microbes Environ.* 32, 300–313. doi: 10.1264/jsme2.ME17017

Hugenholtz, F., and de Vos, W. M. (2018). Mouse models for human intestinal microbiota research: a critical evaluation. *Cell Mol. Life Sci.* 75, 149–160. doi: 10.1007/s00018-017-2693-8

Johansson, M., and Hansson, G. (2016). Immunological aspects of intestinal mucus and mucins. *Nat. Rev. Immunol.* 16, 639–649. doi: 10.1038/nri.2016.88

Keubler, L. M., Buettner, M., Häger, C., and Bleich, A. (2015). A multihit model: colitis lessons from the interleukin-10-deficient mouse. *Inflamm. Bowel Dis.* 21, 1967–1975. doi: 10.1097/MIB.0000000000000468

Kho, Z. Y., and Lal, S. K. (2018). The human gut microbiome—a potential controller of wellness and disease. *Front. Microbiol.* 9:1835. doi: 10.3389/fmicb.2018.01835

Kim, H. J. Li, H., Collins, J. J., and Ingber, D. E. (2016). Contributions of microbiome and mechanical deformation to intestinal bacterial overgrowth and inflammation in a human gut-on-a-chip. *Proc. Natl. Acad. Sci. U. S. A.* 113, E7–E15. doi: 10.1073/pnas.1522193112

Knecht, D., Cholewińska, P., Jankowska-Mąkosa, A., and Czyż, K. (2020). Development of swine's digestive tract microbiota and its relation to production indices-a review. *Animals* 10:527. doi: 10.3390/ani10030527

Laukoetter, M. G., Nava, P., Lee, W. Y., Severson, E. A., Capaldo, C. T., Babbin, B. A., et al. (2007). JAM-A regulates permeability and inflammation in the intestine in vivo. *J. Exp. Med.* 204, 3067–3076. doi: 10.1084/jem.20071416

Linden, S. K., Sutton, P., Karlsson, N. G., Korolik, V., and McGuckin, M. A. (2008). Mucins in the mucosal barrier to infection. *Mucosal Immunol.* 1, 183–197. doi: 10.1038/mi.2008.5

Liu, T., Zhang, L., Joo, D., and Sun, S. C. (2017). NF-κB signaling in inflammation. *Signal Transduct. Target. Ther.* 2:17023. doi: 10.1038/sigtrans.2017.23

Loeuillard, E., Bertrand, J., Herranen, A., Melchior, C., Guérin, C., Coëffier, M., et al. (2014). 2,4,6-trinitrobenzene sulfonic acid-induced chronic colitis with fibrosis and modulation of TGF-β1 signaling. *World J. Gastroenterol.* 20, 18207–18215. doi: 10.3748/wjg.v20.i48.18207

Lopez, P. P., Gogna, S., and Khorasani-Zadeh, A. (2020). "Anatomy, abdomen and pelvis, duodenum," in *StatPearls* (StatPearls Publishing).

Lu, P., Sodhi, C. P., Jia, H., Shaffiey, S., Good, M., Branca, M. F., et al. (2014). Animal models of gastrointestinal and liver diseases. Animal models of necrotizing enterocolitis: pathophysiology, translational relevance, and challenges. *Am. J. Physiol. Gastrointest. Liver Physiol.* 306, G917–G928. doi: 10.1152/ajpgi.00422.2013

Lunney, J. K. (2007). Advances in swine biomedical model genomics. *Int. J. Biol. Sci.* 3, 179–184. doi: 10.7150/ijbs.3.179

Maloy, K., and Powrie, F. (2011). Intestinal homeostasis and its breakdown in inflammatory bowel disease. *Nature* 474, 298–306. doi: 10.1038/nature10208

Martin, A. M., Sun, E. W., Rogers, G. B., and Keating, D. J. (2019). The influence of the gut microbiome on host metabolism through the regulation of gut hormone release. *Front. Physiol.* 10:428. doi: 10.3389/fphys.2019.00428

Marx, U., Akabane, T., Andersson, T. B., Baker, E., Beilmann, M., Beken, S., et al. (2020). Biology-inspired microphysiological systems to advance patient benefit and animal welfare in drug development. *ALTEX* 37, 365–394. doi: 10.14573/altex.2001241

Nakamura, T., and Sato, T. (2017). Advancing intestinal organoid technology toward regenerative medicine. *Cell Mol. Gastroenterol. Hepatol.* 5, 51–60. doi: 10.1016/j.jcmgh.2017.10.006

Panek, M., Grabacka, M., and Pierzchalska, M. (2018). The formation of intestinal organoids in a hanging drop culture. *Cytotechnology* 70, 1085–1095. doi: 10.1007/s10616-018-0194-8

Pearce, S. C., Coia, H. G., Karl, J. P., Pantoja-Feliciano, I. G., Zachos, N. C., and Racicot, K. (2018). Intestinal *in vitro* and *ex vivo* models to study host-microbiome interactions and acute stressors. *Front. Physiol.* 9:1584. doi: 10.3389/fphys.2018.01584

Perše, M., and Cerar, A. (2012). Dextran sodium sulphate colitis mouse model: traps and tricks. *J. Biomed. Biotechnol.* 2012:718617. doi: 10.1155/2012/718617

Pilla, R., and Suchodolski, J. S. (2020). The role of the canine gut microbiome and metabolome in health and gastrointestinal disease. *Front. Vet. Sci.* 6:498. doi: 10.3389/fvets.2019.00498

Pizarro, T. T., Pastorelli, L., Bamias, G., Garg, R. R., Reuter, B. K., Mercado, J. R., et al. (2011). SAMP1/YitFc mouse strain: a spontaneous model of Crohn's disease-like ileitis. *Inflamm. Bowel Dis.* 17, 2566–2584. doi: 10.1002/ibd.21638

Radice, G. L. (2013). N-cadherin-mediated adhesion and signaling from development to disease: lessons from mice. *Prog. Mol. Biol. Transl. Sci.* 116, 263–289. doi: 10.1016/B978-0-12-394311-8.00012-1

Ripken, D., and Hendriks, H. (2015). "Porcine *ex vivo* intestinal segment model," in *The impact of food bioactives on health: in vitro and ex vivo models*. eds. K. Verhoeckx, P. Cotter, I. López-Expósito, C. Kleiveland, T. Lea, A. Mackie et al. (Cham, CH: Springer), 255–262.

Scheinin, T., Butler, D. M., Salway, F., Scallon, B., and Feldmann, M. (2003). Validation of the interleukin-10 knockout mouse model of colitis: antitumour necrosis factor-antibodies suppress the progression of colitis. *Clin. Exp. Immunol.* 133, 38–43. doi: 10.1046/j.1365-2249.2003.02193.x

Sekirov, I., and Finlay, B. B. (2009). The role of the intestinal microbiota in enteric infection. *J. Physiol.* 587, 4159–4167. doi: 10.1113/jphysiol.2009.172742

Shaffiey, S. A., Jia, H., Keane, T., Costello, C., Wasserman, D., Quidgley, M., et al. (2016). Intestinal stem cell growth and differentiation on a tubular scaffold with evaluation in small and large animals. *Regen. Med.* 11, 45–61. doi: 10.2217/rme.15.70

Shanks, N., Greek, R., and Greek, J. (2009). Are animal models predictive for humans? *Philos. Ethics Humanit. Med.* 4:2. doi: 10.1186/1747-5341-4-2

Shortt, C., Hasselwander, O., Meynier, A., Nauta, A., Fernández, E. N., Putz, P., et al. (2018). Systematic review of the effects of the intestinal microbiota on selected nutrients and non-nutrients. *Eur. J. Nutr.* 57, 25–49. doi: 10.1007/s00394-017-1546-4

Simian, M., and Bissell, M. J. (2017). Organoids: A historical perspective of thinking in three dimensions. *Int. J. Cell Biol.* 216, 31–40. doi: 10.1083/jcb.201610056

Simon-Assmann, P., Turck, N., Sidhoum-Jenny, M., Gradwohl, G., and Kedinger, M. (2007). In vitro models of intestinal epithelial cell differentiation. *Cell Biol. Toxicol.* 23, 241–256. doi: 10.1007/s10565-006-0175-0

Smetanová, L., Stětinová, V., Svoboda, Z., and Kvetina, J. (2011). Caco-2 cells, biopharmaceutics classification system (BCS) and biowaiver. *Acta Med. Austriaca* 54, 3–8. doi: 10.14712/18059694.2016.9

Sokolis, D. P., and Sassani, S. G. (2013). Microstructure-based constitutive modeling for the large intestine validated by histological observations. *J. Mech. Behav. Biomed. Mater.* 21, 149–166. doi: 10.1016/j.jmbbm.2013.02.016

Song, K., Li, G., Zu, X., Du, Z., Liu, L., and Hu, Z. (2020). The fabrication and application mechanism of microfluidic systems for high throughput biomedical screening: a review. *Micromachines* 11:297. doi: 10.3390/mi11030297

Srinivasan, B., Kolli, A. R., Esch, M. B., Abaci, H. E., Shuler, M. L., and Hickman, J. J. (2015). TEER measurement techniques for in vitro barrier model systems. *J. Lab. Autom.* 20, 107–126. doi: 10.1177/2211068214561025

Stappaerts, J., Brouwers, J., Annaert, P., and Augustijns, P. (2015). In situ perfusion in rodents to explore intestinal drug absorption: challenges and opportunities. *Int. J. Pharm.* 478, 665–681. doi: 10.1016/j.ijpharm.2014.11.035

Sung, J. H., Yu, J., Luo, D., Shuler, M. L., and March, J. C. (2011). Microscale 3-D hydrogel scaffold for biomimetic gastrointestinal (GI) tract model. *Lab Chip* 11, 389–392. doi: 10.1039/C0LC00273A

Suntharalingam, G., Perry, M. R., Ward, S., Brett, S. J., Castello-Cortes, A., Brunner, M. D., et al. (2006). Cytokine storm in a phase 1 trial of the anti-CD28 monoclonal antibody TGN1412. *N. Engl. J. Med.* 355, 1018–1028. doi: 10.1056/NEJMoa063842

Tuddenham, S., and Sears, C. L. (2015). The intestinal microbiome and health. *Curr. Opin. Infect. Dis.* 28, 464–470. doi: 10.1097/QCO.0000000000000196

Vickerman, V., Blundo, J., Chung, S., and Kamm, R. (2008). Design, fabrication and implementation of a novel multi-parameter control microfluidic platform for three-dimensional cell culture and real-time imaging. *Lab Chip* 8, 1468–1477. doi: 10.1039/b802395f

Weigmann, B., and Neurath, M. F. (2016). Oxazolone-induced colitis as a model of Th2 immune responses in the intestinal mucosa. *Methods Mol. Biol.* 1422, 253–261. doi: 10.1007/978-1-4939-3603-8_23

Westerhout, J., Wortelboer, H., and Verhoeckx, K. (2015). "Using Chamber,," in *The impact of food bioactives on health: in vitro and ex vivo models*. eds. K. Verhoeckx, P. Cotter, I. López-Expósito, C. Kleiveland, T. Lea, A. Mackie et al. (Cham, CH: Springer), 263–268.

Wilk, J. N., Bilsborough, J., and Viney, J. L. (2005). The mdr1a−/− mouse model of spontaneous colitis: a relevant and appropriate animal model to study inflammatory bowel disease. *Immunol. Res.* 31, 151–160. doi: 10.1385/IR:31:2:151

Workman, M. J., Gleeson, J. P., Troisi, E. J., Estrada, H. Q., Kerns, S. J., Hinojosa, C. D., et al. (2017). Enhanced utilization of induced pluripotent stem cell-derived human intestinal Organoids using microengineered chips. *Cell Mol. Gastroenterol. Hepatol.* 5, 669–677.e2. doi: 10.1016/j.jcmgh.2017.12.008

Xiao, L., Feng, Q., Liang, S., Sonne, S. B., Xia, Z., Qiu, X., et al. (2015). A catalog of the mouse gut metagenome. *Nat. Biotechnol.* 33, 1103–1108. doi: 10.1038/nbt.3353

Yamane, M., and Yamane, S. (2007). The induction of colonocyte differentiation in CaCo-2 cells by sodium butyrate causes an increase in glucosylceramide synthesis in order to avoid apoptosis based on ceramide. *Arch. Biochem. Biophys.* 459, 159–168. doi: 10.1016/j.abb.2007.01.008

Yin, X., Mead, B. E., Safaee, H., Langer, R., Karp, J. M., and Levy, O. (2016). Engineering stem cell organoids. *Cell Stem Cell* 18, 25–38. doi: 10.1016/j.stem.2015.12.005

Zheng, D., Liwinski, T., and Elinav, E. (2020). Interaction between microbiota and immunity in health and disease. *Cell Res.* 30, 492–506. doi: 10.1038/s41422-020-0332-7

Ziegler, A., Gonzalez, L., and Blikslager, A. (2016). Large animal models: the key to translational discovery in digestive disease research. *Cell. Mol. Gastroenterol. Hepatol.* 2, 716–724. doi: 10.1016/j.jcmgh.2016.09.003

Conflict of Interest: The authors declare that the research was conducted in the absence of any commercial or financial relationships that could be construed as a potential conflict of interest.

may be evaluated in this article, or claim that may be made by its manufacturer, is not guaranteed or endorsed by the publisher.

frontiers | Frontiers in Microbiology

ORIGINAL RESEARCH
published: 15 April 2022
doi: 10.3389/fmicb.2022.775186

Coronavirus Disease 2019-Related Alterations of Total and Anti-Spike IgG Glycosylation in Relation to Age and Anti-Spike IgG Titer

Christian Schwedler[1,2†], Marta Grzeski[1†], Kai Kappert[1,3], Jörn Rust[4], Guido Heymann[5], Berthold Hoppe[1,5] and Véronique Blanchard[1*]*

[1] Institute of Diagnostic Laboratory Medicine, Clinical Chemistry and Pathobiochemistry, Charité – Universitätsmedizin Berlin, Corporate Member of Freie Universität Berlin, Humboldt-Universität zu Berlin, Berlin, Germany, [2] German Cancer Consortium (DKTK), German Cancer Research Center (DKFZ), Heidelberg, Germany, [3] Labor Berlin – Charité Vivantes GmbH, Berlin, Germany, [4] Department of Anaesthesiology, Critical Care, and Pain Medicine, BG Klinikum Unfallkrankenhaus Berlin, Berlin, Germany, [5] Institute of Laboratory Medicine, BG Klinikum Unfallkrankenhaus Berlin, Berlin, Germany

OPEN ACCESS

Edited by:
Hector Mora Montes,
University of Guanajuato, Mexico

Reviewed by:
Raminta Zmuidinaite,
MAP Sciences Ltd., United Kingdom
Ivan Martinez Duncker,
Universidad Autónoma del Estado de Morelos, Mexico

***Correspondence:**
Christian Schwedler
christian.schwedler@charite.de;
christian.schwedler@outlook.de
Véronique Blanchard
veronique.blanchard@charite.de

† These authors have contributed equally to this work and share first authorship

Specialty section:
This article was submitted to Infectious Agents and Disease, a section of the journal Frontiers in Microbiology

Received: 13 September 2021
Accepted: 02 March 2022
Published: 15 April 2022

Citation:
Schwedler C, Grzeski M, Kappert K, Rust J, Heymann G, Hoppe B and Blanchard V (2022) Coronavirus Disease 2019-Related Alterations of Total and Anti-Spike IgG Glycosylation in Relation to Age and Anti-Spike IgG Titer. Front. Microbiol. 13:775186. doi: 10.3389/fmicb.2022.775186

The coronavirus disease 2019 (COVID-19) caused by the severe acute respiratory syndrome coronavirus-2 (SARS-CoV-2) has been affecting the world since January 2020 and has caused millions of deaths. To gain a better insight into molecular changes underlying the COVID-19 disease, we investigated here the *N*-glycosylation of three immunoglobulin G (IgG) fractions isolated from plasma of 35 severe COVID-19 patients, namely total IgG_1, total IgG_2, and anti-Spike IgG, by means of MALDI-TOF-MS. All analyses were performed at the glycopeptide level to assure subclass- and site-specific information. For each COVID-19 patient, the analyses included three blood withdrawals at different time-points of hospitalization, which allowed profiling longitudinal alterations in IgG glycosylation. The COVID-19 patients presented altered IgG *N*-glycosylation profiles in all investigated IgG fractions. The most pronounced COVID-19-related changes were observed in the glycosylation profiles of antigen-specific anti-Spike IgG_1. Anti-Spike IgG_1 fucosylation and galactosylation showed the strongest variation during the disease course, with the difference in anti-Spike IgG_1 fucosylation being significantly correlated with patients' age. Decreases in anti-Spike IgG_1 galactosylation and sialylation in the course of the disease were found to be significantly correlated with the difference in anti-Spike IgG plasma concentration. The present findings suggest that patients' age and anti-S IgG abundance might influence IgG *N*-glycosylation alterations occurring in COVID-19.

Keywords: IgG glycosylation, *N*-glycopeptides, glycans, Spike, SARS-CoV-2, COVID-19, MALDI-TOF

INTRODUCTION

Coronaviruses have been responsible for three pandemics this century with high mortality although they are usually responsible for only benign colds. The severe acute respiratory syndrome coronavirus (SARS-CoV) and the Middle East respiratory syndrome coronavirus (MERS-CoV) caused nosocomial outbreaks in 2002 and in 2012, respectively, due to a virus transfer from animals to humans (De Wit et al., 2016; Reis et al., 2021). However, in 2019, the severe acute respiratory syndrome coronavirus-2 (SARS-CoV-2) emerged worldwide as the causative agent

of the coronavirus disease 2019 (COVID-19), which can range from a mild disease course to pneumonia requiring hospitalization and to life-threatening multi-organ failure in the most severe cases. So far, around 431 million cases and almost 6 million deaths have been reported worldwide.

Immunoglobulins G (IgG) are the most abundant antibodies present in human blood with concentrations ranging from 7 to 18 mg/ml. Produced by mature plasma cells, they play a crucial role in the regulation of inflammation and immune reactions in humans and animals (Karsten et al., 2012; Hess et al., 2013; Bartsch et al., 2020). In humans, IgG is subdivided into four subclasses named according to their abundance: IgG_1, IgG_2, IgG_3, and IgG_4 (Schur, 1988). Although they share about 90% of amino acid homology, each subclass differs with respect to effector functions and binding affinities toward Fc gamma receptors (FcγRs) (Wang and Ravetch, 2019). Each IgG molecule consists of two parts: fragment antigen binding (Fab) that is sporadically glycosylated and fragment crystallizable (Fc), which is glycosylated at asparagine (Asn) 297 within each heavy chain. IgG glycosylation at Asn297 modulates its interactions with Fcγ receptors (FcγRs). In particular, absence of core-fucosylation was shown to tremendously increase the binding to FcγRIIIa and enhance antibody-dependent cellular cytotoxicity. This principle is used in the production of recombinant monoclonal antibodies by the pharmaceutical industry for anti-cancer therapy (Yu et al., 2017).

IgG glycosylation at Asn297 consists of complex-type biantennary *N*-glycans being highly fucosylated, slightly sialylated and having various degrees of galactosylation (Clerc et al., 2016). IgG glycosylation is age- as well as sex-dependent (Bakovic et al., 2013; Stambuk et al., 2020) and has been widely studied in health and disease. Fucosylation is relatively stable in adulthood and upon aging (Dall'olio et al., 2013; De Haan et al., 2016). On the opposite, sialylation and galactosylation decrease with age (Dall'olio et al., 2013) because their occurrence is related to estrogen regulation both in men and women (Ercan et al., 2017). Moreover, the latter glycosylation features are also gender-dependent: IgG galactosylation and sialylation are higher in pre-menopausal women as compared with men (Bakovic et al., 2013). After menopause, sialylation, and galactosylation levels are similar in men and women (Bakovic et al., 2013). Distinct IgG glycosylation features are also associated with a broad range of inflammatory pathologies. Precisely, IgG glycosylation is modulated during chronic as well as acute inflammation. In rheumatoid arthritis patients, decreased galactosylation was correlated with clinical parameters (Van De Geijn et al., 2009; Schwedler et al., 2018) and with decreased activity of galactosyltransferase in plasma B-cells (Axford et al., 1987). During bacterial and viral infections, decreased IgG galactosylation was observed for hepatitis B and tuberculosis (Pilkington et al., 1995; Ho et al., 2015; Irvine and Alter, 2020).

In COVID-19 patients, however, regulation of glycosylation has not been addressed in detail. Thus, in order to gain a better understanding of IgG glycosylation upon SARS-CoV-2 infection, we studied total IgG and anti-SARS-CoV-2 IgG glycosylation at Asn297 in a cohort of patients hospitalized in Berlin (Germany) during disease course.

MATERIALS AND METHODS

Sample Collection

The study was approved by the Institutional Review Board at Charité – Universitätsmedizin Berlin, Campus Virchow-Klinikum, Germany (no. EA2/095/20) and at the Ärztekammer Berlin, Germany (Eth-23/20). All experiments were performed in accordance with relevant guidelines and regulations. Additional written informed consent was taken for Eth-23/20. The investigated cohort consisted of 35 COVID-19 patients hospitalized Charité – Universitätsmedizin Berlin or Unfallkrankenhaus Berlin between 31.03.2020 and 31.12.2020 and 35 age- and sex-matched healthy controls (HC) (**Table 1**). For each COVID-19 patient, the analysis included three plasma samples, each withdrawn at a different time-point of the hospital stay. Blood withdrawal was performed according to the standard of care and plasma was separated by centrifugation at 2200 × *g* for 10 min using plasma separation tubes with polymer gel and lithium heparin (Becton Dickinson, Medical-Pharmaceutical System, Franklin Lakes, NJ, United States, or Greiner Bio-One, Kremsmünster, Austria). Obtained plasma was aliquoted and stored at −80°C until the time of further analysis. C-reactive protein (CRP) was determined by immunoturbidimetry.

Enzyme-Linked Immunosorbent Assay

Plasma anti-SARS-CoV-2-IgG levels were semi-quantified using a commercially available enzyme-linked immunosorbent assay (ELISA) system [Anti-SARS-CoV-2-ELISA (IgG), EUROIMMUN Medizinische Labordiagnostika AG, Lübeck, Germany]. The system consists of immobilized recombinant SARS-CoV-2 Spike S1 subunit protein, which is specifically recognized and bound by its cognate anti-SARS-CoV-2 Spike S1 IgGs (in the following parts of this work referred to as anti-Spike/anti-S IgGs) contained in COVID-19 positive samples. The binding efficiency was determined based on the value of an extinction sample to extinction calibrator ratio, a relative measure of the anti-S IgG concentration in plasma. Plasma samples with anti-S IgG IU > 1.1 were assessed as COVID-19 positive and those with IU > 4.0 were used for anti-S IgG glycosylation analysis.

Purification of Anti-S IgG From Plasma

A 20-μl aliquot of each COVID-19 patient plasma sample was diluted 1:50 in the sample buffer supplied with the ELISA kit. The resulting mixture was distributed among four consecutive wells of the anti-SARS-CoV-2-ELISA plate and incubated for 1 h at 37°C. Afterward, the supernatants were discarded and the wells were washed with 3 × 300 μl of wash buffer (supplied with the ELISA kit) and 2 × 300 μl of Milli-Q water. The retained anti-S IgG antibodies were eluted with 3 × 100 μl of 100 mM formic acid. For each plasma sample, the eluates from all four wells were pooled together and evaporated in a vacuum centrifuge.

Purification of Total Immunoglobulins G From Plasma

Total IgG antibodies were isolated from human plasma as described previously (Schwedler and Blanchard, 2019). Briefly,

TABLE 1 | Demographics of the cohorts used in this study.

		COVID-19 patients		
Parameter	**HC**	**First detection**	**Middle detection**	**Last detection**
n	35	35	35	35
Age, years	65.0 (53.2–75.6)	64.0 (55.6–75.8)		
Female sex, *n* (%)	14 (40.0)	14 (40.0)		
Hospital stay, days		2 (0–6)	12 (5–17)	20 (13–30)
ICU, *n* (%)		28 (80.0)	24 (68.6)	7 (20.0)
Anti-S IgG, positive (%)		27 (77.1)	29 (82.9)	34 (97.1)
Anti-S IgG, IU		25.4 ± 33.0 (0.1–128.4)	77.3 ± 143.9 (0.1–721.1)	61.7 ± 68.5 (0.1–322.4)
CRP, mg/L		83.5 ± 86.9 (0.6–320.5)	47.8 ± 54.3 (0.6–284.7)	44.7 ± 59.4 (0.6–235.3)

HC, healthy controls; ICU, intensive care unit; CRP, C-reactive protein; Anti-S IgG, anti-SARS-CoV-2 immunoglobulin G; IU, international unit. Age and hospital stay are shown as median (interquartile range), whereas CRP and anti-S IgG are shown as mean ± SD (range).

a 5-μl aliquot of each plasma sample was incubated in a 96-well filter plate (AcroPrep Advance filter plate, 1.2 μm Supor membrane, Pall Life Sciences, Dreieich, Germany) with Protein A Sepharose beads (GE Healthcare, Uppsala, Sweden) for 1 h at 37°C. The beads were washed thoroughly with 1 × PBS and Milli-Q water under vacuum (multi-well plate vacuum manifold, Pall Life Sciences). Afterward, the captured IgG molecules (IgG_1, IgG_2, and IgG_4) were eluted with 2 × 50 μl of 100 mM formic acid, dried by vacuum centrifugation, and stored at −20°C until further use.

Tryptic Digestion and Glycopeptide Purification

Tryptic digestion of IgG followed by glycopeptide purification was performed as described previously (Wieczorek et al., 2020). Briefly, dried antigen-specific anti-S IgG or total IgG fractions were dissolved in 50 μl of 50 mM ammonium bicarbonate (Merck, Darmstadt, Germany). Sequencing grade modified trypsin (Promega, Madison, WI, United States) was reconstituted to a concentration of 0.2 μg/μl in a buffer provided by the manufacturer and 5 μl was added to each sample. After overnight incubation at 37°C, the digested IgGs were dried by vacuum centrifugation and stored at −20°C until further processing.

Immunoglobulins G glycopeptide enrichment was achieved using self-made cotton-HILIC microcolumns (Selman et al., 2011), conditioned with 3 × 50 μl of Milli-Q water and 3 × 50 μl of 85% ACN. Then, the trypsinized IgG samples were resuspended in 50 μl of 85% ACN and applied to the microcolumns. The columns were washed with 3 × 50 μl of 85% ACN containing 0.1% TFA and 3 × 50 μl of 85% ACN. Eventually, retained IgG glycopeptides were eluted with 6 × 50 μl of Milli-Q water, dried in a vacuum centrifuge, and stored at −20°C until MALDI-TOF-MS measurements.

MALDI-TOF Measurements and Data Analysis

Dried total and anti-S IgG glycopeptides were dissolved in 70 and 5 μl Milli-Q water, respectively. Of these, 1 μl was spotted on the stainless steel MALDI target plate (Bruker Daltonics, Bremen, Germany). After drying, each spot was overlaid with 1 μl of 2.5 mg/ml 4-chloro-α-cyanocinnamic acid (ClCCA, Sigma Aldrich, St. Louis, MO, United States) in 70% ACN and was left to air-dry at room temperature. Measurements were performed on Ultraflex III mass spectrometer (Bruker Daltonics, Bremen, Germany) equipped with Smart Beam Laser (laser frequency 100 Hz). Calibration was performed with Peptide Calibration Standard II (Bruker Daltonics, Bremen, Germany). Mass spectra were recorded in reflectron negative ionization mode using the *m/z* range of 1000–5000 and a partial "random-walk" laser movement mode. All IgG glycopeptides were detected as $[M\text{-}H]^-$ species and are listed in **Supplementary Table 1**. The recorded mass spectra were exported as ASCII text files, and the subsequent data processing including re-calibration, baseline subtraction, and peak extraction was performed using the MassyTools software (Jansen et al., 2015). The re-calibration of total IgG_1/anti-S IgG_1 and total IgG_2 mass spectra was performed using the list of six IgG_1 and six IgG_2 glycopeptides (G0F, G1F, G0FN, G2F, G1FN, and G2FS1), respectively. The intensities of the detected glycopeptides were normalized for total IgG_1, total IgG_2, and anti-S IgG_1. Afterward, the subclass-/type-specific IgG glycosylation profiles were represented in a form of four glycosylation traits, i.e., fucosylation, galactosylation, sialylation, and bisection, determined by summing up relative intensities of respective glycopeptide structures as described below:

Fucosylation (Fuc) = G0F + G1F + G2F + G0FN + G1FN + G2FN + G1FS1 + G2FS1 + mono G0F + mono G1F;

Galactosylation (Gal) = (G1F + G1FN + G1FS1 + Mono G1F + G1 + G1N) * 0,5 + G2F + G2FN + G2FS1 + G2 + G2N + G2S1;

Sialylation (Sial) = G1FS1 + G2FS1 + G1S1 + G2S1;

Bisecting GlcNAc (Bisec) = G0FN + G1FN + G2FN + G0N + G1N + G2N.

It should be noted that, in the case of IgG_2, fucosylation could not be determined due to the mass overlap of its afucosylated structures with the major glycopeptides of the IgG_4 subclass.

Statistical Analysis

Statistical analyses were performed using IBM SPSS version 25.0 (IBM, Armonk, NY, United States) and PRISM 6.0 software (GraphPad Software, La Jolla, CA, United States). Two-way ANOVA was performed to test whether total IgG_1-, anti-S IgG_1-, and total IgG_2-specific glycosylation traits change over the course of the COVID-19 disease. Wilcoxon signed-rank test was used to determine whether total IgG_1 and anti-S IgG_1 glycosylation profiles in COVID-19 patients differ between the first and the last time-point of hospitalization. Mann–Whitney *U*-test was used to determine whether total IgG_1 glycosylation differs between COVID-19 patients and HC. Association between the length of COVID-19 patients' hospital stay and age was evaluated by Pearson's correlation. Subsequently, the same statistical tests were performed to determine whether COVID-19-related differences in total IgG_1, total IgG_2, and anti-S IgG_1 glycosylation correlate with patients' age and with the difference in plasma CRP and anti-S IgG concentration recorded in the course of the disease. For each parameter/glycosylation trait, the difference between the last and the first time-point of hospitalization (Δ) was calculated according to the formula: $\Delta X = X_{last} - X_{first}$. To control the Type I Error, all individual *p*-values were adjusted employing the Bonferroni correction method (*p*-values were multiplied by the corresponding number of tests). Eventually, the Bonferroni corrected *p*-values are indicated as $^{*}p < 0.05$, $^{**}p < 0.01$, $^{***}p < 0.001$.

RESULTS

In this study, we investigated the glycosylation profiles of total IgG_1, total IgG_2, and antigen-specific anti-S IgG_1 isolated from plasma samples of COVID-19 patients by means of MALDI-TOF-MS. The investigated cohorts consisted of 35 severe COVID-19 patients and 35 sex- and age-matched HC, whose demographics are presented in **Table 1**. A majority of COVID-19 patients (80%) was treated at intensive care unit (ICU) wards. The hospitalization duration varied from 4 to 57 days (median: 20 days) and a total of 33 patients survived the COVID-19 infection. For each COVID-19 patient, three plasma samples (referred to as first, middle, and last) were analyzed, each of which corresponded to a different time-point of patient's hospital stay, namely the beginning, middle, and the end. The first anti-S IgG glycopeptide detection corresponded to hospitalization day 0–6 and, with few exceptions, matched with the first day when anti-S IgG could be unambiguously detected (≥1.1 IU). Altogether, the investigated material consisted of 140 plasma samples (HC: 35; COVID-19 patients: 105) resulting in 245 IgG glycopeptide samples (total IgG: 140; anti-S IgG: 105) being measured.

The analytical workflow used in this study is presented in **Figure 1**. Inter-day repeatability of the sample preparation was verified by analyzing the same plasma sample in triplicate on three consecutive days. The results of repeatability testing are presented in **Supplementary Figure 1**. The mean coefficient of variation values were 3.11 for total IgG_1, 3.75 for total IgG_2, and 4.71 for anti-S IgG_1, indicating a very good repeatability of the applied method.

The representative MALDI-TOF mass spectra $[M-H]^-$ of total and anti-S IgG glycopeptide fractions are presented in **Figure 2**. In the total IgG fraction, up to 28 glycopeptide signals were detected, of which 17 corresponded to IgG_1 and 11 to IgG_2 subclass (**Figure 2A** and **Supplementary Table 1**). Five IgG_2 structures (i.e., G1, G2, G1N, G2N, and G2S1) could not be unambiguously assigned due to the mass overlap with IgG_4 glycopeptides and hence were not included in the analysis. It should be noted that the anti-S IgG fraction contained solely IgG_1 glycopeptides (**Figure 2B**); this is why it is referred to as anti-S IgG_1 in the following parts of this work. As shown in **Figure 2B** for one representative COVID-19 patient, at the beginning of the disease (hospitalization day 6), the most abundant anti-S IgG_1 glycopeptides are the afucosylated G1 and G2 structures, whereas the fucosylated G0F and G1F glycopeptides become the most abundant structures later in the disease course (day 18 and day 31).

Aiming at performing statistical comparisons between clinical parameters and glycosylation features, the glycosylation profiles of total and anti-S IgGs were represented in the form of four glycosylation traits, namely fucosylation, galactosylation, sialylation, and bisection, calculated separately for each IgG subclass/type, as described in section "MALDI-TOF

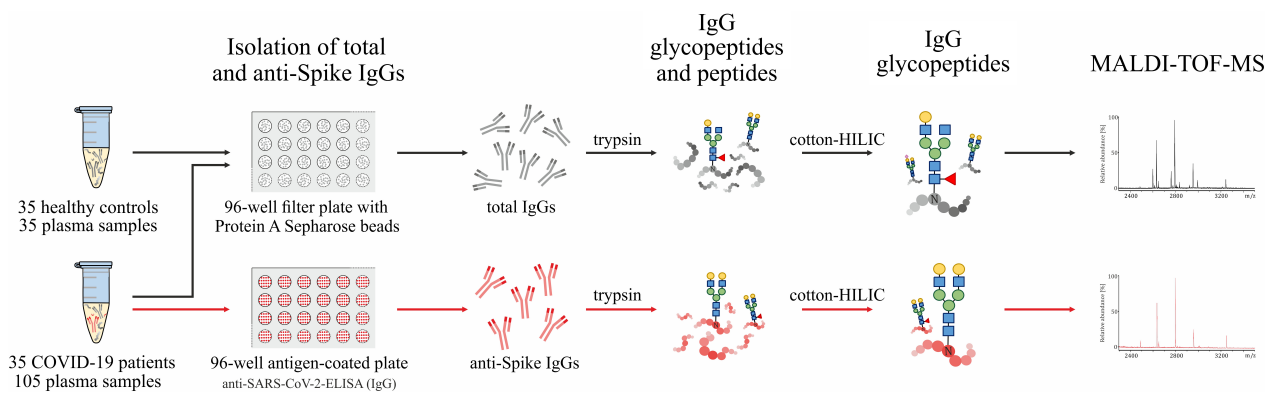

FIGURE 1 | Schematic representation of the analytical workflow used in this study.

Measurements and Data Analysis." The relative abundance and SD values of all total IgG_1, total IgG_2, and anti-S IgG_1 glycosylation traits and individual glycopeptide structures detected in HC and COVID-19 patients are presented in **Supplementary Table 2**.

As visible in **Figure 3**, COVID-19 was found to be associated with significant changes in total IgG_1, total IgG_2, and antigen-specific anti-S IgG_1 glycosylation. In general, all investigated IgG fractions presented similar patterns of COVID-19-related glycosylation alterations, marked by a gradual decrease in galactosylation and sialylation and a concomitant gradual increase in fucosylation (in the case of IgG_2, fucosylation was not determined). Bisection was the only glycosylation trait that showed a distinct profile of COVID-19-related alterations in total IgG_1/total IgG_2 and antigen-specific anti-S IgG_1 antibodies, in which it, respectively, decreased and increased in the course of the disease. IgG_2 was found to be marked by an overall lower galactosylation compared to both IgG_1 fractions, which seems to be a universal feature of IgG_2 glycosylation and is in line with previous reports (Bakovic et al., 2013; Wieczorek et al., 2020). Notably, the strongest COVID-19-related glycosylation alterations were recorded for antigen-specific anti-S IgG_1. Among all glycosylation traits, anti-S IgG_1 fucosylation and galactosylation had a particularly high variation in the course of the disease, with anti-S IgG_1 fucosylation (first: 83.3%; last: 95.9%) showing a 12% increase and anti-S IgG_1 galactosylation (first: 56.4%, last: 42.2%) a 14% decrease. Notably, as visible in **Supplementary Figure 2**, further stratification of COVID-19 cohort based on the length of hospitalization revealed that the above-described alterations prevail in patients with prolonged hospital stay (≥20 days).

Despite similar trends of COVID-19-related alterations, glycosylation profiles of total and antigen-specific anti-S IgG_1 antibodies were found to differ significantly, with the strongest discrepancy being observed at the beginning of hospitalization. Precisely, as visible in **Figure 4**, anti-S IgG_1 antibodies secreted early in the COVID-19 course were marked by significantly lower fucosylation and bisection and significantly higher galactosylation and sialylation as compared to total IgG_1 of COVID-19 patients. Notably, although anti-S IgG_1 glycosylation

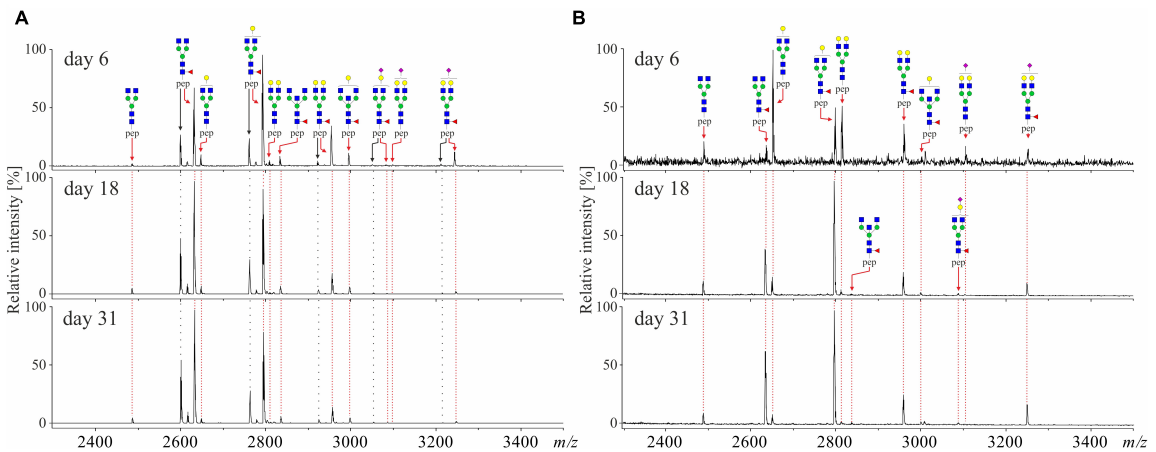

FIGURE 2 | Representative MALDI-TOF-mass spectra $[M-H]^-$ of **(A)** total $IgG_{1/2}$ and **(B)** anti-Spike IgG_1 isolated from plasma of severe COVID-19 patient (male, age 51) at beginning (day 6), midpoint (day 18), and the end (day 31) of the disease. IgG_1 glycopeptides are marked in red and IgG_2 glycopeptides are marked in black.

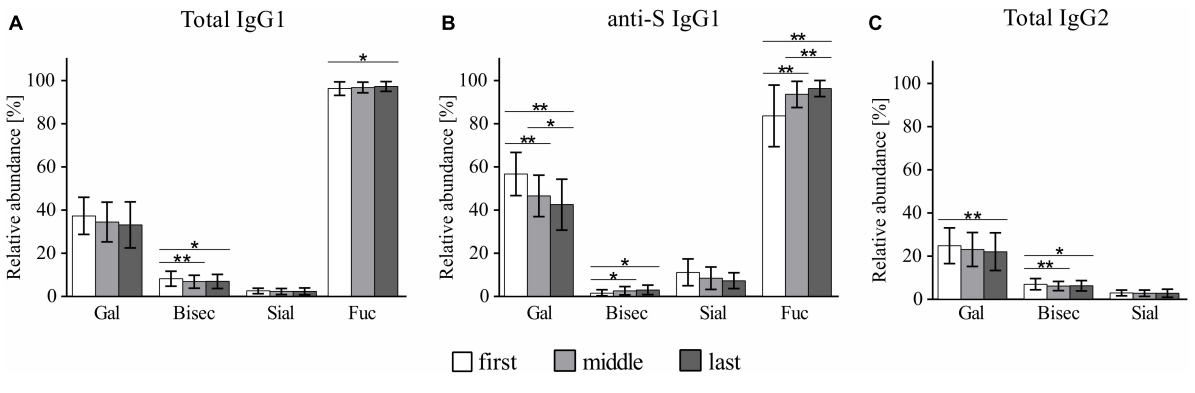

FIGURE 3 | Profiles of COVID-19-related glycosylation alterations in **(A)** total IgG_1, **(B)** anti-S IgG_1, and **(C)** total IgG_2. *$p < 0.05$, **$p < 0.01$. The calculation of the glycosylation traits Gal, Bisec, Sial, and Fuc is given in section "MALDI-TOF Measurements and Data Analysis."

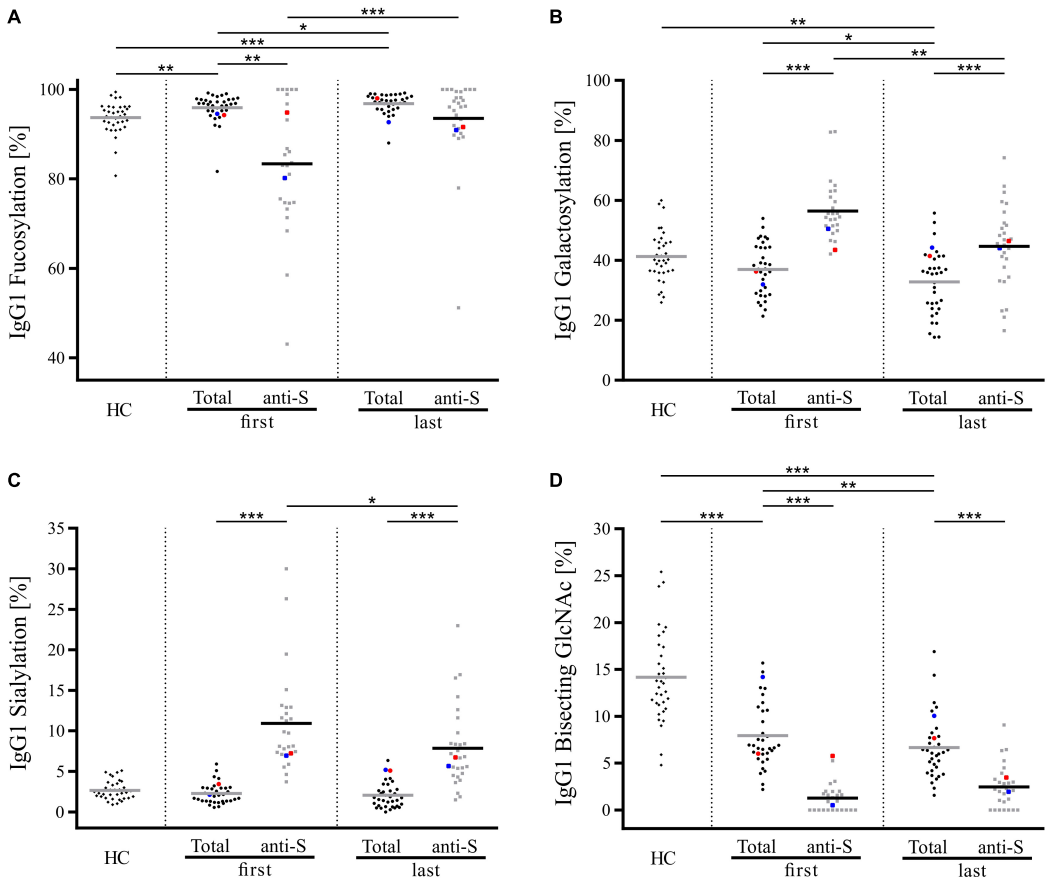

FIGURE 4 | Comparison of Fc glycosylation of total and anti-S IgG_1 in COVID-19 patients at the beginning and the end of hospitalization and total IgG_1 Fc glycosylation of healthy controls (HC). **(A)** Fucosylation, **(B)** galactosylation, **(C)** sialylation, and **(D)** bisecting GlcNAc. The calculation of the glycosylation traits Gal, Bisec, Sial, and Fuc is given in section "MALDI-TOF Measurements and Data Analysis." Data points corresponding to the two deceased COVID-19 patients are indicated in red (patient 1) and blue (patient 2). The Bonferroni corrected *p*-values are indicated as $*p < 0.05$, $**p < 0.01$, $***p < 0.001$.

was observed to alter continuously in the disease course (**Supplementary Figure 3**), statistically significant differences between total and anti-S IgG_1 were as well detected at the end of hospitalization for the following glycosylation traits: galactosylation, sialylation, and bisection. It is also notable that the profile of total IgG_1 glycosylation was found to differ significantly between COVID-19 patients and HC (**Figure 4**). In particular, total IgG_1 glycopeptides of COVID-19 patients were marked by decreased abundance of bisecting GlcNAc and increased fucosylation both at the beginning and at the end of hospitalization. Contrarily, sialylation of total IgG_1 was unaltered in COVID-19 patients as compared to HC, whereas galactosylation was significantly decreased in COVID-19 patients at the end of hospitalization.

In the investigated COVID-19 cohort, the length of hospitalization was expectedly found to correlate with patients' age ($p = 0.038$, Pearson $r = 0.3552$). Since, in line with literature data (Gudelj et al., 2018), IgG *N*-glycan composition in both healthy and COVID-19 patients was likewise observed to differ based on patients' age (**Supplementary Figure 4**), we next tested whether this age-dependency is also reflected at the level of COVID-19-related glycosylation changes recorded in total IgG_1, total IgG_2, and anti-S IgG_1. Among all investigated antibody fractions, age-dependency of COVID-19-related glycosylation alterations could be detected only in anti-S IgG_1. The results of the correlation analyses are presented in **Figure 5**, in which the *X* axes represent patient age, whereas the *Y* axes represent the change (Δ) in the respective anti-S IgG_1 glycosylation trait recorded between the last and first hospitalization time-points. Notably, anti-S IgG_1 fucosylation was the only glycosylation trait, in which the difference between the final and the initial level was significantly correlated with patients' age. Precisely, in the course of COVID-19 disease, younger patients exhibited significantly stronger alteration in anti-S IgG_1 fucosylation level as compared to older ones. Contrarily, in the case of galactosylation and sialylation, a more prominent change between the final and the initial level was observed in older COVID-19 patients, however, the respective correlations were statistically insignificant.

Since altered IgG glycosylation is a common feature of inflammatory conditions, we next tested whether COVID-19-related total and anti-S IgG_1 glycosylation alterations correlate with changes in CRP and plasma anti-S IgG concentration in

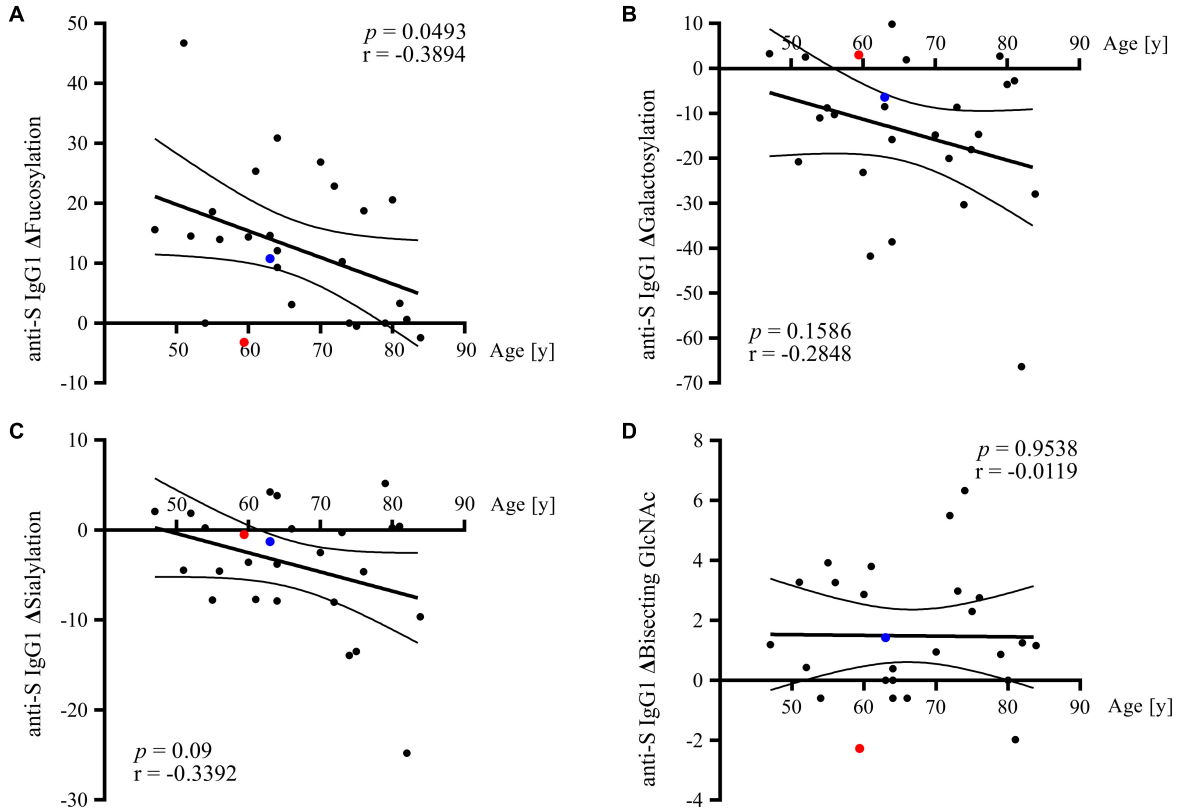

FIGURE 5 | Correlation of anti-S IgG_1 glycosylation alterations with patients' age. In each graph, the *Y* axis represents the difference (Δ) in the relative abundance of the respective glycosylation trait recorded between the last and first hospitalization time-point: **(A)** Δfucosylation, **(B)** Δgalactosylation, **(C)** Δsialylation, and **(D)** Δbisecting GlcNAc. Data points corresponding to the two deceased COVID-19 patients are indicated in red (patient 1) and blue (patient 2).

the course of COVID-19. As compared to physiological CRP concentrations that range between 0.8 and 3.0 mg/L (Shine et al., 1981), CRP levels in COVID-19 patients were strongly increased, with the highest levels being expectedly recorded at the beginning of hospitalization (except for the two patients who did not survive COVID-19) (**Supplementary Figure 5A**). In the course of patients' hospitalization, the CRP and anti-S IgG levels were observed to, respectively, decrease and increase in COVID-19 patients; however, for none of these parameters the difference between the final and the initial level was correlated with patients' age (**Supplementary Figures 5C,F**). As visible in **Table 2**, Pearson's correlation analyses revealed that COVID-19-related changes in total and anti-S IgG_1 glycosylation profiles are not correlated with changes in CRP levels. Contrarily, changes in anti-S IgG_1 galactosylation and sialylation were both found to significantly correlate with changes in plasma anti-S IgG concentration recorded between the last and the first time-point of patients' hospital stay (**Table 2**).

DISCUSSION

An increasing number of evidences suggest that altered IgG glycosylation might be a factor contributing to disease severity in COVID-19. To further deepen the understanding of molecular signatures underlying the SARS-CoV-2 infection, in this work, we performed a longitudinal analysis of total and anti-S IgG Fc-glycosylation in a cohort of 35 hospitalized COVID-19 patients and 35 HC by means of MALDI-TOF-MS. To assure site- and subclass-specificity of determined glycosylation profiles, in this study, all analyses were performed at the level of tryptic glycopeptides.

Upon SARS-CoV-2 infection, virus-specific IgG antibodies are typically detected in blood within 7 days from symptom onset (Long et al., 2020; Dan et al., 2021; Pang et al., 2021; Semmler et al., 2021; Sterlin et al., 2021). In our study, the first detection of SARS-CoV-2-specific anti-S glycopeptides in plasma of affected patients occurred between the hospitalization day 0 and day 6. While this broad range might partly result from the differences in patients' hospital admission time, it might as well reflect the inter-individual variability of the humoral immune response to SARS-CoV-2 infection.

In our study, COVID-19 was found to be associated with significant changes in total and antigen-specific IgG glycosylation. In particular, anti-S IgG_1 produced in the early stage of the disease was found to be marked by strongly decreased core-fucosylation, which is in line with previously reported data (Hoepel et al., 2021; Larsen et al., 2021). Of note, this particular feature of SARS-CoV-2-specific antibodies has important functional consequences. Precisely, although

afucosylation of the IgG Fc portion does not influence the binding toward viral particles, it enhances by several folds the binding affinity toward FcγRIIIa receptors on the surface of innate immune cells (Wang et al., 2017; Chakraborty et al., 2021). These Fc-FcγR interactions are crucial for Fc-mediated effector functions such as antibody-dependent cellular cytotoxity and phagocytosis, which next to viral neutralization are the primarily mechanisms contributing to anti-viral host protection (Taylor et al., 2021). Data reported by Bye et al. (2021) indicate, however, that low fucosylation of anti-SARS-CoV-2 Spike IgG might be a double-edged sword; while it facilitates the recovery process by potentiating anti-viral immune responses, it might contribute to COVID-19 patients' death by enhancing pathogenic platelet activation and thrombosis (Bye et al., 2021). In line with this data, immune complexes engaging afucosylated IgG molecules were shown to stimulate the expression of pro-inflammatory cytokines (e.g., IL-6, TNF, and IL-1β) in macrophages and natural killer cells, generating a prothrombotic environment (Chakraborty et al., 2021; Larsen et al., 2021). In addition, high titers and low fucosylation of anti-S IgG_1 were recently shown to promote inflammation by alveolar macrophages (Hoepel et al., 2021).

Consistent with data of Larsen et al. (2021), in this work, the initially low fucosylation of antigen-specific IgG_1 was found to increase continuously over time, eventually approaching the levels observed in total IgG_1. It seems plausible that this timely restricted production of highly potent afucosylated anti-viral antibodies helps preventing excessive and potentially harmful immune activation. Contrary to the above described findings, in the study of Chakraborty et al. (2021), afucosylation levels were shown to be stable over time. This discrepancy might be caused by the fact that, in the latter study, the investigated samples were not collected at the onset of anti-S IgG_1 expression.

Interestingly, some reports indicate that low fucosylation of antigen-specific IgG antibodies might as well play a role in other acute viral infections. For instance, a longitudinal study of dengue-infected patients showed that, at the early stage of the disease, IgG glycosylation profile is marked by high afucosylation, which decreases in the course of the disease the way we have measured here for anti-S IgG (Wang et al., 2017). Contrarily, antibodies against internal viral proteins such as nucleocapsid in COVID-19 or the parvovirus B19 were not afucosylated but rather highly fucosylated (Larsen et al., 2021). These seemingly contradictory data suggest that the biological function of IgG fucosylation might differ depending on the nature of the infectious agent, but this has not been investigated in details so far.

Besides profiling the COVID-19-related IgG glycosylation changes, the aim of our study was to determine whether observed alterations are associated with patients age and whether they correlate with changes in CRP and anti-SARS-CoV-2 IgG plasma concentrations. Notably, for the vast majority of conducted analyses, statistically significant trends were observed exclusively in antigen-specific anti-S IgG_1, which further confirms that the glycosylation of bulk and anti-viral IgG in COVID-19 might be distinctly regulated. In this work, anti-S IgG_1 fucosylation was the only glycosylation trait whose change was correlated with patients' age during hospitalization. Precisely, in the course of the disease, anti-S IgG_1 antibodies of younger COVID-19 patients displayed a more prominent alteration in the fucosylation level as compared to older patients. In the light of what has been written above, it seems plausible that this dynamic timely restricted transition from highly pro-inflammatory afucosylated phenotype at seroconversion to less pro-inflammatory fucosylated anti-S IgG_1 phenotype observed later in the disease course comprises an innate regulatory mechanism that allows younger individuals to mount a more potent virus-specific immune response that is limited to the early phase of the disease. Following this understanding, a weaker change in anti-S IgG_1 fucosylation observed in older COVID-19 patients could contribute to compromised or less balanced anti-viral response. In line with this rationale, the quality of the humoral response was shown to decline with age, which was linked to diminished potential of aged B-cells to undergo somatic hypermutations (Frasca et al., 2017). Correspondingly, the quantity and glycosylation profile of anti-SARS-CoV-2 antibodies elicited in response to COVID-19 mRNA vaccination were shown to differ in younger and older individuals (Farkash et al., 2021). In line with our data, anti-SARS-CoV-2 antibodies produced after the first and the second vaccination showed higher variation with respect to the fucosylation level in younger as opposed to older individuals (Farkash et al., 2021). Interestingly, in our study, no correlation was observed between the change in anti-S IgG_1 fucosylation and the change in anti-SARS-CoV-2 antibody titer in the course of hospitalization, implying

TABLE 2 | Correlation between COVID-19-related differences in total and anti-S IgG_1-specific glycosylation traits and the difference in CRP and anti-S IgG plasma concentration in COVID-19 patients.

		Total IgG_1				Anti-S IgG_1			
		ΔFuc	**ΔGal**	**ΔSial**	**ΔBisec**	**ΔFuc**	**ΔGal**	**ΔSial**	**ΔBisec**
ΔCRP	*r*	−0.217	0.246	0.032	−0.351	0.166	0.311	0.218	−0.176
	p	1	1	1	0.8	1	1	1	1
Δanti-S IgG	*r*	−0.123	−0.194	−0.033	−0.332	−0.175	−0.717	−0.617	−0.075
	p	1	1	1	0.784	1	0.0016	0.0064	1

The difference between the last and the first time-point of hospitalization (Δ) was calculated for each parameter or glycosylation trait according to the formula: $\Delta X = X_{last} - X_{first}$. For all glycosylation traits, descriptive statistics are shown in terms of r (Pearson's correlation coefficient) and p (p-values). The presented p-values are Bonferroni-adjusted, statistical significance was reached when $p < 0.05$. Representations of glycosylation traits are given in terms of Fuc (fucosylation), Gal (galactosylation), Sial (sialylation), and Bisec (bisecting GlcNAc).

that the above-described age-dependent transformation of IgG fucosylation in COVID-19 patients is independent of anti-S IgG abundancy in blood. Nevertheless, considering that the vast majority of the investigated cohort was represented by severe COVID-19 patients, who presented overall high anti-Spike IgG titers, the latter observation necessitates validation in a larger and more diversified cohort.

In line with the results of Hoepel et al. (2021) and Larsen et al. (2021), anti-S IgG_1 antibodies investigated in the present study were marked by high galactosylation and sialylation as compared to their corresponding levels in total IgG_1. Particularly, this glycosylation profile of anti-SARS-CoV-2 antibodies was specific to the early stage of the disease, as the disparity between total and antigen-specific IgG galactosylation/sialylation diminished continuously toward the end of hospitalization. Notably, this profile was shown to be associated with previous natural infection and recent immunization (Wang et al., 2015; Sonneveld et al., 2017; Hoepel et al., 2021). Interestingly, contrary to the trends observed for fucosylation, COVID-19-related decrease in anti-S IgG_1 galactosylation and sialylation showed no correlation with patients' age; instead, they were found to negatively correlate with changes in anti-S IgG plasma concentration. Considering that, along with previous reports (Hoepel et al., 2021; Larsen et al., 2021), anti-S IgG_1 concentration and anti-S IgG_1 galactosylation/sialylation levels were, respectively, observed to increase and decrease in the course of the disease, the above findings imply that a strong increase in anti-S IgG concentration, reported to occur in severe COVID-19 patients (Larsen et al., 2021; Madariaga et al., 2021), might be accompanied with less prominent decrease in anti-S IgG_1 galactosylation and sialylation. Notably, the persistence of highly galactosylated/sialylated anti-S IgG_1 antibodies that are otherwise limited to acute, early stage of the disease, could potentially contribute to the severity of the disease. This observation is advocated by the fact that platelet-mediated thrombosis that contributes to increased mortality in critically ill COVID-19 patients was shown to require both low levels of fucosylation and high levels of galactosylation in the anti-S IgG Fc domain (Bye et al., 2021).

Expectedly, inflammation accompanying SARS-CoV-2 infection was reflected by strong CRP elevation in COVID-19 patients at the beginning of hospitalization. Afterward, in the COVID-19 patients who survived the disease, CRP levels were found to gradually decrease in the disease course, with the biggest change being observed during the first half of hospitalization. In our study, the difference in CRP level showed no correlation with changes observed in IgG glycosylation traits.

It should be noted that the present study suffers from some limitations. First and foremost, the analyses were conducted on a relatively small number of samples, with COVID-19 cohort consisting predominantly of patients having severe disease symptoms. Therefore, it would be meaningful to validate these findings in a larger and more diversified cohort. Additionally, anti-S IgG fractions investigated in our study contained exclusively IgG_1 glycopeptides, as antibodies of this subclass dominate the immune response directed toward S1 subunits of the viral Spike protein (Yates et al., 2021). It would be of interest to determine whether reported trends are as well observed in IgG_3, whose titers were recently reported to increase upon SARS-CoV-2 infection, particularly in response to SARS-CoV-2 Spike S2 subunit (Luo et al., 2021; Yates et al., 2021).

In conclusion, the results presented in this study confirm previous findings showing that anti-S IgG_1 antibodies produced in COVID-19 patients are marked by differential glycosylation profiles, which normalize gradually in the course of the disease. Using a German cohort, we were able to show that COVID-19-related glycosylation alterations that occur in antigen-specific anti-S antibodies are to some extend dependent on patient's age and anti-S IgG quantity. Further studies are needed to determine whether these observed trends are specific to anti-Spike S1 subunit IgG_1 antibodies and whether they are likewise detected in COVID-19 patients suffering from less severe disease symptoms.

DATA AVAILABILITY STATEMENT

The raw data supporting the conclusions of this article will be made available by the authors, without undue reservation.

ETHICS STATEMENT

The studies involving human participants were reviewed and approved by the Charité – Universitätsmedizin Berlin, Campus Virchow-Klinikum, Germany (no. EA2/095/20) and by the Ärztekammer Berlin, Germany (Eth-23/20). All experiments for EA2/095/20 were performed in accordance with relevant guidelines and regulations. Additional written informed consent was taken for Eth-23/20.

AUTHOR CONTRIBUTIONS

VB contributed to the conception and design of the study. KK, BH, JR, and GH coordinated the collection of samples and database. CS and MG performed the experiments and data analysis. VB, MG, and CS wrote the manuscript. All authors contributed to manuscript revision, read, and approved the submitted version.

FUNDING

This work was financially supported by the Federal Ministry of Education and Research through the project titled "Multimodal Clinical Mass Spectrometry to Target Treatment Resistance (MSTARS)" (grant number 031L0220A), DKTK (RAMTAS) and by the Sonnenfeld Foundation (grant for equipment).

SUPPLEMENTARY MATERIAL

The Supplementary Material for this article can be found online at: https://www.frontiersin.org/articles/10.3389/fmicb.2022.775186/full#supplementary-material

Supplementary Figure 1 | Inter-day repeatability testing of the analytical workflow used in this study. Average is shown as mean ± SD.

Supplementary Figure 2 | Coronavirus disease 2019-related glycosylation alterations in patients with shorter (<20 days) and longer (≥20 days) hospitalization. **(A)** Total IgG_1, **(B)** anti-S IgG_1, and **(C)** total IgG_2. The calculation of the glycosylation traits Gal, Bisec, Sial, and Fuc is given in section "MALDI-TOF Measurements and Data Analysis." $*p < 0.05$, $**p < 0.01$.

Supplementary Figure 3 | Longitudinal changes of (left) anti-S IgG_1 and (right) total IgG_1 Fc glycosylation in COVID-19 patients; **(A,B)** fucosylation, **(C,D)** galactosylation, **(E,F)** sialylation, and **(G,H)** bisecting GlcNAc. Data points corresponding to the two deceased COVID-19 patients are indicated in red (patient 1) and blue (patient 2).

Supplementary Figure 4 | The age-related IgG glycosylation changes in both healthy controls (HC) and COVID-19 patients represented with the two major IgG_1 *N*-glycopeptide structures, namely **(A)** agalactosylated G0F and **(B)** digalactosylated G2F.

Supplementary Figure 5 | Plasma CRP and anti-S IgG concentration in COVID-19 patients. **(A,D)** CRP and anti-S IgG levels at the beginning, in the middle, and at the end of patients' hospital stay. **(B,E)** Longitudinal changes in CRP and anti-S IgG_1 levels in the course of the disease. **(C,F)** Correlation of CRP and anti-S IgG levels with patients' age; the *Y* axes represent the difference (Δ) in the respective parameter recorded between the last and first hospitalization time-point. Data points corresponding to the two deceased COVID-19 patients are indicated in red (patient 1) and blue (patient 2). For patient 1, only one measurement of CRP was performed. $**p < 0.01$, $***p < 0.001$.

REFERENCES

Axford, J. S., Mackenzie, L., Lydyard, P. M., Hay, F. C., Isenberg, D. A., and Roitt, I. M. (1987). Reduced B-cell galactosyltransferase activity in rheumatoid arthritis. *Lancet* 2, 1486–1488. doi: 10.1016/s0140-6736(87)92621-3

Bakovic, M. P., Selman, M. H., Hoffmann, M., Rudan, I., Campbell, H., Deelder, A. M., et al. (2013). High-throughput IgG Fc N-glycosylation profiling by mass spectrometry of glycopeptides. *J. Proteome Res.* 12, 821–831. doi: 10.1021/pr300887z

Bartsch, Y. C., Eschweiler, S., Leliavski, A., Lunding, H. B., Wagt, S., Petry, J., et al. (2020). IgG Fc sialylation is regulated during the germinal center reaction following immunization with different adjuvants. *J. Allergy Clin. Immunol.* 146, 652–666 e11.. doi: 10.1016/j.jaci.2020.04.059

Bye, A. P., Hoepel, W., Mitchell, J. L., Jegouic, S., Loureiro, S., Sage, T., et al. (2021). Aberrant glycosylation of anti-SARS-CoV-2 spike IgG is a prothrombotic stimulus for platelets. *Blood* 138, 1481–1489. doi: 10.1182/blood.2021011871

Chakraborty, S., Gonzalez, J., Edwards, K., Mallajosyula, V., Buzzanco, A. S., Sherwood, R., et al. (2021). Proinflammatory IgG Fc structures in patients with severe COVID-19. *Nat. Immunol.* 22, 67–73. doi: 10.1038/s41590-020-00828-7

Clerc, F., Reiding, K. R., Jansen, B. C., Kammeijer, G. S., Bondt, A., and Wuhrer, M. (2016). Human plasma protein N-glycosylation. *Glycoconj. J.* 33, 309–343. doi: 10.1007/s10719-015-9626-2

Dall'olio, F., Vanhooren, V., Chen, C. C., Slagboom, P. E., Wuhrer, M., and Franceschi, C. (2013). N-glycomic biomarkers of biological aging and longevity: a link with inflammaging. *Ageing Res. Rev.* 12, 685–698. doi: 10.1016/j.arr.2012.02.002

Dan, J. M., Mateus, J., Kato, Y., Hastie, K. M., Yu, E. D., Faliti, C. E., et al. (2021). Immunological memory to SARS-CoV-2 assessed for up to 8 months after infection. *Science* 371:eabf4063. doi: 10.1126/science.abf4063

De Haan, N., Reiding, K. R., Driessen, G., Van Der Burg, M., and Wuhrer, M. (2016). Changes in healthy human IgG Fc-glycosylation after birth and during early childhood. *J. Proteome Res.* 15, 1853–1861. doi: 10.1021/acs.jproteome.6b00038

De Wit, E., Van Doremalen, N., Falzarano, D., and Munster, V. J. (2016). SARS and MERS: recent insights into emerging coronaviruses. *Nat. Rev. Microbiol.* 14, 523–534. doi: 10.1038/nrmicro.2016.81

Ercan, A., Kohrt, W. M., Cui, J., Deane, K. D., Pezer, M., Yu, E. W., et al. (2017). Estrogens regulate glycosylation of IgG in women and men. *JCI Insight* 2:e89703. doi: 10.1172/jci.insight.89703

Farkash, I., Feferman, T., Cohen-Saban, N., Avraham, Y., Morgenstern, D., Mayuni, G., et al. (2021). Anti-SARS-CoV-2 antibodies elicited by COVID-19 mRNA vaccine exhibit a unique glycosylation pattern. *Cell Rep.* 37:110114. doi: 10.1016/j.celrep.2021.110114

Frasca, D., Diaz, A., Romero, M., and Blomberg, B. B. (2017). Human peripheral late/exhausted memory B cells express a senescent-associated secretory phenotype and preferentially utilize metabolic signaling pathways. *Exp. Gerontol.* 87, 113–120. doi: 10.1016/j.exger.2016.12.001

Gudelj, I., Lauc, G., and Pezer, M. (2018). Immunoglobulin G glycosylation in aging and diseases. *Cell Immunol.* 333, 65–79. doi: 10.1016/j.cellimm.2018.07.009

Hess, C., Winkler, A., Lorenz, A. K., Holecska, V., Blanchard, V., Eiglmeier, S., et al. (2013). T cell-independent B cell activation induces immunosuppressive sialylated IgG antibodies. *J. Clin. Invest.* 123, 3788–3796. doi: 10.1172/JCI65938

Ho, C. H., Chien, R. N., Cheng, P. N., Liu, J. H., Liu, C. K., Su, C. S., et al. (2015). Aberrant serum immunoglobulin G glycosylation in chronic hepatitis B is associated with histological liver damage and reversible by antiviral therapy. *J. Infect. Dis.* 211, 115–124. doi: 10.1093/infdis/jiu388

Hoepel, W., Chen, H. J., Geyer, C. E., Allahverdiyeva, S., Manz, X. D., De Taeye, S. W., et al. (2021). High titers and low fucosylation of early human anti-SARS-CoV-2 IgG promote inflammation by alveolar macrophages. *Sci. Transl. Med.* 13:eabf8654. doi: 10.1126/scitranslmed.abf8654

Irvine, E. B., and Alter, G. (2020). Understanding the role of antibody glycosylation through the lens of severe viral and bacterial diseases. *Glycobiology* 30, 241–253. doi: 10.1093/glycob/cwaa018

Jansen, B. C., Reiding, K. R., Bondt, A., Hipgrave Ederveen, A. L., Palmblad, M., Falck, D., et al. (2015). Massytools: a high-throughput targeted data processing tool for relative quantitation and quality control developed for glycomic and glycoproteomic MALDI-MS. *J. Proteome Res.* 14, 5088–5098. doi: 10.1021/acs.jproteome.5b00658

Karsten, C. M., Pandey, M. K., Figge, J., Kilchenstein, R., Taylor, P. R., Rosas, M., et al. (2012). Anti-inflammatory activity of IgG1 mediated by Fc galactosylation and association of FcgammaRIIB and dectin-1. *Nat. Med.* 18, 1401–1406. doi: 10.1038/nm.2862

Larsen, M. D., De Graaf, E. L., Sonneveld, M. E., Plomp, H. R., Nouta, J., Hoepel, W., et al. (2021). Afucosylated IgG characterizes enveloped viral responses and correlates with COVID-19 severity. *Science* 371:eabc8378. doi: 10.1126/science.abc8378

Long, Q. X., Liu, B. Z., Deng, H. J., Wu, G. C., Deng, K., Chen, Y. K., et al. (2020). Antibody responses to SARS-CoV-2 in patients with COVID-19. *Nat. Med.* 26, 845–848.

Luo, H., Jia, T., Chen, J., Zeng, S., Qiu, Z., Wu, S., et al. (2021). The characterization of disease severity associated IgG subclasses response in COVID-19 patients. *Front. Immunol.* 12:632814. doi: 10.3389/fimmu.2021.632814

Madariaga, M. L. L., Guthmiller, J. J., Schrantz, S., Jansen, M. O., Christensen, C., Kumar, M., et al. (2021). Clinical predictors of donor antibody titre and correlation with recipient antibody response in a COVID-19 convalescent plasma clinical trial. *J. Intern. Med.* 289, 559–573. doi: 10.1111/joim.13185

Pang, N. Y., Pang, A. S., Chow, V. T., and Wang, D. Y. (2021). Understanding neutralising antibodies against SARS-CoV-2 and their implications in clinical practice. *Mil. Med. Res.* 8:47. doi: 10.1186/s40779-021-00342-3

Pilkington, C., Yeung, E., Isenberg, D., Lefvert, A. K., and Rook, G. A. (1995). Agalactosyl IgG and antibody specificity in rheumatoid arthritis, tuberculosis, systemic lupus erythematosus and myasthenia gravis. *Autoimmunity* 22, 107–111. doi: 10.3109/08916939508995306

Reis, C. A., Tauber, R., and Blanchard, V. (2021). Glycosylation is a key in SARS-CoV-2 infection. *J. Mol. Med.* 99, 1023–1031. doi: 10.1007/s00109-021-02092-0

Schur, P. H. (1988). IgG subclasses. A historical perspective. *Monogr. Allergy* 23, 1–11.

Schwedler, C., and Blanchard, V. (2019). Measurement of neutral and sialylated IgG N-Glycome at Asn-297 by CE-LIF to assess hypogalactosylation in rheumatoid arthritis. *Methods Mol. Biol.* 1972, 77–93. doi: 10.1007/978-1-4939-9213-3_6

Schwedler, C., Haupl, T., Kalus, U., Blanchard, V., Burmester, G. R., Poddubnyy, D., et al. (2018). Hypogalactosylation of immunoglobulin G in rheumatoid arthritis: relationship to HLA-DRB1 shared epitope, anticitrullinated protein

antibodies, rheumatoid factor, and correlation with inflammatory activity. *Arthritis Res. Ther.* 20:44. doi: 10.1186/s13075-018-1540-0

Selman, M. H., Hemayatkar, M., Deelder, A. M., and Wuhrer, M. (2011). Cotton HILIC SPE microtips for microscale purification and enrichment of glycans and glycopeptides. *Anal. Chem.* 83, 2492–2499. doi: 10.1021/ac1027116

Semmler, G., Traugott, M. T., Graninger, M., Hoepler, W., Seitz, T., Kelani, H., et al. (2021). Assessment of S1-, S2-, and NCP-Specific IgM, IgA, and IgG Antibody Kinetics in Acute SARS-CoV-2 infection by a microarray and twelve other immunoassays. *J. Clin. Microbiol.* 59:e02890-20. doi: 10.1128/JCM.02890-20

Shine, B., De Beer, F. C., and Pepys, M. B. (1981). Solid phase radioimmunoassays for human C-reactive protein. *Clin. Chim. Acta* 117, 13–23. doi: 10.1016/0009-8981(81)90005-x

Sonneveld, M. E., Koelewijn, J., De Haas, M., Admiraal, J., Plomp, R., Koeleman, C. A., et al. (2017). Antigen specificity determines anti-red blood cell IgG-Fc alloantibody glycosylation and thereby severity of haemolytic disease of the fetus and newborn. *Br. J. Haematol.* 176, 651–660. doi: 10.1111/bjh.14438

Stambuk, J., Nakic, N., Vuckovic, F., Pucic-Bakovic, M., Razdorov, G., Trbojevic-Akmacic, I., et al. (2020). Global variability of the human IgG glycome. *Aging* 12, 15222–15259. doi: 10.18632/aging.103884

Sterlin, D., Mathian, A., Miyara, M., Mohr, A., Anna, F., Claer, L., et al. (2021). IgA dominates the early neutralizing antibody response to SARS-CoV-2. *Sci. Transl. Med.* 13:eabd2223.

Taylor, P. C., Adams, A. C., Hufford, M. M., De La Torre, I., Winthrop, K., and Gottlieb, R. L. (2021). Neutralizing monoclonal antibodies for treatment of COVID-19. *Nat. Rev. Immunol.* 21, 382–393. doi: 10.1038/s41577-021-00542-x

Van De Geijn, F. E., Wuhrer, M., Selman, M. H., Willemsen, S. P., De Man, Y. A., Deelder, A. M., et al. (2009). Immunoglobulin G galactosylation and sialylation are associated with pregnancy-induced improvement of rheumatoid arthritis and the postpartum flare: results from a large prospective cohort study. *Arthritis Res. Ther.* 11:R193. doi: 10.1186/ar2892

Wang, T. T., Maamary, J., Tan, G. S., Bournazos, S., Davis, C. W., Krammer, F., et al. (2015). Anti-HA Glycoforms Drive B Cell Affinity Selection and Determine Influenza Vaccine Efficacy. *Cell* 162, 160–169. doi: 10.1016/j.cell.2015.06.026

Wang, T. T., and Ravetch, J. V. (2019). Functional diversification of IgGs through Fc glycosylation. *J. Clin. Invest.* 129, 3492–3498. doi: 10.1172/JCI130029

Wang, T. T., Sewatanon, J., Memoli, M. J., Wrammert, J., Bournazos, S., Bhaumik, S. K., et al. (2017). IgG antibodies to dengue enhanced for FcgammaRIIIA binding determine disease severity. *Science* 355, 395–398. doi: 10.1126/science.aai8128

Wieczorek, M., Braicu, E. I., Oliveira-Ferrer, L., Sehouli, J., and Blanchard, V. (2020). Immunoglobulin G subclass-specific glycosylation changes in primary epithelial ovarian cancer. *Front. Immunol.* 11:654. doi: 10.3389/fimmu.2020.00654

Yates, J. L., Ehrbar, D. J., Hunt, D. T., Girardin, R. C., Dupuis, A. P. II, Payne, A. F., et al. (2021). Serological analysis reveals an imbalanced IgG subclass composition associated with COVID-19 disease severity. *Cell Rep. Med.* 2:100329. doi: 10.1016/j.xcrm.2021.100329

Yu, X., Marshall, M. J. E., Cragg, M. S., and Crispin, M. (2017). Improving antibody-based cancer therapeutics through glycan engineering. *BioDrugs* 31, 151–166. doi: 10.1007/s40259-017-0223-8

Conflict of Interest: KK is partly contractually provided to Labor Berlin – Charité Vivantes GmbH.

The remaining authors declare that the research was conducted in the absence of any commercial or financial relationships that could be construed as a potential conflict of interest.

Publisher's Note: All claims expressed in this article are solely those of the authors and do not necessarily represent those of their affiliated organizations, or those of the publisher, the editors and the reviewers. Any product that may be evaluated in this article, or claim that may be made by its manufacturer, is not guaranteed or endorsed by the publisher.

Advantages of publishing in Frontiers

OPEN ACCESS
Articles are free to read for greatest visibility and readership

FAST PUBLICATION
Around 90 days from submission to decision

HIGH QUALITY PEER-REVIEW
Rigorous, collaborative, and constructive peer-review

TRANSPARENT PEER-REVIEW
Editors and reviewers acknowledged by name on published articles

Frontiers
Avenue du Tribunal-Fédéral 34
1005 Lausanne | Switzerland

Visit us: www.frontiersin.org
Contact us: frontiersin.org/about/contact

REPRODUCIBILITY OF RESEARCH
Support open data and methods to enhance research reproducibility

DIGITAL PUBLISHING
Articles designed for optimal readership across devices

FOLLOW US
@frontiersin

IMPACT METRICS
Advanced article metrics track visibility across digital media

EXTENSIVE PROMOTION
Marketing and promotion of impactful research

LOOP RESEARCH NETWORK
Our network increases your article's readership